UNIVERSIDAD COMPLUTENSE DE MADRID
FACULTAD DE GEOGRAFÍA E HISTORIA

TESIS DOCTORAL

Taphonomic and spatial study of the archeological site DS from Bed I in Olduvai Gorge (Tanzxania)

Estudio tafonómico y espacial del yacimiento DS del Lecho I de la garganta de Olduvai (Tanzania)

MEMORIA PARA OPTAR AL GRADO DE DOCTOR

PRESENTADA POR

Lucía Cobo Sánchez

Directores

Manuel Domínguez Rodrigo
Gonzalo Ruiz Zapatero

Madrid

UNIVERSIDAD COMPLUTENSE DE MADRID

FACULTAD DE GEOGRAFÍA E HISTORIA

TESIS DOCTORAL

Taphonomic and spatial study of the archaeological site DS from Bed I in Olduvai Gorge (Tanzania)

Estudio tafonómico y espacial del yacimiento arqueológico DS del Lecho I de la Garganta de Olduvai (Tanzania)

Lucía Cobo Sánchez

Directores:
Manuel Domínguez Rodrigo
Gonzalo Ruiz Zapatero

Tutor:
Gonzalo Ruiz Zapatero

Madrid, 2020

UNIVERSIDAD COMPLUTENSE DE MADRID

FACULTAD DE GEOGRAFÍA E HISTORIA

TESIS DOCTORAL

TAPHONOMIC AND SPATIAL STUDY OF THE ARCHAEOLOGICAL SITE DS FROM BED I IN OLDUVAI GORGE (TANZANIA) / ESTUDIO TAFONÓMICO Y ESPACIAL DEL YACIMIENTO ARQUEOLÓGICO DS DEL LECHO I DE LA GARGANTA DE OLDUVAI (TANZANIA)

MEMORIA PARA OPTAR AL GRADO DE DOCTOR

PRESENTADA POR

Lucía Cobo Sánchez

DIRECTOR

Manuel Domínguez Rodrigo
Gonzalo Ruiz Zapatero

To my parents, who have given me so
many opportunities,

and

to Manuel, who awoke my interest and
curiosity in human evolution.

If you could interview a chimpanzee about the differences between humans and apes, I think it might say, 'You humans are very odd; when you get food, instead of eating it promptly like any sensible ape, you haul it off and share it with others.'

Glynn Isaac (1937 - 1985)

Acknowledgements

This thesis would not have been possible without the help and support of a large number of people. I wish to express my sincere gratitude to all who have helped.

I am especially thankful to my supervisors, Manuel Domínguez and Gonzalo Ruiz, for their guidance and unwavering support. Manuel Domínguez has been a continuous inspiration to me throughout the years. I am extremely lucky to have had him as a mentor and a teacher, and to have benefited from his extensive knowledge on so many subjects and from his unfailing and contagious enthusiasm. I wish to thank him for his constant guidance and encouragement, his patience and his active involvement in this work through each stage of the process. I also sincerely wish to thank Gonzalo Ruiz for his assistance during the last year and for sharing valuable advice and suggestions. I thank them both deeply for believing in my work and in my abilities.

I also wish to thank Manuel Domínguez and Enrique Baquedano, Codirectors of TOPPP (The Olduvai Paleoanthropology and Paleoecology Project) and the Institute of Evolution in Africa, and Audax Mabulla, Director of the National Museum of Tanzania, for inviting me to participate in their research project at Olduvai Gorge all these years, and for entrusting me with the challenging task of analyzing this invaluable faunal assemblage.

Many people were involved in the recovery, cleaning and restoration of the fossils. I am extremely grateful to all members of TOPPP for their generous assistance during fieldwork and in the lab, and would especially like to thank David Martín, Julia Aramendi, and Elia Organista for their constant support. I am also extremely grateful to the team of Tanzanian excavators for their skilled work and their happy disposition. Many students from different universities in the USA helped in the excavations at DS throughout the years. They also volunteered to clean the fossils in the laboratory, as did several groups of students from the Complutense University of Madrid. I thank them sincerely for their disinterested help. I am also deeply grateful to Aroa Serrano, Laura Gómez Tejerina, Andrea Díaz, Sofía de León, and Laura Gómez Morgado, for volunteering to restore the most delicate fossil remains under the supervision of María Cruz Ortega, and for doing this with extreme care and professionalism. Their help was crucial to complete the analysis.

I would also like to extend my gratitude to José Yravedra, Ainara Sistiaga, Mari Carmen Arriaza, and David Uribelarrea for very helpful advice and practical suggestions. I am also very grateful to Antonio Rodríguez, Charles Egeland, and Abel Moclán, for their very insightful and constructive contributions, and for challenging me with ingenious questions that helped improve my work considerably. David Martín helped with the descriptions of the stratigraphic layers and the geological formation of the site, and Emily Whitney, Elia Organista, and Gabriel Cifuentes helped resolve some technical difficulties at critical moments.

I am thankful to the Complutense University of Madrid and the Banco de Santander for funding my research and a three-months stay in Perth (Australia), where I had great pleasure of working with Adrian Baddeley on the spatial statistical analysis of DS. I am extremely grateful to him and his team for their warm hospitality and for generously sharing their knowledge.

I owe my deepest gratitude to my friends and family, who have stood by me during these past five years, putting up with absences, long working hours and moments of self-doubt and discouragement, and without whose affection, unconditional support and full confidence in my abilities, I could not have done this. I wish to especially thank Alex, Sarah, and Peter for their invaluable friendship and for being near me even though they are far away. Last but not least, I'm deeply grateful to Adrián, for his love, generosity and joyfulness, and for providing support constantly and in all possible forms during the past year.

Abstract

Faunal remains recovered at early archaeological sites dated to around 2 million years (Ma) play a critical role in discussions about the evolution of early hominin behavior. Anthropogenic assemblages from this time period are scarce, however and, until recently, most of the available evidence on the behavior of early *Homo* has been almost exclusively obtained at the FLK *Zinj* site from Bed I in Olduvai Gorge (Tanzania). The recent discovery of DS (David's Site, 1.84 Ma) and two additional hominin-made accumulations on the same paleosurface as the iconic site of FLK *Zinj* provides an invaluable opportunity to address key issues regarding early hominin lifestyles, particularly their subsistence behaviors and their foraging capabilities. The DS site has been extensively excavated and is exceptionally well preserved. Over the past years, significant advances in taphonomic and spatial statistical techniques have been made, which mainly involve the combination of several variables in multivariate approaches and the use of machine learning algorithms. The application of these methods to the faunal fossil record within extended frames of reference helps overcome equifinality when trying to detect the main agent of site formation and interpret site function.

The main objectives of this dissertation are:

a) to assess the processes that led to the formation of the faunal assemblage in Level 22B at DS by evaluating the effect of the abiotic and biotic taphonomic agents involved in the creation and transformation of the original archaeological deposit.

b) to accurately determine the degree of implication of hominins at the site and the kind of interaction that took place between them and the carnivores with which they coexisted.

c) to describe relevant aspects of early *Homo* subsistence and social behavior based on similarities and differences between DS and other Paleolithic sites, ethnographic data from modern hunter-gatherer campsites, and experimental or actualistic assemblages.

The taphonomic study includes analyses of the site's integrity, skeletal part representation, bone breakage patterns, bone surface modifications, and bovid mortality profiles. The spatial analysis explores the differential use of space by

hominins and certain structural aspects of their social behavior.

This study confirms previous interpretations about hominin behavior drawn from earlier taphonomic analyses of FLK *Zinj* and the high explanatory power of the applied taphonomic and spatial approaches. In particular, the results show that the faunal assemblage from Level 22B at DS is an autochthonous largely undisturbed assemblage and that complete fleshed small and medium-sized ungulate carcasses were actively transported and introduced into the site by hominins. These had early access to meat resources. The evidence also points to hunting as the main carcass foraging strategy employed by early humans, probably through ambush techniques, and suggests that carnivore activities were limited at the site. DS seems to have been used by hominins as a central place near locations with easy access to herbivores and water sources. At these places, hominins probably congregated on small areas and consumed food collectively. The regular successful acquisition of large carcasses and their transport to central places likely relied on high levels of group cooperation. The evidence from DS indicates that early *Homo* showed significant behavioral complexity relative to extant primates and a very cohesive social structure that was different from that of other primates, including modern humans.

Resumen

Los restos faunísticos recuperados en algunos de los yacimientos arqueológicos más antiguos, que datan de alrededor de dos millones de años (Ma), desempeñan un papel muy importante en las discusiones sobre la evolución del comportamiento de los homininos. Sin embargo, los conjuntos arqueológicos de origen antrópico de ese periodo son escasos y, hasta hace poco, la mayor parte de los datos disponibles sobre el comportamiento de los primeros miembros del género *Homo* han sido obtenidos casi exclusivamente del yacimiento FLK *Zinj* del Lecho I de la Garganta de Olduvai (Tanzania). El reciente descubrimiento de DS (David's Site, 1.84 Ma) y de otras dos acumulaciones generadas por homininos sobre la misma paleosuperficie que el emblemático yacimiento de FLK *Zinj*, brinda una valiosa oportunidad para abordar cuestiones clave relacionadas con la forma de vida de los primeros *Homo* con nuevos datos, en particular sus comportamientos de subsistencia y sus capacidades depredadoras. El yacimiento se ha excavado en extensión y se encuentra excepcionalmente bien preservado. A lo largo de los últimos años, se han realizado avances significativos en las herramientas tafonómicas y espaciales estadísticas disponibles, que ahora comprenden principalmente la combinación de varias variables en aproximaciones multivariantes y el uso de algoritmos de máquinas de aprendizaje automático. La aplicación de estos métodos al registro faunístico fósil y la utilización de marcos referenciales ampliados permite superar problemas de equifinalidad a la hora de detectar el agente principal de formación del yacimiento e interpretar la funcionalidad de la localidad.

Los objetivos principales de esta tesis doctoral son los siguientes.

En primer lugar, se pretende determinar los procesos de formación del conjunto faunístico del nivel 22B de DS. Para eso se evalúa y mide el efecto de los distintos agentes tafonómicos bióticos y abióticos involucrados en la creación y transformación del depósito arqueológico original.

El segundo objetivo consiste en determinar de manera precisa el grado de implicación de los homininos en el yacimiento y el tipo de interacción que tuvo lugar entre ellos y los carnívoros con los que convivieron.

En tercer lugar, se describen los aspectos relevantes de la subsistencia y el comportamiento social de los primeros *Homo* con ayuda de los datos obtenidos

y de las similitudes y diferencias observadas entre DS y otros conjuntos, principalmente otros yacimientos del Paleolítico, campamentos de cazadores-recolectores actuales y experimentos que simulan diversos escenarios.

El estudio tafonómico incluye varios análisis sobre la integridad del conjunto óseo, la representación esquelética, los patrones de fracturación, las modificaciones de la superficie ósea y los perfiles de mortalidad de los bóvidos representados. El análisis especial explora el uso diferencial del espacio por parte de los homininos y ciertos aspectos estructurales de su comportamiento social.

Este estudio confirma anteriores interpretaciones sobre el comportamiento de los homininos basadas en análisis tafonómicos de FLK *Zinj* y el gran poder explicativo de las herramientas tafonómicas y espaciales aplicadas. En particular, los resultados muestran que el conjunto faunístico del nivel 22B de DS es autóctono, que está prácticamente intacto y que las carcasas, en su mayoría casi completas, de ungulados pequeños y de mediano tamaño fueron transportadas e introducidas en el yacimiento de forma activa por homininos, quienes tuvieron acceso temprano y primario a estos recursos cárnicos. La evidencia también apunta a que la caza, más concretamente la caza por emboscada, fue la principal estrategia empleada por los homininos para adquirir carcasas, y sugiere que las actividades de carnívoros en el yacimiento fueron limitadas. DS parece haber sido utilizado por homininos como un lugar central con fácil acceso a herbívoros y fuentes de agua. En estas localidades, los homininos probablemente se congregaban en áreas pequeñas y consumían los alimentos de manera colectiva. La adquisición exitosa y regular de carcasas de gran tamaño y su transporte a lugares centrales probablemente requirió altos niveles de cooperación. La evidencia recabada en DS indica que los primeros miembros del género *Homo* mostraban una complejidad conductual considerable en relación con los primates actuales y una estructural social muy cohesiva diferente de la de otros primates, incluidos los humanos modernos.

Table of Contents

List of figures

List of tables

1. Introduction

1.1. The early archaeological record from Africa

Research into the evolution of human behavior often draws from behavioral features that differentiate modern humans from other primates, particularly chimpanzees, who are our closest living relatives. Especially useful for archaeologists are the behavioral adaptations that are related to subsistence or the acquisition of food resources by hominins, because these features are the most directly inferred from the archaeological record. One of the most long-standing definitions of human behavior of this kind was proposed by Isaac (1978), who described human behavior by laying special emphasis on food transport to central places, food sharing and cooperation, as well as on an increased dependency on meat and tool use, and who was among the first to realize that these elements were already operating in some African early archaeological sites dating to around 2 Ma.

Early Pleistocene archaeological sites, which are dense concentrations of stone tools and faunal remains accumulated in spatially restricted locations, sometimes preserved within vertically discrete horizons, in fact have yielded evidence of stone tool use and frequent mammal carcass exploitation by hominins. Isaac's ideas served as guiding principles to numerous researchers concerned with the interpretation of early archaeological sites, who have picked up, modified or questioned his hypotheses (Bunn, 1981, Binford, 1981; Blumenschine, 1986; Potts, 1988; Rose and Marshall, 1996; Domínguez-Rodrigo *et al.*, 2007). Most of these researchers have argued since then that meat-eating was a crucial adaptation that could explain the emergence of tool use, brain expansion in hominins, and a number of social adaptations that occurred throughout hominin evolution, including food sharing and increased cooperation, as proposed by Isaac (1978; 1983).

It is important to note that tracing back these behavioral developments and establishing whether they were already shared with certain hominins is key to understanding the evolutionary context and conditions in which they evolved, and the evolutionary implications they had; i.e. what other anatomical, behav-

ioral or socio-reproductive features did these changes enable? As a matter of fact, Isaac (1978; 1983) and others after him (e.g. Lupo, 2013; Domínguez-Rodrigo, 2013) have stressed that behavioral features should not be examined in isolation but rather as sets of functionally linked behaviors that reinforce and intensify each other through natural selection. This means that the emergence of traits like increased meat-eating or tool use should be expected to have had physical, socioecological and cognitive consequences on the lives of hominins and affected broader patterns of adaptation and evolution (Foley, 2001). It is not surprising, therefore, that the high level of carnivory seen in early humans compared to other primates and the foraging capabilities of hominins have long been a subject of debate among researchers, and the early archaeological record has played a critical role in these discussions.

The first three or four million years of human evolution are completely devoid of archaeological record, which limits our knowledge about hominin behavior, and especially subsistence behavior, to inferences drawn from other non-archaeological approaches, mainly from anatomical features of hominin skeletons and from paleoecological reconstructions of their habitats. But the emergence of the genus *Homo*, around 2.8 - 2.5 million years ago (Mya) (Villmoare *et al.*, 2015; Kimbel, 1996; Sherwood *et al.*, 2002; Dominy *et al.*, 2008; Antón *et al.*, 2014), which also coincides "slightly" later with the earliest evidence of stone tool use to butcher carcasses around 2.6 Mya (de Heinzelin et al, 1999; Semaw *et al.*, 1997; 2003; Domínguez-Rodrigo *et al.*, 2005), marks the beginning of a new phase in human evolution, in which some of the foundational elements of human behavior can already be recognized. At this stage, the archaeological record becomes especially important to the task of reconstructing the evolution of human behavior. Recently, Harmand *et al.* (2015; 2019) have claimed to have found the oldest lithic artifacts in a deposit dating to 3.3 Mya at Lomekwi (West Turkana, Kenya). Yet, the stratigraphic provenance of such stone artifacts has been seriously questioned (Domínguez-Rodrigo and Alcalá, 2016; 2019; Archer *et al.*, 2020). Similarly, the purported butchery marks on two specimens from Dikika (3.4 Ma, Ethiopia) (McPherron *et al.*, 2010) have been criticized by several expert taphonomists, and their stratigraphic origin has also been contested (Domínguez-Rodrigo *et al.*, 2010; 2011; Domínguez-Rodrigo and Pickering, 2017). Therefore, the earliest secure and undisputed archaeological traces of stone tools and their use (among other things) to butcher carcasses still stem from the archaeological localities at Gona (Ethiopia) that date to 2.6 Ma (Semaw *et al.*, 2003; Domínguez-Rodrigo *et al.*, 2005). Gona and Bouri (Ethiopia) have both yielded the oldest samples of cut-marked bones (Domínguez-Rodrigo and Baquedano, 2018). At Gona, the placement of cut marks indicates that hominins may have eviscerated and defleshed carcasses, which supports that hominins already may have gained early

access to large ungulate carcasses during this time period (Domínguez-Rodrigo *et al.*, 2005), and at Bouri, cut marks also appear on bones indicating a variety of butchery activities, including filleting, dismemberment and marrow extraction of several different large mammals (de Heinzelin *et al.*, 1999). Additional evidence from early stone tool use from the period from 2.6 to 2.0 Mya comes from several other archaeological sites mainly discovered in the Middle Awash, West Turkana, Hadar, and Kanjera (see Rogers and Semaw (2009) and Domínguez-Rodrigo (2009), who provide a summary of all the excavated, primary context archaeological sites older than 2 Ma). Yet, at many of these sites, the association of lithic and faunal remains is less clear, and the remains constitute small sample sizes. Sites like Hadar and Omo in Ethiopia or Lokalalei in Kenya have yielded slightly younger stone tool assemblages (2.4 – 2.3 Ma) that have also provided important information on hominin early stone tool manufacture and use (Harmand, 2007; Roche *et al.*, 2003).

However, even though the number of the earliest Oldowan sites has increased notably in the past 30 years, most of what is known about early human behavior has come from several more recent sites at Olduvai Gorge, Kanjera South, and Koobi Fora that are dated to 2.0 - 1.6 Ma. The archaeological assemblages uncovered at Kanjera represent the oldest of these best-preserved records of hominin behavior. Excavations from two main sites have shown that hominins selected and transported lithic raw materials over long distances and that they accumulated and butchered carcasses they had obtained through primary access (Plummer and Potts, 1995; Plummer *et al.*, 1999; Plummer *et al.*, 2009; Braun *et al.*, 2009; Plummer and Bishop, 2016). Researchers have interpreted that at least the smaller antelopes were probably acquired through hunting (Oliver *et al.*, 2019). At Koobi Fora, a prolific region that preserves classic early Pleistocene sites, archaeological works began early in the 1970s and included several large-scale excavations, such as FxJj50 and FxJj20 (1.5 Ma and 1.95 Ma, respectively) (Harris and Isaac, 1976; Isaac *et al.*, 1976; Bunn *et al.*, 1980; Braun *et al.*, 2010). These sites provided data for numerous studies, including analyses of the lithic remains (Toth, 1982), taphonomic and zooarchaeological analyses (Bunn, 1982; 1983), spatial analyses (Kroll, 1994; Kroll and Isaac, 1984), and geoarchaeological and experimental studies on site formation (Kaufulu, 1983; Schick, 1984). Braun *et al.* (2010) have reported evidence from FxJj20 of the incorporation of various aquatic animals, including turtles, crocodiles and fish, into the hominin diet, but the most relevant taphonomic and zooarchaeological data was provided by Bunn (1986) in his study of the FxJj50 assemblage, which also indicated that hominins were having primary access to carcasses which they transported to central places. Similar inferences regarding the subsistence behavior of early *Homo* or *Homo ergaster* have been drawn from a number of slightly younger sites in Africa in which ungulate carcass butcher-

ing by hominins is also amply documented. The most important ones are ST4 in Peninj (1.5 Ma, Tanzania; Domínguez-Rodrigo *et al.* 2001a, b; 2009), Ain Boucherit (1.8 Ma; Algeria; Sahnouni *et al.*, 2018) and Swartkrans Member 3 (1.5 Ma; South Africa; Pickering *et al.*, 2004).

Yet, the most informative record of the behavior of early *Homo* comes from Bed I at Olduvai Gorge in Tanzania, in particular from FLK *Zinj*, which was, until very recently, the only anthropogenic site from Bed I (Domínguez-Rodrigo *et al.*, 2007). Years of research at Olduvai since the Leakeys pioneering work in the 1960s and 1970s have yielded important discoveries and large amounts of archaeological data from numerous assemblages. For over 50 years, the discussions about early human behavior and about the interpretations of early sites have mainly revolved around the Bed I assemblages (Domínguez-Rodrigo *et al.*, 2007). Remains have been preserved mostly in undisturbed contexts, which has promoted abundant archaeological excavations at this extremely fossiliferous locality. Nevertheless, ever since the dense concentrations of materials were discovered at Olduvai, their formation history and the role played by hominins in the accumulations have been controversial. It was suggested that the sites could be derived assemblages formed by hydraulic processes or hyena dens where hominin activity had been marginal (Binford, 1981; 1985). At present, a relative consensus has been reached regarding the sites' taphonomic histories, and a wealth of taphonomic analyses have proved that most of these sites represent special locations in the landscape where carcasses were actively accumulated, although not always exclusively by hominins. Numerous arguments have been listed by Potts (1988) and summarized by Domínguez-Rodrigo *et al.* (2007) supporting an active accumulation of carcasses by carnivores and hominins at the sites, and the autochthony of most assemblages. First, the density of faunal remains at these sites is extremely high when compared to natural bone scatters from modern savannas. Under natural circumstances, i.e. when they are not consumed by carnivores, animal carcasses become scattered instead of accumulated (Hill, 1975; 1979; Behrensmeyer, 1983). Second, the sites contain remains from several individuals accumulated in relatively small areas, whereas in modern savannas several individuals are rarely encountered when natural deaths occur (Potts, 1988). Third, the faunal assemblages are characterized by a relatively high taxonomic and ecological diversity, with taxa from different ecological niches (Bunn, 1982; Potts, 1988). Lastly, abundant limb bones relative to axial remains suggest transport of carcass parts (Potts, 1988), although the scarcity of axial remains is also explained by carnivore ravaging and density-mediated attrition.

Once it was established that early sites were the result of active carcass transport, it became an issue to determine whether they represented accumulations made by carnivores or by hominins. Domínguez-Rodrigo *et al.*'s (2007) in-

depth taphonomic analysis of the main Bed I assemblages provided an answer to this question for each of the sites and pointed out that only FLK *Zinj* had been accumulated by hominins. The remaining assemblages represented carnivore accumulations (FLKNN 1-3), background scatters formed in death arenas (FLKN 6), and palimpsests in which contributions from both carnivores and hominins could be identified (FLKN 1-5 and DK 1-3) (Domínguez-Rodrigo *et al.*, 2007). Thus, FLK *Zinj* has played a prominent role in understanding early Pleistocene hominin subsistence behavior. The site has been analyzed by several groups of researchers, and most of them have concluded that hominins were actively accumulating carcasses at FLK *Zinj*, which they probably acquired through hunting or confrontational scavenging (Leakey, 1971; Bunn and Kroll, 1986; Domínguez-Rodrigo *et al.*, 2007; Parkinson, 2013, 2018).

Yet, for years, the evidence coming from this extensive and dense archaeological assemblage has been an anomaly among Bed I assemblages, and the only consistent proof of a significant behavioral shift toward higher behavioral complexity in early humans from the African early Pleistocene. Fortunately, over the past decade, archaeological research at Olduvai Gorge (Tanzania) by TOPPP (the Olduvai Paleoanthropology and Paleoecology Project) has produced numerous fascinating discoveries that are reinforcing our impression that hominins were actively obtaining and sharing meat resources regularly. Among these findings, the most exciting and important ones are probably the three new large anthropogenic sites discovered in Bed I. All three lie on the same paleosurface as FLK *Zinj*, which means they are dated to 1.84 Ma. They have been named PTK (Philip Tobias Korongo), DS (David's Site) and AGS (Alberto Gómez's Site). This dissertation presents the results from the faunal analysis of DS, while excavations and analyses are still on-going at AGS and PTK. The three sites also seem to be the result of the active transport and accumulation of carcasses by hominins, which means that FLK *Zinj* can at last cease to be considered an anomaly in the Olduvai early Pleistocene archaeological record. Hominin agency at these sites, meat-eating and hominin predation can now be examined in greater detail and better reconstructed.

More specifically, the key issues regarding hominin lifestyles with which researchers have been concerned in the past fifty years of archaeological research in Africa include the identification of the main agents of site formation, the hunting or scavenging behavior of hominins reflected at the sites, their socioeconomic function, and the behavioral complexity of hominins relative to extant primates (Domínguez-Rodrigo *et al.*, 2007). All these are intricately interconnected subjects and, as Potts (1988) has put it, they should be addressed in a certain order in order to appropriately make inferences about hominin behavior. The goal is to characterize hominin behavior relative to that of other primates and humans based on the evidence recovered from the sites. In order

to do so, the meaning or function of the sites must be determined; i.e. we want to infer how hominins used these locations. This is usually established by determining the main agents of site formation and identifying the specific activities carried out by hominins and other species at the sites. These activities are connected and, in the end, form a behavioral pattern specific to hominins and different from those of extant apes and modern humans. Each of these inferential steps has constituted an intensely debated issue by itself over the past decades, and all of these interpretive topics have developed in parallel with a significant progress of methodological and taphonomic approaches. The following pages present a summary of the history of each of these hotly debated issues and of the key role played by FLK *Zinj* in their development.

1.2. *Models on the socioeconomic function of early archaeological sites*

The long tradition of archaeological research at Olduvai Gorge is partly due to the fact that the most debated issues of the early Pleistocene, including the socioeconomic characterization of early sites, i.e. whether they were used by hominins as central places, near-kill sites or stone caches for example, have rested almost exclusively on information stemming from the largely undisturbed Bed I assemblages (Domínguez-Rodrigo *et al.*, 2007). In the 1960s and 1970s, when taphonomy was still in its early phase, it was intuitively assumed that these accumulations of bone refuse and stone tools were mainly the result of hominin activity, and they were at first interpreted by Leakey (1971) as hominin campsites, or "living floors", although she also identified other types of sites in her reports of the excavations, including butchering sites, channel sites, and vertically dispersed deposits (Leakey, 1971). Her interpretations of the sites focused on home bases and cooperative hunting and were largely influenced by the hunting paradigm of the 1960s (Domínguez-Rodrigo *et al.*, 2007). So was Isaac's (1978) first "home-base" or "food sharing" model about the functionality of early sites, which he characterized as home bases that resulted of the delayed consumption and transport of carcass parts where hominin social activities, toolmaking, butchery, and intentional food sharing would have taken place. He based this idea also on the evidence discovered at Koobi Fora and maintained that intentional food sharing and cooperation would have resulted in the sexual division of labor (Isaac, 1978).

These ideas prompted in-depth taphonomic studies of the sites as well as methodological and theoretical discussions, which in turn gave rise to critiques and reformulations of Isaac's model that fell under two completely opposed visions of early hominin behavior. On the one hand, Binford's (1981) revisionist interpretation, in which he questioned the basic assumption that hominins had been responsible for the accumulations and suggested that these had been created by carnivores or had formed as the result of natural or hydraulic processes, whereas hominin activity at the sites was only limited to the consumption of some flesh scraps and bone marrow, depicted hominin social behavior as more similar to that of non-human primates. Years later, Sept (1992) would also reject the idea that early sites could have represented home bases and propose a model, inspired in debris patterns of chimpanzee activity, that depicted

early sites as concentrations of debris formed as a result of the frequent reuse through time of the sites for individual feeding or nesting due to the ecological structure and resource configuration in that particular area (Sept, 1992). On the other hand, Bunn's (1982) taphonomic analysis of the FLK *Zinj* site led him to conclude that hominins had had primary access to carcasses through hunting or confrontational scavenging (Bunn, 2001), and Isaac (1983) used this empirical evidence as well as ethological information on foraging behavior to propose a revised model, the "central place foraging" model, in which he left out some of the social inferences of his previous version, and only claimed that hominins used specific locations or central places on the landscape to bring raw materials and carcasses to be shared among the group, while further stressing that delaying food consumption and transporting resources would have had evolutionary advantages (Isaac, 1983). A similar scenario was described in the "favored place" model proposed by Schick (1987), in which hominins' dependence on raw materials for stone tool manufacturing was emphasized and said to have conditioned their selection of *loci*. In the "stone cache" model (later named "resource transport" model) presented by Potts (1988) sites were viewed as having been dangerous for hominins because carnivores would have frequented the same localities. He suggested, therefore, that occupations may have been sporadic to avoid temporal and spatial overlap with carnivores, and that hominins would have left raw materials at several locations in anticipation for the possibility that nearby acquired carcasses would require processing. This would have reduced transport distances and energetic costs, while it would also have helped avoid carnivore competition. These stone caches would only have been used for subsistence-related activities, as opposed to home bases where other social activities could have taken place. Like Binford (1981), Potts also envisioned hominin behavior as more similar to that of extant apes than modern humans, especially by arguing that this behavior would not have required advanced planning and anticipation capabilities. However, it was later shown that such behavior in fact implied relatively complex cognitive abilities (Domínguez-Rodrigo *et al.*, 2007), something reflected among other reasons in the fact that some of the lithic material at the sites had been carried over several kilometers (Hay, 1976; Toth, 1982). The content of the lithic assemblages at Olduvai was also at odds with Potts (1988) expectations. Manuports and unutilized cores were argued to have dominated these assemblages, but de la Torre and Mora (2005) showed that these were actually ecofacts and that the reduction chain was unsupportive because the manuport raw materials did not correspond to the flaked raw materials. Moreover, other stone tool analyses had shown that activities related to plant processing took place at the site apart from carcass butchering (Keeley and Toth, 1981), and the reconstructions of the sites' contexts indicated that they were located in areas associated with

closed-vegetation habitats and therefore lower predation risk (Blumenschine, 1986; Domínguez-Rodrigo, 2001), which suggested more prolonged stays at the sites by hominins than initially suggested by Potts (1988).

Blumenschine (1991) then realized that site use by hominins would have been determined by the amount of carnivore competition or predation risk at the death site and by the amount of food available for hominins. If predation risk was low and food surplus was high, then transport of carcass parts to central places would be viable. If, on the contrary, predation risk was high and carcass yield was low, then hominins would have only moved to nearby spots or trees to seek refuge from predators. He believed that the taphonomic evidence from the sites was consistent with the latter scenario, which was termed "refuge" model. This predator-avoiding strategy, similar to what can be observed in baboons in savanna-woodlands today, would have characterized hominins even if they were not carnivorous (Blumenschine, 1991; Blumenschine *et al.*, 1994). An alternative possibility was suggested by O'Connell (1997), who compared early sites to multiple-carcass assemblages at ambush sites frequently used by the Hadza and proposed the "near-kill location" model. Like Blumenschine (1986), he argued that early sites like FLK *Zinj* and FxJj50 should be interpreted as kill sites or scavenging sites rather than central places resulting from long-distance transport, as had been suggested by Schick (1987), Bunn (1986; Bunn and Kroll, 1986), and Isaac (1983). A later version, the "male-display" model (O'Connell *et al.*, 2002) criticized the emphasis other models put on hunting and male provisioning and stressed the importance of female gathering activities. O'Connell and colleagues argued that male hominins displayed in front of the social group by confronting carnivores at their kills in order to gain mating opportunities rather than to procure meat resources (O'Connell *et al.*, 2002). Blumenschine's (1991) and O'Connell's (1997; O'Connell *et al.*, 2002) models have received substantial criticism from the defenders of the central-place foraging model. As an example, in the "resource defense" model, in which early sites were viewed as focal sites that offered defensible resources including water and plant foods and which were used for a number of other social activities apart from carcass processing, it is considered that the danger posed by carnivores is more likely to have promoted cooperative behaviors and group defense strategies instead of avoidance behaviors, as was suggested by Blumenschine (1991) (Rose and Marshall, 1996). With regard to the "male-display" model, Domínguez-Rodrigo *et al.* (2007) have argued that the aim to gain prestige among the group is probably a recent phenomenon, because in modern foragers like the Hadza it is associated with individual hunting mainly using bow and arrow technology, while hunting or confrontational scavenging in the past with less sophisticated technology would probably have required the collaboration of several individuals. Therefore, collective hunting would have provided less opportunities for display in the early Pleistocene (Domín-

guez-Rodrigo *et al.*, 2007).

Except for the central-place foraging model, all the other models described here are still unsupported by the taphonomic evidence. Thorough analyses of the faunal assemblages at Olduvai Bed I and Koobi Fora have yielded substantial data that undercut and challenge many of the expectations of the proposed interpretations of the sites' functionality (see Table 1.1). For example, Domínguez-Rodrigo and Barba (2007) showed that carnivore tooth marks at FLK *Zinj* had been overestimated significantly by several researchers, who thus also overestimated the importance of carnivore activity at the sites, or that the lack of overlap of carnivore tooth marks and anthropic marks evidenced that carnivores and hominins did not commonly compete for or consume the same carcasses (Domínguez-Rodrigo *et al.*, 2007). Moreover, the Bed I sites contain taxa from various different habitats, whose transport cannot be exclusively explained by short distance transport and carnivore avoidance (Domínguez-Rodrigo *et al.*, 2007). The sites were also situated in areas associated with closed-vegetation habitats and low predation risk (Arráiz *et al.*, 2017). Disagreement between authors clearly came from their opposed views regarding the evidence expressed in the archaeological record (e.g. Blumenschine, 1991; Bunn and Kroll, 1986), but, interestingly, all were based on meat-eating and meat acquisition strategies. It had become clear that the key to understanding how hominins used the landscape and how they behaved socially, lay in determining time of access to carcasses and the regularity of meat consumption by hominins. This is why this debate developed in parallel with the hunting-scavenging debate and why it has greatly influenced archaeological taphonomic studies over the years.

TABLE 1.1. *Main socio-economic models proposed to interpret site function and the expectations regarding the behaviors that would have to be reflected at the site that would confirm each of the hypotheses.*

Main proponent	Model	Site function	Main carcass acquisition strategy	Food surplus	Transport distance	Duration of stay	Predation risk	Implied behavior
Isaac (1978; 1983) (see also Bunn, 1986; Bunn and Kroll, 1986; Leakey, 1971)	"home base"/"food sharing"; "central place foraging"	central place where all kinds of social and collective activities would have taken place, including tool manufacture, carcass butchery, and food sharing	hunting and confrontational scavenging	yes	long*	prolonged	low	delayed consumption of food; cooperation to obtain and transport resources to central place; collective consumption and food sharing
Schick (1987)	"favored place"	sites are loci where stone tools and bones are more likely to accumulate	not discussed	yes	long*	prolonged	low	sophisticated planning capabilities reflected in the procurement of raw materials and its modification; delayed consumption of animal tissues, perhaps food sharing
Potts (1988)	"stone cache" / "resource transport"	used for subsistence-related activities only	not discussed	not rejected	short	short	high	would not require especially advanced planning capabilities; food sharing and cooperation possible, but not verifiable
Blumenschine (1991; Blumenschine *et al.*, 1994)	"refuge"	used to seek temporal refuge from predators and consume bone marrow left by carnivores	passive scavenging	no	short	short	high	similar to that of extant primates; avoidance strategies when encountering carnivores
Sept (1992)	"chimpanzee nesting"	used repeatedly but individually by hominins for feeding and nesting	not discussed	no	short	short	high	social behavior very similar to that of chimpanzees and other extant primates; individualistic rather than collective behaviors
Rose and Marshall (1996)	"resource defense"	like central place, but would also have provided defensible resources like water and plant foods	hunting and confrontational scavenging	yes	long*	prolonged	low	the danger posed by carnivores would have promoted group cohesion, cooperation and defense strategies like those observed in extant primates
O'Connell (1997; O'Connell *et al.*, 2002)	"near-kill location" / "male display"	sites are similar to Hadza ambush kill or scavenging sites; male display	confrontational scavenging (although relatively infrequent)	no	short	short	high	males display in front of group to gain mating opportunities; meat procurement is not as important as the resources obtained through female gathering

*from several hundred meters to a few kilometers

1.3. The hunting and scavenging hypotheses

The idea that meat-eating and hunting could be one of the key differences that separated hominins from other anthropoids dates back to Darwin's time. He envisioned that these had been adaptations to the savanna environment that had triggered hominin intelligence and had resulted in the progressive increase of brain size (Darwin, 1871). Ancient stone tools and bones from old deposits in caves were seen by naturalists from that time as evidence of past predatory behaviors (Boucher de Perthes, 1849), a general belief that probably also inspired Dart's (1953; 1959) vision of aggressive cannibalistic killer hominins. At this time, the hunting paradigm was linked with the sociobiological idea that human aggressive behaviors were inevitable and used to justify colonial policies and warfare (Dennell, 1990; Domínguez-Rodrigo *et al.*, 2002).

In the second half of the twentieth century, anthropologists underpinned the idea that predation had always been an important part of human societies using modern analogs, and the hunting hypothesis started being widely supported and promoted in academic circles, for example at the "Man the Hunter" conference in 1966), to explain the origin of bipedalism or the earliest archaeological record (Lee and deVore, 1968; Ardrey, 1976; Washburn, 1957; Fisher, 1982; Haraway, 1989). Moreover, the first thorough observations of primate behavior in the wild showed that chimpanzees were hunters too (Goodall, 1963; McGrew *et al.*, 1978; 1979), which led to an important modification in the hunting hypothesis: instead of having emerged with hominins, hunting had progressively evolved from small-game acquisition as observed in chimpanzees or, as could have been characteristic of the last common ancestor, to an increased dependency of meat and the obtainment of larger game - as is seen in modern human populations – as a consequence of the spread of savanna habitats. This and other differences observed between humans and other primates, particularly those related to meat-eating and hunting, were the foundation for Isaac's (1971; 1978) home base model, which identified the use of central locations, tool use, food transport, meat sharing, and a sexual division of labor as functionally linked behavioral features reinforcing each other composing a novel adaptive set, as explained above. He also maintained that the archaeological evidence from Olduvai Gorge (in particular FLK *Zinj*) and Koobi Fora represented the use of home bases and kill sites, and therefore that these sites

supported the hunting scenario (Isaac, 1978).

Although there were already some questions and doubts regarding the origin of these and other zooarchaeological assemblages and the timing of hominin access to carcasses at that time, and scavenging from other predators was viewed by some archaeologists as a transitional stage toward hunting (e.g. Leakey, 1967), it was Binford (1981) who systematically described and defended the scavenging hypothesis. He reevaluated the faunal remains from FLK *Zinj*, Klasies River Mouth and several sites in Europe, paying special attention to skeletal part profile analyses, and used ethnoarchaeological observations and carnivore dens for comparison (Binford, 1981; 1984; 1985; 1988). With his work he challenged assumptions derived from the hunting hypothesis, including Isaac's (1978) home base model, and claimed that carnivores rather than hominins were responsible for early site formation. He described hominins as marginal or obligate scavengers who obtained small amounts of marrow and tissue from largely defleshed carcasses abandoned by carnivores and argued that hunting only emerged with the spread of anatomically modern humans. He maintained that there was no evidence of behaviors like food transport to central places or meat sharing by these hominins. This hypothesis gained further steam from Brain's (1981) finding that bone assemblages associated with *Australopithecus* remains from Swartkrans and Makapansgat in the South African cave sites had in fact been accumulated by carnivores. Binford's ideas were further endorsed by other researchers, for example by Potts and Shipman (1981; Shipman 1986), who analyzed bones from Olduvai (Beds I and II) and found carnivore tooth marks on top of cut marks on some specimens, but rejected by other authors, like Bunn and Kroll (1986; Bunn, 1982), who analyzed the fauna from FLK *Zinj* and concluded that hominins were the main bone accumulators at the site, and probably hunters.

Then, Blumenschine (1986; 1988a; 1995) proposed a new passive scavenging model to explain hominin behavior as reflected at the FLK *Zinj* assemblage based on his own actualistic work with carnivores in the Serengeti. He modeled skeletal part survival and bone surface modification patterns in several different scenarios in which hominins could have gained access to carcasses, and concluded that hominins would have had opportunities for scavenging intact and partially defleshed carcass parts from natural death sites or felid kills in wooded and riparian habitats, that available body parts would have been transported a short distance to safer locations to be consumed, and that the remains would have then been ravaged by bone-crunching predators (Peters and Blumenschine, 1995). Blumenschine's work initiated a new phase in the hunting-scavenging debate, marked by experiments and simulations of different scenarios of hominin access to carcasses, in order to gain an understanding of how different taphonomic agents affect bone accumulations and to be able

to recognize them in the archaeological record. This approach was followed up, refined and expanded by many other researchers who started conducting numerous experiments to model the effects of many kinds of taphonomic processes (e.g. Capaldo, 1998; Pobiner and Braun, 2005; Domínguez-Rodrigo and Barba, 2005; Faith, 2007; Gidna *et al.*, 2014; Pante *et al.*, 2015).

At this stage, the hunting-scavenging debate had completely turned into a taphonomic controversy, centered around the questions of whether skeletal parts, bone surface modifications, and bone breakage patterns at FLK *Zinj* reflected that hominins had had primary or secondary access to the carcasses they consumed, and whether they obtained large quantities of meat or just flesh scraps. By then, four main scenarios for early hominin acquisition strategies had been proposed: 1) obligate marginal scavenging, 2) passive scavenging focusing largely on the remains of felid kills; 3) confrontational (or power or aggressive) scavenging that involves driving predators from their kills of large mammals to obtain fleshed carcasses, and 4) active hunting (Lupo, 2013). The first two options meant hominins had secondary access to defleshed carcasses, options 3 and 4 required primary access to fleshed carcasses. As several authors have pointed out, these are not mutually exclusive scenarios, and hominins could have used a combination of these strategies (e.g. Domínguez-Rodrigo, 2002).

Blumenschine's (1995) interpretation of the FLK *Zinj* fauna emphasized a high frequency of tooth marks on the fossils, as well as percussion marks, but largely ignored the evidence of cut marks on meaty long bones from studies by other researchers (Bunn, 1982; 1991; Bunn and Kroll, 1986; Bunn and Ezzo, 1993; Oliver, 1994). In the light of more recent studies, the empirical evidence proposed for the scavenging scenarios turned out to be ambiguous, insufficient or incorrect (e.g. Rose and Marshall, 1996; Potts, 1988; Domínguez-Rodrigo, 1999a, b). In their reanalysis of the FLK *Zinj* assemblage, Domínguez-Rodrigo *et al.* (2007) showed that cut mark patterns in fact matched those from experiments simulating early access to fleshed carcasses, and that Blumenschine had misidentified tooth marks that were actually biochemical marks created by fungus and bacteria (Domínguez-Rodrigo and Barba, 2007). These new counts of cut marks and tooth marks were later corroborated by Parkinson (2013; 2018). An additional point of criticism of the scavenging hypotheses was that secondary scavenging from carcasses at carnivore kills could not yield abundant meat, and only long bone marrow and braincase contents are available after felids consume their prey (Blumenschine, 1986; contra Binford, 1985; 1988 and Blumenschine and Peters, 1998), with the exception of leopard kills (Cavallo and Blumenschine, 1989). Therefore, scavenging could only be feasible if carried out aggressively at felid kills. Other flaws of the scavenging hypotheses, mainly brought forward by Domínguez-Rodrigo and collaborators, were that some of

the experiments in which scavenging was simulated had been carried out with carnivores in conditions of captivity instead of in the wild (Marean *et al.*, 1992; Pobiner, 2015), or that the statistical treatment of the data by some (Pante *et al.*, 2012) had been erroneous or inappropriate (e.g. Domínguez-Rodrigo *et al.*, 2014; Domínguez-Rodrigo and Pickering, 2017).

In spite of the overwhelming evidence for early and primary access, new versions of the scavenging hypotheses have continuously been proposed in more recent years. Pante *et al.* (2012), for example, revived Blumenschine's (1995) model that hominins were passive scavengers from felid kills at FLK *Zinj*, while admitting, however, that hominins might have had earlier access to carcasses than previously suggested (contra Blumenschine, 1995), because cut marks were more abundant on humeral fragments than on femoral fragments (Pante *et al.*, 2012). This statement is an example of the controversial use of data that these authors have been criticized for, as pointed out by Domínguez-Rodrigo *et al.* (2014): an unequal number of defleshing cut marks on humeri and femora does not imply unequal access to these bones, because muscle attachments and the likelihood of scratching the bones with stone tools when extracting flesh are different on these elements (Bunn, 2001; Domínguez-Rodrigo *et al.*, 2014). Further, Pante *et al.* (2012) failed to provide an interpretation that explains the frequencies of cut, percussion, and tooth marks jointly. Other researchers who support scavenging scenarios have suggested that hominins may have acquired carcasses from crocodiles (Njau and Blumenschine, 2006; Sahle *et al.*, 2017), yet without providing evidence of bones with crocodile modifications from the earliest sites at Olduvai (Domínguez-Rodrigo and Baquedano, 2018).

One of the main concerns of the researchers who defend the scavenging hypotheses is that predatory carnivores would have constituted a huge threat for hominins. In general, defenders of the scavenging hypothesis and of the behavioral models resulting from this idea, have suggested that hominins would not have been able to defend themselves from the high predation risk posed by carnivores, that this would have prevented hominins from creating home bases, and posit scenarios in which hominins would have used avoidance strategies to respond to carnivore competition (Binford, 1981; 1985; Potts, 1984; Shipman, 1986; Blumenschine *et al.*, 1994; Blumenschine *et al.*, 2012). Yet, many have argued that predation risk would not have been substantially higher for early Pleistocene hominins than what some extant nonhuman primates experience, and that their responses to predation risk include cooperative defense, aggressive displays, and in general, increased group cohesion (e.g. Rose and Marshall, 1996). It is therefore probable that early hominins would have acted similarly in cases of risk of carnivore predation, and perhaps even used stones or branches as weapons (Isaac, 1987; Kortlandt, 1980; O'Connell *et al.*, 1988; Rose and Marshall, 1996). If hominins engaged actively in competition with carnivores, they

would very likely also have been capable of driving carnivores off their prey and would have been able to use confrontational scavenging as a strategy to acquire fleshed carcasses (Bunn *et al.* 1991), although this carcass acquisition strategy would have been far riskier than hunting, and it also means that hominins would have been able to defend themselves and their resources at their favored or central places (Rose and Marshall, 1996).

In order to better understand hominin activities across the FLK *Zinj* paleolandscape, at a certain point in the debate the need arose to reconstruct the ecology and the environment surrounding the site (Ashley *et al.*, 2010; Blumenschine *et al.*, 2012; Uribelarrea *et al.*, 2014). The resulting works provided further support for the hypothesis of primary access to carcasses and the use of central places by hominins. As already noted by Uribelarrea *et al.* (2014), in the 1980s, Blumenschine (1986) had presented evidence that open vegetation landscapes were the most dangerous for hominins in terms of carnivore predation risk, and that wooded or closed-vegetation habitats would have been the least hazardous locations, which could have provided refuge spots for hominins (Blumenschine, 1991; Blumenschine *et al.*, 1994; Capaldo, 1995). Further research in wooded alluvial environments also confirmed that these are the least frequented by carnivores (Domínguez-Rodrigo, 2001). Therefore, Blumenschine and Masao (1991) had initially proposed that FLK *Zinj* had been a hazardous spot located in the middle of a barren floodplain.

Later evidence showed, however, that FLK *Zinj* was placed in a wooded habitat (e.g. Barboni *et al.*, 2010; Ashley *et al.*, 2010), but Blumenschine *et al.* (2012) argued that the characteristics of the landscape of FLK *Zinj* would have attracted both carnivores and hominins, and that both would have used the land surface intensively. The exhaustive geoarchaeological reconstruction carried out by Uribelarrea *et al.* (2014) showed that the site was located on the edge of an elevated woodland platform by a lake floodplain and that the fossiliferous productivity of the landscape surrounding FLK *Zinj* was significantly lower than at the site itself, which meant that bones were accumulating in very high densities at that particular spot, probably because it would have provided refuge to hominins from carnivore predation and close access to other resources, contrary to the reconstruction yielded by Blumenschine and collaborators, who depicted FLK *Zinj* as lying on a "topographic high point carved out by fluvial incision of the lake margin following a major lake regression" (Blumenschine *et al.*, 2012: 381).

With the incorporation of a broad Okavango-style river into their geoarchaeological reconstruction, these researchers implied that high-energy geological processes were present in the vicinity of FLK *Zinj* (Blumenschine *et al.*, 2012). In fact, parallel to these discussions about the timing of access to carcasses by hominins at FLK *Zinj* and their use of the landscape, other researchers

had been questioning the integrity of the FLK *Zinj* assemblage and other Bed I sites based on purported preferred orientation patterns of bone fragments and lithics retrieved from Leakey's (1971) site plan (Benito-Calvo and de la Torre, 2011; de la Torre and Benito-Calvo, 2013), but had failed to provide a coherent explanation for these results. In their counterarguments, Domínguez-Rodrigo *et al.* (2012; 2014b) showed that Mary Leakey's drawings were inaccurate representations of the actual orientation and shapes of the bones and insisted on the lack of geomorphological and taphonomic data in the Bed I sites that would indicate post-depositional large-scale movement of the archaeological materials (see also Potts, 1988; Capaldo, 1997; Domínguez-Rodrigo *et al.*, 2007). Most assemblages in Bed I are located in low energy deposits corresponding to the lacustrine floodplain of the Olduvai Lake, there is no sedimentary evidence of the existence of high-energy processes, and the deposits are mainly clayey facies associated with lake sediments (Hay, 1976; Leakey, 1971; Uribelarrea *et al.*, 2014; Martín-Perea *et al.*, 2019). Most researchers concur that the assemblages at Olduvai Bed I are autochthonous accumulations and, more recently, Domínguez-Rodrigo *et al.* (2019) have shown that bone composition and shape patterns of several Bed I and Bed II sites resemble those of undisturbed or minimally transported experimental assemblages. The high amount of small bone fragments and splinters recovered from the sites, especially at FLK *Zinj*, also supports autochthony (Bunn, 1982; Domínguez-Rodrigo *et al.*, 2019). This means that: a) the original configuration of bones and lithics was not significantly modified post-depositionally; b) that the site has preserved its spatial properties, and c) that the interpretation of FLK *Zinj* as a safe spot in the landscape to which hominins transported carcasses acquired through primary access (Bunn and Pickering, 2010) still holds.

As a matter of fact, within the last decades, archaeological research in other regions has also demonstrated that the earliest evidence in those geographic areas of hunting dates to much earlier times than previously thought. It certainly predates the appearance of anatomically modern humans, and flexible hunting and scavenging strategies probably characterized foraging among different hominin populations and species of the genus *Homo* throughout its evolution (e.g. Villa *et al.*, 2009; Richards and Schmitz, 2008; Berger and Trinkaus, 1995; Saladié *et al.*, 2014; Rodríguez-Hidalgo *et al.*, 2017; Lupo, 2013). Regarding the zooarchaeological and taphonomic data from 1.8 – 1.6 Mya, the evidence indicates that hominins were already gaining access to complete carcasses of relatively large ungulates regularly, and repeatedly transporting large portions of these carcasses back to favored safer locations, as once proposed by Isaac (1978) (Pickering and Bunn, 2013; Uribelarrea *et al.*, 2014). In spite of the disagreements between researchers regarding the earliest foraging strategies of hominins, most authors acknowledge that the appearance of some early *Homo*

was marked by an increase in body size and cranial capacity, and the emergence of modern gut morphology among other changes, brought about by a dietary shift toward a high-quality diet focused on the consumption of meat (Aiello and Wheeler, 1995).

Such changes could only have been provoked by the regular intake of a substantial amounts of meat. Eating meat regularly would only have constituted a possibility for hominins if they actively hunted or gained early access to carcasses by confrontationally scavenging from felids, since secondary scavenging processes in Pleistocene savanna environments do not yield sufficient meat (Blumenschine, 1986; Domínguez-Rodrigo 1999; 2002). This does not imply that hominins never passively scavenged carcasses from abandoned carnivore kills, but only that the predominant taphonomic signal in Pleistocene anthropogenic sites from across Africa clearly reflects early access to carcasses (Bunn and Ezzo, 1993; Asfaw *et al.*, 2002; Pickering *et al.*, 2004; 2008; Fiore *et al.*, 2004; Pickering and Bunn, 2013).

1.4. The development of taphonomic approaches

The debates surrounding site formation, carcass acquisition, the regularity of meat consumption and the use of referential locations on the landscape by hominins have directly influenced the development of archaeological taphonomy over the last decades. It is thanks to these debates that this discipline now counts with a considerable number of robust methods that allow the scientific contrasting of the hypotheses and assumptions that different researchers have. Here, I divide the trajectory of archaeological taphonomy into four phases, each one of them marked by the addition of a new conceptual advance and by the incorporation of more refined statistical methods to zooarchaeological studies.

Taphonomy originally emerged in the context of paleontological studies in the 1940s and 1950s. The term was coined by Efremov (1940; 1950; 1953) and means "the laws of burial". Taphonomy was originally defined as "the study of the transition of animal remains from the biosphere into the lithosphere" but has since then undergone tremendous development and its objects of reference in the case of the archaeological record now also include non-living elements recovered from the sites, such as lithic remains (Domínguez-Rodrigo *et al.*, 2011). Taphonomy therefore studies site formation processes and in archaeological studies it targets "interpreting taphonomic entities produced by humans, the relations among these entities and with their respective external environments, in order to reconstruct anthropogenic behaviors" (Domínguez-Rodrigo *et al.*, 2011). During the first phase of taphonomic research, archaeologists concerned with the interpretation of fossil bone assemblages generally focused on skeletal part frequencies, taxonomic identification and mortality profiles, which have always been the major approaches used by zooarchaeologists and paleontologists, while they developed new methods for quantifying the anatomical parts and individuals represented in the sites (Binford, 1978; 1981; Bunn, 1982; Bunn and Kroll, 1986; 1988; Bunn *et al.*, 1988; Potts, 1988; Stiner 1991). Other types of analyses, including the assessment of bone breakage patterns and bone surface modifications were only used as complementary methods to reinforce the interpretations drawn from skeletal part profile analyses (Domínguez-Rodrigo 2002; Domínguez-Rodrigo *et al.*, 2007). However, it was soon realized that skeletal part abundance analyses often yielded controversial results, because they are prone to equifinality, i.e. different taphonomic agents can cre-

ate very similar skeletal profiles, and because they are heavily influenced by methodological and taphonomic biases (see methods section 2.2). In contrast, the "physical attributes" of the bone assemblages themselves, including data on fragmentation and surface modifications, were more reliable and it was initially argued that they were less prone to equifinality (e.g. Domínguez-Rodrigo *et al.*, 2007; Blumenschine and Pobiner, 2007; Arriaza and Domínguez-Rodrigo, 2016).

Domínguez-Rodrigo *et al.* (2007) discussed this matter at length and proposed that taphonomic interpretations of early sites would profit from prioritizing the evidence stemming from these "physical attributes (Domínguez-Rodrigo *et al.*, 2007). During this second phase of the development of taphonomy, marked by a shift from laying emphasis on skeletal part frequencies to bone surface modifications and fracture patterns, the importance of experimental research to increase analogical frameworks and avoid equifinality was also soon recognized and promoted. Experimental and replicative studies serve to generate comparative taphonomic data and play a key role in the analyses of early sites. They model time and sequence of carcass acquisition by hominins and non-human carnivores and the intensity of carcass processing resulting from different scenarios (Lupo, 2013). Although experiments are far from perfect and are usually limited by factors related to the design and possibilities of execution of the experiments, and by ecological and behavioral variability in carnivore feeding strategies, many variables can be experimentally controlled. Thus, the creation of referential frameworks through experimentation and actualistic work has significantly increased the usefulness of the analyses of bone surface modifications and breakage patterns. Actually, the utility of constructing and using referential frameworks is reflected in the fact that this line of research, which began in the 1980s and 1990s due to the concern that most archaeological interpretations were founded on ideology rather than on empirical evidence, is currently still being refined and improved decades later.

Experimental work has done much to eliminate equifinality from taphonomic interpretations. General differences detected in fracture angles created through dynamic and static loading (Capaldo and Blumenschine, 1994; Pickering and Egeland, 2006), contrasts in the frequencies of tooth-marked shaft fragments depending on the timing of access to carcasses by carnivores (Blumenschine, 1988; 1995; Blumenschine and Marean, 1993; Capaldo, 1995) or in the frequencies of cut-marked specimens in scenarios of primary and secondary access to carcasses by hominins (Domínguez-Rodrigo 1997; Domínguez-Rodrigo and Barba, 2005) have been useful to support different models of access to carcasses by hominins. Yet, on occasions, the application of experimental data to the archaeological record has generated inconsistent results depending on the analyst, like in the case of FLK *Zinj*. This is in part due to differences in

how researchers quantify different taphonomic attributes, but it is also related to problems of equifinality often caused by small experimental samples and to the examination of one single variable at a time. As a matter of fact, traditionally, taphonomic research has understood assemblages as concentrations of deposited taphonomic entities (Fernández López, 2006), and has placed emphasis on the quantification of taphonomic attributes. Yet, in the last few years, a new complementary view of taphonomy is being advocated, which stresses the fact that additional taphonomic attributes can be detected using more sophisticated approaches that are produced when the association of taphonomic entities is taken into account (Domínguez-Rodrigo *et al.*, 2017a).

Domínguez-Rodrigo *et al.* (2014; 2017a; 2019a) have advocated the combination of variables in multivariate statistical approaches in order to overcome equifinality produced when variables are used independently. When variables are used jointly in multivariate analyses, the results are much more consistent, because the relationships and associations between variable types are captured in addition to the effects of each single variable (Domínguez-Rodrigo *et al.*, 2014). Several studies combining the distributions of all mark types (tooth marks, cut marks and percussion marks on different anatomical portions) or different variables related to skeletal part profiles, have widely demonstrated that viewing assemblage formation as a dynamic system in which the association of taphonomic entities generates emergent properties is far more effective (Domínguez-Rodrigo *et al.*, 2014; Arriaza and Domínguez-Rodrigo, 2016). This approach has also been applied successfully to better model and understand the effect of fluvial processes on bone assemblage formation (Domínguez-Rodrigo *et al.*, 2017a; 2019a). This view of taphonomy could be taken as the beginning of a third stage in the trajectory of taphonomy. It has also opened the door to spatial taphonomy, which is the analysis of the spatial patterning of taphonomic attributes. By analyzing taphonomic attributes produced by different taphonomic agents, for example carnivores and hominins, from a spatial perspective, we can discover hidden spatial patterns in how each agent distorts bone assemblages and make inferences about their interaction and their involvement in site formation (Domínguez-Rodrigo *et al.*, 2017a). Although some experimental analyses of postdepositional disturbance by carnivores already exist (Marean and Bertino, 1994; Camarós *et al.*, 2013; Arilla *et al.*, 2014), experiments modeling the effect of different taphonomic agents are needed in which the exact spatial location of bones and lithics is plotted, so that their spatial patterns can be analyzed and compared among them and with those detected at archaeological sites. Experimental studies in which this line of research is pursued are still few in number, but their results are very promising (Domínguez-Rodrigo *et al.*, 2017a; Arriaza *et al.*, 2019).

Recently, the application of machine learning algorithms to taphonomic

research has been shown to have the power to magnify the advantages of using many variables simultaneously. These methods are much more powerful than traditional frequentist and Bayesian statistical methods. A set of several machine learning algorithms, including Support Vector Machines, Neural Networks, and Random Forests, have been applied in recent years with high success to various areas of taphonomic research like skeletal part profiles, bone surface modifications and breakage patterns, yielding a strong convergence in the classifications (sometimes with 100% accuracy) (Arriaza and Domínguez-Rodrigo, 2016; Domínguez-Rodrigo and Baquedano, 2018; Domínguez-Rodrigo, 2019a; Moclán *et al.*, 2019). These methods could potentially be the beginning of a new phase in taphonomy characterized by much more reliable interpretations of the taphonomic attributes from bone assemblages. Yet, these classifications depend on the correct identification of these attributes by the analyst, particularly of bone surface modifications. Commonly, different analysts report different estimations of tooth marks, percussion marks and cut marks, thereby reaching conflicting conclusions. New methods are needed to steer taphonomic analyses toward higher objectivity. Such new analytical tools have recently been proposed and are currently being developed and improved. They consist in the identification or classification of bone surface modifications using a combination of geometric morphometrics and machine learning, or even deep learning algorithms using convolutional neural networks, and their potential for distinguishing cut marks from trampling marks or for differentiating tooth marks made by different carnivores has already been confirmed (e.g. Courtenay *et al.*, 2019; Cifuentes-Alcobendas and Domínguez-Rodrigo, 2019).

1.5. In-site spatial statistical analysis

The utility of spatial information resulting from the distribution and the relationships between artefacts has long been recognized (Hodder and Orton, 1976; Whallon, 1974; Yellen, 1977; Binford, 1983), as has the need for the development of spatial statistical tests that can be used in order to gain certainty with regard to subjective appreciations of spatial attributes reflected in an assemblage and in order to detect spatial associations that are not perceptible to the naked eye (Kroll and Price, 1991). Even though several analytical techniques have been available for decades to study archaeological debris (summarized by Kroll and Price, 1991 and by Domínguez-Rodrigo and Cobo-Sánchez, 2017b), these quantitative analytical tools commonly failed to produce few interpretable and consistent results according to some researchers (Whallon and Mellars, 1978; Kroll and Price, 1991; Giusti and Arzarello, 2016). This was mainly due to the fact that the difficulties researchers faced in finding universal spatial patterns in forager camp organization eventually created skepticism about the potential of these ethnographic studies as analogs (Hodder, 1987), and this line of research was nearly completely abandoned until a few years ago. In any case, spatial archaeological studies have mostly been descriptive and graphic, and inferences are sometimes drawn from subjective statistically unsupported observations (Bevan *et al.*, 2013). In some cases, spatial patterns of archaeological remains are described, yet not fully interpreted behaviorally. Thus, the main question behind spatial archaeology, namely, how to interpret archaeological spatial patterns, particularly those from Paleolithic sites, has remained largely unresolved. Fortunately, a number of more refined and robust spatial statistical tests that have recently been developed are starting to be applied within the fields of ecology, geology, epidemiology and econometrics (Baddeley and Turner, 2004; Baddeley *et al.*, 2015; Bivand, 2010; Dorman, 2014; Pebesma, 2004; Bivand *et al.*, 2013) and they can also be usefully introduced in spatial archaeology in order to interpret hominin behavior, as has recently been shown in a spatial study of the archaeological assemblages from at FLK *Zinj* and PTK (Domínguez-Rodrigo and Cobo-Sánchez, 2017b).

In fact, one of the most important ideas behind spatial archaeology is that human activities are spatially organized and therefore that social dynamics can

be apprehended from the analysis of the spatial patterns of food refuse. Spatial statistical analyses thus represent an excellent opportunity to approach hominin social structure. However, this is not an easy task, in part because referential frameworks are needed for comparison. A number of ethnoarchaeological studies that recorded the spatial distribution of bone refuse at several modern hunter-gatherer campsites can however be used as referential analogs that reflect human's modern social structure (Domínguez-Rodrigo and Cobo-Sánchez, 2017a). Thanks to these maps of bone refuse, and to new available spatial statistical analytical tools, we now know that humans generate multi-cluster spatial patterns in forager camps that reflect an individualized household social structure (Domínguez-Rodrigo and Cobo-Sánchez, 2017a). Therefore, examining the spatial patterns of different periods throughout human evolution could help establish when the modern human social structure emerged. However, the different forms of hominin social structure that evolved throughout human evolution most likely have no modern counterpart, which is why reconstructing these forms of social organization is a complicated endeavor. Another challenge stems from the fact that extensively excavated, and fully anthropogenic sites are required that have also preserved their spatial properties and are largely undisturbed. Otherwise, spatial analyses might be of limited value to infer hominin social dynamics.

Nevertheless, spatial analyses can also be used for taphonomic purposes and be very useful to understand the effect of postdepositional processes on site formation (e.g. Giusti and Arzarello, 2016; Giusti *et al.*, 2018; Coil *et al.*, 2020; Peters and Kolfschoten, 2020). Spatial analyses often explore the depositional and functional association of stone tools and bones (Giusti and Arzarello; Domínguez-Rodrigo and Cobo-Sánchez, 2017), but can also help differentiate between several different hominin occupations that are stratigraphically indistinguishable or not visible to the naked eye (e.g. Marín *et al.*, 2019). A recent study even uses a combination of spatial data and machine learning algorithms to separate several fossiliferous levels at a paleontological site (Martín-Perea *et al.*, 2020). A further goal of spatial approaches is to address site function and the division of space in areas used for different activities (Clark, 2017; Oron and Goren-Inbar, 2014). It would be interesting to be able to identify the spatial attributes of the patterns created by different taphonomic agents so that taphonomic processes can be better identified in the fossil record. To that effect, experimental studies modeling carcass distortion by different taphonomic agents, such as water currents or carnivores are being expanded (Domínguez-Rodrigo *et al.*, 2017a; Arriaza *et al.*, 2019).

In sum, significant additional knowledge on site formation and hominin behavior can be gained from exploring the spatial distribution of remains and from analyzing the spatial distribution of taphonomic variables. This is also

targeted in the spatial analysis included in the present study. I further examine whether different areas of the site were used for different purposes, i.e. whether certain activities can be identified spatially and I also intend to provide insight regarding hominin socio-economic behavior.

1.6. The relevance of the newly discovered anthropogenic sites from Bed I

As can be appreciated from the previous paragraphs, the hunting-scavenging debate and the discussions about early site functionality mainly revolved around FLK *Zinj*, given that all other Bed I sites from Olduvai represented non-anthropogenic accumulations, including carnivore-collected carcasses, background scatters or palimpsests in which hominins contributed only marginally to the bone clusters (Domínguez-Rodrigo *et al.*, 2007). Other East African sites like Koobi Fora have yielded less informative faunal assemblages due to poorer bone preservation. Thanks to all the controversy concerning the assemblage formation history and its behavioral meaning, the FLK *Zinj* site has been studied by many researchers and from many different viewpoints, and a wealth of detailed information exists about its formation and autochthonous nature, the contribution of hominins and carnivores to the archaeofaunal assemblage, the inferred carcass foraging strategies of hominins, the characteristics of the surrounding environment, and the spatial properties of the distribution of the remains (e.g. Bunn and Kroll, 1986; Oliver, 1994; Blumenschine, 1991; Domínguez-Rodrigo *et al.*, 2007; Bunn and Pickering, 2010; Pante *et al.*, 2012; Parkinson, 2013; Domínguez-Rodrigo *et al.*, 2014; Domínguez-Rodrigo and Cobo-Sánchez, 2017; Domínguez-Rodrigo *et al.*, 2019 a, b, c).

However, given the palimpsestic nature of the other sites at Olduvai and Koobi Fora, and the lack of sites comparable to FLK *Zinj* in terms of preservation and spatial extension, some researchers were reluctant to make generalized assertions about early human behavior being characterized by regular early and primary access to carcasses through hunting (and/or confrontational scavenging) and the use of central places for activities such as food sharing, based on the interpretation of just one archaeological site. To this should be added that there has been some confusion in the past regarding the hominin species with which this behavior should be associated (*Homo habilis* or *Homo ergaster*). The discovery in 2015 at PTK of OH 86, a phalanx of a modern human-like hand, proved that a hominin with a more modern-looking anatomy coexisted with *Homo habilis* and *Paranthropus boisei* in Olduvai during Bed I times (Domínguez-Rodrigo *et al.*, 2015). This phalanx could have belonged to *Homo ergaster* or to its more ancient form.

It should be emphasized that the FLK *Zinj* faunal assemblage could be encompassing two different archaeological levels (levels 22A and 22B). Leakey (1971) did not make a distinction between the two depositional events and could have combined two assemblages with somewhat distinct depositional histories (Domínguez-Rodrigo *et al.*, 2010), although she described in her notes that, at FLK *Zinj*, the uppermost section of the *Zinj* clay, i.e. Level 22A, contained the denser archaeological assemblage. Also, although the spatial location of each bone fragment was recorded, no record exists between these coordinates and the taphonomic attributes of each specimen from FLK *Zinj*, but this information will be easily obtained from the new sites. The taphonomic study of these new sites in the present time also represent a great opportunity because new available statistical and technological developments can be applied, and a growing amount of experiments and actualistic studies can be used to also establish new testable hypotheses within the framework of scientific theories (Domínguez-Rodrigo, 2013). Recent examples of this kind of innovative studies include the attempt to estimate group size and time of occupation of early sites (Domínguez-Rodrigo *et al.*, 2019b, c), and the intent to infer hominin social structure from spatial patterns of archaeological materials (Domínguez-Rodrigo and Cobo-Sánchez, 2017), both of which have yielded interesting results.

Like at DS, a clear anthropic signature can already be observed from the excavations at PTK and AGS. All three faunal assemblages are exceptionally well-preserved, and comparable in the high densities of archaeological remains they have yielded. DS and AGS in particular contain a high proportion of ungulate axial remains compared to FLK *Zinj*, as well as numerous refits and several semi-articulated anatomical elements. At all three sites the faunal remains also show a clear spatial and functional association with a large and diverse sample of stone tools, which have also been analyzed (Díez-Martín *et al.*, in prep.). This association is also apparent in the presence of abundant cut and percussion marks on the bones, which show mostly green fractures. This all indicates a similarly anthropogenic agency as inferred for FLK *Zinj*. It is also worth noting that all three sites have been or are being excavated extensively, which will enable comprehensive spatial analyses of the distributions of archaeological remains. The fact that all four sites contain levels that are located on the same paleosurfaces, which are currently being reconstructed with a high level of detail, represents a great opportunity to reconstruct hominin activities at the landscape level and assess variability in foraging strategies and in the uses of the sites. This means that hominin behavior can now be addressed at a broader scale with greater confidence. The taphonomic and spatial study of DS presented here constitutes the first step in this direction.

1.7. Excavation procedures and data recovery at DS (David's Site)

David's Site (1.84 Ma) is located in the junction between the main and secondary branches of Olduvai Gorge in northern Tanzania (2°59'33"S; 35°21'08"E). It was discovered a few hundred meters away from FLK *Zinj*, in an area covered by a dirt road in 2014 (Figure 1.1). That year, rains had started eroding the archaeological deposit, which lay very close to the surface, and excavations started immediately after its discovery. From 2014 to 2018 intensive excavations exposed an area of 554 m^2 . DS is therefore larger than the penecontemporaneous FLK *Zinj* site and constitutes the biggest open window to the African Early Pleistocene (Appendix Figure 7.14). Over the course of these five fieldwork seasons, more than 15,000 fossil remains and stone tools (including sieve finds) were recovered from Level 22B. Level 22A contained archaeological remains as well, yet in much lower densities. Excavations proceeded quickly during the first two campaigns, because the archaeological deposit was found at a few centimeters right below the surface. Careful excavation of the layers by a large digging crew included plotting the materials larger than 2 cm with laser theodolites. All trenches (3x3 m) were stereo-photographed once they were uncovered in order to obtain a photogrammetric 3D reconstruction of the soil and deposited materials as they were prior to recovery. Azimuth and plunge of the items were measured with a compass and an inclinometer respectively. The removed sediment was sieved in 5 mm and 3 mm meshes.

By the end of the 2015 field season, excavations had already exposed a large area. At this point, a spatial statistical prediction using different regression models and simulations was carried out in order to detect the potentially densest portions of the unexcavated areas of DS (Domínguez-Rodrigo *et al.*, 2017b). The high correspondence between the results obtained from these predictions and subsequent excavations at the site demonstrated the great potential of the application of spatial statistical techniques in archaeological research. Since the density of remains increased towards the south, where the archaeological deposit was covered by a much thicker sedimentary stratigraphic sequence, pneumatic hammers, picks and shovels had to be used to remove the sterile deposits and overburden and prepare the surface for careful excavation.

At the end of the 2016 field season, most of the paleosurface (468 m^2) had been exposed and abundant fossil bones and lithic remains had been retrieved

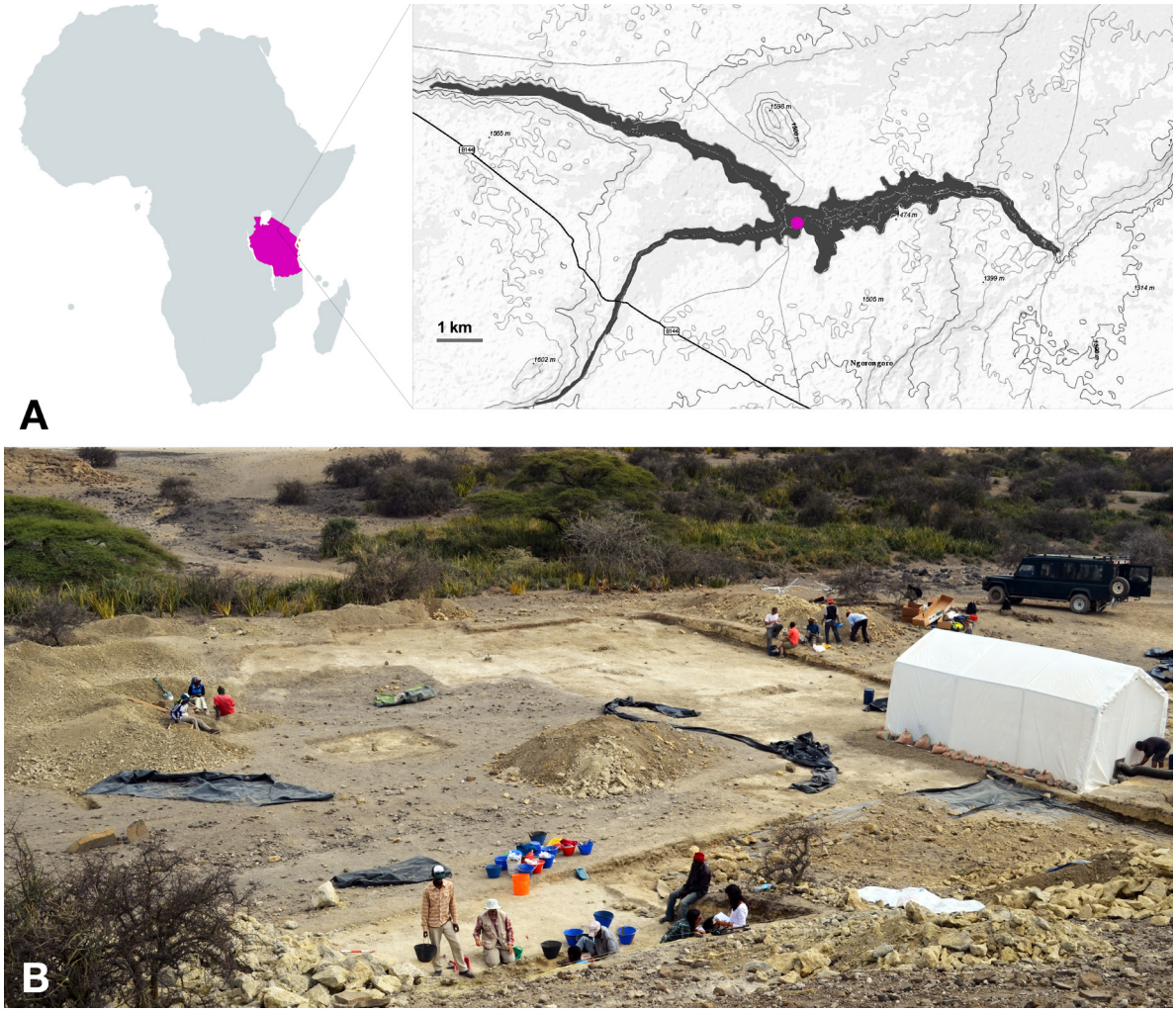

FIGURE 1.1. *A) Location of DS in Olduvai Gorge in northern Tanzania. B) General view of the DS excavation in 2015 from the south. Photo by Elia Organista.*

from both archaeological levels. In addition, a series of sediment samples were taken from some of the trenches to carry out chemical biomarker analyses. Plant biomarker analyses at a very high spatial and temporal resolution have already provided meter scale vegetation patterns and association and correspondence with the fossil remains collected at DS (work in progress). The analysis of nearly 100 samples from the different geoarchaeological levels comprised in the *Zinj* clay at this site suggests that the higher densities of archaeological material are found in a microhabitat dominated by aquatic macrophytes and isolated wooded patches (Sistiaga *et al.*, in prep.). This approach makes it possible to correlate archaeological spatial information with spatial patterns of plants at a very high resolution and can therefore allow archaeologists to address new interesting questions about hominin behavior at the sites. For example, which

ecological factors conditioned hominins to choose DS as a place to carry out their activities. The trenches excavated in 2017 towards the south of the site area yielded somewhat lower fossil densities than those excavated in previous campaigns in level 22B, suggesting that the limits of the site towards that direction could be close. The trend observed for level 22A was the opposite, however. During the removal of Tuff IC in one of these trenches, a fascinating discovery was made. Across the still unexcavated trench, the shape of a fallen tree trunk could be observed, which suggests that DS was located in a wooded area. Before the trench was excavated, samples were taken from the sediment forming this unique find to be analyzed by experts (Figure 1.2).

In 2018, several additional trenches were opened at the edges of the site with the intention of demarcating its limits. Indeed, the excavated trenches yielded lower densities of archaeological materials, and that year the limits of the site were confidently established, and excavations were finalized (Figure 1.3). We determined that some of the edges of the site were delimited by erosion, especially the central area of the site, which had undergone significant erosion due to the erosion and deposition of the Ndutu unconformable sediments and to their subsequent erosion, exposing the underlying clay to the effect of modern rains and the use of the area as a road. In addition, the southern edge of the excavation had started yielding lower densities of materials due to a change in facies from clayey to silty sediments, which probably indicates a change in the paleolandscape. The almost complete absence of bone remains at the southeastern limit of the site could be due to the presence of more water in this area

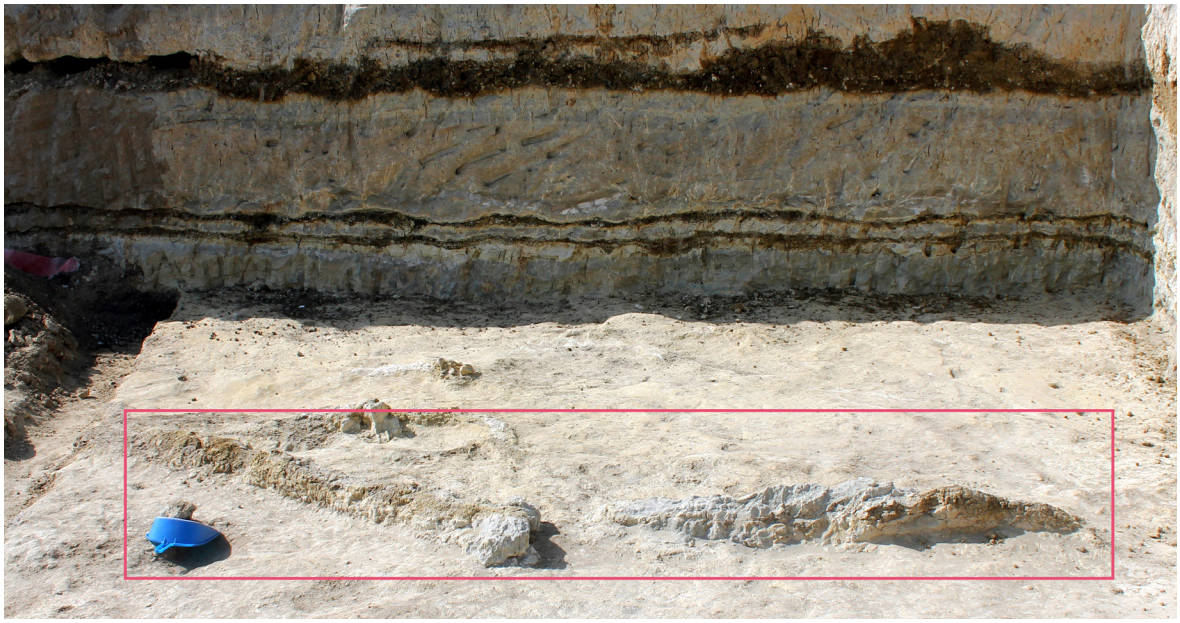

FIGURE 1.2. *Shape of a fallen tree trunk found under Tuff IC in 2017.*

FIGURE 1.3. *Excavations at DS (top left and bottom right) and examples of semi-articulated bone remains and well-preserved axial bones (top right and bottom left).*

– reflected in a higher presence of large carbonate nodules – that could have affected the preservation of fossils. In this area, only large basalts and some stone tools have been found. The remaining areas are limited by the lava flows of the bottom of Bed I that were already part of the paleolandscape when hominins created the site.

There are several aspects that bestow a special value on DS. On one side, preservation of the fossil bones is as good as that at FLK *Zinj*, and reflects that post-depositional processes had a very marginal effect on the assemblage. Also, numerous rib and vertebrae remains have been recovered that usually disappear due to the action of carnivores or hydraulic processes. On the other side, the assemblage was probably formed in a short period of time (Domínguez-Rodrigo *et al.*, 2019c) and the ecological conditions at the site can be reconstructed with very high resolution, not to mention that given its large extension, all aspects, taphonomic, behavioral and ecological, can be explored spatially.

Around 85% of the faunal remains recovered from DS stem from Level 22B,

which has yielded 3458 bone fragments and 1182 lithics (if counting the fraction longer than 20 mm). The average fossil density in this archaeological level is of about 8 pieces per square meter, but archaeological materials cluster around three areas of very high density (around 70 remains per square meter). The remaining archaeological artefacts come from Level 22A. The opposite occurs at PTK and FLK *Zinj*, where the bulk of the archaeofaunal assemblage and the associated lithic tools come from the uppermost section of the *Zinj* clay (i.e., 22A) (Leakey, 1971). In this study, I present the results of the zooarchaeological and taphonomic analysis of the faunal remains from Level 22B at DS. I have focused almost exclusively on the ungulate remains, because they represent the bulk of the bone assemblage (98.8%) and also reflect hominin activity most directly, which is the primary focus of this dissertation. However, a comprehensive analysis of the remaining faunal sample, which mainly includes birds and carnivores, could provide relevant information about the ecological conditions at the site and should therefore be carried out in the future. Level 22A has also provided evidence of hominin activity at the site yet, it seems, not as conspicuous as Level 22B. On-going work pertaining to the lithic assemblage, the biochemical analysis of plant remains, and geoarchaeological studies will soon appear and complement the results presented here. Below, I include basic relevant information about the stratigraphy and geological context of DS.

1.8. Geological and stratigraphic overview of DS

Olduvai Gorge is located southeast of the Serengeti Plains in northern Tanzania. The oldest sediments it contains are around 2 Ma old. Over the past 200 Ka fluvial erosion has carved through the different geological layers creating the gorge, which splits into two branches, the main and the secondary gorge. Hay (1976) defined several geological units within the gorge that are still the foundation for geological studies at Olduvai today: Beds I, II, III, IV, the Masek, Ndutu and Naisiusiu Beds. DS lies in Bed I, which spans from approximately 1.98 Ma to 1.75 Ma, and is formed by the alternating deposition of clayey facies associated to lake sediments and silty layers on the one hand and volcanic tuffs (1A – 1F) that have been securely dated on the other hand (Walter *et al.*, 1991; 1992; Manega, 1994; Blumenschine *et al.*, 2003).

Several important sites are known from the layers occurring between these tuffs, like FLKN, FLKNN and DK, but the four fully anthropogenic sites discovered in Bed I (FLK *Zinj*, PTK, DS, and AGS) all stem from the paleosol underlying Tuff 1C, which contains a clay stratum (<20 cm) that can be traced laterally on a significant portion of the gorge at the junction and on both ends of its trajectory in areas that lay close to an ancient lake. Paleoecological reconstructions of the *Zinj* paleolandscape have repeatedly emphasized the low-energy depositional environment dominating the lower and middle sequence of Bed I around FLK *Zinj* (and the other anthropogenic sites), mainly evidenced by "lake-margin facies, corresponding to a shallow lake with predominantly fine-grained sedimentation … dominated by decantation of clay in mudflats with few or no evaporitic sedimentation" (Uribelarrea *et al.*; 2014, p. 2).

Researchers have identified two important zones in this paleolandscape: a topographically higher supralittoral area dominated by a palm and acacia woodland (Barboni *et al.*, 2010; Arráiz *et al.*, 2017), and a topographically lower littoral with wetland and a freshwater spring (Ashley *et al.*, 2010; Uribelarrea *et al.*, 2014). In other words, the landscape was composed of a raised platform and a shallow depression separated by around 2 m difference in elevation (Uribelarrea *et al.*, 2014). FLK *Zinj*, PTK, AGS, and DS are all located on topographically higher ground in a supralittoral environment and are separated from each other by a few hundred meters (Uribelarrea *et al.*, 2014; Figure 1.4). DS in particular is located between two alluvial inputs. Mineralogical and geo-

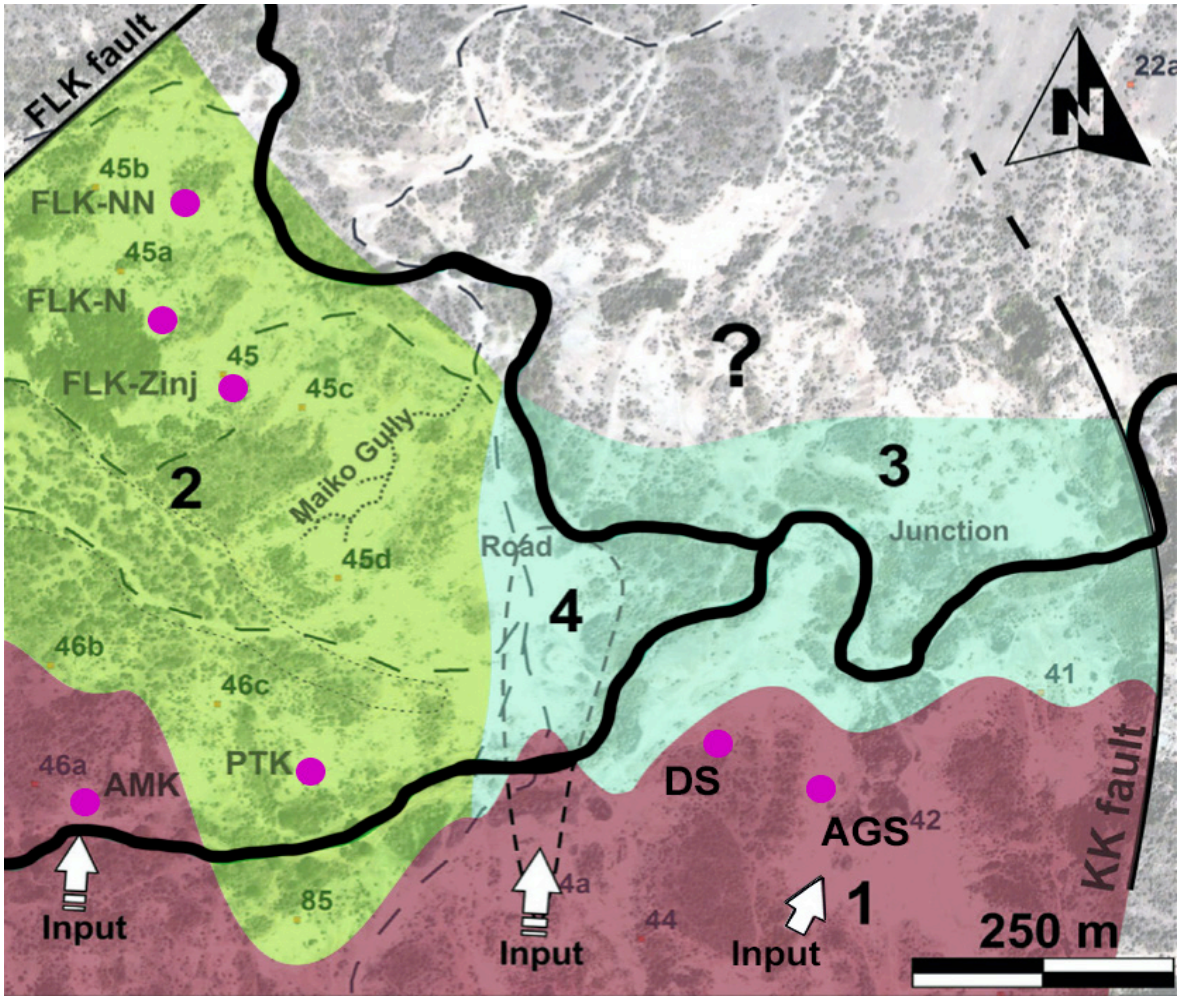

FIGURE 1.4. *Cartography of the main zones identified in the Zinj paleolandscape, within the lake-margin zone of lower-middle Bed I between the FLK and KK faults and the location of the main Bed I sites, including DS (modified from Figure 10 in Uribelarrea et al., 2014). The anthropogenic sites are located on zones 1 and 2, which are the topographically highest areas on the landscape.*

chemical lateral variations throughout the FLK *Zinj* paleolandscape suggest a differential entry of fresh water into the basin, with fresh water entering the system from the surroundings of DS during the deposition of both levels 22A and 22B (Martín-Perea *et al.*, 2019). This suggests that at DS hominins probably had regular access to fresh water and herbivores. Phytolith analyses have shown that like FLK *Zinj* and PTK, DS was located in a wooded environment, which could have provided refuge from carnivore predation. The anthropogenic sites are also contemporaneous with a palimpsest at FLKNN 1, located at the freshwater spring (Domínguez-Rodrigo *et al.*, 2007; Ashley *et al.*, 2010) and AMK, a site that seems to have formed naturally (Aramendi *et al.*, 2017). The stratigraphic

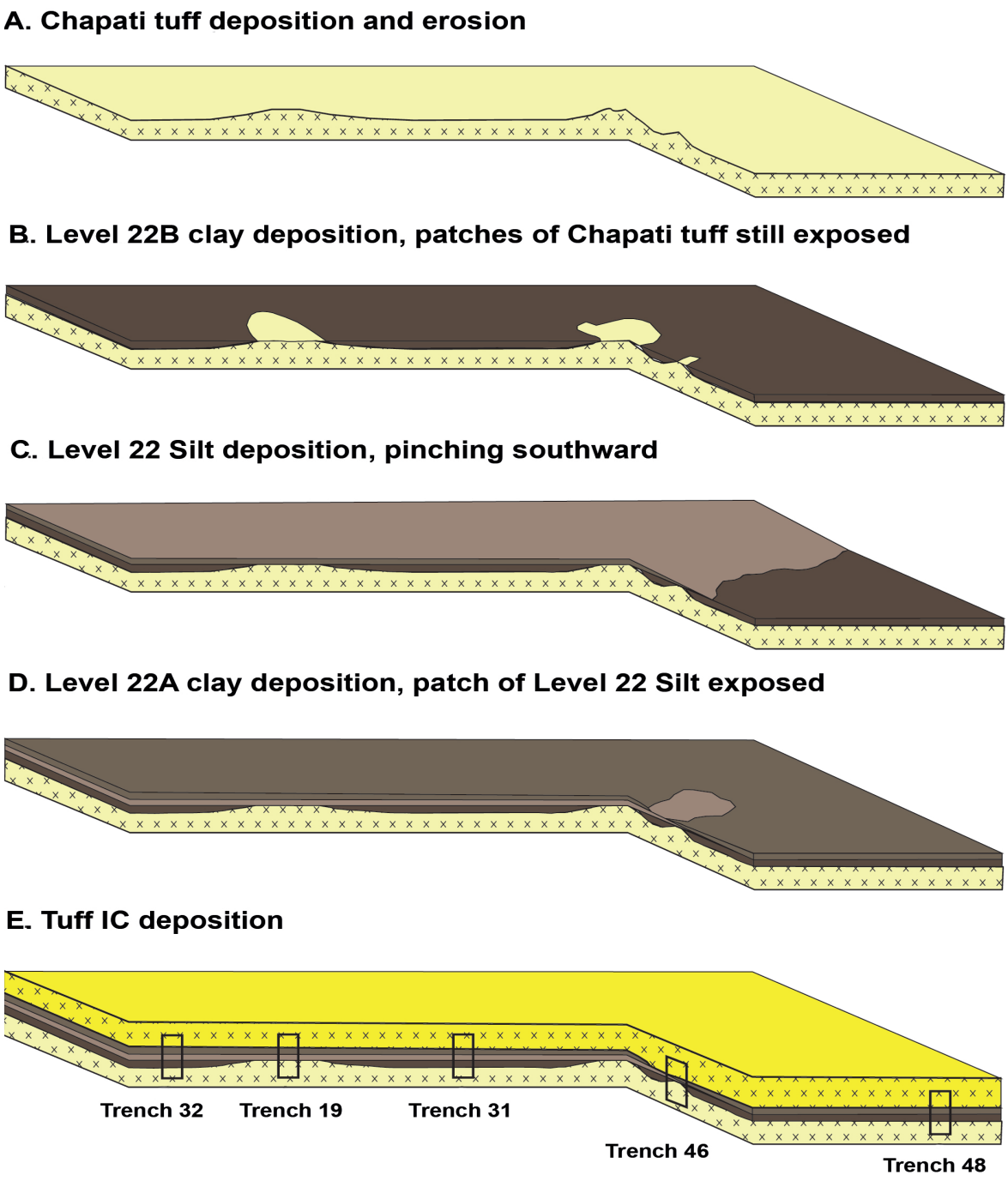

FIGURE 1.5. *Schematic representation of the geological history of DS showing the deposition of the different levels as described in the text.*

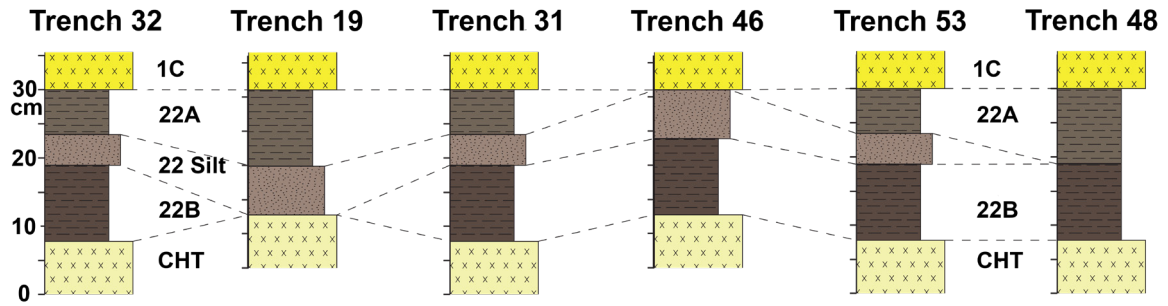

Figure 1.6. *Stratigraphic columns at the trenches highlighted in Figure 1.5.*

sequence is very similar at all these sites, except at FLKNN 1, where it comprises a carbonate layer corresponding to the freshwater spring.

As has been mentioned above, most archaeological remains recovered at DS stem from Level 22B, which is deposited disconformably over an irregular topography of the Chapati Tuff (Uribelarrea *et al.*, 2014; Figure 1.5A). The Chapati Tuff, given its name due to its multilayer composition, is a laminated reworked tuff present throughout the entirety of the Main Junction. From the base to the top, it is composed of three main units (Uribelarrea *et al.*, 2014): a) a 1-5 cm white to light yellow laminated tuffaceous sand and silty sand with some interbedded green tuffaceous clay (1-20 mm thick); b) a 10-20 cm grey massive tuffaceous clay with rounded, medium-sized tephra fragments; and c) a 1-3 cm white massive tuff with thin carbonate laminae. At DS, the Chapati Tuff is reworked and, in some areas, eroded at DS. This palaeotopography leads to some patches of Chapati Tuff still exposed after deposition of level 22B (Figure 1.5B). Therefore, in some areas of the site in which the contact between both levels was not sharp but gradual, the Chapati Tuff has been excavated, although only for stratigraphic purposes. This level has also yielded some archaeological remains. However, in most parts of the site Level 22B overlies the Chapati Tuff with a discrete and sharp contact (Hay, 1976; Uribelarrea *et al.*, 2014; Martín-Perea *et al.*, 2019).

Level 22 consists of two clayey sublevels (level 22A and level 22B) each containing separate archaeological assemblages. Level 22B is a ~10 cm olive gray (5Y 4/2) clay. In this level, archaeological remains are commonly found in the lowermost ~5 cm. Level 22B was deposited under very low energy conditions, as evidenced by clay mineral micro-textures and the absence of large clay aggregates (Martín-Perea *et al.*, 2019). An intercalated, discontinuous <5 cm silty unit, Level 22 Silt, is found between levels 22A and B at DS and surroundings (Uribelarrea *et al.*, 2014; Martín-Perea *et al.*, 2019), and is a windborne, dis-

continuous, low energy deposit (Figure 6), which overlies level 22B and the Chapati Tuff and pinches out southward (Figure 1.5C). The deposition of this level, however, does not seem to have altered the position of the archaeological remains in a meaningful way. Level 22A is a ~10 cm dark olive gray (5Y 3/2) earthy clay, discontinuous, low energy (Martín-Perea *et al.*, 2019) deposit which overlies level 22 Silt in the northern areas of the site, is commonly absent in the center of the site, but overlies level 22B in the southern grids of the site (Figure 1.5D). Archaeological remains embedded in this level are also found in the lowermost ~5 cm of the level. Mineralogically, level 22A and 22B are clay mineral rich, with a significant presence of anorthoclase and albite and variable quantities of zeolites (Martín-Perea *et al.*, 2019). Tuff 1C, which deposited conformably over level 22A and 22silt (Figure 1.5E), is interpreted as an airfall tephra (Hay, 1976; Uribelarrea *et al.*, 2014) and is a 30-40 cm crystal tuff containing over 80% of sharp, <2 mm anorthoclase, hornblende, augite and titanomagnetite juvenile crystals (Uribelarrea *et al.*, 2014; Figure 1.6).

Fortunately, in most of the area in which DS was found Tuff 1C had not been eroded away and has preserved the underlying archaeological deposit. Yet, it should be noted that some erosion occurred in the areas close to the basalt, where Tuff 1C was only partially present, and especially in the central part of the site, which means that a portion of the assemblage could have been washed away by rains or destroyed. Be that as it may, DS is still the largest early Pleistocene site in Africa and the preserved deposit contains substantial information about hominin activities during Bed I times.

1.9. Structure and aims of this study

In this study I build on previous taphonomic analyses of Bed I sites and apply a series of taphonomic approaches to the faunal assemblage from Level 22B at DS in order to unlock the behavioral meaning of the site and examine how it fits into what is already known about early human behavior from the studies of other early Pleistocene sites (mainly the other Bed I sites, Kanjera, and Koobi Fora). From the specific to the general, the objectives of this study are the following: assessing the processes that led to the formation of the faunal assemblage in Level 22B, by evaluating and measuring the effect of the abiotic and biotic taphonomic agents involved in the creation and transformation of the original archaeological deposit; accurately determining the degree of implication of hominins at the site, and the kind of interaction that took place between them and the carnivores with which they coexisted; and interpreting the functionality of the site. A further goal is to describe in detail different aspects of early *Homo* behavior based on the obtained evidence and on similarities and differences observed between the findings at DS and at other Paleolithic sites. Lastly, I will explain how the documented hominin socio-economic behaviors and tested hypotheses fit into the systemic structure of a scientific-realistic theory on the evolution of human behavior, and I will pose further relevant questions about the social organization of early *Homo*.

This dissertation is structured following the composition of scientific publications: after the introduction in this first chapter, I describe the samples and the methods applied in each of the included taphonomic and spatial analyses, along with the used statistical techniques and the selected referential analogs for comparison with the DS sample. In the next chapter, the statistical results and the similarities and differences between DS and other Paleolithic sites are reported following the order exposed in the methods section. The dissertation ends with a chapter including a discussion and the conclusions of the study, where the results and their behavioral implications are organized and discussed around the most relevant issues of early Pleistocene archaeological research.

In a way, this study is halfway between traditional taphonomic methods and groundbreaking approaches. I have included univariate and bivariate statistical methods as well as multivariate approaches and machine learning algorithms

using the same datasets in order to show how the latter really contribute to eliminate equifinality in every analysis. I also use most of the available experimental data modeling different types of access to carcasses by hominins and carnivores, as well as actualistic studies carried out in the wild of modern carnivore ethology as referential frameworks. Additionally, this work includes comparisons of DS with other Paleolithic sites, especially with other Bed I sites, but also with sites from more recent periods and other geographical locations where anthropogenic accumulations were purportedly created by hominins having primary access to carcasses mainly through hunting.

The taphonomic study presented here is structured in the traditional way. First, site integrity is examined using a combination of approaches that include bone orientation patterns, specimen size distribution and a multivariate analysis of the frequencies of different types of bone shapes and composition. The goal of this analysis is mainly to test the hypothesis that the site is autochthonous and that the effect of water currents on the archaeological accumulation can be excluded, and thereby that the spatial properties of the assemblage are intact. Then, I analyze skeletal part abundances and their relationship to food utility and return rates. I further compare long limb bone representation in particular to meaty long bone element ratios at other Paleolithic sites in an effort to address site functionality and hominin carcass transport strategies.

The analysis on bone fragmentation patterns and bone surface modifications are especially useful to assess time of access to carcasses by hominins and carnivores. Elucidating whether hominins had early and primary access to carcasses is necessary to justify food surplus and intentional food sharing. Domínguez-Rodrigo (2013) showed that around 45% of the heuristic power of the theory this study is framed in (see below) depends on demonstrating primary access by hominins to large carcasses, because hypotheses are linked. If primary access to carcasses is confirmed then abundant meat and butchery, active foraging strategies, food transport, food sharing and cooperation are more likely, since primary access is a prerequisite for these behaviors. Thus, this question is addressed continuously throughout the study, and the sections dealing with fracture patterns and bone surface modifications include several different approaches that range from univariate comparisons of cut mark, percussion mark and tooth mark frequencies or of fragmentation ratios and frequencies of breakage angles with experimental data and with data from other sites to machine learning analyses combining several variables.

Bovid mortality profiles are also approached on the one hand following traditional methods using triangular graphs, and on the other hand using a statistically more robust method combining more variables. This study further confirms that these novel methods have a high explanatory power when used to treat taphonomic data, as has been stressed by Domínguez-Rodrigo and col-

laborators (e.g. Domínguez-Rodrigo *et al.*, 2014; Arriaza *et al.*, 2016; Moclán *et al.*, 2019; Domínguez-Rodrigo *et al.*, in prep.), and therefore also seeks to encourage other taphonomists to use them and to try to exploit their potential.

Addressing the same taphonomic problem from different perspectives is also highly advisable. For example, access to carcasses by hominins is addressed additionally by inspecting the anatomical location of cut marks aside from their frequencies, and in addition to these major taphonomic sections of the study, I have also included two minor approaches that could seem of little importance compared to the others, yet are very informative. The first is an assessment of the degree of carnivore ravaging at DS and is used to infer the degree of carnivore competition present in the surroundings of the site (Domínguez-Rodrigo *et al.*, 2007), something that is of crucial importance to interpret site functionality, according to most researchers. The second is the taphotype approach, which is very useful to classify assemblages as hominin-or carnivore-made according to the predominant patterns of long bone portion deletion (Domínguez-Rodrigo *et al.*, 2015).

The advantages and limitations of each of the used taphonomic techniques are discussed in more detail in the methods section. Finally, in all of the presented analyses I have included the data from FLK *Zinj* as well as the data from DS with the intention to find similarities and differences between both penecontemporaneous sites and to try to assess hominin behavioral variability during Olduvai Bed I times. This is also applicable to the spatial analysis.

1.10. Application of a scientific theory on the emergence of human behavior to the fossil record

In order to work scientifically, it is important to frame research in a body of knowledge stated as a theory and supported by several axioms (e.g. Domínguez-Rodrigo, 2013). The application to the empirical record of a wide range and well-structured theory also constitutes the only way to grasp complex issues such as the meaning or functionality of a site like DS, as explained below. The articulated theory for the origin of human behavior that will be put to test in this study is placed within an evolutionary framework and was formulated by Domínguez-Rodrigo (2013) based on Isaac's (1978) diagnostic features of human behavior as compared to non-human primates. The theory states that "human behavior emerged when subsistence was based on a cooperative and solidarious social organization" (Domínguez-Rodrigo, 2013; p.15). Cooperation refers to the coordinated participation of adult individuals in different subsistence activities, while solidarity makes reference to the result of cooperation in communal benefit (Rankin and Taborsky, 2009; Domínguez-Rodrigo, 2013).

This main theory is sustained and defined by a set of axioms or founder hypotheses that are not directly testable but are logically related to a number of factual hypotheses (Bunge, 1998) (Table 1.2). Factual hypotheses act as a bridge between the empirical record and the founder hypotheses and they should be established within a systemic conception of behavior (Brooks and McLennan, 1991), i.e. the hypotheses should be interconnected and dependent on each other, just as different behavioral components in a behavioral system are interrelated (Domínguez-Rodrigo, 2013). The amount of knowledge that can be empirically contrasted increases not only with the number of hypotheses, but also with the number of links or dependent relations between these hypotheses. Importantly, the corroboration of a single hypothesis increases the heuristic value of the hypotheses to which it is associated. For example, stone tool use or meat-eating are not independent from the fact that both activities occur on specific locations where materials accumulate in very high densities, and food sharing requires food to be brought back to a protective spot to be distributed. Therefore, contrasting intertwined hypotheses provides higher heuristic power and can help resolve issues of equifinality, while it allows us to tackle wider questions, such as the functionality of sites. In contrast, working with single

falsifying premises that are contrasted individually limits our capacity to reconstruct past complex behaviors (Domínguez-Rodrigo, 2013; Bunge, 1998). Only the corroboration or rejection of linked hypotheses leads to progressive knowledge, which occurs when the evaluated hypotheses are reformulated to form a new body of knowledge or theory (Bunge, 1998; Niiniluoto, 1987; Popper, 1972; Domínguez-Rodrigo 2013).

Table 1.2 presents the list and a description of the hypotheses that compose the main theory applied in this study, as well as several examples of how these hypotheses would be corroborated if DS was indeed an anthropogenic assemblage that reflected the purported hominin behaviors. The hypotheses relate to the type of access to carcasses by hominins, their use of the landscape and favored locations, as well as their prey selection and carcass transport strategies. If hominins at Olduvai cooperated 1.84 Ma ago in order to obtain and transport sufficient food to be shared amongst the group in central places, and were capable of anticipating future needs to a higher degree than nonhuman primates, this should be reflected in the frequencies and the location of bone surface modifications, in the type of bone breakage patterns, skeletal part abundances and prey mortality profiles at DS, as expressed in Table 1.2. The table is a slightly modified version of the tables 1.3 and 1.4 from Domínguez-Rodrigo's (2013) work. The taphonomic analysis presented in the methods and results sections tests the proposed premises comprehensively.

Table 1.2. *Hypotheses and testing premises that compose a theory of the emergence of human behavior (modified from Domínguez-Rodrigo, 2013: tables 1.3. and 1.4.)*

Founder Hypotheses/ Axioms	Factual hypotheses	Description	Testing premises	Associations
A. Intentional food sharing was the main goal of cooperation				
	A1. Primary access to animal resources			
		Primary access implies that carcasses are fleshed before hominins butcher them and that no other carnivore has already consumed them.		
			Primary access to carcasses would be supported by high frequencies of cut marked and percussion marked bone specimens that coincide with the corresponding experimental scenarios (e.g. Barba and Domínguez-Rodrigo, 2005; Galán *et al.*, 2009), by the location of cut marks on hot zones in long bones evidencing filleting, and on ribs and/or vertebrae evidencing evisceration (Binford, 1981; Bunn, 1982). We would also expect a high proportion of dynamic long bone breakage (including a high number of	

impact flakes and type A notches) (e.g. Moclán and Domínguez-Rodrigo 2018), and lack of typical felid damage patterns on the bones (including taphotypes typically associated with felids). In addition, we should find taxa diversity that would contrast with a highly specialized felid predatory range (Domínguez-Rodrigo, 2013).

A1a, A1b, E1

A1a. Hunting

Hunting refers to strategies in which hominins are actively engaged in killing their prey themselves

Hunting would be supported by bovid age profiles that differ from the preys of carnivores and/or show similarities to prime adult-dominated profiles typical in many sites of more recent periods of human evolution and age profiles generated by modern hunter-gatherers (e.g. Bunn and Pickering, 2010). Hunting would also be corroborated if the taphotypes did not match those created by felids. It could also be supported potentially by impact marks from sharp or pointed objects on the bones (Gaudzinski *et al.*, 2019).

A1b. Confrontational scavenging

Confrontational scavenging refers to carcass obtainment strategies in which hominins confront other carnivores in the early stages of carcass consumption by the latter to snatch it from them.

This would be corroborated if age profiles were similar to the prey targeted by carnivores, especially felids, if a taphotype analyis yielded a predominance of typical felid modification patterns (Domínguez-Rodrigo *et al.*, 2015), and if the anatomical distribution and frequency of cut marks and tooth marks were to correspond with a felid to hominin to hyenid scenario (e.g. Domínguez-Rodrigo, 1997).

A2. Focus on a range of carcass sizes from 1 to 3-4

Food sharing is more justifiable if at any point there is a material evidence for a representation of a resource that would have exceeded the needs of one individual. The redundancy in this pattern, especially if occurring on the same spot repeatedly, would suggest that the finality of such behavior would have been food sharing.

The accumulation on the same spot of several animals spanning carcass sizes from 1 to 3-4, especially of animals that weigh >100 kg, that show evidence of having been defleshed entirely or primarily by hominins, would suggest that meat was sufficiently abundant to be shared collectively.

A1, B1

B. Selection of central places for sharing food and referential places for communal use

B1. Selection of central places

A central place is defined as a locus repeatedly used (on a daily basis), to which resources are transported, processed, and discarded acting as the focal point of group fission/fusion.

The use of the spot as a central place would be supported by the presence of allochthonous taxa and a significantly higher bone density at the site than in the surrounding landscape. Additionally, bone clusters should be qualitatively different from those at nonanthropogenic sites, and the accumulation should involve multiple individuals. Presumably, skeletal part profiles would be relatively unbiased. The environmental context of the location would be characterized by low

trophic dynamics. A central place would also be characterized by food surplus that would enhance food sharing and evidence of other activities not related to animal carcass consumption. The depositional time should be short (no more than one or two years). These points are interdependent (Domínguez-Rodrigo, 2013).

A2, A1

B2. Selection of referential places

A referential place is that to which hominins go with the goal of performing a specific activity (individually or collectively), which will yield communal benefit at some point. Examples of referential places are near-kill location places in some modern foragers as described by O'Con nell (1997), knapping spots near or at the sources of raw material, etc. The site qualifies as referential if it can be shown that it was used more than once.

Evidence of hominin reoccupation could be evidenced in the presence of several weathering stages on anthropically modified bones in addition to the presence of several animal carcasses, and abundant evidence of hominin activity and remains in general. The existence of additional archaeological levels at the site with evidence of anthropic activity would also demonstrate that the site was a referential place for hominins.

C. Importance of meat eating

C1. Abundant evidence of butchery

Abundant means repeated evidence of primary carcass butchery, preferably not just at the same site but in different sites where an anthropogenic origin is taphonomically justified.

Systematic evidence of exclusive hominin flesh exploitation as described above (A1), and evidence of the complete butchering process of several carcasses (>50%,

Domínguez-Rodrigo, 2013), from evisceration to the access to the marrow content of bones, would support that meat was consumed abundantly.

A1

D. Collective obtainment of resources

D1. Transport of (almost) complete size 3-4 carcasses

Transport of complete or partial fleshed sections of animals larger than 100 kg (including access to it and initial butchery to be transported) requires the joint participation of several individuals according to carcass size.

The transport of complete or partial sections of large animals would be evidenced in an even representation of the high-survival set of skeletal elements and, more exceptionally, on an abundance of part of the low-survival anatomical set. Taphonomic evidence regarding the site's integrity would exclude the possibility of the accumulation being a death site or the result of natural processes.

A1

D2. Collective transport of lithic raw material

Collective transport of lithic raw material is inferred when the amount of lithic artifacts discarded at a site exceed the physical capability of having been accumulated by one single individual, provided that the accumulation took place in one occupational episode and not across a dia chronic sequence of various occupational episodes.

Abundant lithic raw material exceeding transport capacity of one individual

B1, E1

E. Dependence of tool use

E1. Tools were needed for every subsistence activity

Dependence means complete reliance on tools for survival. If so, the exploitation of raw material and use of artefacts across the landscape must be curated.

Abundant cutting tools (a minimum of fifteen flakes per MNI should be present), intensively reduced raw materials from a distant source, and materials in various stages of the reduction sequence should be present

A1, F1

F. Planning and forethought

F1. Hominins anticipated adaptive needs

Refers to anticipation of future needs as reflected in raw material procurement and exploitation and is linked to the reduction sequence concept.

The presence of differential reduction sequences and ty

pologies for tools according to raw material type, the presence of tools that were not used on site, as well as the presence of raw materials from distant sources evidencing long-distance transport reflect that hominins had the capacity to anticipate their needs.

B1, B2, F1

G. Systemic nature of these hypotheses

Behaviors from axioms A-F are documented.

Evidence for these behaviors in several anthropogenically supported sites from the same period would constitute even more consistent proof.

2. Methods

Taphonomic analysis

2.1. Site formation

Many actualistic experiments have aimed at explaining the ways in which a taphocenosis can be affected and altered by abiotic post-depositional processes, and in particular by water (e.g. Badgley, 1986 a, b; Badgley and Behrensmeyer, 1980; Behrensmeyer, 1975; 1982; Boaz, 1982; Boaz and Behrensmeyer, 1976; Coard, 1999; Coard and Dennell, 1995; Dodson, 1973; Frison and Todd, 1986; Frostick and Reid, 1983; Gifford and Behrensmeyer, 1977; Petraglia and Nash, 1987; Petraglia and Potts, 1994; Schick, 1984; Voorhies, 1969).

These studies have provided very different approaches to address the issue. Whereas some authors have focused on sedimentary analyses, which have shown that silt and clay deposits are usually indicative of low-energy environments, and that coarser sediments indicate high energy contexts (e.g. Aslan and Behrensmeyer, 1996; Badgley, 1986 a,b; Behrensmeyer, 1975; 1982; Schick, 1984), others have emphasized the fact that water can modify the original location and orientation of archaeological materials, creating allochthonous assemblages and anisotropic orientation patterns (Badgley, 1986 a, b; Behrensmeyer, 1990; Coard and Dennell, 1995; Kreutzer, 1988; Schick, 1984; Toots, 1965; Voorhies, 1969; Domínguez-Rodrigo *et al.*, 2014; Cobo-Sánchez *et al.*, 2014).

Other authors have looked at the effects of water on specimen size distribution (Schick, 1984), differential anatomical representation according to bone type (Voorhies, 1969), or the presence of polishing and abrasion (Behrensmeyer, 1975; Schick, 1984; Stein, 1987; Shipman and Rose, 1988; Fernández-Jalvo and Andrews, 2003; Thompson *et al.*, 2011).

Yet, several of these variables have been found to be equivocal or ambivalent when examined in isolation (Domínguez-Rodrigo *et al.*, 2014; 2019). For

example, chemical weathering and aeolian processes can also polish bones (Schiffer, 1987), and preferential orientations can also be caused by trampling or gravity (Olsen and Shipman, 1988; Bertran *et al.*, 1997; Lenoble *et al.*, 2008; Domínguez-Rodrigo and Martínez-Navarro, 2012, Krajcarz and Krajcarz, 2014). In fact, anisotropy is not necessarily coupled with allochthony (Domínguez-Rodrigo *et al.*, 2014; Cobo-Sánchez *et al.*, 2014). This does not mean that these variables are not useful to determine the effect of water inputs on fossil assemblages, but rather that investigations regarding the post-depositional disturbance of sites should include the examination of more than one of these factors, preferably in joint multivariate analysis. When variables are used independently, results can appear contradictory. Systemic approaches to very different taphonomic problems that take into account the interaction between multiple variables have proven to be much more effective and accurate in explaining post-depositional processes (e.g. Domínguez-Rodrigo *et al.*, 2014), and the analysis of site integrity is no exception (Domínguez-Rodrigo *et al.*, 2018; 2019). By considering the emergent properties resulting from the relationship between variables, and by linking fossil assemblages to experimentally created frames of reference, we can strive for higher resolution from information and objectivity in its interpretation. What is more, referential scales of the different degrees of distortion that can be caused by fluvial processes can be created in order to better define the boundaries between low and high fluvial impact, as has recently been done by Domínguez-Rodrigo *et al.* (2014; 2018; 2019).

Autochthony and site integrity at DS are assessed in this section by means of three different approaches. I examine the intrinsic properties of the recovered bone specimens expressed in their composition and shape, their size distribution, and their orientation patterns.

2.1.1. Composition and shape

Domínguez-Rodrigo *et al.*'s (2014; 2018) recent actualistic fluvial experiments have demonstrated that the resistance of each bone specimen to water is best determined by the shape and the composition or texture of bones. The magnitude of the fluvial disturbance in a given assemblage can thus be evaluated by combining these two variables. As was previously proposed by Domínguez-Rodrigo *et al.*, (2014) and Organista *et al.* (2018), regarding their composition, bone specimens can be classified as either dense, spongy-trabecular or mixed. Regarding its shape, a bone fragment can be classified as either flat (disc and blade), tube (rod) or cube (sphere or polyhedron) (Domínguez-Rodrigo *et al.*, 2019). For example, long bone shafts have a dense cortical composition,

whereas long bone epiphyses and most portions of axial elements are characterized by a cancellous or trabecular structure. Mixed bone composition refers to specimens with both types of bone tissue, for example a complete long bone. In their study, Domínguez-Rodrigo *et al.* (2019) classify several previously published experimental assemblages (Domínguez-Rodrigo and Lezana, 1996; Domínguez-Rodrigo *et al.*, 2014; 2018) into three different degrees of local distortion by water: a) no fluvial input (a Maasai faunal assemblage), b) moderate-low impact (lag assemblage), and c) moderate-high impact (autochthonous resedimented or transported assemblage).

These categories are statistically differentiated by the relative representation of the compositions and shapes defined above. It is important to emphasize that the category "transported" does not imply here allochthonous transported assemblages but locally resedimented autochthonous assemblages which do no longer occupy their original position, although they lie close to it. Allochthonous transported assemblages would not preserve the association of cancellous-dense bone shapes documented in these autochthonous assemblages. Domínguez-Rodrigo *et al.* (2019) used this scale in order to address the degree of fluvial inputs at several archaeological sites from Bed I and Bed II at Olduvai Gorge (FLK *Zinj*, FLKNN1 and 3, FLKN1-2, and FLKN 3-4 from Bed I, and MNK Main, SHK Main, BK3 and BK4c from Bed II), which belonged to different depositional environments (see also Organista *et al.*'s (2017) analysis of BK4c). Their results showed that the selected sites clustered around the less disturbed assemblages regardless of their sedimentary context. The authors caution that there are other taphonomic processes that can affect skeletal profiles, like for example carnivore post-depositional ravaging, which can bias the relative representation of each composition and shape category. Interpretations should take these effects into account (Domínguez-Rodrigo *et al.*, 2019).

This approach is applied in the same way here in order to assess the magnitude of fluvial impact at DS. For this purpose, each specimen was categorized according to its shape and composition. The 22B assemblage was subdivided into small and medium-sized carcasses, and independent analyses were carried out for each carcass size. Each analysis consisted of a multiple correspondence analysis (MCA), which was done using the "FactoMineR" library in R (Lê *et al.*, 2008), and two independent bootstrapped correspondence analyses (CA) to evaluate the effect of the variables separately. The latter were carried out using the "cabootcrs" R library (Ringrose and Ringrose, 2019). Bootstrapped CA were also supported by chi-square tests. The graphic representations of the MCA include the cos2 and contribution values of each variable in the final bidimensional solutions. CA plots include 95% confidence ellipses.

Correspondence analyses are similar to principal component analyses in that they establish relationships between variables and objects in a two-dimen-

sional space (Greenacre, 2010), but they are applied on categorical instead of continuous data. Bootstrapped CA creates simulated samples via re-sampling with replacement from the original data, and performs the analysis on the new sample. The bootstrapped version of CA has proven to be powerful and efficient when applied to archaeological data (Lockyear, 2013; Domínguez-Rodrigo *et al.*, 2015; Domínguez-Rodrigo *et al.*, 2019).

2.1.2. Orientation of archaeological items

Before removing the archaeological objects from the ground during the excavations, the horizontal and vertical orientations were measured with compasses and clinometers along the A axis of the specimens, which divides the object symmetrically along its longitudinal axis. These measurements were only taken on those lithics and bone specimens with a longitudinal axis at least twice as long as its width (Domínguez-Rodrigo and García Pérez, 2013; Domínguez-Rodrigo *et al.*, 2014).

The data obtained from these measurements were graphically displayed using stereograms and rose diagrams (software OpenStereo). The measurements were first transformed from degrees into radians and then into circular objects using R's "circular" library. Subsequently, the Rayleigh test, the Kuiper test, and the Watson test were applied to the dataset. The first test is used to detect isotropy/anisotropy, the other two are omnibus tests that examine whether a certain orientation is bimodal or polymodal in cases of non-uniform distribution. P-values >0.05 indicate that the null hypothesis of isotropy cannot be rejected (Fisher, 1995). In addition, the dispersion and the fabric shape can be evaluated with a concentration parameter K and a force parameter (C), which are ratios stemming from the eigenvalues of the original circular data. K values between 0 and 1 correspond to a uniform or isotropic distribution, k values >1 indicate a trend towards anisotropy. The C value indicates the strength of the cluster or girdle. Woodcock's and Benn's diagrams were used additionally to determine the fabric shape of the DS assemblage (Woodcock, 1977; Benn, 1994). These analyses were carried out for a) the complete 22B assemblage (including bones and lithics), b) for the bone assemblage alone, and c) only considering long bone shafts. These bone portions tend to stabilize more quickly than other elements in the direction of the flow, and their preferential orientation could be indicative of the local rearrangement of an autochthonous assemblage (Domínguez-Rodrigo *et al.*, 2014; Organista *et al.*, 2017).

2.1.3. Specimen size distribution

Disturbance of fossil assemblages by water flows also affects fragment length distribution, because smaller fragments are often carried away by moderate

to high water currents (Badgley, 1986, Domínguez-Rodrigo and Martínez-Navarro, 2012; Domínguez-Rodrigo and García-Pérez, 2013; Pante and Blumenschine, 2010; Petraglia and Nash 1987; Schick, 1984). Thus, assemblages biased by post-depositional processes show a biased preservation of small specimens, whereas a high frequency of small specimens suggests limited post-depositional disturbance, and further supports autochthony at a given site (e.g. Domínguez-Rodrigo and Martínez-Navarro, 2012).

Specimen size distribution was first tallied for the complete bone assemblage, including the bone fragments recovered in the sieved sediment, then for long bone shaft fragments, and lastly for green broken shafts in order to avoid the potential bias created by diagenetic breakage. Following Organista *et al.*'s (2017) methodology, this tally was replicated for small-sized carcasses on one hand and medium-sized carcasses on the other hand, although these categories do not include specimens <20 mm recovered through sieving, since carcass size was often difficult to determine for such small fragments. Size categories were labeled as small (<30mm), intermediate (31- 60 mm), and large (>61mm).

2.2. *Skeletal part representation*

2.2.1. Quantification and analysis of skeletal element abundances

Zooarchaeologists commonly use the relative frequencies of skeletal elements present at Plio-Pleistocene sites to assess carcass-acquisition strategies and transport decisions by hominins, as well as site function (e.g. Blumenschine 1986; Bunn 1986; Grayson 1989; Klein 1989; Marean and Kim 1998). In order to do so, they systematically turn to data on modern hunter-gatherers. Since the 1970s, ethnoarchaeologists have noted that modern foragers often select a limited number of parts of the obtained carcasses for transportation to the consumption site, and have engaged on extensive discussions on the conditions under which carcass transport selectivity occurs, stressing the complexity and high variability that characterizes carcass butchering and transport activities in human groups (Binford 1978; Bunn *et al.* 1988; Lupo 2001; O'Connell *et al.* 1990; Bartram *et al.* 1991; Bartram 1993; Monahan 1996; 1998; Speth 1987).

The realization that different skeletal elements are associated with a certain nutritional content that can be measured by weighing the amount of associated soft tissue, led to the idea that this might condition foragers' transport decisions. Binford (1978) pioneered this initiative by developing a number of hypothetical economic utility curves modelling different human transport strategies. Zooarchaeologists then started applying these utility curves to faunal collections recovered at Paleolithic sites (e.g. Speth 1983; Thomas and Mayer 1983; Emerson 1991), while also attempting to improve the reliability and replicability of the model creating the use of alternative measures of food utility (e.g. Blumenschine and Caro 1986; Blumenschine and Madrigal 1993; Madrigal and Capaldo 1999; Metcalfe and Jones 1988; Grayson 1989; Lyman 1994; Marean *et al.* 2000; Marean and Cleghorn 2003; Faith and Gordon 2007). Utility curves were mainly employed to interpret site function: a positive relationship between food utility and skeletal part abundances, it was argued, could be suggestive of a consumption site, because it would contain an abundance of high-utility bones; i.e. mainly appendicular parts, while inverse curves could be pointing to kill or butchering sites where mostly low-utility parts, especially axial remains, would have been left behind (Thomas and Mayer 1983; Lyman 1985; Bunn 1986).

Furthermore, models drawn from ethnographic studies also suggested that hunters were limited by certain ecological constraints and hazards, and that the degree of selectivity of carcass parts especially reflected transport distance (Bunn *et al.* 1988; Metcalfe and Jones, 1988; O'Connell *et al.*, 1988a, 1990; Faith *et al.* 2009). This meant that transport decisions were not only mediated by the economic value of different skeletal parts, but also by the energetic costs of processing and transporting them. This led to models suggesting that return rates, or the net benefits of nutrient extraction could more realistically predict how carcasses were processed and transported by hominins (O'Connell *et al.* 1988; 1990; Monahan 1998; Metcalfe and Barlow 1992; Egeland and Byerly 2005). Generally speaking, complete carcasses would mean close distances from the kill sites to the consumption site, and the transport of specifically selected parts would be suggestive of longer distances (Faith *et al.* 2009). It is now well established that butchery and transport decisions are conditioned by both the economic value of different body parts and the energetic costs of transporting them (Faith *et al.* 2009). The analysis of skeletal profiles goes far beyond linking the presence of high utility parts, such as meaty long bones, to early access to carcasses, and the presence of low utility parts, such as head and feet, to marginal access to carcasses, but aims to assess the intentions and constraints behind particular butchery and transport strategies, because it is particularly relevant to understand the behavioral significance of Plio-Pleistocene sites and the cognitive and social capabilities of early *Homo*.

However, the use of skeletal profiles to interpret hominin behavior is far from straightforward. Skeletal profiles may well reflect the animal body parts to which hominins had access in the first place, or alternatively, they may reflect the body parts they selected for transport, but they may just as well be biased as the result of taphonomic processes. Density mediated attrition, carnivore ravaging, subaerial weathering and post-depositional alteration including trampling, sediment compaction or chemical leaching, can cause the destruction of the less dense skeletal parts and alter the original skeletal part abundances significantly (Grayson 1989; Lyman 1984; 1985; 1992; 1994; Faith and Gordon 2007). Two different solutions to this problem have been proposed. First, several researchers have recommended making a distinction between high- and low-survival skeletal elements and using only the former in the analysis (Marean and Frey 1997). The high-survival set of elements includes dense bones with thick cortical walls and medullary cavities, such as long limb bones (shafts) and mandibles. The cranium is classified as a high-survival element as well, because it includes the petrosal and teeth. Bones with grease-rich cancellous parts such as axial elements (vertebrae, ribs, pelves, scapulae), long bone epiphyses, phalanges and small compact bones are classified as low-survival elements (Marean and Frey 1997, Marean and Cleghorn 2003, Cleghorn and Marean 2004, 2007; Faith and Gordon 2007). The use of only a part of the

skeletal elements can, however, lead to sample size issues (Faith and Gordon 2007), and it is advisable to subject the data to a bootstrap method prior to the correlations.

The classification between skeletal elements that survive destructive taphonomic processes and those that tend to be deleted from the fossil record more rapidly is mainly based on studies on the impact of carnivore modification (Bartram *et al.* 1999; Blumenschine 1988; Capaldo 1995, 1998; Faith and Behrensmeyer 2006; Marean and Spencer 1991), because there has been much less experimental research done on other destructive processes. The discovery of several assemblages that were characterized by the predominance of low-utility elements led to the realization that these patterns, that have also been called reverse utility curves, can appear when density mediated attrition is not taken into account (Lyman 1985; 1992; Marean and Frey 1997). Lyman (1985; 1992) even proved that bone volume density was negatively correlated with food utility. Addressing the impact of differential bone destruction by taphonomic processes is thus crucial. Therefore, a second approach is usually implemented when analyzing skeletal part abundances that consists in evaluating bone destruction in a bone collection by performing correlations between the skeletal abundance values (as expressed by %MAU) and mineral density values. Bone mineral density is not the only variable that can affect the ability of a bone to resist destruction (Lyman 1993), and the fact remains that there are other effects of attrition that can act on an assemblage that should be considered as well, like fluvial transport. Water can further alter skeletal part abundances, by removing cubic, tubular and trabecular bones first, and should therefore be considered in conjunction with density-mediated attrition (see site formation analysis in this study, sections. 2.1 and 3.1).

The interpretation of skeletal part abundances is further complicated by the fact that non-parametric correlations assume independency between the elements, when in fact some elements are transported to a site simply because they are attached to other more nutritious parts (Rogers 2000); in other words, carcasses are often treated by foragers in terms of units comprised of several skeletal elements. Some utility indices have been created with the aim of solving this, for example the SFUI or Standardized Food Utility Index (Metcalfe and Jones 1988). A few other alternatives to the correlation method have been proposed, which include examining mean utility of the assemblage, and the ABCML approach (Analysis of bone counts by maximum likelihood, Rogers 2000). The latter requires more data and knowledge on attritional processes in order to be effective, which are currently nonexistent (Faith and Gordon 2007).

It is very difficult to assign or associate certain skeletal part profiles to particular taphonomic agents in order to differentiate their actions in a certain accumulation. Humans are especially variable in their carcass transport decisions. Their strategies are often determined by variables that are difficult to

control and model archaeologically, like distance to camp, time of day, or number of carriers (e.g. Binford 1978, Bunn *et al.* 1988; Bartram 1993; Monahan 1998), although they tend to transport complete or mostly complete carcasses (Bartram *et al.* 1991; Monahan 1996), similarly to felids (Arriaza and Domínguez-Rodrigo 2016). Thus, although analyses on skeletal part profiles are a key part in any taphonomic study, their interpretation is often controversial, because they are subject to equifinality. In fact, during the last decades, the use of these analyses to interpret early Pleistocene sites has lost relevance in favor of bone surface modification analyses (e.g. Domínguez-Rodrigo *et al.* 2007). Even so, Arriaza and Domínguez-Rodrigo's (2016) recently reanalyzed skeletal part frequencies of the Bed I sites in Olduvai Gorge and showed that skeletal part profiles can be useful to assess agency at these sites when machine learning methods are applied and appropriate analogs are used. Their model is not applied here, however, because it was particularly effective in discriminating felid and hyenid accumulations, but could not confidently differentiate human from felid accumulations.

Skeletal part abundances are a proxy for the amount of animal food represented at a given site and they are estimated from a number of quantification units, namely NISP (Number of Identified Specimens), MNE (Minimum Number of Elements), MNI (Minimum Number of Individuals), and MAU (Minimum Animal Units) (Binford 1978; Lyman 1994; White 1953; Chaplin 1971). It has been established that skeletal part profiles significantly depend on how MNEs are quantified. Long bone representation should be calculated using ends and long bone shafts, as has been advocated by numerous researchers (e.g. Bunn and Kroll 1986, Todd and Rapson 1988, Marean and Spencer 1991, Morlan 1994, Marean 1995), mainly because the latter are more resistant to destruction (contra Stiner 2002). Quantifying MNEs with shafts also means that MNEs are less dependent on NISP. The following section outlines the methodology followed to estimate quantification for the DS 22B ungulate assemblage and the analyses that were applied to it in order to interpret the skeletal part profiles that resulted for each size class. This study includes all ungulate remains recovered from level 22B during the excavations from 2014 to 2016. The specimens recovered in 2017 (NSP = 184) and in 2018 (NSP = 136) have not been included, because they were not available for study or excavated at the time this analysis was carried out. A subsequent taphonomic exploration of these remains revealed that adding the 2017 and 2018 finds would not significantly alter the results presented here.

2.2.1.1. Number of Identified Specimens (NISP) and Minimum Number of Elements (MNE)

The NISP estimates presented here refer to the number of identified specimens to a specific skeletal element, but not to a specific taxon, although many specimens could be identified to taxonomic family. In contrast with sites where taxa identification is more or less straightforward because the assemblages consist of easily distinguishable species, DS mainly consists of remains of several similarly sized bovid taxa, which can only be confidently differentiated by morphological differences in their dentition. Even though Gentry (1978) also provided some morphological guidelines to further differentiate bovid tribes using the epiphyses of long limb bones, estimating NISP from teeth and complete, well-preserved long bone epiphyses alone, would result in an important loss of information. This is especially true for a site like DS, where the preservation of axial remains is remarkable, and long bone shafts are very abundant. The use of this definition of NISP, which includes specimen identification to size class as defined by Bunn (1982; see also Brain 1974, 1981), increases the identification rate enormously, while it avoids an important bias. Given that the aim of this study is mainly taphonomic and not paleontological or taxonomic, the identification of long bone shafts to a specific element using anatomical landmarks like muscle insertions or foramina, as well as diaphyseal cross-section and medullary cavity shape and size, is crucial (Barba and Domínguez-Rodrigo, 2005). In the present study, an important effort was made to maximize specimen identification according to element.

Estimates of the minimum number of elements (MNE) were made by laying all identified specimens of a particular skeletal element on a large table and arranging them according to bone portion (Yravedra and Domínguez-Rodrigo, 2009). This included all the long bone shaft specimens. The MNE was estimated by counting the number of times the most represented portion of a certain element was present, after comparing overlapping and non-overlapping bone specimens. This is also called the overlap approach (see description in Marean *et al.* 2001). Ageing, as well as siding were also considered in order to establish the minimum number of elements that accounted for the estimated NISP values for each skeletal part. Appendicular elements were approached first, followed by the axial and cranial elements. Estimates were made with ungulate remains only (which make up most of the collection), and for small (size 1-2), medium-sized (size 3-4), and large carcasses (size 5) separately (Bunn, 1982). Isolated teeth were not included in the cranial MNE counts.

Since the number of rib specimens appeared to be notable at DS when compared to other sites, and in particular compared to FLK *Zinj*, the minimum number of ribs was additionally estimated using a different method. These elements are usually highly fragmented, and MNE estimates based on the abun-

dance of heads and neck portions alone will theoretically underestimate the number of ribs represented. This is especially true because carnivores tend to delete these sections from the record and further fragment the rib shafts in the process. The new method consisted in measuring all rib fragments for each size class, then adding these values together, and dividing the result by the average length of a rib from the mid-section of the rib cage from a similarly sized animal to each of the carcass groups described above. This procedure probably still underestimates the total MNE count, especially because most ribs on both sides of the rib-cage are shorter, but provide a conservative minimum estimate, which can exceed that provided by counting rib heads alone. The MNE values resulting from both methods were then compared and the highest value was used for the skeletal part profile derived for each carcass size group.

2.2.1.2. Relationship between NISP and MNE

Some researchers have argued that there is a linear relationship between NISP and the more derived units MNE and MNI, and that skeletal part abundance analysis based on NISP can therefore mimic the results obtained through MNI estimates. By doing so, they advise against the use of MNE and MNI (e.g. Grayson and Frey 2004). However, in their analysis, these researchers presented NISP values from archaeological faunal samples (not experimental samples), which were not estimated including all the potentially identifiable long bone shafts (Klein and Cruz-Uribe 1991, Domínguez-Rodrigo 2009). When the diaphyses of long bones are included in the estimations, the relationship between the units changes creating an asymptote (e.g. Bartram 1993). In order to illustrate this, in the present study a graph was generated by plotting NISP values against MNE values for both small and medium-sized carcasses.

2.2.1.3. Minimum Number of Individuals (MNI)

The minimum number of individuals (MNI) was originally defined to measure the potential amount of meat present at a site (White, 1953), but it is now used to document taxonomic representation in an assemblage, and it constitutes the only valid method taphonomists have in order to determine how many animals (or parts of how many animals) were represented at any given site (Domínguez-Rodrigo 2009). MNI estimates were first calculated using only fragments of mandibles with teeth, as well as isolated teeth. However, this method can bias the number of carcasses accumulated by hominins by potentially increasing it. Since teeth are less affected by postdepositional processes, the dental MNI can include individuals that belong to a background scatter that is not related to the rest of the assemblage (Klein 1986, Domínguez-Ro-

drigo *et al.* 2007). This can also happen when using postcranial elements, but certainly to a lesser degree than when using dentition because of its higher durability through taphonomic transformation of the assemblage. A second more conservative MNI estimate was thus calculated using appendicular elements only. This postcranial MNI provides a more accurate estimate of the minimum number of carcasses that constitute the assemblage where most of hominin processing is documented.

2.2.1.4. Skeletal part profiles

Skeletal part profiles were generated using the post-cranial MNI estimated by the radii-ulnae both for the small and the medium-sized carcasses, given that it was the most abundant appendicular element in the DS assemblage. In order to evaluate the deviation of the observed MNE value with regard to the predicted value according to the MNI estimates, i.e. the relative abundance or survival rate of each skeletal element, the minimum number of elements for each skeletal part was multiplied by 100 and then divided by the number that skeletal part occurs in the skeleton times the post-cranial MNI (Brain 1969). The resulting percentages were plotted as a bar diagram.

2.2.1.5. Minimal Animal Units (MAU)

In order to analyze the assemblage economically MNE frequencies were standardized. For this assessment, the minimal animal units (MAU) were calculated from the MNE values, as was established by Binford (1978, 1981, 1984), by dividing the MNEs of each skeletal part by the number of times that such element occurs in the bovid vertebrate skeleton. Each resulting MAU was subsequently transformed into %MAU by standardizing each MAU with reference to the largest original MAU, also as described originally by Binford (1978, 1981).

2.2.1.6. Skeletal part frequencies in relation to bone mineral density

Lyman (1984; 1992) was the first to note that utility indices were negatively correlated with bone density; i.e. high-utility elements consistently have low volume densities, while low-utility elements tend to have high-volume density. Skeletal element abundances of assemblages that have undergone density-mediated attrition can thus potentially produce curves that suggest a reverse-utility strategy. For this reason, before particular skeletal profiles are attributed to certain processing and transport strategies by hominins, they should be subjected to correlations with bone mineral density. In this study, I use Lam *et al.*'s (1999) density data for wildebeest derived using computed tomography

(CT) for correlations with skeletal part abundances of medium-sized carcasses. I used the average value for an entire bone. Computed tomography produces more accurate results than those derived using other methods, such as photon densitometry. But, since CT data are not available for small carcasses, I have chosen to use the photon densitometry values derived for domestic sheep by Lyman (1982b; 1984a). Spearman's correlations were performed with all skeletal elements first. In order to assess whether density-mediated attrition mainly affected axial remains, a second correlation was carried out with long limb bones only, for which data were bootstrapped first.

2.2.1.7. Skeletal part frequencies in relation to food utility

Skeletal part abundances of medium-sized carcasses (using %MAU) were then compared against economic utility using the SFUI (Standardized Food Utility Index) for complete bones developed by Metcalfe and Jones (1988) using Binford's data for caribou. Since SFUI is only available for medium-sized carcasses, skeletal part abundances of small carcasses were analyzed using the Modified General Utility Index (MGUI) for sheep developed by Binford (1978). Correlations were performed first using all skeletal elements, subsequently only the high-survival portions of the skeleton, in order to account for the potential effect of density-mediated attrition on low-survival body parts, and lastly, a third set of correlations was carried out only with the appendicular elements. Cranial elements were disregarded here because the background scatter could potentially have inflated the minimum number of cranial elements. Spearman's correlations were carried out for small- and medium-sized carcasses separately and Spearman's rho and its associated p-value were used to assess this relationship. Since the number of types of elements is small and decreases significantly when axial elements are excluded from the analyses, I performed a second set of correlations applying a bootstrap method to the data first.

When the relationship with food utility is clear or significant, it is often contrasted with the hypothetical utility curves depicting different transport models: the unbiased strategy, which represents a scenario in which elements are transported in direct proportion to their economic utility; the bulk strategy, whereby the quantity of high utility elements is maximized; and the gourmet strategy, in which the quality of the elements prevails (Binford 1978). Data can also fit a reverse utility curve, in which low utility elements are highly represented (Marean and Frey 1997). Finally, an unconstrained strategy refers to the case where all elements are represented in accordance to their abundance in a skeleton irrespective of their economic utility (Faith and Gordon 2007). Faith and Gordon (2007) pointed out that when using only the high-survival set (or appendicular elements), Type II errors tend to occur because sample

size decreases significantly. In the case of the medium-sized carcasses of DS the total MNE of high-survival elements adds up to 144 and in the total MNE of high-survival elements in small carcasses is 35. According to Faith and Gordon (2007) error rates for sample sizes between 100 and 150 can be of up to 23% and for MNEs below 50 the error can increase to 48% depending on the transport strategy. The unconstrained strategy can yield a Type I error rate of around 10% in all sample sizes. The potential for sample-size effects on the correlations should be taken into account when interpreting the results.

2.2.1.8. Skeletal part frequencies in relation to return rates

Apart from the food utility index, other economic variables have been proposed, which could in theory predict how different skeletal parts are transported to a site more realistically, because they measure the net benefit of nutrient extraction by including data on the costs and benefits of meat and marrow extraction, i.e. they are concerned with the costs associated to carcass processing and transport (Madrigal and Holt 2002, Marean and Cleghorn 2003, Egeland and Byerly 2005). Although there is no study yet to convincingly prove the usefulness of return rates for predicting transport strategies among modern hunter-gatherers, I tested the possibility that return rates instead of food utility could have conditioned transport decisions at DS. Egeland and Byerly (2005) have argued that it is possible that return rates are more useful to explain Plio-Pleistocene hominin behavior, because higher levels of competition and predation risk existed in the past. The danger of encountering carnivores would have put hominins in a position of processing the carcasses as quickly as possible. In contrast, modern savannas present fewer hazards for hunter-gatherers nowadays, which makes it possible for them to spend more time at a near-kill location, for example waiting for a carrying party to arrive (O'Connell 1990). The estimates for composite return rates (defleshing and marrow extraction) and marrow return rates used here stem from the study by Egeland and Byerly (2005), who estimated return rates for meat-bearing appendicular skeletal elements (including the scapula) for taxa of size classes 2, 3 and 4, by dividing energy yield by processing time.

2.2.1.9. Shannon evenness index

An additional way to interpret carcass transport strategies is to examine the evenness of the distribution of specimens across different elements. All mentioned transport strategies differ in the degree of evenness of the distribution of standardized skeletal elements. For example, the gourmet strategy has an uneven distribution of body parts in which high-utility elements predominate,

whereas the unconstrained strategy is characterized by an even distribution of skeletal elements. The evenness of the distribution of skeletal elements is used to infer transport distance. Short and long distance transport have been defined on the basis of observations among the Hadza. Short distance transport of complete carcasses in these human groups occurs between 3 and 5 km, and long distance transport takes place when the distance to the campsite ranges between 5 km to more than 14 km (Bunn *et al.* 1988). When transport distance is long, hunters maximize return rates by spending more time processing the prey at the point of acquisition and selecting parts of the carcass for transport. Modern foragers sometimes even spend the night at a kill site or a near-kill site waiting for the arrival of other members of the group to help carry the prey to the camp (O'Connell 1990). Transport distance is one of the key factors behind carcass transport decisions, and is also critical to understand site function, i.e. whether hominins used the location as a central place or as a near-kill butchering site for example.

In order for it to be used in conjunction to the correlations, Faith and Gordon (2007) introduced the application of the Shannon evenness index to skeletal part abundances, which can be employed to establish the degree of selectivity in carcass transport. It is calculated in the same manner as the Shannon evenness index for taxa diversity (e.g. Magurran 1988; Grayson and Delpech 1998; Grayson *et al.* 2001), but using the standardized proportion of the different types of elements. Interpretations of the index values differ depending on the total MNE used to estimate the index, and Type II errors increase when sample sizes are small (Faith and Gordon, 2007). The evenness index has been estimated for the skeletal part abundances of DS's small and medium-sized carcasses first using the complete high-survival set and then only appendicular bones. Additionally, 95% confidence limits have been obtained by bootstrapping the skeletal element frequencies 1000 times using a bias-adjusted bootstrap method following Faith *et al.*'s (2009) suggestion. The results have been evaluated and interpreted in conjunction with the correlations following Faith and Gordon's (2007; table 4) assessment.

2.2.2. Front vs. hind limb representation: Comparing MNEs from DS to skeletal part abundances at other Paleolithic sites

Skeletal part profiles of the medium-sized carcasses represented at DS, as expressed in terms of MNEs, show a striking feature: front limbs (i.e. humeri and radii) are 70% more abundant than hind limbs (femora and tibiae). This underrepresentation of hind limb bones might be a reflection of particular homi-

nin subsistence strategies and transport decisions or the result of taphonomic processes. The latter seems less likely, because the representation of long bones in carcasses of sizes 1 and 2 is balanced, and because correlations with density yielded a negative relationship. Moreover, currently, no taphonomic process has been documented that has a greater effect on the preservation of hind limbs than on that of front limbs.

In order to examine the relationship between front and hind limbs in more detail, and in order to put the case of DS into perspective, a comparison with other Paleolithic sites was made. A list of anthropogenic sites with published data on the minimum number of long bone elements was compiled. All included faunal assemblages have been interpreted as the result of hominin hunting behavior, but interpretations on the specific function of each site are diverse. Some publications also include interpretations on different hominin hunting strategies. The number of sites in the Paleolithic record that are considered of human origin is much higher than that shown here, but a significant number of the consulted assemblages were not suitable for the analysis for various reasons. A number of sites could not be added to the list because MNE values for limb bones were very low. A minimum of 6 was established as the threshold, and those assemblages that had less than 6 elements of at least one of the four meaty long bones were excluded. As a consequence, a number of faunal assemblages with medium-sized carcass MNE data were left out of the analysis. Other assemblages consisted of accumulations of small-sized animals, and had to be excluded from the comparison, since the focus here is on medium-sized animals. Two examples are Kobeh Cave (Marean and Kim 1988) and El Horno (Costamagno and Fano 2005). Also, Pobiner *et al.* (2008) provided MNE data on several assemblages from Koobi Fora yet without distinguishing between the different carcass sizes. Additionally, I excluded studies where MNE counts had not considered limb bone shafts in the MNE counts.

The final list of selected sites covers a wide chronological and geographical context and is composed of a total of 49 sites or archaeological levels, including 35 Lower, Middle and Upper Paleolithic sites or archaeological levels in Europe and the Middle East, 9 Lower Paleolithic and Middle Stone Age sites from Africa, and 5 Paleoindian sites from North America. Tables 2.1A and B summarize important information of these sites. The MNEs of the four meaty long bones in each site or archaeological level were compared by calculating the ratio between front and hind limbs and by plotting the resulting values in order next to the value for the DS 22B medium-sized carcass assemblage.

Table 2.1. a) *General information and MNE data from the selected anthropogenic Paleolithic sites.*

Site	Chronology (Ka)	Culture	Group	Location	Type	MNE Humeri	MNE Radii	MNE Femora	MNE Tibiae	Front/Hind
Abri du Flageolet V	25	Périgordien	Upper Paleolithic	France (Dordogne)	rockshelter	50	27	31	83	0.6
Abric Romani Ja	50	Mousterian	Middle Paleolithic	Spain (Barcelona)	rockshelter	39	29	35	38	1.03
Abric Romani Jb	50	Mousterian	Middle Paleolithic	Spain (Barcelona)	rockshelter	7	6	7	10	0.7
Agate Basin2	10	post-Clovis	Paleoindian	Northwestern Great Plains	open air	34	39	33	39	1
Aitzbitarte III Level VIa	24	Gravettian	Upper Paleolithic	Spain (Basque Country)	cave	35	14	25	46	0.61
Aitzbitarte III Level Vib	24	Gravettian	Upper Paleolithic	Spain (Basque Country)	cave	11	8	14	18	0.76
Atapuerca Gran Dolina TD10.1	380	Acheulean	Lower Paleolithic	Spain (Burgos)	cave	22	33	19	36	0.92
Atapuerca Gran Dolina TD10.2	400	Acheulean	Lower Paleolithic	Spain (Burgos)	cave	18	21	11	17	1.24
Bolomor IV	>120	Mousterian	Middle Paleolithic	Spain (Valencia)	cave	-	-	-	-	1.6
Bolomor XII	180	Mousterian	Middle Paleolithic	Spain (Valencia)	cave	22	17	21	22	1
Clary Ranch	8-9	post-Clovis	Paleoindian	Northwestern Great Plains	open air	42	25	18	29	1.45
Coimbre 1ab	<17	Magdalenian	Upper Paleolithic	Spain (Asturias)	cave	19	15	27	21	0.7
Covalejos J	>45	Mousterian	Middle Paleolithic	Spain (Cantabria)	rockshelter	16	8	19	14	0.84
Covalejos K	>45	Mousterian	Middle Paleolithic	Spain (Cantabria)	rockshelter	10	12	7	12	1.2
Cueva del Higueral de Motilla	-	Solutrean	Upper Paleolithic	Spain (Andalucía)	cave	10	18	9	17	1.05
Die Kelders Layer 10	70 -130	MSA	MSA	South Africa (Western Cape)	cave	12	8	9	13	0.92
DK	1860	Oldowan	Early Paleolithic	Tanzania (Olduvai Gorge)	open air	25	21	23	30	0.83
FLK *Zinj*	1800	Oldowan	Early Paleolithic	Tanzania (Olduvai Gorge)	open air	14	16	14	19	0.91
FLKN 1-2	1700	Oldowan	Early Paleolithic	Tanzania (Olduvai Gorge)	open air	43	36	38	62	0.69
FLKN 3	1700	Oldowan	Early Paleolithic	Tanzania (Olduvai Gorge)	open air	15	15	8	17	0.88
FLKN 5	1700	Oldowan	Early Paleolithic	Tanzania (Olduvai Gorge)	open air	14	10	12	17	0.88
Grotte de Payre Fa	MIS7	Mousterian	Middle Paleolithic	France (Ardèche)	cave	13	17	15	11	1.13
Jonzac 22	60-70	Mousterian	Middle Paleolithic	France (Charente-Maritime)	rockshelter	24	25	40	36	0.63

Kanjera South 1	2000	Oldowan	Early Paleolithic	Kenya (Lake Victoria)	open air	7	8	6	6	1.33
Kanjera South 2	2000	Oldowan	Early Paleolithic	Kenya (Lake Victoria)	open air	13	16	7	15	1.06
Las Caldas II	15	Magdalenian	Upper Paleolithic	Spain (Asturias)	cave	6	6	4	13	0.46
Las Caldas III	16	Magdalenian	Upper Paleolithic	Spain (Asturias)	cave	13	11	7	32	0.41
Las Caldas VI	16	Magdalenian	Upper Paleolithic	Spain (Asturias)	cave	40	17	33	51	0.78
Las Caldas XI	17	Magdalenian	Upper Paleolithic	Spain (Asturias)	cave	12	14	21	30	0.47
Las Caldas XII	18	Magdalenian	Upper Paleolithic	Spain (Asturias)	cave	31	28	44	60	0.52
Main Folsom	10	post-Clovis	Paleoindian	Northwestern Great Plains	open air	10	13	11	12	1.08
Main Hell	10	post-Clovis	Paleoindian	Northwestern Great Plains	open air	9	3	9	9	1
Maple Leaf	-	Paleoindian	Paleoindian	Canada (Crowsnest Pass)	open air	-	-	-	-	1.69
Mauran	MIS4-3	Mousterian	Middle Paleolithic	France (Haute-Garonne)	open air	-	-	-	-	2.67
Moulin-Neuf	14	Magdalenian	Upper Paleolithic	France (Gironde)	rockshelter	15	11	13	17	0.88
Pincevent	12	Magdalenian	Upper Paleolithic	France (Paris Basin)	open_air	25	41	36	35	1.14
Porc Epic	40-70	MSA	MSA	Ethiopia (Dire Dawa)	cave	12	10	35	16	0.34
Qesem Cave	300	Acheulean	Middle Paleolithic	Israel (near Tel Aviv)	cave	-	-	-	-	0.73
Saint Césaire	33-38	Châtelperronian	Upper Paleolithic	France (Southwest)	rockshelter	9	6	6	7	1.29
Saint Césaire (EGPF)	36-41	Mousterian	Middle Paleolithic	France (Southwest)	rockshelter	8	7	6	9	0.89
Saint Césaire (EJF)	<30	Aurignacian	Upper Paleolithic	France (Southwest)	rockshelter	44	47	38	80	0.59
Saint Césaire (EJM)	<30	Aurignacian	Upper Paleolithic	France (Southwest)	rockshelter	14	9	21	25	0.56
Saint Marcel 7	>46	Mousterian	Middle Paleolithic	France (Ardèche)	cave	41	29	20	87	0.47
Saint Marcel sup	42-46	Mousterian	Middle Paleolithic	France (Ardèche)	cave	7	8	9	17	0.47
Salzgitter Lebenstedt	60 - 130	Mousterian	Middle Paleolithic	Germany (Hannover)	open air	54	55	50	85	0.65
Valdocarros	-	Acheulean	Early Paleolithic	Spain (Madrid)	open air	13	6	10	10	1.3
Verberie II-1	12	Magdalenian	Upper Paleolithic	France (Paris Basin)	open air	45	65	12	39	1.67
Vogelherd	30	Aurignacian	Upper Paleolithic	Germany (Swabian Jura)	cave	39	30	27	78	0.5
Wallertheim	-	Mousterian	Middle Paleolithic	Germany (Mainz Basin)	open air	-	-	-	-	1.84

Table 2.1. b) *Further information about the sites, their interpretation, and the data sources.*

Site	Excavated area	Taxa	Observations	Interpretation on site functionality and subsistence strategies	References
Abri du Flageolet V	32	Mainly Rangifer (95%), but also Cervus, *Equus*	Highly fragmented assemblage that consists of 1900 identifiable specimens. Carnivore damage appears to have played a small role in the attrition of the accumulation. Prime adult dominated age profile and bias for the appendicular skeleton over the axial skeleton. Kills are distributed throughout the winter.	Numerous successive individual hunting episodes (ambush kills) rather than mass kills. Interpreted as a "consumption location", with a strong bias for meat and marrow utility.	Enloe 1993
Abric Romani Ja	250	Cervus, *Equus*, Bovinae	More than 60 combustion structures with associated with the remains.	Residential site. It is interpreted as being the result of an occupation pattern of long duration.	Carbonell 2012 (Ed.)
Abric Romani Jb	250	Cervus, *Equus*, Bovinae	More than 60 combustion structures with associated with the remains.	Residential site. It is interpreted as being the result of an occupation pattern of long duration.	Carbonell 2012 (Ed.)
Agate Basin 2	170	Bison sp.	There is an over-abundance of distal extremities.	Large kill-butchery site. Occupation during early to mid winter. Kill-butchery activities most likely occurred in and around the location of the bonebed. Similar to Main Folsom. Establishing food security as a backup subsistence option as opposed to using the yields of the kill as a regular source of sustenance until depleted.	Hill 2001
Aitzbitarte III Level VIa	42	Bovidae	Specialization on large bovid carcasses	Continuous human occupation of the deepest part of the cave	Altuna et al 2017
Aitzbitarte III Level Vib	42	Bovidae	Specialization on large bovid carcasses	Continuous human occupation of the deepest part of the cave	Altuna et al 2017
Atapuerca Gran Dolina TD10.1	100	Cervus/ Dama, *Equus*	The assemblage is composed almost exclusively of prime-age ungulates. Abundant anthropogenic marks evidencing early primary access to the carcasses through regular hunting.	Hominins used the site as a long-term residential base camp. Selective character of the hominin subsistence strategies.	Rodríguez-Hidalgo et al 2015
Atapuerca Gran Dolina TD10.2	100	Bison sp.	Monospecific assemblage heavily dominated by axial bison elements. Abundant anthropogenic modifications indicate primary access to carcasses by hominins. Focus on exploitation of meat and fat for	Cave is interpreted as having been used as the kill-butchering site for several seasonal events of mass communal hunting. Bison herds were slaughtered and exploited intensively by the hominins that occupied the cave.	Rodríguez-Hidalgo et al 2017

			ransportation of high-yield elements to another location.		
Bolomor IV	14	Mainly *Cervus*	High diversity of species including ungulates, lagomorphs, birds, tortoises and carnivores. Among the herbivores, red deer is most abundant. Predominance of adult animals. Cut marks suggest primary access.	Generalist behavior based on a broad diet.	Blasco 2011; Blasco and Fernandez Peris 2012
Bolomor XII	8	*Cervus, Dama, Equus*	High proportion of skeletal elements with high nutritional value, predominance of adult animals, cutmarks indicating primary access.	Coexistence of different subsistence strategies: multiple predation of horses, individual hunting of red deer.	Blasco *et al.* 2010; Blasco 2011
Clary Ranch	182	*Bison sp.*	Most bones were fragmented. Long bones were hauled to Clary Ranch as part of complete limb or sublimb transport packages removed from carcasses at a nearby multianimal procurement locality.	Kill-butchery site. Late summer early fall secondary processing area.	Hill 2001
Coimbre 1ab	4	*Cervus, Equus, Bos-Bison*	Cut mark frequencies, abundance of adult individuals, significant fragmentation of bones, and representation of all anatomical parts, including axial bones and epiphyses suggest human agency.	Hunting of rabbits and exploitation of river resources as well as small carnivores. Dominance of Iberian ibex and progressive widening of the diet.	Yravedra et al 2017
Covalejos J	10	*Cervus, Equus, Bos-Bison*	Neanderthal hunting strategies do not vary greatly over time. Predominance of deer. Similar mortality profiles. Mainly adults. Bone destruction caused by carnivores.	Probably short occupations. Since at times the cave must have been flooded	Yravedra et al 2016
Covalejos K	10	*Cervus, Equus, Bos-Bison*	Predominance of mainly adult deer. Bone destruction caused by carnivores.	Probably short occupations, since at times the cave must have been flooded. Neanderthal hunting strategies do not vary greatly over time.	Yravedra et al 2016
Cueva del Higueral de Motilla		*Cervus*	Taphonomic evidence suggests hunting	Complete butchering process documented. Short-term home base during spring and autumn.	Cáceres 2003
Die Kelders Layer 10	3	*Bovidae*	Shaft portions of long bones have the highest frequencies of cutmarks. Bone surface modification frequencies point to primary access by hominins. Mostly young and adult eland.	Hominins were the main accumulators of medium-sized mammals, and focused on high ranked prey items.	Marean et al 2000
DK		*Bovidae*	Felids were the primary accumulating agent. Subsequently hyneas ravaged the carcasses.	Palimpsest. Hominins used sporadically the site for independent carcass processing.	Domínguez-Rodrigo et al 2007; Arriaza and Domínguez-Rodrigo 2016

FLK *Zinj*	300	Mainly *Bovidae*	Taphonomic analysis indicates primary access to fully fleshed carcasses by hominins. Axial remains are underrepresented, which is interpreted as a result of postdepositional carnivore ravaging.	Referential place or focal point on the landscape to which hominins regularly transported mostly complete carcasses.	Domínguez-Rodrigo *et al.* 2007; Parkinson 2018
FLKN1_2		*Bovidae*	Felids accumulated most of the bones and hominins a smaller amount.	Palimpsest	Domínguez-Rodrigo et al 2007; Arriaza and Domínguez-Rodrigo 2016
FLKN3		*Bovidae*	Felids were the primary accumulating agent	Palimpsest	Domínguez-Rodrigo et al 2007; Arriaza and Domínguez-Rodrigo 2016
FLKN5		*Bovidae*	Felids were the primary accumulating agent		Domínguez-Rodrigo et al 2007; Arriaza and Domínguez-Rodrigo 2016
Grotte de Payre Fa		*Cervus* and *Equus*	Taphonomic evidence suggests hunting	The level is interpreted as the result of random hunts during autumn and spring	Daujeard 2008
Jonzac 22	6	*Rangifer*	Prey were butchered on-site. With abundant evidence of meat filleting and marrow exploitation. Absence of hearths.	Reindeer were hunted seasonally and the site was occupied during short intervals of time. Frequent short time visits.	Niven et al 2012
Kanjera South 1	170	Mainly *Bovidae*	Surface modification and skeletal element analyses suggest that hominins obtained most or all of these remains relatively early in their resource lives. Medium-sized carcasses were likely not complete.	Hominins had early and probably primary access to both small and medium-sized carcasses at the site.	Ferraro et al 2013
Kanjera South 2	170	Mainly *Bovidae*	Largest Kanjera South assemblage (NISP = 2190). Surface modification and skeletal element analyses suggest that hominins obtained most or all of these remains relatively early in their resource lives. Medium-sized carcasses were likely not complete.	Hominins had early and probably primary access to both small and medium-sized carcasses at the site.	Ferraro et al 2013
Las Caldas II	25	*Cervus*	High diversity of species and hunting strategies.	The site was occupied repeatedly during the Solutrean and the Magdalenian	Corchón et al 2017

Las Caldas III	25	*Cervus*	High diversity of species and hunting strategies.	The site was occupied repeatedly during the Solutrean and the Magdalenian	Corchón et al 2017
Las Caldas VI	25	*Cervus* and *Equus*	High diversity of species and hunting strategies.	The site was occupied repeatedly during the Solutrean and the Magdalenian	Corchón et al 2017
Las Caldas XI	25	*Cervus* and *Equus*	High diversity of species and hunting strategies.	The site was occupied repeatedly during the Solutrean and the Magdalenian	Corchón et al 2017
Las Caldas XII	25	*Cervus* and *Equus*	High diversity of species and hunting strategies.	The site was occupied repeatedly during the Solutrean and the Magdalenian	Corchón et al 2017
Main Folsom	186	*Bison sp.*	Large scale transport of high utility upper limbs. The Main Folsom component at Agate Basin is a camp with bison and pronghorn food packages.	Residential site. The location served as a late winter-early spring residential hub for small, mixed-sex group of hunter-gatherers. The occupation lasted several weeks or perhaps longer.	Hill 2001
Main Hell	48	*Bison sp.*	High incidence of carnivore damage.	Kill-butchery site used during late fall and early winter.	Hill 2001
Maple Leaf	112	*Bison sp.*	Skeletal part representation is provided as %MNI. There are few cut marks and no articulated elements, although some closely associated. Presence of carnivore ravaging.	Middle Prehistoric small bison kill site on the basis of Binford's (1978) summer kill models	Landals 1990; Gaudzinski 1996
Mauran	25	*Bison sp.*	Skeletal part representation is provided as %MNI. High proportion of young and prime-adult individuals (is interpreted as catastrophic age profile)	It is interpreted as a kill site that provides evidence for recurrent occupation of the site over a long period of time. It can be interpreted along the same lines as Il'skaja, Wallertheim and La Borde: a kill site where Bison carcasses were extensively butchered.	Farizy et al 1994; Gaudzinski 1996
Moulin-Neuf	52	*Rangifer* and *Equus*	Taphonomic analysis suggests a human origin for the fauna. Carcass exploitation was intense. Selective transport of horse remains (lacking skulls and lower limb bones) but complete saiga carcasses.	Cemento-chronological analysis of horse specimens indicate that these animals were killed during every season of the year. The site seems to have been occupied for relatively short intervals with the site dedicated to the processing and consumption of carcasses.	Costamagno 2000
Pincevent	4000	*Rangifer*	Monospecific faunal accumulation. Hearth serves as a focal point for the organization of artifactual and faunal debris.	Short term occupation of the site during autumn. But residential or consumption site. The spatial analysis suggests that organization of space use is similar to residential households.	Enloe 2003

Porc Epic	180	*Bovidae*	The faunal remains were accumulated primarily by hominin activity. Hominins exploited a wide range of prey.	Predominance of high-utility elements is interpreted as the result of selected transport of nutritional elements to a residential base. The high location of the cave make it unsuitable as a kill site or an ambush spot.	Assefa 2006
Qesem Cave	300	*Dama. Cervus.* and *Equus*	The assemblage is dominated by adult-aged individuals, but the spectrum age mortality is broad. The skeletal pattern is biased towards the highest-nutritional value elements.	The assemblage appears to have been generated solely by humans occupying the cave, and was primarily modified by their food-processing activities. The broad range in the mortality pattern could be the result of practicing cooperative hunting strategies or possible episodes of incipient multiple predation, which aim to non-selectively kill several individuals in a single hunting event. Develpment of social hunting techniques and seasonal occupations.	Blasco *et al.* 2014
Saint Césaire	29	*Rangifer* and *Equus*	Selective transport of high utility parts and extensive exploitation of elements	Residential campsite	Morin 2004
Saint Césaire (EGPF)	17	*Rangifer* and *Equus*	Selective transport of high utility parts and extensive exploitation of elements	Residential campsite	Morin 2004
Saint Césaire (EJF)	31	*Rangifer* and *Equus*	Selective transport of high utility parts and extensive exploitation of elements	Residential campsite	Morin 2004
Saint Césaire (EJM)	17	*Rangifer* and *Equus*	Selective transport of high utility parts and extensive exploitation of elements	Residential campsite	Morin 2004
Saint Marcel 7	30	*Cervus*	Clear specialization in hunting strategy with predominance of adult red deer. Carcass butchery was especially intensive and extensive.	Long term residential camp	Daujeard 2008
Saint Marcel sup	30	*Cervus*	Clear specialization in hunting strategy with predominance of adult red deer. Carcass butchery was especially intensive and extensive.	Long term residential camp	Daujeard 2008
Salzgitter Lebenstedt	150	*Rangifer*	More than 80 reindeer, mostly adults, that show abundant traces of human butchering activities. Carnivore gnawing marks are marginal. Neanderthals focused on "selection and processing of high quality animals and parts thereof."	There is a remarkable resemblance in the hunting strategies and the treatment of reindeer prey by Neanderthals when compared to Upper Paleolithic sites.	Gaudzinski and Roebroeks 1999

Valdocarros	700	*Cervus*, *Equus*, and *Dama*	Carcasses were often transported fairly evenly, which suggests primary access.	Based on the evenness index, carcasses were probably obtained near the site and transported over short distances.	Yravedra 2006; Yravedra *et al.*, 2017
Verberie II-1	250	*Rangifer*	Monospecific faunal accumulation. Some high utility bones are underrepresented. This is not due to density-mediated attrition. Abundance of medium-utility elements in contrast to very low representation of the femur and the tibia.	Underrepresented high utility elements are "likely to have been transported from the kill site, after some initial processing and partial consumption of meat and marrow from elements not selected to be transported to a residential site from a hunting site". Verberie is interpreted as a "hunting campsite for initial carcass processing".	Enloe 2004
Vogelherd	-	*Rangifer* and *Equus*	Evidence suggests that reindeer and horses were exploited by human groups. Animal-processing activities were probably conducted around hearths.	Aurignacian groups likely obtained these taxa regularly during the late summer and fall." The cave was probably occupied seasonally.	Niven 2007
Wallertheim	451	*Bison sp.*	Skeletal part representation is provided as %MNI. Only bisons were hunted and accumulated by hominins. Prime dominated age profile. The accumulation of other species (mainly horses) is interpreted as natural.	Like Mauran, Il'skaja and La Borde, the site si interpreted as a kill-site used by hominins during a long period of time. Carcasses of bovids were dismembered and exhaustively exploited. They are considered kill and/or habitation sites.	Gaudzinski 1996

2.2.3. Ravaging intensity and degree of competition

Estimating the degree of ravaging intensity in a faunal assemblage can help establish the degree of competition and, by extension, the type of ecological setting in which the site was formed: high ravaging stages might be indicative of high-competition settings like open habitats, whereas low ravaging stages indicate more closed environments. It is true that this relation is not always perfect: low competition can also occur in open environments in absence of nutritional stress of carnivores, while hyena dens, where competition is usually low, can show high degrees of ravaging. However, in general, low competition generates low ravaging stages and high competition creates high ravaging stages, whether in open or in closed environments (Domínguez-Rodrigo *et al.* 2007).

In order to estimate the degree of ravaging intensity in the Bed I assemblages, Domínguez-Rodrigo *et al.* (2007) proposed the use of three indices: the ratio of axial to appendicular remains, the ratio of femur to tibia, and the ratio of proximal humerus and distal radius to distal humerus and proximal radius. The latter is more appropriate for contexts where it is known that long bones were first broken by hominins, while the ratio of femur to tibia is more adequate when carnivores had access to complete bones. Both scenarios are tested here for the case of DS. The representation of the relationship between these ratios yields a theoretical model which can be divided into four different ravaging stages. Stage 0 shows no ravaging and represents an ecological environment where competition is nonexistent. Stage 1 represents minor destruction of axial bones and cancellous bone. In assemblages that fall into Stage 2, moderate ravaging causes the deletion of around half of the axial bones and soft portions and in stage 3 assemblages ravaging is intense and only one third of less dense bones survives.

All three ratios were estimated for the complete DS assemblage and for small and medium-sized carcasses separately. Only ribs and vertebrae were included in the counts of axial remains, sacral and caudal vertebrae were excluded. Indeterminate axial and appendicular specimens were not taken into account in the calculations. The resulting values were represented in two graphs next to those published for the other Bed I sites (Domínguez-Rodrigo *et al.* 2007).

2.3. Bone breakage

The analysis of bone breakage patterns is usually neglected in favor of the analyses of bone surface modifications, which tend to be more informative about the timing of access to carcasses by hominins and carnivores. The issue of whether early *Homo* had primary access to carcasses is generally considered to be more important because the access to significant amounts of meat carries relevant implications regarding the evolution of hominin socio-economic behavior. However, access to the marrow content of bones is an important part of the carcass butchering and consumption process, and must therefore also have been important to hominin diet.

Moreover, the analysis of bone breakage patterns is especially relevant in the studies of those assemblages where poor preservation of the cortical surfaces impedes the identification of bone surface modifications. In the case of DS, poorly preserved surfaces are predominant and most cortical surfaces are affected by biochemical marks, which can sometimes alter other bone surface modifications and make them unidentifiable. This is especially true for scores created by carnivores, which can become irregular on the edges and polished in the interior, when affected by biochemical processes. Marks have been estimated conservatively at DS, but there is a possibility that tooth marks have been underestimated for this reason, and therefore it seems important to address the degree of carnivore involvement in the assemblage by other means as well. Here, I apply traditional methods used to assess bone breakage agency in taphonomic analyses, such as the estimation of fragmentation indeces, the analysis of breakage plane angles and the distribution of notch types, but also a more recently developed approach using machine learning algorithms. The contribution of carnivores to the modification of the assemblage is also further assessed through the use of taphotypes, and by estimating the degree of ravaging.

Interestingly, ever since the beginning of the hunting-scavenging debate, researchers of both sides agreed on the idea that hominins were probably responsible for most bone breakage at the earliest archaeological sites, and especially at FLK *Zinj* (e.g. Blumenschine 1991; Domínguez-Rodrigo 1997). This part of the taphonomic study examines whether this hypothesis is also confirmed in the case of DS.

2.3.1. Data recovery

In order to assess fragmentation and bone breakage at DS, first the type of fractures present (green and/or dry or indeterminate) were determined for each bone specimen. For green-broken long limb bones, I also documented the type of breakage plane (longitudinal or oblique) and the type of circumference of the shaft, following Bunn's (1982) classification system into three types based on the percentage of remaining circumference (type 1: <50%, type 2: >50%, type 3: 100%; see also Marean *et al.* 2004; Pickering *et al.* 2005; Domínguez-Rodrigo *et al.* 2007). In addition, the presence or absence of notches were recorded and classified according to the types proposed by Pickering and Egeland (2006; modified from Capaldo and Blumenschine 1994): a) complete notches, b) incomplete notches, c) overlapping notches, d) double-opposing notches, and e) micronotches. I used a caliper with accuracy up to one millimeter to measure all breakage planes that were longer than 2 cm from the long bone subsample. The angles between the bone cortical surfaces and the fracture planes were also measured at the center of a fracture plane using a goniometer. Additionally, linear measurements of different features of notches on both the cortical and medullary sides of the long bone fragments were recorded following Capaldo and Blumenschine (1994) methodology in order to later characterize notch morphology. These measurements include maximum notch breadth and maximum notch depth on the cortical side, and maximum flake scar breadth and flake scar length on the medullary side of the bone. The platform angle of the notch was also measured whenever possible. I also quantified the number of impact flakes in the assemblage. The different approaches and analytical tools used for this part of the analysis on bone breakage are described in more detail below.

2.3.2. Green vs. dry bone breakage

Before addressing the question of which agent was responsible for most bone breakage at DS, it is necessary to identify the proportion of the assemblage that was broken when bones were still fresh; in other words to discern bone breakage by a biotic agent from diagenetic fragmentation (Brugal 1994). Discrimination between green breakage and breakage that occured when the bone was already dry or mineralized is based on the observation of the features of fracture surfaces. Breakage planes of green fractures are generally smooth and run parallel or oblique (sometimes spiral) to the main axis of long bones, while dry or diagenetic fractures tend to create irregular fracture surfaces that often occur on transversal or longitudinal planes. Green fracture planes also

may present hackle marks, notches, negative flake scars, and impact points (e.g. Johnson 1985; Shipman *et al.* 1981; Villa and Mahieu 1991; Lyman 1993). Types of fractures were determined for each bone specimen using these criteria. Unclear breakage planes, mostly of axial and cranial remains, were left undetermined. Proportions of green and dry broken bones were also estimated for each of the long bone separately for more detail.

2.3.3. Fragmentation indeces

Lyman (1994b, 1994c, 2008) has suggested that fragmentation of an assemblage should be assessed considering two dimensions: the extent and the intensity of fragmentation. The extent of fragmentation refers to the proportion according to NISP of specimens in a faunal collection that are anatomically incomplete. The intensity of fragmentation implies the distribution of fragments according to size, and is measured by estimating NISP:MNE ratios for different skeletal elements. Higher ratios suggest smaller fragments. Both indices were estimated considering the complete assemblage and including dry broken specimens in order to also estimate the degree of impact of diagenetic processes on the assemblage.

Then, NISP:MNE ratios were estimated for long limb bones using green broken fragments only and for small and medium-sized carcasses separately in order to compare the ratios with actualistic hammerstone and carnivore broken assemblages. Since NISP:MNE ratios are also an indirect measure of fragment length (Lyman 1994), I additionally calculated average shaft length for each long bone element and compared both indeces. The percentage of complete bones with respect to MNE is an additional analytical tool used here to assess the degree of bone breakage. A high presence of complete bones at a site can also be indicative of incomplete carcass processing by hominins and low carcass competition. Likewise, the fragment ratio of epiphyses to shafts is a proxy used to assess carcass competition or the extent of carnivore ravaging at a site. This estimate was also calculated for DS for each long bone and separately for each carcass size, and compared to other assemblages. For the Bed I sites they were estimated using the published NISP data, which include green and dry broken specimens. Estimates using green broken specimens only should yield somewhat lower values, but they should not vary significantly given the reported low impact of diagenetic breakage and the predominantly biotic agency in the breakage of those Bed I assemblages (Domínguez-Rodrigo *et al.*, 2007).

Bone breakage agents are not always easily discernible from these ratios, because they sometimes overlap in hammerstone breakage experiments and actualistic hyena dens. Only carnivore-only experiments that have been high-

ly fragmented yield significantly different ranges (Egeland *et al.* 2008). In this regard, it has been suggested that the patterns resulting from the proportions of shaft circumference types can be more useful to assess the contribution of hominins and carnivores to bone breakage at a site (Domínguez-Rodrigo *et al.* 2007; although see Marean *et al.* 2004). Bunn (1982) noted that broken assemblages, by either humans or carnivores, typically produce a pattern of shaft fragment representation in terms of their preserved cross section that is characterized by a ratio of types 3 and 2 (>50% of the shaft cross section) to type 1 (<50%) that ranges from 0.44 to 0.1, i.e. specimens preserving less than half of their circumference outnumber the other types. This occurs in all types of broken assemblages except very low fragmented ones, like the felid accumulations of the Bed I sites. Hominin-to-carnivore and carnivore-only assemblages tend to yield values toward the low end of this range because they are more highly fragmented (Bunn, 1982; Domínguez-Rodrigo *et al.* 2007), while hammerstone-only experiments and hyena dens yield higher values. Apart from this, the percentages of shaft cross section types are an additional way of assessing fragmentation intensity and carcass competition at a given site.

Only green broken bones were used for all these estimations. The resulting values for DS were compared to those reported for several hyena dens, including Syokimau (Bunn 1982; Egeland *et al.* 2008); KND2 (Prendergast and Domínguez-Rodrigo 2008), KFHD1 (Lam 1992); Amboseli hyena den (Potts 1988), assemblages from two modern hunter-gatherer campsites (Prendergast and Domínguez-Rodrigo 2008; Bunn 1982), several experiments modeling hammerstone and carnivore breakage (Marean and Spencer 1991; Marean *et al.* 2004), the Olduvai Carnivore Site (Arriaza *et al.* 2016), and several Bed I sites from Olduvai (Domínguez-Rodrigo *et al.* 2007).

2.3.4. Analysis of breakage plane angles

Experimental studies on bone breakage planes have shown that the relative influence of dynamic loading through hammerstone percussion and static loading by carnivores on the formation of an assemblage can be elucidated using a combination of fracture plane and fracture angle data (Alcántara-García *et al.* 2006; Pickering *et al.* 2005). Alcántara-García *et al.* (2006) showed that there are statistically significant differences in breakage angles between both types of agents. Carnivores usually create fractures with angles between 80º and 110º, while hammerstone percussion often generates more acute (<80º) or more obtuse (>110º) angles. These differences are not so apparent on transverse planes, which are ambiguos indicators of the agent of bone fracture, but are evident on longitudinal, and especially on oblique fractures, which are luckily

also the most common type of fracture imparted by both agents.

As mentioned above, following previous studies (e.g. Pickering *et al.* 2005; Domínguez-Rodrigo *et al.* 2007) all measurable oblique and longitudinal planes were measured to the nearest degree with a goniometer. I calculated the frequencies of oblique and longitudinal fractures in each carcass size and estimated the mean and 95% confidence intervals for the frequencies of acute (<90º) and obtuse (>90º) angles within each type of fracture. The results were compared to the ranges obtained in experimental works modeling static and dynamic loading (Capaldo and Blumenschine 1994; Alcántara *et al.*, 2006).

2.3.5. Notch type distribution

Experimental work has shown that the relative proportion of notch types differs in assemblages that have been broken by humans and carnivores and that it can provide additional information on the agent of breakage in archaefaunal collections (Domínguez-Rodrigo *et al.* 2007; Moclán and Domínguez-Rodrigo 2018). Incomplete and double opposing notches are more abundant in carnivore-broken assemblages than complete notches, whereas the latter tend to be more frequent in assemblages that have been broken by humans.

Notches were classified according to notch type following the typology from Moclán and Domínguez-Rodrigo (2018) (modified from Capaldo and Blumenschine 1994). I distinguished between complete notches (type A), which have two inflection points on the cortical view and a non-overlapping negative flake scar; incomplete notches (type B), which are missing one of the inflection points; double overlapping notches (type C), with negative flake scars that overlap with the adjacent notch; double opposing complete notches (type D), which are composed of two notches that appear on opposite sides of a fragment and result from two opposing loading points; and micronotches of < 1 cm (type E).

Following Moclán and Domínguez-Rodrigo's (2018) approach, I carried out a bootstrapped correspondence analysis using the "cabootcrs" R library (Ringrose 2013) in order to compare the relative distribution of notch types at DS to several experimental samples, which included a spotted hyena den in the Maasai Mara (Domínguez-Rodrigo *et al.* 2007), the Olduvai Carnivore Site (OCS), an accumulation probably made by lions (Arriaza *et al.* 2016), and a set of assemblages of small and large animal carcasses involving different taxa that were broken anthropically (Domínguez-Rodrigo *et al.* 2007; de Juana and Domínguez-Rodrigo 2011; Blasco *et al.* 2014; Moclán and Domínguez-Rodrigo 2018). The correspondence analysis was carried out first including all carcass sizes, then separately again for small and medium-sized carcasses. An

additional correspondence diagram was generated by lumping together all the anthropic breakage samples in a single category in order to visualize the results better. In this graph, the DS sample includes all carcass sizes.

2.3.6. Machine learning analysis of fracture planes and notch types

Recently, Moclán *et al.* (2019) introduced a new method that consists in applying machine learning analysis to a certain combination of variables related to fracture planes and notches to assess bone breakage agency in archaeological assemblages. Their statistical approach enables classifying agency with high accuracy and represents a significant advance in understanding bone breakage processes, which are usually insufficiently studied in taphonomic studies, because they have been poorly understood.

Machine learning is a method of data analysis that is based on programmed algorithms, which are trained through an automated learning process. Supervised algorithms identify patterns in the input data (training set) and apply these patterns to make classifications or decisions in testing sets in order to evaluate their accuracy. Their ultimate goal is to make predictions of new datasets. When the accuracy in the testing sets is good, the applicability of the models to new data guarantees good performance in classification and prediction. Machine learning methods are a type of artificial intelligence (AI) that are systematically being applied for example in medical diagnosis, marketing, economics, musical composition, social networks or online shopping. Arriaza *et al.* (2016) showed the potential of the application of these methods to taphonomic problems by using different powerful machine learning algorithms (decision trees, neural networks, random forests, and support vector machines) to re-analyze skeletal part profiles of Bed I sites. Their study proved that machine learning methods can better extract information from taphonomic data than other statistical approaches used in the past. These methods, thus, also represent an opportunity of recovering and re-analyzing taphonomic data that were assumed to be of little use.

Following the methodology proposed by Moclán *et al.* (2019), I summarized the breakage data from DS in a table including the following columns (as numerical variables): presence or absence of epiphyses, specimen size, number of fracture planes measurable in the fragment, type of fracture (oblique or longitudinal), angle of the fracture plane, type of angle (acute, obtuse or right (85º-95º)), whether the fracture was longer than 4 cm, presence or absence of notches, and presence or absence of notch types A, C, and D. The experimental dataset provided by Moclán *et al.* (2019) is used here as the comparative sample. It includes a bone collection recovered from a spotted hyena den (KND2,

Prendergast and Domínguez-Rodrigo 2008), one generated through hammerstone percussion (Moclán and Domínguez-Rodrigo 2018), and a bone collection fractured by wolves, which in general tend to modify and fracture bones to a lesser degree (e.g. Yravedra *et al.* 2011), and serve here as a proxy for other carnivores such as jackals and canids. I used seven different machine learning algorithms to classify the archaeological sample: neural network (NNET), support vector machines (SVMs), k-nearest neighbor (KNN), random forest (RF), mixture discriminant analysis (MDA), naive Bayes (NB), and partial least squares (PLS) (see section 2.3 for a detailed description of each method). In all seven analyses the same procedure was followed.

First, a non-parametric missing data imputation method using random forests was used. This consists of applying a random forest algorithm over a recursive selection of variables and averaging the resulting tree estimates. The algorithm itself produces an out-of-bag (OOB) imputation error estimate which renders the need of a test set or cross-validation unnecessary. Following this, the imputed data set was bootstrapped 1000 times with a function from the "caret" R library that considers bootstrapping the sample in proportion to the variable representation to each of the factors of the outcome variable (Kuhn and Johnson, 2013). After enlarging the sample, data were pre-processed. The methodological description that follows was initially described in Domínguez-Rodrigo (2019). To minimize variance biases, data were centered (the average predictor is converted to zero mean and a deviation from substracting it from each case) and scaled (values were coerced to a standard deviation of one). The ML algorithms used did not require data transformation to deal with normality, skewness or collinearity (Kuhn and Johnson, 2013). Then, the dataset was divided into a training (70% of the sample) and a testing set (the remaining 30%). The algorithm was trained with the training set, and evaluated with the testing set. This is a standard procedure in predictive models that is carried out in order to avoid bias/variance tradeoff (Hastie *et al.* 2016). Data used to train models usually have a tendency to overfit the data, which creates a potential error (bias) when extending the predictive model beyond the training data. High variance from training data may cause use random noise in the model with a tendency to overfit the training data and underfit additional data. The bias can introduce erroneous estimates of the relations of predictors and hence underfit the data (Hastie *et al.*, 2016). Ideally, the analyst should target building a model that captures most of the important relations of the predictors and the regularities of the training data and produce accurate predictions of general data not used to train the model. This bias/variance tradeoff is best managed when using data to train the model and other data (usually a non-negligible portion of the original data) to verify and validate the degree of accuracy of the prediction stemming from the model.

During the application of ML algorithms, the models were tuned with self-correcting methods (Kuhn and Johnson, 2013), one of the great advantages of ML tests. During model elaboration, several techniques allow estimating the performance of the model. Some statistics (e.g., RSME) enable estimating the performance potential on new data. Wolpert (1996) presented the "no free lunch theorem" whereby the apriori position should be that there is no single model that will always perform better than the rest. This is why for every problem, one should use as many techniques as possible and determine which one(s) is (are) the best for the problem at hand. This is the approach adopted here, where several and very diverse ML algorithms will be compared for efficiency and accuracy.

After one avails of several models, model selection takes place. Several techniques are available, but the most common because of its applicability to most ML tests is cross-validation (Kuhn and Johnson, 2013). Model evaluation takes place through resampling techniques that estimate performance by selecting subsamples of the original data and fitting them in multiple submodels. The results of these submodels is aggregated and averaged. Several techniques can be used for this subsampling and submodeling: generalized cross-validation, k-fold cross-validation, leave-one-out-cross validation or bootstrapping (Hastie *et al.*, 2016). Here I selected 10-fold cross validation, which consists of the original sample being partitioned into 10 similarly-sized sets. A first model is subsequently generated using all subsamples but the first fold. Then the first subset is reintroduced to the training set and the procedure is repeated with the second fold and so on until the tenth one. The estimates of performance of each of the ten processes are summarized and, thus, used to understand the model utility.

Model selection is usually done combining indicators of error (i.e., RSME or root mean square error) or accuracy (Kuhn and Johnson, 2013). Cost values (of bias-variance) were evaluated vis-a-vis accuracy with the caret function "tuneLength" up to 10 (i.e., 2^{-2}….2^{7}). The tuning parameter selected for measuring model performance was the "kappa" parameter. For class predictions, these can come in two forms: a discrete category (showing the factor classification) and a probability of membership to any specific category. This latter can be continuous (as in random forests or discriminant analyses, for example) or binary when using sigmoid classifiers (as in logistic regression or support vector machines). The Kappa statistic (which considers the amount of accuracy generated by chance) can take the form of -1 to 1(as in correlation). It is a proxy of accuracy by indicating perfect match between the model and the documented classes (kappa=1) or less so (kappa=<1) (Kuhn and Johnson, 2013). Kappa values of 0.3-0.6 shows reasonable agreement. Estimates higher than these indicate a high agreement between the expected accuracy and the docu-

mented one. Cohen´s kappa value is a more robust measure of prediction and classification than accuracy, because it does not quantify the level of agreement between different datasets, but it represents the degree of similarity of datasets corrected by chance (Lantz, 2013). The selected model performance was also tabulated with confusion matrices.

Finally, the model was used on a separate dataset that included the DS and FLK *Zinj* values. The model returned a classification of the DS and the FLK *Zinj* assemblages into either primary or secondary access to carcass models. When possible, the probabilities of the outcomes were calculated too. All machine learning analyses were carried out with the "caret" library in R. The following paragraphs provide a description of the classificatory methods used.

2.3.6.1. Support Vector Machines (SVM)

Support Vector Machines are one of the most flexible and effective machine learning methods (Kuhn and Johnson 2013), and were first developed by V. Vapnik in the mid-1960s. The SVM algorithms provide a powerful method for non-linear classification. A SVM classifies data points in a multidimensional space by creating a hyperplane that yields a homogeneous distribution of data on either sides (Arriaza and Domínguez-Rodrigo 2016). When this mathematical boundary is non-linear, kernels and tuning parameters are used to add dimensions to data to improve separation between classes (Cortes and Vapnik 1995; Schölkopf *et al.* 2000). The SVM regression method uses a threshold (via the tuning of kernels) set by the user to determine which residuals contribute to the regression fit. To estimate the model parameters, SVM also uses a loss function. The cost (C) parameter is the cost penalty that is used to penalize models with large residuals. The loss function (the same as the lambda in NN) determines the degree of overfit of the training data. The cost parameter adjusts the structure of the model. A SVM radial kernel was used in conjunction with the C-Classification parameter, which selects the size of the hyperplane. It can produce a small-margin plane to maximize classification (large C values) or a wider margin (low C values), which results in higher missclassification errors (Arriaza and Domínguez-Rodrigo, 2016). Here, a fixed value for the cost function was adopted and the kernel parameter was estimated to $\sigma = 0.3502354$. The model was tuned over >100 cost values. The final cost value selected by the kappa parameter was C=0.25. For the present study, the "e1071" and the "caret" R libraries were used.

2.3.6.2. K-Nearest Neighbors (K-NN)

The K-Nearest Neighbors algorithm works well in samples with many vari-

ables and performs well when there are well-defined labeled sets. This unsupervised (lazy) learning algorithm classifies unlabeled data by assigning them the class of the most similar labeled examples. The algorithm makes no assumption about the distribution of the sample and it is easy to train. KNN identifies k cases in the sample as the nearest in similarity. Unlabeled cases are subsequently assigned by similarity.

To predict the location of testing data in the predictor space, different k models are tested and compared to an error/accuracy parameter. To overcome the bias-variance tradeoff an intermediate k value is usually selected. Larger k values tend to reduce the bias of variance but small patterns may go unnoticed. Here, a final model was produced with k=23. Training and testing datasets were created through boosted subsamples. These were subsequently analyzed using the R "class" and "caret" libraries and the "knn" function.

2.3.6.3. Random Forest (RF)

The Random Forest algorithm produces hundreds of classification trees with random selections of the variables of a data set, instead of all the variables. Each selection produces an independent tree. Bootstrap aggregation or bagging, is the common procedure of random forests, which splits a training data set into multiple data sets derived from bootstrapping. The results are contrasted against a validation test, from the observations (about one third) not used for the training data set. These observations are referred to as out-of-bag (OOB) observations. RF produce estimates on how many iterations are needed to minimize the OOB error. After selecting a number of trees, the algorithm averages the results and produces a robust classification method, which avoids overfitting of results to data, as is more common in standard decision and regression trees (Arriaza and Domínguez-Rodrigo, 2016). Here, forests were built using 500 trees. For the present study, the "randomForest" and the "caret" R libraries were used.

2.3.6.4. Mixture Discriminant Analysis (MXDA)

Initially conceived as an extension of LDA (Linear Discriminant Analysis), MDA is built upon class-specific distributions combined into a single multivariate distribution, i.e. it allows each class to be represented by multiple multivariate normal distributions with similar covariance structures, which effectively work as sub-classes of the data. This is done by creating a per-class mixture, as described by Kuhn and Johnson (2013). This consists of separating the class-specific means from the class-specific covariance structure. Otherwise described, each class has different means but the complete-class data set has

the same covariance. These are sub-classes of the data. They are spatially modelled once it is specified how many distributions should be used. The number of distributions per class is the tuning parameter of the model (Kuhn and Johnson 2013). The MDA algorithm integrates ridge- and lasso- penalties to determine feature selection. Here, the final model selected through the kappa parameter was composed of two sub-classes. MXDA can be useful to determine underlying subclasses in each group, but most importantly, it allows modeling multivariate non-normality within the variables.

2.3.6.5. *Naive Bayes (NB)*

The Naive Bayes algorithm is the most common machine learning method that is based on the application of Bayesian methods. The Bayesian technique uses training data to calculate an observed probability of the possible outcomes based on information of a given data set. The classifier is then applied to new data sets by using the observed probabilities to make predictions. Bayesian methods thus use prior probabilistic knowledge, whereas frequentists approaches draw conclusions from sample data and emphasize frequency or proportion of the data. Bayes´ Rule, as used in the NB algorithm, estimates probabilities of classes on observed predictors (i.e., probabilities of previous outcomes), resulting in dynamic estimates of posterior probabilities of classes. The conditional probability (i.e., the probability of observing specific predictor values in relation to data associated with specific classes) is used to model classification. This machine learning algorithm is called "naive" because it assumes that all the variables in the dataset are equally important and independent (Lantz 2013). Prior probabilities allow the decision of which class any case must be assigned. If no prior estimates are provided, these are derived from the documented occurrence of classes within the training set and their relation to predictors´ properties. Predicted classes are created based on the largest class probabilities for each class as derived from the training set. NB uses a non-parametric density modeling process. Here, the "caret" R library was used. The tuning parameter was held constant at a value of 0 and the kappa parameter was used to select the optimal model.

2.3.6.6. Partial Least Squares Discriminant Analyisis (PLS-DA)

This test classifies classes by identifying the predictor combinations that optimally separate classes. It is commonly used in situations where predictor reduction is necessary (such as in LDA based on PCA scores), but it is more efficient than these two-step data reduction methods. The most important favorable properties of the PLSDA algorithm are its way of dealing with collin-

earity between variables and its ability of ranking variables according to their predictive capacity. PLSDA finds latent variables (components) that maximize classification accuracy, i.e. PLSDA creates linear combinations of predictors that are chosen to maximally summarize the variation of the predictors in a number of components which, at the same time, have a maximum correlation to the outcome (Kuhn and Johnson 2013). Therefore, when data reduction is required for classification, PLSDA is preferred over PCA-LDA. In this test, the tuning parameter is the number of latent components to be retained in the final model. When the number of predictors is short compared to the number of cases, PLSDA can execute classification better than LDA: Predictor importance can be also identified. Here, the "plsr" function within the "pls" R libary was used. Model tuning was carried out with the "caret" R library. The number of components retained in the final model was six.

2.3.6.7. *Neural Network (NN)*

The neural network algorithm (Bishop 1995; Ripley 1996; Titterington 2010) is inspired by the functioning of biological neural networks in the human brain. An artificial neural network is formed of hierarchically layered artificial neurons or nodes, which pass on synthesized information to other layers of nodes through regression methods. Nodes convey the transformed input signal through feedforward networks, which terminate in an output node. The training of the neural network is done by adjusting weights through successive layers of nodes. The input data fed to the neural layers (perceptrons) is transformed via specific nonlinear sigmoidal functions. The parameters of these functions are usually optimized to minimize SQR (Sum of Square Residuals). These parameters exhibit a tendency to overfit the training data set. To avoid this, weight decay is used to reduce the model errors for a given value of lambda. This λ parameter must be specified together with the number of hidden units (perceptrons). Reasonable values for λ range from 0.0 to 0.1. Here, five different weight decay values were tested (0.00, 0.01, 0.1, 1, 2). The models were tuned for an uneven number of units (i.e., neurons) ranging from 1 to 19, in a resampling method involving training and testing subsamples. The final values for the model were size=3 and decay=0.04. For the present analysis, the "nnet" and the "caret" R libraries were used.

The experimental and the archaeological samples were each divided into four databases, according to the breakage plane categories established by Alcántara-García *et al.* (2006) and used also by Moclán *et al.* (2019): longitudinal planes with angles smaller than 90º, longitudinal planes with angles larger than 90º, oblique planes with angles of less then 90º, and oblique planes with angles of more than 90º. The machine learning techniques were applied first to the

complete dataset, then again to each of these subsets separately, in order to establish whether each of these types of breakage planes could be more clearly attributed to hominin or to carnivore activity. Transversal planes were left out of the analysis, since they are usually not very informative. I combined all carcass sizes in the same analysis and the datasets were not bootstrapped, since they were sufficiently large (>50; Chernick 2007; Moclán *et al.* 2019).

The comparative sample was first divided into a training and a testing set (70% and 30% of the sample respectively) in order to test the predictive power of the model. Although the machine learning methods differ mathematically, their results are reported and interpreted in the same way. The predictive capacity of the model is assessed using the following indices. The accuracy value yields the percentage success of the classification of the algorithm. The kappa index accounts for the possibility that a correct prediction occurs by chance. Values between 0.80 and 1 reflect very good predictions (Lantz 2013). Sensitivity and specificity are estimates related to the reliability of the accuracy and kappa values. The first one calculates the proportion of correctly classified positive results, the second estimates the proportion of correctly classified negative results. The balanced accuracy takes these two estimates into account to provide a corrected result.

Predictive models were generated for each dataset using all seven machine learning algorithms. The mentioned indices were reported on an ascending scale from 0 to 1 (Moclán *et al.* 2019). Subsequently, the DS samples were compared to the training sets by estimating the probability for each archaeological breakage plane of having been broken by each of the three agents. Each breakage plane was classified according to this probability into one of the three taphonomic categories. The sum of the classifications in each category yields the percentage of fracturing that can be attributed to each taphonomic agent.

2.4. Bone surface modifications (BSM)

2.4.1. General overview of BSM frequencies in the DS archaeofaunal assemblage

Isolated teeth have been left out of BSM analyses, as this section deals only with the cortical surfaces of bones. The analyzed sample is composed of all the plotted specimens, which are >2cm. It is worth mentioning that seven bone specimens (> 2 cm) from the level bags have also been included in the BSM study, as they were found to bear either cut marks or percussion marks. The exact location of these remains was not recorded with the total station; however, their approximate location can be determined within a square meter. Although a few plotted fragments were found to be smaller than 2 cm once measured in the lab, most of these fragments were bigger than 1.5 cm (65 out of 79, 83%). Moreover, a few level bag specimens that were recovered in the sieve were in fact slightly bigger than 2 cm, albeit most were anatomically indeterminate (58 out of 70, 82%). The latter have not been included in the analysis. Collected surface remains were not taken into consideration here either, since it is not possible to determine their exact stratigraphic origin, although most of them very likely derive from the 22B archaeofaunal assemblage.

Following established work of different taphonomists and analysts (e.g. Bunn 1981; Bunn *et al.* 1986; Blumenschine *et al.* 1996; Domínguez-Rodrigo and Barba 2006; Domínguez-Rodrigo *et al.* 2009; Domínguez-Rodrio and Yravedra, 2009), bone surfaces were carefully and systematically examined with a 20x magnification hand lense under a strong oblique light source. During the inspection of each specimen, the fragment was continuously turned and repositioned in relation to the light source in order to appreciate modifications of different depths and illumination contrasts. The general degree of cortical preservation was recorded, as were different alterations caused by diagenetic processes, like manganese formation and water action (Fernández-Jalvo *et al.* 2002; Fernández-Jalvo and Andrews 2016). Overall, surface condition was evaluated by assigning a weathering stage (Behrensmeyer 1978), and a score of "poor", "moderate" or "good" cortical surface to each specimen, an assess-

ment which is used to determine the level of reliability of frequencies of BSM in relation to cortical surface preservation (Pickering *et al.* 2008; Organista *et al.* 2017). Good preservation refers to an unaffected cortical surface, free from the effect of diagenetic processes and in which the original cortical surface has been preserved. Moderate preservation makes reference to a state of preservation characterized by at least half of the cortical surface being unaffected by modification of the properties of the cortical surface or disappearance thereof. Poor preservation implies that the original cortical surface is either weathered, strongly modified by bioerosion, completely absent, or covered by carbonate.

Several types of bone surface modifications were recorded, including cut marks, percussion marks, tooth marks, biochemical (i.e., conspicuous bioerosive) marks, trampling, and microabrasion (following the guidelines published by Bunn 1981, Domínguez-Rodrigo *et al.* 2009 on cut marks, by Blumenschine 1988; Blumenschine and Selvaggio 1988; Blumenschine 1995; Pickering and Egeland 2006 on tooth, cut, and percussion marks, by Domínguez-Rodrigo and Barba 2006 on biochemical marks, and by Behrensmeyer *et al.* 1986, Domínguez-Rodrigo *et al.* 2009 on trampling marks and microabrasion. Care was taken in recording only those marks that could be identified with certainty, and all marks were also inspected by two experienced taphonomists.

A correct evaluation of the frequency of marks on bone surfaces involves not only the consideration of well-preserved cortical surfaces, but also the adjustment of the bias created by dry breakage of bone fragments, mostly during diagenesis (Pickering *et al.* 2008). Failure to consider this biasing process, which generates a higher degree of fragmentation than originally present in the anthropogenic assemblage, would result in underestimation of the original BSM frequencies, thus rendering comparisons with experimental/actualistic samples of limited value for inferential purposes. In order to correct for this bias, a special correction method was used (Pickering *et al.* 2008). Since each dry fracture implies the creation of at least two fragments, the number of dry fractures in any assemblage needs to be first divided by two. This number is then added to the number of specimens exhibiting only green fractures in the assemblage. The percentage of marks in that bone collection is therefore calculated from the formula X+(Y/2), where X is the number of green broken specimens, and Y the number of dry broken specimens. Specimens with both green and dry factures were counted twice. This results in a more conservative estimate of BSM frequencies. This approach is applied here to the complete ungulate collection of Level 22B, but also each time smaller sets of bones (e.g. limb bones or axial bones) are analysed in more detail. This correction method affects axial bones in a particular way, since green fractures are more ambiguous in flat and irregular bones than in limb bone shafts. Since only clearly distinctive green and dry fractures were recorded, percentages of marked bones may appear more inflated in the NSP, NISP and axial remains samples, than in

the limb bones subsamples.

Estimations of BSM frequencies were initially made on the complete non-dental skeletal assemblage (NSP). Then, estimates were corrected for dry bone breakage. Subsequently, the NSP sample was divided into long limb and axial subsamples. BSM frequencies were then estimated on NISP. The NSP sample was also divided into two subsamples composed of small and medium carcasses (size classes 1-2 and 3-4 respectively, following the size class system for bovids by Brain 1974; 1981). Although BSM on large carcasses (size class 5-6) have been documented (see results section), they are not included in the statistical analyses, because specimens of large carcasses represent a very small portion of the faunal assemblage. BSM calculations were repeated separately on these two samples per NSP and NISP, as well as on their respective long limb and axial subsamples. All estimates were made on the different categories for bone surface preservation, and corrected for dry bone breakage.

The BSM analysis presented below focuses mainly on mark frequencies on long limb bones, given the lack of frames of references for axial and cranial anatomical sections.

2.4.2. Comparing DS to the archaeological record. Cut mark frequencies from the DS archaeofaunal assemblage in relation to a referential set of Paleolithic sites

In this section, statistical analyses deal with cut mark frequencies only, and its aim is to examine similarities and differences between the DS faunal assemblage and a selection of faunal collections in which carcass consumption and accumulation has been taphonomically interpreted as the result of primarily hominin activities through primary access to carcasses. This is especially true for Upper Paleolithic assemblages, where the acquisition of small and medium-sized carcasses is commonly almost unanimously interpreted as hunted. The list of archaeological deposits used for this purpose stems partly from a study by Domínguez-Rodrigo and Yravedra (2009), who carried out a multivariate statistical analysis in order to evaluate the effect of different variables on the variability of total cut mark frequencies across a number of archaeological sites. From the list presented in that study, a total of 46 archaeological levels from 10 sites were grouped into three different chrono-cultural categories for the present analysis: Early Stone Age (ESA), Mousterian, and Upper Paleolithic. Non-Paleolithic sites were excluded because they are beyond the scope and purpose of this study, especially those where butchery was performed with metal tools. The three groups of sites were compared with regard to three variables: A) total frequency of cut-marked specimens (CM-NISP), B) total frequency

of cut marked specimens on long bones (CM-LB), and C) total frequency of cut-marked specimens on long bone shafts (CM-MSH). Although Early Stone Age (ESA) sites were added to this comparative sample, the intention was to add them merely as additional information and additional comparative background, with the main focus on Upper Pleistocene anthropogenic sites, where primary access to carcasses was taphonomically well-supported. The goal with this comparative analysis was to see how the DS sample compared with sites traditionally interpreted as anthropogenic and resulting from hominin hunting. Thus, only ESA sites analyzed by our team were used, given that these selected ESA assemblages are some of the most extensively cut-marked faunal assemblages for the Early Pleistocene.

In order to increase the sample size from that used by Domínguez-Rodrigo and Yravedra (2009), a systematic search for taphonomic studies of anthropogenic sites from the Mousterian and the Upper Paleolithic archaeological records that included data on cut mark frequencies was carried out. Difficulties arose especially when trying to find information on cut mark frequencies on long bones and long bone shafts (CM-LB and CM-MSH). When available, data had to be often calculated by combining the information presented in different tables. In several studies, numbers were presented only on NSP but not on NISP. Information on cut marks was nearly always purely descriptive.

Carcass size was also taken into consideration, and the analysis explained below was therefore carried out twice for each site: on the sample of small sized carcasses (size 1 and 2), and on the sample of medium-sized carcasses (size 3 and 4) (Tables 2.2 and 2.3). The cut mark frequency values for DS were calculated for a) the well-preserved sample, b) the assemblage with good and moderate bone surface preservation, and c) the complete bone collection, which is neither corrected for badly preserved surfaces nor for dry bone breakage (Tables 2.2 and 2.3). Statistics were finally applied to a sample of 33 archaeological levels for small sized carcasses, and a total of 56 archaeological levels for medium-sized carcasses, although sample sizes varied according to the variable at issue. Data were more limited for variables CM-LB and CM-MSH. Information on cut mark frequencies on long bones of small carcasses was available for 19 sites, and values for cut mark frequencies on long bones of medium carcasses was found for 33 sites. Cut mark frequencies on mid-shafts are provided for 19 sites when only small carcasses were taken into account, and 29 sites when medium-sized carcasses were considered (Tables 2.2 and 2.3).

As a first step, a Bartlett's test was applied to test if the groups of ESA, Mousterian, and Upper Paleolithic sites were homoscedastic, i.e. to test if they all shared equal variances (with regard to each one of the three variables). When this was the case, ANOVA was used to test whether or not the means of these groups were statistically similar or not. As a post-hoc analysis, Tukey's HSD

Table 2.2. *List of assemblages used for the comparative analysis (small-sized carcasses)*

Site	Group	A (cm-NISP)	B (cm-LB)	C (cm-MSH)
FLK *Zinj*	Early Stone Age	10.5	14.9	12
BK1	Early Stone Age	5.1	10	10
BK2	Early Stone Age	7.8	5.4	5.4
BK3	Early Stone Age	5.2	13	13
BK4ab	Early Stone Age	10.6	14.3	16.7
BK4c	Early Stone Age	9.3	14.8	11.1
Esquilleu XI	Mousterian	14.3	21.4	26.3
Esquilleu XIII	Mousterian	13.6	27.2	25.8
Esquilleu VI	Mousterian	13.4	19.3	20.5
Esquilleu XII	Mousterian	10.6	17.6	19.1
Covalejos K	Mousterian	8.5	18.1	21
Covalejos I	Mousterian	6.8	12.2	12.5
Covalejos C	Mousterian	10.5	22.2	22.2
Cueva Corazón	Mousterian	6.9	NA	NA
Ambrosio Sol Med	Upper Paleolithic	11.4	20.9	27.1
Ambrosio Sol Sup	Upper Paleolithic	5.5	23.2	25.6
Ambrosio Sol Sup Evo	Upper Paleolithic	5.8	15.4	6.5
Estebanvela I	Upper Paleolithic	10	29.4	34.5
Estebanvela II	Upper Paleolithic	8.8	12.5	14.4
Estebanvela III	Upper Paleolithic	9	18.6	25.7
Las Caldas IX	Upper Paleolithic	7.8	NA	NA
Las Caldas VIII	Upper Paleolithic	12.9	NA	NA
Las Caldas VII	Upper Paleolithic	7.3	NA	NA
Las Caldas V	Upper Paleolithic	6.2	NA	NA
Las Caldas IV	Upper Paleolithic	8.9	NA	NA
El Horno 1	Upper Paleolithic	33.6	NA	NA
Coímbre 1ab	Upper Paleolithic	17.3	NA	NA
Coímbre 1c1	Upper Paleolithic	13.5	NA	NA
Coímbre 1c2	Upper Paleolithic	15.4	NA	NA
Coímbre 1c3	Upper Paleolithic	13.7	NA	NA
Coímbre 2	Upper Paleolithic	17.4	NA	NA

Coímbre 4	Upper Paleolithic	17.8	NA	NA
Coímbre 6	Upper Paleolithic	11.4	NA	NA
DS (a)	Early Stone Age	10.3	11.7	13.5
DS (b)	Early Stone Age	9.2	9	10.5
DS (c)	Early Stone Age	4	6.2	6.8

Table 2.3. *List of assemblages used for the comparative analysis (medium-sized carcasses)*

Site	Group	A (cm-NISP)	B (cm-LB)	C (cm-MSH)
FLK *Zinj*	Early Stone Age	17.2	22.6	17.2
BK1	Early Stone Age	10.3	15.6	15.6
BK2	Early Stone Age	11.6	22.8	23
BK3	Early Stone Age	7.8	11.9	12
BK4ab	Early Stone Age	9.3	14.8	11.1
BK4c	Early Stone Age	7.7	11.4	14.3
Jonzac 22	Mousterian	22	24.8	NA
Abric Romani I	Mousterian	9.6	18.8	NA
Abric Romani M	Mousterian	8.5	19	NA
Cueva Corazón	Mousterian	17.5	NA	NA
Solutré Village	Mousterian	1.9	2.1	NA
Fieux K ouest	Mousterian	1.8	NA	NA
Combe Saunière	Upper Paleolithic	17.4	NA	NA
Castanet	Upper Paleolithic	17.5	NA	NA
Solutré P16	Upper Paleolithic	2.1	NA	NA
Las Caldas IX	Upper Paleolithic	9.5	NA	NA
Las Caldas VIII	Upper Paleolithic	14.5	NA	NA
Las Caldas VII	Upper Paleolithic	10.6	NA	NA
Las Caldas V	Upper Paleolithic	7.6	NA	NA
Las Caldas IV	Upper Paleolithic	7.3	NA	NA
El Horno 1	Upper Paleolithic	44.4	NA	NA
Roc de Combe 5	Upper Paleolithic	14.5	17.5	NA
Roc de Combe 6	Upper Paleolithic	7.3	11.5	NA
Roc de Combe 7	Upper Paleolithic	12.7	14.3	NA
Roc de Combe 8	Upper Paleolithic	20	32.1	NA
Cuzoul de Vers	Upper Paleolithic	12.8	NA	NA
Coímbre 1ab	Upper Paleolithic	20.2	NA	NA
Coímbre 1c1	Upper Paleolithic	23	NA	NA
Coímbre 1c2	Upper Paleolithic	31.4	NA	NA
Coímbre 1c3	Upper Paleolithic	20.6	NA	NA

Coímbre 2	Upper Paleolithic	24.1	NA	NA
Coímbre 4	Upper Paleolithic	22.4	NA	NA
Coímbre 6	Upper Paleolithic	25	NA	NA
Vogelherd	Upper Paleolithic	16.1	21.3	22.7
Amalda VII	Mousterian	11.2	26.8	29.2
Esquilleu XI	Mousterian	9.6	25.5	31.8
Esquilleu XIII	Mousterian	6.2	18.6	22.4
Esquilleu VI	Mousterian	12.3	24.5	27.2
Covalejos J	Mousterian	8.6	24.6	24.9
Covalejos K	Mousterian	9.5	23.4	25.9
Covalejos I	Mousterian	5.3	21.8	25.4
Covalejos D	Mousterian	14.6	40.5	50
Covalejos C	Mousterian	14.3	21.7	21.7
Ambrosio Sol Med	Upper Paleolithic	11.8	22.4	25.8
Ambrosio Sol Sup	Upper Paleolithic	8.7	55.9	28.9
Ambrosio Sol Sub Evo	Upper Paleolithic	15.3	34.4	39.1
Estebanvela I	Upper Paleolithic	16.4	30.9	32.7
Estebanvela II	Upper Paleolithic	5	7.5	8.4
Estebanvela III	Upper Paleolithic	7.3	17.4	12.2
Amalda IV	Upper Paleolithic	23.9	40	41.9
Amalda VI-V	Upper Paleolithic	17.3	37.6	45.4
Linar	Upper Paleolithic	9.8	20.7	18.6
Ruso 3	Upper Paleolithic	19	27.2	29.7
Ruso 4a	Upper Paleolithic	15	30	33.3
Ruso 4b	Upper Paleolithic	6.1	17.8	13.3
Cofresnedo	Upper Paleolithic	16.6	28.3	30.2
DS (a)	Early Stone Age	19.8	25	25.5
DS (b)	Early Stone Age	16	17.5	17.4
DS (c)	Early Stone Age	5.9	10.3	10.7

test was used on the samples. In the case of heteroscedasticity, the non-parametric Kruskal-Wallis test was applied in conjunction with a pairwise comparison using Wilcoxon rank sum test. Given that samples were small, and due to the possibility that the statistical analysis could overestimate the real difference between groups, results were interpreted conservatively. In addition, a bootstrapping T-test method was used to calculate the mean differences of groups in pairs by randomly resampling the data 5000 times. This method involved a nonparametric bootstrap bias-corrected-and accelerated (BCa) method, which provided 95% percentile intervals. A robust standardized effect size measure was used. The effect size of the mean difference was established using Cohen's

δ value (small: δ=0.2, medium: δ=0.5, large: δ=0.8). Effect sizes can also be interpreted in terms of the percent of nonoverlap of one group's scores with those of the other group. An effect score of 0.0 indicates that the distribution of scores for one group overlaps completely with the distribution of scores for the other group. An effect value of 0.8 indicates a nonoverlap of 47.4% in the distributions of both groups (Cohen 1988).

As a complement, a t-test was applied to the homoscedastic samples that showed significant differences between groups in order to compare the cut mark frequency values of DS to the means of each group. Mann-Whitney U test was applied to heteroscedastic samples. The comparison was first made with the well-preserved sample, then with the moderately well preserved sample, and lastly with the complete assemblage. Confidence interval plots for the differences between means were generated using the "gplot" library in R, with the purpose of showing the similarities and differences between the DS samples and the groups of paleolithic sites regarding CM-NISP, CM-LB, and CM-MSH, and in order to assess whether the DS sample falls within the confidence intervals of the different groups. All statistical tests were carried out using R (www.r-project.org).

2.4.3. Comparing DS to dual and multi-patterned experimental assemblages and FLK Zinj

Type of access to carcasses by hominins at DS is addressed in this section by comparing cut mark, percussion mark, and tooth mark frequencies on long limb bones separately to experimental data sets, as was standardized by Blumenschine (1995). Available models simulating primary and secondary access to animal carcasses stem from different studies from the past 30 years (see Blumenschine 1988; Blumenschine 1995; Capaldo 1995, 1997; Domínguez-Rodrigo 1997a; Domínguez-Rodrigo 1997b; Domínguez-Rodrigo and Barba 2005; Pante *et al.* 2012; Gidna *et al.* 2014) for experiments involving cut marks; Blumenschine 1988, 1995; Capaldo 1995, 1997; Pante *et al.* 2012 for experiments involving percussion marks, and Blumenschine 1988, 1995; Capaldo 1995, 1997; Domínguez-Rodrigo *et al.* 2007b; Pante *et al.* 2012, Gidna *et al.* 2014; Organista *et al.* 2016) for experiments involving tooth marks). Percentages of bone surface modifications resulting from these experiments have previously been applied to the African early Pleistocene archaeological record at sites like FLK *Zinj* (e.g. (Domínguez-Rodrigo *et al.* 2007) or BK (Domínguez-Rodrigo *et al.* 2014; Organista *et al.* 2017) in Olduvai to address early human subsistence behavior.

The experimental studies were carried out by different authors following slightly different methodologies, and therefore some of the models are used

separately in this analysis, i.e. treated as different models, although they are named the same. For example, although Blumenschine (1988, 1995), Capaldo (1995), Domínguez-Rodrigo (1997), and Gidna *et al.* (2014) all simulated carnivore scavenging (model H-C, first hominins, then carnivores) by completely processing several carcasses removing flesh and marrow before bones were exposed to the action of carnivores, only the last two researchers used stone flakes to deflesh the animals, as opposed to the other authors, who employed metal knives. Since the type of butchering tool material has been shown to significantly influence the percentage cut mark frequencies (Domínguez-Rodrigo and Yravedra 2009), these experiments will not be combined in the same model. Furthermore, bone element division into different sections to tally bone surface modifications was conducted in different manners by these researchers: whereas Domínguez-Rodrigo (1997) and Gidna *et al.* (2014) categorized fragments as either midshafts or proximal/distal shafts (including the respective epiphyses), Blumenschine (1988, 1995) and Capaldo (1995) designated specimens as "epiphyseal fragment", "near-epiphyseal fragment", or "midshaft fragment" (not documenting the exact location on which marks occurred, since some of the epiphyseal fragments also included near-epiphyseal portions, and even mid-shafts; see discussion in Domínguez-Rodrigo 1997, 1999). By distinguishing between different experimental methodologies we gain accuracy and detail in the comparisons, yet this has the major drawback that sample sizes of the different models will remain small. Combining them, however, could potentially introduce a bias in the comparison.

Other similar experiments are not considered here, because it would be wrong to establish an analogy between them and archaeological data, due to important methodological flaws. For example, some authors have made experiments with captive lions (Pobiner 2007, 2015; Parkinson *et al.* 2014) or applied data derived from experimental models on captive spotted hyenas to the archaeological record (Marean *et al.* 1992; Faith *et al.* 2007), yet these models are inadequate proxies for wild carnivore behaviors (Gidna *et al.* 2013; 2015). Lupo and O'Connell's (2002) ethnographic work with the Hadza also contained substantial bias, namely that bones were boiled before they were exposed to carnivores. This would have made carcasses less attractive to scavengers (Domínguez-Rodrigo *et al.* 2007a). The different methodologies and the characteristics of the experimental models that can be applied to DS are summarised below and in Table 2.4.

As has been pointed out before, the use of correction methods for the biases created by differential bone surface preservation and the impact of dry breakage in the Plio-Pleistocene record guarantees that experiments can be used properly as proxies of archaeological sites. Thus, as in the previous section, apart from the complete DS sample (DSc), two additional DS subsamples that account for

Table 2.4. a) *Description of the different experiments with small carcasses including cut mark data modeling primary and secondary access to carcasses by hominins. HO: Hammerstone/Hominin only; WB-C: Whole bone to carnivore; H-C: Hominin-Carnivore; CO: Carnivore only; LO: Lion only; V-H-C: Vulture-Hominin-Carnivore; F-H: Felid-Hominin; F-H-H: Felid-Hominin-Hyenid; N: number of assemblages.*

Model	Type	Marks	References	Description	N
HO	Primary access	CM	Domínguez-Rodrigo and Barba 2005	- Defleshing was carried out with stone flakes and aimed to remove all small scraps of flesh. Hammerstone-on-anvil technique was used to break the bones. - Bone fragments were classified as either midshafts or proximal/distal shaft following Domínguez-Rodrigo 1997. - The butchering process was carried out by students (unexperienced butchers).	4
HO	Primary access	CM, PM	Blumenschine 1988, 1995; Pante *et al.* 2012	- Complete metal-knive defleshing by the author, and hammerstone-on-anvil technique to break the bones and remove marrow. - Long bones are divided into epiphyseal, near-epiphyseal and midshaft portions following Blumenschine 1988, and marks are tallied accordingly. - CM percentages for midshafts and for the total number of specimens are from Pante *et al.* 2012. - PM percentages are from Blumenschine (1995).	6
WB-C	Primary access	CM, TM	Capaldo 1995, 1997; Pante *et al.* 2012	- Complete metal-knive defleshing. - Bones were fragmented by carnivores. - A total of 30 experiments were conducted, but carnivores completely consumed or removed 11 of them. Eight of them were composed of less than five bone fragments and were not included in the study. - Long bones are divided into epiphyseal, near-epiphyseal and midshaft portions following Blumenschine 1988 and marks are tallied accordingly. - CM percentages are for midshafts and for the total number of specimens are from Pante *et al.* 2012, who summarized Capaldo's results and removed those assemblages made of few specimens.	7
H-C	Primary access	CM	Domínguez-Rodrigo 1997	- The small bovids had been defleshed by poachers. - Bone fragments were classified as either midshafts or proximal/distal shaft following Domínguez-Rodrigo 1997.	1

H-C	Primary access	CM, PM, TM	Blumenschine 1988, 1995; Capaldo, 1995, 1997; Pante *et al.* 2012	- Complete metal-knive defleshing, and hammerstone-on-anvil technique to break the bones and remove marrow. - Long bones are divided into epiphyseal, near-epiphyseal and midshaft portions following Blumenschine 1988 and marks are tallied accordingly. - CM percentages for bone portions are taken from Pante *et al.* 2012, TM and PM percentages are from Blumenschine 1995; Capaldo, 1997; Domínguez-Rodrigo *et al.* 2007a. - Blumenschine's and Capaldo's experiments are discussed separately when TM and PM are considered. - Spotted hyenas were the major if not exclusive scavengers of these simulated sites.	32
CO	Carni-vore only	TM	Blumenschine 1988, 1995; Pante *et al.* 2012	- Bones were defleshed by different mammalian carnivores and then fragmented by spotted hyenas, and in one case by a lion (maybe also mongooses and jackals).	2
F-H	Second-ary access	TM	Domínguez-Rodrigo *et al.* 2007b	- Bones stem from Brain's (1981) experimental collection of carcasses from cheetah/leopard kills. - Bones were virtually fragmented - The assemblages are composed of a steenbok, a goat, a sheep, and three impalas.	6
F-H	Second-ary access	TM	Gidna *et al.* 2014; Or-ganista *et al.* 2016	- The sample is composed of warthogs, juvenile zebras and wildebeest. - Bones were virtually fragmented in order to preserve the bone collection. - Tooth marks were quantified by element and bone section, i.e. bone fragments were classified as either midshafts or proximal/distal shaft following Domínguez-Rodrigo 1997.	13
V-H-C	Second-ary access	CM. PM. TM	Blumenschine. 1988. 1995 (Pante *et al.* 2012)	- Long bones from four carcasses were eaten by vultures. some were also defleshed by carnivores. - Reduced hyena consumption of epiphyseal fragments. - Defleshing was carried out with a metal knife. and hammerstones were used to extract marrow. - Assemblages are variable in type of initial consumers. and the number and type of elements included. - Long bones are divided into epiphyseal. near-epiphyseal and midshaft portions following Blumenschine 1988. - CM, TM, and PM percentages for midshafts and all specimens are from Pante *et al.* 2012	1

Table 2.4. b) *Description of the different experiments with medium-sized carcasses including cut mark data modeling primary and secondary access to carcasses by hominins. HO: Hammerstone/Hominin only; WB-C: Whole bone to carnivore; H-C: Hominin-Carnivore; CO: Carnivore only; LO: Lion only; V-H-C: Vulture-Hominin-Carnivore; F-H: Felid-Hominin; F-H-H: Felid-Hominin-Hyenid; N: number of assemblages.*

Model	Type	Marks	References	Description	N
HO	Primary access	CM	Domínguez-Rodrigo 1997	- Basalt flakes were used to deflesh the four legs of a zebra. - Disarticulation was carried out with metal knives. but cut marks resulting from disarticulation were not counted. - Hammerstones were used to break the bones. - Bone fragments were classified as either midshafts or proximal/distal shaft following Domínguez-Rodrigo 1997, and marks were tallied accordingly. - Focus was placed on defleshing. which aimed removing all small scraps of flesh. - Carcass processing was carried out by the author.	1
HO	Primary access	CM, PM	Blumenschine. 1988. 1995; Pante *et al.* 2012	- Complete metal-knive defleshing. and hammerstone-on-anvil technique to break the bones and remove marrow. - Long bones are divided into epiphyseal. near-epiphyseal and midshaft portions following Blumenschine 1988, and marks are tallied accordingly. - CM percentages for midshafts and for the total number of specimens are from Pante *et al.* 2012. - PM percentages are from Blumenschine (1995).	1
WB-C	Primary access	CM, TM	Capaldo. 1995, 1997; Pante *et al.* 2012	- Complete metal-knive defleshing. - Bones were fragmented by carnivores. - A total of 30 experiments were conducted. but carnivores completely consumed or removed 11 of them. Eight of them were composed of less than five bone fragments and were not included in the study. - Long bones are divided into epiphyseal. near-epiphyseal and midshaft portions following Blumenschine 1988, and marks were tallied accordingly. - CM and TM percentages for midshafts and for the total number of specimens are from Pante *et al.* 2012.	4
H-C	Primary access	CM, TM	Domínguez-Rodrigo 1997. Gidna *et al.* 2014	- Defleshing was carried out with stone flakes and aimed to remove all small scraps of flesh. Hammerstone-on-anvil technique was used to break the bones.	5

				- Bones were disarticulated with metal knives. but these marks were not counted. - Gidna *et al.*'s (2014) bones were virtually fragmented in order to preserve the bone collection. - Bone fragments were classified as either midshafts or proximal/distal shaft following Domínguez-Rodrigo 1997, snd marks were tallied accordingly. - Gidna *et al.*'s (2014) defleshing aimed to remove the bulk of the flesh, not all flesh scraps.	
H-C	Primary access	CM. PM, TM	Blumenschine. 1988. 1995; Capaldo, 1995 (Pante *et al.* 2012)	- Complete metal-knive defleshing. Hammerstone-on-anvil technique to break the bones and remove marrow. - Long bones are divided into epiphyseal, near-epiphyseal and midshaft portions following Blumenschine 1988, and marks were tallied accordingly. - CM percentages for midshafts and all specimens from Pante *et al.* 2012. - Spotted hyenas were the major scavengers involved in this experiment. - TM and PM percentages are from Blumenschine 1995; Capaldo, 1997 - Blumenschine's and Capaldo's experiments are discussed separately when TM and PM are considered. - Spotted hyenas were the major if not exclusive scavengers of these simulated sites.	14
CO	Carnivore only	TM	Blumenschine 1988, 1995; Pante *et al.* 2012	- Bones were defleshed by different mammalian carnivores and then fragmented by spotted hyenas, and in one case a lion (maybe also mongooses and jackals).	7
F-H	Secondary access	CM, TM	Domínguez-Rodrigo 1997 for CM; Domínguez-Rodrigo *et al.* 2007b for TM	- Scraps from nearly defleshed carcasses from lion kills were removed with stone flakes. - Gidna *et al.*'s (2014) bones were virtually fragmented in order to preserve the bone collection intact. Domínguez-Rodrigo 1997 broke one of the two carcasses with a hammerstone. - Butchery was performed by the authors - Bone fragments were classified as either midshafts or proximal/distal shaft following Domínguez-Rodrigo 1997, and marks were tallied accordingly. - TM percentages are provided for one cow (Domínguez-Rodrigo *et al.* 2007b)	15-CM; 1-TM
F-H	Secondary access	TM	Gidna *et al.* 2014; Organista *et al.* 2016	- The sample is composed of adult zebras and wildebeest.	16

				- Bones were virtually fragmented in order to preserve the bone collection. - Bone fragments were classified as either midshafts or proximal/distal shaft following Domínguez-Rodrigo 1997, and as epiphyseal, near-epiphyseal, or midshaft fragments following Blumenschine 1988.	
F-H-H	Secondary access	CM	Domínguez-Rodrigo 1997	- Scraps from nearly defleshed carcassees from lion kills were removed with stone flakes and broken with hammerstones. - Then they were exposed to scavengers. - Butchery was performed by the author - One of the four carcasses had only been half-defleshed by lions. - Bone fragments were classified as either midshafts or proximal/distal shaft following Domínguez-Rodrigo 1997, and marks were tallied accordingly.	4
V-H-C	Secondary access	CM, PM, TM	Blumenschine, 1988, 1995; Pante *et al.* 2012	- Long bones from four carcasses were eaten by vultures, some were also defleshed by carnivores. - Reduced hyena consumption of epiphyseal fragments. - Defleshing was carried out with a metal knife, and hammerstones were used to extract marrow. - Assemblages are variable in type of initial consumers, and the number and type of elements included. - CM, PM and TM percentages were only found available for midshafts and all specimens (Pante *et al.* 2012)	4

bad preservation and dry fractures (DSa and DSb) are used for comparison with the experimental models, and comments are made primarily regarding the similarities and differences between the well-preserved sample (DSa) and the experimental models. Mark frequencies documented at FLK *Zinj* (Domínguez-Rodrigo *et al.* 2007a) have been included in this comparison as well.

2.4.3.1. Univariate analysis of BSM

Cut marks

In all experiments, cut mark data were recorded for all six long bones, with the exception of Gidna *et al.*'s (2014) study on carcass consumption by lions in Tarangire (Tanzania), which did not include metapodials. However, Pante *et al.* (2012), who summarised Blumenschine's (1988, 1995) and Capaldo's (1995) experiments, do not include mean percentages on cut mark frequencies on all different appendicular and bone sections, only cut mark percentages on mid-shafts and on the complete assemblages are provided. While Blumenschine (1988, 1995) and Capaldo (1995) processed the carcasses completely with metal knives, Domínguez-Rodrigo (1997), Domínguez-Rodrigo and Barba (2005), and Gidna *et al.* (2014), defleshed carcasses with stone flakes. Metal knives were only used by these researchers for disarticulation, but the cut marks inflicted on the bones with metal knives were not counted.

Whereas Domínguez-Rodrigo's (1997) and Gidna *et al.*'s (2014) experiments focused therefore mainly on defleshing, the data presented by Pante *et al.* (2012) might also be including cut marks related to the disarticulation of bone elements. With the exception of Domínguez-Rodrigo and Barba's (2005) study, in which carcass defleshing was done by students, the butchering process was carried out by more experienced butchers (e.g. Maasai and Mwalangulu people or researchers). When it came to modeling primary access, none of the experiments involved boiling the bones before carnivores accessed it, thus ensuring that greasy long bone ends were still attractive to carnivores. Although Blumenschine (1988, 1995) and Capaldo (1995) categorized fragments bearing marks as either epiphyseal, near-epiphyseal or mid-shaft portions of bones, in this analysis marks are tallied only according to mid-shafts and end portions (which include epiphyses and near-epiphyses) of long bones, as was done in all other experiments.

Two types of 95% confidence interval plots were generated, one with mark frequencies of each model and the archaeological sites (DS and FLK *Zinj*) in each skeletal part (ULB, ILB, LLB) and bone section (MSH, Ends) with regard to NISP, the other with regard only to the cut-marked specimen sample. Com-

parisons were made for small-sized (size 1-2) and medium-sized (size 3-4) carcasses separately. Additionally, the relationship between the NICMSP (number of identified cut-marked specimens):NISP ratio and the NCMMSSP (number of cut-marked midshaft specimens): NICMSP ratio in all experiments was examined graphically. Confidence ellipses (alpha=95%) were plotted in order to be able to differentiate statistically all the groups. A bootstrapped version of this graph was created for further clarification. These analyses were made with R and the graphs were produced with the "ggplot2" R library.

Percussion marks

Percussion mark frequencies were available for Blumenschine's (1988; 1995) and Capaldo's (1995; 1997) experimental models simulating the HO (Hominin-Only), H-C (Hominin- Carnivore), and V-H-C (Vulture-Hominin-Carnivore) scenarios. The experiments classified as WB-C (Whole-Bone to Carnivore) did not involve hammerstone percussion, since bones were broken by carnivores in these simulations. Naturally, those experiments involving virtual fragmentation (Domínguez-Rodrigo *et al.* 2007b; Gidna *et al.* 2014; Organista *et al.* 2016) also lacked information on percussion marks. Mean percentages of percussion-marked specimens of all experiments were provided for different long bone portions (mid-shafts, epiphyses, and near-epiphyses, following Blumenschine's [1988] methodology), but marks were not tallied according to different long bone elements because this information is missing in the published experimental works available. Percussion mark frequencies for each appendicular anatomical section (ULB, ILB, LLB) for DS and for FLK *Zinj* are provided in the results section.

Tooth marks

Some of the experimental studies used above to address type of access to carcasses by hominins and carnivores by means of quantifying mark frequencies also contain information on tooth-marked specimens. Tooth marks were tallied according to bone portions by all researchers, yet they followed different methodologies, as was the case for cut marks. However, Blumenschine's (1988) epiphyseal fragments (EP) could be grouped with the category named "ends" by Domínguez-Rodrigo 1997. Near epiphyseal fragments (NEP) were to be grouped with mid-shafts; however, raw data were not available in their original publications (only mean percentages were provided) and these categories are therefore held separate. Only mid-shafts are represented in the graphs, the values for NEP can be found in the results section. Data on tooth mark frequencies per appendicular section (ULB, ILB, LLB) could seldom be collected. Gidna *et al.* (2014) and Organista *et al.* (2016), however, do provide these mark

frequencies for Felid-Hominin models. Yet, tooth mark percentages on metapodials are not included in this experimental set, since these bones are usually left unmodified and ignored by felids, particularly by lions. Domínguez-Rodrigo's (2007b) work with Brain's (1981) bone collection of carcasses ravaged by leopards and cheetahs includes tooth mark percentages on metapodials, and they were virtually always close to zero. Tooth mark percentages on ULB, ILB, and LLB were estimated for the DS assemblage, and their mean values are included in 95% confidence interval plots, whenever there is at least one experimental model to compare them to.

It is important to point out that the experimental set documents the action of different carnivores, including mainly hyenas, lions, cheetahs and leopards. All experiments were carried out with wild carnivores, experiments with captive animals or carnivores not in their natural ecosystems have not been included (e.g. Pobiner 2007, 2015; Parkinson, 2014; Marean, 1992). Selvaggio's (1994) study simulating a three-stage model was excluded, mainly because she did not make a distinction between different carcass sizes and, most importantly, carnivore types. Gidna *et al.* (2014) also simulated a LO (lion only) model, yet the fact that archaeological sites such as DS are fragmented assemblages, and that lions do not generally fragment bones, renders this model inappropriate for our purpose. High tooth mark percentages in a sample of carcasses consumed by lions drop drastically when bones are fragmented, because each complete element often bears very few tooth marks. These are especially low on shafts (Organista *et al.* 2016).

2.4.3.2. Multivariate analysis of BSM

Cut mark, percussion mark, and tooth mark data were analyzed simultaneously by means of a mixed multiple discriminant analysis (MXDA) following the methodology in Domínguez-Rodrigo *et al.*'s (2014 a, b) and in Organista *et al.*'s (2017) taphonomic studies of FLK *Zinj* and BK. This method was used to differentiate among experimental models (H-C, F-H, and F-H-H; experimental data from Domínguez-Rodrigo 1997a,b; Pante *et al.* 2012; Gidna *et al.* 2014), and to classify DS data accordingly. MDA was used because it maximizes intergroup variance, therefore enabling factor discrimination, as opposed to Principal Component Analysis (PCA) which maximizes individual sample variance. The MXDA analysis was also selected over other non-linear alternatives, such as quadratic discriminant analysis, because it captures best the discriminant matrix by using linear regression models to transform the response variable and multiple adaptive regression splines to create the discriminating space. This is does not require that the covariance matrix of groups is identical, as LDA does.

Bone surface mark data were bootstrapped prior to MDA through a step-

wise procedure that allows minimization of the error bias. Bootstrapping was carried out by column and for each experimental model separately. A total of 5000 replications were made. Since the analytical variables did not follow a normal distribution and were not homogeneous, a mixture discriminant analysis (MXDA), which allows the use of non-normal distributions, was carried out using the "mda" library of R. The graphic representation of the corresponding biplot was made with the "BiplotGUI" library. This multivariate approach was carried out only on surface mark data of medium-sized carcasses, given that these are most represented at DS, but also due to the fact that no experimental studies on small-sized carcasses exist for the F-H-H model (Domínguez-Rodrigo *et al.* 2014).

2.4.3.3. Machine learning analysis of BSM

In this final section dealing with bone surface modifications, a selection of the most powerful machine learning algorithms available are applied to the experimental dataset on bone surface modification frequencies used previously, with the aim of classifying the DS and the FLK *Zinj* assemblages once more as the result of either primary or secondary access to carcasses by hominins (see section 2.4.6 for a detailed description of each machine learning algorithm). The dataset consisted of 11 features or independent variables (cutmarked upper long bones [CM-ULB], cutmarked intermediate long bones [CM-ILB], cutmarked lower long bones [CM-LLB], cutmarked midshafts [CM-MSH], cutmarked ends [CM-Ends], total number of cutmarked specimens [CM-Total], percussed midshafts [PM-MSH], total number of percussed specimens [PM-Total], tooth-marked midshafts [TM-MSH], tooth-marked ends [TM-Ends], total number of tooth-marked specimens [TM-Total]). Seven machine learning algorithms (Support Vector machines, K-nearest Neighbors, Random Forests, Mixture Discriminant Analysis, Naive Bayes, Partial Least Squares Discriminant Analysis, and Neural Networks) were applied to the bone surface modifications dataset. In all seven analyses the same procedure was followed.

2.4.4. Analysis of the anatomical distribution of BSM on long limb bones using the Hot Zone approach

The exact anatomical location of cut marks, percussion marks, and tooth marks on long limb bones at DS was recorded whenever possible, and plotted on plates depicting each long bone from different sides. Additionally, notes were taken on the distribution of cut marks on hot and cold zones.

The hot zone approach (Domínguez-Rodrigo *et al.* 2007) was conceived for the purpose of creating a frame of reference to address the issue of primary or secondary access to carcasses by hominins using the exact distribution of cut marks on long bones. As such, it constitutes a complementary method to the analysis of cut mark frequencies by element and bone section.

Domínguez-Rodrigo *et al.* (2007) designated different parts of meaty long bones as either a hot or a cold zone, depending on whether flesh scraps were available on those areas after lions had consumed their prey. Hot zones were defined as areas on limb bones where flesh scraps are not present after lion consumption, whereas cold zones represented areas were flesh scraps were observed. Scraps of flesh occur on different parts of the bone on each bone type, since muscles are attached differently to each bone element. The surviving scraps are actually the reflection of the location of muscle attachments to bone. Carnivores pulling flesh off the bone will leave scraps where muscle is most attached to bone surface. This results in areas of each long bone where scraps are documented after carnivore (namely, felid) defleshing (cold zones) and areas without any scrap (hot zones). The occurrence of cut marks on the latter are most indicative of primary access to fully fleshed carcasses.

Thus, zones were assigned numbers depending on bone type: hot and cold zones 1 occur on humeri, zones 2 and 3 on radii-ulnae, zone 4 on femora, and zones 5 and 6 on tibiae (see Domínguez-Rodrigo *et al.* 2007 for a detailed description of each zone). The hypothesis tested is that in secondary access scenarios, the placement of marks is conditioned by the anatomical location of the flesh scraps remaining from felid kills. If hominins were scavenging from defleshed carcasses, cut marks in archaeofaunal assemblages should not appear on areas that do not preserve flesh scraps after lion consumption (i.e. hot zones).

Domínguez-Rodrigo (1999) found that carcasses from lion kills were practically devoid of flesh scraps and that, when present, scraps generally occurred on particular anatomical sections. Flesh remains were present for example on the neck and on the proximal sections of rib cages, and the cranium as well as the metapodials were often left intact. Of those limb bones that preserved scraps, only 8% were upper limb bones, and only 10% of the appendicular bones bearing flesh, presented scraps on the midshaft section, i.e. most of the scraps occurred on proximal or distal sections of the long bones. In experiments modeling primary access to carcasses by hominins, hot zones were cutmarked in broadly similar frequencies than cold zones, although frequencies varied according to bone type (Domínguez-Rodrigo *et al.* 2007). The application of this approach to the *Zinj* archaeofauna served as additional compelling evidence to support the primary access hypothesis, because hot and cold zone frequencies practically mimicked those obtained in experiments of butchery of completely

fleshed carcasses (Domínguez-Rodrigo *et al.* 2007).

Following the guidelines established by Domínguez-Rodrigo *et al.* (2007), cut mark distribution in the DS archaeofauna was analyzed in relation to the defined hot and cold zones. Cut marks potentially inflicted during disarticulation were identified following Nilssen's (2000) and Galán and Domínguez-Rodrigo´s (2013) criteria and removed from this analysis, since these are not related to flesh removal.

2.4.5. The taphotype approach

In a recent study, Domínguez-Rodrigo *et al.* (2015) proposed a new analytical method to study bone damage patterns in faunal assemblages, in order to determine the main taphonomic agent responsible for a certain accumulation, infer hominin-carnivore interactions, and detect the types of carnivores involved in the formation of a site. The approach consists in classifying each meaty long limb element as a certain taphotype, following a morphotypic definition, and comparing the types statistically to actualistic and experimental assemblages using a correspondence analysis.

The term taphotype refers to the form of modification that results from the deletion of a specific portion of a long bone. Carnivores usually gnaw on epiphyseal portions, causing furrowing and the partial disappearence of these soft parts. Domínguez-Rodrigo *et al.* (2015) showed that different carnivore groups create specific taphotypes, while they also share some generic taphotypes. Therefore, they can be differentiated by taphotype frequency and by the distribution of other taphotypes. Carnivores also create different taphotypes depending on carcass size and type, and depending on whether they live in captivity or in the wild. Furthermore, the method reliably discriminates between anthropogenic and non-anthropogenic accumulations. The major advantage of the taphotype approach is that it enables a rapid and automatic classification of a given faunal assemblage. However, further analogical frameworks are needed, especially on bovids belonging to different carcass sizes.

In their paper, Domínguez-Rodrigo *et al.* (2015) distinguished between two classification systems. The first one aims at classifying mainly paleontological and neo-taphonomic assemblages and is used to compare different non-human carnivore types The approach consists in classifying only long limb bone portions or complete limb bones (excluding metapodials) that preserve the complete shaft circumference into one of 15 different taphotypes defined based on the deleted bone portions. The second classification system, also called the single-epiphyses approach, is used on very fragmented human-made assemblages. It is applied by documenting the degree of carnivore damage and furrowing on

epiphyseal portions. Both classifications can occur as one single taphotype or in combination, when damage is documented on independent portions of an element.

The classification of long bone portions as taphotypes was carried out for DS using both classification systems (Tables 2.5 and 2.6), although the second approach is the most appropriate. Since the second classification system creates many taphotypes and hinders the interpretation of the correspondence diagram, I simplified it by combining the taphotypes. The epiphyses characterized by presenting tooth marks (1-4) were merged in category A, all those that presented furrowing (5-8) in category B, and those that presented both type of damage in category C. I left epiphyses without bone damage as category 0 (Table 2.6). All carcass sizes were lumped together for the analysis and no distinction was made between carcass types either in order to avoid small sample sizes.

The DS sample consists of 111 long bone specimens that preserve the complete shaft circumference. Bootstrapped correspondence analyses were carried out using the "cabootcrs" library in R for each element type, and for upper and intermediate limb bones separately. The experimental samples used for comparison are the same samples used in the original study on taphotypes (Domínguez-Rodrigo *et al.* 2015, table 3, p.39). These samples are assemblages com-

Table 2.5. *Description of each of the taphotypes of the first classification system (from Domínguez-Rodrigo et al. 2015).*

Taphotype	Description
0	Complete bone
1	Almost complete bone, including modification of the proximal epiphysis, and involving the preservation of part of it.
2	Deletion of the proximal epiphysis. The following types (up to taphotype 7) assume deletion of the proximal end.
3	Destruction of a part of the shaft, involving at least a minimum of one fourth of the proximal half of the shaft. A second modality of this taphotype is that the destruction of the shaft does not have to be restricted to the proximal half, but can extend to the distal half of the shaft as long as a large portion of the proximal shaft is still surviving.
4	Deletion of approximately half of the proximal half of the shaft.
5	Destruction of the proximal half of the shaft, involving at least also the destruction of a minimum of one fourth of the distal half of the shaft.
6	Complete destruction of the shaft with only the distal end surviving and, possibly, a portion of the immediate near-epiphysis.
7	Same as 6 but with part of the distal epiphysis modified or deleted.
8	Complete bone with partial deletion of the distal epiphysis. This type involves the preservation of part of the distal epiphysis.

9	Complete deletion of the distal epiphysis. The following taphotypes (from 10 to 14) assume the deletion of the distal end.
10	Semi-complete bone with deletion of at least one fourth of the distal half of the shaft. A second modality of this taphotype is that the destruction of the shaft does not have to be restricted to the distal half, but can extend to the proximal half of the shaft as long as a large portion of the distal shaft is still surviving.
11	Deletion of the distal half of the bone.
12	Deletion of the distal half of the bone and a minimum of one fourth of the proximal shaft.
13	Deletion of the complete shaft with only the proximal epiphysis surviving.
14	Proximal epiphysis with part of it deleted or furrowed.
15	Cylinder; shaft complete or semi-complete with both ends missing.

Table 2.6. *Description of the taphotypes of the second classification system and the new categories defined in this study (table modified from Domínguez-Rodrigo et al. 2015).*

Type	Description	New category
0	Lack of modification	0
1	Presence of tooth marks on cranial side	A
2	Presence of tooth marks on caudal side	
3	Presence of tooth marks on medial side	
4	Presence of tooth marks on lateral side	
5	Furrowing on cranial side	B
6	Furrowing on caudal side	
7	Furrowing on medial side	
8	Furrowing on lateral side	
	Presence of tooth marks and furrowing	C

posed of different carcass types (equids, bovids and suids) modified in captivity or in the wild by three different carnivores (lions, jaguars and hyenas). In the analysis using the first classification system, I also included the sample from the Olduvai Carnivore Site (OCS, Arriaza *et al.* 2016). In addition, I also determined the taphotypes of the long bone sample of the KND2 spotted hyena den, which was initially described by Prendergast and Domínguez-Rodrigo (2008). As in the original study on taphotypes, the Sonai assemblage, a bone collection of medium-sized carcasses from a Hadza camp, which was probably also modified by pastoralists (Prendergast 2008), served as the referential framework representing a human-made assemblage.

Domínguez-Rodrigo *et al.* (2015) also included two archaeological samples

from Olduvai Gorge (medium-sized carcasses from BK4 and small carcasses from FLKN) to test the applicability of the method. During a short stay of one week at the National Museum of Dar es Salaam I continued putting together a database documenting the taphotypes for the other Bed I assemblages. I analysed epiphyseal portions of several levels of FLKN, FLKNN, and FLK. However, this task could not be accomplished due to lack of time and the unavailability of some of the fossil boxes. I reached a sufficiently large sample size for FLKN 1-2, but failed to find the boxes with the complete long bones, which were probably stored separately from the rest of the assemblage. Similarly, for FLK *Zinj* the analysed sample is not representative. Therefore, I have not been able to compare DS to the Bed I sites in this analysis, as was originally intended.

2.5. *Mortality profiles*

Mortality profile analyses are useful to assess hominin meat-foraging capabilities as well as their specific prey preferences (e.g. Stiner 1990; Bunn and Gurtov 2014; Marín *et al.* 2017). By comparing mortality patterns generated by the predators with which hominins would have competed, to the age profiles from DS, we can address the issue of whether hominins hunted the carcasses that were accumulated at the site or whether they confrontationally scavenged them from felid kills. This approach entails assuming that modern felids behaved similarly to extinct ones, but studies on predator ecology suggest that the age ranges hunted by large carnivores naturally fall into either a catastrophic or an attritional mortality pattern (e.g. Klein 1982; Stiner 1990), and it seems safe to assume the same for large carnivores in the past. Mortality profiles from ethnographic and archaeological case studies reveal a preference for hunting prime adults, an age range normally not exploited by other predators (e.g. Stiner 1990; Bunn and Gurtov 2014). This means that mortality profiles with a clear bias towards prime-adult individuals would constitute compelling evidence of hominin hunting. However, this assumption must be taken with caution in the light of a prime-adult dominated mortality profile recently obtained in a purportedly lion-accumulated assemblage (Arriaza *et al.*, 2015).

Age profiles have commonly been used to infer hunting strategies. Whereas persistence hunting by endurance running (Bramble and Lieberman 2004; Liebenberg 2006) should yield similar mortality profiles to other forms of cursorial predation, i.e. attritional mortality patterns in which vulnerable young juveniles and old adults predominate, ambush hunting should yield a living-structure mortality profile (if non-selective) or an abundance of prime adults (if selective) (Bunn and Pickering 2010), as is described in more detail below. Thus, mortality profile analyses target two important issues, namely, hunting capability and prey selectivity by hominins.

Mortality profile analyses require careful evaluation. Age profiles can be affected by prey socioecology and environmental factors, and there can be significant variability in prey selection by predators. Thus, I include more than one comparative sample for the same predator when available, and I target age profiles by analyzing them using different grouping systems and statistical methods. The approach is explained in the following sections in detail.

2.5.1. Estimation of the age at death of the sample of ungulates at DS

Ages at death of the bovids represented at DS were estimated through an assessment of teeth eruption and attrition, following the approaches detailed in the following references on modern ungulates. Studies by Spinage (1967; 1976) provide ageing criteria for waterbuck and gazelle; Talbot and Talbot (1963) and Atwell (1980) were used to classify wildebeest remains. The study by Huntley (1979) on ageing criteria for tsessebe (Damaliscus L. lunatus) was consulted also, since it could be used as a proxy for the dental specimens attributed to the extinct species *Parmularius altidens*. However, in this study, ages are only presented for juveniles. Since maturity is reached in tsessebe approximately at the same time as in wildebeest, I used Attwell (1980) also as a reference for *Parmularius*. In fact, Atwell's (1980) method served as a reference for all three Alcelaphini species represented at the site, including *Megalotragus* sp. I also considered using age determination methods for buffalo for this species, but since their longevity is very similar to, if not the same as, that of wildebeest (Grimsdell 1973; Sinclair 1977; Taylor 1988), I aged these specimens using Atwell's (1980) criteria. This decision is of little relevance here, because *Megalotragus* sp. specimens could only be aged approximately. In the case of *Antidorcas*, a complementary method of age determination was used that is based on correlations of age with decreasing molar height in gazelles (Spinage 1976). Accurate age determination of kudu remains was difficult, because the cranial remains of kudu at DS comprise a few fragmented isolated teeth and a few upper molars embedded in a carbonate matrix. Some were visible and two kudu specimens could at least be broadly classified as adult or subadult individuals. A study on ageing criteria in greater kudu (Tragelaphini) by Simpson (1966) uses tooth eruption and wear, skull shape and weight, as well as horn length in males to establish several age classes in this species. However, he only provided details of tooth eruption and wear for subadult individuals and not for adults, the same way Huntley (1979) does for tsessebe, arguing that tooth wear can be significantly influenced by environmental factors (Simpson 1966). He classified adult individuals using skulls and horns only, and the study is therefore of limited use here.

In his studies on the ageing of waterbuck and gazelle, Spinage (1967; 1976) explains his preference for using maxilla for ageing individuals rather than mandibular fragments, because the former show more marked differences with age than the latter. Maxillary fragments are, however, considerably less abundant than mandibles at DS. Therefore, although it is known that tooth eruption rates and wear patterns can diverge slightly between maxillae and mandibles - maxillary dental attrition typically lagging behind mandibular attrition - we also applied these methods to mandibles and included them in the age estima-

tions. This means that there is a possibility that those individuals that were aged using mandibles were in reality somewhat older than what I report here. However, it was necessary to include mandibular specimens, because otherwise, the sample available to determine the MNI would have remained too small. Atwell (1980) does, however, provide diagrams for both upper and lower jaws of wildebeest. Apart from mandibles and maxillae, I also established the approximate age of several isolated well-preserved teeth.

Age determination of *Equus* is usually established using the decreasing height of incisors and the first upper molars (Spinage 1972). Unfortunately, this was not possible at DS, because these elements do not appear to be preserved. Most equid teeth were covered by carbonate, which hindered accurate identification, as well as the visual assessment of wear patterns and crown height in general. However, the visible occlusal surfaces of some molars and premolars, as well as the wear patterns of the incisors, indicate that all three represented individuals had already reached adulthood when they died.

Eruption and attrition scores were recorded for each dental specimen following Bunn and Pickering's (2010b) methodology consisting in distinguishing between not fully erupted or shed teeth, worn teeth, and loss of infundibula, as well as a forth category used to determine whether a specific tooth seemed to be missing due to preservational issues. The results include an absolute age estimation in years for each specimen. This was done in order to facilitate replicating the analysis and, in the case that in the future, detailed studies allow categorizing individuals into different or more adequate age classes than the ones included here. Subsequently, all dental remains for which age could be estimated were laid on a table and arranged by side and taxon in order to estimate the minimum number of individuals (MNI).

2.5.2. Grouping of bovid prey into age classes

Bunn and Pickering (2010b) recommend classifying fossil faunas according to their age into the following stages: "young juvenile", "subadult juvenile", "early prime", "late prime", and "old". The end of the juvenile period is defined by the replacement of the deciduous dentition by the permanent teeth in occlusal wear. Among the juveniles, young juveniles are characterized by possessing worn deciduous premolars and erupting first and second molars, and subadult juveniles by having worn or shed deciduous premolars and erupting or erupted permanent premolars and molars (Bunn and Pickering 2010b). The subdivision into three adult stages Is based on attrition, cementum increments and percentage of PEL (Potential Ecological Lifespan). From this point of view, prime adulthood is divided into early prime, from around 20% to 50% of PEL

(following Klein 1978; 1999), and late prime, from around 50% to 75% of PEL. The boundary between late prime and old individuals is related to the progressive loss of molar infundibula, which represents a challenge, because the timing of the loss of infundibula varies considerably across taxa, and even among the same species within local populations. For example, smaller bovid size groups 1 and 2 present a rapid and early loss of the mesial infundibulum of the lower first molar within the early prime age class, while the same landmark marks the boundary between late prime and old individuals in wildebeest (Sinclair 1977), waterbuck (Spinage 1967), or eland (Atwell and Jeffrey 1981) (Bunn and Pickering 2010b). For example, the loss of the mesial infundibulum from the lower first molar in waterbuck occurs around 9 or 10 years, i.e. similar to wildebeest, which occurs between ages 13 and 15 (at least 72%-83% of PEL, Sinclair 1977), in view of the shorter longevity of the waterbuck. Therefore, the advanced occlusal wear that defines old, physically more vulnerable individuals, and which occurs at around 75% of PEL, is the loss of the mesial infundibulum on the lower first molar of the larger bovids (size 3-4), and of both infundibula on the second molar of some smaller bovids (size 1-2) (Bunn and Pickering 2010). Table 2.7 shows the boundaries between the five different age classes, based on the percentage of PEL and on the timing of loss of infundibula, in waterbucks, gazelles, and wildebeest, which is used as proxy for all alcelaphines. I use this

Table 2.7. *Subdivision into five different life stages of PEL (after Bunn and Pickering 2010) and their correspondence with the absolute ages in years of waterbuck, wildebeest and gazelle.*

	PEL	Wildebeest	Waterbuck	Gazelle
Longevity in years		18	12	11
Age class		**Age in years**		
Young juvenile	0-20%	0 – 2	0 – 1	0 – 1
Subadult juvenile		2 – 3.5	1 – 2.5	1 – 2.2
Early prime	~20 - 50%	3.5 – 9	2.5 – 6	2.2 – 5.5
Late prime	~50 - 75%	9 – 13.5	6 – 9	5.5 – 8
Old	~75% - 100%	13.5 – 18	9 – 12	8 – 11

classification method in this study in order to categorize bovids according to their age and in order to analyze the mortality data from DS, but the categories early and late prime had to be combined for the analysis, because age could not be accurately determined for all adult individuals. Therefore, the age classification system I used for analysis is composed of four age classes: "young juvenile",

"subadult juvenile", "prime adult", and "old". Additionally, for comparative purposes, I lumped the bovids from DS into the three commonly used age classes "young", "prime", and "old" (Stiner 1990), and used the mortality profiles in ternary diagrams, as is usually done in mortality profile analyses (e.g. Bunn and Gurtov 2014; Marín *et al.* 2017; Oliver *et al.* 2019).

Recently, in their age profile analysis of the Olduvai Carnivore Site (OCS), Arriaza *et al.* (2015) proposed adopting a different age class subdivision into five life-stages for wildebeest that was first suggested by Sinclair and Arcese (1995) and which is also based on tooth eruption and toothwear patterns, as well as on cementum growth rings in tooth roots (Watson 1967; Attwell 1980). These five age classes are: yearling (1-2 years), young adult (2-4 years), mature adult (5-8 years), old (8-12 years) and very old (>12 years). According to Arriaza *et al.* (2015) this subdivision including four adult stages is very accurate in determining the most important life changes in wildebeest, and it facilitates the detection of shifts in the diets of lions and spotted hyenas, since they prey on different adult classes (see also Sinclair and Arcese 1995). For this reason, and because some of the available samples of modern carnivore kills are provided following this classification (e.g. Sinclair and Arcese 1995; Mduma 1996; Mduma *et al.* 1999), I additionally grouped the alcelaphines from DS into these age classes.

2.5.3. Comparing age profiles at DS with modern African bovid samples

The bovid age profiles from DS were compared to prey mortality data from several literature sources. On the one hand, I collected data on gazelle and wildebeest kills by lion, leopard, cheetah, spotted hyena and wild dog from the works by Schaller (1972), Sinclair (1977) and Kruuk (1972) from Bunn and Pickering (2010), who provide the information already categorized into their five age class system described above (Table 2.8). These mortality profiles from carnivore kills stem from studies in the Serengeti and were collected during the 1970s. Following the comparative analyses presented in later publications by Bunn and Gurtov (2014) and Oliver *et al.* (2019), I also included several other samples of medium-sized prey of lions, leopards, cheetahs, and wild dogs from a study at the Kafue National Park in Zambia (Mitchell *et al.* 1965), although these were mostly only used for the ternary diagram, because some of the samples lacked information on subadult juvenile prey, which made them less useful for the four-age class multivariate analysis. Prey animals of leopard, cheetah, and wild dog reported by Mitchell *et al.* (1965) were pooled with the Serengeti sample, since the different samples of the same predators showed significant

overlap (Oliver *et al.* 2019). The lion samples showed higher variability and were therefore included as separate samples.

Additionally, I included the age mortality profiles from kudu and impala bow hunting kills by the Hadza in Tanzania and gemsbok kills by the Kua from the Kalahari in Botswana (Bartram *et al.*, 1991; Bartram, 1997) reported by Bunn and Gurtov (2014). With regard to the Kua, these authors state that "hunters employed persistence hunting and snaring, and they used small bows and powerful arrow poison to kill large prey" (Bunn and Gurtov, 2014; p. 48). Since they were very similar, I combined them in a single sample of mortality profiles (in the case of medium-sized carcasses) generated by modern hunter-gatherers. These are samples that have previously been compared to FLK *Zinj* using triangular graphs (Bunn and Pickering 2010; Bunn and Gurtov 2014).

In the following sections, the mortality profiles for small and medium-sized

Table 2.8. *Frequency distribution of carcasses by age (following Bunn and Pickering's (2010b) age classification method) in modern samples of carnivore and human kills used to compare to the age profiles at DS. Samples collected in the Serengeti are from Schaller (1972) and Kruuk (1972), the sample from lion from Zambia was collected by Mitchell (1965), the data from modern hunter-gatherers is presented by Bunn and Gurtov (2014). Data and table structure from Bunn and Pickering (2010b) and Bunn and Gurtov (2014).*

Predator	Prey size	Taxon	Total	Age				
				Young juvenile	Sub-adult juvenile	Early prime	Late prime	Old
						Prime		
Lion	1	Gazelle	204	67	12	82	11	32
						93		
Lion	3b	Wildebeest	262	72	50	78		62
						78		
Leopard	1	Gazelle	30	9	4	15		2
						15		
Cheetah	1	Gazelle	192	124	2	36	8	22
						44		
Spotted hyena	1	Gazelle	98	42		10	25	21
						35		
Spotted hyena	3b	Wildebeest	86	31	15	15		25
						15		
Wild dog	1	Gazelle	65	34	2	19	2	8
						21		

Lion (Zambia)	3	Hartebeest, Kudu, Wildebeest, Waterbuck, Roan, Sable	116	35	4	54	23
Hadza	2	Impala	50	6	9	31	4
Hadza	3b	Greater Kudu	18	3	3	10	2
Kua	3	Gemsbok	13	3	2	7	1

carcasses from DS are included in these comparisons using the three age classes in triangular graphs first, and they are subsequently analyzed using Principal Component Analysis (PCA) and Canonical Variate Analysis (CVA) using four age classes. Wildebeest kills by predation collected by Sinclair and Arcese (1995) and Mduma (1996) in the 1980s and 1990s followed the other classification system into five age classes and were therefore analyzed in a separate comparison using PCA and CVA also. The data are summarized in the work by Mduma *et al.* (1999) (Table 2.9).

By using four or five age classes instead of three and by using more robust statistics, I hope to overcome the limitations of equifinality sometimes yielded by triangular graphs and gain more insight into the differences between carni-

Table 2.9. *Frequency distribution of wildebeest carcasses by age (following Sinclair and Arcese's (1995) age classification method) in modern samples of carnivore kills (lions and hyenas) used to compare to the Alcelaphini age profiles at DS. Data stems from studies by Sinclair and Arcese (1995) – population increase and stationary numbers - and Mduma (1996) - population decline (see also Mduma et al. 1999).*

Predator	Size	Taxon	Total	Yearling	Young adult	Middle age	Old	Very old
Sample from Sinclair and Arcese (1995): collected from 1968 to 1991								
Lion	3b	*Connochaetes taurinus*	57	3	14	20	15	5
Hyena	3b	*Connochaetes taurinus*	43	3	16	9	4	11
Sample from Mduma 1996: collected from 1992 to 1994								
Lion	3b	*Connochaetes taurinus*	29	5	3	12	9	0
Hyena	3b	*Connochaetes taurinus*	13	3	1	3	6	0

vores and humans in prey distribution by age. Simply put, in the next sections, I test the following hypothesis: if hominins scavenged from carnivore kills, more specifically, from lion and/or leopard kills, mortality profiles should coincide with what these felids are known to kill. Beyond this, if the scavenging hypothesis should be falsified, these analyses could help make predictions about the hunting strategies used by hominins. Persistence hunting by endurance running should yield mortality profiles dominated by weaker and more vulnerable individuals (young juveniles and old adults), while ambush hunting should yield mortality profiles that fit the living-structure mortality profile (non-selective ambush hunting) or an abundance of prime adults (selective ambush hunting).

In this analysis, I compare the mortality profiles from DS to those of FLK *Zinj* and FLK background (FLKN 1-2, FLKN 6, FLKNN 2), both in the ternary diagrams and in the multivariate analysis using PCA and CVA. I also include the recently reported age profiles from Kanjera South in the latter (Oliver *et al.* 2019).

2.5.3.1. Triangular graph

In order to visually compare different mortality samples, Stiner (1990) developed a methodology that consists in classifying individuals as juveniles, prime adults or old adults, and in plotting the proportion of each age class on a triangular graph. This method is the most commonly used approach to mortality profile analyses. I generated a ternary diagram with the DS and FLK *Zinj* samples, and the sets of carnivore kills, Hadza and Kua kills. I followed the approach of Bunn and Pickering (2010) and included the sample "FLK background" also, which is composed of mortality data from FLKN 1-2, FLKN 6, and FLKNN2, sites that have little or no significant anthropogenic input and are interpreted as natural background (Domínguez-Rodrigo *et al.* 2007; see also Domínguez-Rodrigo *et al.*, in prep.). Density contours approximating 95% confidence intervals were produced around each sample point using maximum likelihood methods in order to control for differences in sample sizes (Weaver *et al.* 2011). I used the computer software modified triangular graph program developed by Steele and Weaver (2002) to generate separate triangular graphs for small and medium-sized carcasses. The carnivore and modern hunter-gatherer samples used for comparison are presented in Table 2.8.

In their application of this approach to some of the fossil faunas from Olduvai (including FLK *Zinj*), Swartkrans, Kromdraai and Gondolin, Bunn and Pickering (2010a) discarded the first of the five age classes (young juveniles) arguing, among other things, that the teeth of newborns and yearlings are usually not as well preserved in the fossil record as those of older individuals. I believe

that this assumption is flawed since we have found that juvenile teeth and mandibles/maxillae are well-preserved at DS and other Bed I sites. Indeed, very few bones of juveniles are preserved at DS, because they are fragile, but the same is not true for teeth. Hence, including young juvenile dentition in this analysis represents an opportunity to better account for young individuals. What is more, as acknowledged already by Bunn and Pickering (2010) and explained by Domínguez-Rodrigo *et al.* (in prep.), when excluding young juveniles, mortality patterns appear skewed toward adult predominance and are therefore biased. For this reason, I have chosen to include the category of young juveniles in both the fossil sample and the modern carnivore and modern hunter-gatherer referential samples in this analysis, so that, in contrast to the previous mortality profile analysis applied to Olduvai (Bunn and Pickering 2010) for this part of the analysis, I have grouped the first two age classes (young juvenile and subadult juvenile) in a single "juvenile" category, and combined the two prime adult classes (early prime and late prime) into one called "prime adults", as is commonly done (see e.g. Marín *et al.* 2017 or Rodríguez-Hidalgo *et al.* 2015).

In order to interpret triangular graphs it is important to note that the corners of the triangle correspond to strong biases toward each of the three age groups. Since old individuals are usually rare in living populations, cases falling in the upper part of the triangle should be interpreted as significantly biased toward the old age class (Stiner 1990). The lower central region of the triangle represents two important mortality profile models, the U-shaped or attritional pattern occurs on the left part, and the living-structure or catastrophic model, which occurs in the right side of the region. Mortality profiles characterized by a predominance of juveniles (and old) individuals can be produced by disease, malnutrition and accidents, or any process that can have a greater effect on more vulnerable individuals. The catastrophic profile mimics the structure of a living population, which is characterized by a predominance of prime adults. Cases of mass deaths can create such profiles (e.g. Klein 1978; 1982; Voorhies 1969; Stiner 1990).

Large carnivores can also be broadly classified into these two mortality profile groups based on the way they usually select and capture prey. Cursorial predators like hyenas, cheetahs and wild dogs produce attritional mortality patterns, while ambush predators are often associated with catastrophic mortality patterns, because the selection of prey is determined by chance encounter (e.g. Bertram 1979; Kruuk 1972; Schaller 1972; Stiner 1990). The fact remains that there can be considerable variation in predator behavior depending on environmental conditions or prey population structure, but this approach has proven to be useful to contrast human patterns of prey selection (Stiner 1990)

2.5.3.2. Principal Component Analysis (PCA) and Canonical Variate Analysis (CVA)

In addition to the triangular graph, I applied Principal Component Analyses (PCA) and Canonical Variate Analyses (CVA) to the same samples using the four age class system explained above. As with the triangular graph, I carried out separate analyses for small and medium-sized carcasses. Subsequently, I compared the Alcelaphini subsample from DS and the carnivore samples from Table 2.9, following the procedure outlined by Arriaza *et al.* (2015) using the five age class system they used to analyze the age profiles from the wildebeest accumulation at OCS.

Prior to these analyses, the original data of each variable in each sample was bootstrapped 100 times. A CVA transforms the original variables (in this case the four or five different age classes) into canonical variables defined by square distances between the means of the groups obtained by Mahalanobis's D. Like a PCA, a CVA then produces factors that result from the reduction of dimensionality of these multiple variables. Biplot axes are determined by the group means. The degree of separation that is produced by a CVA between these group means is higher than in a PCA. A PCA produces results that maximize sample variance (Arriaza *et al.* 2015). Analyses and biplots were carried out using the "BiplotGUI" R library and each sample was displayed with a 95% confidence interval ellipse.

Spatial analysis

2.6. General spatial assessment of the DS point pattern

The spatial statistical analysis of DS explained here draws ideas and methods from two previous spatial studies on DS, PTK, and FLK *Zinj* (see Domínguez-Rodrigo *et al.*, 2017b, and Domínguez-Rodrigo and Cobo-Sánchez, 2017b). In the first study, spatial statistical regression models were used to predict where the densest unexcavated concentrations of materials might lie at DS at a time when the site was not yet clearly delimited (Domínguez-Rodrigo *et al.*, 2017b). In the other study, the application of spatial statistical tools to the sites of PTK and FLK *Zinj* proved to be a very useful and insightful approach to understand hominin socio-economic behavior at these sites. Based on the dense single cluster pattern that characterizes both sites, the study showed that the socio-economic organization of early humans differed from that of modern foragers (Domínguez-Rodrigo and Cobo-Sánchez, 2017b).

The present study addresses similar issues and is subdivided into three parts, which incorporate some novelties with regard to the aforementioned analyses. In the first part, the DS point pattern is explored by examining the point process intensity and the effect of the paleosurface topography on the spatial distribution of archaeological remains. Complete Spatial Randomness (CSR) and interpoint interaction are also evaluated. Initially, all points are considered together, then the point pattern is split by mark type with the purpose of comparing the spatial patterning and the probability densities of stone tools and bones separately and addressing their spatial inter-dependence or covariation. In addition to this non-parametric approach, several regression models are fit to the data in order to make predictions of the distribution of the archaeological materials in the eroded part of the site.

2.6.1. Estimating the intensity of the DS spatial point pattern using non-parametric methods

2.6.1.1. Testing for Complete Spatial Randomness

The first step in exploring a spatial point pattern dataset is usually to estimate the intensity function of the point process. Intensity refers to the expected density of points per unit area, and it can be constant or spatially varying. Deciding whether points are distributed throughout the spatial window homogeneously, with points lacking spatial preference lying proportionally in a given region, or whether the density is a function of spatial location, is part of testing if the point pattern is the result of a completely random process (Baddeley *et al.*, 2015). Complete Spatial Randomness (CSR) is an important term in spatial statistics. The concept implies that the probability density function of an observed point pattern is constant over the study window and that points are independent, which means that the outcome in one region is not influenced by the outcome in other regions (Diggle, 2003; Illian *et al.*, 2008; Baddeley *et al.*, 2015; Smith *et al.*, 2015). Usually, CSR serves as a null hypothesis and reference against which other models can be compared.

Given that the intensity variation throughout the window is very marked in this case, formal tests are not strictly necessary here to reject the null hypothesis of CSR. However, the following tests can be used. One option is using power divergence tests based on quadrat counts (Cressie and Read, 1984), which involves dividing the spatial window into tessellations of the same area. Due to the irregularity of the DS window and its somewhat semicircular shape, we created a function using the arc-tangent to calculate the angle between the x-axis and the vector from the origin to a certain coordenate (x,y) and divide the window in the same way as a cake. We divided the spatial object into five tessellations. Each tessellation should have enough points, otherwise the test can yield unreliable estimates. Apart from the chi-squared test, the Freeman-Tukey statistic (CR=-1/2) and Neyman's modified statistic (CR=-2) were used.

Other tests for CSR use Monte Carlo simulations, like the quadrat test or the Clark Evans test, which is based on the Clark Evans aggregation index (Clark and Evans, 1954). The latter calculates the ratio of the observed mean nearest neighbour distance to that expected for a Poisson or CSR process of the same intensity. We used the cumulative distribution function method for the edge correction. In theory, K=1 indicates clustering (the closer to one the more marked the cluster is) . However, the Clark Evans index is very sensitive to inhomogeneity, which means that a significant result from this test does not necessarily indicate clustering in this case, because the pattern is very inhomogeneous. A better alternative is to use the Hopkins-Skellam test, which is much

less sensitive to edge effect bias and spatial inhomogeneity. It calculates the nearest-neighbour distances and compares them with the nearest-neighbour distances of completely random patterns (Hopkins and Skellam, 1954). A significant result would indicate that the point pattern is not completely random, and that the following analysis should choose methods that assume an inhomogeneous Poisson process as the null-hypothesis.

2.6.1.2. Kernel estimation and density maps

The fact that intensity is spatially varying means that it can be described as a function of spatial location, which can be estimated from the data. This is done here non-parametrically by using kernel estimation choosing different smoothing bandwidths. The smoothing bandwidth is the standard deviation of the kernel function. A larger bandwidth gives more smoothing, and a smaller bandwidth means higher variance. There are several algorithms which perform automatic bandwidth selection. Any bandwidth selection rule is based on assumptions about the dependence between the points, therefore choosing an appropriate bandwidth can be challenging. For example, the likelihood cross-validation function assumes an inhomogeneous Poisson process, and the Diggle and Berman's mean square error cross-validation method assumes a Cox process, which is more clustered than a Poisson process (Baddeley *et al.*, 2015).

The methods used here to produce an accurate estimate of the DS point pattern intensity are described in Table 2.10. Apart from fixed-bandwidth smoothers, which use the same kernel and the same bandwidth to produce intensity estimates at different spatial locations, we can use variable bandwidth smoothing or adaptive smoothing, with the intention of avoiding the problem of oversmoothing in the areas of high intensity and undersmoothing in the low intensity areas. This is especially an issue when intensity varies greatly across the spatial window, as is the case at DS.

2.6.1.3. Statistical significance of hot spots

The density maps show that observations concentrate in three high density areas of the excavation window. These zones of elevated intensity can be seen as anomalies, so-called hot spots, in the point pattern. A scan test (Kulldorff 1997; Baddeley *et al.*, 2015) was performed to look for evidence of elevated intensity inside circles of fixed radius and to test whether the intensity in these areas is statistically different from the intensity outside the circles. The scan test uses a likelihood ratio test statistic to assess whether the intensity is similar inside and outside the circle. The test was performed with a fixed radius two times the sig-

ma value yielded by the likelihood cross-validation method, and the p-values were computed for all locations.

2.6.2. *Measuring the effect of the paleosurface topography on the distribution of archaeological materials*

We also tested whether the distribution of points could be correlated to the paleosurface topography. If archaeological materials were to be found preferentially on higher topographic areas, this would be indicative of low post-depositional disturbance, and the topography could then be used to describe or model the spatially varying intensity. For this purpose, the elevation values (z-values) of the archaeological objects were first interpolated into an expand-

Table 2.10. *Selected smoothing bandwidth methods to estimate the DS point pattern intensity*

Fixed bandwidth	**References**
a) Likelihood cross-validation method. The bandwidth is chosen to maximise the point process likelihood cross-validation criterion. This algorithm assumes an inhomogeneous Poisson point process. (We adjusted the selected bandwidth by multiplying it by 2, which provides a more appropriate density map.)	Berman and Diggle, 1989; Baddeley *et al.* 2015
b) Cronie and van Lieshout's criterion based on Cambell's formula. The bandwidth is chosen to minimise the discrepancy between the area of the observation window and the sum of reciprocal estimated intensity values at the points of the point process.	Cronie and van Lieshout, 2018
c) Diggle and Berman's mean square error cross-validation method. The bandwidth is chosen to minimise the mean-square error. This algorithm assumes a Cox process	Berman and Diggle, 1989; Diggle 2003; Baddeley *et al.* 2015
Variable bandwidth	**References**
d) The adaptive version of this function computes Abramson's (1982) variable-bandwidth estimator using a fixed bandwidth (in this case the one computed using the likelihood cross-validation method)	Abramson, 1982; Davis and Baddeley, 2018
e) This density function computes an adaptive estimate of the intensity function of the point pattern using Voronoi/Dirichlet tessellation. For each tessellation the number of points are counted and divided by the area of the same tile. Then an estimate of the intensity of the point pattern is calculated by dividing the result by 1-f (the fraction of the point pattern used to create the tessellations)	Ogata *et al.*, 2003; Ogata 2004; Baddeley 2007
f) This function estimates the intensity using the distance from each spatial location to the kth nearest data point. It can handle wide variation in the intensity function. It implicitly assumes that points are independent, so it does not perform well if the pattern is strongly clustered or strongly inhibited.	Baddeley *et al.*, 2015

ed grid using kriging to create the topography covariate. As a first exploratory step, the excavation area was split into four different sub-regions of equal area according to the topography to count the points at different topographic elevation intervals. Then the "rhohat" function was applied, which estimates the intensity of the point pattern as a function of the covariate and generates a plot that shows the estimated function together with 95% confidence bands assuming an inhomogeneous Poisson point process. Three tests of goodness-of-fit were used to compare the observed and predicted distributions of the values of the spatial covariate: the Kolmogorov-Smirnov test, the Cramer-von Mises test and the Anderson-Darling test. The ROC curve and the area under the curve (AUC) were calculated as well in order to estimate the strength of the influence of the topography on the point pattern intensity.

2.6.3. Correlation and point inter-dependency

2.6.3.1. Testing the type of inhomogeneity of the DS point pattern: correlation-stationary or locally-scaled?

Correlation and inter-dependency between points is usually approached using empirical summary functions, such as the K-function, because they convey information across a range of spatial scales. The K-function, for example, yields the average number of observed points lying within a distance r of each data point, standardized by dividing by the intensity (Baddeley *et al.*, 2015). A weakness of this function is that it requires the intensity function to be accurately estimated, an inaccurate estimate of intensity could lead to a false significant result. The inhomogeneous K-function further assumes that the process is correlation-stationary, i.e. the inhomogeneous K-functions from different quadrats or subpatterns are similar, so its use is only recommended if this is true. The way of testing this assumption is to divide the spatial point pattern into several point patterns using quadrats or tessellations and to estimate the inhomogeneous K-function in each point pattern. If the process is correlation-stationary, then these functions should yield similar results. I transformed the DS point pattern into a hyperframe containing a series of subpatterns, which were grouped into patterns with high and low intensity. Tessellations were again created by cutting the window as a cake, at different angles from a point of origin outside the excavation window. Then, a studentised permutation test was applied. Since this test also requires an accurate estimate of the intensity, several tries were made using most of the above-mentioned smoothing bandwidth selectors.

An alternative to the inhomogeneous K-function would be the locally-scaled K-function, which assumes that the point pattern is a locally scaled version of

a stationary process (Baddeley *et al.*, 2015). The difference between the two functions is that the inhomogeneous K-function assumes that the scale of interaction between points remains constant at different spatial scales, while the intensity varies, whereas the locally-scaled K-function assumes that the point process is in small regions a rescaled version of a stationary and isotropic process. Here only the rescaling factor varies from place to place. A studentised permutation test was performed for this function using different sigma values as well.

2.6.3.2. Application of the inhomogeneous K-function, the locally-scaled function and further summary functions to the DS point pattern

Some of the results of the tests described above indicated that the inhomogeneous K-function and the locally-scaled K-function could be used to determine whether the point pattern is random, clustered or regular, if certain intensity estimates are used.

The inhomogeneous K-function was calculated using Cronie and van Lieshout's criterion for the intensity estimate and compared to the K-function of an inhomogeneous Poisson process made with the intensity function of DS. The procedure used to compute an inhomogeneous K-function is exactly the same for the simulated Poisson pattern as for the data. In order to test whether the deviation from the inhomogeneous Poisson line was statistically significant I used the envelope function creating a number of Monte Carlo simulations (nsim = 39) of inhomogeneous Poisson processes whose intensity functions were estimated using the same bandwidth as for the DS point pattern. This ensures that the DS and the inhomogeneous Poisson curves are comparable, and that the corresponding envelopes support a valid Monte Carlo test of the null hypothesis.

The same procedure was followed to calculate the locally-scaled K-function and several other summary functions that are analogous to the inhomogeneous K-function or derived from it. The inhomogeneous L-function is the square-root transformation of the K-function. The G-function calculates the nearest-neighbor distances, the F-function estimates the distances from the empty spaces to the nearest points, and the J function is the combination of both (Baddeley *et al.*, 2015). It is possible that bones and lithics have completely different spatial distributions, and that their different types of inhomogeneity are blurring the results. Thus, I applied these summary functions again to the point patterns of bones and lithics separately.

2.6.3.3. The inhomogeneous pair-correlation function

The K-function is often difficult to interpret or ambiguous because its values contain contributions for all interpoint distances less than or equal to r. An alternative is the pair-correlation function (which is effectively a standardized derivative K-function) (Baddeley *et al.*, 2015). I applied the inhomogeneous version of this function to the DS point pattern using the divide-by-d estimator, which performs better for small r values.

2.6.4. The relative spatial distribution of bones and lithics

2.6.4.1. Estimating the intensity and the spatially-varying type distribution of bones and lithics

The intensities of the spatial patterning of bones and lithics were estimated using the bandwidth selection methods from above. As for the overall DS point pattern, the scan test and hot spots analysis were applied to the separate spatial pattern of bones and that of lithics. These tests were again performed with a fixed radius two times the sigma value yielded by the likelihood cross-validation method, and the p-values were computed for all locations.

We estimated the spatially-varying type distribution or relative risk of the multitype point pattern including fossil bones and stone tools. The estimation of relative risk uses cross-validation to select an appropriate smoothing bandwidth. I tried the three different available cross-validation methods. Tolerance contours for the relative risk or type probability distribution, which are curves drawn around the regions where the estimated probability of a given type is significantly different from the average proportion, were also computed (Hazelton and Davis, 2009). Significance was assessed by a Monte Carlo test. The procedure is as follows: The point pattern is first randomly relabeled (i.e. the marks attached to the points are randomly permuted) and the type probability or relative risk is computed for the relabeled data. This is repeated n times, yielding n images of the probabilities of the mark types. A Monte Carlo test is computed at each pixel. I carried out 19 simulations, which produces values that are multiples of 1/20 = 0.05 (Baddeley, in prep.).

2.6.4.2. Correlation between bones and lithics using approaches based on nearest neighbors

Methods like the inhomogeneous K-function are unstable in some cases and depend on a very accurate estimation of the intensity. Since spatial varia-

tion in the DS point pattern is extreme and hard to estimate accurately, it is a challenge to determine the type of correlation between bones and lithics using methods like the inhomogeneous cross-type K-function or the i to any Kdot function. The use of summary functions and other methods depending on spatial location yielded different conclusions in our analysis depending on bandwidth selection and other operational choices (like edge correction estimates). Since they are vulnerable to the choices we make, the answer is very sensitive in terms of robustness. Approaches based on nearest neighbor distances should be more robust against spatial variation, because they do not involve estimating the intensity of the point pattern.

The nearest neighbor equality function is a newly developed tool that is analogous to the inhomogeneous cross-type K-function, but uses counts of nearest neighbors of a certain type. The method counts the proportion of neighbors of a certain type against the order of the neighbor. It is based on the nearest-neighbor correlation, which is a robust method that can be applied to stationary and non-stationary processes. The nearest neighbor equality function has two versions: cumulative and non-cumulative. The non-cumulative version is equivalent to computing the nearest-neighbor correlation, but when the cumulative proportion is calculated, the graph shows the fraction amongst the kth nearest neighbors, which have a specified type. This use of this function is very convenient, since it does not operate with the spatial location of the points or their distances, and is therefore not dependent on the intensity of the point pattern. The envelopes are effectively generated by keeping the positions of the points fixed and shuffling only the labels of the points (Baddeley, in prep.).

The mark connection function calculates the ratio of the bivariate pair correlation (gij) and the unmarked pair correlation (g) and shows the resulting conditional probability that two points lying together are of the same or different types. The mark equality function is defined as the sum of the mark connection functions between all pairs of points of the same type. It also measures the dependence between types of two points lying at a distance r. When f=1 there is a lack of correlation, i.e. the marks attached to the points of the point pattern are independent and identically distributed (Baddeley *et al.*, 2015). I also performed a Monte Carlo test of spatial segregation of the two types of remains with 39 simulations (Kelsall and Diggle, 1995; Diggle *et al.*, 2005).

2.6.5. Simulation of the point pattern outside the excavation window through statistical modelling

In this section I use parametric statistical models to describe the point process. The aim here is to understand how the point pattern depends on certain covariates and find a good approximation to reality by comparing models that include or omit particular terms that refer to these variables. The model that

fits the data best can then be extrapolated to the area surrounding the site, in order to make predictions of the part of the site that might have been lost to erosion or in order to predict where dense concentrations of archaeological materials may lie that have not yet been uncovered (Domínguez-Rodrigo *et al.*, 2017b). There are several other advantages of statistical modelling when compared to summary statistics. A very important one is that there are no implicitly imposed assumptions about the point pattern, these are stated openly as the analysis progresses (Baddeley *et al.*, 2015). It is also a very powerful and flexible way to analyze the data, because it allows to adjust for effects that could alter or bias the analysis. For example, from the previous analyses we know that the point pattern is strongly inhomogeneous, that the effect of the topography has a significant effect on the distribution of remains, that the point pattern is clustered, and that bones and lithics have different intensity functions. I therefore primarily explore models that take these aspects into account.

2.6.5.1. Inhomogeneous Poisson models

Table 2.11 lists the regression models that were fit to the DS data. The first regression (F1) is a linear model dependent on the covariate topography, which can be measured at all spatial locations. To account for the great amount of inhomogeneity of the point pattern, we turned this model into a cubic polynomial regression (F2), and we added the Cartesian coordinates as covariates in models F3-F6. The fact that bones and lithics have different intensity functions is included in models F5-F7 by adding a term of interaction between the marks (Table 2.11). The first four models were compared using Analysis of Variance (ANOVA) and the Akike Criterion (AIC). Regression model F4 was then used to simulate a spatial pattern inside the window of DS.

Table 2.11. *Different regression types used.*

Regression type	Formula
Linear	F1 <- ppm(DS~top)
Cubic polynomial	F2 <- ppm(DS~polynom(top,3))
Cubic polynomial	F3 <- ppm(DS~polynom(x,y,3))
Cubic polynomial	F4 <- ppm(DS~polynom(x,y,3) + top)
Cubic polynomial with interaction between marks	F5 <- ppm(DSm~polynom(x,y,3)*marks + top)
Cubic polynomial with interaction between marks	F6 <-ppm(DSm~polynom(x,y,3)*marks
Cubic polynomial with interaction between marks	F7 <- ppm(DSm~polynom(top,3)*marks
Cox process; cubic polynomial	F8 <- kppm(DS~polynom(x,y,3) + top, "LGCP")

2.6.5.2. Simulation of Cox Process

Clustering was detected in previous sections using non-parametric methods, which suggests that points are not independent as would be required by Poisson process modelling. Therefore, following Domínguez-Rodrigo *et al.*'s (2017b) methodology, we also produced a Cox process model, which takes this inferred dependency between points into account (Guan 2006; Waagepetersen 2007). A Cox process is produced in two stages. First, a certain intensity surface with clusters is generated and then the point pattern is produced using that intensity surface. We used the method Log Gaussian Cox Process to generate the intensity function based on random fields, which have spatially varying intensity with high and low point density areas (Moller *et al.*, 1998). Then we simulated a random point pattern outside the excavated window. This simulated point pattern uses the calculated spatial trend to produce a Cox process outside the window, but each simulation uses a different intensity function. Ideally, however, simulations should be data-dependent. This means that a conditional simulation of the point pattern in the new window given the point pattern in the excavated window would more realistically reproduce the distribution of archaeological materials. This method is not yet available in the "spatstat" R library at the moment of writing, and this type of simulation is therefore not implemented. However, differences between one simulation and the other would probably only be detectable at the locations near the edges of the window, but would not affect the general spatial trend. We consider the presented simulation therefore adequate and sufficient in this case.

2.7. Spatial analysis of high density areas

One of the most relevant results of the previous section of the spatial analysis is that three significant cluster areas of archaeological material at DS (level 22B) were identified, as opposed to the single cluster documented at FLK *Zinj* and at PTK (Domínguez-Rodrigo and Cobo-Sánchez, 2017a) (Figure 2.1). The clusters at DS occur on different regions of the site, they appear to be separated by similar distances, and seem to be of similar sizes. But are they really that similar and what does this type of spatial pattern represent in terms of hominin behavior? It is possible that the multi-cluster spatial distribution of remains at DS is a direct result of having been occupied for a longer period of time or more intensively than the two other sites. Alternatively, this spatial pattern could be reflecting the use of this location for several different socioeconomic activities that may or may not have been completely synchronic. Fortunately, the extension of the site and the large amount of recovered remains allow for further detailed spatial exploration.

In modern hunter-gatherer campsites food refuse also appears in multiple clusters; however, these are directly correlated to the number of households or domestic areas that exist in the camp (Domínguez-Rodrigo and Cobo-Sánchez, 2017b). It is rather unlikely that Oldowan hominins were organized socially in nuclear families, as modern foragers do, so the multi-cluster pattern at DS should be explained along different lines. The single cluster pattern documented at PTK and FLK *Zinj* would support that food was probably processed and consumed collectively on a communal area rather than on separate areas resulting from a household-like individual use of the space by split units of the hominin group. Moreover, since archaeological sites are palimpsests, it is probable that the clusters reflect redundant occupations, maybe more so than modern campsites (Domínguez-Rodrigo and Cobo-Sánchez, 2017b). This should produce significant differences between cluster areas in hunter-gatherer campsites and those from early Pleistocene archaeological sites, which would reflect differences in the social dynamics of early Pleistocene hominins and modern humans.

The spatial properties of debris accumulated in the Olduvai hominin sites also involve clustering patterns, which in itself constitutes evidence of the

non-random spatial organization of hominin behavior. What are the characteristics of these clustering areas at early archaeological sites, as opposed to the cluster patterns in modern forager camps, and can these spatial features be used to infer different behaviors, site functions or site formation processes? The following section presents a new approach to address these questions.

2.7.1. Spatial comparison of the high intensity spots at DS to the clustering areas of FLK Zinj, PTK and several modern hunter-gatherer campsites

In this comparative analysis, the objectives are twofold: to find and describe the main differences between the clusters generated by modern foragers and by hominin groups, and to contrast the clustering areas from DS to the ones observed at FLK *Zinj* and PTK, and examine whether the three clusters at DS are more similar to each other than they are to the other sites or vice versa. Given that these anthropogenic sites not only share similar taphonomic histories, but also occur on the same stratigraphic clay unit as DS and even in very similar environments, it makes sense to expect that they might also share similarities in their spatial configuration. In this respect, the joint spatial analysis of these three sites represents an exceptional opportunity to try to understand the use of space and the social behavior of Oldowan hominins.

The approach applied consists of isolating the major statistically significant clustering areas of each spatial pattern and comparing them based mainly on a number of selected cluster parameters. The list of spatial features used in this section includes absolute and relative variables related directly with the cluster areas, the spatial distribution of the points they contain, such as the perimeter, diameter, and area of the cluster, or the mean intensity and the mean distance between the points inside the clustering zone, as well as variables that account for the relation between the cluster and the remaining spatial window. I initially considered including summary function estimates and several p-values from different statistical tests used to describe all the point patterns, yet these values turned out to be too similar to be useful to detect differences. Moreover, a preliminary comparison between FLK *Zinj* and PTK showed that based on these variables, both assemblages share a very similar spatial configuration characterized by a positive correlation between the points and one main large cluster area (see previous section and Domínguez-Rodrigo *et al.* (2017b) for the results of these estimations and more information on the spatial analysis of DS, and Domínguez-Rodrigo and Cobo-Sánchez (2017a, b) for the spatial analyses of FLK *Zinj*, PTK, and several modern forager campsites). This is why it seems

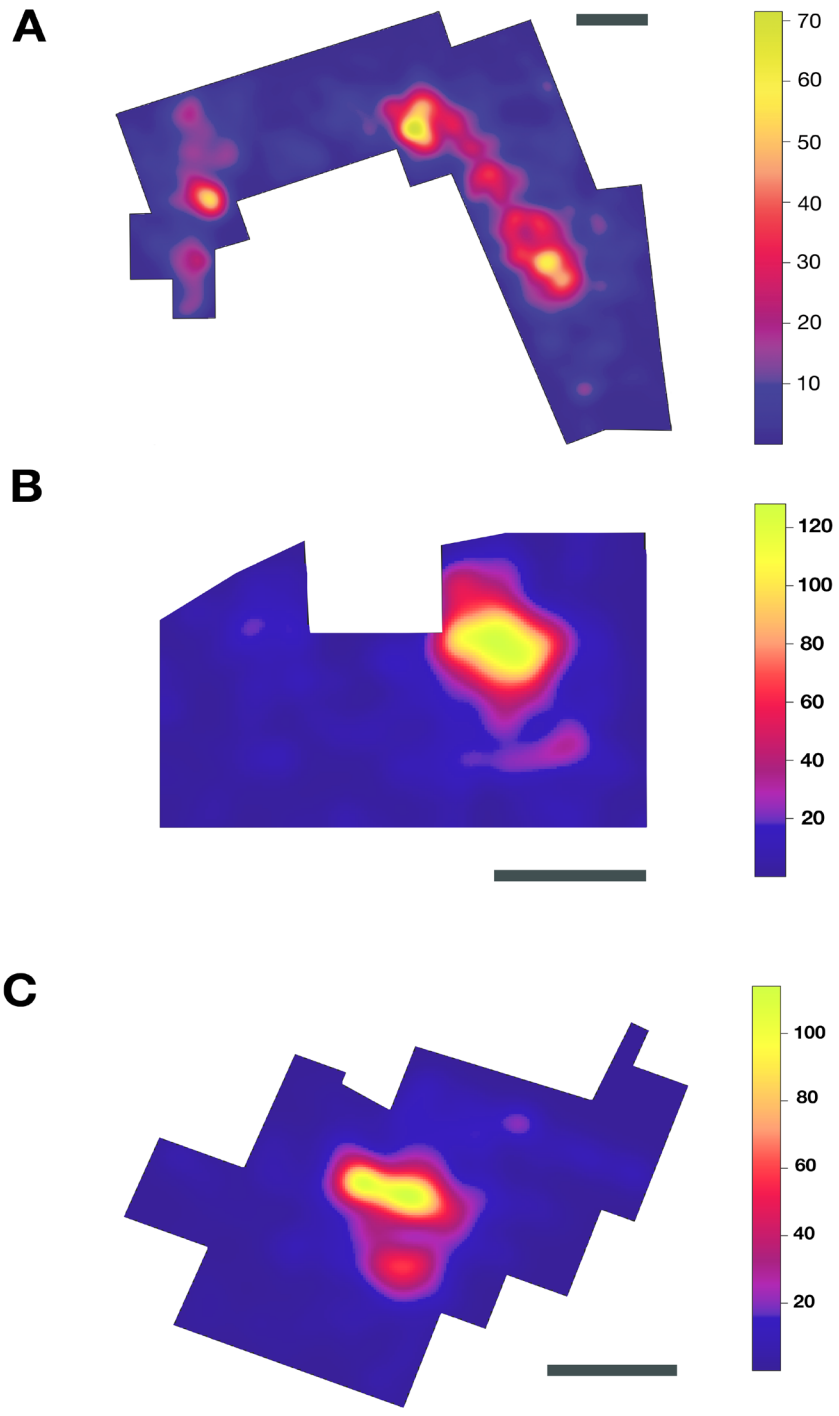

FIGURE 2.1. *Density maps of the archaeological materials at a) DS b) FLK Zinj and c) PTK. Scales: 5 meters.*

appropriate to expand the number of variables used in these spatial analyses to include more specific measurements in order to examine the singularities of each site and the links among the assemblages more closely. In addition, clusters contain most of the archaeological materials and we expect them to be more informative about the behavioral processes that generated them than the scattering areas or the overall spatial patterns.

The selected set of Kua (Bartram *et al.*, 1991) and !Kung (Yellen, 1977) foraging camps has also been previously spatially analyzed by Domínguez-Rodrigo and Cobo-Sánchez (2017b). These camps were selected, because maps of material debris (bone fragments) and information about the camp, the number of occupants, and the duration of the occupation were available. Camp 1 (Kanni//am//odi: household 7) was occupied by three households (each with their own hearth) during a dry season (Bartram *et al.*, 1991). Camp 2 (oabe 1) was occupied by 14 people during a rainy season and had three main hearths that were used as the location for butchery and consumption of carcasses. Interestingly, Bartram *et al.* (1991) found that axial and appendicular remains had a different spatial distribution. Whereas axial bones appeared clustered around nuclear

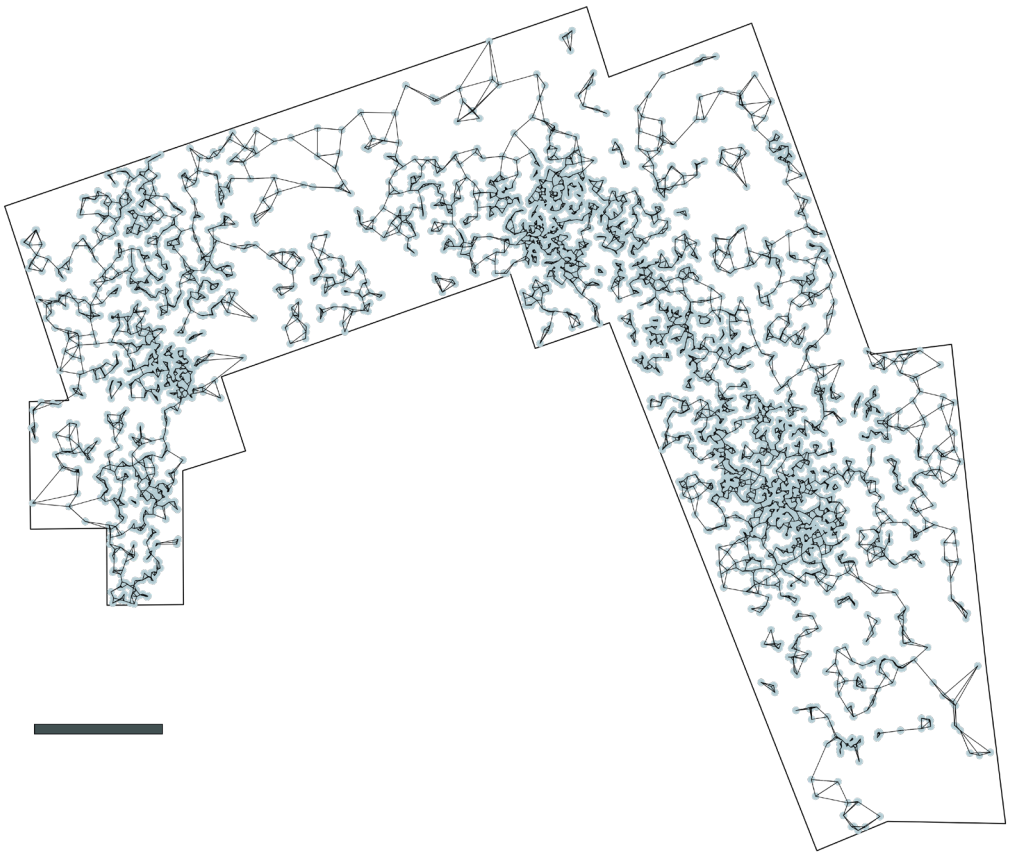

FIGURE 2.2. *K-nearest neighbor graph of the DS point pattern generated with a K value of 3.Scale: 5 meters.*

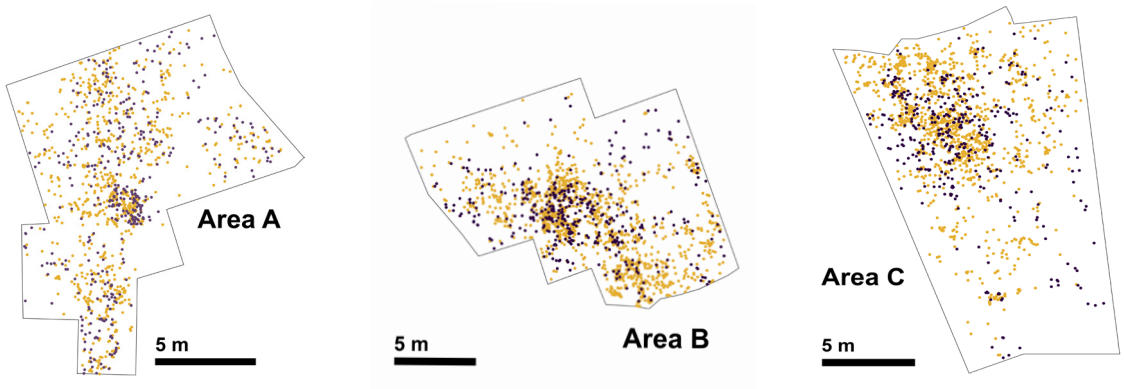

FIGURE 2.3. *From left to right, areas A, B, and C from DS. Yellow dots represent bone remains, purple dots represent lithic artifacts.*

areas, appendicular elements were found more scattered in the areas of primary refuse close to the hearths. Camp 3 (Kunahajina) was first occupied for a few days and later reoccupied for three months. Most carcasses (over 20) were introduced in the camp and accumulated by seven domestic areas in clusters associated with food consumption. Secondary refuse areas in the form of scatters were generated when cleaning the front of the huts. Finally, Camp 4 (//Gakwe Dwa 2), the !Kung camp, was occupied by seven households for a few days in July. Honey gathering took place more often than hunting, but enough remains were deposited on the ground to make the spatial patterns of the households visible. The four selected camps represent a range of short (days) single occupation and long (months) multiple occupation camps (Domínguez-Rodrigo and Cobo-Sánchez 2017b).

Prior to estimating the cluster variables of DS, the assemblage was subdivided into three similarly-sized areas, each one containing one cluster. In order to find an appropriate subdivision of DS into clusters I used a k-nearest neighbor graph, although there are other similar techniques that can be used, like the sphere of influence-graph or the DBSCAN algorithm (Ester *et al.*, 1996; Argote-Espino *et al.*, 2012), which help detect holes or gaps in the spatial pattern and identify clusters of points in space (Illian *et al.*, 2008; Chiu and Mochanov, 2003; Smith *et al.*, 2015). The K-nearest neighbor graph connects the points with segments to their K nearest neighbors. I used a K value of 3, in line with recommendations by others (e.g. Illian *et al.* 2008; Smith *et al.*, 2015), and cut the DS spatial pattern into zones A, B, and C through the emptiest areas of the spatial object (Figures 2.2 and 2.3).

In order to calculate the cluster parameters of the main clusters in each spatial pattern, the statistically significant cluster areas were first isolated by performing a spatial scan test (Kulldorf, 1997) with a sigma value two times

Table 2.12. *List of variables used for classifying the three sites and the four hunter-gatherer campsites according to their form of clustering. A) Variables related with the main clusters. B) Variables related with the overall spatial window. C) Variables used to describe the relation between the clustering area and the overall window. D) Variables used to describe the correlation between the cluster of bones and the cluster of lithics in the overall spatial point patterns including both types of material debris.*

A

Cluster parameters		
	Name	**Description**
1	Area cluster	Area of significant clustering
2	Diameter cluster	Cluster diameter
3	Perimeter cluster	Cluster perimeter
4	Intensity cluster	Mean intensity inside the cluster
5	Peaks cluster	Number of peaks inside the cluster
6	Distance boundary cluster	Standardized value of the mean distance of the points inside the cluster to the cluster boundary (in relation to the cluster diameter)
7	Distance centroid cluster	Standardized value of the mean distance of the points inside the cluster to the cluster centroid (in relation to the cluster diameter)
8	Distance neighbors cluster	Standardized value of the mean distance between the nearest neighbors inside the cluster (in relation to the cluster diameter)
9	Perimeter/diameter	Ratio between the perimeter and the diameter of the cluster
10	Length/breadth	Ratio between the maximum length and maximum breadth of the cluster

B

Spatial window parameters		
	Name	**Description**
11	Number clusters window	Total number of clusters
12	Distance neighbors window	Mean distance between nearest neighbor points in the complete spatial window
13	Area window	Total area of the spatial window
14	Distance centroid window	Standardized value of the mean distance of all the points in the spatial window to the cluster centroid (in relation to the site's diameter)
15	Intensity window	Mean intensity of the spatial window
16	Area secondary clusters window	Mean area of the secondary areas in which clustering is significant (each cluster area must be > 1m2)

C

Relation between cluster and window		
	Name	**Description**
17	Percentage area cluster	Percentage of the cluster area in relation to the area of the complete spatial window
18	Percentage diameter cluster	Percentage of the cluster diameter in relation to the diameter of the complete spatial window
19	Percentage perimeter cluster	Percentage of the cluster perimeter in relation to the perimeter of the complete spatial window
20	Intensity cluster/Intensity window	Ratio between the mean intensity inside and outside the cluster
21	Area secondary clusters/Area cluster	Ratio between the mean area of the secondary clusters and the main clustering area

D

	Name	**Description**
22	Overlap bone cluster and lithic cluster/No overlap area	Ratio between the area where bones and lithics overlap (intersection) and the area in which they do not overlap (i.e. intersection of bones with the complement of lithics)
23	Area bone cluster/ Area lithic cluster	Ratio between the cluster area of bones and the cluster area of lithics
24	NN-correlation (norm.)	Nearest neighbor correlation (normalized value)
25	NN-correlation (unnorm.)	Nearest neighbor correlation (unnormalized value)
26	Percentage overlap	Percentage of intersection or overlap area between the bones and the lithics cluster areas in relation to the total area of the spatial window
27	Percentage no overlap	Percentage of the area where the clusters of bones and lithics do not overlap in relation to the total area of the spatial window
28	Intensity bone cluster/ Intensity lithic cluster	Ratio between the mean intensity inside the bone cluster and the mean intensity inside the lithics cluster

the value estimated using the likelihood cross-validation method employed throughout the whole spatial analysis (see section 2.6). The statistically significant clustering areas at each site and hunter-gatherer campsite are presented in the appendix (section 7.3). These areas were then treated as new separate point patterns. Then, the variables outlined in Table 2.12. were estimated using functions from the "spatstat" library in R. Calculations were made for the overall

point patterns, including bones and lithics, as well as separately for the bones and the lithics spatial patterns. The modern hunter-gatherer campsites were only included in the comparison of the spatial patterns of bone remains, since stone tools are absent in these camps.

Two statistical analyses were carried out with all the estimations for each of the three groups of clustering areas (the overall point patterns, the bone point patterns, and the lithic point patterns). On the one hand, I performed a cluster analysis with R based on Euclidean distances and the "average" agglomeration method in order to find associations between the different clustering areas. Additionally, I used random forests (R library "caret", see section 2.3 for a detailed description of this method) in order to examine the importance of each of the variables in the classifications and understand the differences between these groups of high intensity areas. We used random forests because they perform well when the number of variables is high. Random forests are made with different variable combinations using split-variable randomization to identify the most important variables for the prediction. In the case of the bone point patterns, the cases were first subdivided into two groups – hominin-made sites and modern foraging camps -, then forager campsites were excluded, and the subdivision was made into three types of clusters based on the groups yielded by the cluster analysis. The same subdivision was made for the overall and the lithic point patterns. After that, the samples were bootstrapped 1000 times and subdivided into training (70%) and testing (30%) sets for the analysis.

2.7.2. Comparing the high intensity spots at DS from a taphonomic perspective: Are the clusters taphonomically homogeneous?

The results of the previous analysis have shown that the three cluster areas at DS present some meaningful differences from a spatial point of view. The next section of this analysis explores whether these differences are coupled with variability in the taphonomic content of these clusters, or whether the discrepancies represent just random spatial variations of the same type of spatial cluster patterning that are not caused by any behavioral or taphonomic disparities. Unfortunately, the available spatial data from FLK *Zinj* is not linked to the taphonomic data, and the taphonomic analysis of PTK is being completed at the moment (Organista *et al.*, in prep.), which means that the spatial analysis of the taphonomic variables can only be applied to DS for now.

Therefore, in this final section of the analysis, elements from the spatial and taphonomic analyses of DS are combined in order to address the following question: Are the three clusters taphonomically homogeneous or is the taphonomic signal of each cluster different from the others? On the one hand, if

the three clusters are statistically indistinguishable from each other in their taphonomic content - i.e. if the amount of bone surface modifications or the amount of certain skeletal elements do not vary significantly between clusters-, each area with its own cluster could be interpreted as a different depositional moment or "site" resembling FLK *Zinj* or PTK, depending on the cluster area. If this were the case, we could also expect that some of the variables related with the preservation of these subassemblages, in particular subaerial weathering, would present spatial variation. This would indicate that DS was formed in at least two or three (or more) successive events. On the other hand, if there were significant variations in the content of the three regions, these could be indicating that different activities took place in these areas that may reflect different aspects of the formation or the functionality of the site or even the social use of space by hominins. Interpretations could maybe then serve as hypotheses to be tested for the other sites (FLK *Zinj* and PTK) based on the spatial similarity between the cluster areas.

This section analyzes a selection of taphonomic variables from a spatial perspective in order to contrast the following possible scenarios:

1. DS was formed at least in three similar depositional events, which is reflected spatially in three areas of high intensity that are taphonomically homogeneous. (The only variable that could in theory present variation in this case is subaerial weathering of faunal remains.)

2. DS can be considered a single large assemblage in which different depositional events cannot be distinguished. The three areas of high intensity are largely taphonomically homogeneous and characterized by the same or very similar carcass butchering behaviors. However, certain distinctive properties of the clusters would suggest that some areas were used predominantly over others, or that some areas were subject to higher postdepositional disturbance than others.

3. Regardless of the number of occupations that may have taken place at DS, hominins used different areas for different activities, which is reflected in that the three areas of high intensity are clearly taphonomically distinctive. Each cluster formed as the result of clearly different taphonomic processes. Should activities among areas differ, it would be expected that the properties of the lithic assemblages associated to each of them would also differ (Díez-Martín *et al.*, in prep.). The spatial similarities of the clusters to the ones at FLK *Zinj* and PTK would suggest that these interpretations might also be appropriate for these sites.

Given that more than 30 variables were used in the taphonomic analysis of the bone assemblage (lithics are not included in this section), it would not have been effective to explore and analyze each variable separately or to include all variables combined into one single multivariate analysis. I chose to classify

Table 2.13. *List of variables used in each of the multinomial logistic regression models used to test whether the three areas at DS are taphonomically distinctive.*

Regression model	Type	Variables
1	Preservation	Presence/absence of trampling marks, presence/absence of microabrasion, presence/absence of biochemical marks, presence/absence of water disturbance, presence/absence of carbonate, presence/absence of abrasion, presence/absence of manganese, presence/absence of chemical weathering, presence/absence of dry fractures, preservation of cortical surface (good, moderate or poor), weathering stage (0, 1 or 2)
2	Anatomical/ Taxonomic profile	Skeletal part (appendicular, axial or cranial), animal size (small, medium-sized or large), animal age (juvenile, prime adult or old), presence/absence of teeth, taxa (Alcelaphini, Antilopini, Reduncini, Tragelaphini, Equidae, Carnivora)
3	Skeletal part	Type of limb bone (front or hindlimb), side (left or right), type of epiphysis (proximal or distal), presence/absence of horns
4	Activities	Presence/absence of cut marks, presence/absence of cut marks on hot zones, presence/absence of cut marks on cold zones, presence/absence of defleshing marks, presence/absence of disarticulation marks, presence/absence of impact flakes, presence/absence of percussion marks, presence/absence of impact points, presence/absence of toot marks, presence/absence of furrowing, shaft circumference type (1, 2 or 3), presence/absence of green fractures

each taphonomic variable as either related with the preservation of the site, (i.e. preservation of the cortical surface, or presence/absence of biochemical marks), to anthropic or carnivore activity (i.e. cut marks, percussion marks, tooth marks or furrowing), or to skeletal part or taxa representation, including age and size of the carcasses, and to carry out various regression models with different variables separately for each of the three groups.

The method applied here was inspired by the analysis performed by Smith *et al.* (2015) to a Bronze Age cemetery in Thailand. Following the approach of these authors, I explored

the spatial distribution of these taphonomic variables in multinomial logistic regressions, which are used to model nominal outcome variables, in which the log odds of the outcomes are modeled as a linear combination of the predictor variables. The three groups of points or areas of DS (A, B, and C) act here as the dependent variable. The principles of multinomial logistic regression are very similar to those of the binary logistic regression, the difference being that one of the categories of the response or dependent variable is chosen as the reference category (in this case area A). Consequently, coefficients, standard errors, and p-values of the coefficients are determined for each category of each response variable, except for the reference category. The interpretation of the odds ratios has to be made in relation to the reference category, i.e. the odds ratios represent the change in odds of the outcome being a particular category versus the reference category, for differing factor levels of the corresponding explanatory variable.

Several multinomial logistic regression models, each including a different number of variables, were carried out for each of the three variable groups using the "multinom" function from the "nnet" R library (Venables and Ripley, 2002). For each group of regressions, the best model was selected based on the lowest residual deviance and AIC values. The variables related to the skeletal part and taxa representation had to be further split and used in two different models. The resulting groups of variables included in the four final multivariate regressions are shown in Table 2.13.

The variables that contributed significantly to the regression models (p-value < 0.05) were selected to be examined spatially in more detail by plotting their spatial distribution and the spatial variation of the intensity using sigma values estimated using Cronie and van Lieshout's criterion, because it yields clearer density maps for spatial patterns with fewer points. In fact, this method was observed to capture the size of the clusters of DS well, and the details of the smoothing bandwidths yielded by the likelihood cross-validation method, which was used in the previous section for the overall DS point pattern, are unnecessary here (Cronie and van Lieshout, 2018). I also calculated the spatially-varying type distribution or relative risk of the multitype point pattern generated by each of the variables in question. Tolerance contours for the relative risk or type probability distribution were estimated using a Monte Carlo test (see section 2.6 for the detailed description of the method).

3. Results

Taphonomic analysis

3.1 Site formation

3.1.1. Composition and shape

3.1.1.1. Small carcasses

The MCA on the sample of small-sized carcasses provides a bidimensional solution that explaines 44.1% of the inertia. The first dimension accounts for 23.4% of inertia, the second dimension for 20.7% of inertia. The variables that most contribute to the first dimension are mixed composition and tubular shape (Table 3.1). The cos2 values for these variables are also the highest (Figure 3.1A). Cube shape contributes most to the second dimension. The cos2 values add to this factor the dense composition. The Maasai sample, DS and the lag assemblage are distributed along the second dimension axis, while the transported assemblage differs from all other assemblages in the frequency of tubular fragments and bones with a mixed composition and is separated from the others in the first dimension axis. The DS assemblage appears closest to the Maasai experimental sample, where trabecular bone fragments are more represented with respect to the other assemblages. The fact that DS also contains a large amount of spongy bones, brings it closer to the Maasai sample than to the transported experimental assemblage. There is a clear separation over the second dimension axis between the experimental lag assemblage and the other samples. This is probably due to the fact that bones from smaller carcasses that have been affected by a water current will tend to form a transported assemblage, while in the case of heavier bones from medium-sized or large carcasses, the same fluvial impact would first form a lag assemblage. The position of DS close to the Maasai sample and next to the categories dense and flat suggests that the small carcass sample was not affected by water disturbance.

Table 3.1. *Loading scores of factor/variable contribution in the MCA according to carcass size.*

Factor/ Variable	Small carcasses				Medium-sized carcasses			
	Dim 1	cos2	Dim 2	cos2	Dim 1	cos2	Dim 2	cos2
dense	-0.188	0.022	0.868	0.477	-0.766	0.397	0.350	0.083
mixed	3.504	0.728	0.042	0.000	3.178	0.054	4.243	0.097
trabecular	-0.221	0.062	-0.609	0.465	0.495	0.354	-0.278	0.111
cube	-0.436	0.071	-1.166	0.506	0.815	0.206	-1.122	0.390
flat	-0.285	0.129	0.560	0.496	-0.523	0.578	0.184	0.072
tube	2.521	0.836	-0.230	0.007	1.917	0.339	1.658	0.254
DS	-0.036	0.001	0.429	0.108	-0.292	0.176	0.009	0.000
lag	0.288	0.003	2.555	0.221	-0.162	0.001	2.974	0.214
Masai	-0.131	0.018	-0.388	0.158	0.404	0.056	-0.719	0.176
transported	0.842	0.065	-0.519	0.025	2.039	0.210	2.215	0.248

The solution of the CA on the composition variable explains 100% of inertia. The first dimension alone accounts for 85.45% of inertia (Figure 3.2A, Table 3.2A). The assemblage of the DS small-sized carcasses appears very close to the Maasai assemblage; the confidence ellipses of both samples overlap and are clearly separated from the lag and transported assemblages. The slight difference between the Maasai and the DS assemblage is probably due to a higher representation of bone specimens with a trabecular structure in the former (Figure 3.2A). The CA on the shape variable shows a solution also explaining 100% of inertia. The first dimension accounts for 51.66%, the second dimension for 48.34% of inertia (Figure 3.2B, Table 3.2B). Although the assemblages do not overlap when only shape is considered, DS resembles the Maasai sample more than the transported one. The higher percentage of bones with a cubic shape is characteristic of the Maasai experimental assemblage and accounts for the separation from DS, which contains a high proportion of flat specimens (Figure 3.2B). These results are supported by chi-square tests (Table 3.4).

3.1.1.2. Medium-sized carcasses

The MCA for medium-sized carcasses accounts for 38.7% of inertia. The first dimension explains 19.8% of inertia, the second dimension 18.9%. Mixed composition and tube contribute most to the first axis, the cos2 values add flat, dense, and trabecular to these factors (Table 3.1, Figure 3.1B). The variables mixed and tube contribute the most to the second dimension, as well as cube when the cos2 values are taken into account. As was the case with small carcasses, DS appears

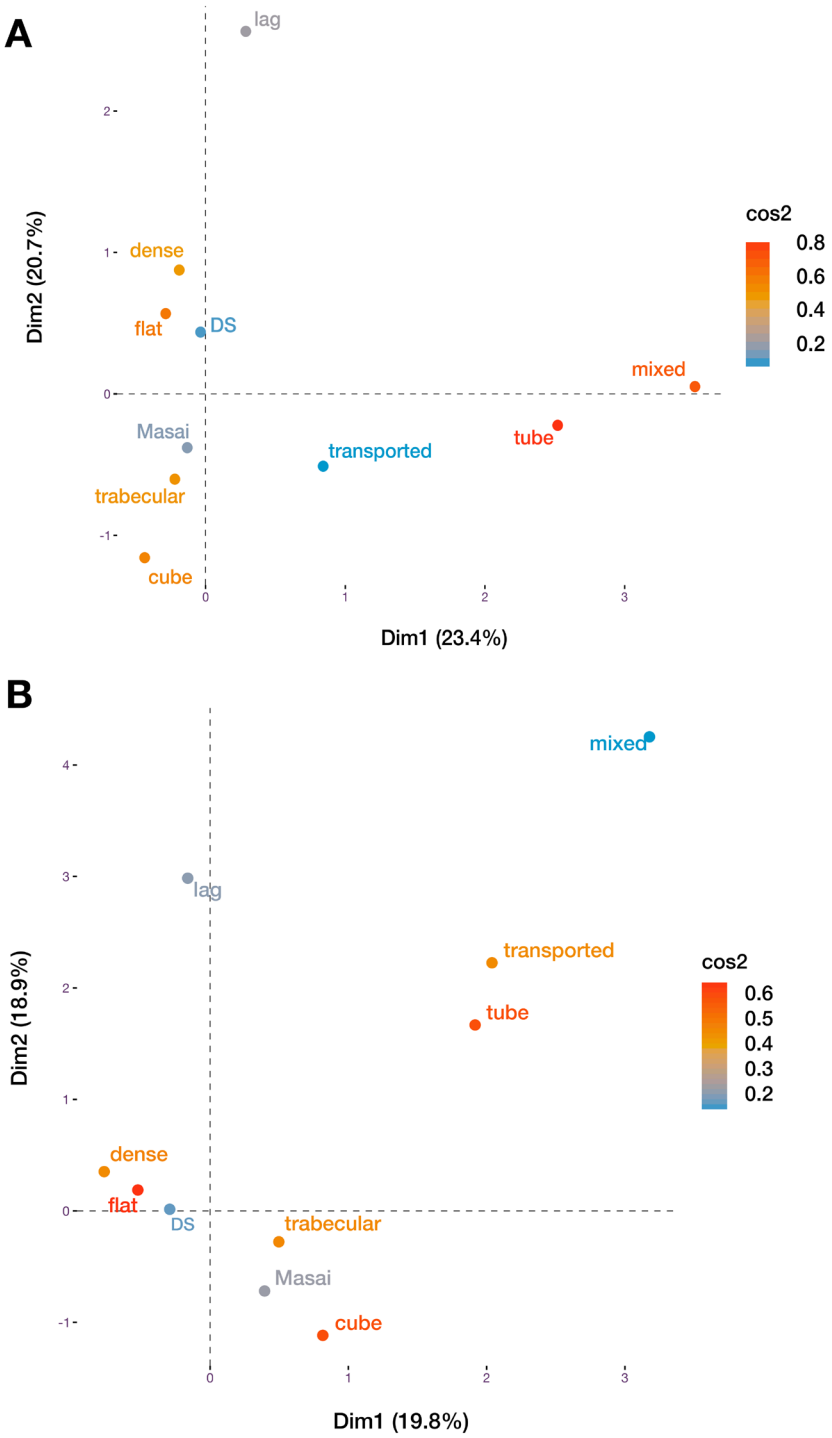

FIGURE 3.1. *Bidimensional solution of the MCA on the samples of small carcasses (top) and medium-sized carcasses (bottom), explaining 44% and 39% of inertia, respectively.*

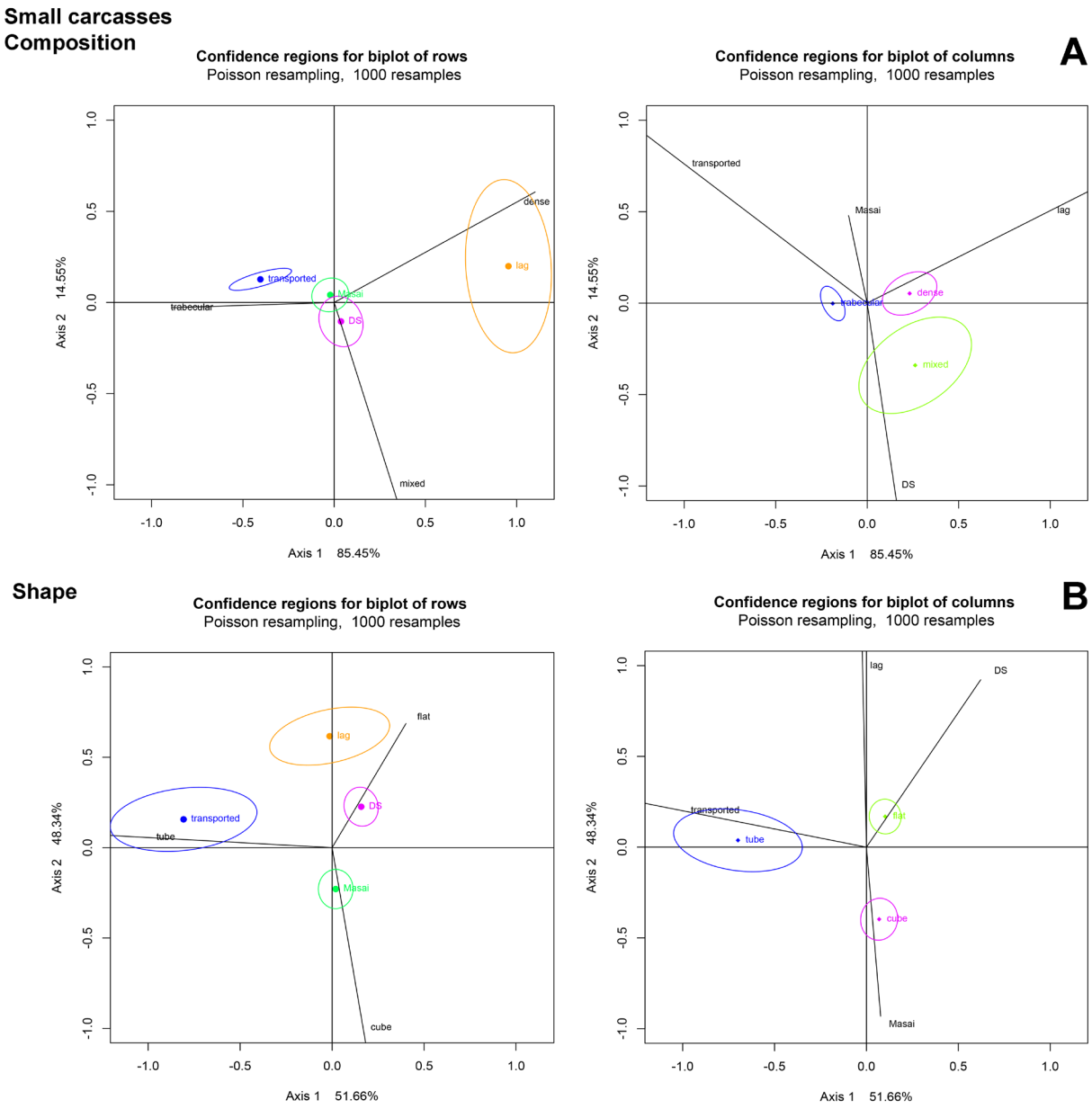

FIGURE 3.2. *CAs explaining 100% of inertia in small carcasses considering A) the composition variable and B) the shape variable.*

closest to the Maasai experimental assemblage, both being characterized mostly by dense, flat and trabecular bone specimens, as well as compact spongy bones, and both samples are clearly separated from the lag and transported assemblages, which indicates that the sample of medium-sized carcasses at DS was not affected in any meaningful way by hydraulic inputs either. The separation between the three autochthonous assemblages and the transported assemblage is effective especially over the first axis dimension (Figure 3.1B).

When considering variables separately, the CA on composition yields a solution explaining 100% of inertia. The first dimension alone explains 85.98% of in-

ertia (Figure 3.3A, Table 3.3A). Chi-square tests for the contingency tables yielded significant results in this case too (Table 3.4). DS appears within the Maasai sample confidence ellipse. Both samples are also within the much bigger ellipse that confines the variability of the transported assemblage. A CA on the shape variable also shows a solution explaining 100% of inertia (67.62% is accounted for by the first dimension), and very similar results to the CA on small carcasses (Table 3.3B; Figure 3.3B). DS appears closest to the Maasai sample and most separated from the transported assemblage, indicating that the archaeological

TABLE 3.2. *Loading scores for the CA and the corresponding values of inertia of each dimension of A) bone composition in small carcasses, B) bone shape in small carcasses.*

A

	axis 1	st dev	rep	ctr	axis 2	st dev	rep	ctr	quality
DS	0.037	0.048	114	12	-0.104	0.056	886	531	1000
lag	0.955	0.104	958	673	0.199	0.196	42	172	1000
Masai	-0.021	0.038	209	5	0.042	0.037	791	117	1000
transported	-0.404	0.083	910	311	0.127	0.030	90	180	1000
dense	0.232	0.060	951	470	0.053	0.048	49	142	1000
mixed	0.262	0.126	373	87	-0.340	0.111	627	857	1000
trabecular	-0.188	0.027	1000	443	-0.002	0.038	0	0	1000

	Inertia	%	Cum%
1	0.044	85.45	85.45
2	0.008	14.55	100.00

B

	axis 1	st dev	rep	ctr	axis 2	st dev	rep	ctr	quality
DS	0.158	0.039	327	143	0.226	0.044	673	315	1000
lag	-0.013	0.157	0	0	0.617	0.076	1000	206	1000
Masai	0.020	0.037	7	3	-0.229	0.045	993	445	1000
transported	-0.808	0.160	964	854	0.157	0.075	36	34	1000
cube	0.069	0.039	30	20	-0.397	0.049	970	708	1000
flat	0.102	0.035	268	99	0.169	0.039	732	289	1000
tube	-0.660	0.139	997	881	0.038	0.069	3	3	1000

	Inertia	%	Cum %
1	0.064	51.66	51.66
2	0.060	48.34	100.00

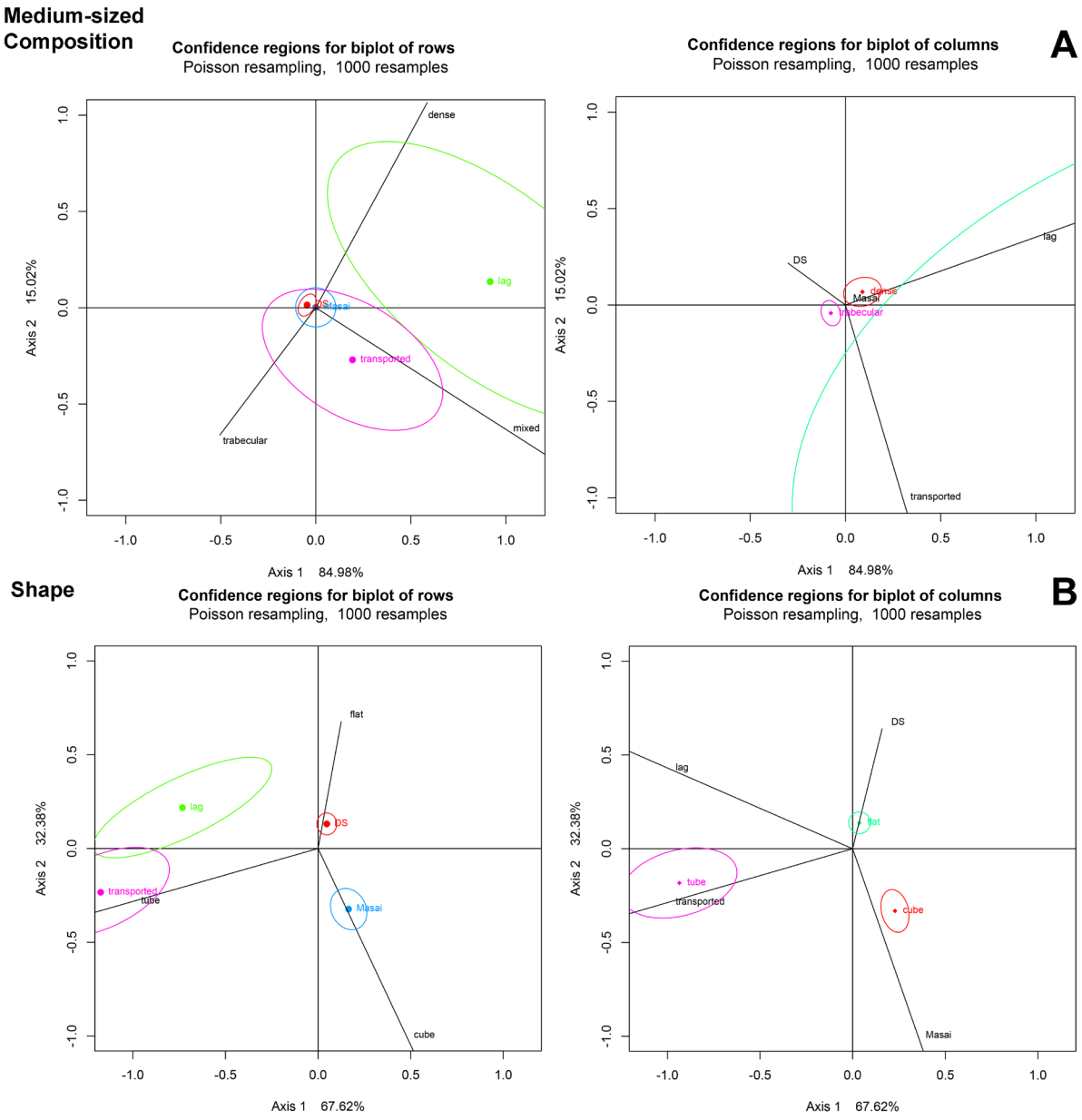

FIGURE 3.3. *CAs explaining 100% of inertia in medium-sized carcasses considering A) the composition variable and B) the shape variable.*

assemblage has not undergone any significant post-depositional disturbance by water inputs. DS is clearly characterized by flat specimens, the Maasai sample by polyhedral elements and the transported assemblage by bones with a tubular shape.

In sum, these results indicate that DS is an autochthonous assemblage that has not been significantly affected by water. Minor divergences from the Maasai experimental assemblage could be due to other biasing taphonomic processes present at DS, such as some minor carnivore ravaging or density mediated attrition.

Table 3.3. *Loading scores for the CA of A) bone composition in medium-sized carcasses, B) bone shape in medium-sized carcasses*

A

	axis 1	st dev	rep	ctr	axis 2	st dev	rep	ctr	quality
DS	-0.046	0.019	916	61	0.014	0.023	84	32	1000
lag	0.918	0.380	979	861	0.136	0.278	21	107	1000
Masai	0.000	0.043	23	0	0.002	0.041	977	0	1000
transported	0.193	0.190	338	78	-0.270	0.139	662	862	1000
dense	0.089	0.040	631	139	0.068	0.033	369	458	1000
mixed	1.752	0.756	934	711	-0.465	0.624	66	284	1000
trabecular	-0.077	0.020	767	151	-0.042	0.026	233	259	1000

	Inertia	%	Cum %
1	0.023	84.98	84.98
2	0.004	15.02	100.00

B

	axis 1	st dev	rep	ctr	axis 2	st dev	rep	ctr	quality
DS	0.047	0.022	115	17	0.131	0.024	885	276	1000
lag	-0.732	0.201	919	145	0.218	0.104	81	27	1000
Masai	0.165	0.040	207	79	-0.323	0.047	793	634	1000
transported	-1.174	0.164	962	759	-0.233	0.098	38	63	1000
cube	0.229	0.032	322	142	-0.332	0.046	678	622	1000
flat	0.037	0.023	67	11	0.138	0.023	933	310	1000
tube	-0.936	0.124	963	848	-0.183	0.082	37	68	1000

	Inertia	%	Cum %
1	0.087	67.62	67.62
2	0.041	32.38	100.00

Table 3.4. *Chi-square results for the CA contingency tables.*

	Shape		Composition	
	X2	p-value	X2	p-value
Small (Size 1-2)	144.95	2.2e-16	60.331	3.856e-11
Medium (Size 3-4)	290.16	2.2e-16	60.988	2.835e-11

3.1.2. Orientation of archaeological items

The null hypothesis of isotropy could not be rejected for either of the analyzed DS sub-assemblages (a, b or c, see Methods). Statistical tests indicate that they all present uniform distributions (Table 3.5). Likewise, stereograms and rose diagrams all show uniform distributions of the orientations of archaeological material with no preferential horizontal trend (Figure 3.4). Additionally, Woodcock diagrams show an isotropic fabric for all three assemblages (Figure 3.5). The von Mises distribution k concentration value is below 0.03 for all three samples (Table 3.5). Finally, the position of DS in the Benn's diagrams equally indicates that the site is basically undisturbed (Figure 3.5).

3.1.3. Specimen size distribution

When considering all the bone fragments recovered at DS, including the specimens retrieved from the sieved sediment, the specimens <20 mm are the most abundant, indicating minor post-depositional effects by sedimentary processes. Small fragments constitute more than half of the complete assemblage. Specimens smaller than 30 mm constitute slightly less than 80% of the whole assemblage. When only green long bone shafts are considered, however, the frequency of small specimens decreases drastically, partly because many small fragments are the result of diagenetic breakage, but also due to the difficulty of identifying green fractures in very small specimens (Figure 3.6; Table 3.6). When small fragments are left out, it can be noticed that medium-sized fragments (31-60 mm) are almost twice as abundant as large ones (>61 mm). A similar pattern of specimen size distribution can be observed when small and medium-sized carcasses are considered independently. As is expected, Figure 3.6 shows that small carcasses yield smaller specimens than larger carcasses. With respect to the remaining size categories both carcass sizes show a very similar pattern of specimen size distribution. Interestingly, whereas some deviation can be appreciated in the distribution lines from small carcasses between the lines depicting the distribution of long bone shafts and long bone green shafts in medium-sized carcasses (red and orange lines, Figure 3.6) and the line showing the distribution of all specimens, all three lines follow practically the same pattern in medium-sized carcasses. This suggests that long bone shafts follow the same distribution as the remaining skeletal elements and that dry breakage is not a biasing factor of size distribution in medium-sized carcasses. The latter is also true for small carcasses, however it appears that the difference between the curves is caused by skeletal elements other than long bone shaft fragments (whether considering all shafts or only those with green fractures), like cranial and axial elements or long bone epiphyses, which may have fragmented into smaller pieces.

TABLE 3.5. *Statistical tests applied to the three DS assemblages (A: bone and lithics; B: bones; C: long bone shafts) and their significance. All values indicate isotropy.*

	Rayleigh		Kuiper		Watson		von Mises d.	
	Z	p-value	V	p-value	U2	p-value	k	c
A	0.0214	0.3095	15.511	0.10<p<0.15	0.1003	>0.10	0.00	2.11
B	0.0083	0.8543	11.569	>0.15	0.0519	>0.10	0.02	2.19
C	0.0182	0.7642	11.527	>0.15	0.0495	>0.10	0.03	2.14

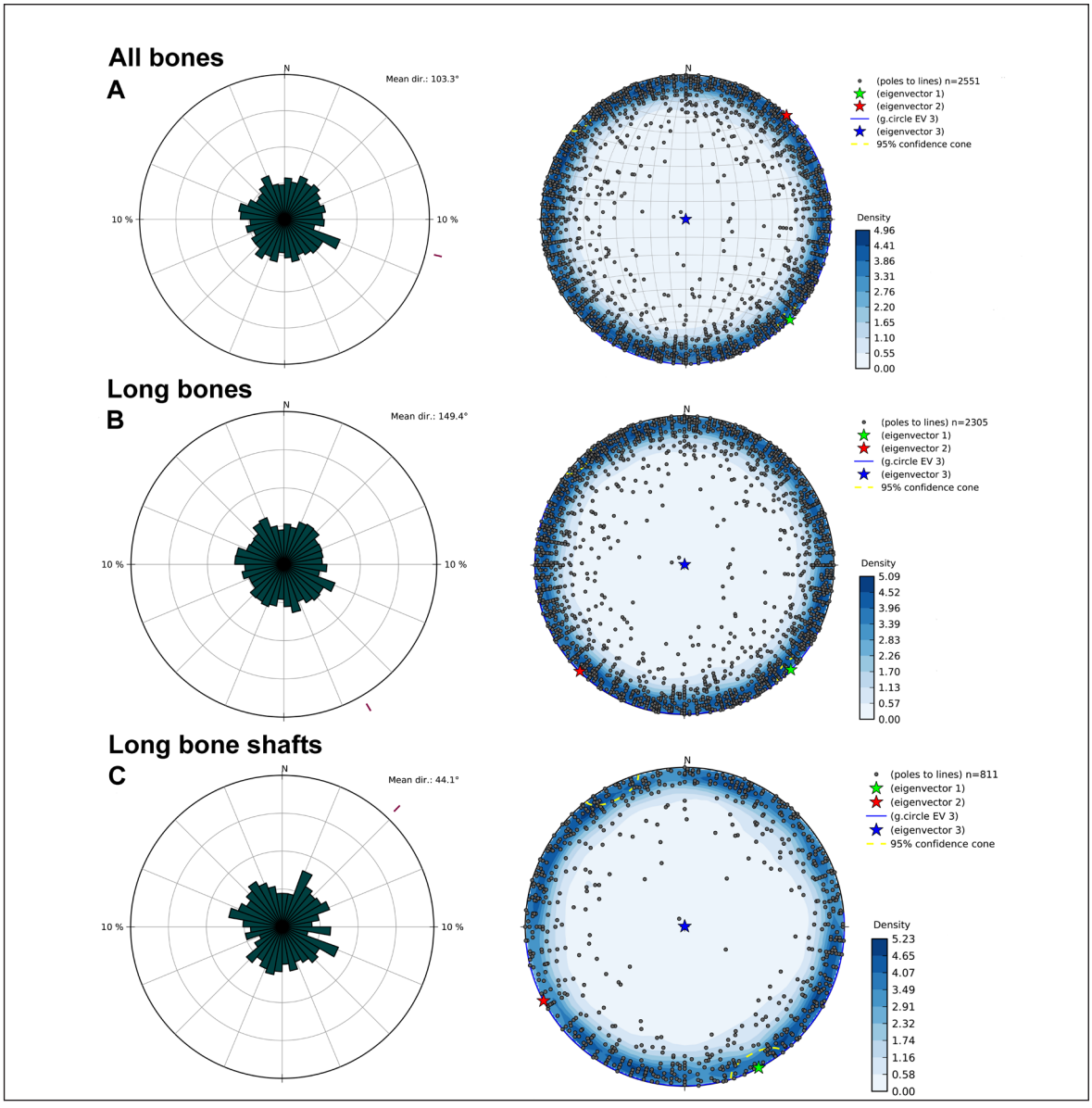

FIGURE 3.4. *Stereograms and rose diagrams showing uniform distributions and horizontal trends in A) the complete 22B assemblage, B) the long bone subassemblage, and C) the shafts subassemblage.*

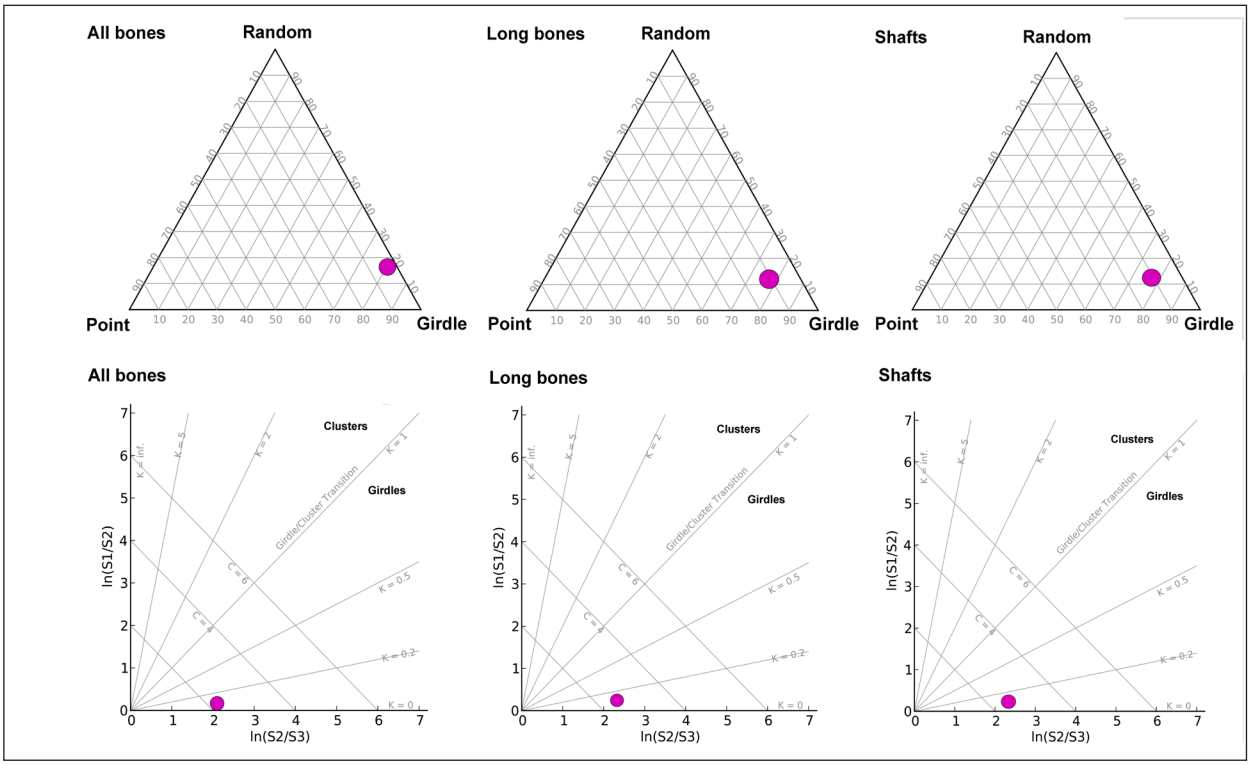

FIGURE 3.5. *Woodcock and Benn's diagrams of the complete 22B assemblage, the long bone subassemblage, and the shafts subassemblage showing isotropic fabrics.*

3.1.4. Summary

The sedimentary matrix in which the DS assemblage was recovered is composed of clay and silty clay, which demonstrates that it was formed in a very low-enery depositional environment. Polished or abraded specimens were very infrequent (less than 0.3%) and this alteration when documented did never affect the entire specimen. Evidence of water-induced and chemical modifications on bone surfaces were rare (less than 0.5%), but around 10% of the fossils showed a carbonate matrix, which 60% of the times hindered the identification of the bone specimen. Subaerial weathering was almost non-existent (99.9% of specimens fall into stage 0, Behrensmeyer 1978), which means that the assemblage formed probably in less than a year or just slightly more if a dense vegetation cover existed at the site.

The DS assemblage lacks any evidence indicative of transportation by water flows. Judging by the analyses included here, the assemblage was not affected by significant post-depositional disturbance. Specifically, the completely uniform distribution of the orientation of bones including long bone shafts, and the overwhelming presence of small bone specimens are not consistent with the distur-

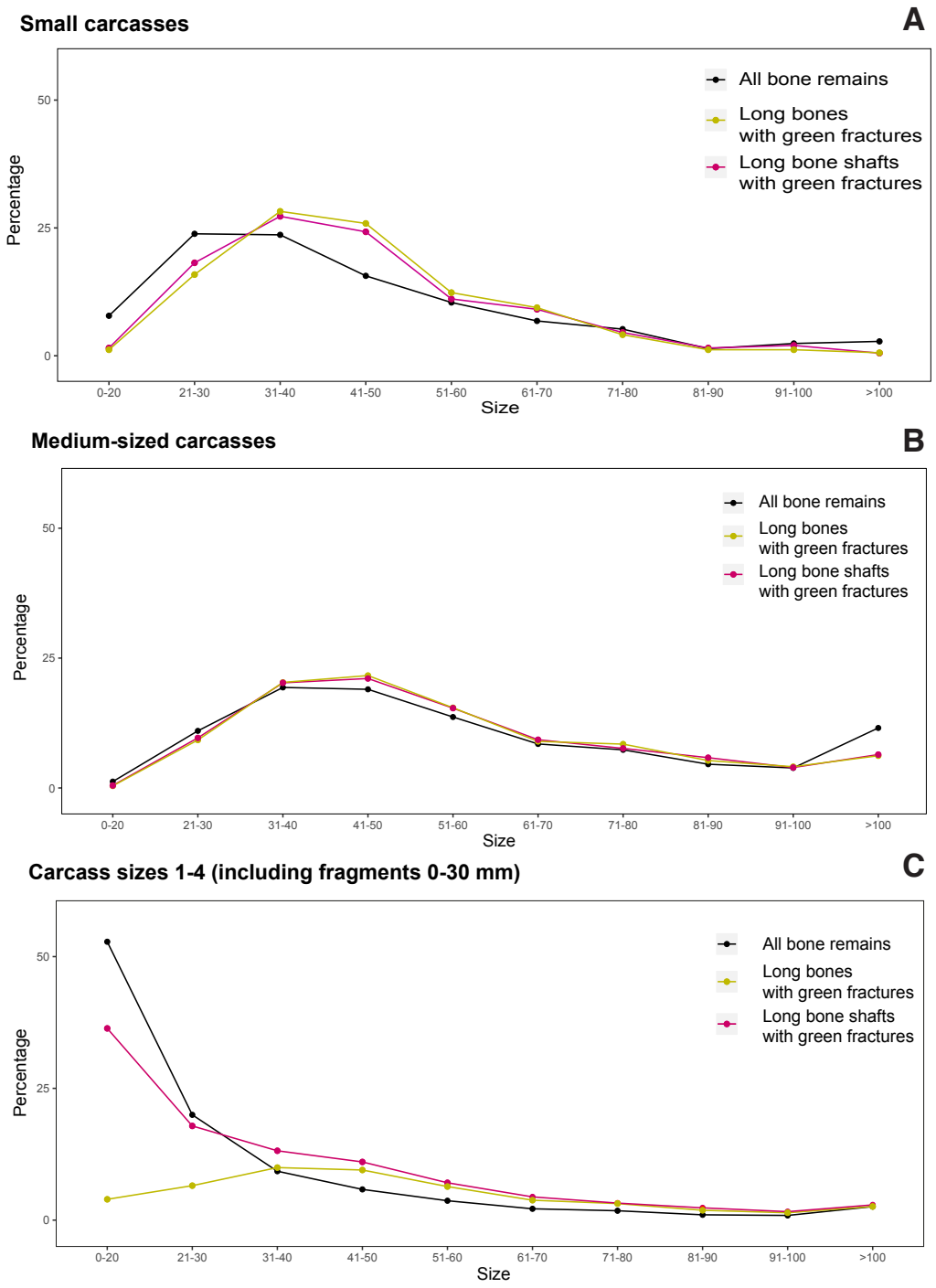

FIGURE 3.6. *Specimen size distribution of all bone remains and green broken long bones and long bone shafts from a) small carcasses and b) medium-sized carcasses excluding specimens <30 mm. c) Specimen size distribution of all bone remains and green broken long bones and long bone shafts including specimens <30 mm.*

Table 3.6. Specimen size distribution in DS level 22B quantified per NISP and %NISP. Percentages appear in parentheses.

Size	Level	Category		Carcass size	Category		Carcass size	Category	
	22B			1-2			3-4		
		LB shafts	LB green		LB shafts	LB green		LB shafts	LB green
0-20	5622 (52.82)	857 (36.38)	93 (3.95)	39 (7.82)	3 (1.52)	2 (1.18)	24 (1.23)	4 (0.48)	3 (0.40)
21-30	2126 (19.98)	421 (17.87)	154 (6.54)	119 (23.85)	36 (18.18)	27 (15.88)	214 (10.99)	82 (9.64)	70 (9.23)
31-40	988 (9.28)	310 (13.16)	235 (9.97)	118 (23.65)	54 (27.27)	48 (28.24)	377 (19.35)	170 (20.24)	154 (20.32)
41-50	621 (5.83)	260 (11.04)	224 (9.51)	78 (15.63)	48 (24.24)	44 (25.88)	370 (18.99)	177 (21.07)	164 (21.64)
51-60	392 (3.68)	167 (7.09)	150 (6.37)	52 (10.42)	22 (11.11)	21 (12.35)	266 (13.66)	129 (15.36)	117 (15.44)
61-70	229 (2.15)	104 (4.41)	89 (3.78)	34 (6.81)	18 (9.09)	16 (9.41)	165 (8.47)	78 (9.29)	68 (8.97)
71-80	189 (1.78)	76 (3.23)	74 (3.14)	26 (5.21)	9 (4.55)	7 (4.12)	143 (7.34)	64 (7.62)	64 (8.44)
81-90	108 (1.01)	55 (2.33)	44 (1.87)	7 (1.40)	3 (1.52)	2 (1.18)	89 (4.57)	49 (5.83)	40 (5.28)
91-100	95 (0.89)	38 (1.61)	33 (1.40)	12 (2.40)	4 (2.02)	2 (1.18)	75 (3.85)	33 (3.93)	31 (4.09)
>100	273 (2.57)	68 2.89)	61 (2.59)	14 (2.81)	1 (0.51)	1 (0.59)	225 (11.55)	54 (6.43)	47 (6.20)
Total	10643	2356	1157	499	198	170	1948	840	758

bances created in accumulations by water inputs. Moreover, the similarities in the frequencies of bone specimen composition and shape types between DS and an undisturbed experimental accumulation is further suggestive of completeness and overall integrity of the site. Minimal divergence from the experimental sample is mainly due to the lack of representativeness of cubic or polyhedral bones (mostly vertebrae or compact bones) and, to a lesser extent, of trabecular or cancellous bones (long bone epiphyses and axial elements) in DS as opposed

to the Maasai settlement. This difference could however be accounted for by density-mediated attrition and some, although limited, carnivore ravaging. The exceptional preservation of the site also suggests that the spatial properties of the assemblage, as hominins might have left it, might to a great extent be intact. This will be further elaborated in subsequent sections on bone refitting and spatial analysis.

3.2. Skeletal part representation

3.2.1. Quantification and analysis of skeletal element abundances

3.2.1.1. Number of Identified Specimens (NISP) and Minimum Number of Elements (MNE)

Table 3.7. shows the NISP estimates per element for each animal size class of the part of the 22B assemblage that was available to calculate skeletal element frequencies, which includes 3055 ungulate specimens that were recovered between 2014 and 2016. The total NISP is 1790 (58% of NSP).

Small carcasses (NISP=347) are represented by all elements of the skeleton, and especially by long limb bone shafts. Long bone epiphyses of all long bones are also present, albeit in much smaller numbers than midshafts. Most axial remains are rib fragments, although cervical, thoracic, and lumbar vertebrae have been found in small numbers. Pelvis fragments are slightly more

Table 3.7. *NISP estimates per element and animal size class of the 22B ungulate assemblage used in the analysis of skeletal part abundances (2014-2016). Appendicular elements are subdivided into proximal, midshaft, and distal portions. Epiphyseal portions with a significant part of midshaft attached were counted twice, once as a shaft and once as an epiphysis.*

	NISP				
Element	Size 1-2	Size 3-4	Size 5	Size indet	Total
Skull	7	50	1	4	62
Mandible	9	48	1	1	58
Teeth	8	46	1	34	89
Vertebrae					
Atlas	0	2	0	0	2
Axis	0	1	0	0	1
Cervical	2	13	0	0	15
Thoracic	7	48	0	0	55
Lumbar	5	17	0	0	22

	Sacra	0	8	0	0	8
	Caudal	0	9	0	0	9
Ribs		102	406	2	1	511
Scapula		7	41	0	0	48
Pelvis		11	42	2	4	59
Humerus	Complete	0	0	0	0	0
	Proximal	1	8	0	0	9
	Midshaft	25	138	2	8	170
	Distal	4	20	0	0	24
Radius-Ulna	Complete	0	0	0	0	0
	Proximal	6	36	0	0	42
	Midshaft	14	70	5	2	91
	Distal	2	4	0	0	6
Metacarpal	Complete	0	1	0	0	1
	Proximal	1	16	0	0	17
	Midshaft	7	34	2	0	43
	Distal	2	7	0	0	9
Femur	Complete	0	0	0	0	0
	Proximal	8	7	0	0	15
	Midshaft	35	67	3	2	107
	Distal	1	5	1	0	7
Tibia	Complete	0	0	0	0	0
	Proximal	1	5	0	0	6
	Midshaft	35	113	5	2	155
	Distal	4	2	0	0	6
Metatarsal	Complete	2	1	0	0	3
	Proximal	4	8	0	0	12
	Midshaft	12	23	0	0	35
	Distal	0	5	0	0	5
Carpals		4	9	1	0	15
Tarsals		4	9	0	0	13
Phalanges		15	28	0	0	43
Other						
	Sesamoid	0	7	0	0	7
	Patella	2	6	0	0	8
	Sternum	0	3	0	0	3
Total		347	1363	23	51	1790

abundant than specimens belonging to scapulae. Compact bones have been recovered as well. The cranial skeleton is also represented by several skull and mandibular fragments, as well as some isolated teeth. Medium-sized carcasses are much more abundant than small carcasses (NISP=1363). Among this size class, long limb bones constitute 42% (N=570) of the sample. Around 80% of these 570 specimens are long bone shafts. The proximal epiphyses from radii-ulnae are the most abundant long bone ends (N=36), followed by the distal humeri (N=20). Femora and tibiae ends are less abundant. All elements from the axial skeleton are represented, including all types of vertebrae and even the sternum. Rib fragments are very abundant, and scapulae and pelves are represented by almost the same number of specimens. Cranial elements, including skull, mandible, and tooth fragments, make up around 10% of the total number of remains. Large carcasses are only represented by a few cranial and appendicular fragments, as well as two rib fragments.

The subdivision of the appendicular elements into proximal, midshaft, and distal portions shows that shafts are much more abundant than epiphyseal specimens in all size classes and that, with the exception of a few complete metapodials (N=4), long bones were always fragmented. The high number of recovered fragmented rib fragments and axial specimens in general is remarkable (Table 3.7).

The long bone MNE estimates per size class were derived using both epiphyses and shaft fragments, depending on which was most representative. For example, for medium-sized carcasses, the highest estimates for the minimum number of humeri and tibiae resulted from shaft portions with landmarks or muscle insertions: the minimum number of humeri was calculated using the insertion of the Teres muscle, and the minimum number of tibiae was estimated counting the number of tibial crests on the cranial side of the proximal shafts. However, the minimum numbers of radii-ulnae and femora were estimated using proximal epiphyses. The radius-ulna is the most represented long limb bone in medium-sized carcasses, followed by the humerus (Table 3.8). Among the axial skeleton elements, scapulae were abundant, mostly represented by the glenoid fossa, and several were found fairly complete, without any evidence of carnivore ravaging on the blades. Vertebrae were also fairly complete. Pelves appeared more fragmented than scapulae. Ribs were more abundant than vertebrae. When estimating the minimum number of ribs using the alternative measuring method described in the methods section (2.2), the value increased by 27% in medium-sized carcasses and by 81% in small carcasses. MNEs were estimated similarly for small carcasses, although most of the MNEs of long bones were estimated using either proximal or distal ends.

3.2.1.2. *Relationship between NISP and MNE*

Correlations between NISP and MNE for small and medium-sized carcasses result in a relatively high correlation coefficient (Spearman's rho = 0.6 for small carcasses, and rho = 0.8 for medium-sized carcasses), but they explain only 46% and 69% of the sample variance, respectively. The graph that results from plotting the NISP values against the MNE estimates illustrates that the relationship between both variables is far from linear (Figure 3.8A and B). For both the small and the medium-sized carcasses, the linear relationship only exists while NISP values are low. But, as of a certain point, the curve becomes an asymptote or even declines, and the correlation between both variables disappears. This means that after a certain threshold, the MNE and MNI estimates do not necessarily increase with the increase in NISP. Contrary to what is sometimes claimed, NISP and MNE/MNI estimations are subjected to different independent errors (Domínguez-Rodrigo, 2012). Bartram (1993) noticed that analysts who reported positive tight correlations between the variables were leaving out many identifiable shaft fragments from their counts. In other words, they were

Table 3.8. *MNE estimates per element and animal size class of the 22B assemblage used in the analysis of skeletal part abundances (2014-2016).*

Element		Size 1-2	Size 3-4	Size 5
Skull		4	10	1
Mandible		1	21	1
Vertebrae				
	Atlas	0	1	0
	Axis	0	1	0
	Cervical	1	11	0
	Thoracic	7	23	0
	Lumbar	5	15	0
	Sacra	0	5	0
	Caudal	0	9	0
Ribs		29	112	1
Scapula		5	23	0
Pelvis		2	13	1
Humerus		6	24	1
Radius-Ulna		6	29	3
Metacarpal		3	16	2
Femur		4	15	3

Tibia		5	17	4
Metatarsal		6	12	0
Carpals		4	9	1
Tarsals		4	9	0
Phalanges		14	16	0
Other				
	Sesamoids	0	7	0
	Patella	2	6	0
	Sternum	0	1	0

FIGURE 3.7. *Several examples of scapulae, pelves and vertebrae preserved in several stages of completeness. Note the fairly complete ribs and scapula blades as well as the intact apophyses of the throacic vertebrae.*

estimating MNEs and MNIs out of a NISP sample composed of more or less complete elements or end portions, while disregarding the more fragmentary shaft specimens. When including the more fragmented part of the assemblages, as is done in this study, the relationship is nuanced. This demonstrates that the MNE and MNI estimates reported in this analysis do not necessarily depend on the NISP estimations.

3.2.1.3. Minimum Number of Individuals (MNI)

There are a minimum of 27 individuals that reach size 3-4 in their adult stage, 5 size 1-2 bovids, and 1 size 5 carcass represented in level 22B at DS that could be identified to species using the dental remains (Table 3.9). These values constitute the dental MNI. The bovid dental remains belong to *Kobus sigmoidalis*, *Parmularius altidens*, *Connochaetes sp.*, *Tragelaphus strepsiceros*, *Megalotragus sp.*, and *Antidorcas recki.* The remaining ungulate dental specimens belong to *Equus olduvayensis*, *Kolpochoerus heseloni*, and *Hippopotamus sp*. When considering only limb bones in order to estimate the minimum number of carcasses represented, the radii-ulnae yield a MNI of 4 small carcasses, and 16 medium-sized carcasses. The MNI of large carcasses is 5 and is yielded by the tibiae.

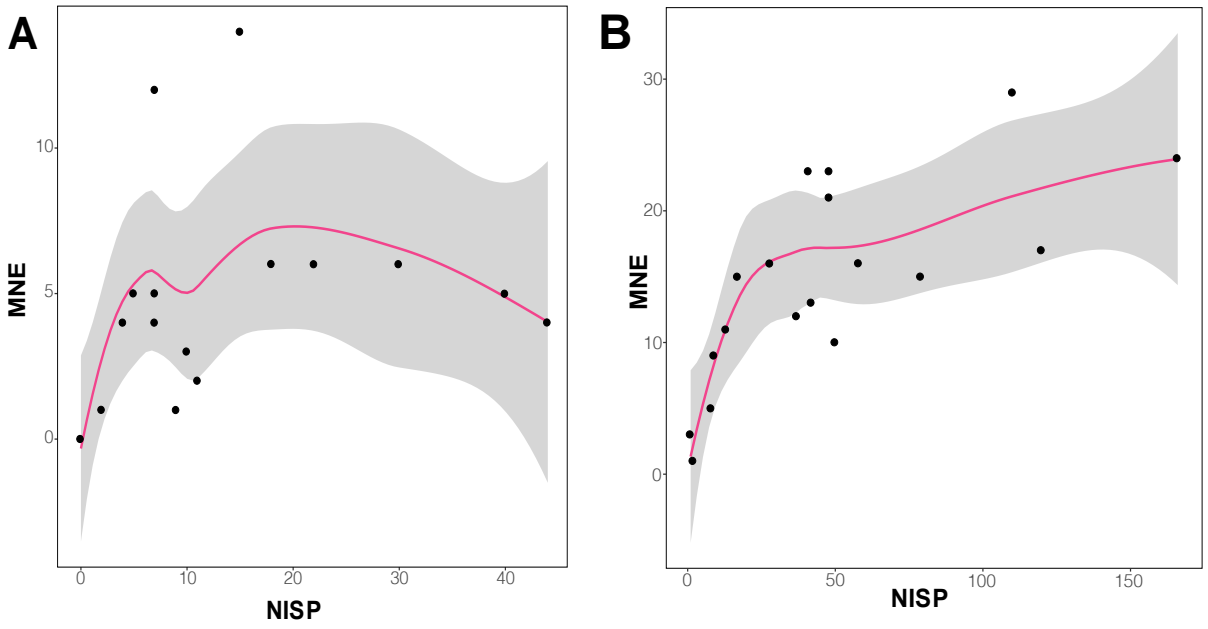

FIGURE 3.8. *Relationship between NISP and MNE considering a) small carcasses and b) medium-sized carcasses*

Interestingly, similar results were obtained at FLK *Zinj*. The comparison of the MNIs from size 1-2 and size 3-4 bovid carcasses between FLK *Zinj* and DS shows that almost the same bovid species are represented at both sites in similar proportions (Table 3.10). The difference between the dental and the post-cranial bovid MNIs is not too marked, which suggests that most carcasses were possibly transported the same way to the site.

3.2.1.4. Skeletal part profiles

The resulting skeletal part profiles for each carcass size are shown in Figure 3.9. Interesting observations can be drawn from them. Whereas all skeletal parts are represented similarly in small carcasses, which suggests that they were transported complete to the site, medium-sized carcasses are represented unevenly by anterior and posterior limb bones, with front limbs being more abundant than hind limbs (Figure 3.9). This pattern is also observed between the scapula and the pelvis. The frequencies of axial remains, even though higher than at FLK *Zinj*, are less well represented than appendicular elements as expected according to MNI due to preservation biases. Ribs are more abundant than vertebrae, which could be due to some extent to the fact that water transports cubic-shaped cancellous bones more easily than flat ones, or it could be explained by the fact that carnivores tend to ravage preferentially on these

Table 3.9. *Minimum number of individuals represented by mandibular elements at DS (Level 22B).*

Taxon	MNI
Kobus	11
Parmularius	4
Megalotragus	2
Connochaetes	4
Tragelaphus	2
Antidorcas	5
Equus	3
Hippopotamidae	1
Kolpochoerus	1
Size	
Size 1-2	5
Size 3-4	27
Size 5	1

Table 3.10. *Minimum number of bovids represented by cranial/mandibular elements at FLK Zinj (Domínguez-Rodrigo et al. 2007) and DS*

	Zinj	DS
Antidorcas	7	4
Parmularius	4	4
Connochaetes	2	2
Kobus	7	9
Tragelaphus	0	1
Megalotragus	0	2
Syncerus	1	0

bones (Arriaza *et al.*, 2019). In fact, some of the vertebral apophyses show ambiguous fractures that could be due to carnivore gnawing; however, this cannot be assured because the fractures are not clear, and tooth marks have not been observed on the bone surfaces.

3.2.1.5. Skeletal part frequencies in relation to bone mineral density

When applied to the complete skeleton, correlations of skeletal part frequencies with bone density yielded significant results for both small and medium-sized carcasses. In both cases the correlation was positive and Spearman's rho yielded medium to high values (Table 3.11, Figure 3.10A and B). When considering only long limb bones, the correlation coefficient for small carcasses becomes much lower, which means that density-mediated destruction mostly affected the preservation of the axial skeleton, and had a much lower effect on long limb bone preservation. In medium-sized carcasses the relationship is inverted (rho = - 0.78) and points to a higher presence of low-density appendicular elements, which could mean a higher presence of high-utility elements (Table 3.11). The relationship to food utility is further detailed in the following section.

3.2.1.6. Skeletal part frequencies in relation to food utility

Small carcasses

When considering carcasses of sizes 1 and 2, the first set of correlations yielded non-significant results, but the analysis performed with the bootstrapped data on the high-survival parts and on long bones yielded significant p-values. The Spearman's rho value is negative but denotes a weak relationship (- 0.44) when the complete skeleton or the high-survival set is considered; the correlation produces a reverse utility curve (Figure 3.11A). Finally, no correlation is found between appendicular element frequencies and MGUI, which points to an unconstrained strategy, suggesting that most of the appendicular elements are represented in accordance with their abundance in the skeleton, regardless of their economic utility. Indeed, the removal of the axial skeleton reveals this lack of relationship with food utility more clearly (Table 3.12). According to these results, small carcasses were probably transported complete to the site.

Medium-sized carcasses

As with small carcasses, correlations performed on %MAU values of medium-sized carcasses only yielded significant p-values when the bootstrapping method was applied first. Contrary to what would be expected due to the neg-

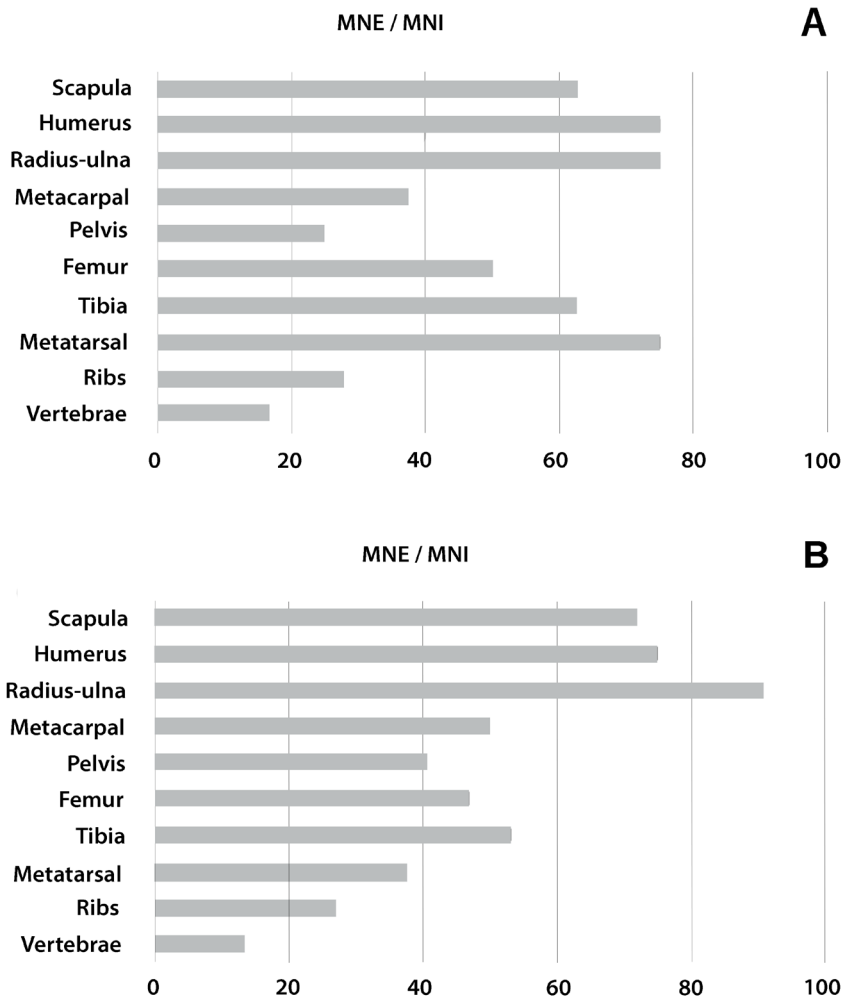

FIGURE 3.9. *Resulting skeletal part profiles for a) small carcasses, and b) medium-sized carcasses*

TABLE 3.11. *Spearman's rho and p-values of the correlations between bone mineral density and skeletal part abundances of small and medium-sized carcasses (density values after Lam (1999) for medium-sized carcasses and Lyman (1982) for small carcasses).*

	Size 1-2 Spearman's rho	p-value	Size 3-4 Spearman's rho	p-value
Complete skeleton	0.801	0.001	0.5268	0.0436
	Size 1-2 Mean	**p-value**	**Size 3-4 Mean**	**p-value**
Appendicular skeleton (bootstrapped data)	0.3133	< 0.0001	-0.7840	< 0.0001

ative coefficient resulting from the correlation with bone density, the relationship with food utility was negative and very weak in all three cases (Table 3.12). The elimination of the axial skeleton from the correlations did not produce an increase in the effect of food utility on skeletal part abundances; in fact, Spearman's rho values decrease a bit when only appendicular (and cranial) elements are considered. This suggests that density-mediated attrition on the axial skeleton is not the only factor affecting skeletal part abundances of medium-sized carcasses. In other words, the appendicular skeleton itself appears to present a bias that is not explained in terms of food utility or density-mediated attrition (**Table 3.12; Figure 3.11B**). Since the relationship with food utility is weak, no clear link can be established with any of Binford's utility curves.

3.2.1.7. Skeletal part frequencies in relation to return rates

Small carcasses

Skeletal part abundances of small carcasses show no statistically significant correlation to composite return rates, but when marrow return rates are considered, the correlations with the bootstrapping method yield a relatively low but positive significant result (0.34, Tables 3.13 and 3.14). Correlations with food utility suggested that small carcasses were transported complete to the site. MGUI and marrow return rates for small carcasses are highly correlated (rho= 0.86, p-value = 0.03), which indicates that for small carcasses, high-utility bones are also those most efficiently processed in terms of marrow extraction (femur and tibia). The positive result of this correlation points to a slightly

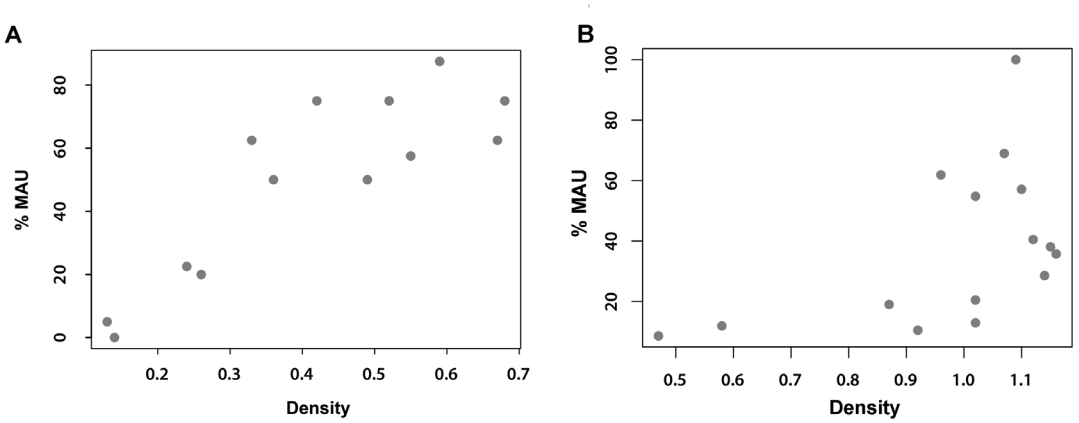

Figure 3.10. *Scatterplot showing skeletal part frequencies in relation to bone mineral density of a) small carcasses, and b) medium-sized carcasses*

Table 3.12. *Spearman's rho and p-values of the correlations of skeletal part abundances of small- and medium-sized carcasses with food utility values. The %MAU values of small carcasses are compared against the Modified General Utility Index (MGUI) for sheep (Binford 1978), and the %MAU values of medium-sized carcasses are compared against the Standardized Food Utility Index (SFUI) for caribou (Metcalfe and Jones, 1988).*

	Size 1-2		Size 3-4	
	Spearman's rho	p-value	Spearman's rho	p-value
a)				
Complete skeleton	- 0.4591	0.0638	- 0.2451	0.3417
High-survival set	- 0.2927	0.4816	- 0.4048	0.3268
Appendicular skeleton	0.0304	0.9545	- 0.3189	0.5379

Bootstrapped sample	Mean	p-value	Mean	p-value
b)				
Complete skeleton	- 0.4365	< 0.0001	- 0.2422	< 0.0001
High-survival set	- 0.2479	< 0.0001	- 0.3871	< 0.0001
Appendicular skeleton	0.0731	0.0002	- 0.2862	< 0.0001

more frequent transport of hind limbs. However, given that there are very few ungulate carcasses of size classes 1 and 2 at DS (MNI = 5), that the correlation coefficient is low and that the composite return rate correlation is non-significant, it is probably safest to assume that it is unclear that a relationship between body part abundances of small carcasses and economic utility exists at DS.

Medium-sized carcasses

In the case of medium-sized carcasses, composite return rates yield a significant although very weak positive relationship with skeletal part abundances when the data is subjected to bootstrapping first (rho = 0.12, Table 3.13), suggesting that return rates have a slight effect on skeletal part abundances, but are probably not enough to account for the observed skeletal pattern. Similarly, correlations with the bootstrapping method between marrow return rates and skeletal part abundances yield a significant but low Spearman's rho value (0.15, Table 3.14). Both correlation coefficients are not high enough to establish a connection between the two variables confidently, but they suggest that return rates are more useful to explain skeletal part abundances at DS than food utility values.

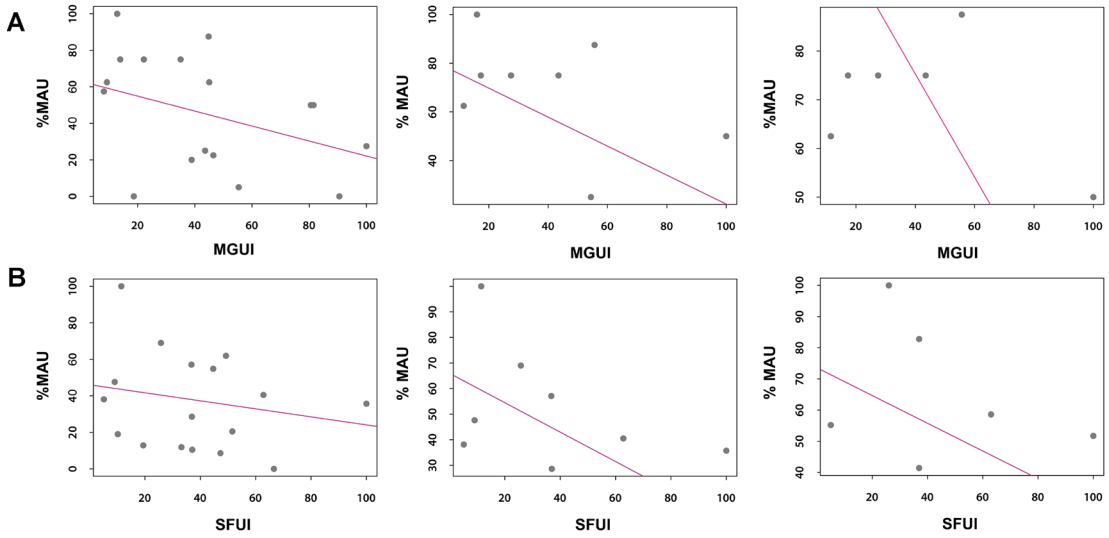

FIGURE 3.11. *Scatterplot showing skeletal part frequencies in relation to food utility of A) small carcasses, and B) medium-sized carcasses. From left to right, correlation with the complete skeleton, high-utility parts and the appendicular specimens.*

3.2.1.8. Shannon evenness index

Small carcasses

Evenness values for small and medium-sized carcasses at DS were estimated in two different ways: using high-survival elements and using long bones only. **Table 3.15** shows the results along with the total MNEs from which they were estimated, and the transport strategies that would in theory correspond to them according to Faith and Gordon (2007). For small carcasses the evenness index points to an unconstrained strategy. This result is at odds with the corresponding correlation of high-survival elements with food utility, which yielded a negative low value, but agrees with the results of the correlation made using only long bones elements, which points to a lack of relationship between transported elements and food utility. Given that all found relationships with food utility and return rates are weak, it is safe to assume that small carcass transport followed an unconstrained strategy. Small carcasses entered the site complete and were entirely processed at DS. This might be suggestive of short-distance transport from the kill site.

Medium-sized carcasses

Skeletal part abundances of medium-sized carcasses are distributed slightly more unevenly than small carcasses according to the evenness index. The esti-

mation of the index with the high-survival set yields a value of 0.96, and the estimation with long bones yields an evenness index of 0.97, both of which reflect a bulk strategy (**Table 3.15**). However, the results of the correlations are not consistent with any of these behaviors since the utility curve for medium-sized carcass skeletal part abundances resembles an inverse bulk strategy (Figure 11B). The bulk strategy is characterized by the maximization of the quantity of high and medium-utility elements, and suggests some degree of selectivity, which in turn indicates longer transport distances (Faith *et al.*, 2009). This interpretation should be considered tentatively, due to the fact that correlation coefficients are weak as well as negative in the case of food utility, and that data do not fit a bulk utility curve.

In their analysis of carcass selectivity at other Bed I sites, Faith *et al.* (2009) argued that there was a lack of evidence for selective transport, because the 95%

Table 3.13. *Spearman's rho and p-values of correlations between skeletal part abundances of small- and medium-sized carcasses and composite return rates (Egeland and Byerly 2005)*

	Size 1-2		Size 3-4	
	Spearman's rho	**p-value**	**Spearman's rho**	**p-value**
a)				
Appendicular skeleton	- 0.2994	0.5142	0.1429	0.7825

Bootstrapped data	**Mean**	**p-value**	**Mean**	**p-value**
b)				
Appendicular skeleton	- 0.0002	0.3176	0.1163	< 0.0001

Table 3.14. *Spearman's rho and p-values of the correlations between skeletal part abundances of small- and medium-sized carcasses and marrow return rates (Egeland and Byerly 2005)*

	Size 1-2		Size 3-4	
	Spearman's rho	**p-value**	**Spearman's rho**	**p-value**
a)				
Appendicular skeleton	0.3339	0.5177	0.2	0.7139

Bootstrapped data	**Mean**	**p-value**	**Mean**	**p-value**
b)				
Appendicular skeleton	0.3402	< 0.0001	0.1537	< 0.0001

Table 3.15. *Evenness index for small and medium-sized carcasses calculated a) with all high-survival elements b) only with appendicular elements. Interpretation is given according to the mean values at different MNEs provided by Faith and Gordon (2007: table 4)*

	Size 1-2				Size 3-4			
	Evenness	2.5%-97.5% CI	Total MNE	Strategy	Evenness	2.5%-97.5% CI	Total MNE	Strategy
High-survival elements	0.967	0.948– 0.977	35	**Unconstrained**	0.962	0.934– 0.973	144	**Bulk**
Appendicular elements	0.984	0.968– 0.991	30	**Unconstrained**	0.974	0.951– 0.987	113	**Bulk**

confidence limits of the skeletal element evenness did not exclude the value 1, which marks the perfectly even distribution of skeletal elements. They argued that confidence limits that exclude this value should be interpreted as significant evidence for selective transport. These researchers concluded that transport costs were low at other Bed I sites and had not reached the point where energetic returns could be increased by processing some elements at the point of prey acquisition. Therefore, transport distances must have been relatively short in general. According to this, the skeletal part abundances of medium-sized carcasses at DS would provide evidence for slight selective transport, since the confidence intervals (0.934 – 0.973) estimated by bootstrapping skeletal frequencies 1000 times exclude the value 1.000. One reason that may be impacting this index is the unevenness in the representation of front and hindlimbs. This bears no relationship to transport distance but to part selection. Additionally, the idea that only the value 1 signifies an even distribution is a theoretical statistical argument. In reality, skeletal part profiles from Pleistocene sites only rarely yield such homogeneous distributions and are still interpreted as even. The evenness value for medium-sized carcass sizes is very close to 1, and the estimation with appendicular elements yields an even higher value. This means that carcass element selectivity must have been low and, as with FLK *Zinj*, we cannot assume with certainty that hominins transported medium-sized carcasses across long distances at DS either. The mean values for evenness index of medium-sized carcasses of both sites are very similar.

We have already argued why we think that skeletal part abundances of small carcasses agree with an unconstrained strategy and short distance transport, and no evidence to the contrary has been found. It is true that evenness values for medium-sized carcasses are slightly lower than those for small carcasses and that skeletal part profiles of medium-sized carcasses seem to suggest some degree of selectivity, albeit low, in that front limbs are notably more abundant than hind limbs (Figure 3.9). Most of the medium-sized carcasses at DS were

probably complete, since all elements of the skeleton are represented, so the distortion might be caused by only a limited part of the assemblage. If we assume that most carcasses are complete, i.e. all transported pairs of hind limbs have a corresponding pair of front limbs at the site, then there are at least 9 complete medium-sized carcasses and 6 incomplete medium-sized carcasses, or pairs of hind limbs, represented at DS.

In sum, the correlations and the evenness index do not provide a clear answer to the problem of differential representation of skeletal parts at DS, but some inferences can be drawn from them. First, density-mediated attrition affects axial remains especially, but it is not the only factor that produces the reverse pattern in medium-sized carcasses, and therefore, skeletal profiles of medium-sized carcasses are probably the result of hominin transport decisions. Second, while it appears that small carcasses were consistently transported complete to the site, which is indicated by a clear unconstrained pattern, when density-mediated attrition on the axial skeleton is taken into consideration, the pattern of medium-sized carcasses is far less clear. It is very likely that the skeletal profile of medium-sized carcasses represents a collection of individual transport episodes that formed under very different situations, and that this hinders the observation of any predominant strategy. Since all skeletal elements are represented at the site, it can be assumed that on some occasions all parts of the carcasses were transported to the consumption site, whereas other times hominins only transported selected parts. This bias, which is not reflected in the evenness index, might have implications regarding transport distance. Whereas the pattern of small carcasses is indicative of short distances to the site, incomplete carcasses point to longer distances or different acquisition strategies. If hominins indeed transported some carcasses across longer distances, this would contrast with what is known of FLK *Zinj*, where no such bias in the skeletal profiles was observed. Given that correlations with food utility and return rates do not yield clear results and leave this matter unresolved, the relation between front and hind limbs in medium-sized carcasses is further explored using a different approach in the following analysis.

3.2.2. Front vs. hind limb representation: Comparing MNEs from DS to skeletal part abundances at other Paleolithic sites

The low representation of hind limbs with respect to front limbs in medium-sized carcasses does not seem to be related to the effect of density-mediated attrition or to any other taphonomic processes. First, the analyses reported in previous sections demonstrated that DS was only minimally affected by water. Variations from a completely undisturbed assemblage were reflected in differences in the overall lower representation of axial remains (mainly verte-

brae), compact bones and long bone epiphyses. There is no reason to believe that the mentioned underrepresentation of hind limbs is the reflection of a lack of epiphyses, first because the MNE of the femora was estimated using proximal epiphyses and not shafts, and second because when the ratio between shafts and the best represented epiphysis (proximal or distal) is calculated for each long bone element, the results are very similar for the humerus, the radius and the femur (0.1, 0.5 and 0.1 respectively). The tibia, however, yields a very low value (0.04), which suggests that there is an underrepresentation of tibia epiphyses with regard to the other meaty long bones. In fact, it is surprising that proximal tibia epiphyses are more abundant than distal epiphyses, which are denser and are usually better preserved. Be that as it may, the MNE value for the tibiae as estimated using shafts is still higher than that for the femora. A further argument against the hypothesis that the unbalance of front and hind limbs resulted from the effect of taphonomic processes is that skeletal part abundances of small carcasses are not biased. Although the sample size of small carcasses is small, front and hind limbs are clearly equally represented in these types of carcasses. Finally, the relationship between bone mineral density and long bones of medium-sized carcasses was negative, so the most plausible explanation is that the reason for the underrepresentation of hind limb bones is behavioral.

Figure 3.12 show the proportion between front and hind limbs of a selected group of Paleolithic sites that are interpreted as anthropogenic accumulations resulting from hunting. The left side of the graph represents the case of a higher representation of hind limbs than front limbs, while the right part shows the sites with a higher proportion of front limbs than of hind limbs.

If we assume that hominins had primary access to the accumulated animals, it is reasonable to expect most points to cluster around the center or on the left part of the graph, thus reflecting the presence of complete carcasses or the predominance of higher utility elements, i.e. hind limbs. However, there is high variability and the sites cover almost the complete spectrum, from a clear overrepresentation of hind limbs at Porc Epic to more than twice the number of front limbs than hind limbs at Mauran. DS ranks third from the right after Wallertheim and is followed by Maple Leaf and Verberie II-1 (Figure 3.12). Interestingly, the four sites surrounding DS have all been interpreted as kill or near-kill butchering sites. The assemblages that seem to represent residential sites appear on the left part of the graph most of the times. Other sites' functionalities are less clear, and have been left unspecified as "consumption sites" (Figure 3.13).

Mauran and Wallertheim are both Mousterian assemblages interpreted as kill sites where bison carcasses were extensively butchered. The sites seem to have been occupied recurrently for a long period of time (Farizy *et al.*, 1994; Gaudzinski, 1996). Maple Leaf was interpreted as a small Paleoindian bison kill

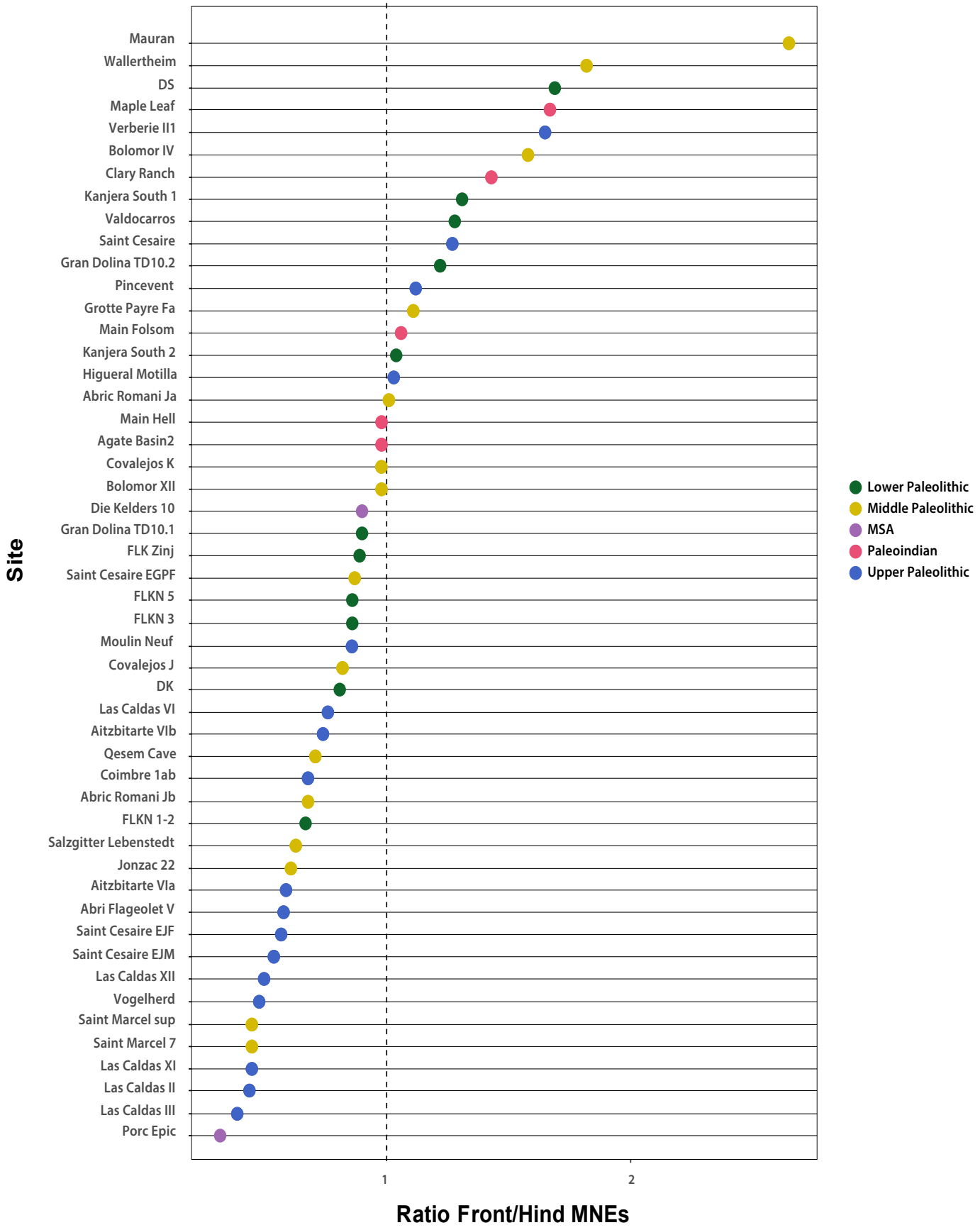

FIGURE 3.12. *Graph showing the proportions between front and hind limbs at each of the selected anthropogenic Paleolithic sites. On the left part of the diagram are the cases with a higher representation of hind limbs, the right part shows the sites with higher proportion of front limbs.*

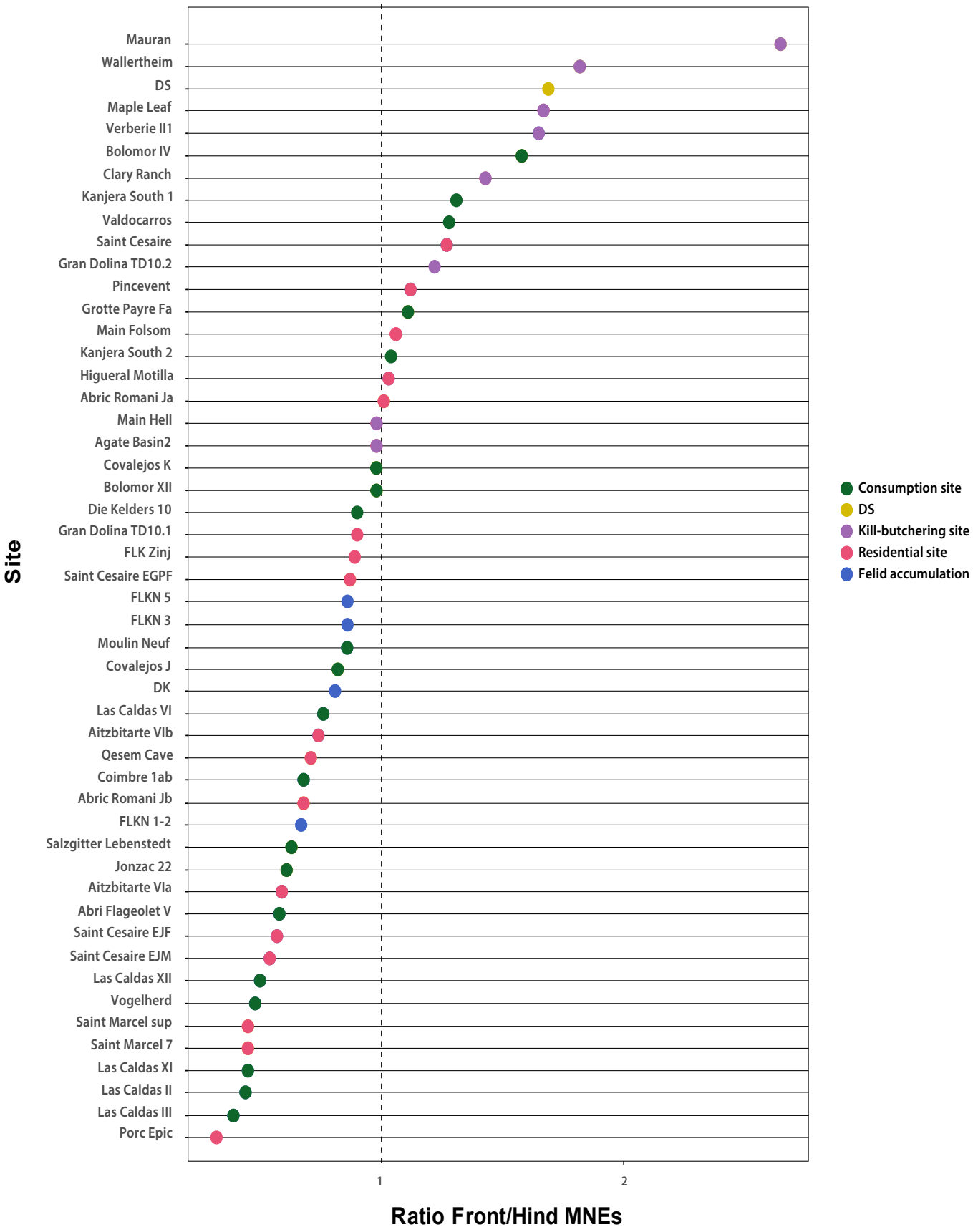

FIGURE 3.13. *Graph showing the proportions between front and hindlimbs at each of the selected anthropogenic Paleolithic sites, as well as their interpretation as either consumption places, residential sites, or kill sites.*

site on the basis of Binford's (1978) summer kill models (Gaudzinski, 1996), and the Magdalenian site Verberie II-1 (12 Ka) is interpreted as a hunting campsite for initial carcass processing. The abundance of medium-utility elements in contrast to a very low representation of femora and tibiae is also not due to density-mediated attrition: this pattern is explained as the result of the selection of high utility parts to be transported to a residential site and the partial processing and consumption of other parts at the hunting or near-kill butchering site (Enloe, 2004). Verberie II-1 is a monospecific faunal accumulation of reindeer, and the other mentioned sites consist mainly of bison carcasses. Clary Ranch, another Paleoindian assemblage, and Gran Dolina TD10.2 (Atapuerca) are also interpreted as near-kill sites or initial processing areas (Hill, 2001; Rodríguez-Hidalgo *et al.*, 2017). Both are characterized by greater abundance of front limbs with regard to hind limbs. The bonebed uncovered at Gran Dolina TD10.2, also consists of bison carcasses and is also interpreted as a place where some of the meat and fat was selected for transportation to another location (Rodríguez-Hidalgo *et al.*, 2017). Based on other taphonomic evidence, these bison accumulations formed as the result of one or several seasonal events of mass communal hunting.

The proximity of DS to these sites in these graphs suggests that DS could also have served the function of a near-kill butchering site. Were hominins partially processing and consuming the carcasses at a near-kill location and selecting the higher utility parts for transport to a central place? Although it is a valid hypothesis, the following remarks should be taken into consideration. First, the use of DS as a near-kill butchering site would imply that hominins would have had to travel long distances to the central place, otherwise spending time and energy using a near-kill location would not be advantageous. This would in turn stand in marked contrast with FLK *Zinj*, which was previously interpreted as a central place to which hominins transported complete carcasses from short distances (Faith *et al.*, 2009). Furthermore, all the sites that show similarities with DS in the ratio between front and hind limbs in this comparison are characterized by being monospecific, whereas DS is not. More specifically, most of them are bison kill sites. At DS, in addition to being taxonomically varied, there are small carcasses hat were transported presumably complete and consumed on the spot. This makes the interpretation of DS more challenging. In fact, it may also be risky to compare DS to Paleoindian sites formed often as a result of mass communal hunting, which have special features and are interpreted according to a number of theoretical models that are not applicable to DS.

There are several other sites that appear on the right part of the graph next to DS and which present a skeletal profile similar to that of medium-sized carcasses at DS, also characterized by a higher frequency of front limbs with regard to hind limbs. In contrast to the aforementioned kill or near-kill sites, these other locations are interpreted as residential sites (Pincevent and Saint Césaire)

or consumption places (Bolomor IV, Kanjera South 1, Valdocarros) (Figures 3.12 and 3.13). At Bolomor IV, hominins primarily accumulated carcasses of adult deer, next to a variety of other species including lagomorphs, tortoises and birds (Blasco, 2011; Blasco and Fernández Peris, 2012). Valdocarros is a very large site (700 m^2) that also has evidence of primary access to carcasses by hominins and includes different species, namely Cervus, *Equus*, and Dama. Their skeletal representation is also slightly biased according to the ratio between front and hind limbs presented here, although this is not reflected in the evenness index, which suggests that carcasses were transported fairly evenly over short distances (Yravedra 2005). Ferraro *et al.* (2013) also report skewed skeletal element abundances for medium-sized carcasses at Kanjera South 1, and suggest that these carcasses were likely not complete. The same is true for the Upper Paleolithic sites Saint Césaire and Pincevent. Both these assemblages are dominated by one species, adult red deer at Saint Césaire and reindeer at Pincevent, and it is well established that both were used as residential sites. At Pincevent, the spatial analysis suggests that organization of space use resembles modern hunter-gatherer residential households (Enloe, 2003). Skewed skeletal profiles at residential sites are the product of a higher carcass part selectivity at the kill sites – when they are not biased by taphonomic processes –, which in turn may be the convenient decision when distance to camp is long. This inference is unproblematic when skeletal profiles reflect incomplete carcasses at Upper Paleolithic sites, because this type of behavior is observed in modern hunter-gatherers, but it seems more uncertain when dealing with older sites, in particular sites that date to the Early Paleolithic. Interestingly, though, apart from DS, the two Early Paleolithic examples reported here, Kanjera South 1 and Valdocarros, present a more marked contrast in the representativity of front and hind limbs than Pincevent and Saint Césaire (Figures 3.12 and 3.13), which means that if the inference of carcass part selectivity and long distance transport is made for these sites, it should equally be valid for DS and other similar Early Paleolithic sites. Kanjera South 2, which is a larger assemblage than Kanjera South 1, also falls on the right side of the graph. Although it falls closer to the central vertical line than Kanjera South 1, Ferraro *et al.* (2013) have also suggested that medium-sized carcasses might have been introduced incomplete to this site as well, because there is an overrepresentation of cranial remains compared to the postcranium.

3.2.3. Behavioral implications

There are a number of matters that complicate the interpretation of skeletal part profiles of archaeological sites. Among them, the most problematic ones seem to be the high variability that may have existed in carcass part selection and transport decisions in hominin groups and our inability to account for

many of the factors and constraints that might have influenced them in these decisions. On the other side, however, a series of methods and approaches have been developed that enable zooarchaeologists to formulate hypotheses and work around some of the difficulties, like the biases caused by taphonomic processes, especially carnivore destruction and density mediated attrition. Skeletal part profiles of African Plio-Pleistocene sites in particular pose a major challenge, because they are the best evidence we have to address their functionality, which is the subject around which one of the hottest paleoanthropological debates has revolved since the 1970s. Understanding site function is key to comprehend many other aspects of hominin behavior. It is tightly related to topics such as hominin subsistence and transport strategies, their cooperation and planning capabilities, their use of the landscape or food sharing.

The skeletal part representation analysis applied to the DS ungulate assemblage has yielded clearer results for small carcasses than for medium-sized carcasses. The former present a relatively unbiased skeletal profile, when density-mediated attrition on the axial skeleton is considered, which is in accordance with the skeletal part profiles documented at FLK *Zinj* and points likewise to short distance transport and the use of DS as a consumption or central place. However, the appendicular skeletal representation of medium-sized ungulates shows some degree of unevenness in carcass transport, whereby this interpretation is neither confirmed nor rejected.

The near-kill location hypothesis outlined above implies that transport distances would have been costly on some occasions, and also that hominins had enough time to process and consume some parts of the carcasses at these locations as modern foragers do. Hadza and Kua hunters have been observed to do this: they maximize the nutritional intake at the site and minimize the energetic costs of transportation by eliminating inedible parts at the near-kill site. Often, those skeletal elements that are more easily processed, such as limb bones, are eaten and discarded at the site, while the rest (axial skeleton) is transported (Monahan 1998; Bartram and Marean, 1999). It has been pointed out, however, that modern savannas probably do not pose as many hazards derived from carnivore competition for humans nowadays as they did for hominins during the Pleistocene, and that it is thus less likely that hominins had the time to remain next to the carcass for long periods of time, so as to process almost an entire carcass before returning to the central place (Egeland and Byerly, 2005). Although this is possible, it seems more likely that DS served as a central place, where most small and medium-sized carcasses were introduced complete, and only a few carcasses entered incomplete. This interpretation receives support from the fact that DS taxonomic composition, faunal assemblage size and spatial pattern (see below) are similar to those of FLK *Zinj*, where this skeletal representation contrast between front and hind limbs does not exist. Moreover, a similar skeletal representation is documented at other sites that are confidently

interpreted as residential sites, like Pincevent for example.

From this perspective, the fact that some hind limbs are missing at the site could hypothetically also be explained in two different ways. One possibility is that a few of the carcasses were not acquired by hominins through hunting but by confrontationally scavenging from felids. Hominins would have accessed these carcasses partly defleshed and would maybe have been able to steal almost the complete carcass except viscera and hind limbs. Alternatively, the observed skeletal pattern could result from hominin butchery and discard at the kill site of those elements that are more efficiently processed, i.e. those that have higher return rates (hind limbs: femora and tibiae), as a strategy to maximize their individual energetic gain, and minimize the transport load. DS would thus be dominated by elements associated with lower return rates and we would expect to find a negative association between skeletal element abundances and return rates. This is not the case (correlations yielded very weak coefficients), again probably because the pattern only affects part of the assemblage. It is important to bear in mind that the assemblage is the result of the superposition of many different independent butchery and transport events. Only if one strategy is predominant over the others will it leave a pattern in the archaeological record that can be uncovered.

We have already speculated that the comparison of the DS appendicular skeletal profile to that of other Paleolithic sites suggests that the location could also have served as a near-kill butchering site instead of as a consumption site. Hominins would have acquired carcasses at the site or very near to the site and then butchered and prepared them for further transportation, selecting high-utility elements (i.e. hind limbs) to be transported back to the referential place, which would have been at least some kilometers away (according to models on transport strategies by modern foragers, Bunn *et al.*, 1988; Bartram, 1993), thus creating a skeletal pattern at DS characterized by a deficiency of hind limbs. However, this interpretation is at odds with the transportation into the site and consumption of small carcasses. Additionally, hind limbs from medium-sized carcasses are not missing. They are merely less represented than front limbs, and it can be assumed that some carcasses would have been transported complete to the site. This is also supported by the evenness index. If several carcasses were butchered completely at the site, as is the case with small carcasses, DS must have served as a consumption place, where complete carcasses would have been shared among the group. Other carcasses could have been transported more selectively into the site, especially if they were carried over longer distances, and consumption and discard of the highest marrow-yielding bones (i.e., femur and tibia) could have been done at those sites. This would fit with many Upper Pleistocene sites where this pattern is also documented, including Pincevent and Saint Césaire (Figures 3.12 and 3.13).

One could view this as a contradiction: skeletal part abundances of medium-sized carcasses at DS and other sites seem to be fairly even according to the evenness index, but skewed when only the ratio between meaty front and hind long bones is taken into account. Short and long transport distances are traditionally only inferred through the first approach, which includes more skeletal elements that also differ in their varied economic utility values. From this, it follows either that the assessment of transport distance should include more detailed aspects of skeletal profiles or that the contrast observed between front and hind limb bone frequencies could be pointing to something different from the effect of long-distance transport.

In conclusion, DS appears to have been used at least in part as a central place and was probably formed as the result of the systematic short-distance transport of complete small and several medium-sized carcasses to the site, and the occasional input of partial medium-sized carcasses, which were probably processed and consumed at the location of their acquisition or simply acquired incomplete. I have outlined all the possibilities and cannot conclude anything without further taphonomic analysis. Below I will use further taphonomic evidence to test all these possible interpretations.

3.2.4. Estimating ravaging intensity and degree of competition using skeletal part ratios

Most Bed I sites show low to moderate ravaging. FLKN 4 and FLKNN 1 fall into stage 1 when using the first ratio (femur to tibia), while FLKN 3, FLKN 6 and FLKN 1-2 fall into stage 2. FLKNN 3, FLK *Zinj* and all three samples of DS fall in between stages 1 and 2, due to the higher presence of axial remains (**Figure 3.14**). The Maasai Mara hyena den and the data from the experimental sample modeling hammerstone-to-carnivore (Capaldo, 1995; Domínguez-Rodrigo *et al.*, 2007) show higher degrees of ravaging, given their low axial to limb ratios. When the ratio of femur to tibia is replaced with the other ratio (proximal humerus and distal radius to distal humerus and proximal radius), sites remain in similar stages, although some are displaced by one stage. The actualistic assemblages again show the highest ravaging stages and fall into stage 3, along with FLKN 3, while FLKNN 3 and FLKN 6, which shows a high presence of complete bones, fall into stage 1. FLK *Zinj*, FLKN 1-2 and FLKN 4 are displaced into stage 2, and DS falls between stages 2 and 3 (**Figure 3.15**).

Overall, most Bed I sites show low degrees of ravaging, which would mean that carcass competition was relatively low, especially at FLK *Zinj*, FLKN 1-2, 4 and 6, and FLKNN 3. At DS, however, it seems that competition could have

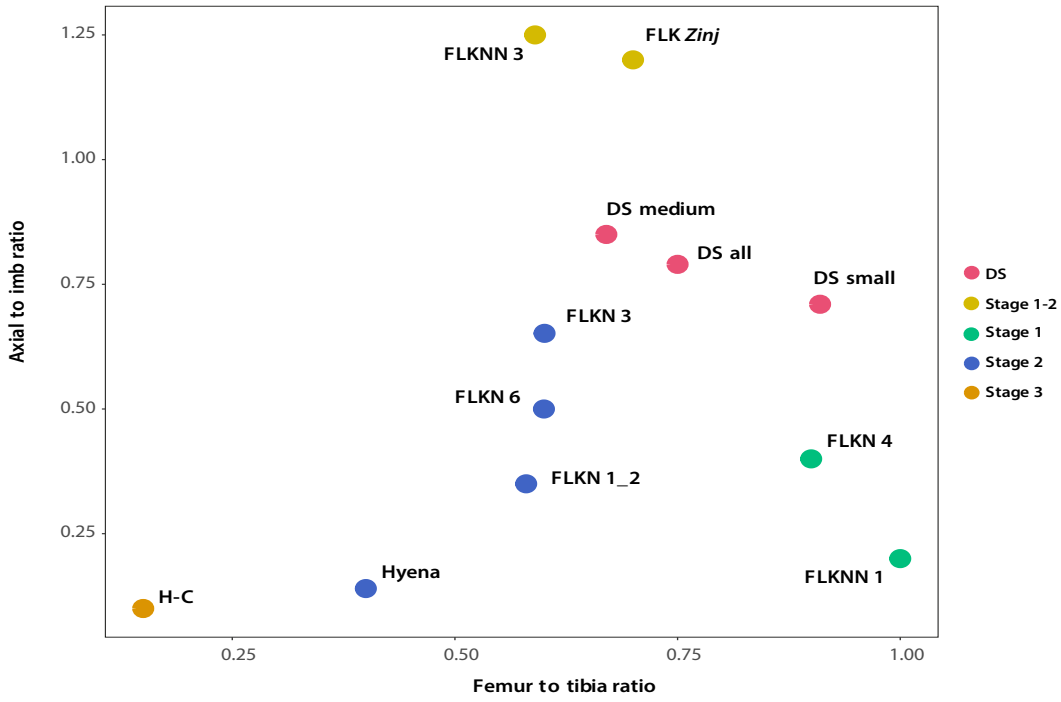

FIGURE 3.14. *Ravaging stages of the DS 22B assemblage and some of the other bone assemblages from the Olduvai Bed I sites using the femur to tibia ratio.*

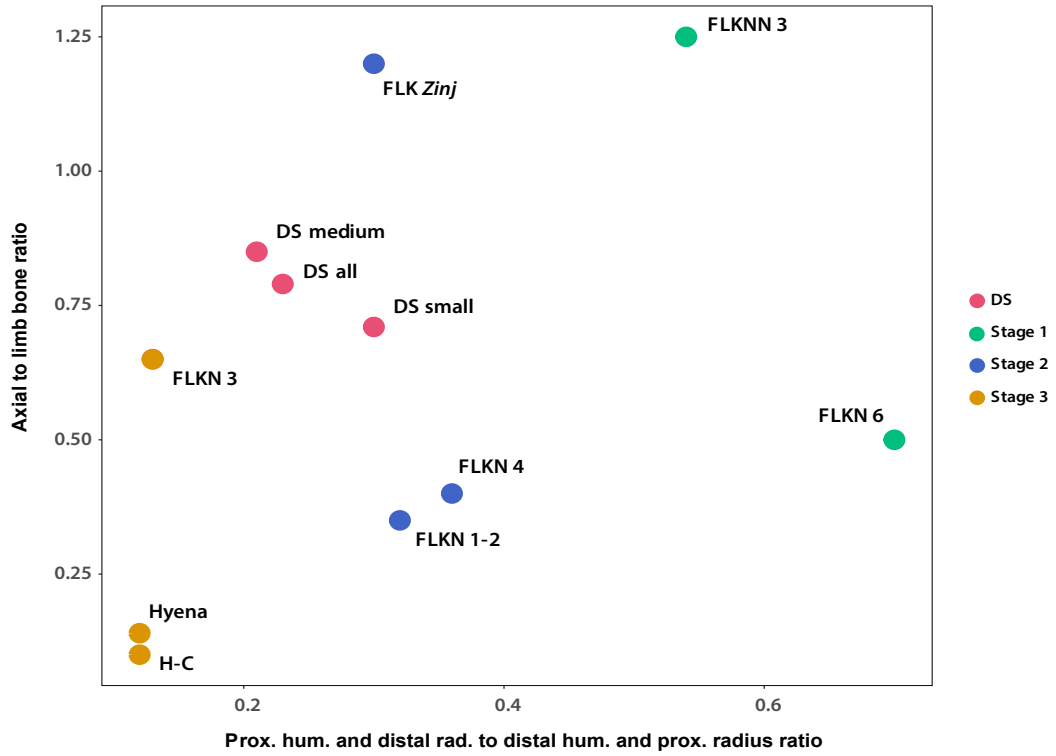

FIGURE 3.15. *Ravaging stages of the DS 22B assemblage and some of the other bone assemblages from the Olduvai Bed I sites using the proximal humerus and distal radius to distal humerus and proximal radius ratio.*

been moderate. The degree of ravaging intensity can point to the ecological context in which the sites were formed. FLK *Zinj* shows a low degree of ravaging, and it has been established that it was probably located in a more closed environment, judging also by the presence of palm trees and its location on an elevated platform (Uribelarrea *et al.*, 2014; Arráiz *et al.*, 2017). DS seems to have been subjected to slightly higher degrees of ravaging, yet we know that the vegetation was similar to that of FLK *Zinj*. However, the site seems to have been formed in an area close to two rivers, which would have attracted game and where carnivore competition for access to carcasses would evidently have been higher. The predatory guild from 2 Mya was larger and more diverse than that of modern savannas today. The probabilities that carcasses could have been left undisturbed is therefore very low, which has implications regarding the amount of passive scavenging opportunities that hominins could have encountered. However, closed-vegetation areas would probably still have remained the lowest competition settings (Domínguez-Rodrigo *et al.*, 2007).

3.3. Bone breakage

3.3.1 Green vs. dry bone breakage

Table 3.16 shows the frequencies of green and dry broken bone fragments in the assemblage. The proportions of each type of fractures are very similar in all three carcass sizes, and also when all animal sizes (including indeterminates) are considered together. Green fractures are much more abundant than dry fractures regardless of carcass size and they are unequivocal on around 42-66% (depending on carcass size) of the bone collection. Diagenetic dry breakage is found in around 9-15% of the assemblage. A small percentage (2-6%) presents both types of fractures. These percentages do not add up to 100% because in a significant proportion of the collection (around 44%) fractures were either indeterminate or absent. About 84% of this latter fraction of the assemblage is composed of teeth and other cranial elements, axial remains, compact bones and more poorly preserved unidentified fragments. When considering long bones exclusively, only around 10% of them present indeterminate fractures. This percentage is reduced to 5% when only long bone shafts are considered. The difficulty of determining the type of fracture in these shaft specimens is probably related to poor preservation and the presence of carbonate concretions covering some of the breakage planes. In any case, among long bones, green breakage is overwhelmingly more abundant than diagenetic breakage in both small and medium-sized carcasses, and the proportions of each fracture type are very similar across long bones, especially in medium-sized carcasses. In small carcasses, metapodials, particularly metatarsals, present a less marked contrast between the frequencies of green and dry breakage than the other limb bones, which could be due to the fact that they contain less marrow (Figure 3.16A and B; 3.17).

DS is very similar to some Bed I sites in the percentages of green and diagenetic breakage of limb bones, such as FLKN 1-2 and FLKN 3, however it shows some differences with other Bed I sites in this regard, like FLKN 5 for example, where especially medium-sized carcasses show much higher frequencies of diagenetic breakage. FLKN 4 and DK levels 2 and 3 also show higher rates of dry breakage (20-30%), although the pattern at FLKN 4 could be related to the fact that sample size is small. (Domínguez-Rodrigo *et al.*, 2007).

Table 3.16. *Proportions of green and dry fractures in the DS 22B assemblage for each carcass size and for the complete faunal assemblage. Percentages do not add up to 100% because for a significant portion of the assemblage consisting mainly of axial and cranial remains, fracture type could not be determined confidently.*

	Green fractures	Dry fractures	Both
Small carcasses	228/483 (47.2%)	48/483 (9.9%)	13/483 (2.7%)
Medium-sized carcasses	1008/1913 (52.7%)	300/1913 (15.7%)	90/1913 (4.7%)
Large carcasses	42/63 (66.7%)	9/63 (14.3%)	4/63 (6.3%)
All	1460/3458 (42.2%)	409/3458 (11.8%)	75/3458 (2.1%)

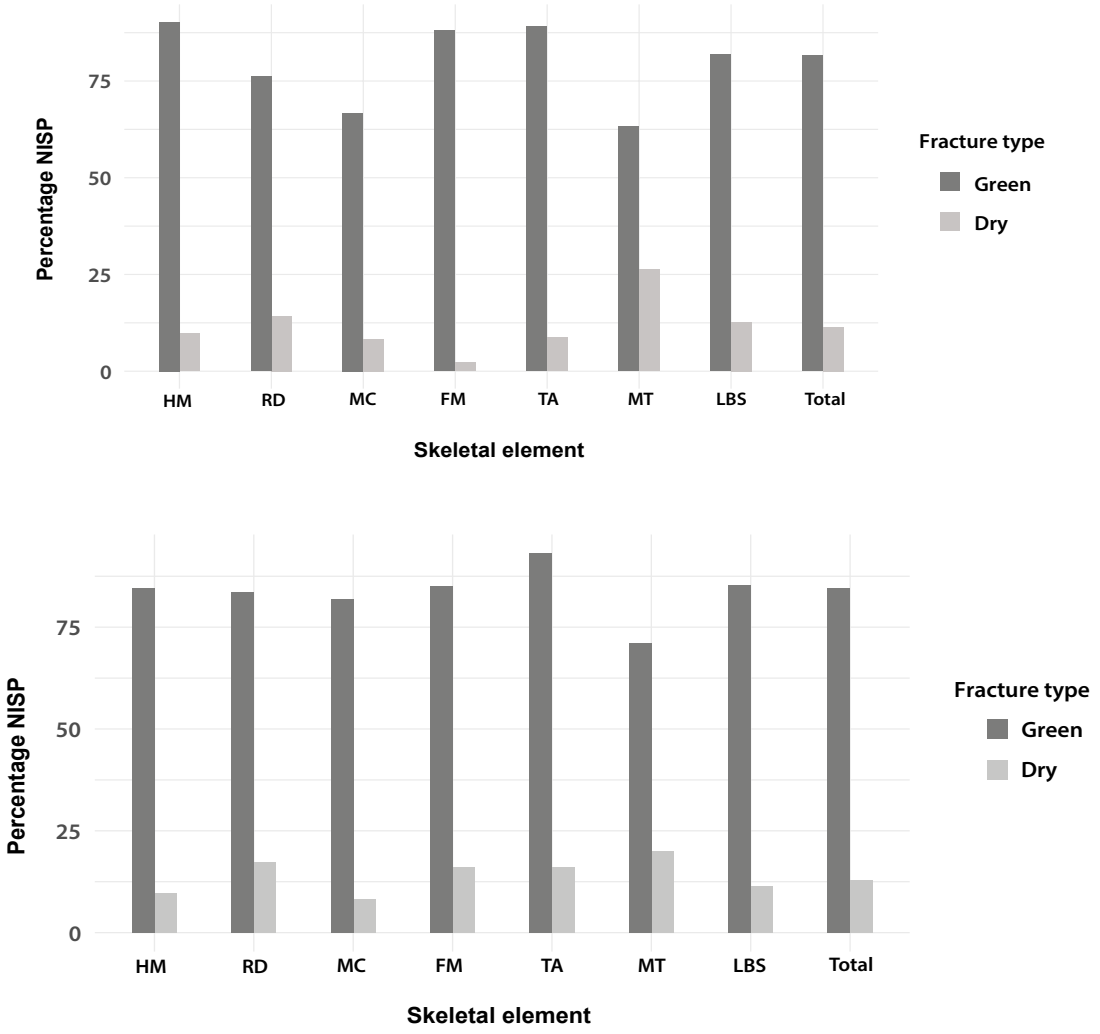

Figure 3.16. *Frequencies of green and diagenetic fractures on limb bones from a) small and b) medium-sized carcasses at DS. LBS: unidentified limb bone shaft*

FIGURE 3.17. *Examples of green fractured long bones shafts.*

3.3.2. Fragmentation indices

3.3.2.1. Extent and degree of fragmentation

For DS, the extent of fragmentation, or %fragmentary (after Lyman 2008), has first been estimated by calculating the proportion of the total NISP that are incomplete skeletal elements, regardless of type of fracture. Fragmented bone specimens make up 98.2% of the faunal collection and only 1.8% of the collection is made up of complete elements. Complete elements are mostly teeth, compact bones and caudal vertebrae. Intensity of bone fragmentation was estimated per element for small and medium-sized carcasses separately, in order to determine whether it differed across the two animal size classes and how it varied across skeletal elements. The results of the ratios of NISP:MNE for each skeletal element and size class are shown in Table 3.17. The highest NISP:MNE ratios can be found among long bones. Small and medium-sized carcasses are similarly fragmented, although the first seem to have fragmented into slightly more pieces than medium-sized carcasses, because ratios are slightly higher for small carcasses. The average ratios of NISP:MNE are 2.97 and 2.83 for small and medium-sized carcasses respectively, and 5.67 and 4.96 when only long bones are considered.

3.3.2.2. Ratio of NISP:MNE for green broken long bones

On the whole, the bone assemblage is highly fragmented and green fractures account for most of the fragmentation at the site. Ratios of NISP:MNE for only green broken long bones yield high values also; the average NISP:MNE ratios for green broken long bones of small and medium-sized carcasses at DS are 4.93 and 4.39 respectively (Table 3.18A). These numbers are much closer to the ratios documented for experiments modeling hammerstone breakage by hominins (3a-3b; Monahan, 1996), than to long bone NISP:MNE values of carnivore-modified assemblages, which typically yield much lower values (probably due to a higher presence of complete bones), although these ratios vary with the degree of carcass competition. Midshaft NISP:MNE ratios estimated for FLK *Zinj* also yielded values more similar to anthropogenic than to carnivore breakage: 2a for small carcasses and 3b for medium-sized carcasses (Domínguez-Rodrigo *et al.*, 2007). Hyena dens, which are typically settings characterized by low competition, generally produce low NISP:MNE ratios as compared to hammerstone broken assemblages (Egeland *et al.*, 2008). Table 3.18B shows the NISP:MNE ratios documented at Syokimau, KFHD1 and KND2, which are close to 1.5-1.6 (Egeland *et al.*, 2008; Prendergast and Domínguez-Rodrigo, 2008), indeed significantly lower than those reported for DS.

Table 3.17. *Ratios of NISP:MNE for each skeletal element for small and medium-sized carcasses.*

Skeletal element	Size 1-2	Size 3-4	Size 5
Skull	1.75	5	1
Mandible	9	2.29	1
Atlas	0	2	0
Axis	0	1	0
Cervical vertebra	2	1.18	0
Thoracic vertebra	1	2.09	0
Lumbar vertebra	1	1.13	0
Sacrum	0	1.6	0
Caudal vertebra	0	1	0
Scapula	1.4	1.78	0
Pelvis	5.5	3.23	2
Ribs	3.52	3.6	2
Humerus	5	6.92	2
Radius-ulna	3.67	3.79	1.33
Metacarpal	3.33	3.63	2
Femur	11	5.27	1.33
Tibia	8	7.06	1.25
Metatarsal	3	3.08	0
Carpals	1	1	1
Tarsals	1	1	0
Phalanges	1.07	1.75	0

The femur and tibia in small carcasses, and the tibia in medium-sized carcasses, are the most fragmented limb bones, while radii-ulnae and metatarsals show the lowest NISP:MNE ratios in small and medium-sized carcasses, although especially in the latter. The NISP:MNE values for large carcasses (size 5) have been estimated with a very small sample size, which renders them less reliable. In theory, lower NISP:MNE ratios reflect larger pieces. This can partly be corroborated in the average shaft length for each long bone presented in Table 3.19, which shows that the shafts of the radius-ulna and the metatarsal are larger than those of femora and tibiae, which are the elements that show the lowest NISP:MNE ratios. The low mean values of the metapodial shafts is probably related to their low marrow content, and low NISP:MNE value of the

humerus shafts is probably related to their smaller size with regard to radii, femora and tibiae.

Pickering and Egeland (2006) and Moclán and Domínguez-Rodrigo (2018) have suggested that, in experiments modelling anthropic hammerstone bone breakage, hindlimb bones, and especially the tibiae, seem to generate a higher number of specimens than front limbs. This is also observed in spotted hyena dens, for example in Syokimau (Bunn, 1982; 1983; Egeland *et al.*, 2008), in

Table 3.18.a. *Ratios of NISP:MNE for green broken long limb bones for small, medium-sized and large carcasses.*

Skeletal element	Size 1-2	Size 3-4	Size 5
Humerus	4.67	5.75	4
Radius-ulna	2.83	2.76	1.33
Metacarpal	2.67	3.13	2
Femur	9.25	4.93	1.33
Tibia	8.2	7.12	1.25
Metatarsal	2	2.67	0

Table 3.18.b. *Ratios of NISP:MNE and the percentages of complete bones reported for the Syokimau (Bunn 1982, 1983; Egeland et al. 2008), Koobi Fora (KFHD1, Lam 1992) and Eyasi (KND2) hyena dens (Prendergast and Domínguez-Rodrigo 2008). The values were estimated including bone specimens of small and medium-sized carcasses, with the exception of KND2, where the values correspond to Ovis/Capra.*

Skeletal element	Syokimau		KFHD1		KND2	
	NISP:MNE	%MNE complete	NISP:MNE	%MNE complete	NISP:MNE	%MNE complete
Humerus	1.33	15.2	1.14	0	1.5	16
Radius-ulna	1.35	20.6	1.40	14.3	1.4	15
Metacarpal	1.38	61.9	1.11	44.4	1.0	67
Femur	1.24	12.0	2.36	0	2.0	31
Tibia	2.26	7.4	1.96	19.0	2.1	16
Metatarsal	1.52	14.8	1.39	42.9	1.0	33
Total	1.51	20.4	1.56	20.0	1.5	29.7

Table 3.19. *Average length of shaft fragments for all long bone elements in small and medium-sized carcasses.*

Skeletal element	Size 1-2	Size 3-4	Size 5
Humerus	41.73	53.68	63.09
Radius-ulna	51.05	78.36	151.5
Metacarpal	47.78	56.66	105
Femur	48.11	62.67	149.29
Tibia	46.12	68.48	114.09
Metatarsal	45.47	72.14	-

the den of Koobi Fora (KFHD1) studied by Lam (1992), and in the less intensely fragmented hyena den at Eyasi (KND2) described by Prendergast and Domínguez-Rodrigo (2008), who also report higher fragmentation ratios for hindlimbs than front limbs (Table 3.18B). Higher fragmentation ratios of these elements could be caused by intrinsic properties of these bones that make them break into more pieces, or they could be related to the fact that marrow content is higher in hindlimbs than in front limb bones, which would in theory drive hominins and carnivores to fragment these bones more intensively (Egeland *et al.*, 2008).

3.2.2.3. Percentage of complete bones

The overall lower NISP:MNE ratios in assemblages created by carnivores are probably related to a higher presence of complete bones at these sites than in anthropogenic assemblages. At DS 5.5% and 3.5% of the long bone MNEs are complete in small and medium-sized carcasses respectively. In contrast, around 20% of the long bone MNE at Syokimau and at KFHD1, and around 30% at KND2 were complete (**Table 3.18B**). Similarly, at the modern lion accumulation at OCS 47% of the long bones were complete (Arriaza *et al.*, 2016).

At other Bed I sites that have been interpreted as felid accumulations or palimpsests, where hyenas partly ravaged the collections and hominin input was only sporadic, the percentage of complete bones is higher than at DS. To name a few examples, in Level 6 at FLKN, almost half of the appendicular bones are complete (41%). Here, carnivore ravaging was not at all intense, and hominins were not involved in bone breakage. The overall proportion of the limb bone MNE made up of complete limb bones at FLKN 1-2 is 14%, which suggests that this site was a low competition setting. This assemblage presents a mixture of very complete bones and other very fragmented ones that point to differ-

ent depositional moments with different degrees of carnivore ravaging. This is partly reflected in the marked difference of complete bones of *Antidorcas* (27%) and *Parmularius* (8%) (Domínguez-Rodrigo *et al.*, 2007). Percentages of complete bones at FLKN 3, FLKN 4 and FLKN 5 are 15%, 10% and 16% respectively. At FLKNN 1 about 20% of the limb bones are complete, at the natural assemblage of FLKNN2 around 28% of MNE are complete and at FLKNN

Table 3.20.a. *Ratios of epiphyses to shafts for green broken long limb bones in each carcass size class.*

Skeletal element	Size 1-2	Size 3-4	Size 5
Humerus	0.12	0.11	0.14
Radius-ulna	0.55	0.45	0
Metacarpal	0.33	0.43	0
Femur	0.16	0.07	0.33
Tibia	0.14	0.06	0
Metatarsal	0.33	0.33	-
All	0.27	0.24	0.07

Table 3.20.b. *Ratios of epiphyses to shafts in several experimental, natural carnivore and Bed I assemblages (from Monahan 1996; Egeland et al. 2008; Domínguez-Rodrigo et al. 2007)*

	Epiphyses:shafts	Data sources
Experimental assemblages		
Carnivore-only (bovid 1-4)	0.03-0.02	Blumenschine 1988; 1995
Carnivore-only (sheep/cow 1-3)	0.08	Marean (cited in Monahan 1996)
Hammerstone-only (bovid 1-4)	0.33-0.5	Blumenschine 1988; 1995
Hammerstone-only (cow 3)	0.42	Bunn 1989
Hammerstone-only (size 1-4)	0.70	Selvaggio 1994
Hammerstone-to-carnivore (bovid1-4)	0.01-0.02	Blumenschine 1988; 1995
Hammerstone-to-carnivore (sheep/cow 1-3)	0.11	Marean (cited in Monahan 1996)
Natural carnivore assemblages		
Koobi Fora hyena den 1 (size 1-3)	1.19	Lam 1992
Syokimau hyena den (size 1-2)	0.36	Egeland *et al.* 2008
Syokimau hyena den (size 3)	0.45	
Makweding leopard (size 1-3)	0.64	Bunn 1982

Amboseli hyena (size 1-3)	0.41	Potts 1988 a
Bed I assemblages		
FLKN1-2 (size 1-2)	0.78	Domínguez-Rodrigo *et al.* 2007
FLKN1-2 (size 3)	0.65	
FLKN 6 (bovid size 1-4)	2.57	
FLKN 3 (size 1-2)	1.49	
FLKN 3 (size 3)	0.88	
FLKNN 2 (size 1-2)	0.08	
FLKNN 2 (size 3)	1.03	
FLKNN 3 (size 1-3)	0.42	

3 over 40%. Another example is DK, where in levels 2 and 3 8.5% of the long bone MNEs are complete. In average, complete limb bones make up 9-10% of the total limb bone MNE at sites in Bed I (Domínguez-Rodrigo *et al.*, 2007).

At some of these assemblages, complete bones are explained as the result of low competition between carnivores and low carnivore ravaging in general; on the other side, those sites that bear more stone tools and evidence of hominin activity, such as DK, the presence of complete limb bones suggests that hominins might not have been exploiting all limb bones for marrow, because encounter rates might have been high and because hominins might have had access to significant amounts of meat (Domínguez-Rodrigo *et al.*, 2007). In fact, at Koobi Fora, Bunn (1994) observed cut marks on several complete bones, suggesting incomplete carcass processing. Be that as it may, fragmentation at DS is intense in any case and the percentage of complete bones is very low, which either indicates that hominins exploited carcasses completely at DS or that in those cases where hominins left some elements intact, bone-crunching hyenids broke them subsequently to access their marrow content and consumed the grease-bearing cancellous bone.

3.2.2.4. Epiphyses-to-shaft fragment ratio

Intense bone fragmentation at DS, especially of femora and tibiae is also reflected in the ratio of epiphyses to shafts, which are considerably lower for these elements than for the other long bones in both small and medium-sized carcasses (Table 3.20A). Ratios of epiphyses to shafts are also low for the humeri, while radii-ulnae and metapodials present the highest values. The sample of size 5 carcasses is not sufficient to be described confidently in this regard.

Table 3.20B shows epiphysis-to-shaft ratios for several experimental assem-

blages and carnivore accumulations. Experimental hammerstone breakage yields epiphysis-to-shaft ratios that range between 0.33 and 0.70. The average ratios estimated for DS are 0.7 and 0.4 for small and medium-sized carcasses respectively. Due to the lower values of humeri, femora and tibiae (**Table 3.20A**), these average estimates do not fall into the range of experimental anthropic breakage. The ratios for humeri, femora and tibiae fit into the ranges of carnivore-only and hammerstone-to-carnivore models, which are generally much lower than those of hammerstone-only models (0.01-0.1, Table 3.20B). However, in both small and medium-sized carcasses the epiphysis-to-shaft fragment ratios of radii-ulna and metapodials do fall inside the range of hammerstone-only experiments. Yet, hyena dens also yield values in a similar range to hammerstone-only experiments (0.34 – 1.9). For example, at Syokimau the epiphyses to shafts ratio is 0.36 for small carcasses and 0.46 for medium-sized carcasses (**Table 3.20B**). But hyena dens are generally reduced competition settings. In samples resulting from carnivores feeding in contexts of high competition, carnivores destroy and consume many more epiphyses, resulting in the values mentioned above (Monahan, 1996; Egeland *et al.*, 2008).

The only Bed I assemblage that presents such low values similar to carnivore-only experiments in open high competition settings is the collection of small carcasses at FLKNN 2 (**Table 3.20B**), which has the highest input from hyenas in bone modification among all the Bed I sites (Domínguez-Rodrigo *et al.*, 2007). Yet, some of the epiphysis-to-shaft fragment ratios obtained for the other Bed I assemblages are significantly higher than the ratios of carnivore-only or hammerstone-only models. The other obtained ratios fall close or in the range of hammerstone-only experiments, the hyena dens and the leopard site (**Table 3.20B**). FLKN 3 and the natural accumulation at FLKN 6 yield even higher ratios, as they are among the sites that show less degree of ravaging in Bed I. The fact that most Bed I sites were created by felids and that they present a high amount of complete bones also explains these high ratios.

Epiphyseal representation can thus potentially be used as a proxy to infer carcass competition and to determine whether the site was located in a high competition setting or whether it was a safe refuge (Monahan, 1996). Based on the values obtained for DS, bone breakage at the site was probably the result of hominin breakage (see values for radii and metapodials) and some degree of carnivore ravaging (reflected in the ratios of humeri, femora and tibiae), although postdepositional disturbance by sedimentary processes can also be a cause of fragmentation and epiphyses removal, and must therefore be taken into account as well. The lower values of humeri, femora and tibiae could thus also be the result of preservational bias, especially since femora and tibiae tend to generate a greater amount of smaller fragments (Moclán and Domínguez-Rodrigo, 2018).

3.2.2.5. Shaft circumference

Shaft circumference types as defined by Bunn (1982; 1983) can also be used to differentiate low-competition settings from high-competition settings in open spaces, while they also provide an indication of the degree of fragmentation of the accumulation. Highly fragmented assemblages yield very high frequencies of type 1 circumferences and very low type 2 and type 3 shafts, while a large number of the latter is indicative of low fragmentation rates. Shaft circumference types do not vary according to skeletal element, nor do they fully discriminate between the taphonomic agents that might have caused the fracturing at a site, as can be observed in the shaft type proportions for the hammerstone-only, hammerstone-to-carnivore and carnivore-only experiments in Figure 3.18 and Tables 3.21A and B (see also Marean *et al.*, 2004). All three are characterized by a predominance of type 1 shaft fragments and much lower percentages of type 2 and 3 circumferences. However, it is true that in their dens hyenas often leave a significant amount of cylinders or complete shafts, which results in a higher proportion of type 3 circumferences (**Figure 3.18**).

The Bed I sites show mixed patterns in the proportions of shaft circumference types, probably reflecting different carnivore ravaging stages. FLK *Zinj* has not been included in the figure, because types 2 and 3 were not differentiated originally in the taphonomic analysis. However, the ratio of types 3 and 2 to type 1 for small and medium-sized carcasses yield values that are most similar to the Khwee hunter-gatherer camp (Bunn, 1982), the hammerstone-to-carnivore, and the carnivore-only model (**Table 3.21B**), as well as to DS. As mentioned above, FLKN1-2, FLKN3, FLKN6 and FLKNN 3 present higher ratios of complete bones and lower degree of ravaging. This is reflected also in a predominance of complete circumferences. Similarly, Level 2 at AMK, a recently discovered natural accumulation in Bed I, where carcass competition was low, also shows a shaft pattern dominated by type 3 specimens (Aramendi *et al.*, 2017). The other Bed I sites (FLKN4, FLKN5, FLKNN1, DK2 and DK3) also present high percentages of type 3 shafts, but type 1 specimens are more abun-

Table 3.21.a. *Frequencies of each type of shaft circumference at DS for small and medium-sized carcasses considering only green broken specimens, including complete bones and epiphyseal fragments.*

	Type 1	Type 2	Type 3
Small	154/192 (80.2)	13/192 (6.7)	25/192 (13.1)
Medium-sized	702/799 (87.9)	51/799 (6.4)	46/799 (5.7)
Large	26/28 (92.9)	2/28 (7.1)	0/28 (0.0)
All	945/1083 (87.3)	66/1083 (6.1)	72/1083 (6.6)

Table 3.21.b. *Available data of frequencies of each type of shaft circumference at several experimental assemblages, hyena dens, and other Bed I sites.*

	Type 1 (%)	Type 2 (%)	Type 3 (%)	Ratio 3+2:1	References
Syokimau (small)	58	15	27	0.72	Egeland *et al.* 2008
Syokimau (medium)	63	14	23	0.59	
Syokimau (large)	0	25	75	-	
Syokimau (total)	60	14	26	0.66	
KND2	18	55	26	4.5	Prendergast and Domínguez-Rodrigo 2008
Sonai camp	71	16	12	0.39	
Khwee camp	80	19	1	0.22	Bunn 1982
CO	88	7	5	0.14	Marean and Spencer 1991; Marean *et al.* 2004
H-C	87	7	6	0.15	
HO	70	9	21	0.43	
FLK Zinj (small)	147	36		0.24	Domínguez-Rodrigo *et al.* 2007
FLK Zinj (large)	442	52		0.12	
FLKN 1-2	23	22	55	3.34	
FLKN 3	33	29	38	2.03	
FLKN 4	58	35	7	0.72	
FLKN 5	70	5	25	0.43	
FLKN 6	7	13	80	13.29	
FLKNN 1	47	22	31	1.13	
FLKNN 3	29	15	56	2.45	
DK 2	76	4	20	0.32	
DK 3	84	4	12	0.19	
AMK Level 1	69	0	31	0.45	Aramendi *et al.* 2017
AMK Level 2	36	5	69	2.06	
OCS (size 3)	23	5	72	3.35	Arriaza *et al.* 2016

dant. With the exception of OCS, which shows the highest number of complete shafts, and KND2, where type 2 is most predominant, Syokimau hyena den, Level 1 at AMK and the hunter-gatherer campsites are all dominated by type 1 specimens, although in the human camps type 3 shafts are less frequent than at Syokimau and AMK I, both of which present a very similar pattern

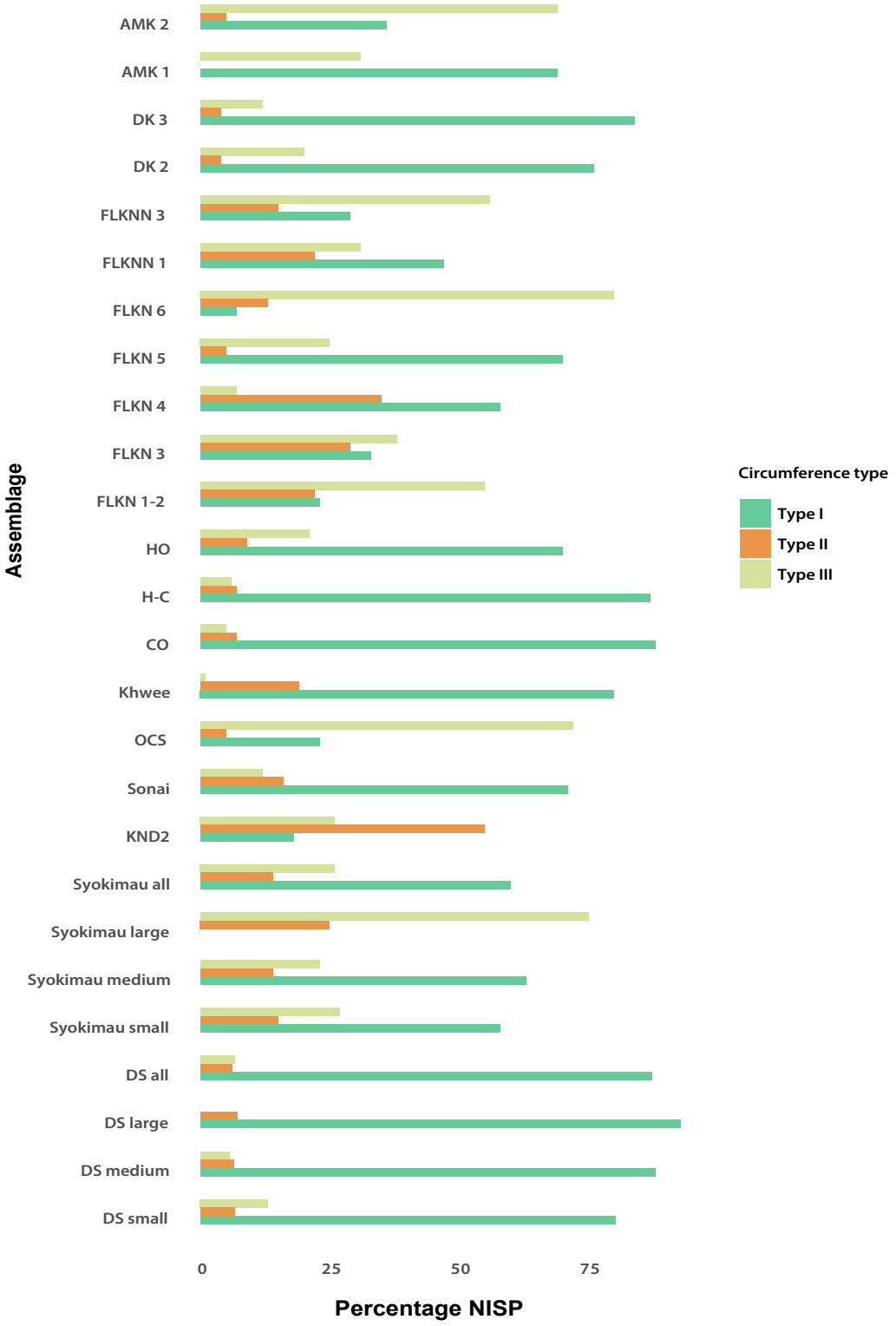

FIGURE 3.18. *Bunn's (1982) shaft circumference types for DS, several actualistic assemblages, including experimental models, hyena dens and hunter-gatherer campsites, and the Bed I sites. FLKNN2 is not included because the percentages added up to more than 100% (probably due to a typing error).*

(Figure 3,18). As expected from the results obtained so far, which indicate a significant degree of bone breakage occurred at DS, type 1 shafts are extremely more abundant than the other two types. Interestingly, the shaft pattern for medium-sized carcasses fits perfectly with the hammerstone-to-carnivore experiments, while the pattern obtained for small carcasses is more similar to the hammerstone-only model (Figure 3.18). The difference between the two carcass sizes lies mainly in the amount of type 3 shafts, which is reduced when more fragmentation (i.e. carnivore ravaging) occurs. This can also be appreciated in the ratio of types 3 and 2 to type 1 (Table 3.21B). According to this assessment, medium-sized carcasses were ravaged by hyenas after hominins had processed the carcass, while small carcasses were not, a possible reason being that there was more meat or grease left in medium-sized carcasses. This could tentatively be taken as an indication of incomplete carcass processing of medium-sized animals by hominins.

In sum, DS presents NISP:MNE ratios on long bones that are similar to those reported in hammerstone breakage experiments and the percentage of complete bones reflects a high degree of fragmentation and bone marrow extraction at the site. Epiphysis-to-shaft fragment ratios yield lower values than those documented in hammerstone-only models, but the values for humeri, femora and tibiae fall into the ranges of carnivore-only and hammerstone-to-carnivore models. The ratio of shaft types 3 and 2 to type 1 yields a value of 0.15, which coincides with the value for hammerstone-to-carnivore model. The pattern of circumference types of small carcasses is more similar to the hammerstone-only model, while medium-sized carcasses seem to have been ravaged more intensely by carnivores. Hominins were probably responsible for most bone breakage at the site, although there appears to have been contribution from hyenas to some degree. This is mostly reflected in the epiphysis-to-shaft ratio and the proportions of shaft circumference types. Both variables are combined in the scatterplot presented in Figure 3.19, which shows that small and medium-sized carcasses at DS fall closest to the hammerstone-only and hammerstone-to-carnivore models. The involvement of hyenas in bone breakage is reflected in lower ratios of epiphysis-to-shaft and shafts type 3 and 2 with regard to type 1 with regard to the hammerstone-only model. This hypothesis is further tested in the following sections, which deal with breakage planes and notches.

3.2.3. Analysis of breakage planes

The frequencies of longitudinal and oblique green fracture planes present in long bone fragments of small and medium-sized carcasses at DS are shown in Table 3.22. Figure 3.17 shows some examples of green fracture planes on long bones. Angles could be measured for a significant proportion of these fractures. The means, ranges, and 95% confidence intervals for each fracture

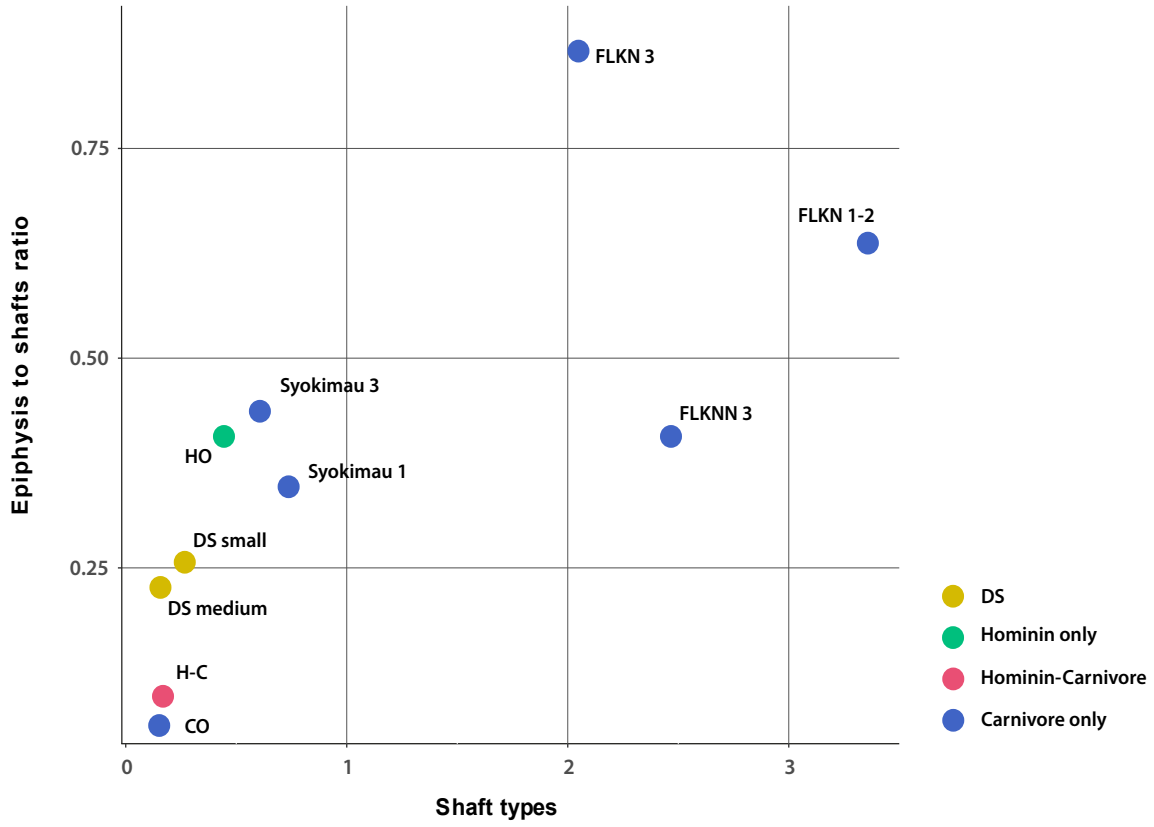

FIGURE 3.19 *Scatterplot combining shaft type proportions and epiphysis-to-shafts ratios from DS, the HO and H-C experiments and several carnivore assemblages.*

type and carcass size are presented in **Table 3.23**. In **Figures 3.21A and B** the DS breakage planes are compared to the mean frequencies of acute and obtuse angles obtained in experiments modeling dynamic and static loading (Capaldo and Blumenschine, 1994; Alcantara-García *et al.*, 2006). The obtained results are different for small and medium-sized carcasses. In small carcasses, angles <90° are more similar to those generated through dynamic loading in both longitudinal and oblique planes, and angles >90° are more similar to static loading. In medium-sized carcasses, however, acute angles were ambiguous as to the agent of bone breakage, because angles fall between the dynamic and static experimental samples, while obtuse angles fall within the range of static loading for both types of fractures. Importantly, whereas in small carcasses there is clear evidence of dynamic loading, acute breakage planes in medium-sized carcasses are more ambivalent.

Overall, the results of this analysis do not clearly point to a single bone breakage agent and suggest that both hominins and hyenas contributed to frac-

Table 3.22. *Frequencies of longitudinal and oblique fracture planes. (The remaining are either transverse, ambiguous or could not be measured and are therefore not included)*

	Longitudinal	Oblique
Small carcasses	321/505 (63.56)	113/505 (22.38)
Medium-sized carcasses	754/1905 (39.58)	597/1905 (31.34)
All (regardless of carcass size)	1028/3326 (30.91)	764/3326 (22.97)

Table 3.23. *Fracture attribute data for green broken limb bone shaft specimens (excluding metapodials)*

		<90°	>90°
Small carcasses			
Longitudinal			
	Mean	75.47	99.30
	SD	8.91	5.65
	95% CI	73.47-77.46	97.19-101.41
	n	79	30
	Range	55-90	91-113
Oblique			
	Mean	68.20	104.71
	SD	12.44	8.91
	95% CI	64.70-71.69	99.95-109.48
	n	51	21
	Range	32-89	92-132
Medium-sized carcasses			
Longitudinal			
	Mean	74.54	101.96
	SD	10.37	10.07
	95% CI	73.11-75.98	100.10-103.81
	n	202	115
	Range	44-90	90-140
Oblique			
	Mean	70.18	107.03
	SD	13.69	14.82

	95% CI	68.25-72.10	104.30-109.77
	n	197	115
	Range	28-90	91-165

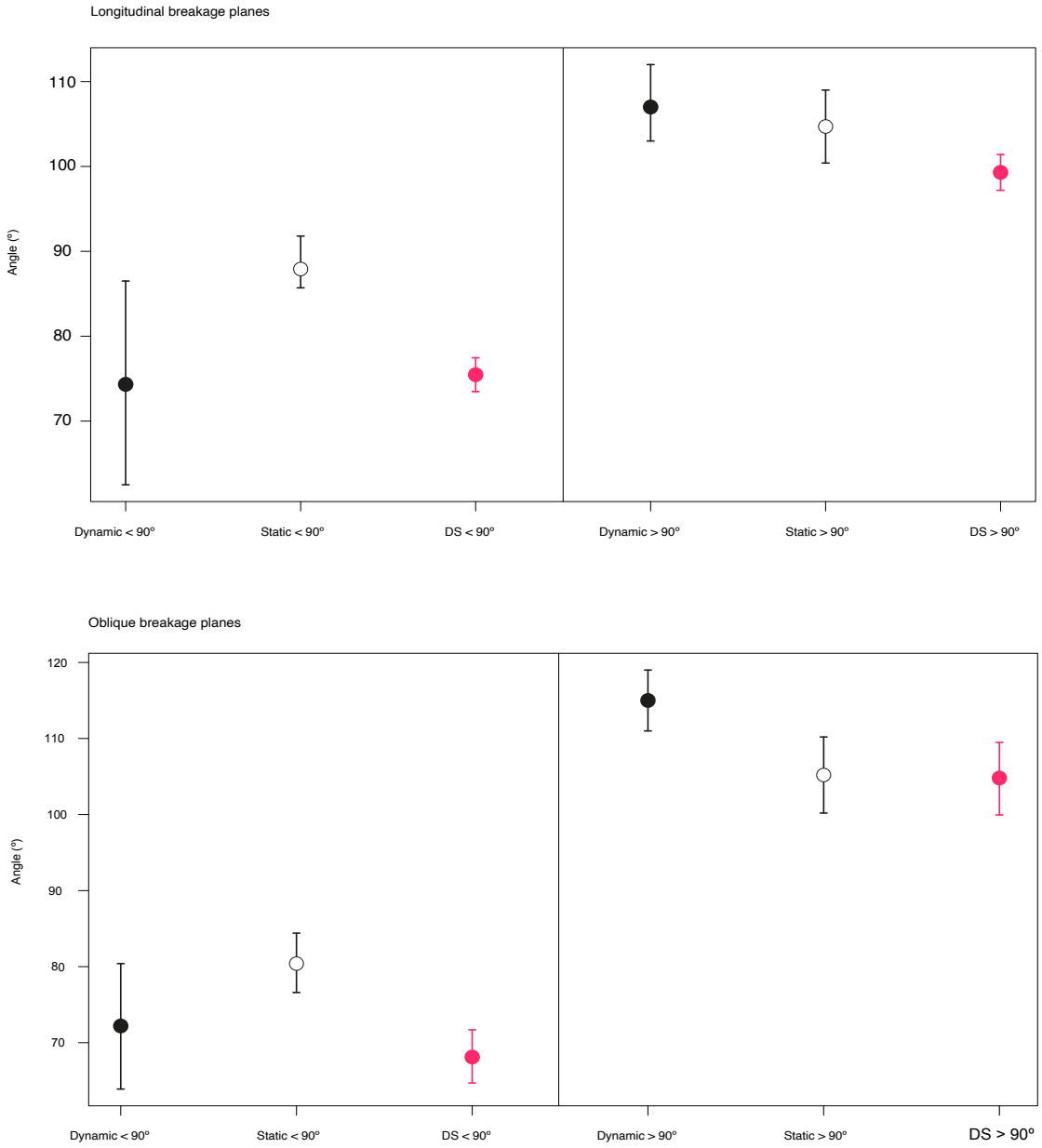

FIGURE 3.20. *Comparison of mean percentages and 95% confidence intervals of the angles created through dynamic and static loading for the different types of fracture planes on small carcasses: longitudinal <90º, longitudinal >90º, oblique <90º, and oblique >90º. Experimental data for static loading stem from Capaldo and Blumenschine (1994) and for dynamic loading from Alcántara García et al. (2006).*

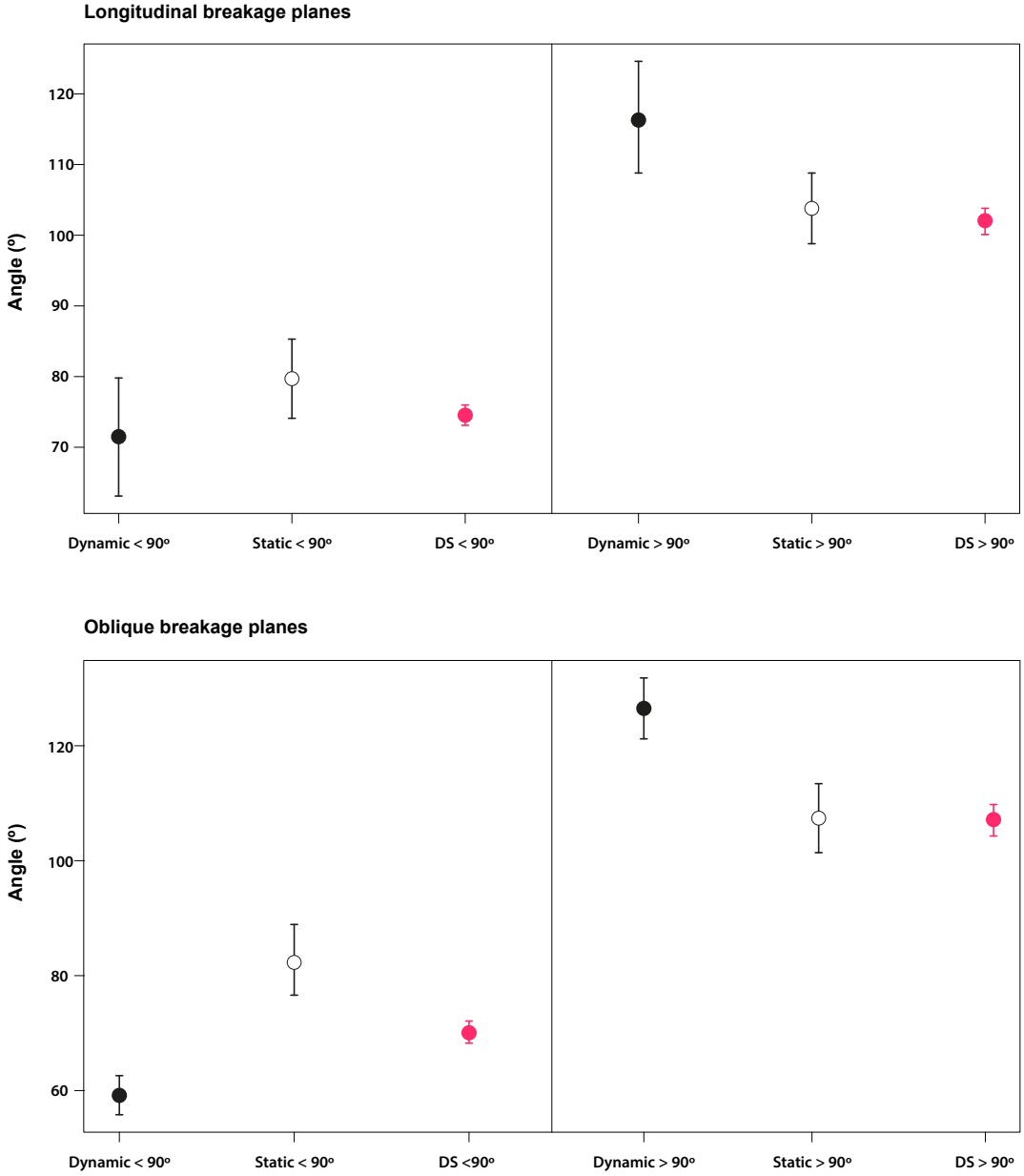

FIGURE 3.21. *Comparison of mean percentages and 95% confidence intervals of the angles created through dynamic and static loading for the different types of fracture planes on medium-sized carcasses: longitudinal <90°, longitudinal >90°, oblique <90°, and oblique >90°. Experimental data for static loading stem from Capaldo and Blumenschine (1994) and for dynamic loading from Alcántara García et al. (2006).*

turing at DS. According to the outcome of this approach, the role of hyenas in bone breakage was not negligible. At FLK *Zinj*, the analysis of bone breakage yielded most plane angles fell within the range of dynamic loading rather than

static loading in small carcasses. In larger carcasses, the results were slightly more ambiguous as occurs with DS, still most of the angles fell outside the range of static loading with some angles falling within the range of dynamic loading (Domínguez-Rodrigo *et al.*, 2007).

3.2.4. Notch type distribution

A total of 132 notches could be identified in the DS long bone sample. Figure 3.22 shows some examples of conspicuous notches in the sample of green broken long bone shafts. The predominant type are micronotches (57%), which are very common in carnivore-broken assemblages (Capaldo and Blumenschine, 1994; Domínguez-Rodrigo *et al.*, 2007; Egeland *et al.*, 2008). These are followed by complete notches, which constitute around 25% of the notch sample. Notch types are distributed very similarly across the different carcass sizes (Table 3.24). The proportions of each notch type in the experimental samples are presented in Table 3.25.

Figure 3.23 shows the two-dimensional solutions of the bootstrapped correspondence analyses carried out on a) the complete notch sample including all carcass sizes, b) only the notches found on small carcasses, c) only the notches on the medium-sized carcasses. The solution accounts for 100% of inertia in all three cases, and more than 50% is accounted for by the first dimension, which separates battering from hammerstone percussion. The second dimension distinguishes between dynamic and static loading. This shows that bone breakage by humans and carnivores can be distinguished by the distribution of notch types, although hammerstone percussion on equid bones overlaps with the notch patterns created by carnivores (de Juana and Domínguez-Rodrigo, 2011). The DS sample, which consists mainly of bovid and not equid bones, also overlaps with both the anthropic and carnivore-broken assemblages when all carcass sizes are considered. The sample of notches inflicted on small carcasses is too small and the confidence ellipse covers all samples except the one created through battering. The solution for medium-sized carcasses is ambiguous, and practically identical to the one which summarizes all carcass sizes: both point to a scenario in which bone fracturing was produced by both hominins and hyenas. This can be observed with more clarity in the correspondence diagram in **Figure 3.24** in which anthropic breakage samples are lumped into the same category. The solution of this correspondence analysis also explains 100% of inertia, most of which is contained in the first axis, which separates sets dominated by notch type A (anthropic breakage) and those in which notch type D (breakage by carnivores) is predominant. The DS sample falls in between both

Table 3.24. *Frequencies of each type of notches on long limb bone fragments in DS (Level 22B). Percentages are in parentheses.*

	Type A	Type B	Type C	Type D	Type E	Total
Small carcasses	7 (25)	1 (3.5)	4 (14.3)	3 (10.7)	13 (46.5)	28
Medium-sized carcasses	21 (23.6)	3 (3.4)	6 (6.7)	7 (7.9)	52 (58.4)	89
Large carcasses	2 (22.2)	1 (11.1)	0	0	6 (66.7)	9
All	33 (25)	4 (3)	10 (7.6)	10 (7.6)	75 (56.9)	132

Table 3.25. *Frequencies of the different types of notches in each experimental sample used for comparison in the multiple correspondence analysis (from Moclán and Domínguez-Rodrigo 2018).*

Sample	Type A	%	Type C	%	Type D	%	Data source
Large bovids (Bos)	59	77.63	10	13.16	7	9.21	Domínguez-Rodrigo *et al.* 2007
Large bovids (Bos)	103	70.07	41	27.89	3	2.04	Blasco *et al.* 2014
Small bovids	42	76.36	9	16.36	4	7.27	Domínguez-Rodrigo *et al.* 2007
Battering (bovid)	30	30	70	70	0	0	Blasco *et al.* 2014
Equid	10	52.63	4	21.05	5	26.32	de Juana and Domínguez-Rodrigo 2011
Deer	23	65.71	10	28.57	2.	5.71	Moclán and Domínguez-Rodrigo 2018
Hyena Den (Maasai Mara)	42	38.53	46	42.20	21	19.27	Domínguez-Rodrigo *et al.* 2007
Lion den (OCS)	8	29.63	7	25.93	12	44.44	Arriaza *et al.* 2016

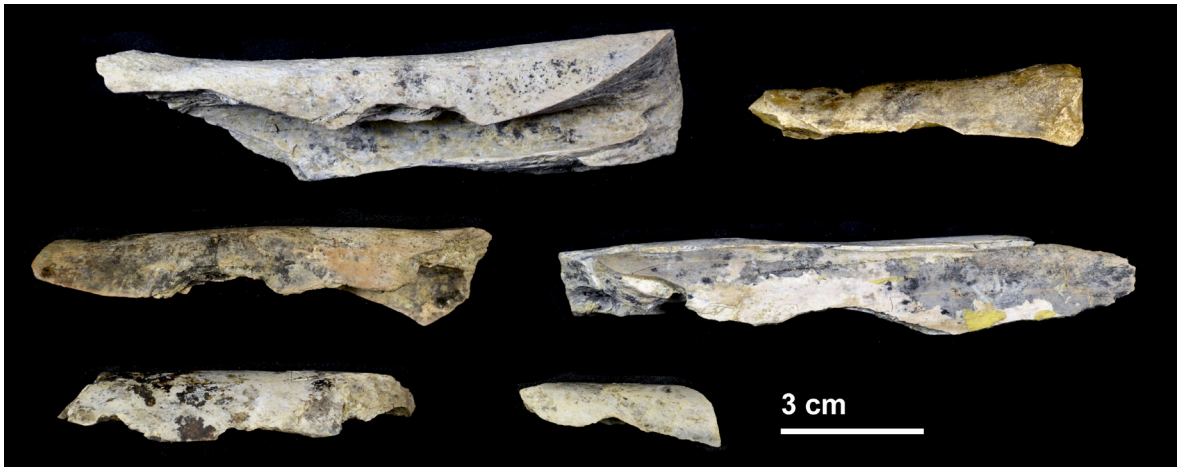

Figure 3.22. *Several examples of long bone shafts with different types of notches.*

sets: it is similar to the hammerstone broken assemblages because complete notches predominate, but it also presents a certain amount of double-opposing notches that are typical of carnivore-broken assemblages. DS differs from the actualistic assemblages in that it presents less type C notches, especially when compared to the Maasai Mara hyena den. Bone breakage at DS seems to have resulted from both anthropic and hyena activities, as has already been concluded in the previous analyses on fragmentation indices and breakage plane angles, although hominin breakage activities seem to have been predominant.

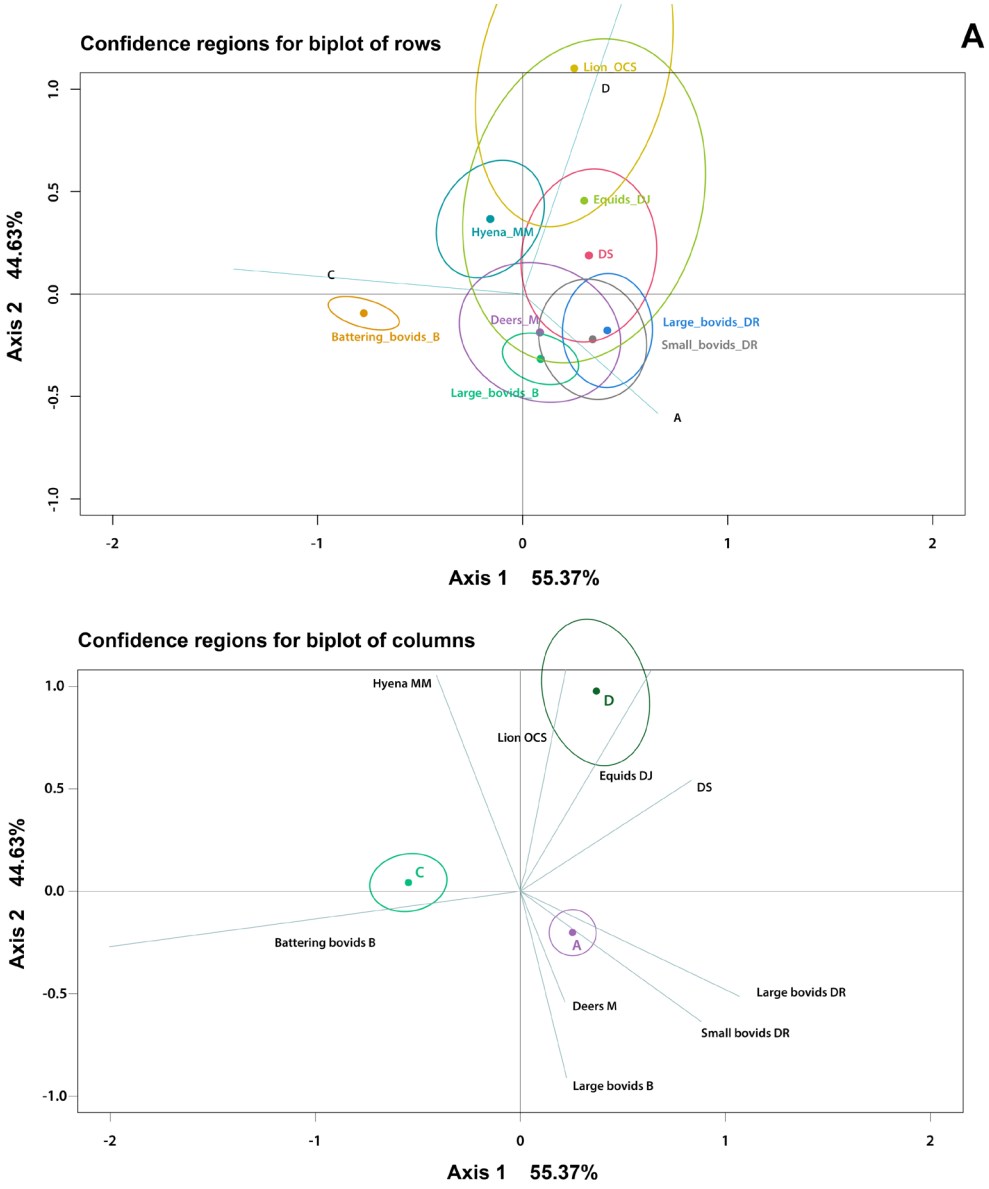

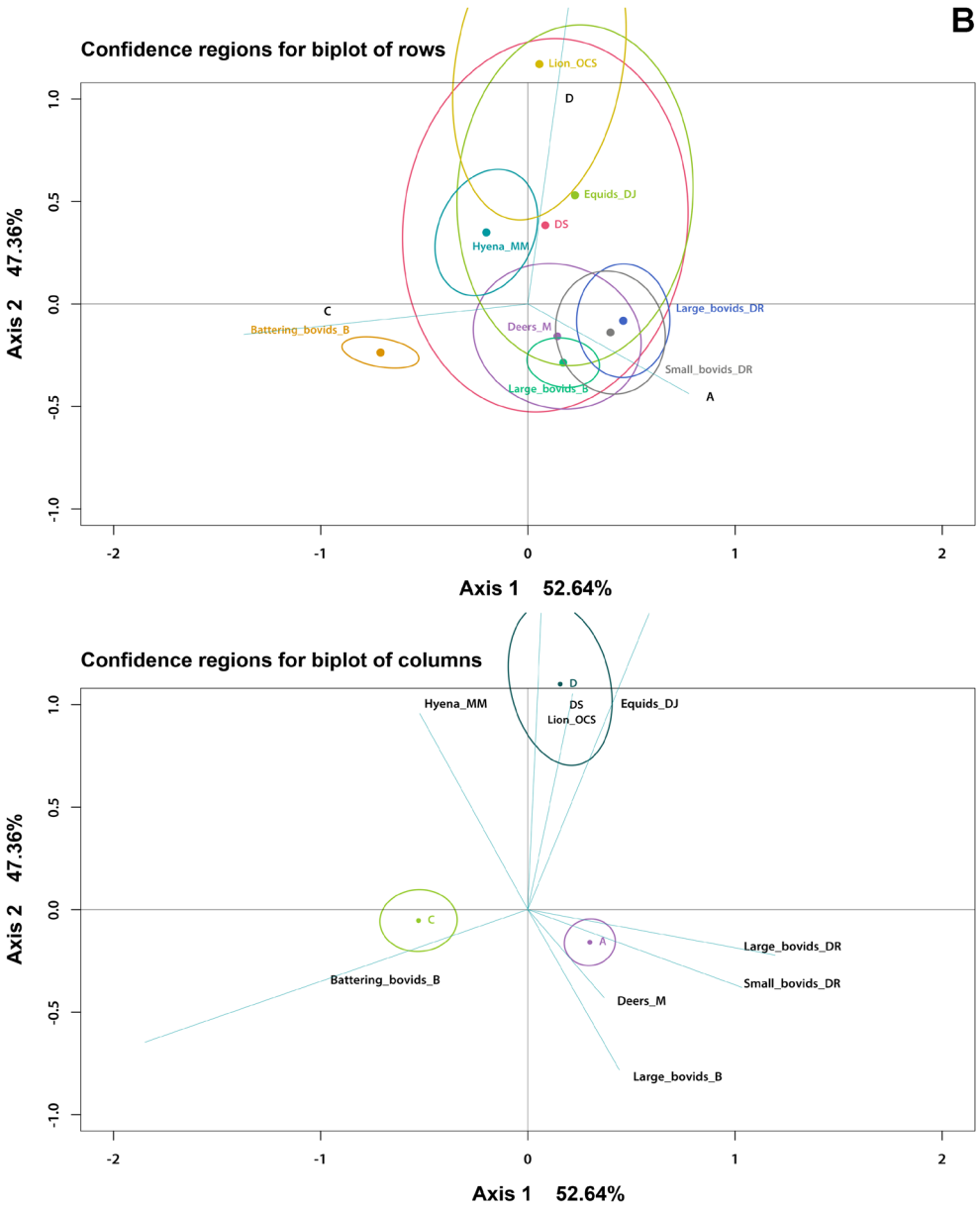

3.2.5. Machine learning analysis of fracture planes and notch types

We reproduced Moclán *et al.*'s (2019) machine learning analysis using the complete dataset and the four subsets of longitudinal and oblique fracture planes in order to generate the predictive models to be used to classify the DS samples. We obtained very similar overall classification results (Appendix Tables 7.1-7.5). The joint analysis of all fracture planes (longitudinal and oblique) produced a classification with more than 80% accuracy; the highest value was yielded with the random forest algorithm (accuracy = 0.88; kappa = 0.80), the lowest were obtained with the naive Bayes method (accuracy = 0.65; kappa =

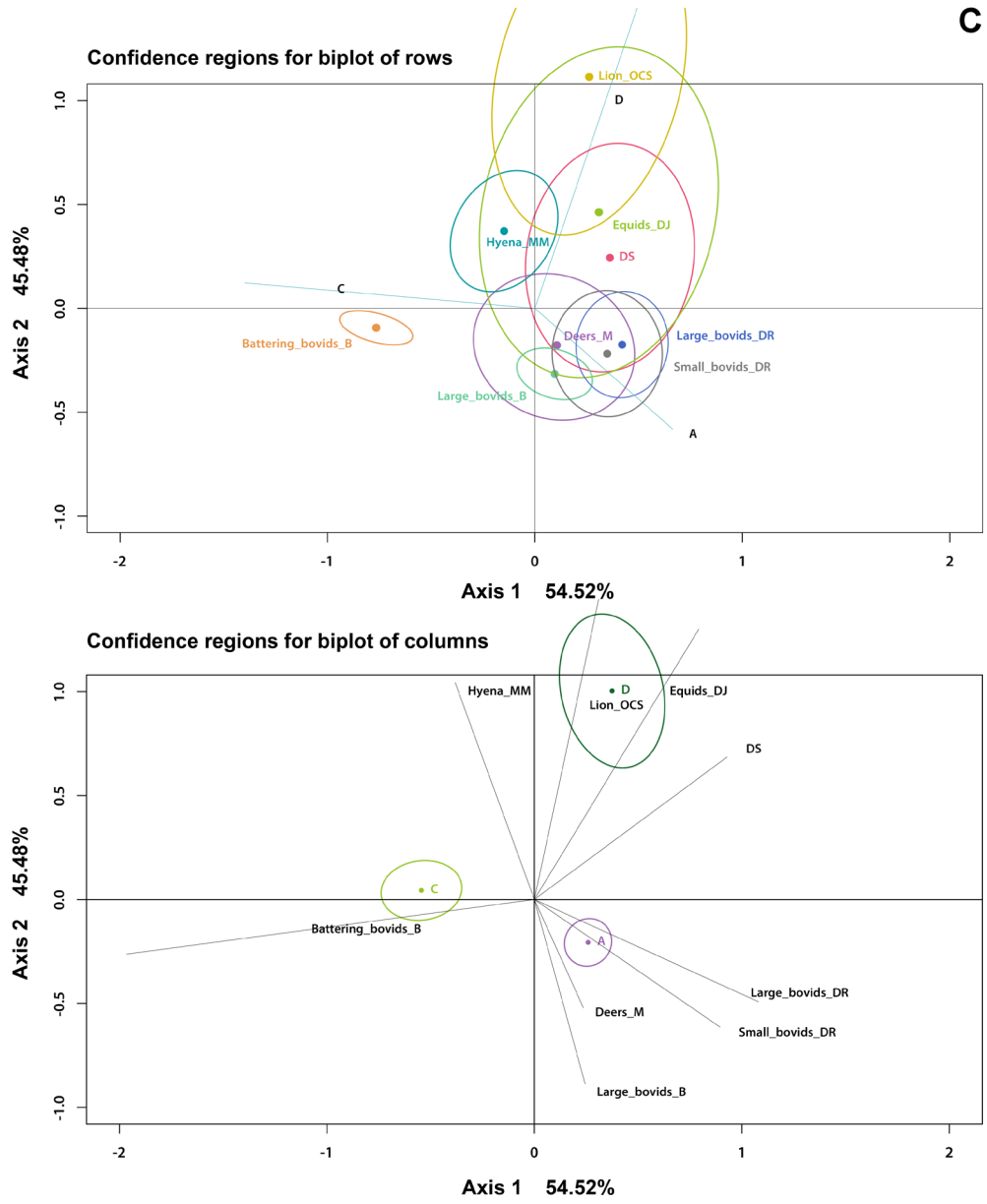

FIGURE 3.23. *Correspondence diagrams comparing notch distribution in experimental samples and A) the complete notch sample of DS including all carcass sizes, B) the notch sample in small carcasses, C) the notch sample in medium-sized carcasses.*

0.30; Appendix, table 7.1A). The sample of longitudinal fracture planes with angles <90° produces classification rates with accuracy between 70% (naive Bayes) and 82% (neural network; Appendix Table 7.2A). Similarly, on average, longitudinal planes >90° are classified successfully with an accuracy of 73% (Appendix Table 7.3A). Oblique fracture planes <90° present slightly higher

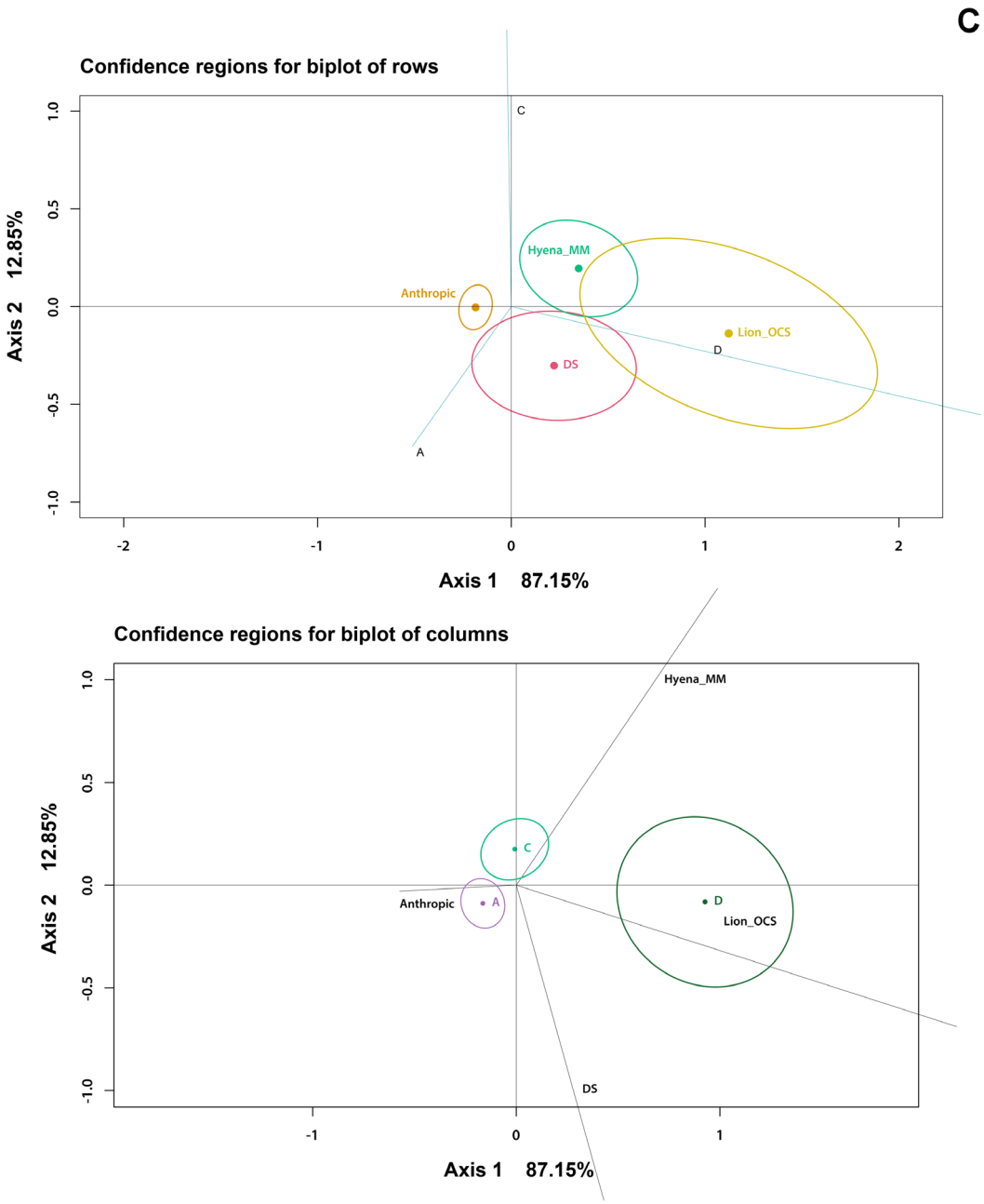

FIGURE 3.24. *Two-dimensional solution of the correspondence analysis using all anthropic experiments as one single category.*

degrees of accuracy in classification (>75%; Appendix Table 7.4A), but the classifications with the highest accuracy values were obtained for oblique fracture planes >90º, which show accuracy values between 78% (naive Bayes) and 91% (mixture discriminant analysis; Appendix Table 7.5A). Overall, most predic-

tive models yielded accuracy values between 75% and 85%. Tables 7.1-7.5 in the Appendix also provide the corresponding kappa, sensitivity, specificity, and balanced accuracy estimates.

According to the combined analysis of longitudinal and oblique planes, bones were predominantly broken through hammerstone percussion by hominins. Depending on the algorithm, the probabilities vary between 87.4% (random forest) and 95.2% (naive Bayes). The probability for hyenas ranges between 3.3% (naive Bayes) and 8.4% (random forest). As mentioned above, the results obtained using the random forest algorithm yielded higher accuracy when considering all fracture planes, which makes the corresponding values slightly more reliable. All types of breakage planes were predominantly created by hominins: longitudinal planes <90° yield percentages of hammerstone percussion between 73.6% and 92.2% (Appendix Table 7.2B), oblique planes <90° between 86.8% and 100% (Table 7.4B), oblique planes >90° between 86.7% and 97.7% (Appendix Table 7.5B), and longitudinal planes >90° between 55.8% and 91.2% (Appendix Table 7.3B). Among the latter, in some cases, the differ-

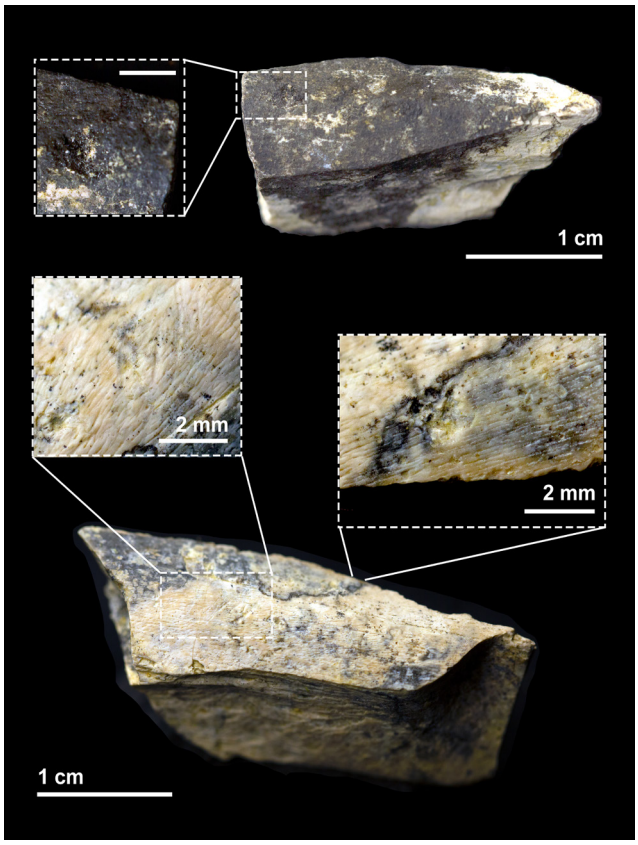

FIGURE 3.25. *Two impact flakes with percussion pits on the cortical surface.*

ence between percentages of hammerstone and hyena breakage is less marked than in the other types of planes (e.g. naive Bayes attributes 44.2% of the breakage planes to hyena breakage and 55.8% to hammerstone percussion; Appendix Table 7.3B). The impact of canids is often negligible; overall percentages range between 1.5% and 5.9% (Appendix Table 7.1B).

In conclusion, all bone breakage assessments applied to DS in this analysis point to a scenario in which hyenas contributed to some degree to bone breakage at the site, but most of the fracturing was clearly the result of anthropic activities. Hominins used hammerstones to break open most of the long bones at the site to access their marrow content. A further argument to support this hypothesis is the high number of impact flakes documented (83) (Figure 3.25), which are usually attributed to anthropic breakage. Similarly, at FLK *Zinj*, the study of notches and platform angles demonstrated that carnivores were involved in bone fracturing, although hammerstone percussion was clearly predominant, especially for large-sized carcasses (Domínguez-Rodrigo *et al.*, 2007).

3.4. Bone surface modifications

3.4.1. General overview of BSM frequencies in the DS archaeofaunal assemblage

Cortical surfaces of bones were generally poorly preserved and sometimes absent. Only one third of the surfaces of the bone collection showed good or moderate preservation and two thirds were badly preserved (Table 3.26). A significant number of specimens was covered by a carbonate layer that hindered its observation, and 190 specimens (14.5%) of all indeterminate specimens could not be identified because of it. Interestingly, long limb bones and axial remains present very similar degrees of preservation of bone surfaces,

Table 3.26. *NSP, NISP values and percentages of bones with good, moderate or poor cortical surface preservation in the complete 22B bone assemblage and in ungulate long limb bones and axial bones of the same level*

Cortical surface preservation	Level 22B	Long limb bones			Axial bones	
	NSP	NSP	NISP to specific element	NISP to limb bone section	NSP	NISP
Good	591/3228 (18.31%)	288/1421 (20.27%)	194/824 (23.54%)	220/960 (22.92%)	179/862 (20.77%)	172/821 (20.95%)
Moderate	478/3228 (14.81%)	245/1421 (17.24%)	155/824 (18.81%)	181/960 (18.85%)	147/862 (17.05%)	141/821 (17.17%)
Poor	2159/3228 (66.88%)	888/1421 (62.49%)	475/824 (57.65%)	559/960 (58.23%)	536/862 (62.18%)	508/821 (61.88%)
Good+Moderate	1069/3228 (33.12%)	533/1421 (37.51%)	349/824 (42.35%)	401/960 (41.77%)	326/862 (37.82%)	313/821 (38.12%)
Total	3228/3228 (100%)	1421/1421 (100%)	824/1421 (57.99%)	960/1421 (67.59%)	862/862 (100%)	821/862 (95.24%)
Number of specimens/Total ungulate bones		1421/3191 (44.53%)	824/3191 (25.82%)	960/3191 (30.08%)	862/3191 (27.01%)	821/3191 (25.73%)

with only slightly more than 20% of the sample being well-preserved, and more than 60% being poorly preserved.

3.4.1.1. BSM frequencies per NSP

When considering NSP, the archaeological deposit of Level 22B has yielded 124 (3.9%) cut marked specimens, 85 (2.7%) percussion marked specimens, and 46 (1.4%) tooth marked specimens (Table 3.27A). Due to the taphonomic processes that affect cortical surface preservation, and therefore also condition the survival of marks, percentages of marks in specimens with poorly preserved cortical surfaces are clearly lower than percentages in the well-preserved sample (e.g. CM, 8.3% vs. 2.6% or PM, 7.1% vs. 0.8%, Table 3.27A). When values of the well-preserved sample are further corrected for dry-fractured bones, the percentage of cut-marked specimens results in 14% of NSP, percussion-marked bones make up 12% of the NSP sample, and only 6% of the specimens bear tooth marks (Table 3.27A).

3.4.1.2. BSM frequencies per NISP

When non-identified specimens are left out of BSM estimations, percentages increase notably. Cut marks are present in 20 unidentified specimens, which leave 104 (5.54%) cut marks, 68 (3.62%) percussion marks, and 36 (1.92%) tooth marks in a total of 1878 identifiable specimens (59% of the NSP sample). In the well-preserved and corrected subsample, more than 18% of the specimens bear cut marks, and more than 14% have percussion marks. Tooth mark frequencies remain relatively low in that same unbiased sample (slightly above 8%, Table 3.27B). The dependence of BSM survival on cortical preservation is evident here as well: the poorly preserved sample bears 60% fewer cut marks than the well preserved sample, i.e. only 7% of the specimens bear cut marks, and only around 2.5% are percussion-marked fragments (Table 3.27B).

3.4.1.3. BSM frequencies per NISP in long limb bones and axial bones

When comparing the occurrence of these types of marks in the subassemblage composed of long limb bones and in the subassemblage of axial bones, the data show that the majority of the specimens with either cut marks or percussion marks are long limb bones (64% and 78%, respectively). Although in very low frequencies (1-2%), tooth marks appear slightly more often on limb bone portions too. Anthropogenic marks are relatively abundant in the well-preserved sample of long limb bones: cut marked and percussion marked specimens make up more than 40% of the BSM sample (when the correction for dry breakage is applied, Table 3.28). Percussion marks are completely absent in the axial skeleton (Table 3.29).

Table 3.27.a) *Cut-marked, percussion-marked, and tooth-marked ungulate bone specimens in each cortical bone surface preservation category in Level 22B (NSP). Values are also for corrected for dry broken bone fragments.*

Cortical surface preservation	Correction for dry broken bones (X+(Y/2))		Number of specimens (NISP)	CM	PM	TM
Good			442/1878 (23.54%)	44/442 (9.95%)	34/442 (7.69%)	20/442 (4.52%)
	Green (X)	**Dry (Y)**	241.5	44/241.5 (18.22%)	34/241.5 (14.08%)	20/241.5 (8.28%)
	232	**19**				
Moderate			329/1878 (17.52%)	20/329 (6.08%)	20/329 (6.08%)	9/329 (2.74%)
	Green (X)	**Dry (Y)**	180	20/180 (11.11%)	20/180 (11.11%)	9/180 (5%)
	170	**20**				
Good+Moderate			771/1878 (41.05%)	64/771 (6.55%)	54/771 (8.30%)	29/771 (3.76%)
	Green (X)	**Dry (Y)**	421.5	64/421.5 (15.18%)	54/421.5 (12.81%)	29/421.5 (6.88%)
	402	**39**				
Poor			1107/1878 (58.95%)	40/1107 (2.13%)	14/1107 (1.26%)	7/1107 (0.63%)
	Green (X)	**Dry (Y)**	569	40/569 (7.03%)	14/569 (2.46%)	7/569 (1.23%)
	437	**264**				
Total			1878	104/1878 (5.54%)	68/1878 (3.62%)	36/1878 (1.92%)

Table 3.27.b) *Cut-marked, percussion-marked, and tooth-marked ungulate bone specimens in each cortical bone surface preservation category in Level 22B (NISP). Values are also for corrected for dry broken bone fragments.*

Cortical surface preservation	Correction for dry broken bones (X+(Y/2))		Number of specimens (NISP)	CM	PM	TM
Good			442/1878 (23.54%)	44/442 (9.95%)	34/442 (7.69%)	20/442 (4.52%)
	Green (X)	**Dry (Y)**	241.5	44/241.5 (18.22%)	34/241.5 (14.08%)	20/241.5 (8.28%)
	232	**19**				
Moderate			329/1878 (17.52%)	20/329 (6.08%)	20/329 (6.08%)	9/329 (2.74%)

	Green (X) **170**	**Dry (Y)** **20**	180	20/180 (11.11%)	20/180 (11.11%)	9/180 (5%)
Good+Moderate			771/1878 (41.05%)	64/771 (6.55%)	54/771 (8.30%)	29/771 (3.76%)
	Green (X) **402**	**Dry (Y)** **39**	421.5	64/421.5 (15.18%)	54/421.5 (12.81%)	29/421.5 (6.88%)
Poor			1107/1878 (58.95%)	40/1107 (2.13%)	14/1107 (1.26%)	7/1107 (0.63%)
	Green (X) **437**	**Dry (Y)** **264**	569	40/569 (7.03%)	14/569 (2.46%)	7/569 (1.23%)
Total			1878	104/1878 (5.54%)	68/1878 (3.62%)	36/1878 (1.92%)

3.4.1.4. BSM in small carcasses (size 1-2)

The sample of small ungulate carcasses constitutes around 15% of the 22B NSP sample. Anthropogenic marks are two times more abundant than tooth marks, however these appear slightly more often than in medium-sized carcasses (2.45% vs. 1.35%, Appendix Tables 7.6A and 7.9A). Corrected estimations in the well-preserved NSP assemblage result in around 10% of the specimens bearing cut marks, around 5% specimens bearing percussion marks, and around 9% of them being tooth-marked (Table 7.6A). With respect to NISP, results turned out to be very similar, since more than 80% of the specimens were identifiable to specific element (Table 7.6B). Dry-broken specimens occur more frequently in bones with bad surface preservation, which implies that percentages of marked specimens remain low in this category. When considering long limb bones (NISP), cut marks are present in around 12% of the well-preserved subassemblage, percussion marks are found in around 8% of the specimens and around 6% bear evidence of having been gnawed by carnivores (Table 7.7). Axial remains are almost as abundant in this size class as long limb bone specimens, and both skeletal parts bear the same amount of tooth marks (Tables 7.7 and 7.8). All the cut marks were recorded on either long bone specimens (69%) or on axial bones (31%), as were all the tooth marks. Percussion marks were only recorded in long limb bones.

3.4.1.5. BSM in medium-sized carcasses (size 3-4)

Most recovered bone specimens in Level 22B are medium-sized ungulates. When considering the well-preserved sample, and when applying the correc-

Table 3.28. *Cut-marked, percussion-marked, and tooth-marked ungulate long limb bone specimens in each cortical bone surface preservation category in Level 22B (NISP). Values are also for corrected for dry broken bone fragments.*

Cortical surface preservation	Correction for dry broken bones (X+(Y/2))		Number of specimens (NISP)	CM	PM	TM
Good			194/824 (23.54%)	38/194 (19.59%)	32/194 (16.49%)	9/194 (4.64%)
	Green (X) 170	**Dry (Y)** 7	173.5	38/173.5 (22.90%)	32/173.5 (18.44%)	9/173.5 (5.19%)
Moderate			155/824 (18.81%)	11/155 (7.10%)	20/155 (12.90%)	5/155 (3.23%)
	Green (X) 134	**Dry (Y)** 6	137	11/137 (8.03%)	20/137 (14.60%)	5/137 (3.65%)
Good+Moderate			349/824 (42.35%)	49/349 (14.04%)	52/349 (14.90%)	14/349 (4.01%)
	Green (X) 304	**Dry (Y)** 13	310.5	49/310.5 (15.78%)	52/310.5 (16.75%)	14/310.5 (4.51%)
Poor			475/824 (57.65%)	30/475 (6.32%)	14/475 (2.95%)	5/475 (1.05%)
	Green (X) 371	**Dry (Y)** 97	419.5	30/419.5 (7.15%)	14/419.5 (3.34%)	5/419.5 (1.19%)
Total			824	79/824 (9.59%)	66/824 (8.01%)	19/824 (2.31%)

Table 3.29. *Cut-marked, percussion-marked, and tooth-marked ungulate axial bone specimens in each cortical bone surface preservation category in Level 22B (NISP). Values are also for corrected for dry broken bone fragments.*

Cortical surface preservation	Correction for dry broken bones (X+(Y/2))		NISP	CM	PM	TM
Good			172/821 (20.95%)	6/172 (3.49%)	0	8/172 (4.65%)
	Green (X) 49	**Dry (Y)** 12	55	6/55 (10.91%)	0	8/55 (14.55%)
Moderate			141/821 (17.17%)	9/141 (6.38%)	0	3/141 (2.13%)

	Green (X)	**Dry (Y)**	34.5	9/34.5 (26.09%)		3/34.5 (8.70%)
	28	13				
Good+Moderate			313/821 (38.12%)	15/313 (4.72%)	0	11/313 (3.51%)
	Green (X)	**Dry (Y)**	63.5	15/63.5 (23.62%)	0	11/63.5 (17.32%)
	25	77				
Poor			508/821 (61.88%)	9/508 (1.77%)	0	2/508 (0.39%)
	Green (X)	**Dry (Y)**	112	9/112 (8.04%)	0	2/112 (1.79%)
	46	132				
Total				24/821 (2.92%)	0	13/821 (1.58%)

tion for dry-broken specimens, cut marks are present in around 15% of the NSP assemblage (Table 7.9A). The percentage increases to almost 20% when considering only NISP (Table 7.9B), and to 25% when long limb bone specimens are considered separately (Table 7.10). Likewise, percentages of bones that show evidence of having been broken by hominins with stone tools increase from around 16% in the NSP sample (Table 7.9A) to around 24% when considering long limbs (NISP) (Table 7.10). In contrast, percentages of tooth marks remain similar in all three subassemblages (4-7%, Tables 7.9A, B, and 7.10). Tooth marks appear slightly more often on axial elements (10% when considering well-preserved cortical surfaces and green broken bones, Table 7.11). Cut marks show the same frequencies as tooth marks in this skeletal part (Table 7.11).

3.4.1.6. BSM per element in small and medium-sized carcasses

Tables 7.12A and 7.12B of the appendix**,** as well as Tables 7.13A and 7.13B show the frequencies of marked specimens according to long bone element and section for small and medium carcasses. Most cut marks and percussion marks appear on midshafts of meaty long bones (around 90% in small carcasses and more than 75% in medium carcasses). In small carcasses, tooth marks appear more often on lower limb bones than on upper and intermediate long bones, but they cluster on intermediate long bones in medium carcasses (Table 7.13B). Around 90% of all BSM appear on midhsafts in both carcass sizes. Upper limb bones have higher percentages of cutmarked specimens in small carcasses. In medium carcasses, intermediate long bones present the highest cut mark frequencies, closely followed by upper limb bones.

Tables 7.14A and 7.14B provide the percentages of cut marks and tooth marks in all axial elements, as well as in skull and mandible fragments. Cut

marks appear mostly on ribs, but several were recorded on vertebral apophyses and even vertebrae bodies. A small number of tooth marks appeared on ribs, vertebrae and pelves (Figure 3.27). Cut marks and percussion marks were observed on two skull fragments, which suggests that hominins might occasionally have been accessing and consuming the brains of these mammals (Figure 3.26).

Evidence for overlap of carnivore and hominin activity was found only in one shaft fragment of a metacarpal of a medium-sized bovid, which showed both cut marks and tooth marks, and two tibia fragments from medium-sized bovids, which bore percussion and tooth marks. This could be reflecting a very low degree of competition between carnivores and hominins at the site. A combination of cut marks and percussion marks was observed on a number of specimens of the small and the long limb bone subassemblages from small and medium-sized carcasses (1 and 15 specimens, respectively), suggesting that hominins were carrying out the complete butchering process at this site.

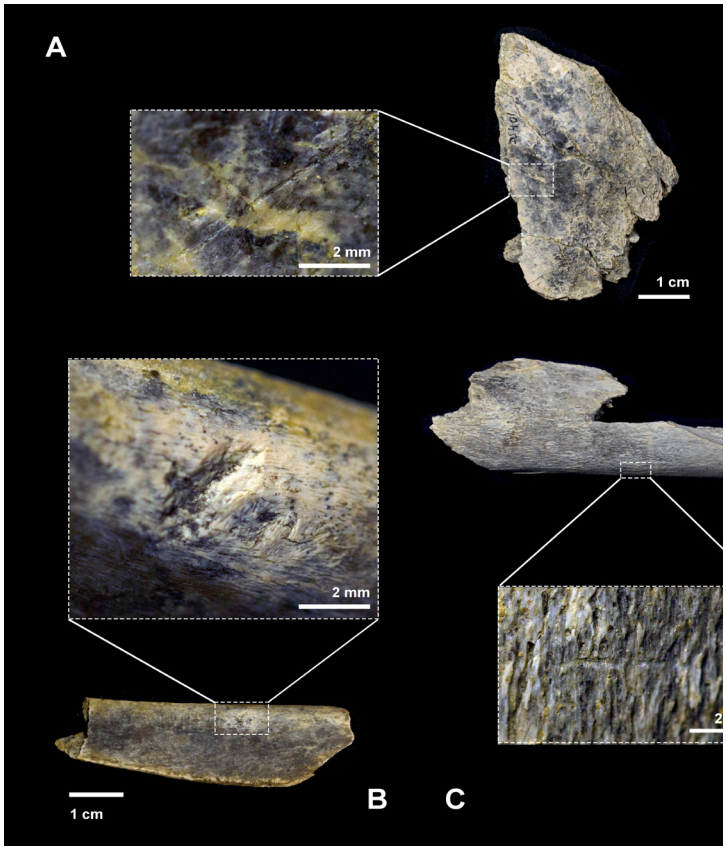

FIGURE 3.26. *Several cranial fragments displaying anthropic damage in the form of cut marks (A, C) and percussion marks (B)*

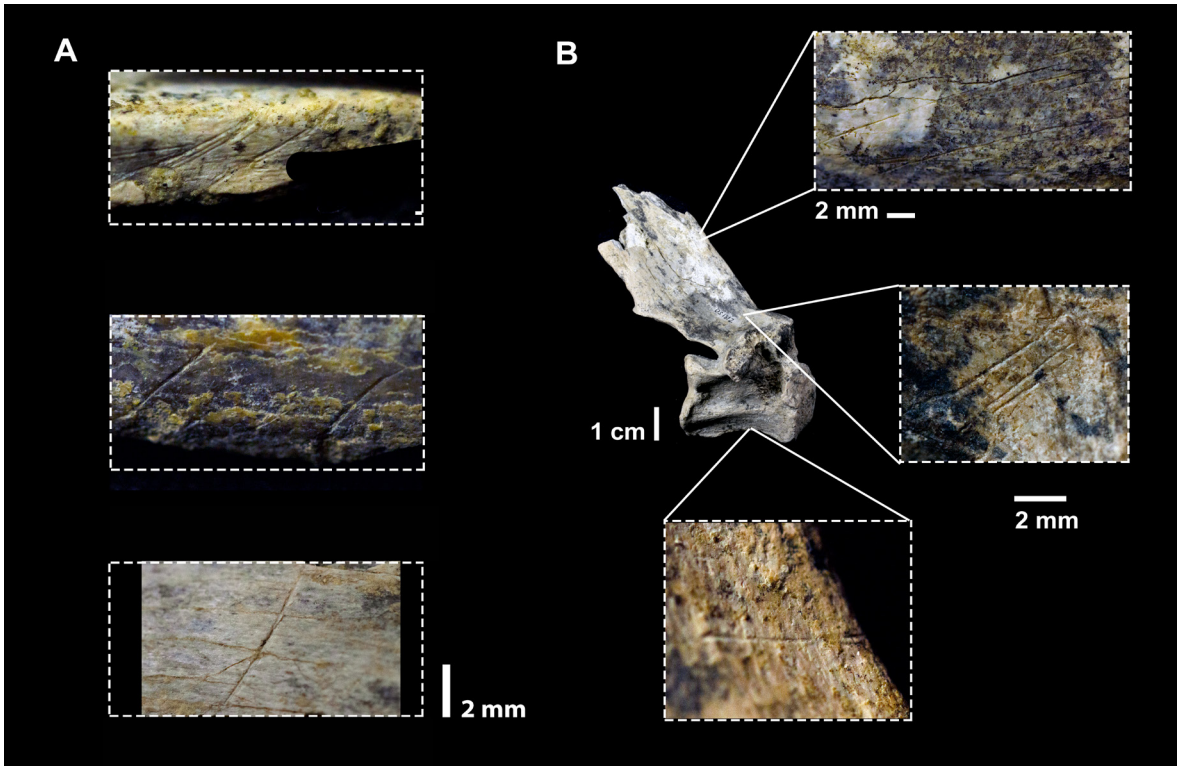

Figure 3.27. *A) Cut marks on the dorsal and ventral sides of ribs. B) Location of documented cut marks on vertebrae.*

3.4.2. Comparing DS to the archaeological record

3.4.3.1. The reference sample: Carcass sizes 1-2: Similarities and differences among the selected ESA, Mousterian, and Upper Paleolithic assemblages with regard to CM-NISP, CM-LB, and CM-MSH

CM-NISP

Both ANOVA and a Kruskal-Wallis test on the CM-NISP heterocedastic set (Table 3.31) show that there is no significant difference among the three subsamples, yet Cohen's δ suggests that mean differences are of medium effect (i.e. >0.5) between ESA sites on the one hand, and Mousterian and Upper Paleolithic sites on the other hand. Cohen's δ value for the mean difference between Mousterian and Upper Paleolithic yielded a value >0.2 but <0.5, indicating a smaller effect size (Table 3.36).

CM-LB

ANOVA results report no statistical difference in the mean values for CM-LB in the three comparative samples. However, when considering this variable,

Cohen's δ indicates a very large effect of the mean differences between ESA and the other two groups, as is suggested also for CM-NISP, and a negligible effect of the mean difference between Mousterian and Upper Paleolithic assemblages.

CM-MSH

With regard to CM-MSH, the ANOVA results indicate a statistically significant difference between the three groups (F-value = 3.7021, p-value = 0.04771, Table 3.31), but the results of the Tukey's HSD test were non-significant, probably because the ANOVA p-value is close to the non-significant 95% boundary. This might also be due to the fact that this test does not assume *Homo*geneity of variances. However, the variable cm-MSH yielded low p-values that suggest that the difference in cut mark frequency on long bone shafts might be between ESA sites and the other two groups (Table 3.32). In fact, Cohen's δ values show very similar effect sizes for the differences between the groups to the ones reported for CM-NISP, and CM-LB: very high significances in the differences between ESA and the other two groups, and a smaller effect size regarding Mousterian and Upper Paleolithic sites, suggesting that cut mark frequencies are significantly higher in Mousterian and Upper Paleolithic assemblages when compared to the selected ESA sites.

3.4.3.2. Comparative analysis of the DS small-size carcass subsamples to the referent assemblages

Tables 3.34 and 3.35 show the results of the application of the t-test and the Mann-Whitney U test to the means of the different groups, and to the cut mark frequencies in the DS samples "a" (good preservation), "b" (good and moderate preservation), and "c" (complete assemblage regardless of preservation).

CM-NISP

According to the Mann-Whitney U test applied to the heteroscedastic CM-NISP sample, none of the DS samples are different from the means of the three referent groups. The confidence intervals plot for the differences between means is consistent with this with regard to DSa and DSb, yet DSc falls outside the 95% confidence intervals (Figure 3.28).

CM-LB

The sub-samples DSa and DSb are both significantly different from the Mousterian and the Upper Paleolithic samples regarding CM-LB, and similar to ESA assemblages (Table 3.35). This can also be observed in the correspond-

ing 95% confidence intervals plot for the differences between means for this variable, which also shows that whereas DSa and DSb fall within the ESA sample, DSc is statistically different from all three groups (Figure 3.28).

CM-MSH

The well-preserved sample of DS shows similarities in the frequency of cut marked specimens on long bone shafts to the ESA and to the Upper Paleolithic, and it is significantly different from the Mousterian sample. DSb is significantly different from the Upper Paleolithic sample, as well as from the Mousterian sample, and DSc is significantly different from all three sets. T-test results are consistent with the 95% confidence intervals. Again, differences between DS and the different groups are clearly less marked when only the well-preserved sub-sample of DS is considered (Table 3.35 and Figure 3.28).

3.4.3.3. The reference sample: Carcass sizes 3-4: Similarities and differences among the selected ESA, Mousterian, and Upper Paleolithic assemblages with regard to CM-NISP, CM-LB, and CM-MSH

CM-NISP

The null hypothesis of homoscedasticity was rejected in the case of the variable CM-NISP (p-value = 0.04403, Table 3.30), the other two variables had equal variances among all three groups.

The ANOVA results show a significant difference among groups when considering CM-NISP. Since ANOVA results are not necessarily reliable in the case of heteroscedasticity because the test assumes *Homo*geneity of variances, a Kruskal-Wallis test is preferred for the variable CM-NISP. This test also yielded a significant result (KW chi-squared = 6.6716, p-value = 0.03559), suggesting that groups are statistically different. A pairwise comparison using Wilcoxon rank sum test for this variable yielded almost significant differences between Mousterian, and Upper Paleolithic sites (Table 3.33). Cohen's δ value is >0.5 when this pair is considered, and also when ESA and Upper Paleolithic are evaluated, suggesting a considerable effect size between these groups. The smallest effect size is yielded for the mean difference between ESA and Mousterian (Table 3.36), which according to the Wilcoxon rank sum test is practically non-existent.

CM-LB

A non-significant result (although a very low p-value) is yielded by the

ANOVA test with regard to cut mark frequencies on long bones (CM-LB) for medium-sized carcasses, meaning that no differences exist between groups regarding this variable (Table 3.31). Tukey's HSD test also provided non-significant results, yet the value referring to the differences between ESA and Upper Paleolithic sites is close to significant (Table 3.32). Indeed, Cohen's δ yielded a value >0.8, suggesting a large significance effect. The mean differences in the other pairs had a medium effect size (Table 3.36).

CM-MSH

Differences in cut mark frequencies between groups were significant with regard to long bone shafts according to ANOVA (Table 3.31). Values yielded by the Tukey's HSD test were statistically significant when ESA sites were compared to the other two groups. As a matter of fact, the effect size provided by Cohen's δ value for these paired groups was very large, as opposed to the effect size for the mean differences between Mousterian and Upper Paleolithic sites (Table 3.36).

3.4.3.4. Comparative analysis of the DS medium-sized carcass subsamples to the referent assemblages

CM-NISP

The Mann-Whitney U test indicates similarities between DS and all three groups with regard to CM-NISP (Table 3.34). The 95% confidence intervals plot, however, suggests differences in means between DSc and all three groups, as was the case for the small-size carcass subsample. DSa also falls outside the ranges of the 95% confidence intervals of the three groups. DSb, however falls within the Upper Paleolithic 95% confidence interval, yet outside the other two groups, both of which showed a marked difference to the Upper Paleolithic sample, as is explained above.

CM-LB

Contrasting results were again obtained when the CM-LB mean values of each sample set were compared to the well-preserved DS sub-sample on the one hand, and to the not so well-preserved DS sub-samples on the other hand. The well-preserved sample of medium-sized ungulates is statistically similar to the Mousterian and Upper Paleolithic means, and significantly different from the ESA sites. The moderately and well-preserved DSb assemblage is statistically indistinguishable from the ESA and Mousterian groups and differs from

Table 3.30. *Bartlett test results for homogeneity of variances in the three comparative sets (ESA, Mousterian and Upper paleolithic) applied to the subassemblages of small and medium-sized carcasses.*

	Size 1-2			Size 3-4		
	Bartlett's K squared	df	p-value	Bartlett's K squared	df	p-value
cm-NISP	7.3657	2	0.02515*	6.2457	2	0.04403*
cm-LB	0.40257	2	0.8177	4.3982	2	0.1109
cm-MSH	4.2282	2	0.1207	4.6617	2	0.09721

Table 3.31. *ANOVA and Kruskal-Wallis results*

ANOVA results				
	Size 1-2		Size 3-4	
	F-value	Pr(>F)	F-value	Pr(>F)
cm-NISP	1.2823	0.2922	3.6746	0.03203*
cm-LB	2.8012	0.09056	3.1378	0.05789
cm-MSH	3.7021	0.04771*	4.1078	0.02817*

Kruskal-Wallis			
	KW chi-squared	df	p-value
cm-NISP (Size 1-2)	2.7566	2	0.252
cm-NISP (Size 3-4)	6.6716	2	0.03559*

the Upper Paleolithic set. This trend is visible in the use of the complete DSc subsample. This provides such a low frequency of cut marks that makes it statistically different from all three groups, as can be appreciated also in the 95% confidence interval plots for the differences between means for this variable (Figure 3.28).

CM-MSH

Contrasting results were also obtained when the CM-MSH mean values of each sample set was compared to the DS sub-samples. The well-preserved DSa sample is statistically similar to the Mousterian and Upper Paleolithic means, and significantly different from the ESA sites. The moderately and well-pre-

Table 3.32. *Tukey's test results.*

Size 1-2					
	Tukey's test				
		diff	lwr	upr	p adj
cm-NISP					
	MOU-ESA	2.191667	-4.945025	9.328358	0.7317365
	UP-ESA	3.916667	-2.271630	10.104963	0.2781666
	UP-MOU	1.725000	-3.844467	7.294467	0.7278675
cm-LB					
	MOU-ESA	6.2642857	-1.601925	14.130496	0.1313404
	UP-ESA	6.5500000	-1.613152	14.713152	0.1278329
	UP-MOU	0.2857143	-7.580496	8.151925	0.9951705
cm-MSH					
	MOU-ESA	8.507143	-1.270985	18.28527	0.0937042
	UP-ESA	9.750000	-0.397243	19.89724	0.0606403
	UP-MOU	1.242857	-8.535271	11.02099	0.9426394
Size 3-4					
cm-NISP					
	MOU-ESA	-0.4033333	-8.8844375	8.077771	0.9927776
	UP-ESA	5.1557143	-2.6022234	12.913652	0.2535298
	UP-MOU	3.0683761	0.1406689	10.977426	0.0431558*
cm-LB					
	MOU-ESA	5.952564	-5.7749086	17.68004	0.4331543
	UP-ESA	11.440476	-0.1539774	23.03493	0.0536929
	UP-MOU	5.487912	-3.6641956	14.64002	0.3154008
cm-MSH					
	MOU-ESA	13.188889	0.8121149	25.565663	0.0350688*
	UP-ESA	11.766667	0.3080005	23.225333	0.0433027*
	UP-MOU	-1.422222	-11.4553734	8.610929	0.9340677

served DSb assemblage is statistically indistinguishable from the ESA and differs from the Mousterian and Upper Paleolithic groups. When the complete DSc subsample is used, differences from all three groups are significant. The

graphics show the same results. DSc falls outside the confidence intervals for all groups, whereas the well or moderately preserved DS sub-samples fall within the confidence ranges (Figure 3.28).

3.4.3.5. Summary

Taphonomic studies of Paleolithic sites commonly do not use correction methods, which means that the impact of dry breakage or differential bone cortical preservation are not properly taken into account. This biases the original frequencies of bone surface modifications (BSM) by deflating them. Given that BSM are not ubiquitous on the whole surface of any given bone specimen, the use of even moderately preserved specimens do not guarantee that all the original BSM are intact. Therefore, experimental or recent (i.e., Upper Paleolithic) bone assemblages, which have frequently undergone limited diagenetic modification (and, hence, restricted loss of cortical bone and dry breakage) are

Table 3.33. *Pairwise comparisons using Wilcoxon rank sum test*

cm-NISP (size 1-2)		
Pairwise Wilcoxon rank sum test		
	Early Stone Age	**Mousterian**
Mousterian	0.54	-
Upper Paleolithic	0.33	0.69

cm-NISP (size 3-4)		
Pairwise Wilcoxon rank sum test		
	Early Stone Age	**Mousterian**
Mousterian	1.000	-
Upper Paleolithic	0.270	0.056

not proper proxies of ESA assemblages, unless corrections methods for these biases are introduced. The most aseptic one is the use of well-preserved (and, ideally, dry breakage corrected) subsamples.

Although ANOVA and Kruskal-Wallis tests were only significant in some cases, differences between the means of the three sets of sites could be further addressed by means of a bootstrap method and the Cohens' δ value. A clear trend was observed regarding the differences between groups in both the small-sized and the medium-sized carcasses, with the exception of the vari-

Table 3.34. *Mann-Whitney Wilcoxon results*

cm-NISP Size 1-2					
	Mann-Whitney U	W	p-value	mean DS	mean
DS (a)					
	ESA	3	1	10.3	8.383333
	MOU	5	0.8889		10.575
	UP	10	1		12.3
DS (b)					
	ESA	3	1	9.2	8.383333
	MOU	5	0.8889		10.575
	UP	11	0.8623		12.3
DS (c)					
	ESA	6	0.2857	4	8.383333
	MOU	8	0.2222		10.575
	UP	19	0.1184		12.3

cm-NISP Size 3-4					
	Mann-Whitney U	W	p-value	mean DS	mean x
DS (a)					
	ESA	0	0.2857	19.8	10.65
	MOU	1	0.1927		10.24667
	UP	10	0.5003		15.80571
DS (b)					
	ESA	1	0.5714	16	10.65
	MOU	2	0.2777		10.24667
	UP	17	1		15.80571
DS (c)					
	ESA	6	0.2857	5.9	10.65
	MOU	12	0.3852		10.24667
	UP	33	0.1486		15.80571

Table 3.35. *T-test to compare DS to the means of the groups UP, MOU, and ESA. First, the comparison is made with the value for the well-preserved subsample of DS (DS (a)), second with the value of the subsample Good+Moderate (DS (b)) and third for the complete assemblage (DS (c)).*

cm-LB						
Size 1-2						
	T-test	**t**	**df**	**p-value**	**mean DS**	**mean x**
DS (a)						
	ESA	0.72905	5	0.4987	11.7	13.45
	MOU	4.577	6	0.003782*		19.71429
	UP	3.4	5	0.01925*		20
DS (b)						
	ESA	1.8539	5	0.1229	9	13.45
	MOU	6.119	6	0.0008698*		19.71429
	UP	4.506	5	0.006364*		20
DS (c)						
	ESA	3.0204	5	0.0294*	6.2	13.45
	MOU	7.7181	6	0.0002481*		19.71429
	UP	5.653	5	0.002406*		20
Size 3-4						
	T-test	**t**	**df**	**p-value**	**mean DS**	**mean x**
DS (a)						
	ESA	-4.1107	5	0.009258*	25	16.51667
	MOU	-1.1009	12	0.2925		22.46923
	UP	0.93134	13	0.3687		27.95714
DS (b)						
	ESA	-0.47649	5	0.6538	17.5	16.51667
	MOU	2.1616	12	0.05156		22.46923
	UP	3.2934	13	0.005821*		27.95714
DS (c)						
	ESA	3.0124	5	0.02968*	10.3	16.51667
	MOU	5.2936	12	0.0001903*		22.46923
	UP	5.5611	13	9.211e-05*		27.95714

cm-MSH Size 1-2						
	T-test	t	df	p-value	mean DS	mean x
DS (a)						
	ESA	-0.50238	5	0.6367	13.5	12.55
	MOU	4.3178	6	0.004995*		21.05714
	UP	2.1419	5	0.08511		22.3
DS (b)						
	ESA	1.0841	5	0.3278	10.5	12.55
	MOU	6.0319	6	0.0009381*		21.05714
	UP	2.8721	5	0.03491*		22.3
DS (c)						
	ESA	3.0407	5	0.02873*	6.8	12.55
	MOU	8.1459	6	0.000184*		21.05714
	UP	3.7727	5	0.01299*		22.3

Size 3-4						
	T-test	t	df	p-value	mean DS	mean x
DS (a)						
	ESA	-5.6854	5	0.002346*	25.5	15.53333
	MOU	1.1279	8	0.2921		28.72222
	UP	0.59923	13	0.5593		27.3
DS (b)						
	ESA	-1.0648	5	0.3357	17.4	15.53333
	MOU	3.9631	8	0.004159*		28.72222
	UP	3.2958	13	0.005795*		27.3
DS (c)						
	ESA	2.7571	5	0.03997*	10.7	15.53333
	MOU	6.3083	8	0.0002307*		28.72222
	UP	5.5262	13	9.77e-05*		27.3

able CM-NISP in the second reference sample. In nearly all cases, considerably large effect sizes ($\delta>0.5$) were provided by Cohen's δ for the mean differences

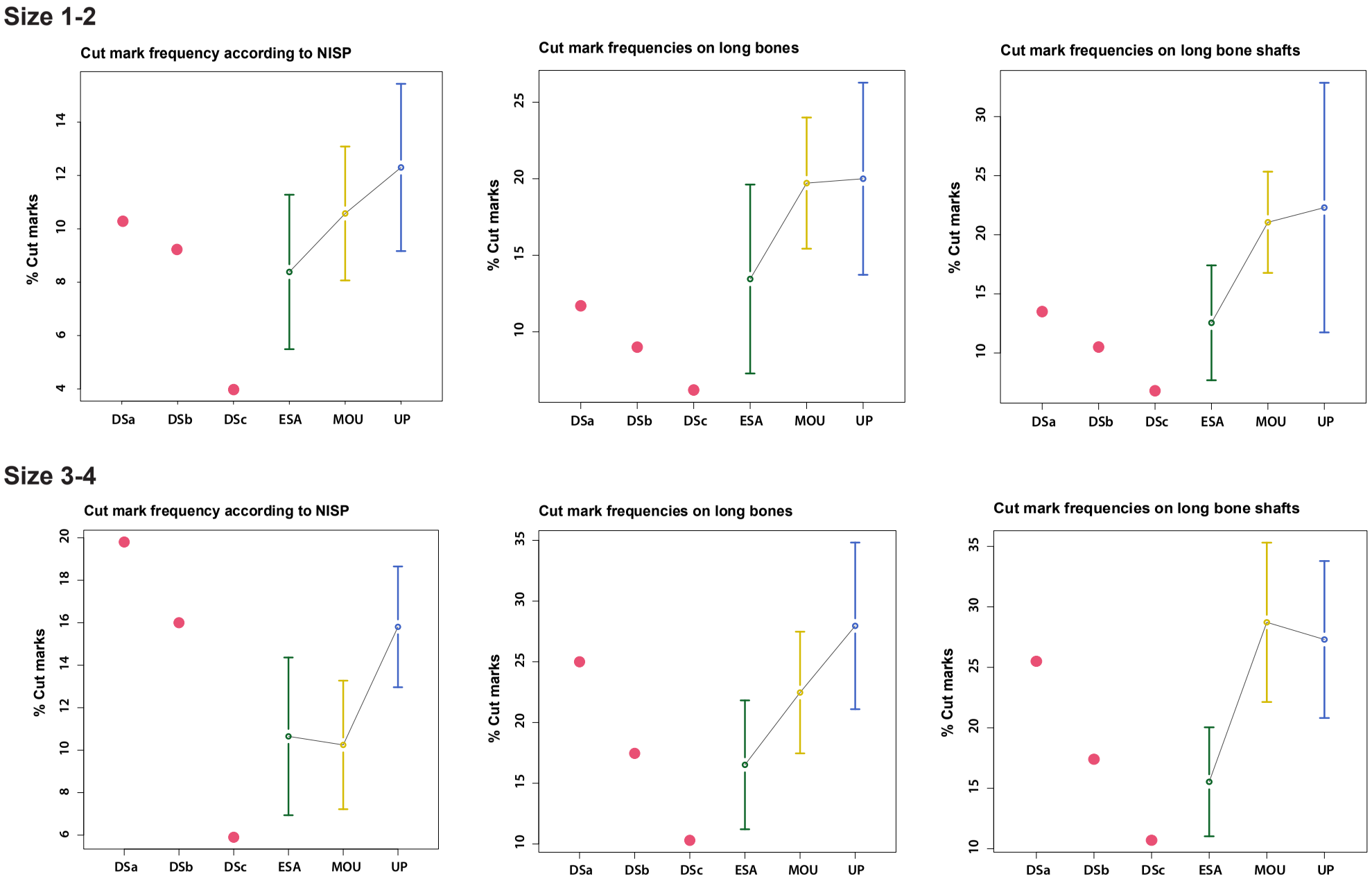

FIGURE 3.28. *Cut mark percentages documented for FLK Zinj (Domínguez-Rodrigo et al. 2007) and the three subsamples of DS (this study) compared to the mean and 95% confidence intervals of the selected anthropogenic Early Stone Age, Mousterian and Upper Paleolithic sites a) considering small carcasses, b) considering medium-sized carcasses.*

between ESA on one side, and Mousterian and Upper Paleolithic sites on the other side, whereas very small effect sizes were yielded by Cohen's δ for the difference between Mousterian and Upper Paleolithic sites. Cut mark frequencies are overall lower in ESA sites, yet this could be the result of none of the ESA sites used here having been tallied only based on the subsample of well-preserved cortical surfaces. Most of them also include moderate preservation and this deflates percentages. The fact that these assemblages are generally worse preserved and have been longer influenced by diagenetic processes, could also be a major reason for these differences. Thus, differences between cut mark frequencies in ESA assemblages and more recent sites are potentially not behavioral, but taphonomic. Indeed, when the DS sub-samples are compared to each of the three sets, results are strongly affected by the type of sample used for comparison. While the well-preserved samples are nearly always statistically similar to Upper Paleolithic assemblages (and often also to Mousterian assemblages), the complete DS sample (regardless of preservation and dry fractures)

Table 3.36. *Results for bootstrapped mean differences, standard deviation, and confidence intervals, as well as Cohen's δ.*

Size 1-2				
	Mean difference (boots.)	**Standard dev. (boots.)**	**Confidence interval (boots.)**	**Cohen's δ (effect size)**
CM-NISP				
MOU-ESA	2.206355	1.414012	(-0.477 - 4.991)	0.7550616 - medium
UP-ESA	3.910664	1.772669	(1.143 - 8.525)	0.6645567 - medium
UP-MOU	1.715621	1.757703	(-1.092 - 6.074)	0.3004743 - small
CM-LB				
MOU-ESA	6.216039	2.75107	(0.832 – 11.547)	1.196287 - large
UP-ESA	6.597453	3.213742	(0.350 – 12.746)	1.104575 - large
UP-MOU	0.2945932	2.734085	(-4.5784 – 6.0134)	0.05403454 - small
CM-MSH				
MOU-ESA	8.45088	2.339559	(3.933 – 13.045)	1.836904 - large
UP-ESA	9.737071	4.08805	(1.127 – 17.067)	1.244636 - large
UP-MOU	1.205774	4.093528	(-7.689 – 8.545)	0.1635754 - small
Size 3-4				
CM-NISP				
MOU-ESA	0.3666033	1.882249	(-3.1924 – 4.2109)	0.08018762 - small

UP-ESA	5.160767	1.880793	(1.410 – 8.874)	0.6583344 - medium
UP-MOU	5.589472	1.960456	(1.944 – 9.707)	0.7347744 - medium
CM-LB				
MOU-ESA	5.843209	2.898451	(0.036 – 11.364)	0.795363 - medium
UP-ESA	11.40276	3.572475	(4.99 – 19.05)	1.095631 - large
UP-MOU	5.353085	3.751571	(-1.302 – 13.758)	0.5321041 - medium
CM-MSH				
MOU-ESA	13.08126	3.110409	(8.70 – 22.42)	1.823785 - large
UP-ESA	11.77382	3.330411	(4.96 – 17.99)	1.198708 - large
UP-MOU	1.43179	3.951392	(-5.277 - 10.480)	0.1380283 - small

presents very low percentages and always falls outside the ranges of the 95% confidence intervals of Mousterian and Upper Paleolithic sites. The fact that in most cases, the well-preserved DS subsample is statistically similar to the cutmarked assemblages from the Upper Pleistocene (i.e., Mousterian and Upper Paleolithic), implies probably a similar butchering behavior. This, initially, suggests that the hypothesis of primary access to carcasses by early Pleistocene hominins is reinforced. This hypothesis will be tested in subsequent analyses.

3.4.3. Comparing DS to dual and multi-patterned experimental assemblages and FLK Zinj

3.4.3.1. Univariate analysis of BSM

Cut marks

Carcass size 1-2

Available experiments carried out with small-sized carcasses have simulated models HO (Hominid-only), WB-C (Whole bone to carnivore), H-C (primary access; Hominid-Carnivore), and V-H-C (secondary access; Vulture-Hominid-Carnivore) (Table 3.37, Figure 3.29A and 3.30A). The first thing that stands out is that cut mark frequencies of the well-preserved and the moderately-preserved samples of DS are very similar to the frequencies documented at FLK *Zinj*, especially when considering cut marks per NISP. When only cut-marked specimens are considered, DS shows a very marked contrast between very high percentages on cut-marked mid-shafts, and very low percentages of cut marks on long bone ends, a feature that is not observed at FLK *Zinj*, and does not

seem to be characteristic of the H-C model either (Figure 3.29A and 3.30A), with which both assemblages show some similarities. This aspect is also characteristic of the distribution of cut marks on medium-sized carcasses at the site (Figure 3.29B and 3.29B), and could be signalling the absence of the butchering activity of disarticulating bone elements at DS.

Both archaeological assemblages also show a more marked contrast in cut mark frequencies than do experimental models HO and H-C (DR) between ULB and ILB on one side, and LLB on the other side, although cut mark percentages at the sites are somewhat lower in general than frequencies reported from these two experiments. Even though it is to be expected that DS and FLK *Zinj* both will present lower frequencies than the HO (DR) model, since carnivore action is documented at both sites, it is interesting to note that when only cut-marked specimens are considered, cut marks are distributed very similarly in DS and in both models representing primary access (HO and H-C (DR)), with higher percentages of cut marks on ULB and ILB, and much lower values in LLB.

The DS and FLK *Zinj* values fall close to all other experiments that model primary access (HO WB-C, H-C (P)) when all bone fragments or only midshafts are considered, and neither of them coincide with the V-H-C (P) model. However, given that no other experiments modeling secondary access (e.g. F-H [felid-hominin] or F-H-H [felid-hominin-hyenid]) were available for this size class, and due to the fact that the sample size of small-sized carcasses at DS is relatively small, especially when only the well-preserved and corrected sample is taken into account (NISP: 54), no definitive statements should be made only on the basis of cut mark frequencies regarding small-sized carcasses at DS. All the same, it is worth emphasizing that the DSa cut mark estimates are very similar to the ones reported for FLK *Zinj*, which is interpreted as the result of hominins having had access to small-sized carcasses before carnivores (Domínguez-Rodrigo *et al.* 2007).

Carcass size 3-4

Most of the experiments model primary or secondary access to medium-sized carcasses, and the comparative sample used for this size class thus comprises two additional models for secondary access, namely F-H, and F-H-H (Tables 3.37 and 3.38**;** Figure 3.29B and 3.30B).

On the whole, the well-preserved and the moderately preserved subsamples of DS and FLK *Zinj* again present very similar cut mark frequencies, as was the case with smaller carcasses. With the exception of the already mentioned low number of cut-marked long bone ends that stand in contrast with a remarkably high number of cut-marked midshaft specimens in DS, all the cut mark values for the well-preserved sample of DS and for FLK *Zinj* fall within the 95% con-

Table 3.37. *Mean percentages of cut marked specimens in each skeletal section per NISP for small and medium-sized carcasses in each experimental model. DR: Domínguez-Rodrigo; P: Pante; G: Gidna (see exact references in table x)*

Size 1-2			ULB	ILB	LLB	MSH	Ends	Total
Primary access	HO (DR)	mean	53.5	37.6	20.4	37.2	49.3	40.4
		95% CI	(27.9-79.2)	(18.3-56.8)	(-16.5-57.2)	(22.5-51.9)	(6.6-91.9)	(18.7-62.1)
	HO (P)	mean				10.3		27.2
		95% CI				(3.1-17.6)		(20.3-33.7)
	WB-C (P)	mean				16.4		18.4
		95% CI				(2.5-36)		(5.5-34.8)
	H-C (DR)	mean	47	41.6	0	46.6	37.5	41.9
		95% CI	-	-	-	-	-	-
	H-C (P)	mean				15.4		18.9
		95% CI				(10.9-20.6)		(14.4-24.4)
Secondary access	V-H-C (P)	mean				0		0
		95% CI				0		0

Size 3-4			ULB	ILB	LLB	MSH	Ends	Total
Primary access	HO (DR)	mean	65.5	65.2	38.1	52.9	61.5	57.5
		95% CI	-	-	-	-	-	-
	HO (P)	mean				20.1		45.9
		95% CI				(0-40)		(25-66.7)
	WB-C (P)	mean				40		41.9
		95% CI				(13-80.1)		(22.1-69.5)
	H-C (DR+G)	mean	43.7	36.9	18.1	37	41.8	36.2
		95% CI	(11.8-75.6)	(12.5-61.2)	(-8.8-44.9)	(9-64.9)	(23.2-60.3)	(12.7-59.7)
	H-C (P)	mean				12.2		16.8
		95% CI				(7.9-16.9)		(12.1-21.9)

fidence interval of models H-C (DR), and in the case of cut-marked midshaft specimens and that of all bone fragments, DS also falls within the 95% confidence range of models HO (P) and WB-C (P). Only the non-corrected samples of DS (b, c) coincide with models of secondary access to carcasses by hominins (F-H, F-H-H, and V-H-C), which cautions once more against the use of biased estimates of bone surface modifications.

Although the experiments modeling primary and secondary access are generally clearly distinguishable in the different skeletal and bone sections, some overlap between their 95% confidence intervals exists in ILB and LLB, which render both skeletal parts less discriminatory of primary and secondary access to carcasses. This is in part due to the fact that confidence intervals tend to be large due to small sample sizes of the experimental studies, and therefore less reliable statistically. Yet, the cut mark estimates of DSa lie in both cases closer to the mean of the model H-C, than to the means of the experiments modeling secondary access to carcasses.

When considering only cut-marked specimens, the interpretation of the type of access to medium-sized carcasses at DS is even clearer, especially in the case of ULB and LLB, in which DSa values perfectly match the percentages reported in those experiments modeling primary access, as do the estimates of FLK *Zinj*, particularly in the case of mid-shafts and all bone specimens (Tables 3.37-3.39; Figure 3.30A and B).

Summary

It is important to stress that the high percentages of badly preserved bone surfaces at DS generally deflate frequency estimates of cut-marked specimens (Figure 3.32). When correction methods are not applied to the assemblage, DS values are commonly slightly lower than in the well-preserved subsample. Although the results are often similar when these percentages are compared to the experiments (especially in small-sized carcasses), it is the corrected sample which shows unequivocal results, as further discussed below.

Figure 3.31, which presents the relationship between the NICMSP: NISP ratio and the NICMMSSP: NICMSP ratio for medium-sized carcasses, as well as its bootstrapped version, show that DSa and DSb unambiguously fall within the confidence ellipse that groups all experiments simulating primary access, and outside the other two groups representing secondary access, whereas DSc lies in the overlap area of the ellipses representing primary access (H-C) and secondary access (F-H). These ellipses are large because of the small experimental sample. When this is corrected by bootstrapping, the spatial distribution of experiments and archaeofaunal assemblages becomes even clearer. FLK *Zinj*, for example, lies on the zone of overlap between the model H-C and the model F-H-H in the uncorrected sample, yet in the bootstrapped version of the graph the doubt is solved in favor of primary access.

Secondary access	**F-H (DR+G)**	mean	1.8	5.4	33.6	3.6	9.4	5.5
		95% CI	(-0.1-3.7)	(0.1-10.6)	(17.1-50)	(-1-8.2)	(4.5-14.2)	(0.4-10.6)
	F-H-H (DR)	mean	4.2	17.3	19.3	8.7	15.6	12.1
		95% CI	(-1.4-9.9)	(-4.5-39)	(11.8-26.7)	(1-16.4)	(5.5-25.7)	(3.7-20.5)
	V-H-C (P)	mean				0		8.5
		95% CI				0		(0-18.4)

Table 3.38. *Mean percentages of cut marked specimens in each skeletal section per total number of cutmarked specimens for small and medium-sized carcasses in each experimental model. DR: Domínguez-Rodrigo; P: Pante; G: Gidna (see exact references in table x)*

Size 1-2			**ULB**	**ILB**	**LLB**	**MSH**	**Ends**
Primary access	**HO (DR)**	**mean**	26.4	15.1	5.1	25.3	14.2
		95% CI	(-11.6-64.4)	(5.5-24.6)	(-0.6-10.7)	(11.3-39.3)	(3.3-25.1)
	H-C (DR)	**mean**	61.6	38.4	0	53.8	46.2
		95% CI	-	-	-	-	-

Size 3-4			**ULB**	**ILB**	**LLB**	**MSH**	**Ends**
Primary access	**HO (DR)**	**mean**	45.2	35.7	19	43	57.1
		95% CI	-	-	-	-	-
	H-C (DR)	**mean**	52	43.8	6.9	62.1	37.9
		95% CI	(32.6-71.5)	(23.7-63.9)	(-10-23.8)	(52.5-71.7)	(28.3-47.5)
Secondary access	**F-H (DR+G)**	**mean**	14.3	58.2	55.5	29.8	49.1
		95% CI	(2.6-26.1)	(36.4-80)	(41.6-70)	(16-43.6)	(31.1-67.1)
	F-H-H (DR)	**mean**	13.3	46.4	40.4	26.5	73.5
		95% CI	(-6.3-32.8)	(21.3-71.4)	(12.6-68.2)	(8.6-44.4)	(55.5-91.4)

In short, cut mark estimates of the DS assemblage point to a scenario in which hominins had primary access to the carcasses they consumed at the site. These results are complemented with the comparison of other bone surface

Table 3.39. *Mean percentages of cut marked specimens in each skeletal section per NISP (A) and per total number of cut marked specimens (B) for small and medium-sized carcasses in the DS subassemblages, and in FLK Zinj 22.*

A

Size 1-2		**ULB**	**ILB**	**LLB**	**MSH**	**Ends**	**Total**
DS a	**mean**	12.5	15.8	0	13.3	7.1	11.7
DS b	**mean**	10.7	12	0	10.7	4.7	9.03
DS c	**mean**	6.49	7.14	3.23	6.92	4.17	6.18
FLK Zinj	**mean**	20	19.7	6.2	11.9	21.8	14.9

Size 3-4		**ULB**	**ILB**	**LLB**	**MSH**	**Ends**	**Total**
DS a	**mean**	24.2	30.8	18.2	27.3	17.9	25
DS b	**mean**	13.8	21.7	18.6	18.6	35.2	17.5
DS c	**mean**	8.59	12.16	9.71	10.3	10.17	10.26
FLK Zinj	**mean**	25.5	23.1	12.3	17.2	46.6	21.9

B

Size 1-2		**ULB**	**ILB**	**LLB**	**MSH**	**Ends**
DS a	**mean**	50	50	0	83.3	16.7
DS b	**mean**	57.1	42.9	0	85.7	14.3
DS c	**mean**	45.5	45.5	9.1	81.8	18.2
FLK *Zinj*	mean	37	48.1	14.8	55.6	44.4

Size 3-4		**ULB**	**ILB**	**LLB**	**MSH**	**Ends**
DS a	**mean**	41.4	41.4	17.2	82.8	17.2
DS b	**mean**	35.9	43.6	20.5	84.6	15.4
DS c	**mean**	34.9	49.2	15.9	79.4	20.6
FLK *Zinj*	mean	37.1	52.9	10	64.3	38.6

modification estimates (i.e. percussion marks and tooth marks) to experimental data, and are further combined in multivariate statistical analyses in the following sections.

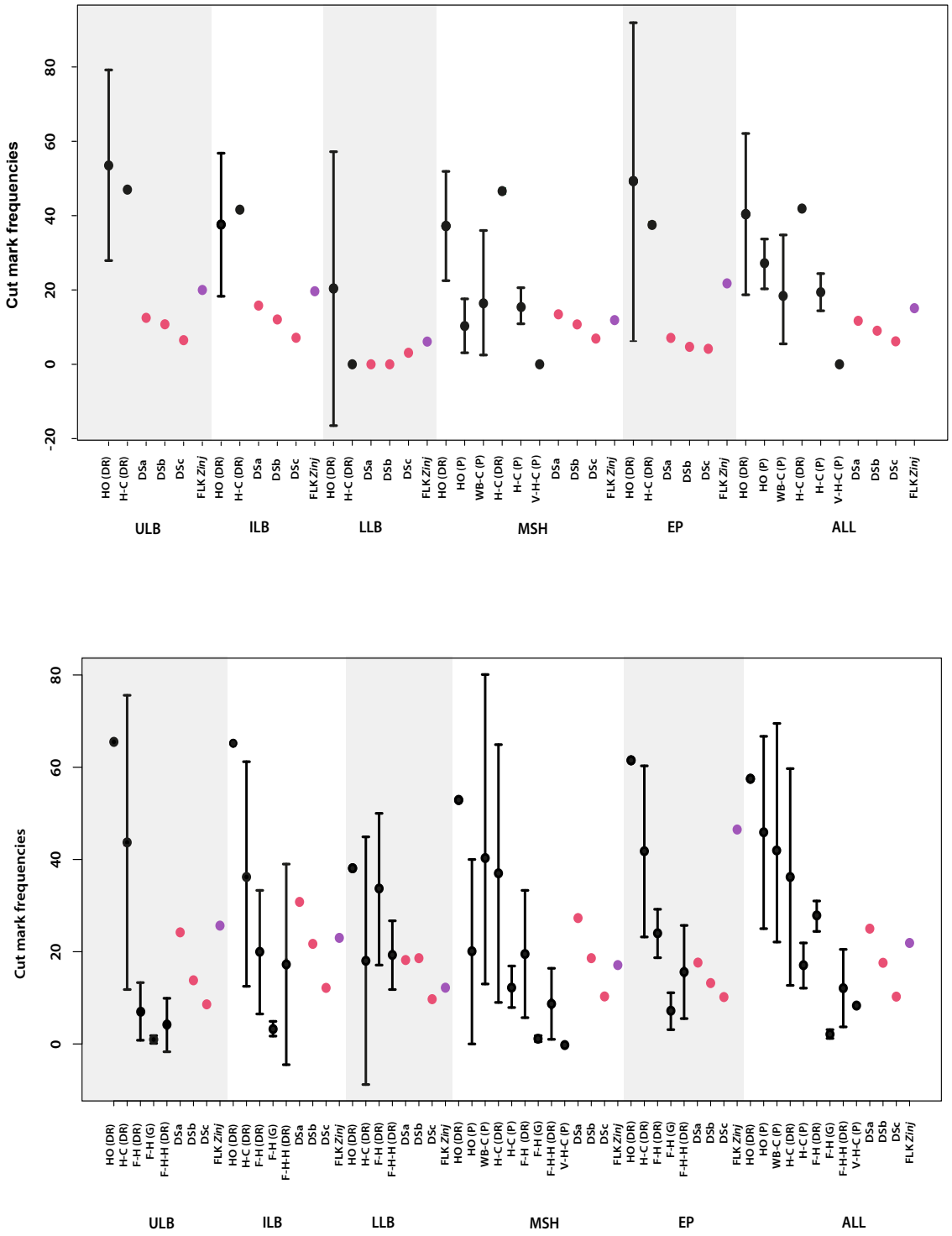

FIGURE 3.29. *Distribution of the 95% confidence intervals for the frequency of cut-marked specimens per NISP for each bone portion from a) small and b) medium-sized carcasses in experimental assemblages and at FLK Zinj and DS.*

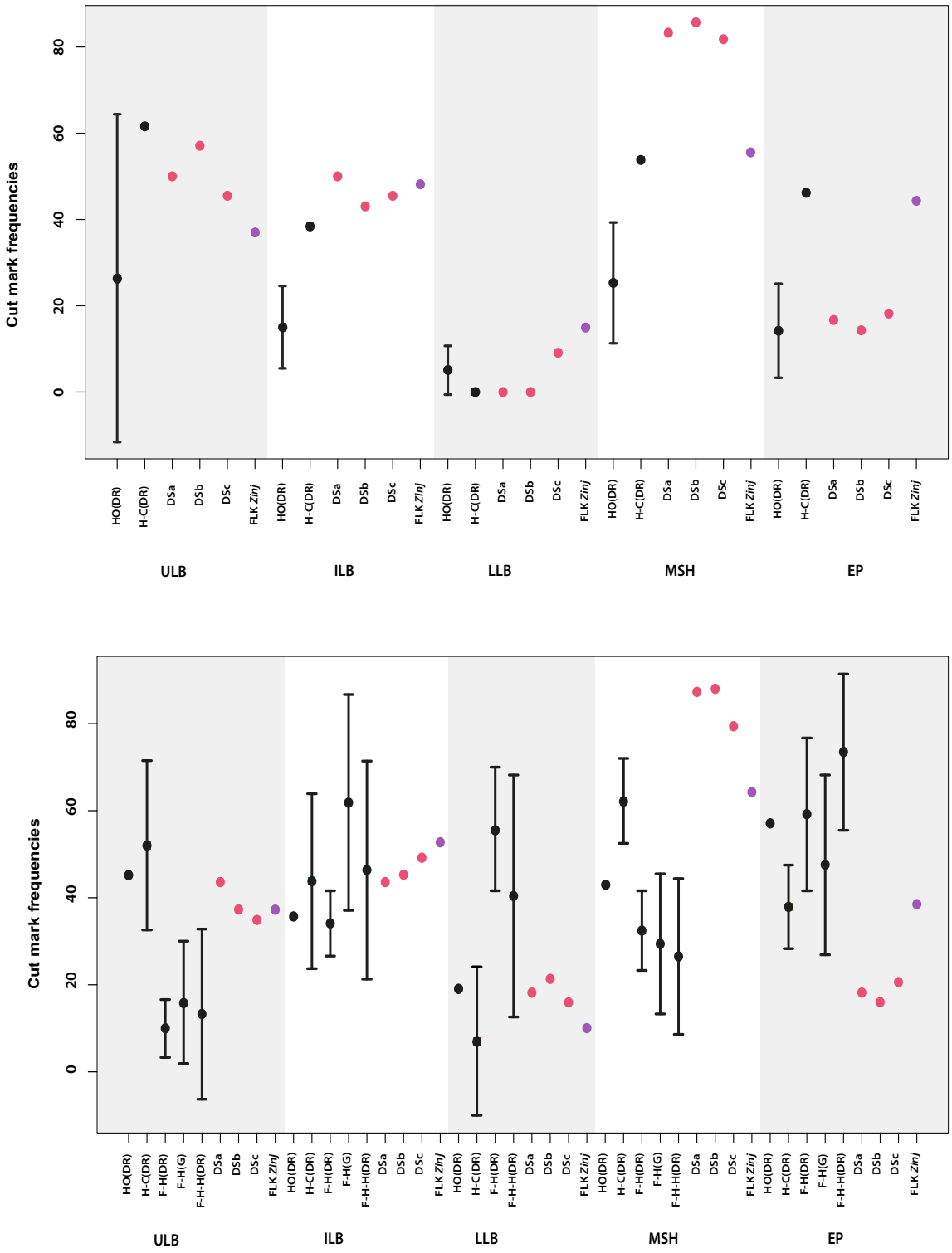

FIGURE 3.30. *Distribution of the 95% confidence intervals for the frequency of cut-marked specimens per total number of cut-marked specimens for each bone portion from a) small and b) medium-sized carcasses in experimental assemblages and at FLK Zinj and DS.*

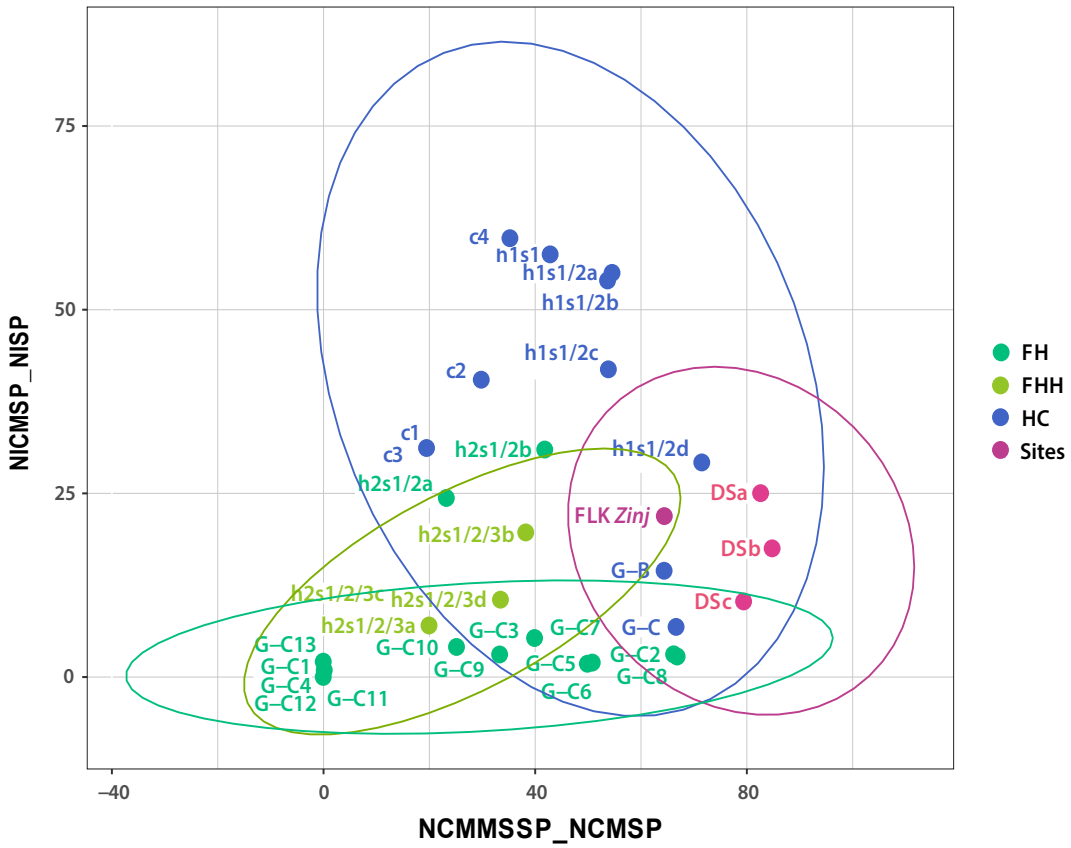

FIGURE 3.31. *Relationship between the NICMSP:NISP ratio and the NICMMSSP:NICMSP ratio for the medium-sized carcass assemblage at DS and FLK Zinj, as well as for the experimental assemblages from the H-C, F-H, and F-H-H models.*

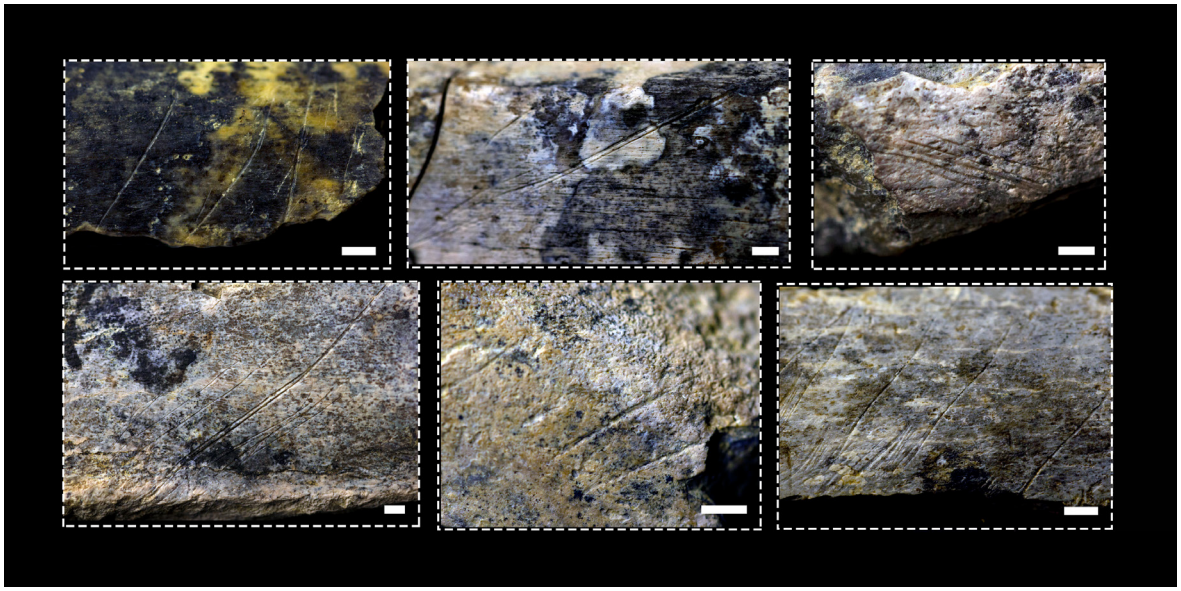

FIGURE 3.32. *Several examples of cutmarked long bone shafts.*

Percussion marks

Carcass size 1-2

As has been pointed out before, the sample size for small-sized animals at DS is relatively small. Percentages of percussion-marked specimens are relatively low and generally below 10%, as can be seen in Table 3.40, and Figure 3.34A. Although the values for DS fall within the 95% confidence interval of the model of secondary access V-H-C, this model's confidence interval overlaps almost entirely with those of the primary access experiments. The frequency of PM on epiphyseal portions coincide with all experimental models. This is, however, lower regarding shaft specimens, where PM frequencies only show correspondence with the V-H-C model. Given that all models reproduce access to complete bones, the mismatch between the DS data and the experiments may be caused by the unrepresentativeness of the sample size. Therefore, the use of percussion mark frequencies on bone portions alone would not allow making a clear distinction between primary and secondary access at DS. In contrast, the values for FLK *Zinj* are higher and more clearly within the range of hominin only and hominin to carnivore experiments.

Carcass size 3-4

Percussion marks are more abundant at DS when considering medium-sized carcasses. Values are even higher than those of FLK *Zinj* on mid-shafts and when all fragments are considered, and they fall within the ranges of H-C (Hominin-Carnivore) and V-H-C (Vulture-Hominin-Carnivore) experiments, which overlap completely (Figure 3.34B). It has been argued that V-H-C experiments present some issues because they are variable in the type of initial consumers and in the number of elements that are included per assemblage (referencia). Additionally, the sample is composed of several assemblages that had been only partially defleshed by vultures and carnivores before humans intervened, and it consists of complete, i.e. non-fragmented, bones (Pante *et al.* 2012). These facts could account for a fairly large confidence interval, and maybe also for the fact that they are indistinguishable from primary access models. Percussion mark frequencies would only be very low in a hypothetical scenario in which hominins would have accessed carcasses after durophagous carnivores such as hyenas, since felids do not usually fragment bones. Thus, HO (Hominin Only), H-C (Hominin-Carnivore), and F-H (Felid-Hominin), as well as V-H-C (Vulture-Hominin-Carnivore) models are expected to yield similar percussion mark frequencies. The percussion mark data obtained at DS, and their distribution indicates that most long bones were broken by hominins at the site, as has been demonstrated also in the analysis of bone breakage patterns (section 3.3; Table 3.40, Figure 3.33; Figure 3.34 A and B; 3.40).

Table 3.40. *Mean percentages of percussion-marked specimens in each bone portion per NISP for small and medium-sized carcasses in each experimental model and in DS and FLK Zinj. B: Blumenschine; C: Capaldo; P: Pante (see exact references in table x)*

Size 1-2			**ULB**	**ILB**	**LLB**	**MSH**	**NEP**	**EP**	**Total**
Primary access	**HO (B)**	**mean**	-	-	-	26.6	43.3	54.4	36.6
		95% CI				(13.1-40.1)	(0-91.6)	(35.7-73.1)	(26-47.2)
	H-C (B)	**mean**	-	-	-	33.6	17.7	25	31.1
		95% CI				(17.7-49.5)	(0-35.9)	(0-100)	(17-45.2)
	H-C (C)	**mean**	-	-	-	28.3	30.2	-	29.6
		95% CI				(22.4-34.2)	(18.9-41.5)		(23.2-36)
Secondary access	**V-H-C (P)**	**mean**	-	-	-	23.6	-	-	17.5
		95% CI				(5.9-47.1)			(4.4-34.8)
FLK Zinj		**percent**				22.9		20	22.1
		nm/total				(32/140)		(10/50)	(42/190)
DS a		**percent**	8	10.5	0	7.9		6.3	7.4
		nm/total	(2/25)	(2/19)	(0/10)	(3/38)		(1/16)	(4/54)
DS b		**percent**	7.1	10	0	7.9		3.7	6.7
		nm/total	(3/42)	(3/30)	(0/18)	(5/63)		(1/27)	(6/90)
DS c		**percent**	6.5	5.7	0	6		2.3	5.1
		nm/total	(5/77)	(4/70)	(0/31)	(8/134)		(1/44)	(9/178)

Size 3-4			**ULB**	**ILB**	**LLB**	**MSH**	**NEP**	**EP**	**Total**
Primary access	**HO (B)**	**mean**	-	-	-	33.3	100	75	50
		95% CI				(-)	(-)	(-)	(-)
	H-C (B)	**mean**	-	-	-	20.6	45.5	35.7	26
		95% CI				(6.4-34.8)	(3.2-87.8)	(0-98.8)	(8.6-43.4)
	H-C (C)	**mean**	-	-	-	13.1	22		16.8
		95% CI				(4.7-21.5)	(9.4-34.6)		(8.7-24.9)

Secondary access	**V-H-C (P)**	**mean**	-	-	-	19.2	-	-	26.9
		95% CI				(3.7-38.3)			(7.7-49.1)
		percent				12.8		20	12.5
FLK Zinj		**nm/total**				(57/446)		(12/60)	(63/506)
DS a		**percent**	16.4	16.3	36.7	21.5		19.5	20.1
		nm/total	(9/55)	(8/49)	(11/30)	(20/93)		(8/41)	(28/134)
DS b		**percent**	14	17.2	27.1	19.5		12.7	17.7
		nm/total	(15/107)	(16/93)	(13/48)	(36/185)		(8/63)	(44/248)
DS c		**percent**	6.6	8.2	14.6	9.2		7	8.6
		nm/total	(17/256)	(21/255)	(15/103)	(42/456)		(11/158)	(53/614)

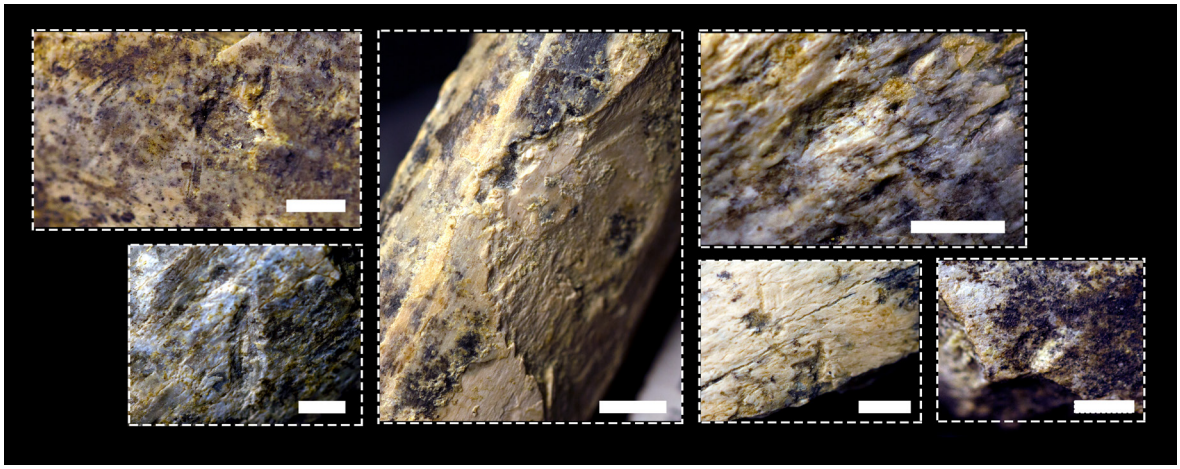

FIGURE 3.33. *Several examples of percussion-marked long bone shafts.*

Tooth marks

Carcass size 1-2

The CO (Carnivore Only) and the WB-C (Whole Bone to Carnivore) models bear the highest amount of tooth marked specimens, since they also include tooth marks generated during the breakage of bones by carnivores for marrow extraction (Table 3.41, Figure 3.35A). The V-H-C (Vulture-Hominin-Carnivore) model is also characterized by a significantly high percentage of tooth marked specimens, probably due to the fact that carnivores intervene at two different stages of carcass consumption. Lower percentages are yielded by sec-

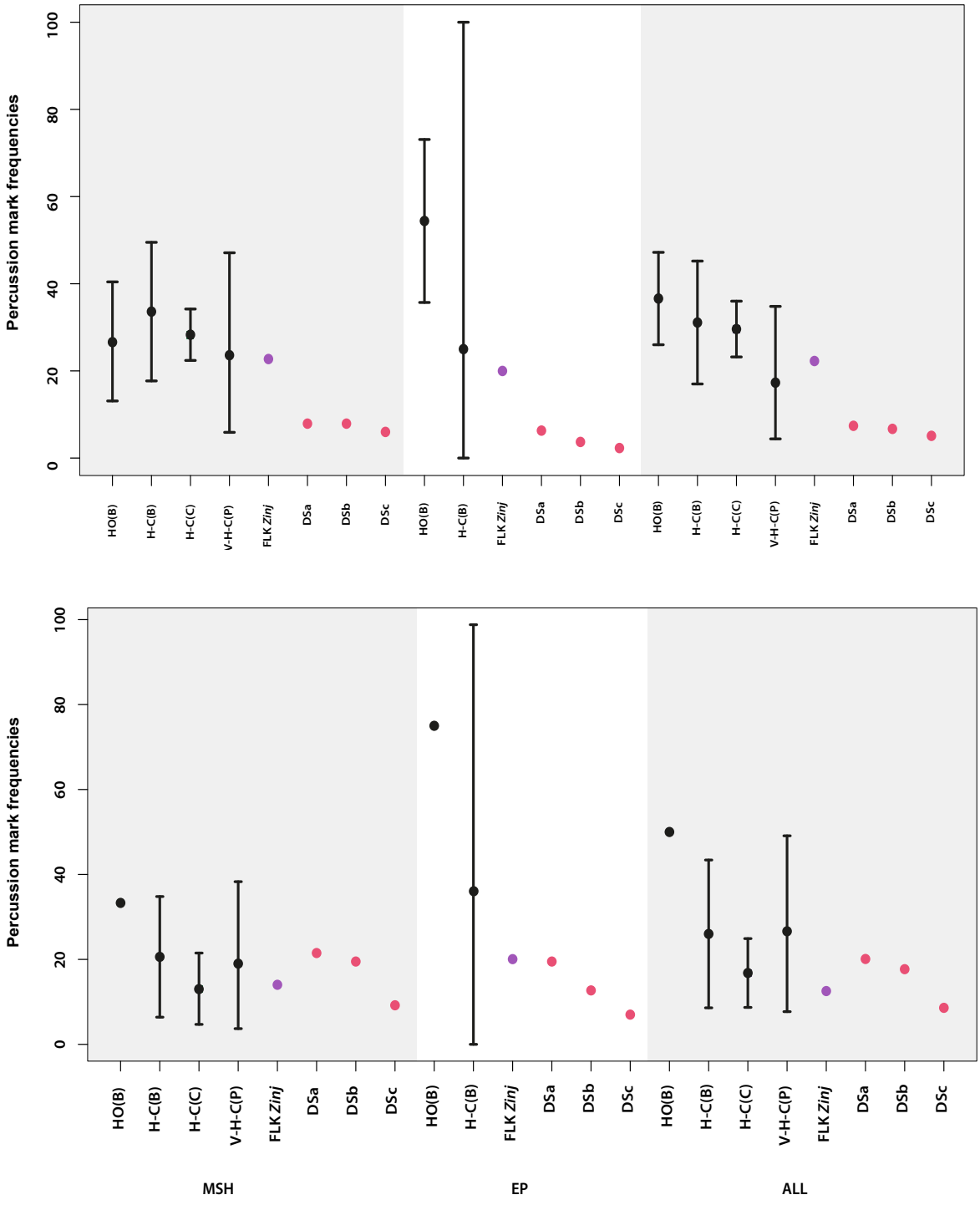

FIGURE 3.34. *Distribution of the 95% confidence intervals for the frequency of percussion-marked specimens per NISP for each bone portion from a) small and b) medium-sized carcasses in experimental assemblages and at FLK Zinj and DS.*

Table 3.41. *Mean percentages of tooth marked specimens in each skeletal section per NISP for small and medium-sized carcasses in each experimental model. B: Blumenschine; C: Capaldo; DR: Domínguez-Rodrigo; G: Gidna*

Size 1-2			**ULB**	**ILB**	**LLB**	**MSH**	**NEP**	**EP**	**Total**
Primary access	**WB-C (C)**	**mean**	-	-	-	70.6	-	-	70.5
		95% CI				(55.7-84.3)			(56.1-84.7)
	H-C (B)	**mean**	-	-	-	15.9	60.7	50	21.9
		95% CI				(2.6-29.2)	(29.3-92.1)	(0-100)	(5.1-38.7)
	H-C (C)	**mean**	-	-	-	14.9	31.4	-	19.4
		95% CI				(11.2-18.6)	(19.9-42.9)		(15.5-23.3)
Secondary access	**CO (B)**	**mean**	-	-	-	69.1	75	100	70.9
		95% CI				(54.8-81.0)	(0-100)	-	(56.7-82.5)
	F-H (DR)	**mean**	18.9	19.9	3	6.8	24.4	17.4	13.2
		95% CI	(-0.3-38)	(8.9-30.8)	(-5.3-11.3)	(1.1-12.5)	(6.4-42.5)	(-0.2-34.9)	(4.1-22.3)
	F-H (G)	**mean**	17.2	13	-	8.8		60.3	15.8
		95% CI	(9.4-25.1)	(3.9-22)		(0.9-16.8)		(47.4-73.1)	(7.9-23.8)
	V-H-C (P)	**mean**	-	-	-	35.5	-	-	43.4
		95% CI				(11.8-58.8)			(21.7-65.2)
FLK Zinj		**percent**	17.9	23.1	10.3	15		24	17.3
		nm/total	(10/56)	(15/65)	(8/78)	(21/140)		(12/50)	(33/190)
DS a		**percent**	4	5.3	10	5.3		6.3	5.6
		nm/total	(1/25)	(1/19)	(1/10)	(2/38)		(1/16)	(3/54)
DS b		**percent**	2.4	3.3	5.6	3.2		3.7	3.3
		nm/total	(1/42)	(1/30)	(1/18)	(2/63)		(1/27)	(3/90)
DS c		percent	2.6	1.4	6.5	2.2		4.5	2.8
		nm/total	(2/77)	(1/70)	(2/31)	(3/134)		(2/44)	(5/178)

Size 3-4			ULB	ILB	LLB	MSH	NEP	EP	Total
Primary access	WB-C (C)	mean	-	-	-	57.3	-	-	78.9
		95% CI				(18.1-89.8)			(61.9-95.0)
	H-C (B)	mean	-	-	-	5.1	39.5	85.7	16.4
		95% CI				(0.2-10)	(8.4-70.6)	(35.6-100)	(10.5-22.3)
	H-C (C)	mean	-	-	-	16.2	48.4	-	27
		95% CI				(10.4-22.8)	(40.5-56.3)		(22.5-31.5)
Secondary access	CO (B)	mean	-	-	-	86.5	90.5	100	87.6
		95% CI				(75.7-95.8)	(76.5-100)	-	(77.9-95.5)
	F-H (G)	mean	15.1	9.7	-	6		53.3	13
		95% CI	(11.7-18.5)	(6.3-13.1)		(3.1-8.8)		(44.1-62.4)	(10.2-15.8)
	F-H (DR)	percent	-	-	-	11.7	23.1	33.3	21.4
		nm/total				(2/17)	(3/13)	(4/12)	(9/42)
	V-H-C (P)	mean	-	-	-	5.6	-	-	18.5
		95% CI				(0-14.4)			(9.1-28.7)
FLK Zinj		percent	16.3	18.6	10	12.1		28.3	14
		nm/total	(26/160)	(26/140)	(5/50)	(54/446)		(17/60)	(71/506)
DS a		percent	1.8	6.1	3.3	3.2		4.9	3.7
		nm/total	(1/55)	(3/49)	(1/30)	(3/93)		(2/41)	(5/134)
DS b		percent	0.9	7.5	4.2	3.8		4.8	4
		nm/total	(1/107)	(7/93)	(2/48)	(7/185)		(3/63)	(10/248)
DS c		percent	0.8	3.5	1.9	2		2.5	2.1
		nm/total	(2/256)	(9/255)	(2/103)	(9/456)		(4/158)	(13/614)

ondary access experiments such as those simulated by Gidna *et al.* (2014), Organista *et al.* (2016) and Domínguez-Rodrigo *et al.* (2007b), in whose experiments felids were involved as primary flesh consumers. These carnivores leave significantly fewer tooth marks on bones than do hyenas. Their values are in some cases similar, and even lower, than those reported for human primary access models (with carcasses scavenged post-depositionally almost exclusively

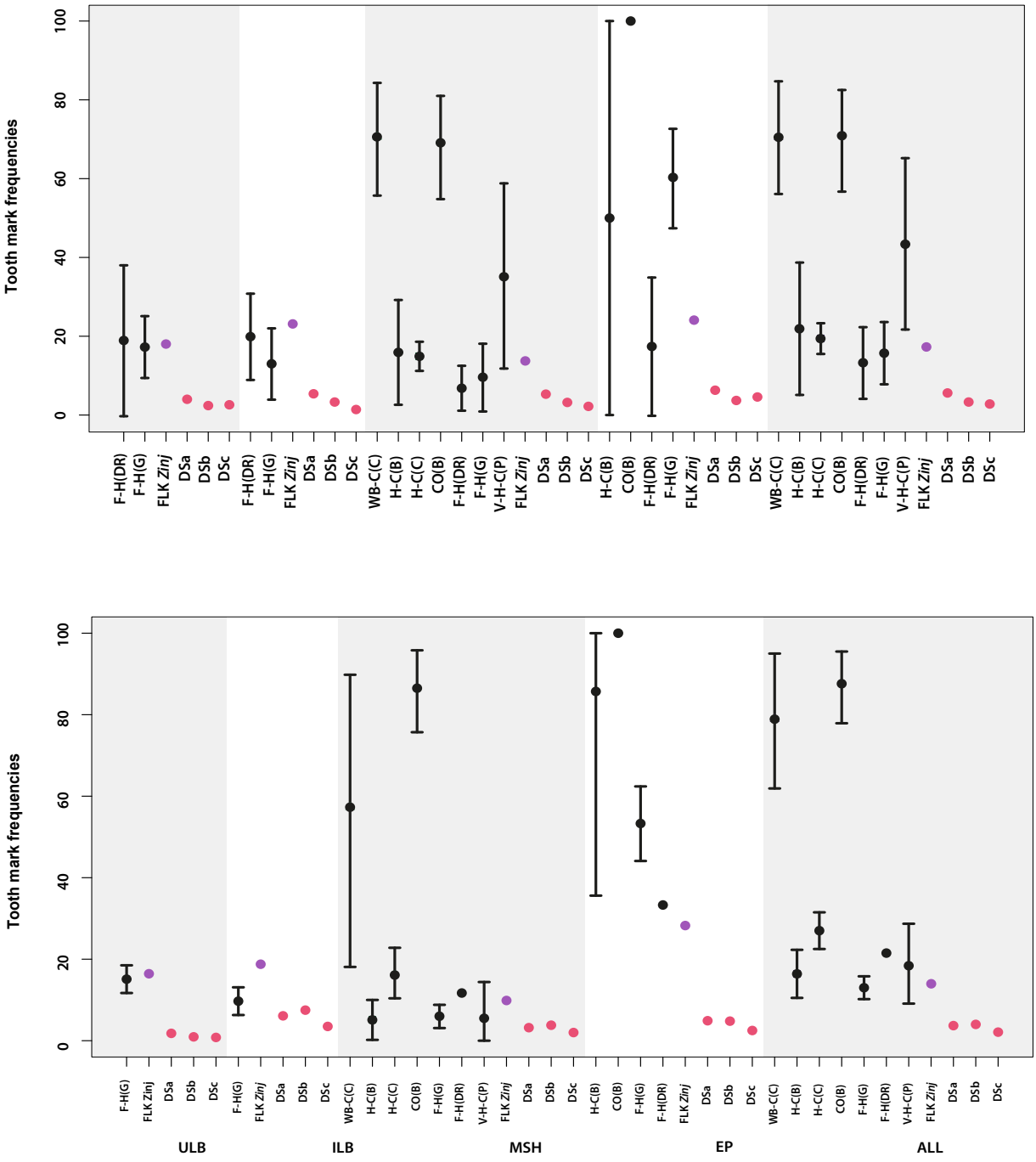

FIGURE 3.35. *Distribution of the 95% confidence intervals for the frequency of percussion-marked specimens per NISP for each bone portion from a) small and b) medium-sized carcasses in experimental assemblages and at FLK Zinj and DS.*

by hyenas). The DS assemblages yielded the lowest tooth mark percentages in all bone portions, and fall in the lower range of the H-C and F-H models for mid-shafts, ends and all NISP (Figure 3.35A). The tooth mark values for FLK *Zinj*, which are higher than those of DS, show a similar distribution. Higher percentages of tooth marked specimens appear on ends when a felid-hominin scenario is modeled, but not on mid-shafts. These bone portions are characterized by low percentages in both types of experiments. Thus, these two models cannot be differentiated by using bone portions alone. This is why the distribution of tooth marks per anatomical section is also of utmost importance. In this case, the data for the small carcass sample of DS shows low values of tooth marking in ULB, only reproduced in the H-C model.

Carcass size 3-4

Very similar results are obtained when considering medium-sized carcasses. DS yields the lowest percentages of tooth marks of all the reference sample (Table 3.41, Figure 3.35B). Frequencies for DS are very similar in all bone portions, even in long bone ends, which are characterized by bearing the highest percentages of these marks in all experimental models. FLK *Zinj* values are within the 95% confidence intervals of both primary (H-C) and secondary models (F-H), which are not statistically distinguishable, as indicated above, when using only long bone portions. However, the very low occurrence of tooth marks on upper limb bones is suggestive of access to carcasses as modelled by H-C models and not F-H models (Organista *et al.*, 2016).

The overall low frequency of tooth marks in the DS faunal assemblage may be a reflection of the overall low carnivore impact in the assemblage perceived by the analysis of skeletal part profiles. The high survival of axial elements (namely, ribs) in this assemblage, as well as pelvic and scapular fragments is rather suggestive of very limited access to these resources by scavenging hominins. As a matter of fact, scapulae very often appear not only in high numbers but also complete, without any of the typical carnivore modifications affecting the scapular blade. Ribs are also unfragmented in large parts of their section, thus, further suggesting that durophagous carnivore access to the assemblage was limited. If carnivores played a minimal part in the post-depositional modification of the DS bones, it is, thus, not unexpected that the tooth marks frequencies are substantially lower than reported for experiments in which carnivores are more actively involved in bone modification. Additionally, the high frequency of biochemical marks in the DS assemblage may have obscured some of the original tooth marks. However, this should not affect the well-preserved subsample, which displays also a very low tooth mark incidence (Figures 3.36; 3.37; 3.41).

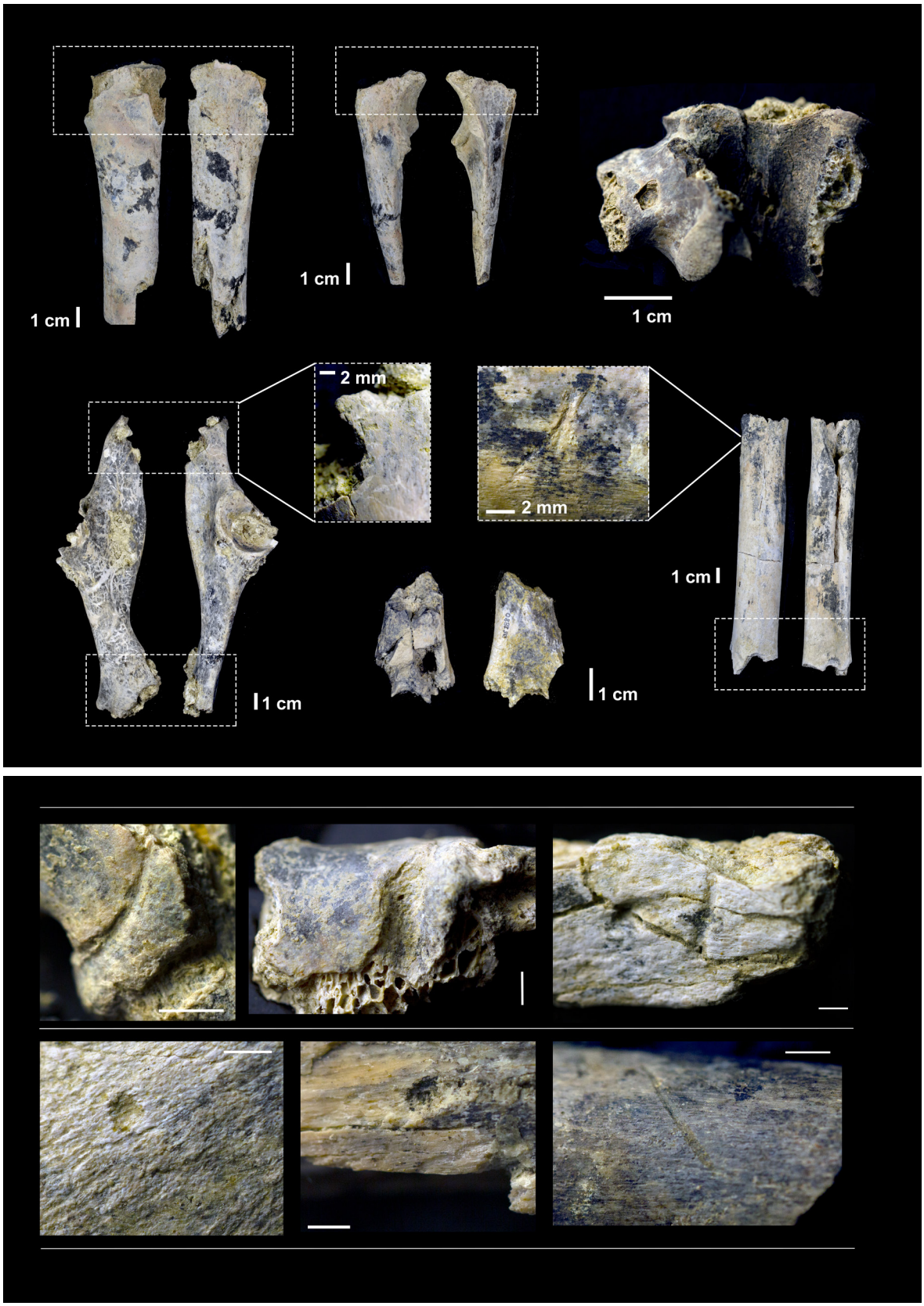

FIGURE 3.36. *Several examples of the documented tooth marked specimens on the DS bone sample.*

In the present analysis, it can be concluded that BSM indicate that hominins had primary access to carcasses (especially from medium-sized animals) as supported by cut marks and tooth marks. Bones were almost exclusively broken by hominins also, as demonstrated by percussion mark frequencies and distribution.

However, very commonly, the independent use of BSM variables does not produce the degree of coincidence displayed in the present study. For this reason, it has been argued that only a conjoint use of all BSM variables using multivariate methods can more efficiently capture the emergent properties of all the information combined (Domínguez-Rodrigo *et al.*, 2014). It has also been argued that independent use of BSM variables is frequently used to support biased interpretations of archaeological assemblages (Domínguez-Rodrigo *et al.*, 2014). In the following section, a multivariate approach is used in order to analyze all mark types simultaneously in order to overcome this problem.

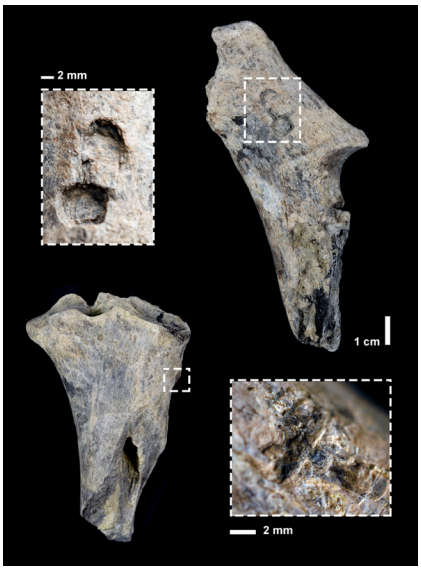

Figure 3.37. *Refitting radius and ulna specimens. The ulna bears large (felid-like) tooth pits, the radius presents hammerstone-inflicted percussion damage.*

3.4.4. Multivariate analysis of BSM

The MDA correctly classified 91.9% of the experimental sample. The first two factors explained 92% of the sample. The first factor explained 78% of the variance alone and was determined mainly by the variables cut mark frequencies on shafts and cut mark frequencies on all bone portions (Table 3.42). These two variables also have more discriminant power in factor 2 than do tooth marks and percussion marks, which are clearly less discriminatory. However, these variables explain most of the third function. When the third factor is

Table 3.42. *Discriminant coefficient scores for the first three functions of the MXDA test.*

	Function 1	Function 2	Function 3
Total CM	0.037373360	0.0243881326	0.028237409
CM shafts	0.020723473	0.0507520323	0.001495505
PM shafts	0.002731512	0.0009340008	0.072427193
Total TM	0.011428745	0.0058899413	0.012719631
TM shafts	0.002328794	0.0022947592	0.012956717

Table 3.43. *Predictions of the model. Classification of DS samples in the three experimental models.*

	H-C	F-H	F-H-H
DSa	0.9988483697	4.177981e-05	0.001109851
DSb	0.9568070866	1.516845e-05	0.028024462
DSc	0.0008254285	6.590731e-05	0.340101439

added, the model explains 98.2% of the sample variance.

The well-preserved DS assemblage appears classified within the 95% confidence alpha bag of the H-C model, therefore suggesting primary access to carcasses by hominins (Figure 3.38). When dry-broken and badly preserved specimens are included in the DS sample (DSb and DSc), a different result is obtained: both samples fall outside the 95% confidence alpha bags of all three experimental scenarios. However, DSb is classified by the MXDA also as primary access with a probability of 96%, and DSc is classified with the F-H experiments (Table 3.43). Similarities between DSa and FLK *Zinj*, which also appears within the primary access 95% confidence alpha bag, as was reported by Domínguez-Rodrigo *et al.* (2014), are mainly due to the percentages of cut-marked and percussion-marked specimens. The distance between them comes as a result of the differences in tooth mark frequencies, which are very low at DS. As is the case for FLK *Zinj*, DSa is placed towards the right elongation of the H-C alpha bag, which includes experiments reproducing bulk flesh removal, which leaves fewer marks than intensive butchery of even small flesh scraps (left side of the H-C alpha bag) (Domínguez-Rodrigo *et al.*, 2014). The larger size of the alpha bags of the H-C and the F-H-H models when compared to that of the F-H model are accounted for by a higher variability in the methodologies of the experimental studies (e.g. the F-H-H model also included a partially fleshed carcass [Domínguez-Rodrigo, 1997a; Domínguez-Rodrigo *et al.*, 2014]).

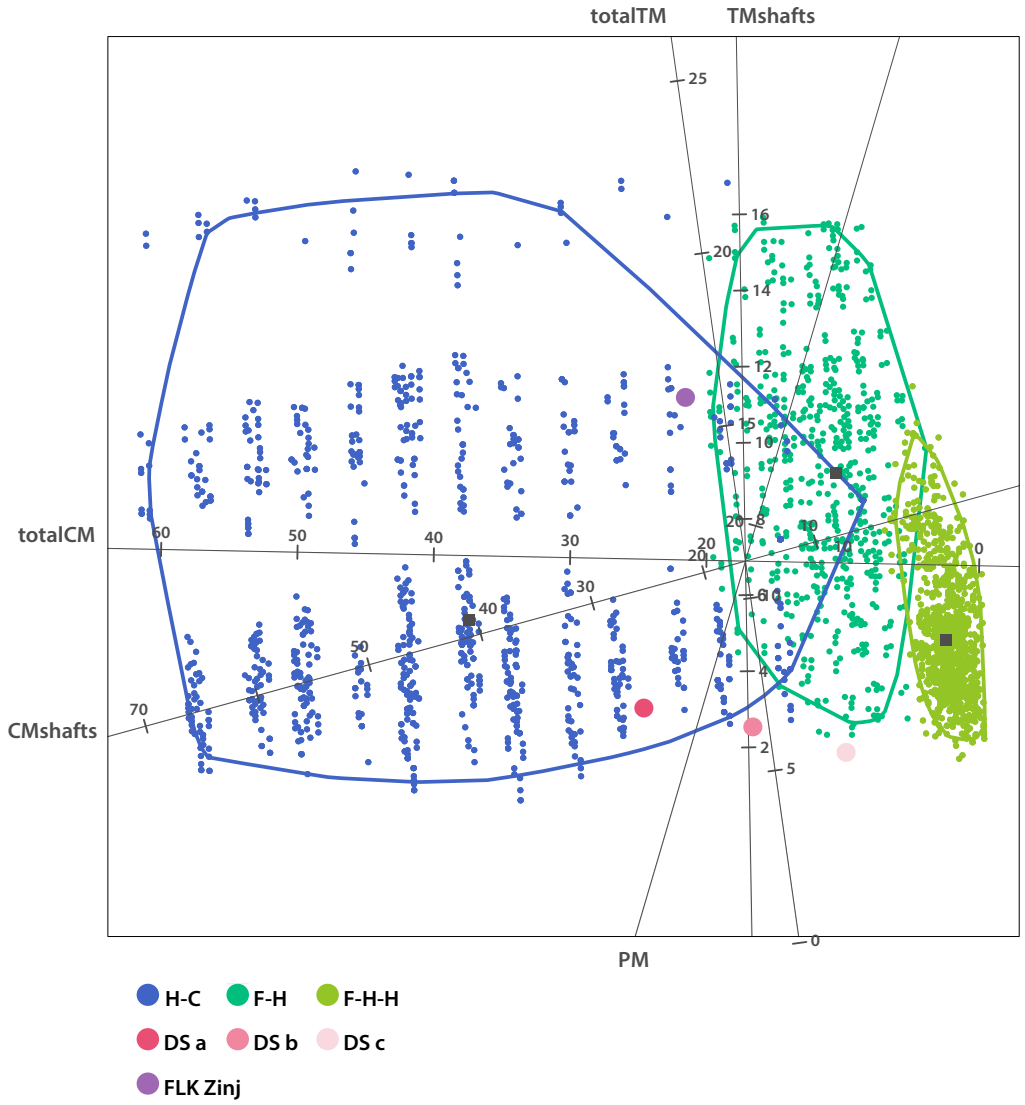

FIGURE 3.38. *Multiple discriminant analysis using a canonical variate approach on a bootstrapped sample of the experimental assemblages of the H-C (color alpha bag), F-H (color alpha bag), and F-H-H (color alpha bag) models. Data from Domínguez-Rodrigo et al. (2014a).*

3.4.5. Machine learning analysis of BSM

Table 3.44 shows the accuracy of correct classification of the machine learning algorithms (SVM, *K*-NN, RF, MXDA, NB, PLS, and NN), as well as their classifications of the FLK *Zinj* and DS assemblages (a, b and c) into primary or secondary access, based on the percentages of bone surface modifications on

different anatomical sections and bone portions of long bones. All methods yielded 100% accuracy. FLK *Zinj* was classified by all algorithms as primary access. The DSa and DSb assemblages were classified as hominin-made (i.e., primary access) almost by all algorithms, the only exception being *K*-NN, which is the least robust method. The RF and the NB algorithms yielded different results for DSc than for the other assemblages, and classified this sample in secondary access. Classification probabilities were nearly always higher than 95% (Table 3.44). If we consider the algorithms jointly, DSa and DSb are classified as primary access 86% of the times, and DSc is classified as primary access more than 70% of the times. Therefore, based on bone surface modifications alone, both FLK *Zinj* and DS can confidently be identified as sites created by hominins in which primary access to carcasses explains most variance.

Table 3.44. *Accuracy percentages of correct classification of each statistical algorithm and classification of FLK Zinj and DS*

Method	Accuracy	DS a	DS b	DS c	FLK Zinj
Support Vector Machine (SVM)	100	primary (NA)	primary (NA)	primary (NA)	primary (NA)
K Nearest Neighbor (KNN)	100	secondary (1)	secondary (1)	primary (1)	primary (1)
Random Forest (RF)	100	primary (0.684)	primary (0.580)	secondary (0.730)	primary (0.640)
Mixture Discriminant Analysis (MXDA)	100	primary (1)	primary (1)	primary (1)	primary (1)
Naive Bayes	100	primary (1)	primary (1)	secondary (0.99)	primary (1)
Partial Least Square (PLS)	100	primary (0.995)	primary (0.981)	primary (0.999)	primary (0.998)
Neural Net (NN)	100	primary (0.997)	primary (0.996)	primary (0.997)	primary (0.999)

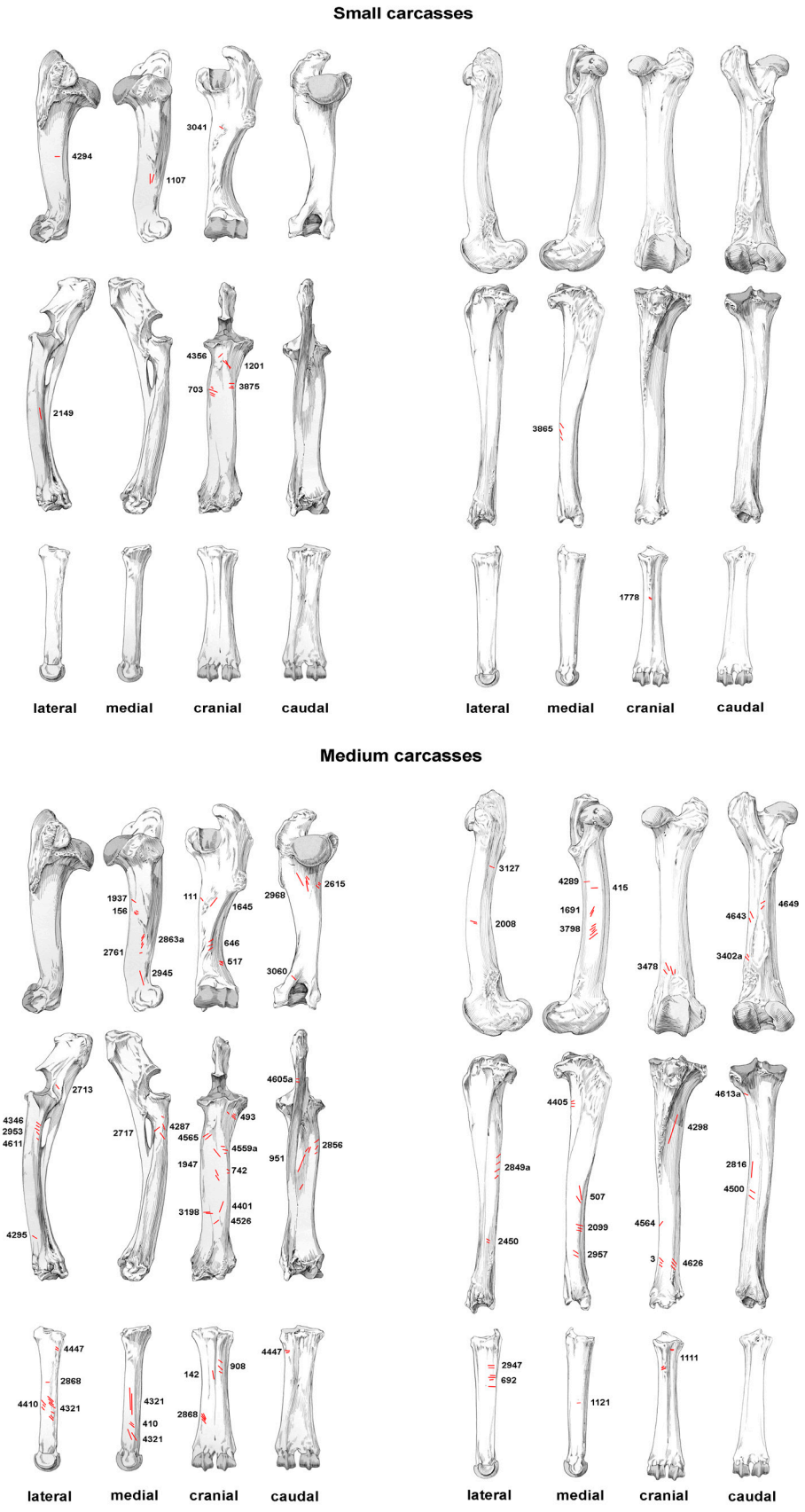

FIGURE 3.39. *Exact location of cut marks in each long bone in small carcasses and in medium-sized carcasses from DS.*

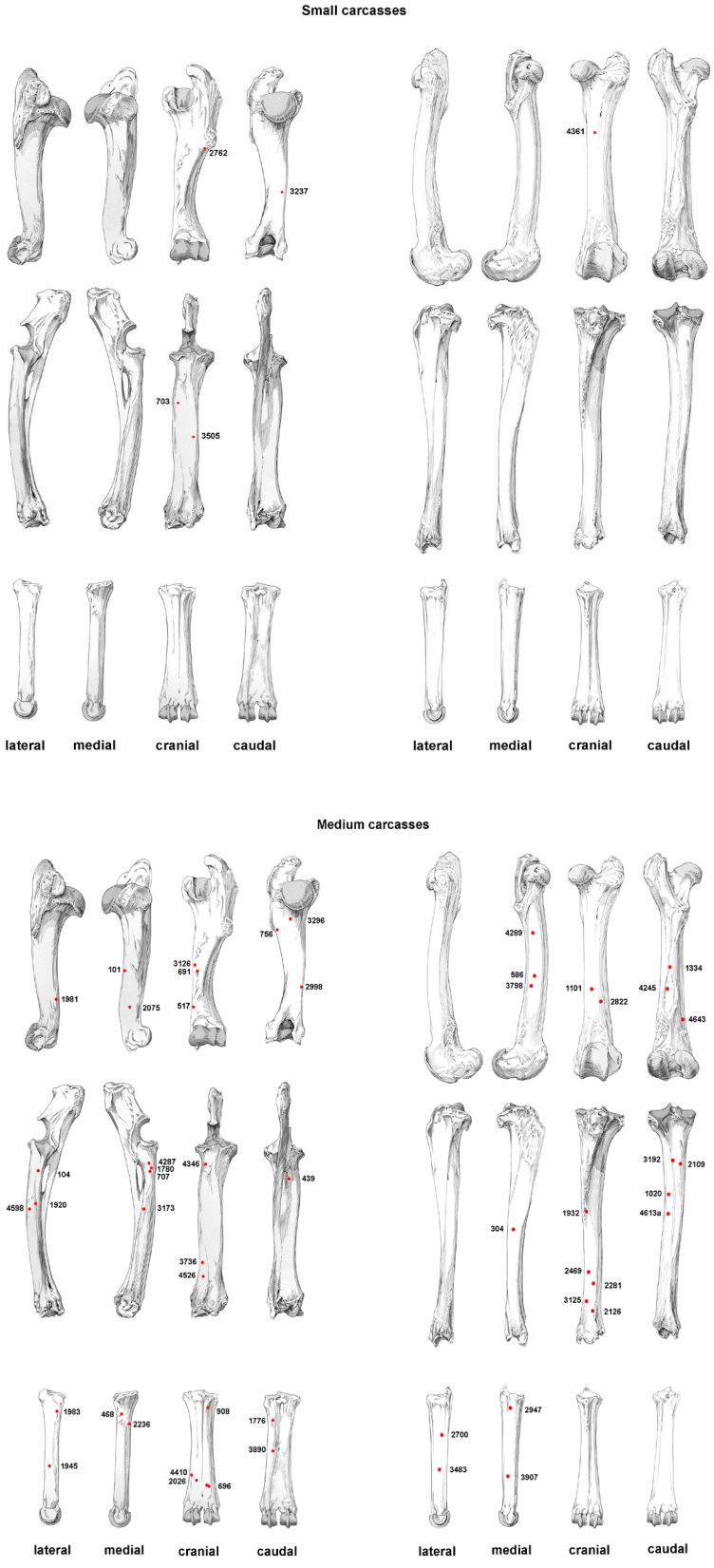

FIGURE 3.40. *Exact location of percussion marks in each long bone in small carcasses and in medium-sized carcasses from DS.*

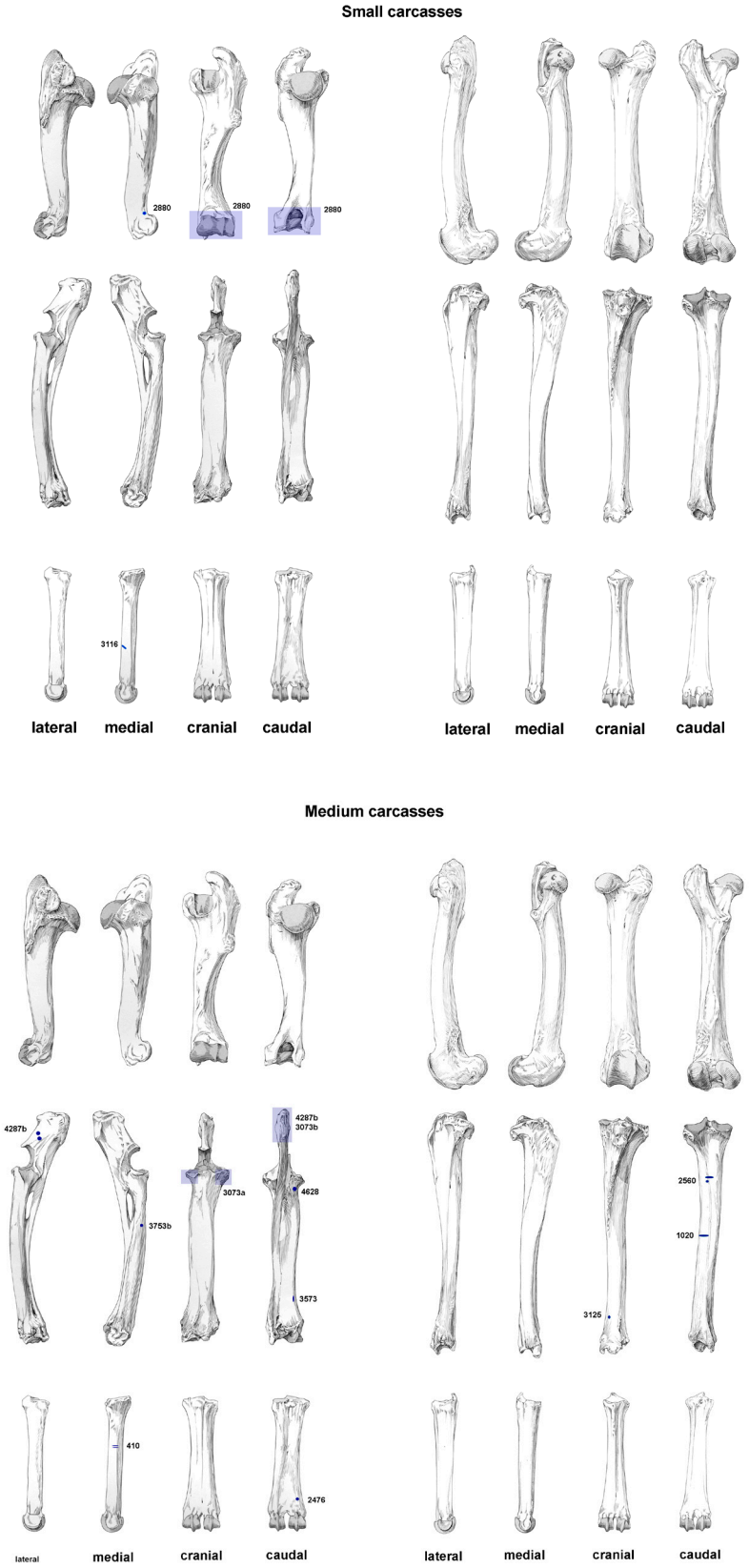

FIGURE 3.41. *Exact location of cut marks in each long bone in small carcasses and in medium-sized carcasses from DS.*

3.4.6. Analysis of the anatomical distribution of BSM on long limb bones using the Hot Zone approach

Table 3.45 shows the percentages of cut marks on hot and cold zones at DS for small and medium-sized carcasses as compared to FLK *Zinj*. Figure 3.39 shows the exact location of cut marks on long bones of small and medium-sized carcasses. For small carcasses, cut marks on humeri are as frequent in hot zones as in cold zones, and cut marks on radii appear on hot zones 80% of the times. The single cut marks that were observed on femora and tibiae appear on hot zones. The number of cut marks in the subsample of small carcasses is relatively low, and decreases when only those marks that can be clearly located in a specific bone section are considered. Therefore, a closer look is taken only at the subsample of cut-marked specimens of medium-sized carcasses.

The bar chart on Figure 3.42 provides the comparison of the distribution of cut marks on hot and cold zones at DS and FLK *Zinj* for carcasses of size 3-4. In this sample, cut marks from DS on the humerus are also similarly represented in both zones, which means they occur more frequently in the hot zones than in experimental assemblages. Cut marks are found mainly on the cranial, caudal, and medial aspects of humeri, but they also appear on the ends, maybe reflecting disarticulation (Nilssen 2000). As is the case at FLK *Zinj*, most of the marks observed on the radius cluster in hot zone 2 (cranial side), which is a very clear sign of filleting as observed in the experimental sample. Some evidence of disarticulation could also be reflected in the presence of cut marks on the caudal aspect of the olecranon of the ulna. Furthermore, nine out of ten cut marks on femora appear on hot zones at DS, clearly indicating filleting, and tibiae are also characterized by a clearly higher frequency of cut marks in the hot zones at both DS and FLK *Zinj* (Figure 3.42). This is especially revealing, because hind limbs have been observed to be defleshed by lions and leopards immediately after prey capture and evisceration (Blumenschine, 1986; Domínguez-Rodrigo *et al.*, 2007). The systematic presence of cut marks on hot zones at DS indicates that hominins were accessing carcasses before carnivores, as cut marks should never be found in hot zones after carnivore defleshing, especially with this proportion. Furthermore, chi-square and Fisher's Exact tests performed on the sample of medium-sized carcasses to find out whether DS differs significantly in the distribution of cut mark frequencies per element from FLK *Zinj* and the experiments modeling primary access yielded non-significant results (Table 3.46). Thus, based on the application of the Hot Zone approach to the DS assemblage, it seems clear that hominins were removing complete muscles from the bones, rather than flesh scraps.

Table 3.45. *Distribution of cut marks per hot and cold zone in small and medium carcasses at DS, FLK Zinj, and experiments modeling primary access to carcasses by hominins. Data for FLK Zinj and experiments from Domínguez-Rodrigo et al. 2007.*

DS	Hot zone	Cold zone	Hot zone	Cold zone
	Small		Medium	
Zone 1	2/4 (50)	2/4 (50)	5/10 (50)	5/10 (50)
Zone 2/3	4/5 (80)	1/5 (20)	13/16 (81.3)	3/16 (18.7)
Zone 4	1/1 (100)	0/1 (0)	9/10 (90)	1/10 (10)
Zone 5/6	1/1 (100)	0/1 (0)	8/13 (61.5)	5/13 (38.5)

FLK Zinj	Small		Medium	
Zone 1	4/7 (57.1)	3/7 (42.9)	6/18 (33.3)	12/18 (66.7)
Zone 2/3	4/5 (80)	1/5 (20)	14/17 (82.4)	3/17 (17.6)
Zone 4	1/3 (33.3)	2/3 (66.7)	5/8 (62.5)	3/8 (37.5)
Zone 5/6	2/9 (22.2)	7/9 (77.8)	10/15 (66.7)	5/15 (33.3)

Experiments	Small		Medium	
Zone 1	11/40 (30)	29/40 (70)	16/58 (27.6)	42/58 (72.4)
Zone 2/3	14/20 (70)	6/20 (30)	25/31 (80.6)	6/31 (19.4)
Zone 4	12/24 (50)	12/24 (50)	13/21 (61.9)	8/21 (38.1)
Zone 5/6	16/40 (65)	14/40 (35)	12/26 (46.2)	14/26 (53.8)

Table 3.46. *Non-significant results of chi-square and Fisher's Exact tests carried out to test whether cut mark distribution on hot and cold zones per element are significantly different when comparing DS and FLK Zinj, and DS to the H-C experiments.*

Chi-square tests	Fisher's Exact tests		
	DS - FLK Zinj		
	X2	p-value	p-value
Humerus	0.21295	0.6445	0.4443
Radius-Ulna	1.1698e-31	1	1
Femur	0.67902	0.4099	0.2745
Tibia	1.762e-31	1	1

	DS - Experiments		
	X2	p-value	p-value
Humerus	1.3722	0.2414	0.1449
Radius-Ulna	6.3429e-31	1	1
Femur	1.2395	0.2656	0.21
Tibia	0.32072	0.5712	0.5006

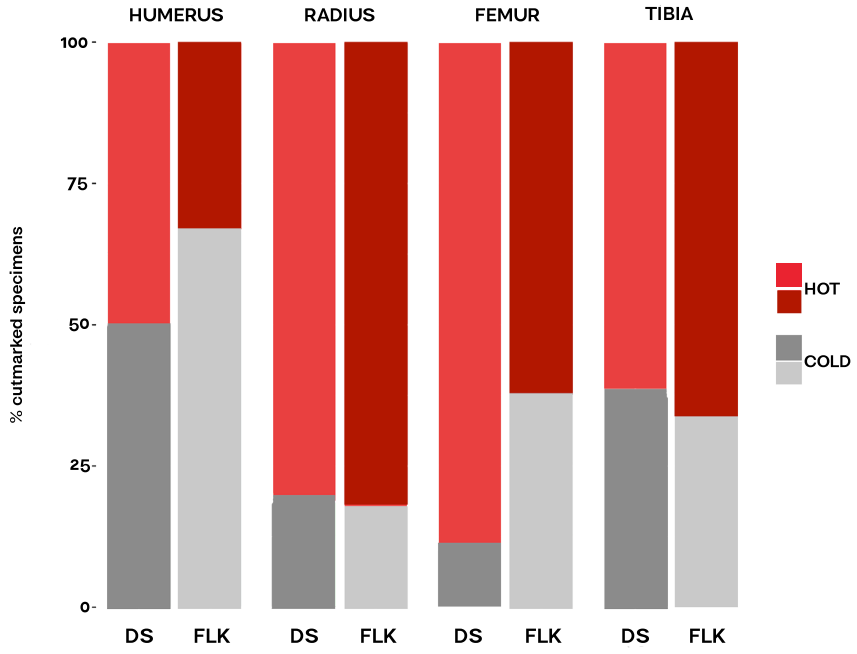

FIGURE 3.42. *Bar chart comparing the distribution of cut marks on hot and cold zones in each long bone of the medium-sized carcasses at DS and FLK Zinj.*

3.4.7. Taphotypes

3.4.7.1. Classification System I

The results of the bootstrapped correspondence analyses of the taphotypes for each long bone element using the first classification system all explain between 50% and 60% of inertia. Figures 3.43 - 3.46 show the obtained correspondence diagrams when considering the taphotypes of the humerus, the femur, the radius and the ulna, and the tibia separately. The DS sample falls inside the confidence ellipse of the anthropogenic assemblage in all the diagrams except in the case of the tibia, where it overlaps with the samples that

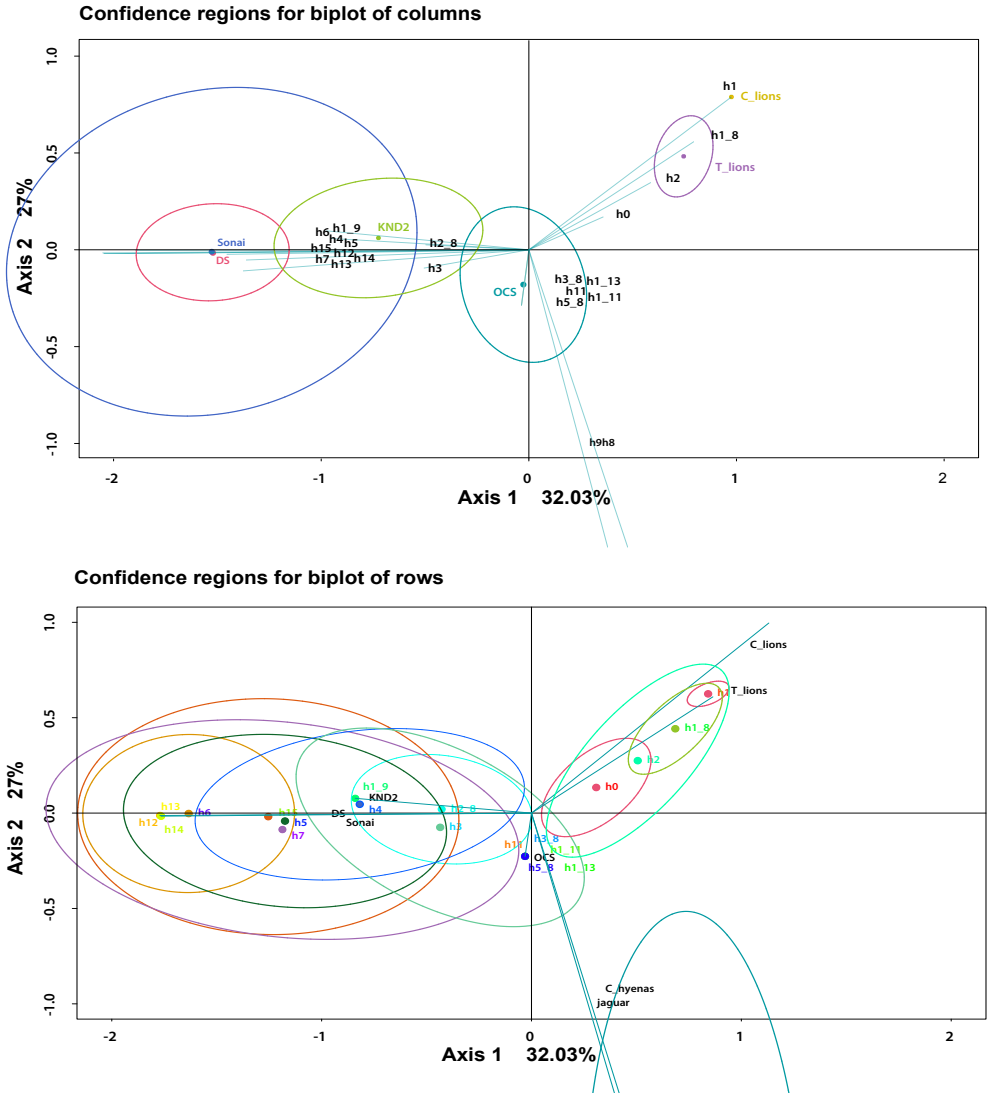

FIGURE 3.43. *Biplots of the bootstrapped CA showing the relationship between the referential carnivore and anthropic humerus CSI taphotypes and the humerus CSI taphotypes documented at DS. Reference data from Domínguez-Rodrigo et al. 2015. Ellipses with 95% confidence intervals are displayed. The length of the axes shows the importance of the contribution of each variable to the inertia.*

were modified by hyenas. This indicates that most epiphyseal fragments were probably created by hominins (Figure 3.50), while a small proportion, mostly composed of tibiae were maybe broken by hyenas. There is a clear separation in all diagrams between the anthropogenic sample, Sonai, the samples modified by felids (Tarangire lions, captive lions, jaguars, and the OCS sample), and the ones in which hyenas were involved.

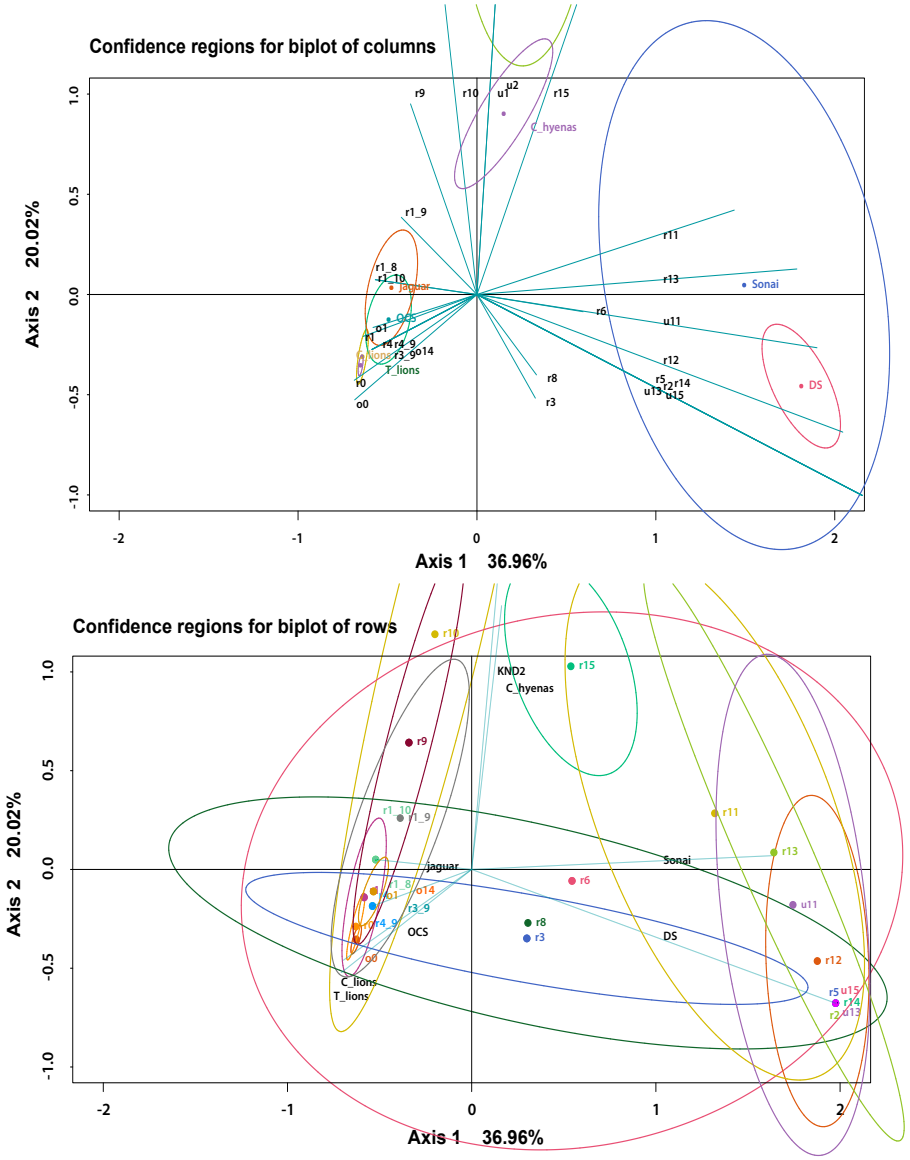

FIGURE 3.44. *Biplots of the bootstrapped CA showing the relationship between the referential carnivore and anthropic radius-ulna CSI taphotypes and the radius-ulna CSI taphotypes documented at DS.*

3.4.7.2. Classification System II

The bootstrapped correspondence analyses using the second classification system and the new categories yielded correspondence diagrams that explain between 50-70% of inertia. Figures 3.47-3.49 present the correspondence diagrams for upper limb bones, intermediate long bones, and the complete assemblage. The bone damage pattern documented at DS again consistently overlaps with the pattern of the Sonai sample, which indicates that DS is of anthropo-

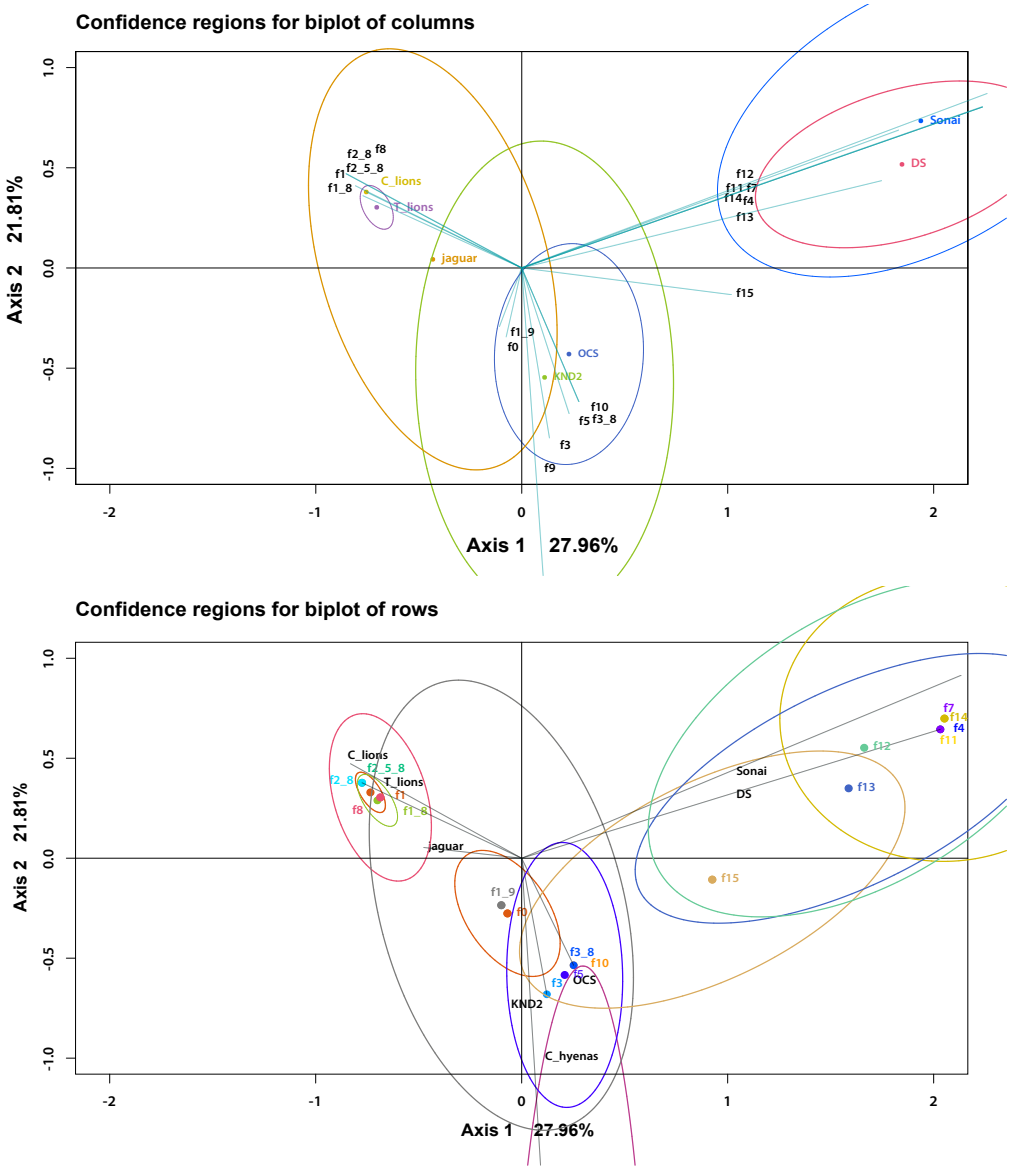

FIGURE 3.45. *Biplots of the bootstrapped CA showing the relationship between the referential carnivore and anthropic femur CSI taphotypes and the femur CSI taphotypes documented at DS.*

genic origin. Intermediate long limb bones also show some overlap with the spotted hyena den KND2, which means that DS was affected by hyena ravaging to some degree. This overlap also occurs when all long limb bones are considered together. Importantly, no overlap occurs between the DS sample and the samples modified by felids, which rules out that felids could have accumulated or modified carcasses at DS, and even that hominins might have confronted felids in order to steal their prey. As was the case when using the first classification system, this second approach also discriminates between samples mod-

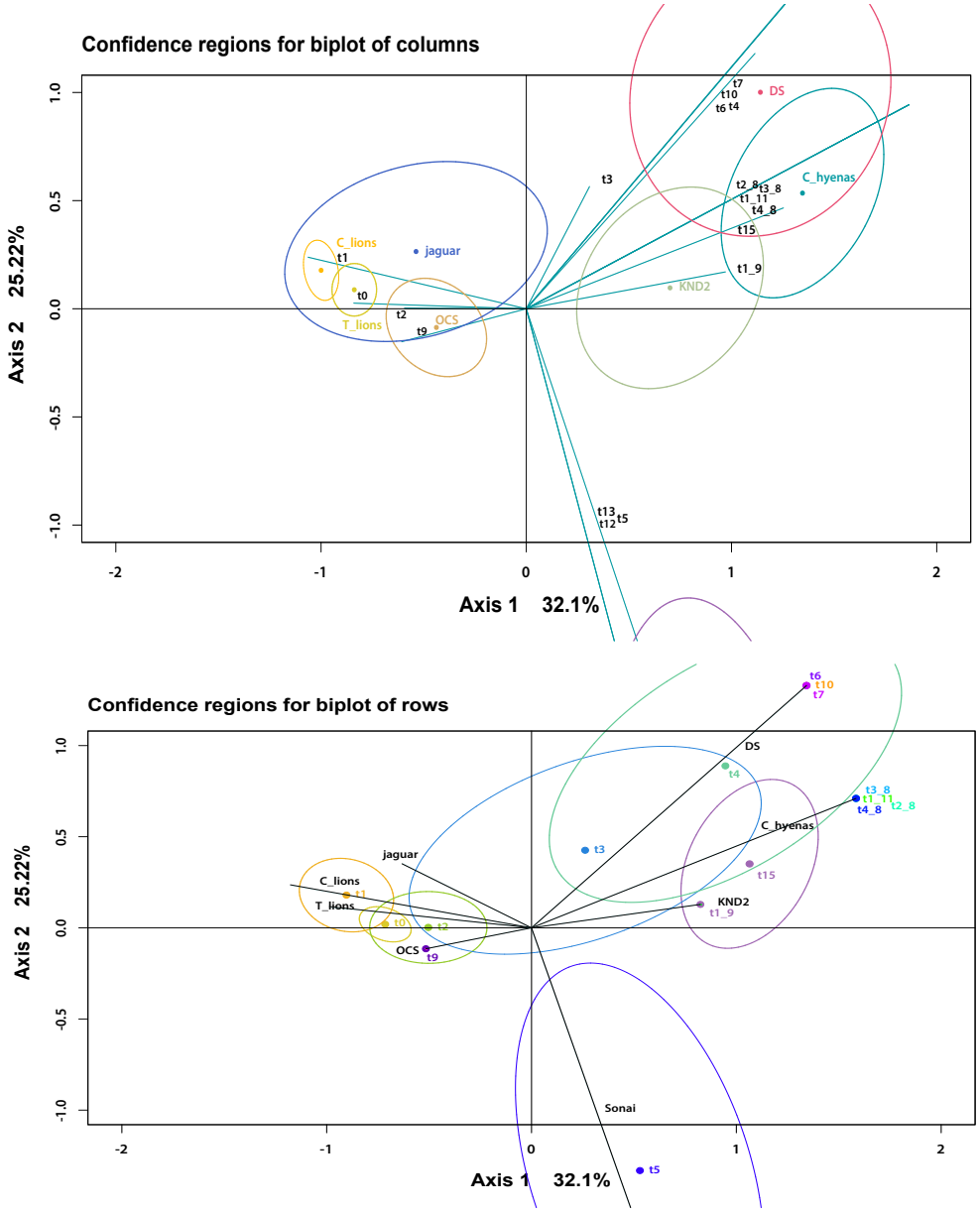

FIGURE 3.46. *Biplots of the bootstrapped CA showing the relationship between the referential carnivore and anthropic tibia CSI taphotypes and the tibia CSI taphotypes documented at DS.*

ified by felids, hyenas and humans, which renders the taphotype approach a very useful method that can be applied objectively and automatically to any assemblage in which taphonomic agency is unclear.

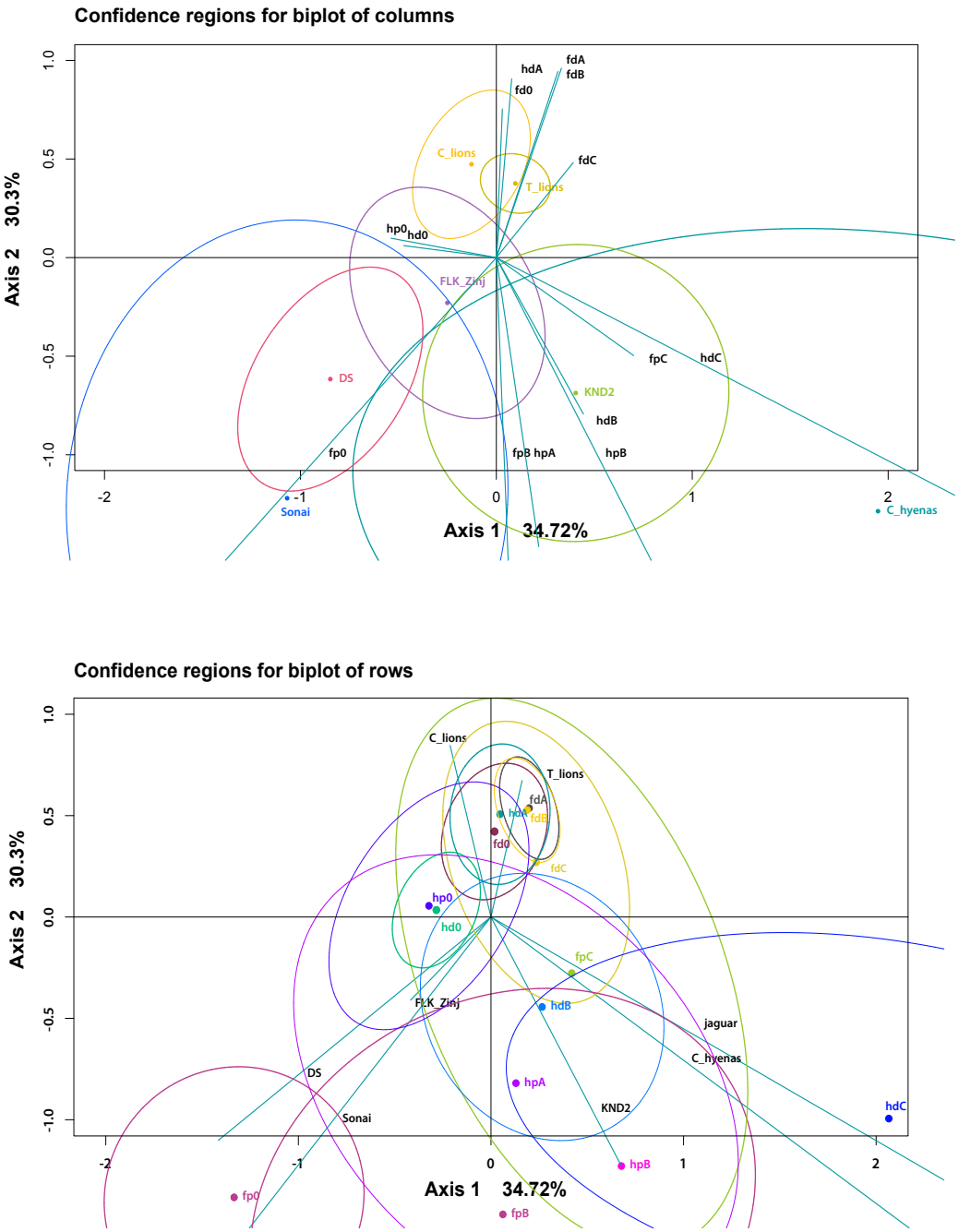

FIGURE 3.47. *Biplots of the bootstrapped CA showing the relationship between the referential carnivore and anthropic simplified ULB CSII taphotypes and the ULB CSII taphotypes documented at DS.*

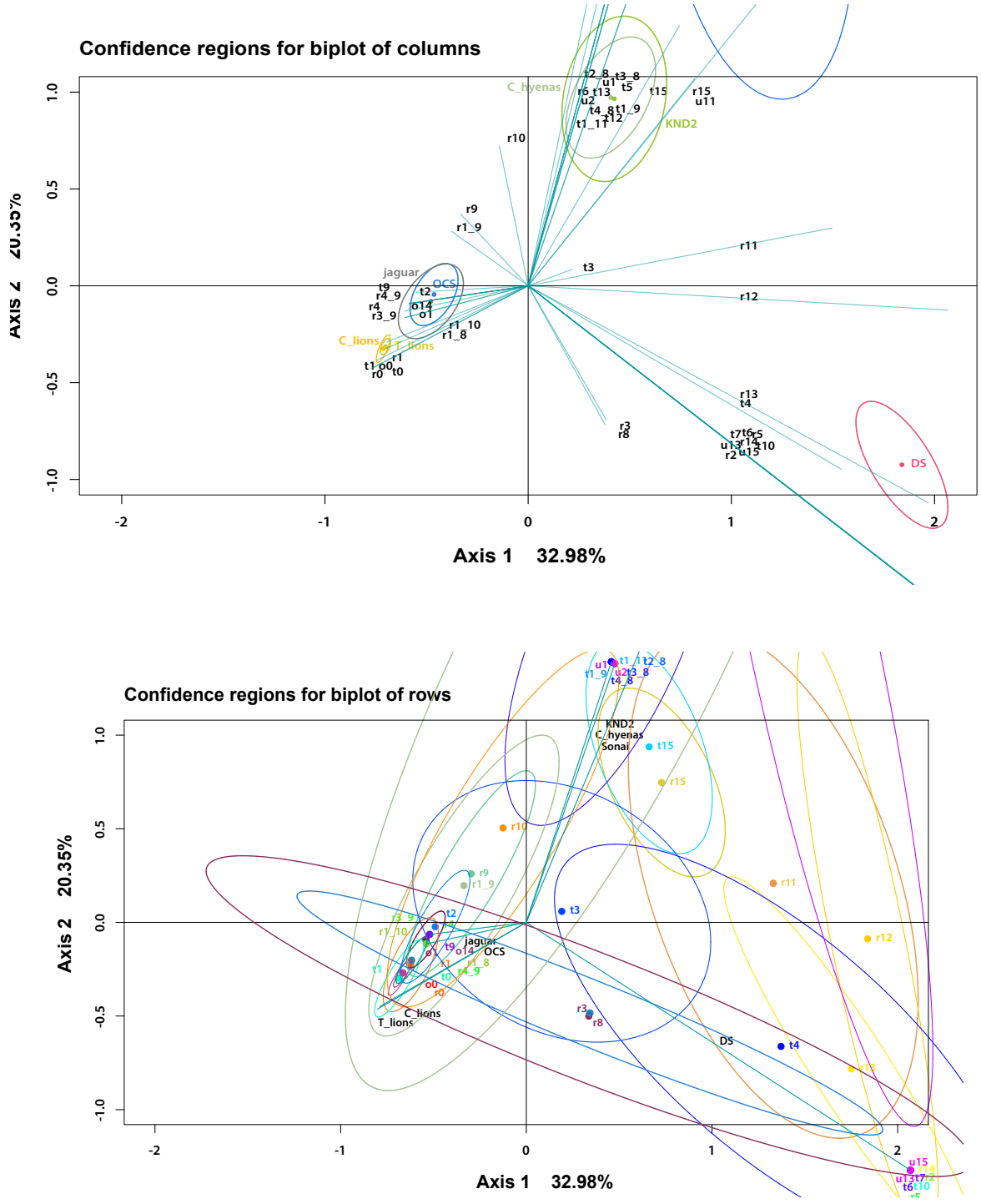

FIGURE 3.48. *Biplots of the bootstrapped CA showing the relationship between the referential carnivore and anthropic simplified ILB CSII taphotypes and the ILB CSII taphotypes documented at DS.*

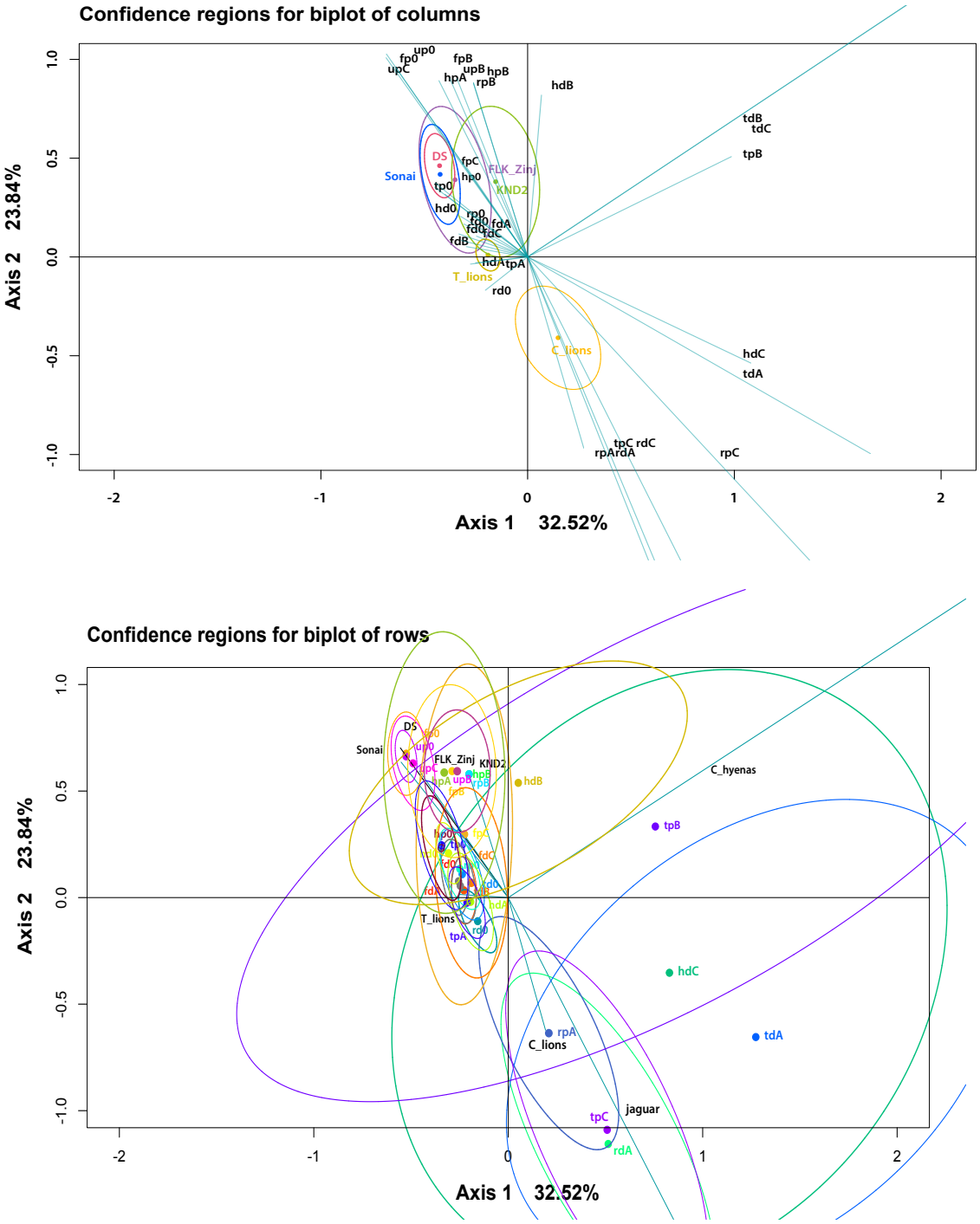

FIGURE 3.49. *Biplots of the bootstrapped CA showing the relationship between the referential carnivore and anthropic simplified CSII taphotypes and the CSII taphotypes documented at DS, considering all long bones.*

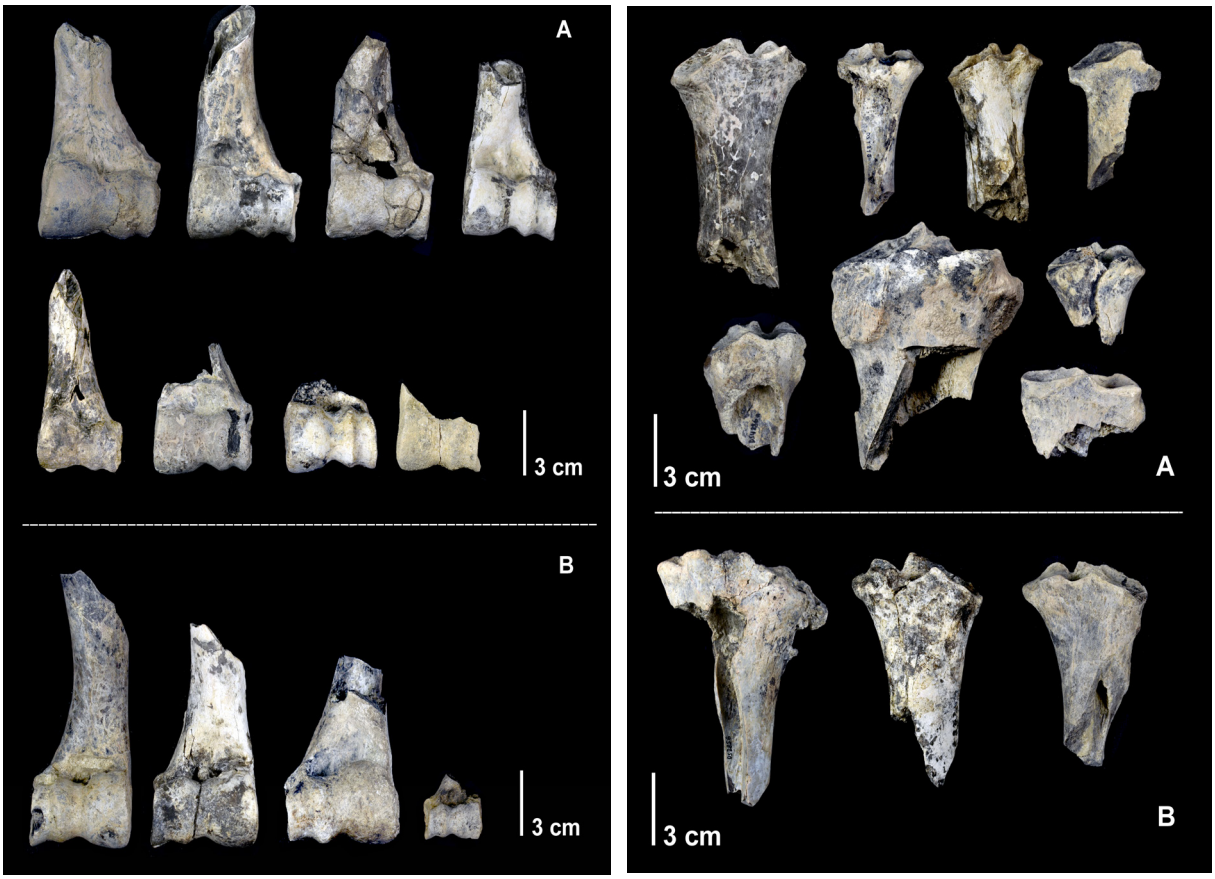

FIGURE 3.50. *Examples of the documented taphotypes of the most abundant epiphyses: distal humeri and proximal radii. A) Left specimens, B) Right specimens.*

3.5 Mortality profiles

3.5.1. Estimation of age at death of the sample of ungulates at DS

The eruption and attrition scores of the dental specimens preserved at DS are shown in Table 3.47, along with an approximate estimate of the individual's age in years. Most recovered bovid dental remains belong to Reduncini, more specifically to waterbuck (*Kobus sigmoidalis),* which is represented by at least eleven individuals with ages that range from less than a year to more than ten years. The tribe Alcelaphini is also abundant, and represented by at least four wildebeest (*Connochaetes sp.)*, four *Parmularius altidens*, and two *Megalotragus sp*. The ages for *Parmularius altidens* range between 0.5 years and 6 years; and although the ages of the remaining Alcelaphini could not be estimated as accurately as for *Parmularius*, they could all still be classified confidently as adults. The kudus (*Tragelaphus*) are represented by a subadult and an adult individual. A nearly complete skull with horns was found at DS in 2015, but it was embedded in carbonate, which would need to be removed in order to establish its age accurately. From the parts that were visible, we could determine that it belonged to an adult. The ages of *Antidorcas* range from less than a year to five years. In addition, visual assessment of the wear pattern on several incisors and back teeth, enabled classifying a minimum of three equid individuals as prime adults. Based on the presence of a completely erupted third molar, one of them was at least five years old. Among the appendicular elements we also found a juvenile equid, which means that the minimum number of equid carcasses adds up to four. The total minimum number of bovids is **28.** Figures 3.51 and 3.52 show some of the best preserved bovid maxillae and mandibles.

3.5.2. Grouping of prey into age classes

The mortality profile data from DS is shown in Tables 3.48A, B, and C. When considering small and medium-sized carcasses together, most bovids are prime adults (57%), followed by juveniles (36%), and only 7% fall into the category

Table 3.47. *Eruption/attrition scores of dental specimens from DS. Table follows the structure of Bunn and Pickering (2010b, table 1). Apart from mandibular and maxillary fragments, several single teeth are included, for which an approximate age could be determined. Each specimen does not represent a separate individual, MNIs are provided in Table 2. Each preserved tooth was given a score using the following code: - = a shed dp4 or permanent tooth not yet fully erupted; m = tooth missing as a result of poor preservation, not necessarily from lack of its development or eruption; w = occlusal wear of varying degrees but no loss of infundibula; ++ = loss of mesial and distal infundibula for permanent molars (Bunn and Pickering 2010b). A cumulative age was then assigned to the complete specimen as in Bunn and Pickering (2010b) following the age determination methods by Spinage (1967; 1976) for waterbuck and gazelle, and Attwell (1980) and Talbot and Talbot (1963) for wildebeest.*

Catalog	Taxon	Maxilla/ Mandible	Isolated tooth	Side	dP4	P4	M1	M2	M3	Age (years)
2428	Reduncini (*Kobus*)	Mandible	No	R	-		-			0 – 0.5
831	Reduncini (*Kobus*)	Maxilla	No	R		w	w	-		1
1760	Reduncini (*Kobus*)	Maxilla	Yes	R				w		4 – 10
3849	Reduncini (*Kobus*)	Maxilla	Yes	L				++		>10
1704	Reduncini (*Kobus*)	Maxilla	Yes	L				-		1
2071	Reduncini (*Kobus*)	Maxilla	Yes	R				w		4 – 10
3168	Reduncini (*Kobus*)	Maxilla	No	R		m	m	w		4 – 10
3037	Reduncini (*Kobus*)	Mandible	No	R	w		-			<1
4629	Reduncini (*Kobus*)	Mandible	No	L	w		-			<1
4247	Reduncini (*Kobus*)	Mandible	No	L	w		w	-		~1
4716	Reduncini (*Kobus*)	Mandible	No	L	w	w	m			3
3133	Reduncini (*Kobus*)	**Mandible**	**No**	**L**	**w**		**w**	**w**	-	**3**
1953	Reduncini (*Kobus*)	**Mandible**	**No**	**L**	-	**w**	**w**	**w**	**w**	**3 – 4**
973	Reduncini (*Kobus*)	**Mandible**	**No**	**R**		**w**	**w**	**m**	**m**	**3 – 4**

2067	Reduncini (*Kobus*)	**Mandible**	**No**	**R**		**m**	**w**	**m**		**3**
3033	Reduncini (*Kobus*)	**Mandible**	**Yes**	**L**				**w**		**3**
3593	Reduncini (*Kobus*)	**Mandible**	**No**	**R**	**w**		**-**			**8 – 12**
782	**Antilopini (Antidorcas)**	**Maxilla**	**No**	**L**			**w**	**w**		**1.3 – 1.5**
3581	**Antilopini (Antidorcas)**	**Maxilla**	**No**	**L**			**m**	**w**		**5**
333	**Antilopini (Antidorcas)**	**Maxilla**	**No**	**R**			**m**	**w**	**m**	**1**
4360	**Antilopini (Antidorcas)**	**Maxilla**	**No**	**R**			**w**			**0.5**
814	**Antilopini (Antidorcas)**	**Maxilla**	**No**	**L**			**w**			**<1.5**
683	**Antilopini (Antidorcas)**	**Maxilla**	**No**	**L**			**w**	**w**	**-**	**1.5 – 2.5**
1461	**Alcelaphini (Parmularius)**	**Mandible**	**No**	**L**	**w**		**-**			**0.5**
2474	**Alcelaphini (Parmularius)**	**Mandible**	**No**	**R**	**w**		**-**			**0.5**
1047	**Alcelaphini (Parmularius)**	**Mandible**	**No**	**R**		**w**	**w**	**m**		**2 – 4**
4288	**Alcelaphini (Parmularius)**	**Mandible**	**No**	**R**	**w**		**-**			**0.5**
561	**Alcelaphini (Parmularius)**	**Mandible**	**Yes**	**R**					**w**	**3 – 4**
2218	**Alcelaphini (Parmularius)**	**Maxilla**	**No**	**R**		**m**	**w**	**w**		**3 – 6**
3382	**Alcelaphini (Connochaetes)**	**Mandible**	**Yes**	**R**				**w**		**6-Oct**
766	**Alcelaphini (Connochaetes)**	**Mandible**	**Yes**	**R**				**w**		**11 – 14**
286	**Alcelaphini (Connochaetes)**	**Mandible**	**Yes**	**R**					**w**	**3 – 15**

2545	**Alcelaphini (Connochaetes)**	**Mandible**	**Yes**	**L**			**w**			**3 – 6**
607	**Alcelaphini (Connochaetes)**	**Maxilla**	**Yes**	**L**				**w**		**3 – 11**
2541	**Alcelaphini (Connochaetes)**	**Maxilla**	**Yes**	**R**					**w -**	**3**
4546	**Alcelaphini (Megalotragus)**	**Mandible**	**Yes**	**R**				**w**	**w**	**4 – 14**
3859	**Alcelaphini (Megalotragus)**	**Mandible**	**No**	**R**		**m**	**w**	**w**	**w**	**4 – 14**
1187	Alcelaphini (*Megalotragus*)	Mandible	Yes	L					w	4 – 14

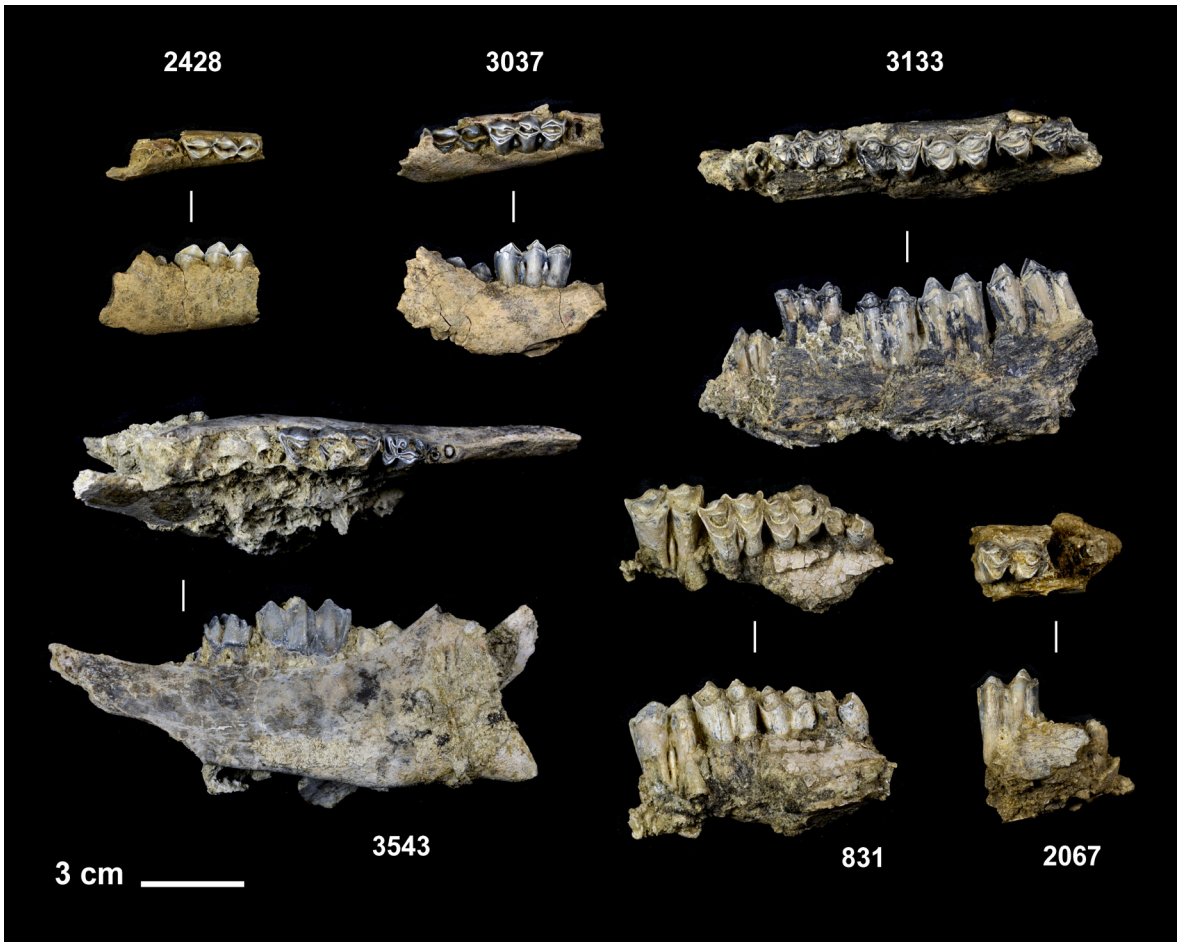

FIGURE 3.51. *Some of the well-preserved mandible and maxilla fragments belonging to* Reduncini *(Kobus).*

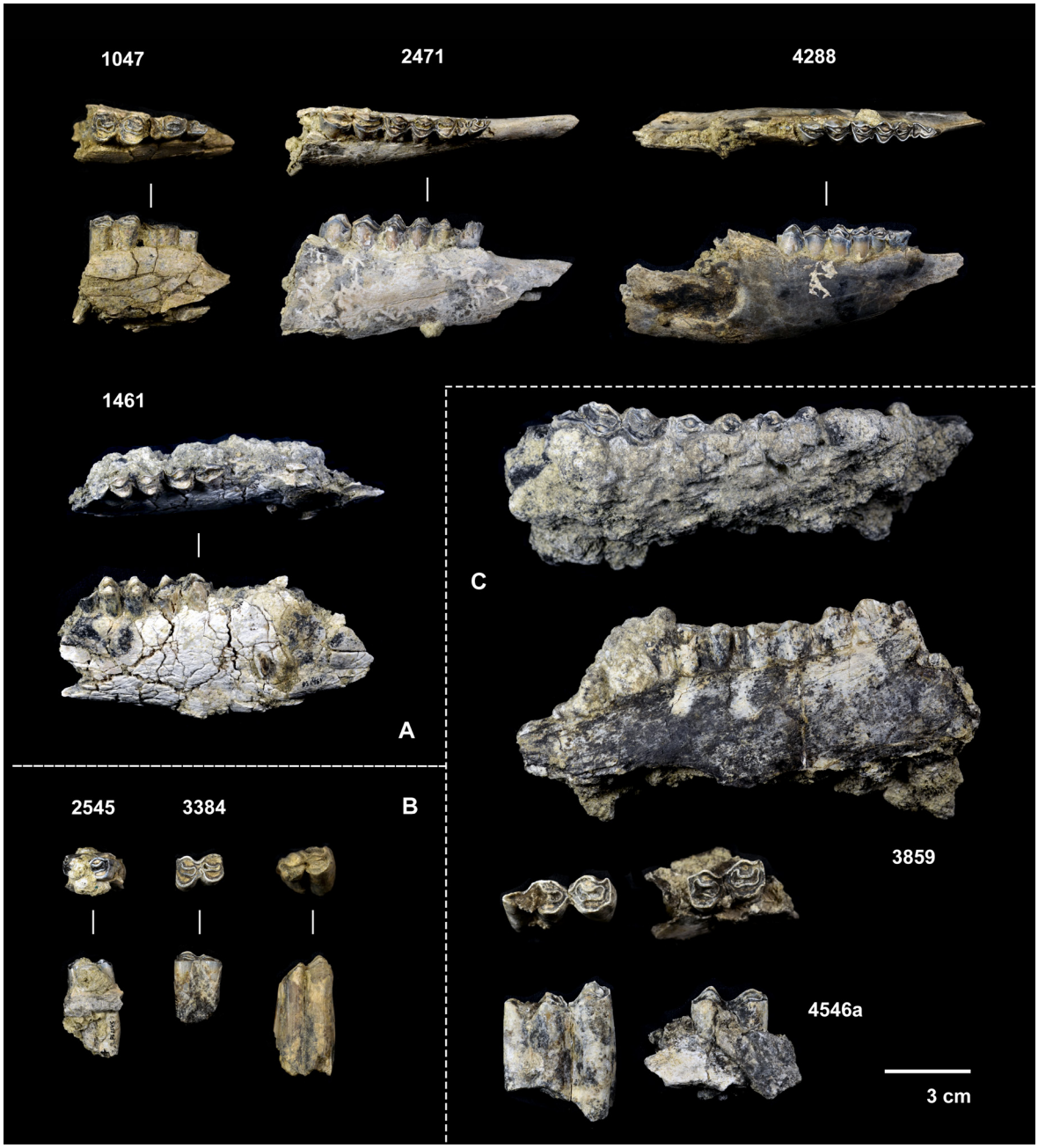

FIGURE 3.52. *Some of the well-preserved mandible and maxilla fragments belonging to* Alcelaphini*: A) Parmularius, B) Connochaetes, C) Megalotragus..*

of old individuals (Table 3.48B). More specifically, prime adults are predominant among *Kobus*, *Connochaetes*, and *Megalotragus sp*. Among smaller bovids, i.e. *Parmularius altidens* and *Antidorcas*, juveniles are more represented than adults (Table 3.48A). The *Tragelaphus* remains most probably belong to a subadult juvenile and a prime (early or late) adult. Only two waterbucks are classified as old using this classification system, and one wildebeest is relocated

Table 3.48. *Age frequency distributions of bovid MNIs at DS based on dental remains. a) MNI estimates for each of the five prey age classes defined by Bunn and Pickering (2010b) and for each represented bovid taxon at DS. The additional category "prime" combines the classes "early prime" and "late prime" and is added in order to enable the classification of those individuals that could not be confidently classified into one of the two adult categories. b) MNIs for each bovid taxon classified into the commonly used three age classes "young", "prime", and "old". c) Age frequency distributions of* Alcelaphini *(Parmularius, Connochaetes, and Megalotragus) according to the five age classes for wildebeest as defined by Sinclair and Arcese (1995) (see also Arriaza et al. 2015).*

A)

Taxon	Size	MNI	Age				
			Young juvenile	Subadult juvenile	Early prime	Late prime	Old
					Prime		
Kobus	3b	11	2	1	3		2
						3	
Parmularius	3a	4	2	1	1		
Connochaetes	3b	4			3	1	
Megalotragus	4	2				2	
Tragelaphus	3b	2		1		1	
Antidorcas	1	5	1	2	1	1	
Total		28	5	5	8	2	2
						6	

B)

Taxon	Size	MNI	Age		
			Young	Prime	Old
Kobus	3b	11	3	6	2
Parmularius	3a	4	3	1	
Connochaetes	3b	4		4	
Megalotragus	4	2		2	
Tragelaphus	3b	2	1	1	
Antidorcas	1	5	3	2	
Total			10	16	2

C)

Taxon	Size	MNI	Age				
			Yearling	Young adult	Mature adult	Old	Very old
Parmularius	3a	4	2	2			
Connochaetes	3b	4			3		1
Megalotragus	4	2				2	
Total		10	2	2	3	2	1

into the category "very old" when using the five age classes defined by Sinclair and Arcese (1995). The distribution of alcelaphines across the five age classes appears to be relatively even: out of a total of 10 alcelaphines, two have been classified as yearlings, another two as young adults, three individuals were mature adults, two carcasses belonged to old individuals, and one was very old (>12 years) (Table 3.48C).

3.5.3. Comparing age profiles at DS with modern African bovid samples

3.5.3.1. Triangular graph

Small bovids

The triangular graph including small bovids (mainly Antilopini) shows age profiles of gazelles generated by lion, spotted hyena, cheetah, leopard, and wild dog, apart from the three archaeological samples from DS, FLK *Zinj* and the background of FLK, and the sample including mortality profiles of impala killed by the Hadza. In this graph, all mortality profiles generated by carnivore predators fall for the most part into the areas that correspond to the attritional (U-shaped) pattern, on the lower left-central region of the triangle, or into the living-structure (catastrophic) pattern on the lower right-central part of the graph (Figure 3.53A). The two broad categories of carnivores according to prey age selection (cursorial and ambush predators) are distinguishable. As would be expected, on the one hand, spotted hyenas, wild dogs, and cheetahs, show a tendency to hunt younger and vulnerable individuals and create an attritional pattern. The cheetah shows the greatest bias toward the juvenile cohort. On the other hand, ambush or short chase predators like leopards and lions fall into the center and right part of the region that illustrates the structure of a living population (Figure 3.53A).

The samples of FLK *Zinj* and DS are extremely small when compared to the referential samples, and thus their confidence ellipses are much larger. The

sample of DS shows a very slight bias toward young individuals, but encompasses all carnivore samples and is therefore statistically indistinguishable from any of them using this method, contrary to the age profiles from FLK *Zinj*, which fall in the upper part of the triangle, above the intersection of the three axes, showing a significant bias toward old age individuals (Figure 3.53A, see also Domínguez-Rodrigo *et al.*, in prep., and Bunn and Pickering, 2010). Finally, the small carcasses of the background of FLK fall mostly in the area of the catastrophic model, but the sample is also slightly biased toward prime adult individuals and overlaps only in part with the lion and leopard samples. The impala killed by the Hadza largely overlap with the leopard and lion kills, but show a greater predominance of prime adults and fall entirely inside the confidence ellipse of the background of FLK (Figure 3.53A). This could either be indicating that hominins might have been more involved in the accumulation of small carcasses in these Bed I assemblages than previously thought (at least at FLKN 1-2 were hominin input is clearer), and support the hypothesis that these sites were palimpsests or, more probably, if we assume that FLK background was formed mostly by felids (Domínguez-Rodrigo *et al.*, 2007), that modern hunter-gatherers can generate mortality profiles of smaller carcasses that are very similar to those created by felids. Taphonomic evidence for small-carcass processing by hominins from the FLK background assemblages is missing and argues against the first option (Domínguez-Rodrigo *et al.*, 2007).

Medium-sized bovids

The age profiles of bovids of size groups 3 and 4 from DS and FLK *Zinj* are almost identical (Figure 3.53B). The 95% confidence ellipses of both samples overlap almost completely and fall mostly in the area representing the living-structure mortality pattern, although both mortality profiles are characterized by a clear predominance of prime adult individuals. Neither one of the two samples overlap with the age profile generated by spotted hyena, but they overlap partly with one of the samples generated by lions and with the sample of the FLK background, although the biggest overlap occurs with the Hadza/Kua kills. Interestingly, the age profiles of wildebeest kills generated by lions in the Serengeti do not resemble the living-structure mortality pattern, as would be expected from an ambush predator, but they overlap partly with the sample of wildebeests that were hunted by spotted hyenas. It is true, however, that the distinction between cursorial and ambush predators is a very general one, and there can be considerable variation in prey selection by predators depending on environmental conditions, the time of year or the structure of the wildebeest population (e.g. Stiner, 1990; Mduma, 1996; Arriaza *et al.*, 2015).

Be that as it may, from this triangular graph, we can deduce that there are important similarities in prey selection of medium-sized bovids between DS and

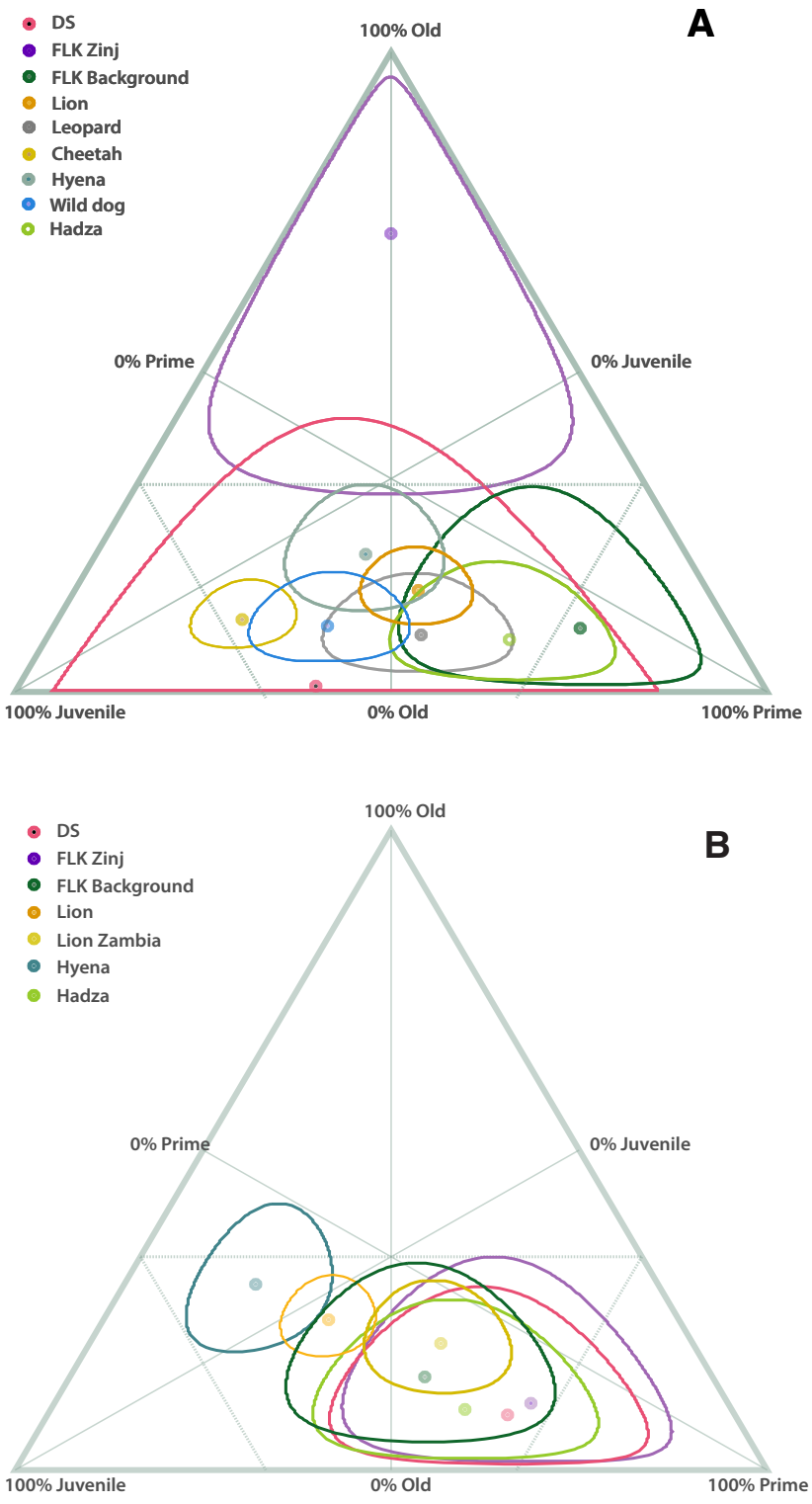

FIGURE 3.53. *Triangle graphs showing the mortality patterns for A) small bovids, and B) medium-sized bovids killed by lions, hyenas, cheetahs, leopards, wild dogs, and Hadza and Kua hunter-gatherers, as well as the mortality profiles documented at DS, and FLK Zinj*

FLK *Zinj*, and that the predominance of prime adult individuals at DS suggests that if hominins hunted these bovids, they probably did so using ambushing strategies, which tend to produce a living-structure mortality pattern because often prey selection is determined by chance encounter (Schaller, 1972; Stiner, 1990). The same has already been hypothesized for the prime-adult-dominated mortality profile of large bovids in the FLK *Zinj* assemblage (Bunn and Pickering, 2010; Bunn and Gurtov, 2014).

However, according to this triangular graph, both felids and humans can create very similar mortality patterns that resemble the structure of a living population and show a predominance of prime adults. The triangular graphs therefore present a case of equifinality and makes it impossible to distinguish between two possible scenarios: a) that the carcasses at the sites were in part acquired by hominins through hunting and in part through confrontational scavenging from felids, b) that the sites are completely anthropogenic, but hominins and lions simply competed for the same types of carcasses in Bed I at DS, FLK *Zinj* and FLK background. Nevertheless, it is possible that this case of equifinality is merely methodological, and that felid and hominin prey choices do differ in some respect, but that this gap cannot be identified using only triangular graphs. For this reason, in the next section, I include a fourth variable and more robust statistics.

3.5.3.2. Principal Component Analysis (PCA) and Canonical Variate Analysis (CVA)

Small bovids

The mortality profile generated by the cheetah differs extremely from all other samples and has therefore been removed from this analysis so that the discrepancies and similarities between the remaining samples can be fully appreciated. The biplots resulting from the PCA and the CVA analyses including the mortality profiles generated by all other carnivores, the three archaeological sites as well as FLK background, and the hunter-gatherer sample, yield solutions with several distinct groups that coincide in both analyses (Figures 3.54A and B). One separate group consists of the DS and FLK *Zinj Antidorcas* samples, which overlap significantly, probably due to the similar proportion of subadults and prime adults. This similarity could not be appreciated in the triangular graph, which showed mainly that the predominant age class in FLK *Zinj* were old adults. The clear separation between these two sites and all the other predators indicates that the carcasses at DS and FLK *Zinj* were most probably hunted by hominins. The second group of predators is composed of the samples of lion and hyena, which also overlap slightly. The mortality pattern created by wild dog resembles that of hyenas but does not overlap with them.

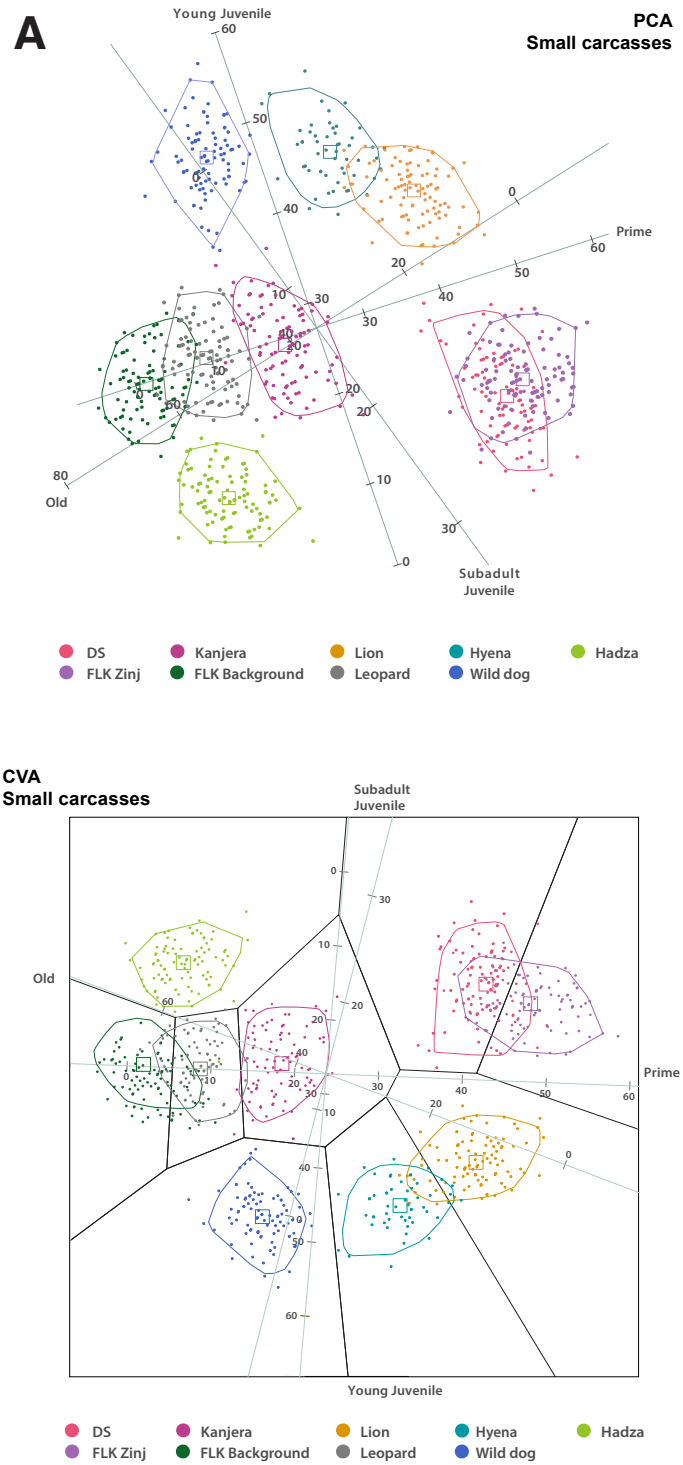

FIGURE 3.54. *Multiple discriminant analysis using A) Principal Component Analysis (PCA) and B) Canonical Variate Analysis on the bootstrapped samples of the mortality profiles generated by carnivores and modern hunter-gatherers, as well as the age profiles documented at DS (this study), FLK Zinj (Bunn and Pickering 2010) and Kanjera (Oliver et al. 2019), regarding small bovids and using four age classes.*

Finally, the third group of mortality patterns that share similarities is composed of the leopard, the FLK background, the Hadza, and the Kanjera age profiles (Figure 3.54A and B). It is interesting that the leopard sample should fall close to the mortality pattern on impala created by the Hadza (as well as to the sample from Kanjera). This relationship could be explained by the lower proportion of old adults with respect to the other age classes in all samples, and again suggests that humans sometimes generate age profiles that resemble those of felids. This is sometimes explained as a result of the fact that both predators use ambush strategies and thus both generate a mortality pattern that is similar to the structure of a living population (Figures 3.54A and B). However, when plotted in ternary diagrams, the age profiles from Kanjera are more similar to those of cursorial predators, suggesting that if these profiles were indeed generated by hominins, they most likely practiced persistence hunting (Oliver *et al.*, 2019).

The samples also fall very close to the mortality pattern from FLK background, and it is especially interesting that the FLK background sample lies closer to the leopard than to the lion sample. In fact, this makes sense considering that bones recovered from FLKN 6 bear similar kinds of modifications to those made by leopards (Domínguez-Rodrigo *et al.*, 2007), and that at FLKN 1-2, the same authors established that "about 40% of the carcasses (*Antidorcas* and juvenile *Parmularius*) could easily have been transported and stored into trees by leopards". What is more, they added that "the remaining carcasses could have been transported either by leopards (…) or by any other felid slightly bigger than a leopard, but smaller than a lion. The best candidate is *Dinofelis*" (Domínguez-Rodrigo *et al.* (2007: 157). It is believed that *Dinofelis* might also have been an ambush hunter and might have behaved similarly to leopards, who prey on smaller mammals and are unique among felids in that they usually transport carcasses into caves, rockshelters and trees, although *Dinofelis* would have had a wider predatory range. *Dinofelis* remains have in fact been found at the site, including a canine that perfectly fits into a tooth puncture on a *Parmularius* humerus (Domínguez-Rodrigo *et al.*, 2007).

Medium-sized bovids

The PCA and CVA diagrams resulting from the age profile analysis of the four age classes of medium-sized bovids point to a very similar scenario. As with small bovids, samples appear classified into three main groups: one is composed of FLK *Zinj* and DS, which overlap almost entirely, as could already be seen in the triangular graphs, the second includes the mortality profiles created by lions and hyenas in the Serengeti, and the third is composed of the age profiles created by lions in the Kafue National Park in Zambia, FLK background, and

the Hadza and Kua kills, which overlap entirely with Kanjera South, supporting the hypothesis that the assemblage of Kanjera South was the result of hominin hunting (Figures 3.55A and B). Previous analysis of the mortality profiles of Kanjera South using ternary diagrams did not yield such clear results, leading researchers to conclude that at Kanjera medium-sized carcasses were probably partly hunted and partly scavenged (Oliver *et al.*, 2019). These results do not completely rule out confrontational scavenging, because age profiles from Kanjera also fall close to profiles generated by lions, but the absolute coincidence with the Hadza and Kua profiles strongly suggests that carcasses could have been acquired in similar ways. The argument is even more compelling when we realize that the Kua sample was acquired through persistence hunting (Bunn and Gurtov, 2014), and that Oliver *et al.*, (2019) explain the attritional age profile and a predominance of juvenile prey at Kanjera arguing that carcasses were acquired by hominins after short chases in order to overcome the challenges of a more open environment than the one present at FLK *Zinj* and DS.

Hadza and Kua prey selection also fall close to the background of FLK, as well as to this sample of lions (that falls in a similar place to leopards in small carcasses), which again demonstrates that human and felid mortality profiles can be very similar. In fact, Bunn and Gurtov (2014) explain that Hadza and Kua hunters are opportunistic hunters who, even though they have sophisticated bows and arrows to hunt, do not pass up shots at young or old individuals expecting to encounter prime adults. Thus, they create non-selective, living-structure mortality profiles.

One of the main novelties with respect to the triangular graph (and the analysis presented by Bunn and Gurtov, 2014) is the clear separation that can be established between the group that includes the FLK background, the Hadza-Kua, Kanjera South, and the lions from Zambia on one hand, and the assemblages DS and FLK *Zinj* on the other hand. These two archaeological sites present the most prime-adult-dominated mortality profiles among all included mortality profiles, which might be indicating a tendency towards selective ambush hunting. Stiner (1990) was the first to note that mortality profiles generated by humans are often prime-dominated, and established this as the characteristic of the human predatory niche. Many Early, Middle, and Upper Paleolithic sites are known that demonstrate this preference by hominins. Some examples include Abric Romaní (Marín *et al.*, 2017), Moscerini (Stiner, 1990b), Lazaret, Breuil (Valensi and Psathi, 2004), Pech de l'Azé (Rendu, 2010), Cuesta de la Bajada (Domínguez-Rodrigo *et al.*, 2015b), Gabassa, Combe Grenal (Steele, 2004) or Kevara (Marín *et al.*, 2017), as well as TD10.1 (Rodríguez-Hidalgo *et al.*, 2015) or Gesher Benot Ya'aqov (Rabinovich *et al.*, 2008). From this analysis, it seems clear that the bovid accumulations at DS and FLK *Zinj* were created by the same type of predator and, based on the fact that their mortality profiles

do not overlap with any of the carnivore samples and on the fact that they are dominated by prime adults, something untypical among carnivores but that occurs in many other archaeological sites that are anthropogenic, it is reasonable to infer that hominins acquired the carcasses through hunting and not confrontational scavenging.

3.5.3.3. The Alcelaphini *subsample*

Figures 3.56A and B show the results of the PCA and CVA applied to the Alcelaphini subsample of DS and the wildebeest kills from Mduma *et al.* (1999) using the five age class system. In this case, the PCA and the CVA show different results. The PCA diagram shows an overlap between the mortality profiles generated by lions and hyenas during a wildebeest population increase and stationary phase, while there is no overlap between mortality profiles generated by the same predators. This shows that changes in wildebeest population dynamics can have great effects on prey selection by predators and may result in significant variations in mortality profiles generated by lions and hyenas (Mduma *et al.*, 1999; Arriaza *et al.*, 2015; Domínguez-Rodrigo *et al.*, in prep.).

All the lion samples used in this study differ considerably, and it is therefore not so surprising that the mortality profiles from Alcelaphini at DS and one of the lion samples match in the CVA (Figures 3.56A and B). There is a possibility that alcelaphines from DS were acquired through confrontational scavenging from lions. It is true that *Connochaetes* is a preferred lion prey (e.g. Scheel, 1993; Domínguez-Rodrigo *et al.* 2019c), in contrast to waterbucks, which are the most abundant taxon at DS. However, as we have seen, humans can create mortality profiles that match those created by felids when they use non-selective ambush strategies. Lions are prone to generate patterns that resemble a living population structure, which in normal conditions is dominated by prime adults (see above), and modern hunter-gatherers have been observed to do this too, as is evidenced by the Hadza and Kua samples. Hominins could have followed a less selective hunting strategy to hunt wildebeest, *Parmularius* and *Megalotragus* than they did for the other bovid taxa, perhaps because these species were encountered less often, or only seasonally (in particular *Connochaetes*), in contrast to the local waterbucks.

It is also possible that this lion sample represents an exceptional mortality pattern. Lions are considered unusual among ambush predators, because they often cooperate with each other to prevent prey from escaping, instead of always relying on geographical features to ambush their prey, and this can also yield variable mortality profiles (Stiner, 1990). What is more, although it is typical for lions and hyenas to prey on younger individuals, lions have also been observed to select older prey and generate prime-dominated assemblages

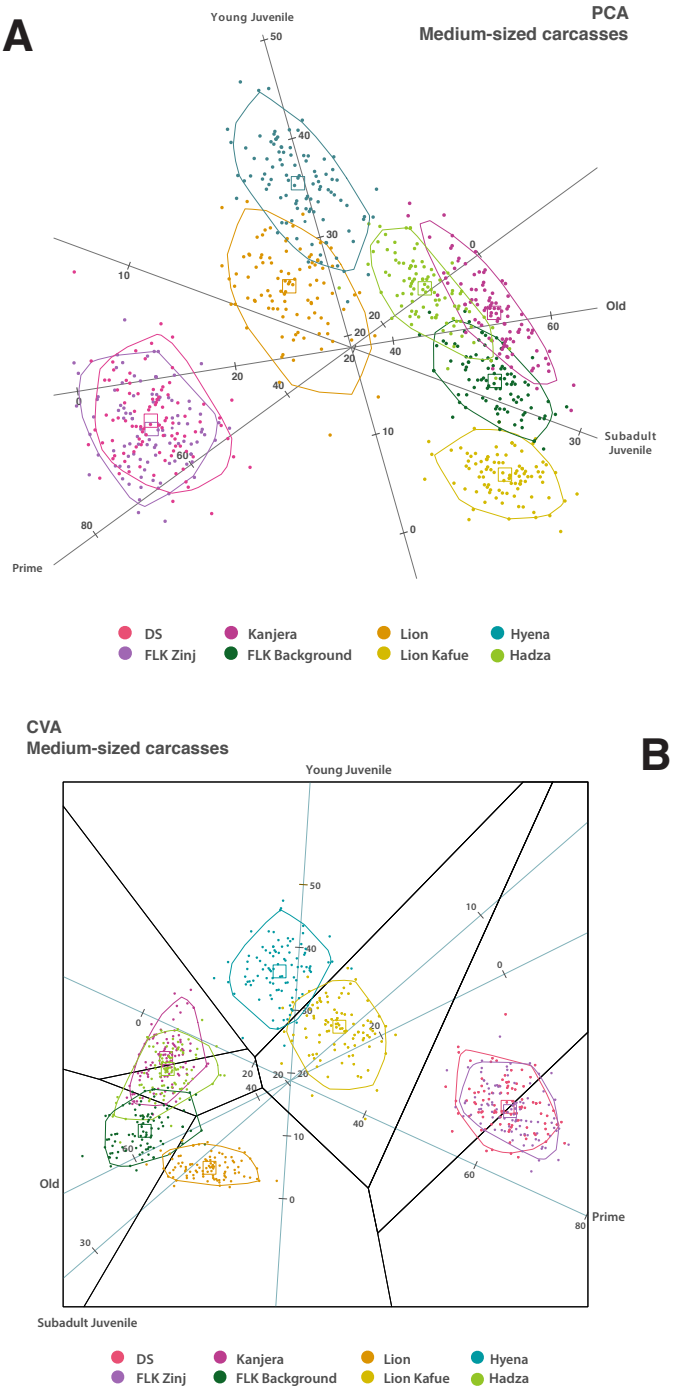

FIGURE 3.55. *Multiple discriminant analysis using A) Principal Component Analysis (PCA) and B) Canonical Variate Analysis on the bootstrapped samples of the mortality profiles generated by carnivores and modern hunter-gatherers, as well as the age profiles documented at DS (this study), FLK Zinj (Bunn and Pickering 2010) and Kanjera (Oliver et al. 2019), regarding medium-sized bovids and using four age classes.*

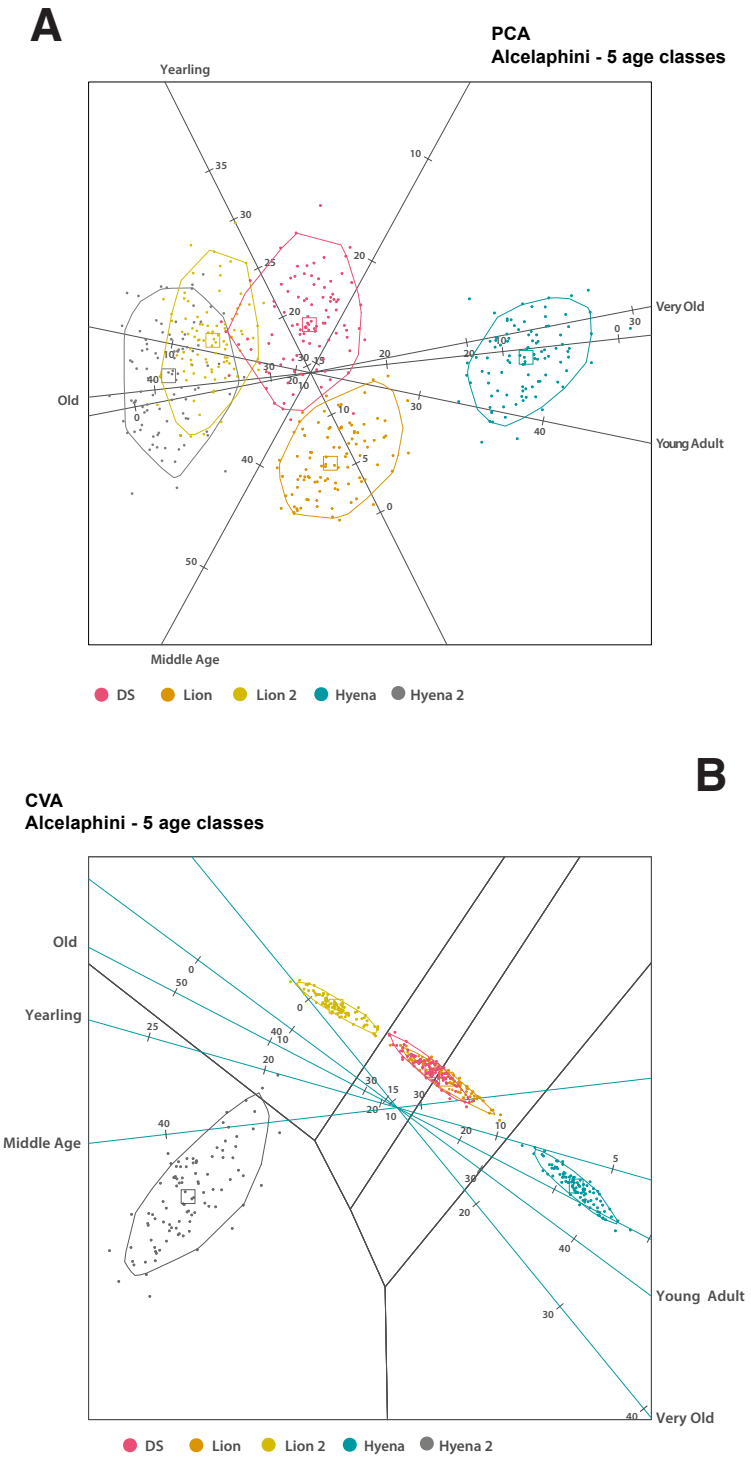

FIGURE 3.56. *Multiple discriminant analysis using A) Principal Component Analysis (PCA) and B) Canonical Variate Analysis on the bootstrapped samples of the mortality profiles generated by lions and hyenas on alcelaphines, as well as the age profiles documented at DS regarding the same bovid tribe and using five age classes.*

(Arriaza *et al.*, 2015). Thus, given the high variability in age mortality profiles generated by lions (and humans), confrontational scavenging of Alcelaphini at DS seems no more likely than hunting.

Furthermore, as mentioned earlier, felid modifications have not been found on these carcasses at DS. In fact, the only specimen bearing felid tooth marks belongs to a waterbuck. The difference between the dental MNI (28) and the appendicular MNI (16) in medium-sized carcasses is relatively marked. Therefore, it is also possible that the Alcelaphini sample constitutes part of a background scatter probably caused by non-anthropogenic agents. In any case, using five age classes instead of three or four probably also evens the numbers in each variable in the sample, and predominant age groups may become less prominent. Also, it is to be expected that mortality profiles from hominins and lions should coincide to a certain point, for the reasons mentioned above. Be that as it may, when medium-sized carcasses are analyzed as a whole using four age classes, the separation between the felid samples and DS points to hominin hunting.

In sum, the analysis of mortality profiles from the bovids accumulated at DS illustrates two things, both of which were already pointed out for FLK *Zinj* (Bunn and Pickering, 2010; Bunn and Gurtov, 2014), namely ambush hunting and a tendency to hunt prime adult prey. Between 60% and 70% of the medium-sized animals from DS and FLK *Zinj* are prime adults, in contrast to around the 50 to 60% that are common in living-structure profiles (Bunn and Gurtov, 2014). Prime adult biased mortality in prey is uncommon in nature but typical in the archaeological and ethnographic record, and many authors have associated this pattern with selective ambush hunting (Binford, 1978; Stiner, 1990; Bunn and Pickering, 2010; Bunn and Gurtov, 2014). Stiner (1990) proposed a model in which hominin hunting would have evolved from non-selective to selective hunting, and that a tendency can be observed in the archaeological record towards more prime-adult-dominated mortality profiles during the Upper Paleolithic and the Holocene. However, this tendency can already be seen at DS and FLK *Zinj*, as well as in many other Lower and Middle Paleolithic sites in Eurasia (see above), which suggests that early *Homo* were already efficient, experienced and regular hunters, as they had the ability to select and hunt the highest ranking prey.

3.6. General spatial assessment of the DS point pattern

3.6.1. Estimating the intensity of the DS spatial point pattern using non-parametric methods

3.6.1.1. Testing for Complete Spatial Randomness

The spatial distribution of archaeological materials was plotted within the excavated window of DS next to a simulated *Homo*geneous Poisson process within the same spatial window and with the same number of points as are present at the site (Figures 3.57A, 3.57B). Two observations can be made when looking at this CSR simulation and the observed DS pattern. The first one is that density of the DS point pattern is notably high (the average intensity of the point pattern is 9 pieces per square metre), the second is that some areas are much denser than others: the DS pattern appears to be inhomogeneous and therefore not completely random.

Figure 3.57**C** shows the division of the DS window into five tessellations and the counts for each tessellation of the observed number of points, the expected number of points if the points were uniformly distributed, and Pearson's residuals. The absolute values of the residuals are larger than 2, which indicates that the point pattern is inhomogeneous. The three tests based on quadrat counts, the chi-squared test, the Freeman-Tukey statistic and Neyman's modified statistic, yielded significant results, but extremely low p-values (< 2.26 e-16), which suggests that performing these tests was unnecessary in the first place. Likewise, the results of the tests that use Monte Carlo simulations, the Clark Evans test (R = 0.67, p-value = 0.025) and the Hopkins-Skellam test (A = 0.14, p-value = 0.001), are statistically significant and suggest that the point process is clustered. The null-hypothesis of CSR does not hold, since points are not uniformly distributed in the study region.

3.6.1.2. Kernel estimation and density maps

The most accurate intensity estimates are yielded by the variable or adaptive smoothing methods, because they account for wide or abrupt changes in

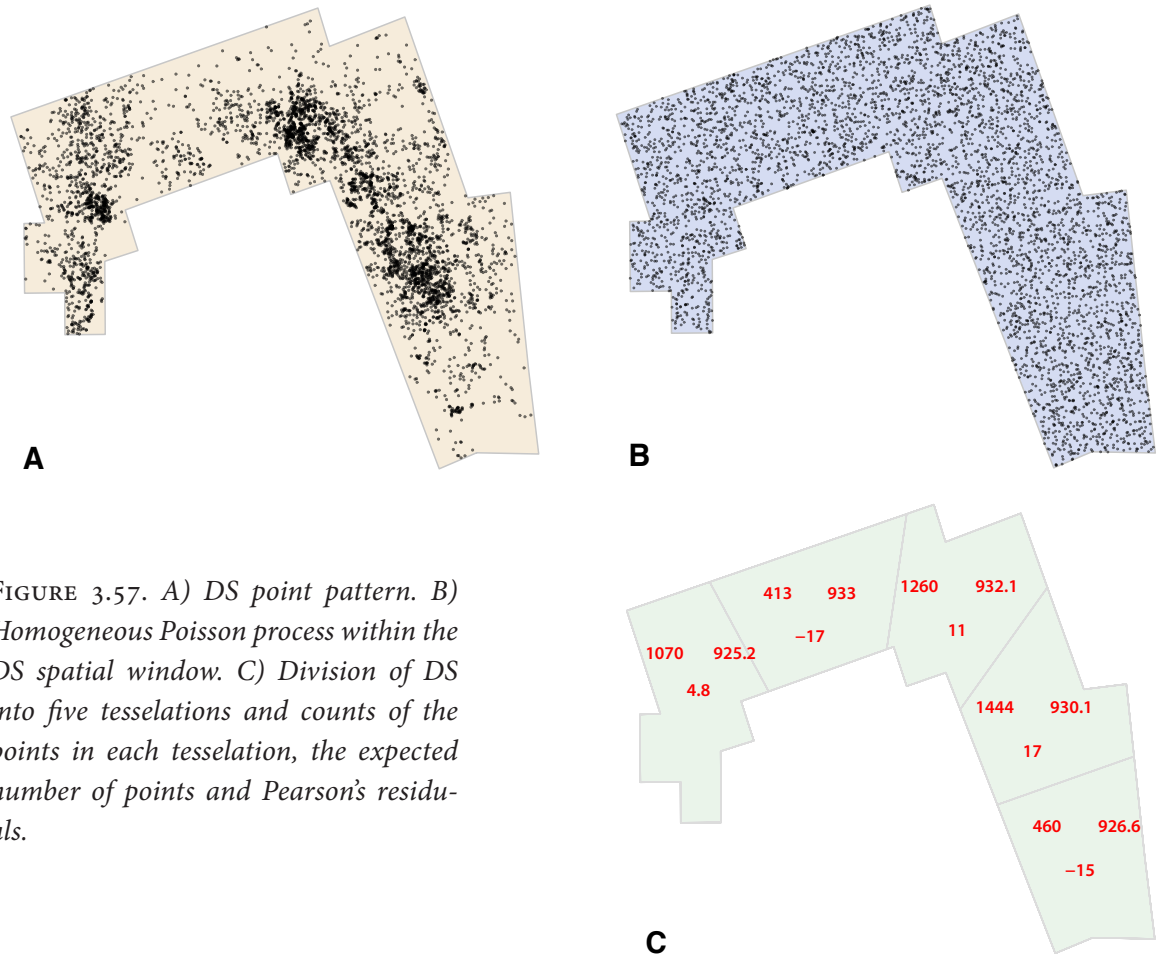

FIGURE 3.57. *A) DS point pattern. B) Homogeneous Poisson process within the DS spatial window. C) Division of DS into five tesselations and counts of the points in each tesselation, the expected number of points and Pearson's residuals.*

the intensity. Among the fixed bandwidth smoothing methods, the likelihood cross-validation method appears to be the most appropriate approach. The corresponding density map indicates that the peak density areas contain more than 50 remains per square meter. Similar to the variable smoothing methods, Diggle and Berman's mean square cross-validation method provides a lot of detail, although it could be overestimating the density in the high density areas. The Cronie and van Lieshout's method seems to capture the size of the clusters well, although it underestimates the real intensity in these areas. The density maps all show that there are at least three high density areas at DS (Figure 3.58).

3.6.1.3. Statistical significance of hot spots

Figure 3.59. shows the areas in which the density of points is significantly higher than in the remaining scatter. In other words, there is a significant excess of points inside these regions.

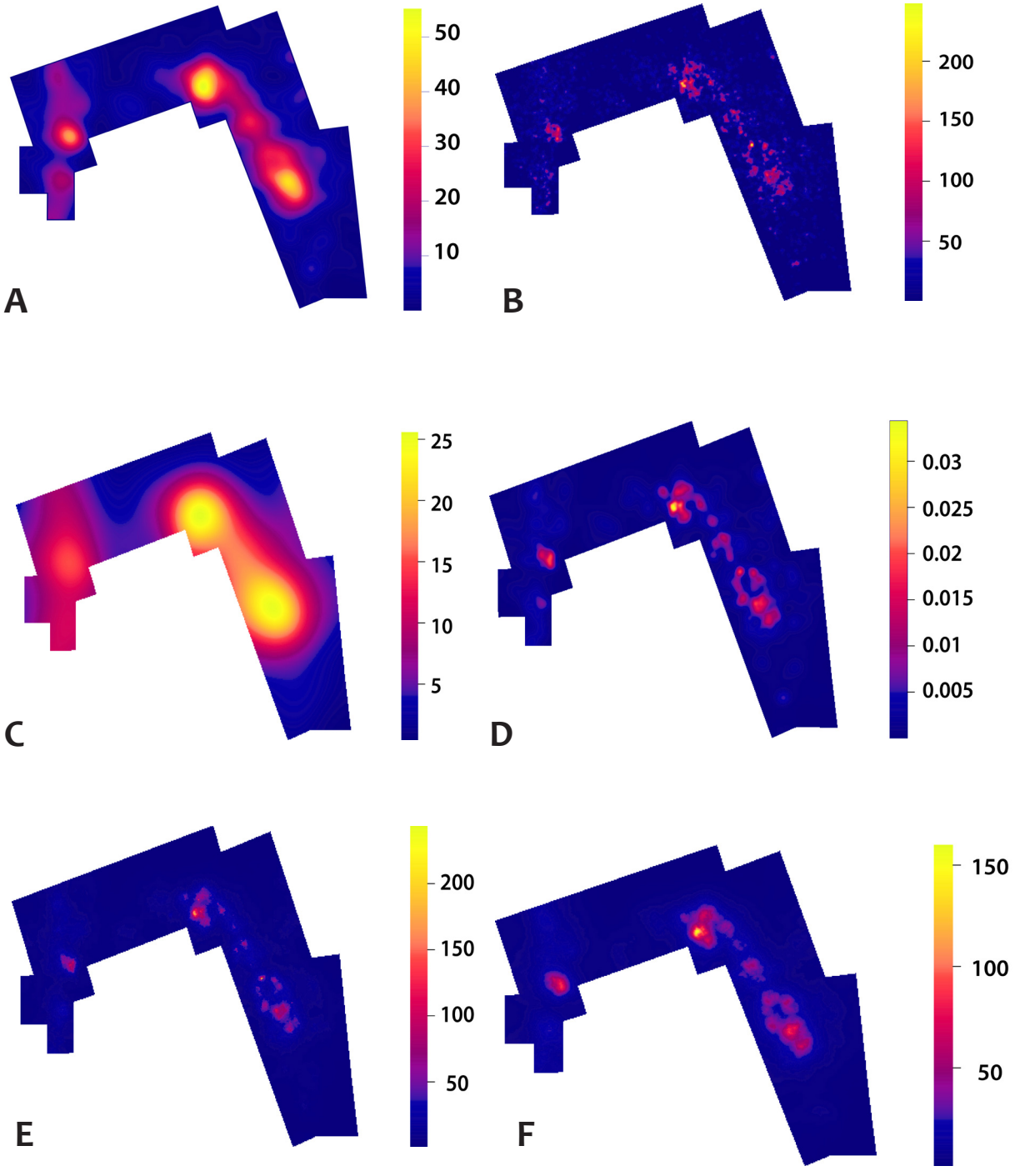

FIGURE 3.58. *Density maps generated using different fixed and adaptive bandwidth smoothing methods. Letters A-F refer to table 2.10. in the methods section.*

FIGURE 3.59. *Areas of significant clustering at DS.*

3.6.1.4. Measuring the effect of the paleosurface topography on the distribution of archaeological materials

The counts of points using the chosen tessellation shows that there are many more archaeological materials on higher topographic areas than on depressed zones (Figure 3.60B; tile 1: 357, tile 2: 925, tile 3: 1577, tile 4: 1788). The barplot in Figure 3.60A shows the average intensity for each topographic elevation interval. The result of the rhohat function indicates that this estimation is not very reliable at the lowest and highest topographic points, probably because intensity at both extremes is very low (Figure 3.60B). This function confirms that higher density probabilities are documented in places where topography is higher. For example, at height 490.7 m the estimated intensity is of around 5 pieces per square meter and at height 490.9 m the estimated intensity is 15 observations per square meter. The predicted intensity map yields clearly higher intensities on higher topographic zones, but the function fluctuates, suggesting that the effect of the covariate on the point pattern is not strong.

The spatial Kolmogorov-Smirnov test, the Cramer-von Mises test and the Anderson-Darling test yielded significant results, indicating that the topography has a significant influence on the point pattern (Table 3.49). The graph associated to the Berman's test (Z2 = 24.95; p-value = 2.2 e-16) shows that there are less points at a certain height than expected if the point process was not dependent on topography, which again means that points tend to be on higher ground (Figure 3.61C).

The ROC curve suggests, however, that the effect of the covariate on the point process intensity is weak, because the curve does not lie substantially above the diagonal line. The index of the area under the curve (AUC) also indicates a small discriminatory power of the covariate. The topography has thus an influence on the point pattern, but is clearly not enough to explain the spatially varying intensity (Figure 3.62). In fact, when we subtract the prediction of the intensity made using the topography from the density map estimated using the likelihood cross-validation method for bandwidth selection (sigma = 0.4), we see that the spatial pattern of the resulting map is very similar to the first density map. The covariate topography mainly fails to predict the high intensity of remains at the hot spots, which suggests that the spatial patterning at DS was not constraint by topographic features and is therefore probably mainly the result of hominin behavior (Figure 3.63).

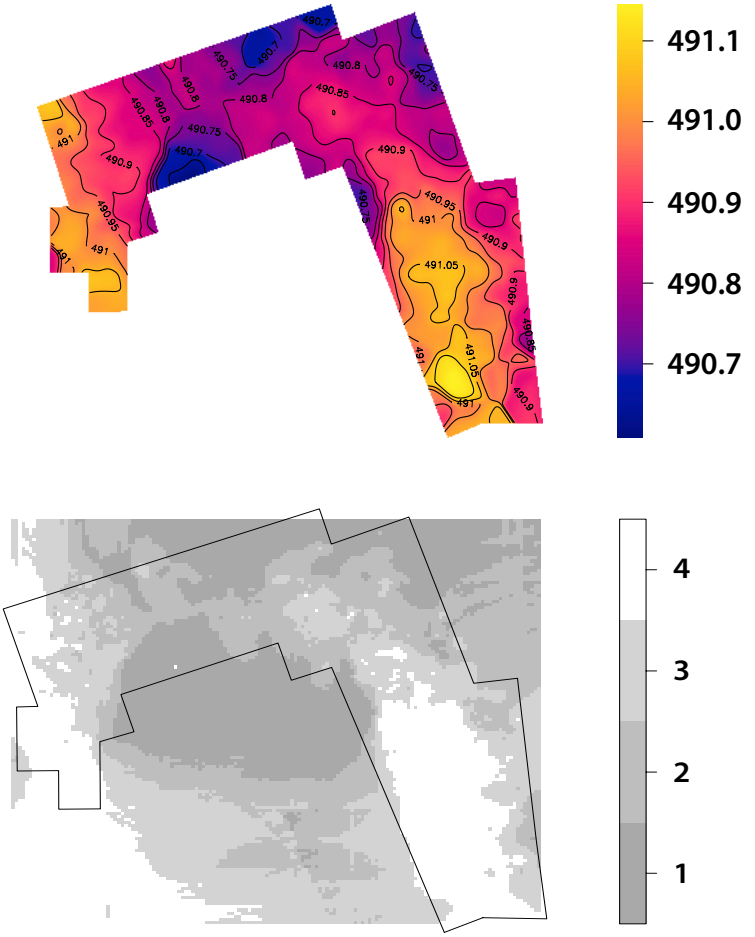

FIGURE 3.60. *Top: Contour map of the topography at DS. Scale in meters. Bottom: Subdivision of the topography into four levels.*

TABLE 3.49. *Results of the spatial versions of the Kolmogorov-Smirnov, Cramer-von Mises and Anderson-Darling tests to assess the influence of the covariate topography on the spatial point pattern of DS.*

	Kolmogorov-Smirnov	Cramer-Von Mises	Anderson-Darling
Statistic	**D = 0.19**	**omega2 = 65.09**	**An = 341.3**
p-value	2.2 e-16	0.001	1.3 e-07

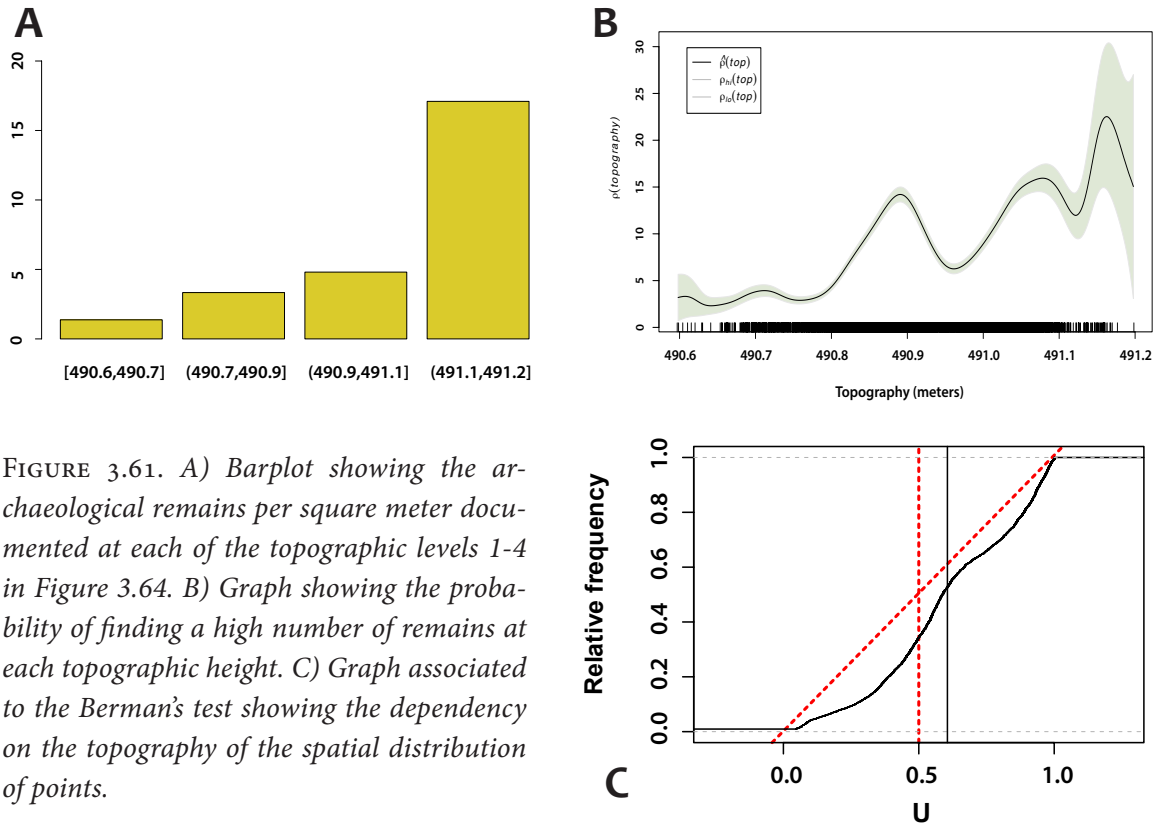

FIGURE 3.61. *A) Barplot showing the archaeological remains per square meter documented at each of the topographic levels 1-4 in Figure 3.64. B) Graph showing the probability of finding a high number of remains at each topographic height. C) Graph associated to the Berman's test showing the dependency on the topography of the spatial distribution of points.*

3.6.2. Correlation and point inter-dependence

3.6.2.1. Testing the type of inhomogeneity of the DS point pattern: correlation-stationary or locally-scaled?

The outcomes of the studentised permutation tests using the different bandwidth smoothing methods described in section X for the inhomogeneous K-function and the locally-scaled function yield conflicting results. Half of the trials suggest that the assumption of correlation-stationarity is not appropriate, and that the inhomogeneous K-function cannot be applied, while the other half suggests that the inhomogeneous K-functions of the subpatterns differ sig-

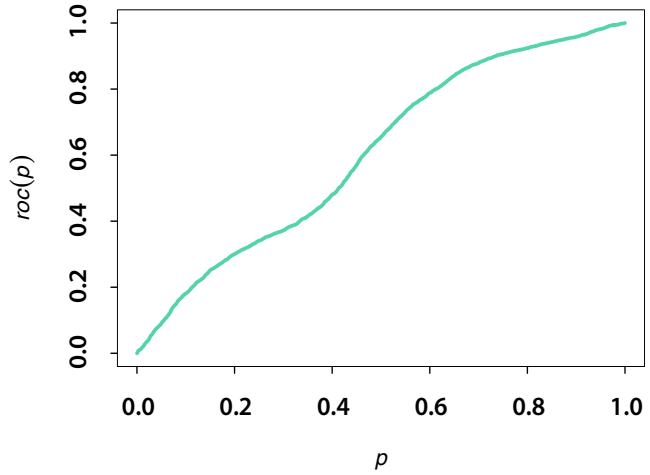

FIGURE 3.62. *ROC curve showing a small discriminatory power of the topography covariate*

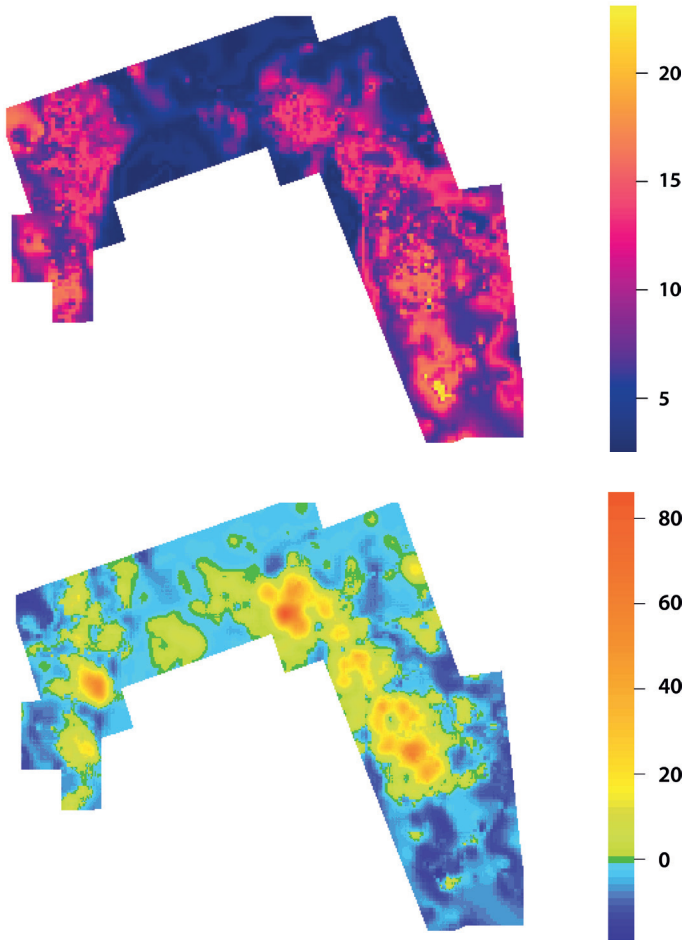

FIGURE 3.63. *A. Prediction of the intensity taking into account the effect of the topography. B. Subtraction of the map A from the real density map using the likelihood cross-validation method for bandwidth selection.*

nificantly. The same happens with the locally-scaled K-function (Table 3.50). The outcome of the tests depends on the estimation of the intensity. It is unclear therefore, whether the point pattern can be described as correlation-stationary or locally-scaled, or whether its in*Homo*geneity is of a different sort. The clearest result is probably yielded by the intensity estimate c, which points to correlation-stationarity. The following summary functions therefore use bandwidth selection method c to estimate the intensity of the point pattern.

3.6.2.2. Application of the inhomogeneous K-function, the locally-scaled function and further summary functions to the DS point pattern

The inhomogeneous K-function yields a positive association between points in short distances (r < 3 m), which means that points are clustered, and a negative correlation at larger distances, i.e. the point pattern displays a regular or more inhibited pattern at larger distances (Figure 3.64). The other remaining summary functions mostly point to clustering, although they also yield ambiguous results. However, the fact that different conclusions are reached depending on our operational choices (in this case bandwidth selection methods), suggests that the method has reached the breakdown point and that the answer will be very sensitive in terms of robustness.

Based on these results, it is likely that the assumptions under which the K-function and the other summary functions are defined do not hold. Some of the characteristics of the point pattern, like the high degree of inhomogeneity, make it difficult to correct for inhomogeneity, and it seems that the K-function is not applicable. The diverging outcomes of the different edge corrections also suggest that the function is unstable, and that it is effectively breaking down. The interpretation of the type of point pattern that characterizes DS is therefore not straightforward, but the point pattern appears to be clustered to some degree, at least at small distances. Results are clearer when bones and lithics are assessed separately (Table 3.51, Figures 3.65, 3.66).

The locally-scaled K-function, on the other side, indicates that the point pattern is clearly clustered, as the curve falls above the inhomogeneous Poisson line, and outside the significance envelopes (Figure 3.67). However, there is no clear signal that the assumption that the point pattern is locally-scaled really holds, because in those cases where the outcome of the studentized test for the locally-scaled K-function is non-significant (therefore supporting the hypothesis of local scaling), the studentized test for the inhomogeneous K-function is non-significant as well.

Table 3.50. *P-values for the studentised permutation tests for the inhomogeneous K-function and the locally-scaled K-function showing ambiguous results.*

Bandwidth smoothing method	p-value of studentised permutation test – inhomogeneous K-function	p-value of studentised permutation test – locally-scaled K-function
a	0.037	0.001
b	0.001	0.001
c	0.178	0.025
d	0.069	0.543
e	0.401	0.108
f	0.583	0.067

3.6.2.3. The inhomogeneous pair-correlation function

The results of the pair-correlation function confirm the outcome of the inhomogeneous K-function. They indicate that for r values smaller than 2 or 3 meters the point pattern is clustered. The curve then declines to values below the Poisson line, suggesting that there is negative association between the points at larger distances (r > 4m, Figure 3.68).

3.6.3. The relative spatial distribution of bones and lithics

2.6.3.1. Estimating the intensity and the spatially-varying type distribution of bones and lithics

As would be expected, the bones and lithics spatial point patterns are also inhomogeneous. Since average intensity is lower in the case of the lithics point pattern (2.1 pieces per square meter) than in that of the bones (6.3 pieces per square meter; there are three times more bones than lithics at DS), the chosen smoothing bandwidth varies (it is smaller for the bones point pattern). Figure 3.69 shows the estimated intensities for both types using the likelihood cross-validation bandwidth selection method (adjusted by multiplying it by 2), which assumes an inhomogeneous Poisson process. The scan test also points to the existence of two to three significant dense areas or hot spots of bones and lithics (Figure 3.70). The result of the bones point pattern is very similar to the overall pattern, since fossil bones make up most of the assemblage. Lithics

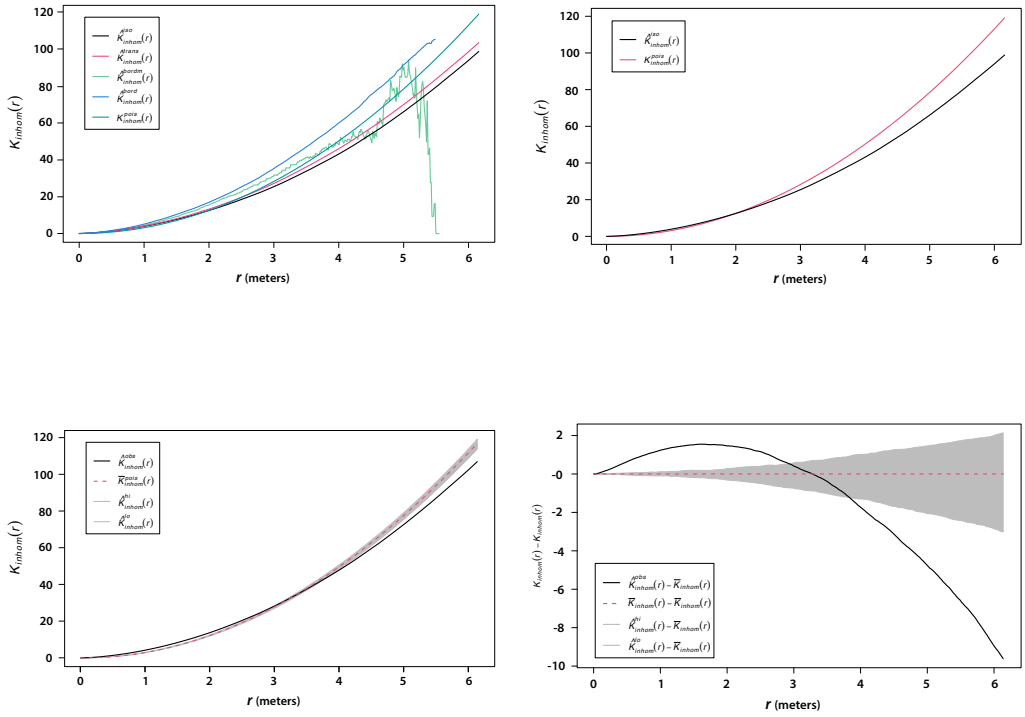

FIGURE 3.64. *Inhomogeneous K-function applied to the DS point pattern.*

appear more clearly concentrated in three distinct clusters, whereas bones are slightly more scattered across the excavation.

It is important to note that the hot spots of both types of finds overlap in space. This indicates that bones and lithics are functionally associated. In the next section, I will test the type of correlation between bones and lithics and whether both point patterns in fact have similar spatial distributions.

The three different available cross-validation methods for the estimation of the spatially-varying type distribution yielded very similar results. Figure 3.71 shows the relative probabilities of finding bones or lithics throughout the DS point pattern. Bones have higher probabilities than lithics in most areas of the excavation, with the exception of two areas close to the edge of the excavated window where bones are absent. The tolerance contours show that the areas with a significantly higher proportion of bones with respect to lithics do not occur directly at the hot spots, but mostly the areas of scattered material. This is also an indication of stronger clustering of lithics on the three hot spots than of bones.

TABLE 3.51. *Interpretations of the summary functions using significance envelopes applied to the DS bones and lithics spatial patterns separately with intensity estimate based on Cronie and van Lieshout's bandwidth selection method.*

	Bones	**Lithics**
Inhomogeneous K and L functions	Clustered, then regular	Clustered, then regular
Inhomogeneous F-function	Random	Random
Inhomogeneous G-function	Random	Clustered
Inhomogeneous J-function	Clustered	Clustered

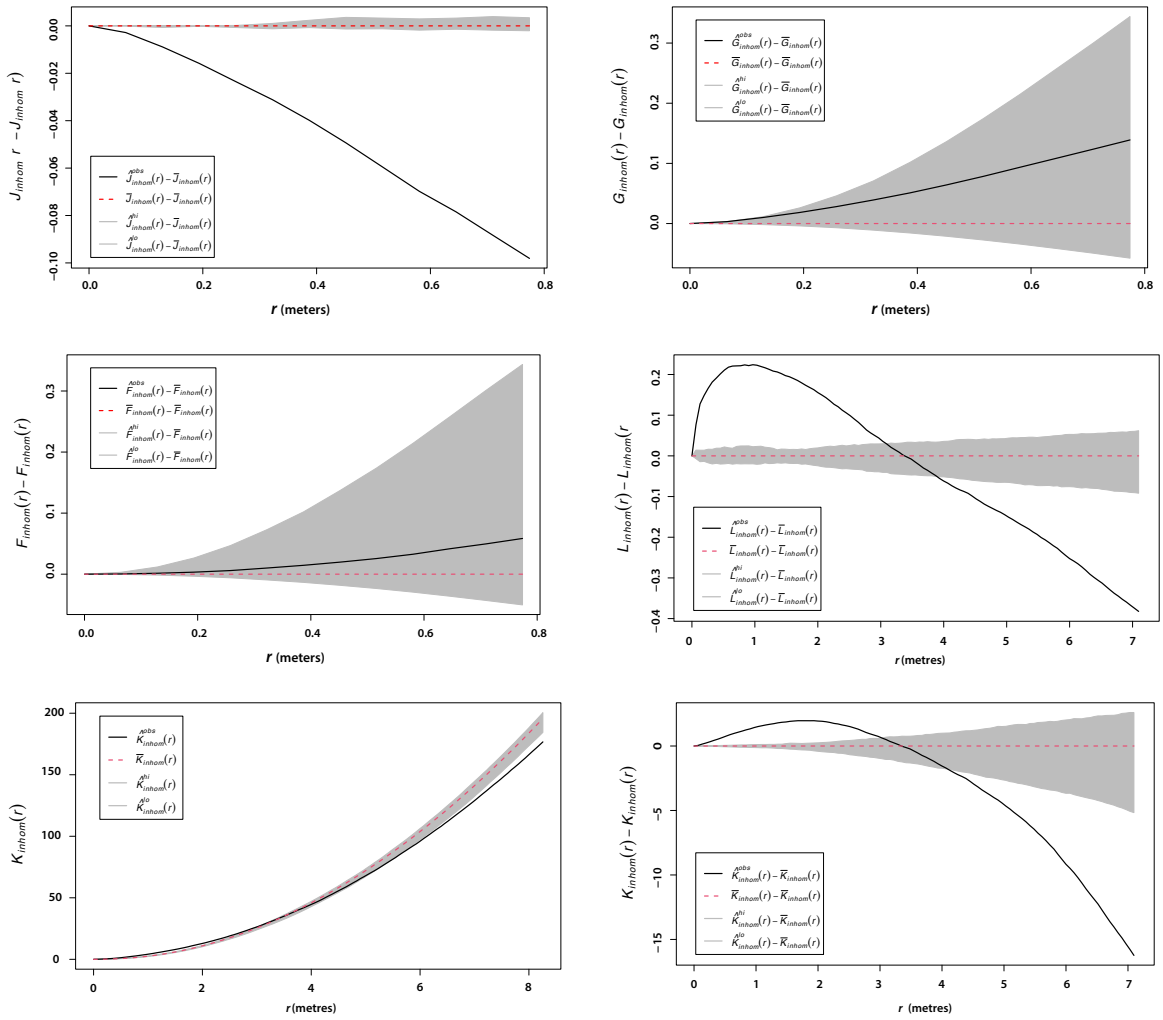

FIGURE 3.65. *Summary functions using significance envelopes applied to the DS bones spatial pattern.*

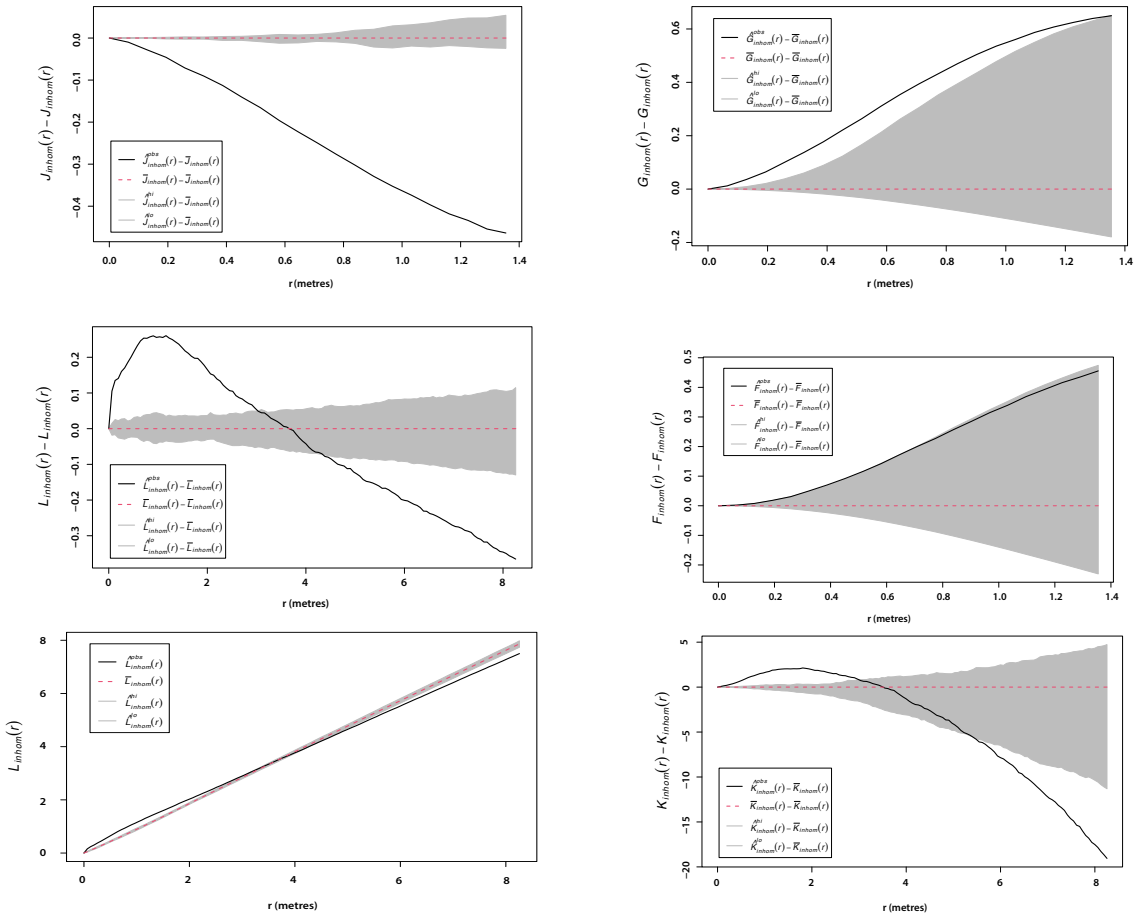

FIGURE 3.66. *Summary functions using significance envelopes applied to the DS lithics spatial pattern.*

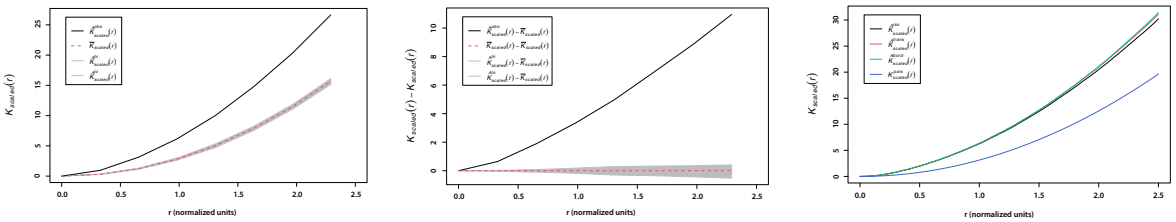

FIGURE 3.67. *Locally-scaled K-function applied to the DS point pattern.*

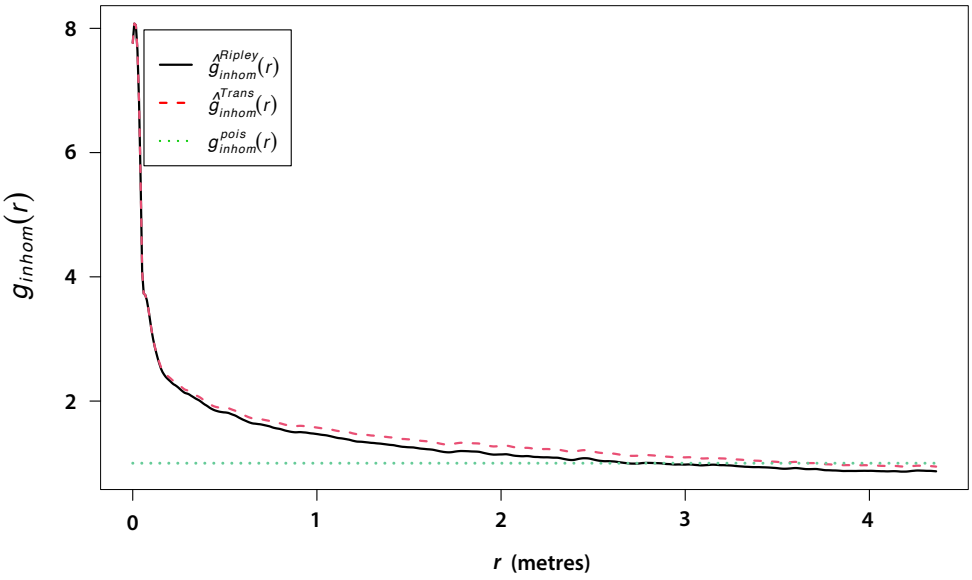

FIGURE 3.68. *Inhomogeneous pair-correlation function of the overall DS point pattern.*

3.6.3.2. Correlation between bones and lithics using approaches based on nearest neighbors

The results of the nearest-neighbour correlation are ambiguous. The unnormalised value, which gives the probability that a point and its nearest neighbour belong to the same type, yields point to point inter-dependence (0.69). The normalised value gives the probability that a random mark value has the same probability as another mark value. This value in turn suggested independence (1.11).

Figure 3.72A shows the cumulative proportion of lithics that are observed at the kth nearest neighbors when measured from bones. The theoretical line represents the expected proportion if both types of points were randomly mixed. There are much lower proportions of lithics observed around bones than would be expected if they were randomly mixed. Figure 3.72B show the fraction amongst the kth nearest neighbors that are of the same type as the point of origin. These fractions are much higher than the theoretical line. Figure 3.72C provides a summary of these last two plots and shows the proportion of points of the same type as the original point (lithics plus bones). In all three cases the observed pattern falls outside the envelopes, which means that the results are statistically significant.

Bones tend to be close to other bones, and lithics tend to be closer to other lithics than to bones. This means that there are patches of bones and patches of lithics, and it suggests that both point pattern distributions are segregated,

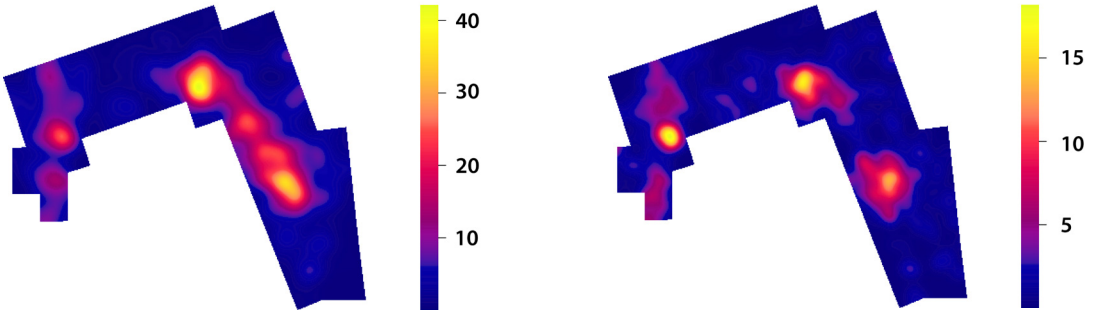

FIGURE 3.69. *Density maps of a) bones and b) lithic remains using the bandwidth obtained with the likelihood cross-validation method multiplied by 2.*

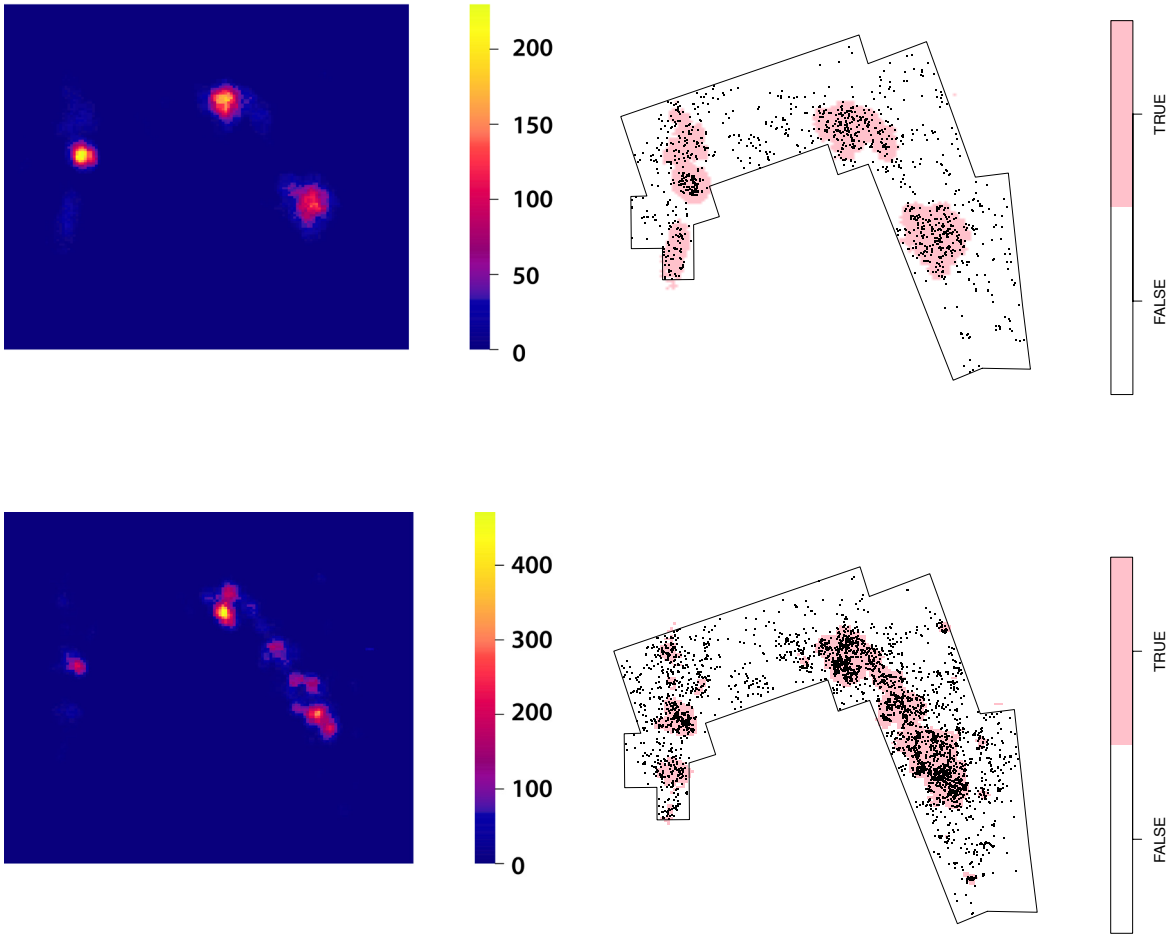

FIGURE 3.70. *Highest density areas of the bones point pattern (a) and the lithics point pattern (b)*

as opposed to randomly mixed. There is a strong positive correlation between points of the same type. A further segregation test also shows significant results (T = 0.14; p-value = 0.025), indicating that both spatial patterns are not independent and have significantly different probability distributions. The results of the mark connection and of the mark equality function also show that two points lying close together or nearby are more likely to be of the same type than would be expected under random labelling (Figure 3.73). This could be a sign of positive correlation between points of the same type, of negative association between points of different types or both.

3.6.4. Simulation of the point pattern outside the excavation window through statistical modelling

3.6.4.1. Inhomogeneous Poisson models

The first model (F1) shows that the topography covariate is significant, as expected from the previous analyses. However, the relationship between topography and intensity is not linear, as indicated by the "rhohat" function (see Figure 3.74A). Figure 3.74B shows the smoothed partial residual diagnostic graph for the transformation of the topography covariate in the cubic polynomial Poisson point process model (F2). Although there is an important divergence between both functions in low topographic areas, this model seems more suitable (Figure 3.74B). An ANOVA and the comparison between both AICs confirms this. When the Cartesian coordinates are added, the models

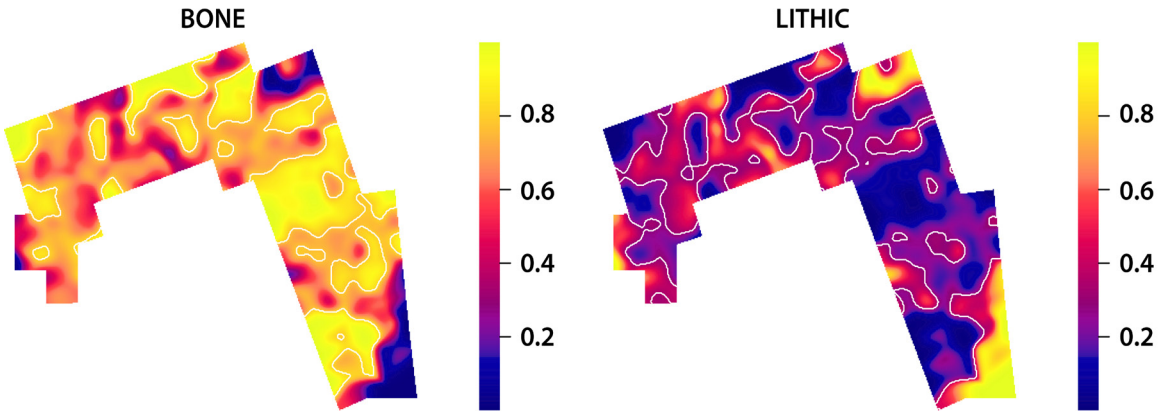

FIGURE 3.71. *Relative risk maps showing the relative probability of finding bones and lithics throughout the excavated area at DS. Bones occur in a significantly higher proportion, but lithics are more strongly clustered on the three high density spots.*

become more accurate (Table 3.52). The differences between the intensities of bones and lithics are significantly relevant as well but cannot be included in the simulations. Therefore, I made the simulation using the intensity function of regression model F4. The predicted simulation shows a very similar spatial intensity variation, but fails to predict the highest density areas, hot spots or clusters (Figure 3.75).

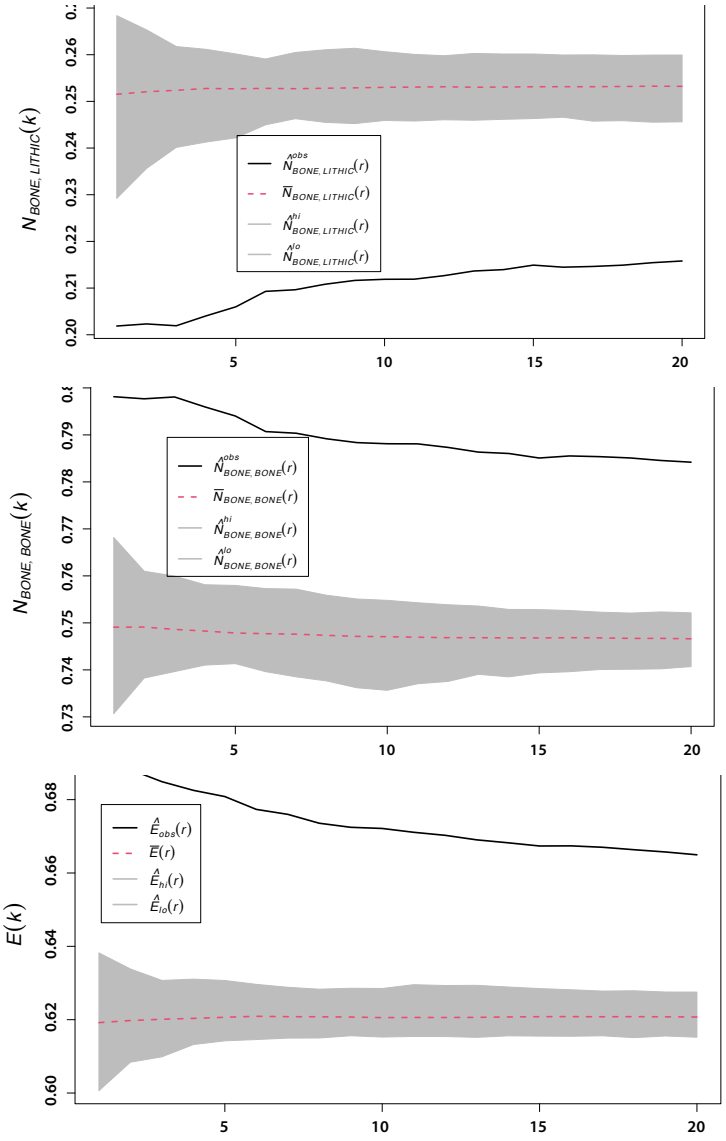

FIGURE 3.72. *A) Cumulative proportion of lithics that are observed at the kth nearest neighbors when measured from bones. The theoretical line represents the expected proportion if both types of points were randomly mixed. . B) The fraction amongst the kth nearest neighbors that are of the same type as the point of origin.. C) Summary of plots A and B showing the proportion of points of the same type as the original point.*

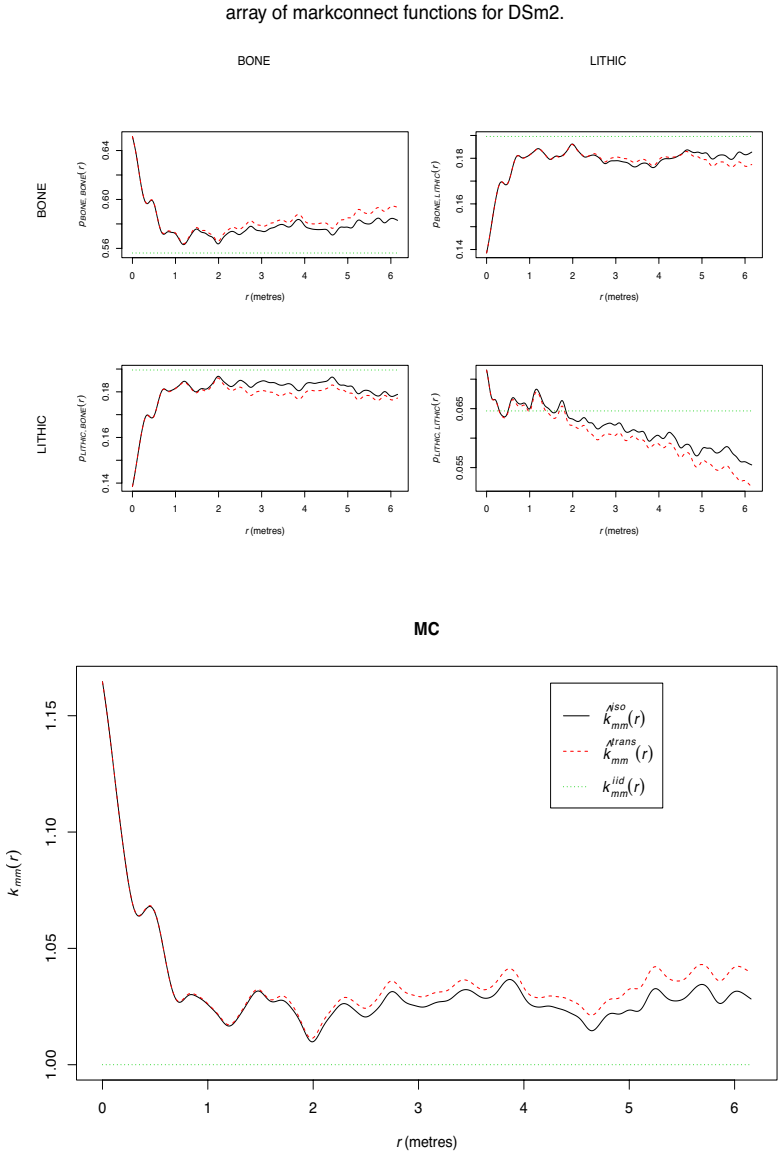

FIGURE 3.73. *Mark connection function. Points lying close together are more likely of the same type.*

TABLE 3.52. *AIC values for models F1-F4*

Formula	AIC
F1 <- ppm(DS~top)	-11199.23
F2 <- ppm(DS~polynom(top,3))	-11308.58
F3 <- ppm(DS~polynom(x,y,3))	-12687.42
F4 <- ppm(DS~polynom(x,y,3) + top)	-13798.09

3.6.4.2. Simulation of Cox Process

Figure 3.76 shows the intensity maps of several different simulations of the spatial patterning of archaeological materials in and outside the excavation window at DS based on the same Cox process model. Based on this model, the spatial patterning at the site is characterized by multiple clusters or concentrations of materials. According to these predictions, the most significant clusters have been preserved and excavated, since they very often appear inside the limits of the site, whereas the eroded part of the site would have been much lower than in the preserved excavated locations. This would indicate that not so much archaeological material has been lost to erosion.

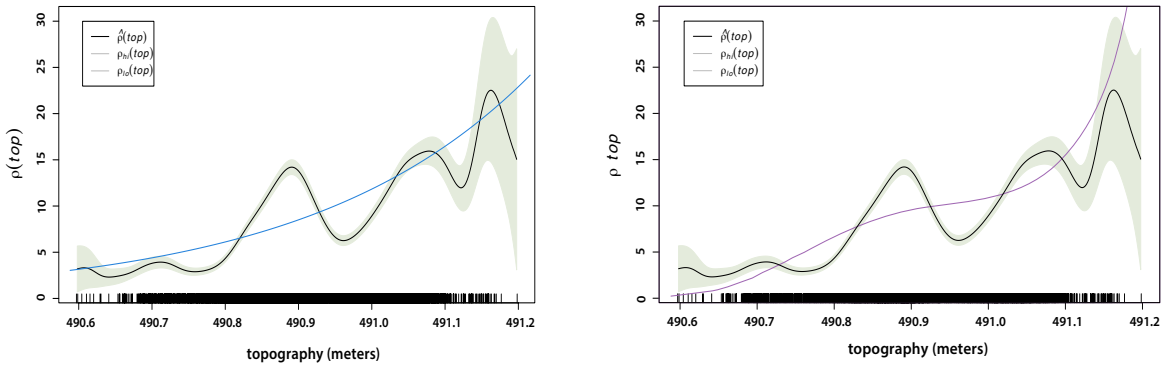

FIGURE 3.74. *A) Rhohat function showing that the relationship between topography and intensity is not linear. B) Rhohat function with the transformation of the the topography covariate in the cubic polynomial Poisson point process model.*

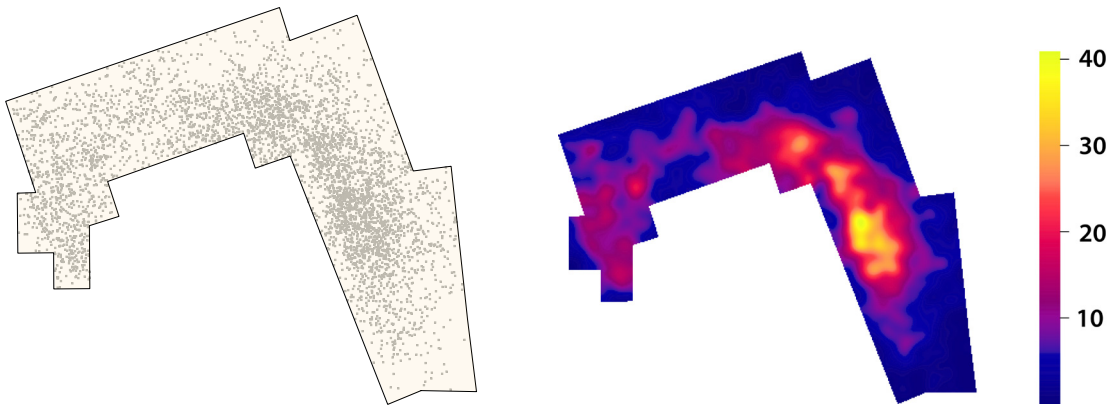

FIGURE 3.75. *A) Point pattern of the simulation made using the intensity function of the regression model F4 (table 3.61.) B) Density map resulting from the same simulation model.*

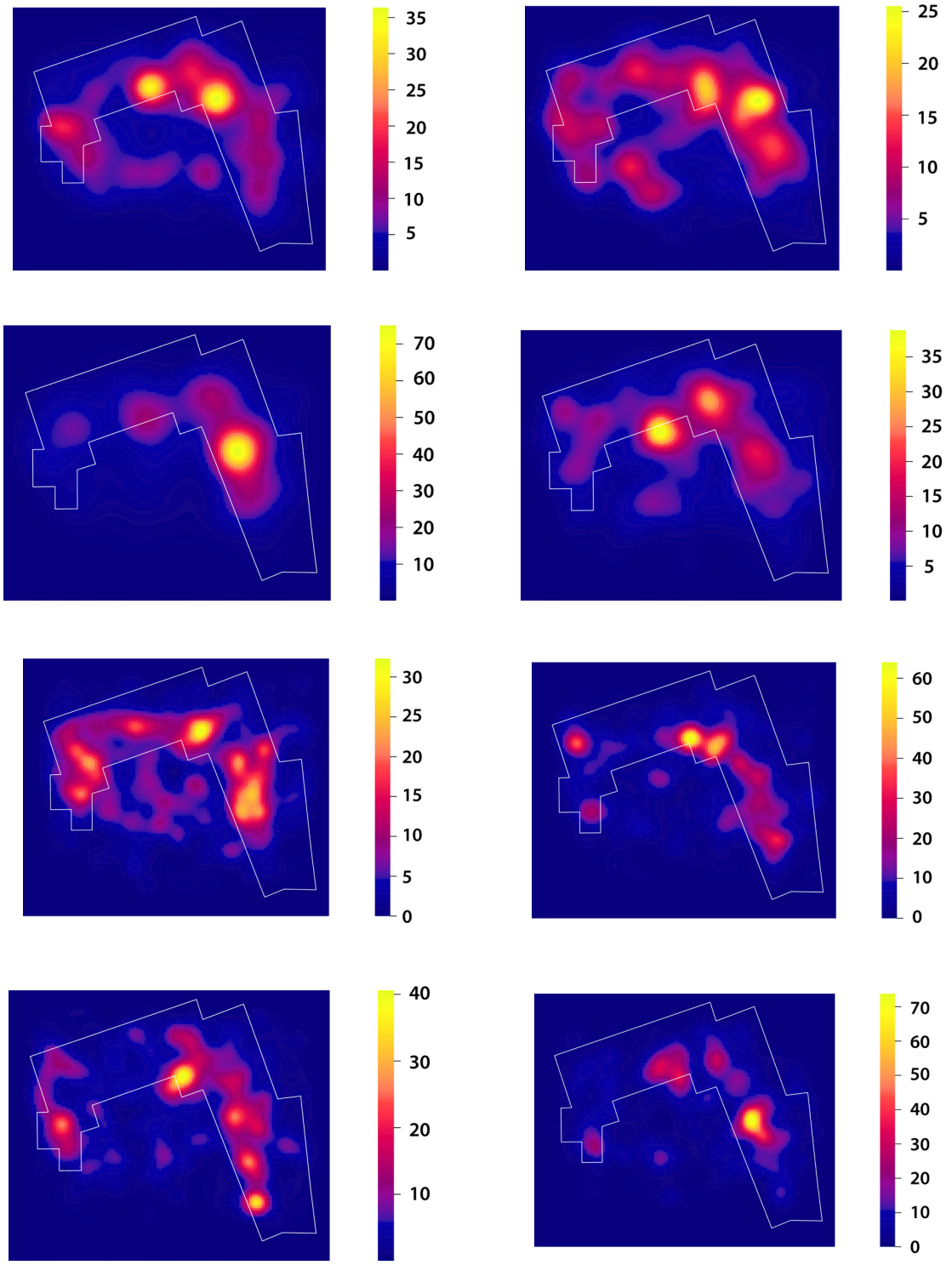

FIGURE 3.76. *Intensity maps of several simulations made of the spatial pattern inside and outside of the DS excavation window based on the same Cox process model.*

3.7. *Spatial analysis of high density areas*

3.7.1. *Spatial comparison of the high intensity spots at DS to the clustering areas of FLK* ***Zinj,*** *PTK and several modern hunter-gatherer campsites*

Tables 3.53 - 3.56 show the estimated cluster parameter values organized according to variable type for the spatial point patterns of bones, lithics, and for both types of remains combined for each site, as well as the resulting values for the multiple cluster patterns of bone remains of modern hunter-gatherer campsites. The results obtained in each cluster analysis and in the random forest models are illustrated in Figures 3.77 and 3.78 and described below.

3.7.1.1. Bone clusters at hominin sites vs. clusters at modern forager campsites

The most notable difference among all the bone clusters analyzed is found between the hunter-gatherer campsites and the archaeological sites (Figure 3.77A). This means that, as expected, the multiple-cluster pattern at DS is not similar in any way to the spatial patterning created by modern humans. The differences can be appreciated mainly in the total area of the site and the mean intensity of the sites, according to the random forest model (Balanced accuracy: 1, Kappa: 1) (Figure 3.78A). Hunter-gatherer campsites are almost ten times bigger than archaeological sites, but the intensity of accumulated bone remains is on average about seven times lower than that documented at hominin sites. This is probably the most remarkable difference of early hominin sites and modern forager camps, and this discrepancy must have profound behavioral meaning. Clusters at forager camps also present lower intensities and longer distances between nearest neighbors than those documented at the Olduvai sites. Interestingly, the ratio between the mean intensity of points inside the clusters and the mean intensity of the complete window is higher at foraging camps and, although the main cluster area is bigger in general, it represents a smaller percentage of the total forager campsite area (Tables 3.53A, 3.54B, and 3.55A). The higher value of this ratio in modern forager camps would indicate that debris-discarding behaviors are less spatially restricted and more widespread and focalized at modern camps than at the Olduvai sites.

Table 3.53. *Estimated cluster parameter values for A) the spatial patterns of bones, including hunter-gatherer camps, B) the spatial patterns of lithics, and C) the overall spatial patterns. 1. Area of cluster, 2. Diameter of cluster, 3. Perimeter of cluster, 4. Intensity of cluster, 5. Number of peaks inside cluster, 6. Mean distance of points to the boundary of the cluster, 7. Mean distance of points to the centroid of the cluster, 8. Mean distance of nearest neighbors inside cluster, 9. Perimeter/Diameter, 10. Length/Breadth*

A

Site	1	2	3	4	5	6	7	8	9	10
Area_A	22.562	9.850	24.747	15.023	2	7.847	25.493	1.086	2.512	2.211
Area_B	20.465	8.004	26.482	31.272	2	7.486	21.660	0.897	3.309	1.044
Area_C	28.438	8.517	29.549	28.377	2	8.371	25.454	0.932	3.469	1.333
FLK_Zinj	18.250	6.486	19.738	41.589	3	12.420	21.616	1.215	3.043	1.353
PTK	24.966	7.747	24.344	27.477	3	10.817	22.274	0.890	3.142	1.161
KANI	56.250	11.574	37.841	1.689	3	11.838	26.287	2.907	3.269	1.298
KUNAH	34.505	9.331	30.882	4.086	2	8.951	27.249	2.548	3.310	1.711
KUNG	9.648	5.038	15.718	3.11	2	12.193	23.815	4.685	3.120	1.063
OABE	81.228	13.165	40.265	3.152	2	12.460	24.391	1.722	3.059	1.164

B

Site	1	2	3	4	5	6	7	8	9	10
Area_A	7.123	3.419	9.716	13.478	3	20.580	23.217	3.226	2.842	1.054
Area_B	33.824	10.109	27.524	7.214	4	10.419	19.767	1.605	2.723	0.783
Area_C	35.081	8.549	25.754	7.212	3	13.595	23.729	1.825	3.013	1.200
FLK_Zinj	16.489	5.565	16.223	30.628	5	15.549	23.702	1.456	2.915	1.061
PTK	27.262	6.623	20.811	13.315	4	18.184	24.022	1.670	3.142	1.051

C

Site	1	2	3	4	5	6	7	8	9	10
Area_A	8.516	4.465	14.793	35.699	4	12.495	21.676	1.600	3.313	0.923
Area_B	25.272	8.845	25.369	36.087	2	8.742	21.417	0.765	2.868	0.887
Area_C	30.891	8.501	24.865	33.473	2	10.545	24.669	0.892	2.925	1.327
FLK_Zinj	17.842	6.370	18.619	71.180	4	12.837	21.676	1.038	2.923	1.349
PTK	22.029	7.398	22.305	41.128	1	10.377	22.093	0.826	3.015	1.136

Table 3.54. *Estimated values for the variables related with the overall spatial window regarding A) the spatial patterns of bones, including hunter-gatherer camps, B) the spatial patterns of lithics, and C) the overall spatial patterns.*

A

Site	11	12	13	14	15	16
	Number clusters window	Distance neighbors window	Area window	Distance centroid window	Intensity window	Area secondary clusters window
Area_A	3	0.757	159.451	21.108	5.356	8.088
Area_B	3	0.524	211.644	17.781	6.677	5.835
Area_C	3	0.541	193.815	15.581	6.584	1.268
FLK_Zinj	2	0.248	145.390	6.991	9.671	3.002
PTK	3	0.479	183.774	13.302	7.651	1.47
KANI	8	1.187	1197.162	17.472	0.249	11.496
KUNAH	22	0.607	1264.515	21.042	0.423	3.812
KUNG	12	0.750	925.640	18.760	0.215	4.241
OABE	3	0.628	1165.117	11.645	0.352	30.885

B

Site	11	12	13	14	15	16
Area_A	4	1.179	159.451	21.339	2.509	5.411
Area_B	1	1.128	211.644	15.783	1.942	0
Area_C	1	1.025	193.815	15.439	1.914	0
FLK_Zinj	2	0.316	145.390	6.204	5.199	3.021
PTK	1	0.183	183.774	2.483	2.601	0

C

Site	11	12	13	14	15	16
Area_A	6	0.132	159.451	20.886	7.864	4.883
Area_B	3	0.115	211.644	17.144	8.708	5.714
Area_C	5	0.114	193.815	18.081	8.498	1.319
FLK_Zinj	2	0.100	145.390	6.726	14.870	2.685
PTK	1	0.093	183.774	12.770	10.252	1.138

Table 3.55. *Estimated values for the variables that describe the relation between the cluster areas and the overall spatial window regarding A) the spatial patterns of bones, including hunter-gatherer camps, B) the spatial patterns of lithics, and C) the overall spatial patterns.*

A

Site	17	18	19	20	21
	Percentage area cluster	Percentage diameter cluster	Percentage perimeter cluster	Intensity cluster/ Intensity window	Area secondary clusters/Area cluster
Area_A	14.150	47.776	39.233	2.805	0.717
Area_B	9.670	33.534	40.733	4.622	0.570
Area_C	14.673	37.636	48.711	4.310	0.089
FLK_Zinj	12.552	11.282	12.184	4.301	0.164
PTK	13.585	34.708	33.080	2.680	0.059
KANI	4.699	23.221	27.106	6.785	0.204
KUNAH	2.729	18.248	21.538	9.658	2.320
KUNG	1.042	11.676	12.899	14.469	4.560
OABE	6.972	26.752	29.245	8.956	0.380

B

Site	17	18	19	20	21
Area_A	4.467	16.583	15.403	5.373	2.279
Area_B	15.982	42.354	42.336	3.715	0
Area_C	18.100	37.777	42.455	3.768	0
FLK_Zinj	11.341	9.680	10.014	5.890	0.165
PTK	14.834	29.669	28.280	5.119	0

C

Site	17	18	19	20	21
Area_A	5.341	21.657	23.452	4.539	0.465
Area_B	11.941	37.058	39.021	4.144	0.157
Area_C	15.938	37.565	40.989	3.939	0.128
FLK_Zinj	12.272	11.080	11.493	4.787	0.150
PTK	11.987	33.143	30.310	4.012	0.052

TABLE 3.56. *Estimated values for the variables used to describe the correlation between bone and lithic clusters of the overall spatial patterns.*

D

Site	22	23	24	25	26	27	28
	Overlap bone cluster and lithic cluster/No overlap area	Area bone cluster/ Area lithic cluster	NN-correlation (norm.)	NN-correlation (unnorm.)	Percentage overlap	Percentage no overlap	Intensity bone cluster/Intensity lithic cluster
Area_A	0.429	3.167	0.638	1.129	0.228	0.532	1.115
Area_B	13.825	0.605	0.705	1.079	0.343	0.025	4.464
Area_C	4.549	0.811	0.739	1.135	0.367	0.081	3.935
FLK_Zinj	5.336	1.107	0.650	1.192	0.442	0.083	1.712
PTK	5.624	0.905	0.676	1.088	0.446	0.079	2.941

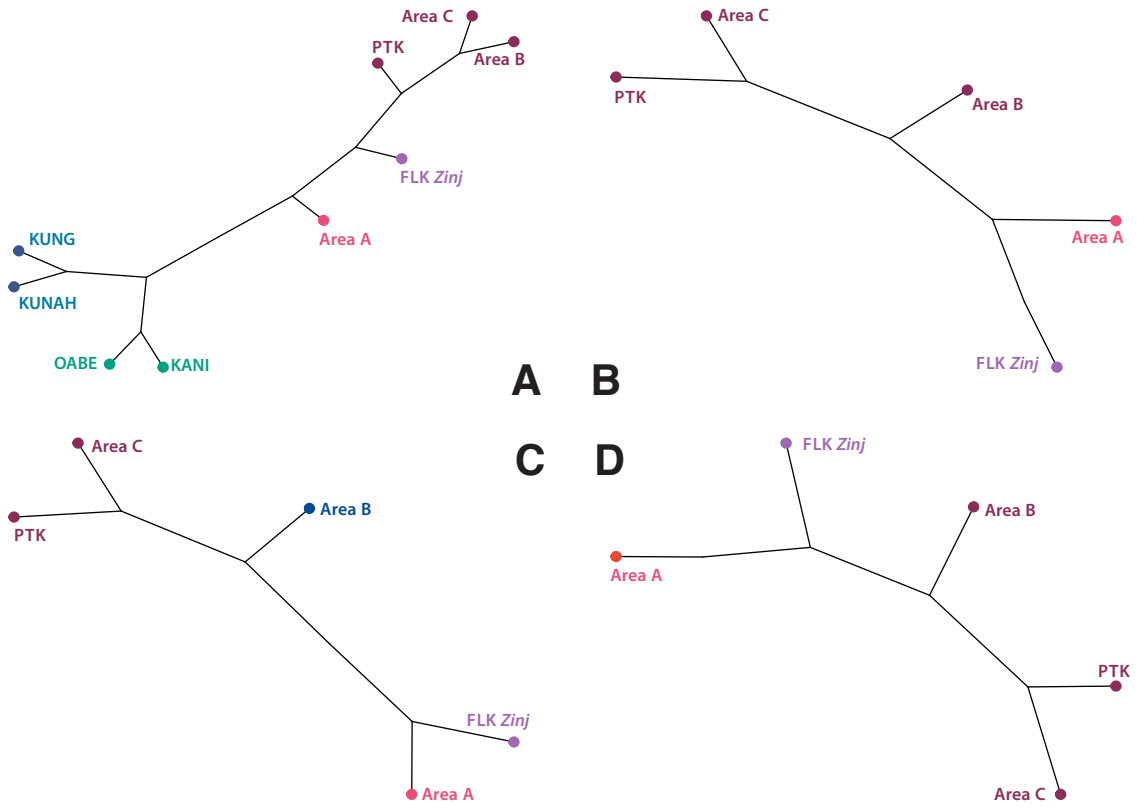

FIGURE 3.77. *Classification of the A) bone (including campsites), B) bone (excluding campsites), C) lithic, and D) overall clusters from areas A, B, C from DS, FLK Znj and PTK.*

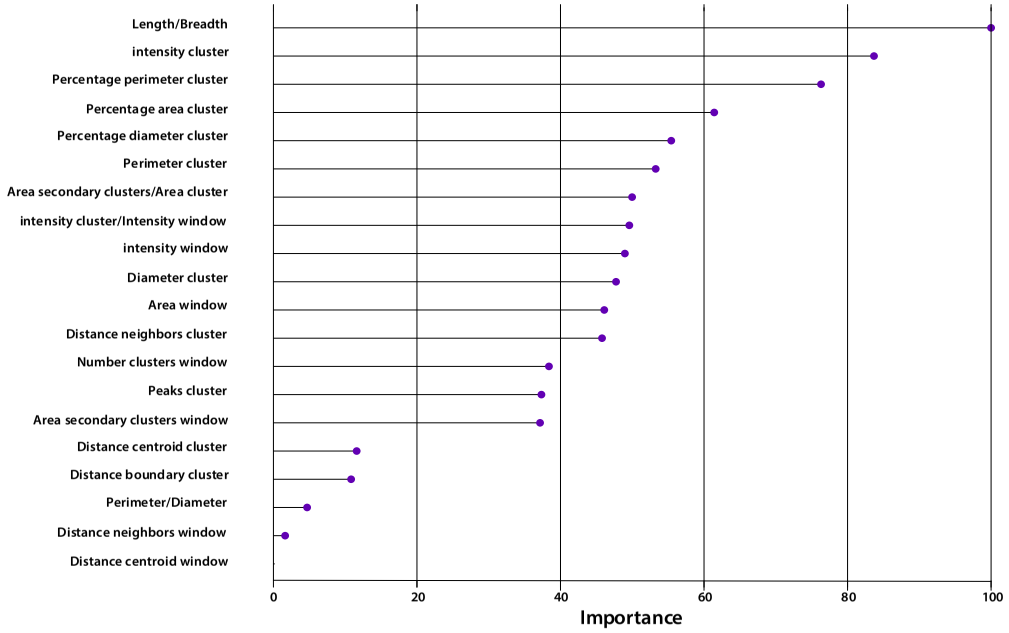

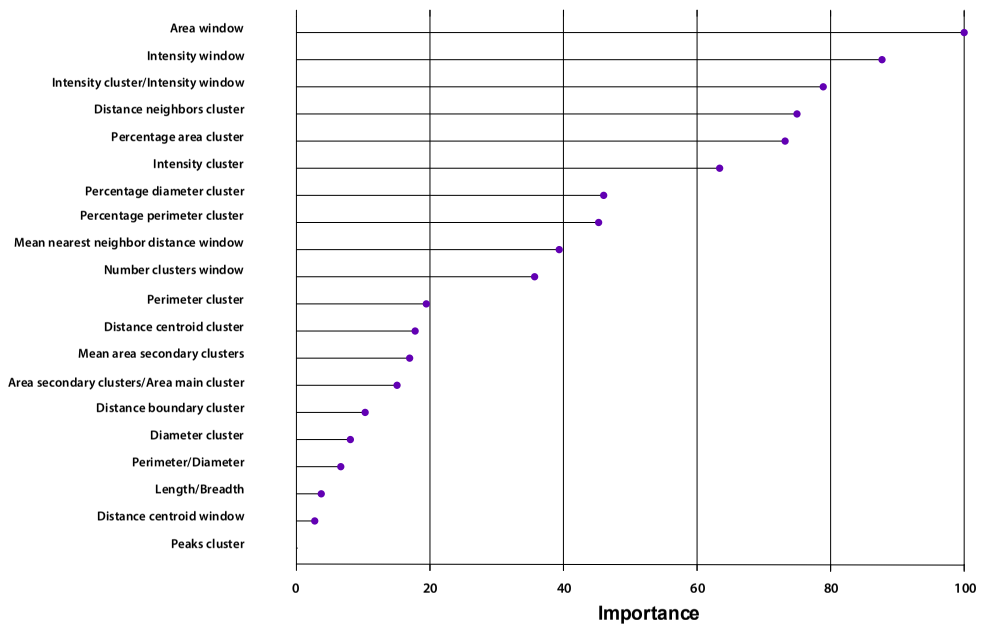

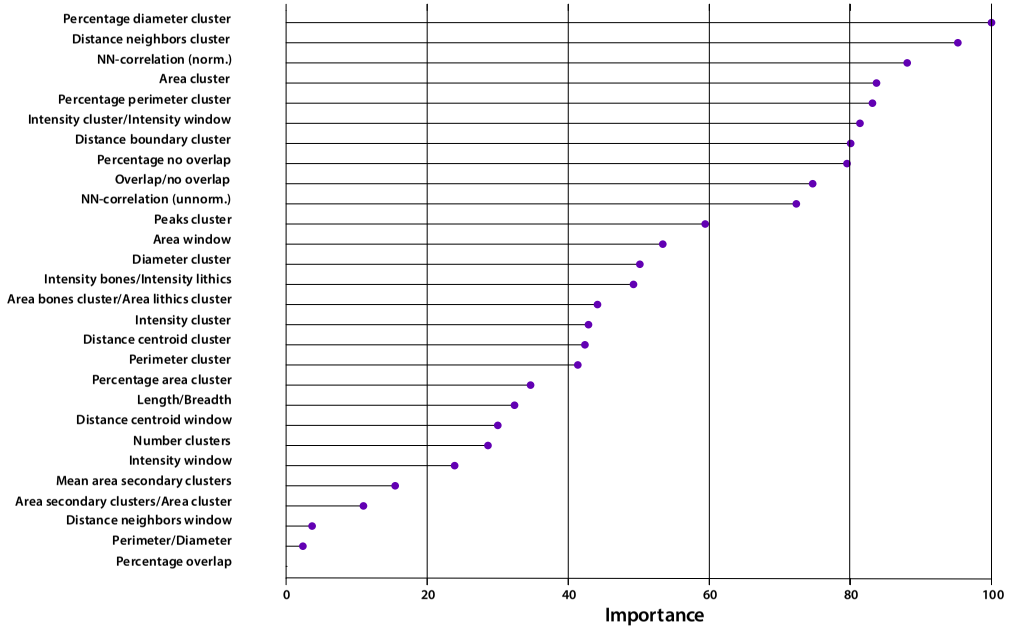

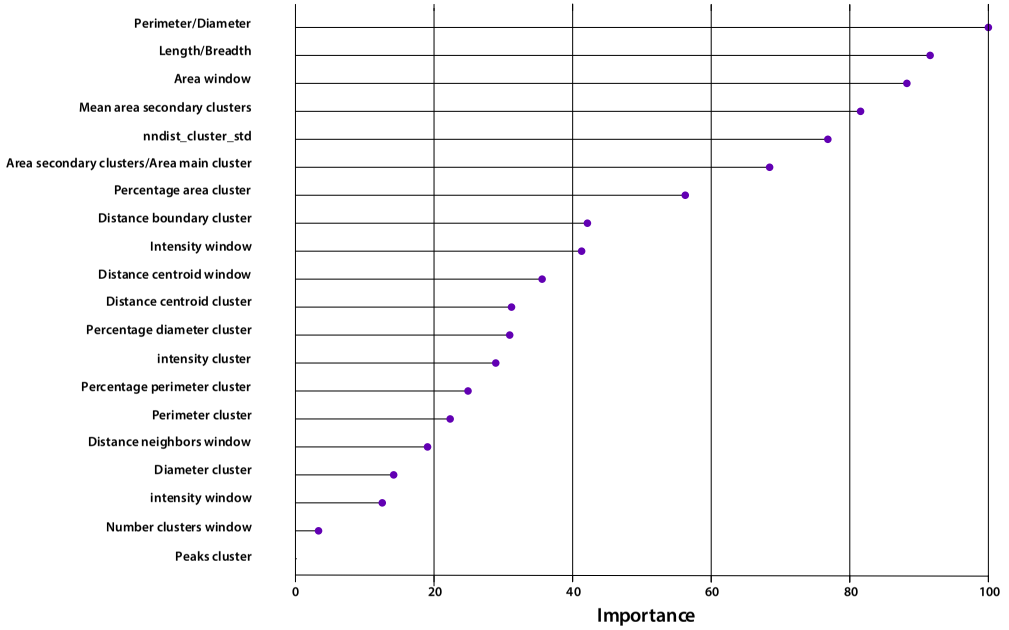

FIGURE 3.78. *Importance of the variables used in the random forests models carried out to establish the most discriminating variables.*

The forager campsites appear further subdivided into two groups, one includes the Kua camps 1 and 2 (Kanni//am//odi: household 7 and oabe 1), the other group the Kua camp 3 and the !Kung camp 4 (Kunahajina and //Gakwe Dwa 2). The camps in the first group share the facts that they were occupied only seasonally and by a similar number of people, and that food remains were accumulated around three hearths. These factors result in similarly sized campsites and clusters, as well as in similar densities inside the clusters of material debris (Tables 3.53A and 3.54A). The other two foraging camps do not share similarities in their formation at first glance, since one was occupied for months and the other only for a few days. However, the fact that the main cluster areas in front of the huts were cleaned in camp 3, and that main activity at camp 4 was honey gathering and not carcass butchering, probably resulted in smaller clustering areas as well as lower material densities, which are two of the factors these camps have in common (Table 3.53A and 3.54A).

3.7.1.2. Bone cluster patterns at DS, FLK Zinj and PTK

On the other end of the cluster dendrogram, areas B and C from DS are grouped together. These two clusters are also closely linked to the bone cluster found at PTK, which in turn lies close to the bone cluster from FLK *Zinj*. These four clusters form a group separate from Area A at DS (Figure 3.77A). In order to approach the potential differences inherent in the variability of the patterns documented at the Olduvai sites, a second analysis was made excluding the modern forager camps. When foraging camps are left out of the cluster analysis, the classification varies slightly (Figure 3.77B): area C is grouped with PTK, both lie closer to area B than to area A and FLK *Zinj*, which present more distinct spatial features. FLK *Zinj* appears the most isolated (Figure 3.77B). The variation with respect to the previous analysis occurs because this classification is based on the effect of other variables, as shown in the corresponding random forest model (Balanced Accuracy: 1, Kappa: 1; Figure 3.78B). While the contrast between foraging camps and anthropogenic sites is mainly related to the overall spatial window and differences in the intensities of the clusters, the archaeological bone assemblages are separated primarily based on variations in the shape of the clusters, as described by the ratios between perimeter and diameter, as well as between maximum length and breadth. Areas B and C, PTK, and FLK *Zinj* show irregular but round shapes, whereas area A presents an elongated shape (Table 3.53A). The total area and the percentage of the total area comprised by the main cluster, as well as the mean nearest neighbor distance inside the clusters and the areas of the secondary clusters also play an important role in the classification (Figure 3.78B). FLK *Zinj* and area A stand away from the other sites mainly because nearest neighbors inside their main clusters are separated by longer distances than at the other locations, and be-

cause the size of its second biggest bone cluster is dissimilar to the secondary clusters at the other sites (Tables 3.53A and 3.55A).

3.7.1.3. Lithic cluster patterns at DS, FLK Zinj and PTK

The cluster analysis of the lithic point patterns shows that the spatial distribution of lithic remains at DS is different in each of the three areas: Area C resembles PTK and they form a distinct pair, while Area A shows similarities to FLK *Zinj*, and the lithics in Area B appear more isolated, although their distribution bears some similarities with the cluster in Area C (Figure 3.77C; Tables 3.53B, 3.54B, and 3.55B). The random forest model (Balanced accuracy: 1, Kappa: 1) shows that the most relevant factors in this analysis are the shape, the intensity, and the size of the clusters in relation to the complete site (Figure 3.78C).

The main similarity between the lithics cluster at PTK and the cluster in Area C is their irregular shape, as described in the ratio between the perimeter and the diameter of the cluster (Figure 3.78C, Table 3.53B). The lithics cluster in Area B is characterized by the most elongated shape, as well as the smallest distances of the points inside the cluster to the cluster boundary and to the cluster centroid with regard to cluster diameter (Table 3.53B), although these last two variables do not have a great effect in the classification (Figure 3.78C). The main common factors between the clusters in area A and in FLK *Zinj* are their size and the size of the surrounding smaller secondary areas with regard to the size of the overall spatial window and the main cluster area, respectively (Tables 3.54B, and 3.55B). Area A yields the lowest values for cluster area, perimeter, and diameter followed by FLK *Zinj*, which presents the smallest mean distance between the nearest neighbors inside the cluster (Table 3.53B). This variable also shows that stone tools appear concentrated in a smaller area. This is probably also related to the fact that the highest intensity of lithic remains per square meter is found at FLK *Zinj*. The ratio between the intensity of stone tools inside the cluster area and the overall mean lithic intensity is very similar to that obtained for area A, and both are higher than in any of the other lithic assemblages.

3.7.1.4. Overall cluster patterns at DS, FLK Zinj and PTK

The cluster analysis of the overall point patterns includes both bones and lithics as well as several additional variables accounting for the correlation between the two types of points and the overlap of their clusters (see Methods). The diagram depicting the importance of the variables according to the respective random forest model (Balanced accuracy: 1, Kappa: 1), indicates that the

most important variables constitute a mixture of the different types of variables included, except variables related to the overall spatial windows (Figure 3.78D). The most relevant variables related to the clusters are percentage diameter, cluster area, and percentage perimeter, as well as the mean nearest neighbor distance inside the cluster, and the important variables related to the correlation between the bones and lithics include the results obtained for the nearest neighbor correlation and the overlap area between bone and lithic clusters. Interestingly, the shape of the clusters, the overall intensity of the point pattern or the number of secondary clusters which were important in the classifications when bones and lithics were analyzed separately, seem to play a less significant role in this analysis (Figure 3.78D**;** Tables 3.53C, 3.54C, 3.55C, and 3.56).

The cluster analysis yields a very similar classification to the one for the lithics clusters: area C and PTK appear on one end of the diagram separated from area B - which appears on a separate branch-, and FLK *Zinj* and area A on the other end of the dendrogram, which are not completely grouped together (Figure 3.77D). The position of each cluster may have been conditioned by the small sample size with which this analysis was carried out, or by the minor variation of the classification of area A, which appears closer to FLK *Zinj* in the case of the lithic spatial patterns than when regarding the spatial distribution of bones.

In sum, these analyses suggest that clusters A, B and C at DS are different from each other regarding the spatial distribution of bone and lithic remains. Area A appears to be more related in general to FLK *Zinj*, especially in the spatial distribution of lithics, and area C is very similar to PTK, while area B only clusters in between both sets of clusters. This could suggest that the formation of these clusters of materials differed in some respects. For example, cluster B could have been used for stone tool knapping activities in addition to butchering activities, which would have resulted in a different spatial distribution of lithics. Regardless of the archaeological significance of these differences, however, the similarities between the areas of DS and the clusters from FLK *Zinj* and PTK suggest that the formation of these three sites does indeed share some important commonalities.

All this gives rise to the next questions: are the differences between the three observed groups of clusters (type 1: Area A and FLK *Zinj*, type 2: Area C and PTK, and type 3: Area B) only spatial or do they reflect different formation histories? Were the clusters formed as the result of different behaviors or activities or did a generally similar behavior generate the spatial variability represented at these three sites? This last question seems justified given the small sample size with which this analysis was carried out. Bootstrapping a very small sample can artificially create greater disparities between the groups. Future efforts will focus on increasing the sample size to include more anthropogenic sites, but also palimpsests and carnivore accumulations. For now, it is worthwhile

Table 3.57. *Coefficients, standard errors and p-values for the coefficients of the levels of the factor variables included in the first multinomial regression model regarding the site's preservation.*

Residual Deviance	806.5928
AIC	862.5928

Variables	Factor level		Coefficient	Standard error	p-value
Trampling	true	B	0.9454123	0.7521014	0.2087436
		C	0.7701987	0.7899043	0.3295339
Microabrasion	**true**	**B**	-0.5909273	0.6314445	0.3493586
		C	-0.7489244	0.6785082	0.2696882
Biochemical marks	**true**	**B**	-0.3144294	0.4116398	0.4449590
		C	0.4144265	0.4593740	0.3669746
Affected by water	**true**	**B**	0.1653749	1.423642	0.9075232
		C	-12.2529529	1.036705e-05	0
Abrasion	**true**	**B**	-33.20003	1.019994e-07	0
		C	-38.44405	1.72537e-09	0
Chemical weathering	**true**	**B**	0.4544937	0.7211582	0.5285457
		C	-1.5955714	0.9762133	0.1021645
Dry fractures	**true**	**B**	0.2560979	1.118897	0.8189589
		C	1.7011606	1.080728	0.1154673
Cortical preservation	**moderate**	**B**	-0.5989367	0.4013971	0.1356651
		C	-0.5907467	0.4290334	0.1685355
	poor	**B**	-2.054326	1.680538	0.2215482
		C	1.086672	1.443226	0.4514821
Carbonate	**true**	**B**	0.550579	1.402480	0.6946333
		C	-17.236168	2.699638e-07	0
Manganese	**true**	**B**	0.005267645	0.6116538	0.9931286
		C	0.037412394	0.6483540	0.9539847
Weathering	**1**	**B**	15.83444	0.6737519	0
		C	14.10619	0.6737522	0
	2	**B**	-0.2344290	1.426533	0.8694676
		C	-0.4060059	1.464424	0.7815911
Intercept		**B**	1.6479216	0.6801613	0.01539974
		C	0.6733512	0.7323228	0.35784812

Table 3.58. *Coefficients, standard errors and p-values for the coefficients of the levels of the factor variables included in the second multinomial regression model regarding the anatomical and taxonomic profiles represented at DS*

Residual Deviance	**228.0584**

Variables	**Factor level**		**Coefficient**	**Standard error**	**p-value**
Skeletal part	axial	B	2.289060	0.8496734	0.00705902
		C	1.039566	0.9531042	0.27539792
	cranial	**B**	-0.6144787	1.446598	0.6710006
		C	1.6529123	1.100377	0.1330629
Animal size	**medium**	**B**	0.2038104	1.122946	0.8559782
		C	-1.3058256	1.066412	0.2207622
	large	**B**	25.741298	2.88e-10	0
		C	-7.715307	4.64e-14	0
Taxon	**Antilopini**	**B**	-1.037486	1.369251	0.4486287
		C	-1.879181	1.327856	0.1570101
	Carnivora	**B**	2.1609540	1.649295	0.1901185
		C	0.4888813	1.652359	0.7673304
	Equidae	**B**	-0.9400959	0.7352918	0.2010611
		C	-1.1165317	0.7349162	0.1286961
	Reduncini	**B**	1.2616233	1.020932	0.2165492
		C	-0.1311977	1.036784	0.8993021
	Tragelaphini	**B**	0.009665271	1.163635	0.9933728
		C	-21.5268884	6.16e-09	0
Animal age	**old**	**B**	-9.213839	7.96e-10	0
		C	13.313835	1.079309	0
	prime	**B**	-0.8090866	0.8144663	0.3205176
		C	-1.1080551	0.8480887	0.1913717
Tooth/Bone	**tooth**	**B**	2.7499225	1.2454737	0.02724894
		C	0.2209685	0.8613803	0.79754290
Intercept		B	-0.6014504	1.583663	0.7041055
		C	1.3439258	1.494578	0.3685457

Table 3.59. Coefficients, standard errors and p-values for the coefficients of the levels of the factor variables included in the third multinomial regression model regarding skeletal part representation.

Variables	Factor level		Coefficient	Standard error	p-value
Front/Hind	hindlimb	B	0.4454488	0.8579257	0.6036101
		C	0.5784101	0.9016210	0.5211833
Side	right	B	0.6382675	0.6825102	0.3496974
		C	0.6794709	0.7292504	0.3514715
Proximal/	proximal	B	0.11871260	0.6705248	0.8594736
distal epiphysis		C	0.07851271	0.7212881	0.9133209
Horn	false	B	0.4489565	0.2891165	0.1204574
		C	0.1598595	0.3155885	0.6124748
Intercept		B	0.4489565	0.2891165	0.1204574
		C	0.1598595	0.3155885	0.6124748

to further trace the observed tendencies and explore whether the differences between the clusters are detectable at a taphonomic level as well.

3.7.2. *Comparing the high intensity spots at DS from a taphonomic perspective: Are the clusters taphonomically homogeneous?*

Tables 3.57 – 3.60 show the coefficients, the standard errors, and the p-values of the levels of the factor variables included in the four final regression models. Overall, only ten of a total of 32 variables are significant in the models, which indicates that there are more similarities than differences between the groups, and that it is probable that the three subassemblages produce a relatively similar taphonomic signal.

In the regression model that uses variables related to the site's preservation, only the coefficients of presence/absence of carbonate, presence/absence of water disturbance, subaerial weathering (stage 1), and presence/absence of abrasion were significant, although the small sample size of abraded specimens makes this variable less relevant for the interpretation. It should be emphasized that abraded bones make up only a small fraction of the bone assemblage at DS (see chapter X). The remaining factors included in the model of the preservation of the assemblage (presence/absence of trampling, presence/absence of microabrasion, presence/absence of biochemical marks, presence/absence of

Table 3.60. *Coefficients, standard errors and p-values for the coefficients of the levels of the factor variables included in the fourth multinomial regression model regarding the activities performed at the site by hominins and carnivores.*

Variables	Factor level		Coefficient	Standard error	p-value
CM	true	B	0.21090996	0.4671890	0.6516692
		C	0.03862504	0.5176889	0.9405246
Hot_zone	true	B	-0.3195843	0.9063829	0.7243935
		C	-0.5004423	0.9871148	0.6121725
Cold_zone	true	B	-0.088959455	1.073425	0.9339514
		C	0.008871197	1.140928	0.9937962
Defleshing	true	B	0.9735451	0.8995202	0.2791220
		C	0.7989052	0.9644113	0.4074517
Disarticulation	true	B	1.153618	1.199766	0.3362826
		C	0.337500	1.359784	0.8039788
Impact_flake	true	B	0.1580744	0.3648443	0.6648219
		C	-0.1576761	0.4212598	0.7081836
PM	true	B	1.2020160	0.3589383	0.0008115958
		C	0.3230414	0.4153993	0.4367667577
Impact_points	moderate	B	-0.47843736	0.4347598	0.2711301
		C	-0.01506638	0.4579988	0.9737574
TM	poor	B	2.160164	1.158826	0.06230813
		C	2.256980	1.173920	0.05453018
Furrowing	true	B	-1.255465	1.648199	0.4462278
		C	-2.048613	1.814088	0.2587798
Circumference	2	B	0.3122079	0.3220152	0.3322738
		C	0.4105776	0.3363541	0.2222106
	3	B	0.6633446	0.2946313	0.0243576977
		C	0.9885108	0.2902735	0.0006605589
Green fractures		B	0.3406448	0.2152000	0.1134392
		C	-0.1703359	0.2090592	0.4152020
Intercept		B	-0.14724647	0.2055548	0.4737833
		C	0.05027019	0.1973048	0.7988896

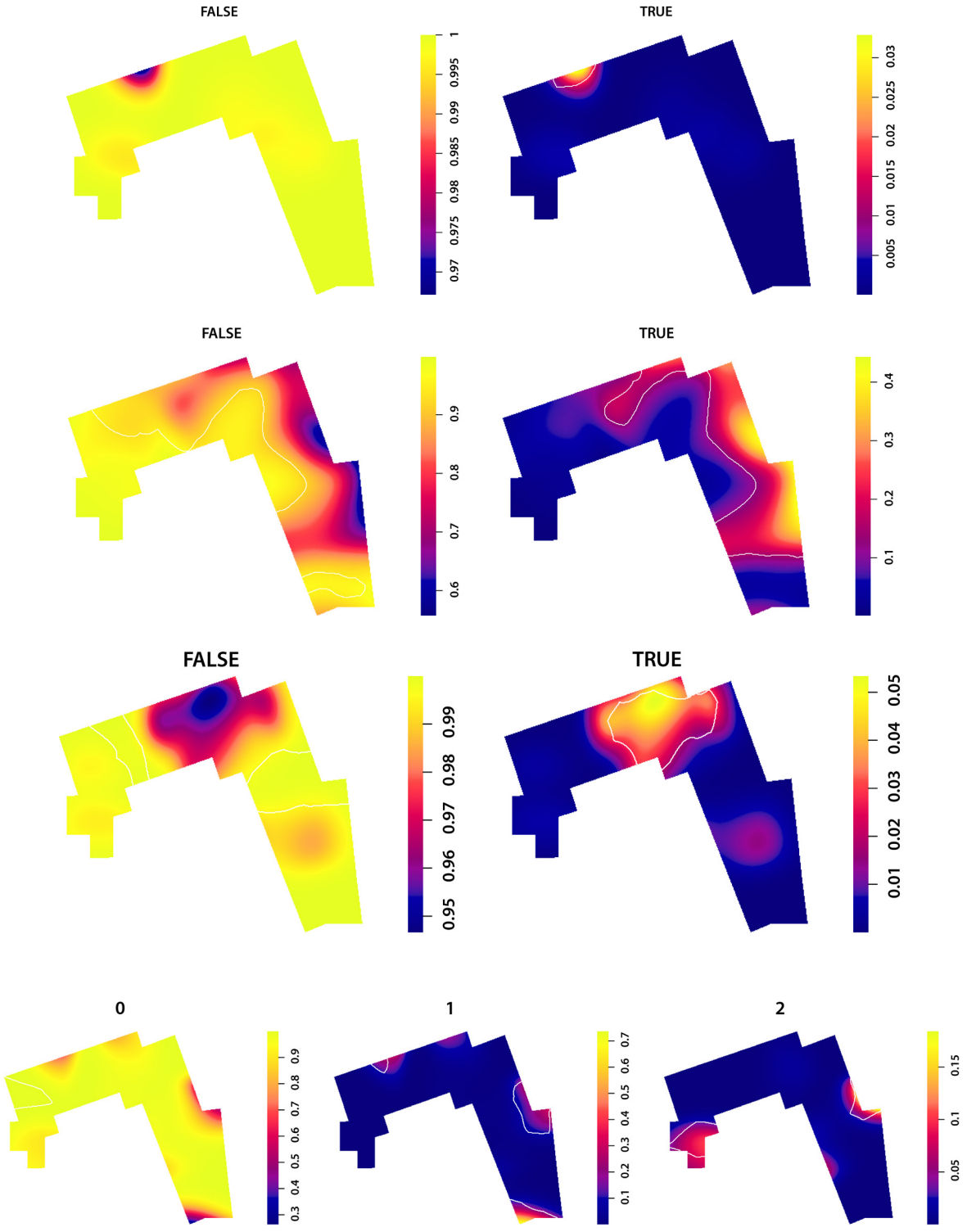

FIGURE 3.79. *Relative risk maps of the spatial distribution of different taphonomic variables. A) abraded and non-abraded specimens, B) bone specimens partially or completely covered with carbonate, C) bone specimens affected by water, D) different stages of weathering documented at the site.*

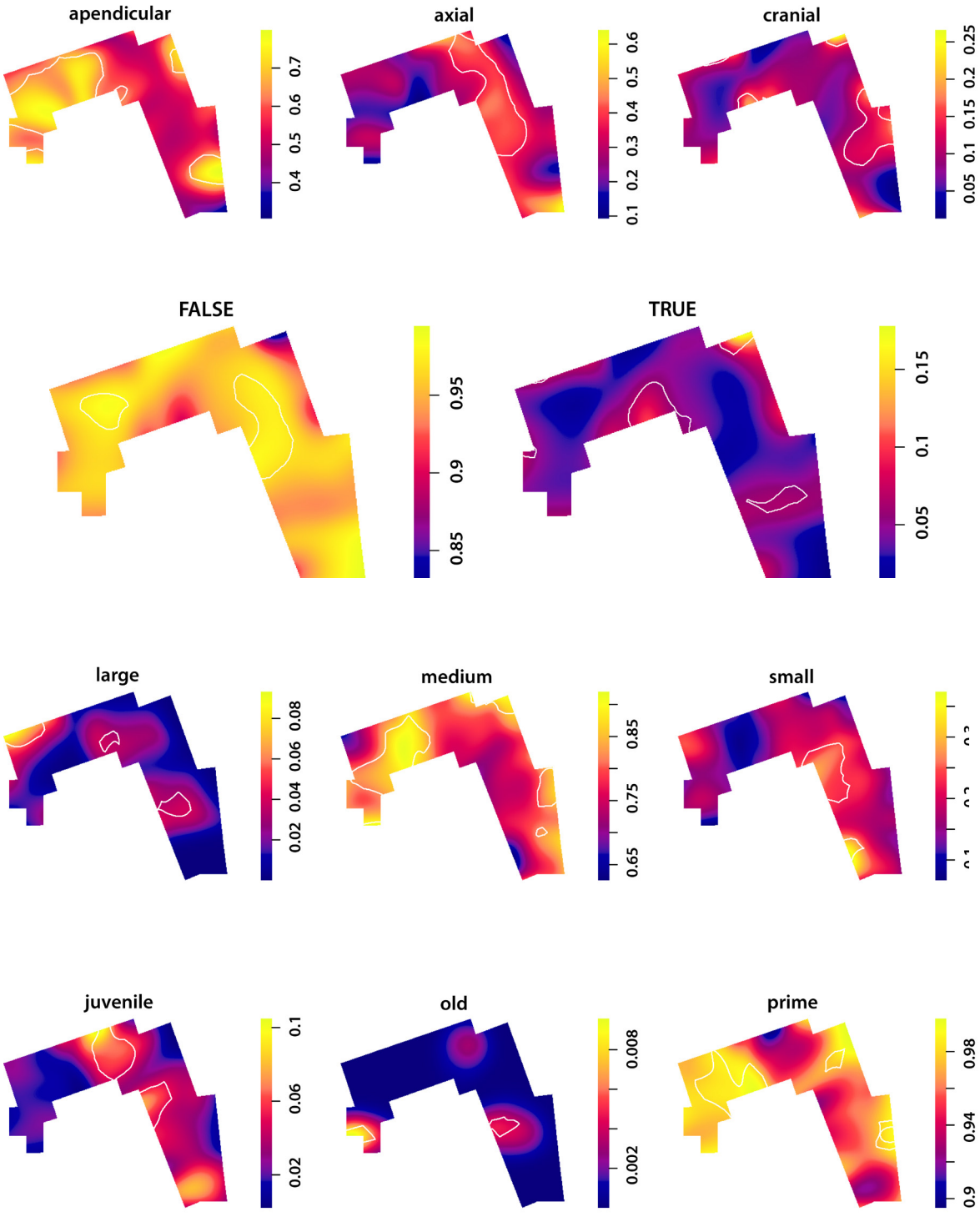

FIGURE 3.80. *Relative risk maps of the spatial distribution of different taphonomic variables. A) different skeletal parts, B) teeth, C) different carcass sizes, and D) different bovid ages.*

chemical weathering, presence/absence of dry fractures, cortical preservation – good, moderate or poor -, and presence/absence of manganese) do not vary significantly between zones A, B, and C.

The distribution, density and relative risk maps of each of the significant variables are presented in Figures 3.79- 3.81 and Figures 7.5-7.13 in the Appendix. Contour lines on the relative risk maps show the regions where the estimated probability of a given type of the variable is significantly different from the average proportion. The number of specimens that present any of the significantly spatially varying features (abrasion, carbonate, water disturbance and weathering stage 1) is relatively low compared to the total number of bone specimens, but some tendencies can be observed (Figure 3.79A-D). For example, water disturbance seems to have affected bone specimens in area B the most, which is also where the majority of abraded specimens are found. There are a number of abraded specimens that fall in a small area of zone A, which is marked as the only location on the site where the proportion of abraded and non-abraded specimens is not kept, and where abraded bones are significantly more abundant than non-abraded bones. The area where the density of water-affected bones is significantly higher than the density of non-affected bones occurs close to this spot, but in area B (Figure 3.79C). Carbonate is most abundant in area C, coinciding with the second densest spot of water-affected

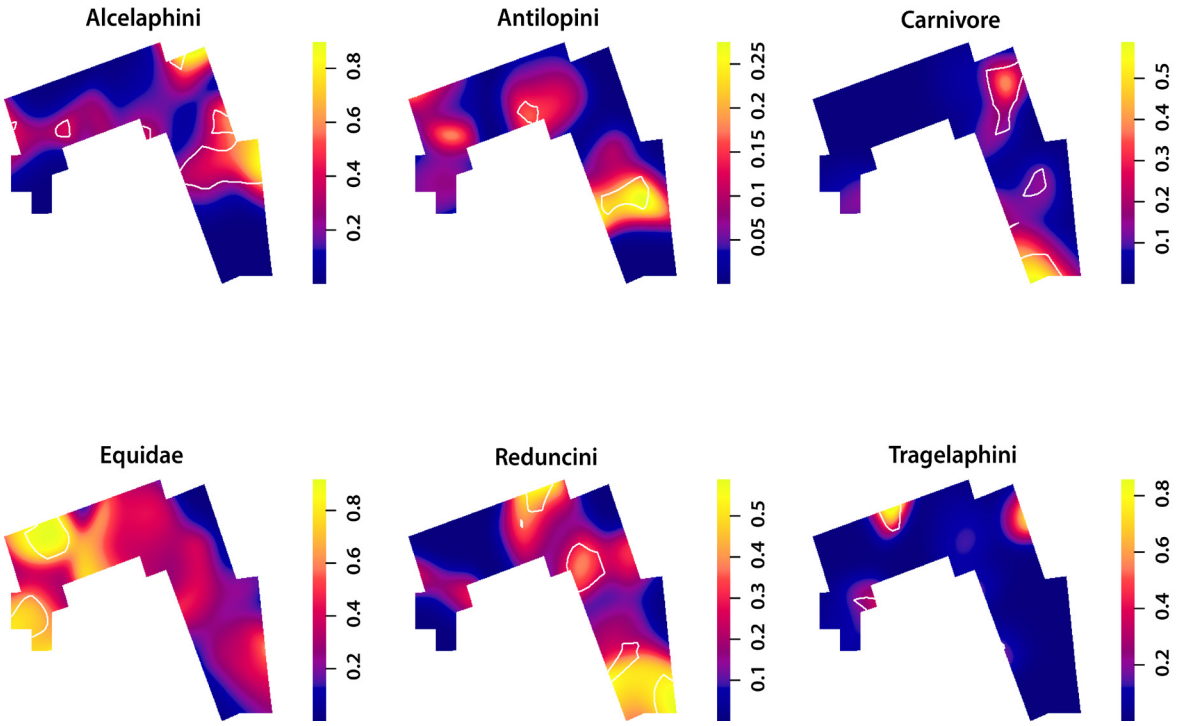

FIGURE 3.81. *Spatial probability distribution of the different represented bovid taxa.*

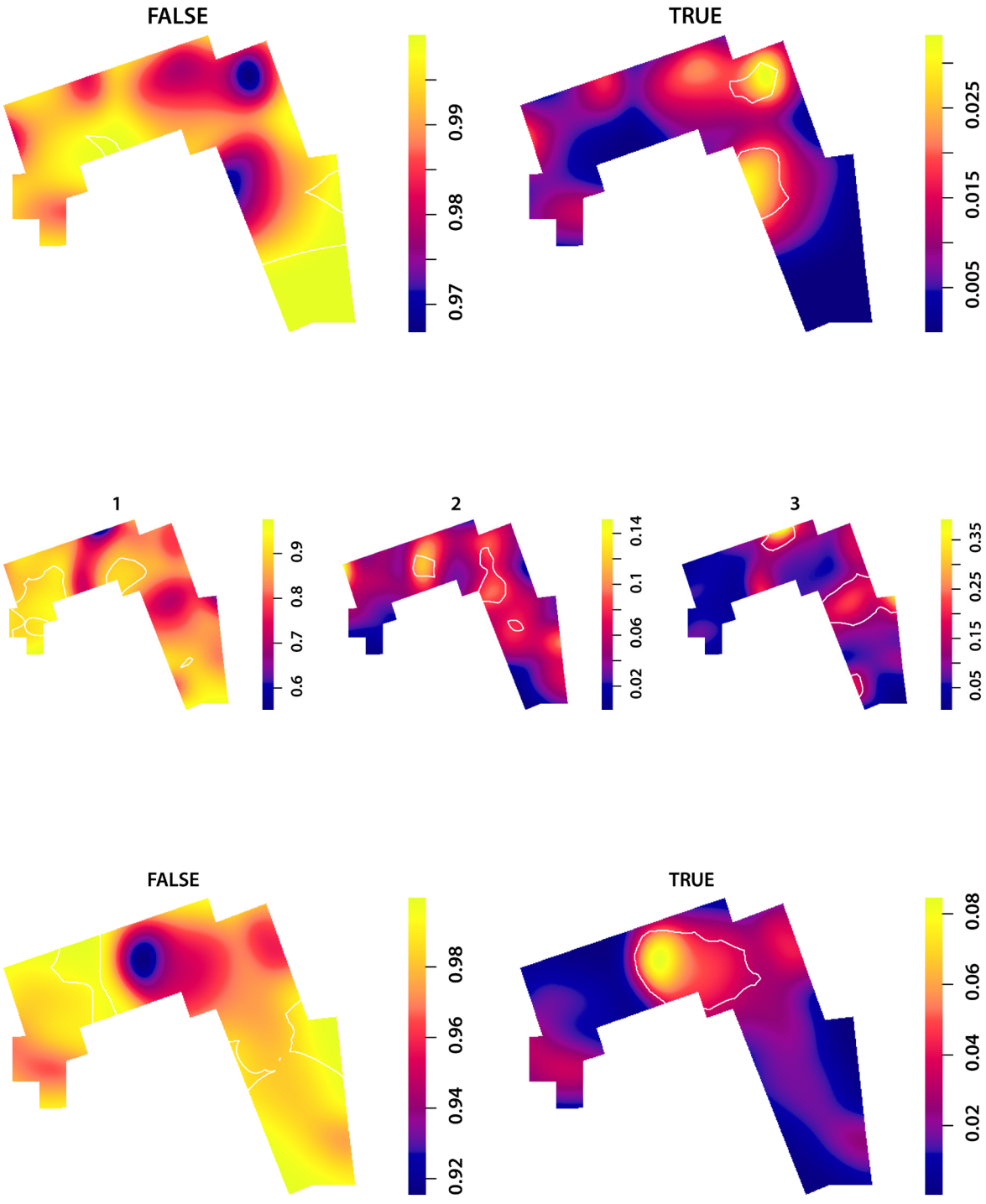

FIGURE 3.82. *Spatial probability distribution of the taphonomic variables A) tooth marks, B) shaft circumference, and C) percussion marks.*

fossils, and B, especially on the edges of the excavated area, where the density of remains is lower (Figure 3.79B).

The majority of recovered bone specimens of level 22B do not show signs of subaerial weathering, although there are around 15 bone fragments classified in weathering stages 1 and 2. Weathered specimens occur only in areas B and C (Figure 3.79D), but in such low density that they do not form a bone accumulation, and should rather be classified as a natural background scatter. Thus, as previously mentioned in the analysis of the site's preservation (section X), different moments of occupation of DS by hominins cannot be identified using weathering stages.

The second regression model, which uses skeletal and taxa representation variables, points to other statistically significant differences between the three areas, as opposed to the third multinomial test, where the four anatomical variables included (presence/absence of horns, side of skeletal element, location of front and hindlimbs, as well as proximal and distal epiphyses), are all homogeneously distributed across the three spatial groups (Table 3.59). According to the second multinomial regression, appendicular and axial elements overlap in the same clusters in areas B and C, but not in area A, where the proportion of appendicular elements is much higher than that of axial remains. By contrast, in areas B and C, axial elements are predominant (Table 3.58**,** Figure 3.80A). Cranial elements can be found in all three zones, and they occur mostly on peripheral areas rather than inside the highest density areas (Figure 3.80A). However, the model also shows that teeth are more predominant in area B than in the other two. The relative risk map of cranial and dental elements both illustrate that these elements tend to occur more abundantly on the edges of the site than appendicular and skeletal elements (Figure 3.80A). Additionally, of the different taxa documented at DS, Tragelaphini yielded a significant p-value. However, the sample size of kudus is very low, which is why this aspect is not further described.

The spatial distribution of carcass sizes and ages also presents some variation across the three areas. Large carcasses predominate in area A, and small carcasses are predominant over medium-sized and large carcasses in some areas of regions B and C, while there is an over-representation of medium-sized carcasses in the same area (A) where appendicular elements stand out with respect to axial and cranial elements (Figure 3.80B). Similarly, Figure 3.80C illustrates that this same area in region A yields a very high probability of finding prime adult individuals (although the coefficient for this factor yielded a non-significant p-value), whereas juveniles predominate in some parts of areas B and C. Therefore, it appears that area A presents an abundance of appendicular elements from medium-sized prime adults, whereas in areas B and C the probability of the points of belonging to the axial skeleton of small and juvenile carcasses is higher than the average proportion.

This described spatially-varying type distribution of skeletal parts suggests that carcass processing by hominins, particularly carcass disarticulation and dismembering, might leave spatial patterns in the archaeological record that can be detected using statistical methods. At DS, the spatial window comprising area B and most of area C could have been used by hominins as the main location of the site, the spot where most carcasses would have been deposited once they entered the site, and where most carcass processing would have taken place. Small carcasses, including juvenile individuals, would have been largely consumed on this processing area, whereas larger carcasses, in particular their appendicular skeleton, would have, on occasions, been subjected to more dispersion into secondary or more peripheral areas of the site, including area A. This part of the site could thus be seen as an extension of the main cluster or clusters in zones B and C.

In fact, when only axial remains are considered, in particular ribs and vertebrae, the fossils appear concentrated in several clusters, not scattered around the site (Appendix Figure 7.8). What is more, during the excavations, some areas were exposed where axial remains appeared nearly in anatomical position, reflecting the deposition of more or less complete ribcages. It is possible, therefore, that these clusters represent at least 6 to 8 single individualized ribcages of carcasses, that again reveal that several carcasses entered the site complete (Figure 3.80A).

Areas B and C also present the highest amount of carnivore activity, as is evidenced by the fourth multinomial regression model, which includes variables directly related to hominin and carnivore activity, such as the presence/absence of cut marks, percussion marks or tooth marks. Only the variables presence/absence of percussion marks and shaft circumference (type 3) yielded significant p-values, although presence/absence of tooth marks was nearly significant and is therefore examined in more detail too (**Table 3.60**). The highest concentrations of both tooth marks and complete shaft circumferences overlap in the area between zones B and C, and secondarily in cluster B (Appendix Figures 7.11 and 7.12), which makes sense considering that both features can probably be attributed to the action of hyenas. The corresponding relative risk maps show a very similar result (Figure 3.82A and B).

The coefficients of the regression and the spatial maps illustrating the distribution of percussion marks indicate that, although this activity is documented across the whole excavated area, the probability of percussion activity is highest in area B (Figure 3.82C). Accessing marrow through bone fracturing comes last in the carcass processing sequence, which means that most carcasses were completely butchered in cluster B, where they had been deposited in the first place. It further suggests that the three areas were not used for different activities (like defleshing or marrow extraction), but rather that all activities related to carcass butchering took place in the same areas. Carcasses were probably

mostly processed and consumed collectively in areas B and C, while partial carcass consumption took place in area A. Tentatively, it could also be argued that carnivore activity, which is most notable between areas B and C, could have caused some distortion in this area through the removal or dispersion of some bone specimens, and created a gap between what we now see as two clusters but what was originally one large bone accumulation.

In short, this analysis has shown that, although two thirds of the taphonomic variables used in the regressions are *Homo*geneously distributed across the three high density areas, some important differences exist between them that enable us to reconstruct the site's formation and functionality (Scenario 2, Methods). Carcass processing took place in all three areas, although the clearest evidence of the complete carcass butchering process is documented in area B, which could be considered the main accumulation. Most differences occur between areas B and A. Area A could be interpreted as an extension or secondary refuse area of the main assemblage in areas B and C where mostly appendicular elements or incomplete carcasses were processed.

3.7.3. Summary and behavioral implications

The results of this second part of the spatial analysis have shown that a further level of detail in the interpretation of a site's formation is possible when taphonomic and spatial analyses are combined. Three distinct areas from a spatial and taphonomic point of view have been detected at DS in the final sections of this study.

Area B seems to constitute the main bone accumulation of the site. The spatial distribution of bone remains and the anatomical representation of the assemblage are similar to those in Area C, which suggests that both accumulations could also be considered one single large cluster that was subjected to slightly higher carnivore ravaging activity in its middle section. The identification of several clusters of axial remains suggests that a number of complete carcasses were collectively butchered by hominins in this part of the site. What is more, at area B, percussion activity stands out particularly, which means that these areas were used for the complete carcass butchering process, including marrow extraction. Extensive percussion activity could also be having an effect on the spatial distribution of lithic remains, which is distinctive in area B. The different lithic types are also currently being analyzed from a spatial perspective in order to understand the classification of lithic spatial patterns better (Díez Martín *et al.* in prep.).

The spatial patterning of the bone clusters from areas B and C resemble the main bone cluster at PTK, which suggests that a similar interpretation can be expected from the taphonomic study of this site (Organista *et al.* in prep.). This bone spatial pattern is also not far from the one obtained for FLK *Zinj*, which

in fact is classified in between the described group (B, C, and PTK) and Area A. The distinctiveness of area A could be related to several taphonomic aspects, like the overrepresentation of appendicular remains in this area. Importantly, the lack of axial remains in this area does not appear to have been caused by carnivore ravaging or disturbance by water, since most carnivore activity and water-related taphonomic features are documented in areas B and C (see above). Thus, it appears that the high presence of limb bones with regard to other anatomical elements in area A is due to behavioral reasons. The presence of mostly appendicular remains instead of appendicular and axial remains could explain the spatial variation between the groups, which lies mainly in the facts that clusters are more elongated and that points inside the clusters do not lie as close together as in the other sites.

At FLK *Zinj*, the overall lower representation of axial remains with regard to limb bones and the distinctive spatial distribution of bone remains could be related to the effect of carnivore ravaging, but the fact that FLK *Zinj* presents similarities to areas B and C and PTK on the one hand and to area A on the other hand can also be interpreted differently, namely as the result of FLK *Zinj* presenting features from both types of spatial patterns. The difference between DS and FLK *Zinj* would then be that remains at FLK *Zinj* were more clustered than at DS. In fact, the spatial patterns of FLK *Zinj* and PTK present higher mean intensities than any of the cluster areas at DS. PTK would then mostly resemble the main bone accumulation at DS (areas B and C), also due probably to the effect on the spatial distribution of remains of carnivore activity, but lack the taphonomic signal from area A at DS.

Area A could be seen as a secondary refuse area from the primary accumulation at the site. As a matter of fact, that area contains large amount of lithic debris produced while knapping, which indicates elaboration of tools as butchery proceeded. The consumption of smaller carcasses would have taken place on the spot in which they were deposited, while the processing of some of the larger carcasses would have taken place along a larger area, including area A. In fact, Bartram *et al.* (1991) observed that at modern forager campsites limb bones often appear dispersed in refuse areas around hearths separated from the nuclear areas much more than other skeletal elements. The spatial distribution of refitting bones shows one connecting line between area A and B, which suggests that both areas could have actually been linked (Figure 3.83). Furthermore, the low-density area separating area A from areas B and C might be related to its proximity to the eroded section of the site and the fact that the ground is topographically lower in this area, which means that this gap between the areas could have been created postdepositionally. Alternatively, area A could have been formed as a result of several independent events, where mostly incomplete carcasses from medium-sized prime adult individuals would have been processed, and where carnivore ravaging was limited. A further difference

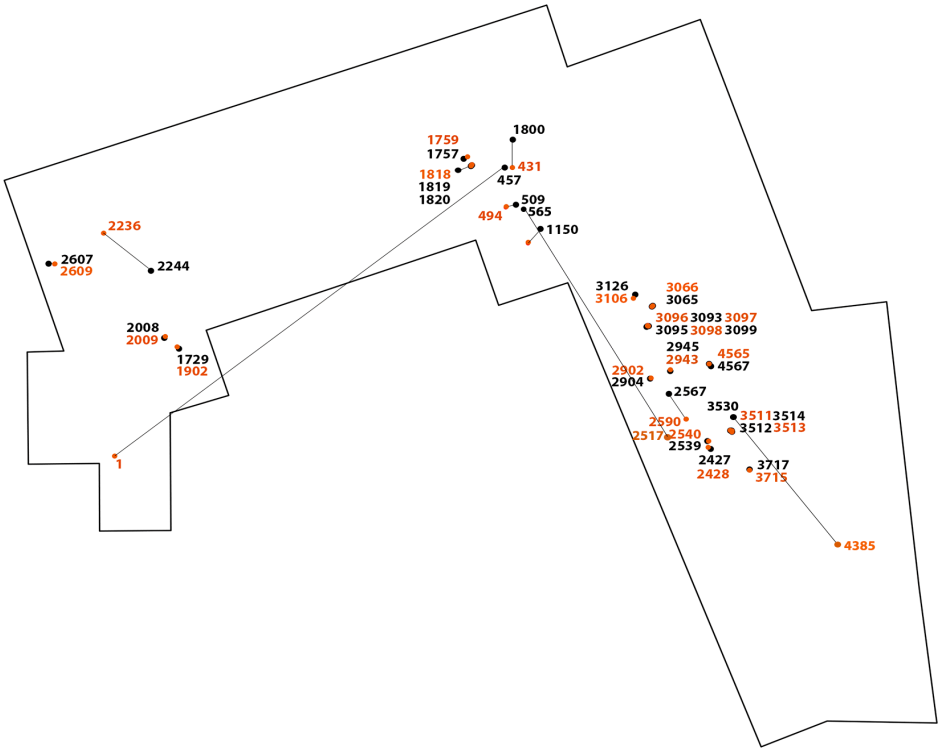

FIGURE 3.83. *Bone refits in level 22B at DS.*

between areas B and C and area A is the existence in the former of some specimens presenting subaerial weathering stages 1 and 2. This might be indicating that B and C formed over a longer period of time or that the main accumulation includes some background scatter, as opposed to area A. Since the total amount of refitting bones between both areas found so far is very limited, I believe the information is insufficient to discard the independence of area A. I expect that the spatial analysis of stone tools will add further indications to help interpret the formation of area A and its relation to areas B and C.

A very promising result of these analyses is the fact that spatial variation seems to be coupled with taphonomic variation among the analyzed assemblages. This means that taphonomic studies would probably greatly benefit from including this spatial component in the interpretations of a site's formation and functionality. All in all, it appears that the three analyzed assemblages present more similarities than differences, even though there are mild spatial and taphonomic variations between them, which seem to be related to the very local differences in the environmental context in which each assemblage formed, rather than to significant variations in hominin behavior. The fact that areas B and C from DS are more similar to PTK than to area A from DS, suggests that these anthropogenic sites in Bed I formed under very similar conditions and as the result of a generally very similar hominin foraging and social behavior,

characterized by the procurement probably by means of ambush hunting of mostly small and medium-sized carcasses that were repeatedly transported, in general over short distances, to the same sites to be processed, consumed and shared collectively.

The present spatial analysis has revealed that early hominin sites were smaller in size and denser in number of bone remains than modern hunter-gatherer camps, even when compared to those modern camps where foragers lived for months. This was also remarked by Domínguez-Rodrigo *et al.* (2019b) when quantifying the minimum number of elements and animals consumed at FLK *Zinj*. If this more intense number of remains at early sites was the result of a prolonged redundancy in the occupation over extensive periods of time, this would be expected to be reflected in diverse subaerial weathering pattern in the archaeofaunal assemblage (Potts, 1988). This is not what is documented at these early anthropogenic sites, where the bulk of the fossil assemblages show no traces of subaerial weathering (Domínguez-Rodrigo *et al.*, 2007). Therefore, this shows that carcass consumption and accumulation must have taken place in very short time intervals spanning no more than one or two years. This resulted from either multiple short reoccupations or very few prolonged reoccupations during this time. Recent preliminary work on dental microwear of DS and FLK *Zinj* is suggestive of the latter option (Domínguez-Rodrigo *et al.*, 2019c).

The higher intensity documented at early anthropogenic sites coupled with the smaller size of the area occupied indicates a very different social organization during carcass consumption from modern foragers. The latter show a centrifugal behavioral pattern, reflecting the individual household use of the camp space. In contrast, at early sites, the behavioral pattern was centripetal, with hominins basically congregating on a very reduced area for repeated carcass consumption. This not only indicates a more cohesive group social structure, but it also stresses the existence of a cognitive partitioning of space, which resulted in the repeated transport, processing and consumption of carcasses over the same small focal spots, despite the inexistence of physical barriers that would have enabled the scattering of carcasses around the same areas where early sites were formed. The present spatial analysis shows how the clusters of bones and stone tools resulting from this behavior are not only similar in intensity, but also in size and shape. This additionally shows that none of these assemblages were resedimented from other *loci*. It also underscores that we are probably underestimating hominin group sizes because their centripetal carcass consumption (reflecting such high amounts of food over so little time) invalidates the use of modern regression proxies for estimating accurate hominin group size and time of occupation represented at sites (Domínguez-Rodrigo *et al.*, 2019b).

The message to take home is that there was a social structure among early

hominins that was different from those documented among modern humans and that it enabled the accomodation of typically structurally human behavioral features such as high degree of cooperation and intentional food-sharing. The challenge now is to define this extinct form of social behavior.

4. Discussion

There are three fundamental conclusions that can be drawn from the results of the taphonomic and spatial analysis of DS that have implications for our understanding of the origins of human behavior. The first one, which appeared self-evident since the beginning of this study, is that the archaeofaunal assemblage in Level 22B at DS represents without a doubt an anthropogenic assemblage. The importance of the fact that hominins were responsible for the accumulation of numerous carcasses and lithic remains at DS as well as for other accumulations at FLK *Zinj* or PTK cannot be overemphasized. It means that early humans, at least sometimes, systematically transported food and raw materials and accumulated them on certain locations of the landscape. From this statement, it follows that early *Homo* very likely engaged in collective and collaborative activities, because the accumulation of such an amount of carcass remains and stone tools requires the participation of several individuals. It also implies that hominins had the cognitive capacity of planning ahead and anticipating the future beyond the immediate needs. The second key component of their socially complex behavior that is reflected at the site is the fact that hominins obtained meat in large quantities by having primary access to carcasses. The third important consequence is that hominins did so mostly through hunting, which implies that meat, and probably also other collectively-obtained resources were intentionally shared among the group. Thus, a high degree of cooperation must have been relevant in the sociality of early *Homo* since the early moments of this genus.

The theory and axioms presented in the introduction, stating that obtaining food collectively and sharing it in central places is at the core of human behavior is reinforced by all the empirical evidence presented in this study. Table 4.1. summarizes all the specific arguments from the results of the applied analyses that corroborate the factual hypotheses that were put to test, and in the following paragraphs the exposed conclusions are discussed in their archaeological and evolutionary context.

4.1. Hominin agency

The first thing to be pointed out is that DS certainly does not constitute part of a natural bone scatter, because the density of archaeological materials at the site contrasts significantly with the overall archaeological productivity of the landscape (Uribelarrea *et al.*, 2014). The highest density areas in the archaeological level 22B at the site contain around 50 to 70 remains (>20mm) per square meter, as opposed to densities smaller than five bone specimens per square meter documented on average in a number of trenches that were excavated in the Olduvai junction that serve as approximate indicators of the general productivity of the paleolandscape (Domínguez-Rodrigo *et al.*, 2010; Uribelarrea *et al.*, 2014; Cobo-Sánchez and Domínguez-Rodrigo, 2017a). In perspective, the types of sites that can be uncovered in Olduvai Bed I include carnivore accumulations, assemblages formed as the result of other natural processes, anthropogenic referential places, sites of "common amenity" as described by Isaac (1983), i.e. palimpsests formed throughout several independent depositional events in which carnivores and hominins would have alternated using the space and accumulating carcasses, and potentially also death sites, such as seasonal mass drownings from ungulate herds.

It is important to underline the fact that the stratum in which the DS faunal assemblage was recovered is stratigraphically discrete (about 20 cm), and there is a clear sedimentary hiatus between the archaeological layers contained therein. Further, most of the assemblage is not affected by weathering (subaerial stage 0; Behrensmeyer, 1978). Occupation was, therefore, probably not longer than one or two years (Behrensmeyer, 1978; Bunn, 1986), as is discussed below. Equally relevant is the fact that the site is largely undisturbed. Along with the lack of water-induced modifications on the bone surfaces and the completely uniform bone orientation patterns, the immense amount of small bone fragments also indicates that the site's integrity is largely intact, and that the assemblage was not conditioned or disturbed by water inputs. The similarities in bone type regarding bone composition and shape with undisturbed experimental accumulations are suggestive of an overall completeness of the site, although some degree of density-mediated attrition (caused biostratinomically by biotic actors) should be taken into account when inferring behaviors from the faunal record at DS.

The diversity of represented taxa, including six different bovid species, the predominance of animal sizes 3-4 that weigh more than 100 kg, particularly prime adult bovids, as well as the fact that some of the medium-sized carcasses are slightly unevenly represented, suggest that carcasses were actively transported and introduced into the site, which rules out that DS could represent a death site. The possibility of the accumulation having been created exclusively by carnivores is also excluded, because the properties of the assemblage do

Table 4.1. Empirical evidence documented at DS supporting the hypotheses outlined in the introduction

Factual hypotheses	Empirical evidence supporting the hypotheses	Conflicting evidence
A1. Primary access to animal resources	Both small and medium-sized carcasses show high frequencies of cut marked and percussion marked bones that coincide with hominin-to-carnivore scenarios.	
	When cut mark frequencies are corrected for poor cortical preservation and dry breakage, percentages coincide with those documented at Upper Paleolithic sites as well as those reported for FLK *Zinj*.	
	Cut marks are located on all skeletal parts, including ribs (indicating that animals were eviscerated by hominins), vertebrae and skulls.	
	Most cut marks appear on midshafts of meaty long bones, which suggests not much disarticulation was carried out.	
	Lower cut mark percentages are documented on LLB than on ULB and ILB.	
	The systematic presence of cut marks on hot zones reveals that hominins were accessing fleshed carcasseses.	
	The low tooth mark percentages documented on different portions of the bones, also mostly coincide with hominin-to-carnivore models.	
	The lack of typical felid damage on bones or taphotypes associated to felids indicate that hominins were not confronting felids for their prey.	
	Two bone fragments present both anthropic and carnivore modifications that show there was almost no competition between hominins and carnivores.	
	In sum, univariate, multivariate and machine learning analyses of BSM yield consistent and uniform results pointing overwhelmingly to primary access to carcasses by hominins.	
A1a. Hunting	Taphotypes at DS do not coincide with those typical for felids.	
	Most overlap in the documented mortality profiles of medium-sized bovid carcasses occurs with the Hadza/Kua kills when using the triangle graphs.	
	The CVA and PCA analyses with four age classes show a clear separation between the age profiles generated by carnivores and the two anthropogenic sites FLK *Zinj* and DS in both small and medium-sized carcasses.	

	The sample from Kanjera also points to hunting.	
	The bovid accumulations at DS and FLK *Zinj* are both dominated by prime adults (60-70%), something typical in many other archaeological sites that are anthropogenic, which is consistent with ambush hunting.	
A1b. Confrontational scavenging	One ulna specimen shows two large tooth marks, potentially attributable to a felid.	Low frequencies of tooth marks are a reflection of the overall low carnivore impact at the site.
	The uncorrected sample of cut marks is classified in the multiple discriminant analysis with the felid-to-hominin experiments.	The high percentage of cut marks indicating primary access (including evisceration and removal of large muscles) suggests hominins accessed carcasses before any other carnivore.
	There is a bias in the representation of front and hind limbs consisting in a lower representation of the highest utility parts (hind limbs) that could indicate that some medium-sized carcasses where acquired from confrontational scavenging from felids.	The bias in the representation of front and hind limbs is not necessarily explained by confrontational scavenging. It could also be related to transport distance or simply to variability in hominin transport decisions, and does not exclude hunting.
	When using the triangle graph, mortality profiles from DS and FLK *Zinj* overlap partly with one of the age profile sample created by lions and with the FLK background sample. According to this graph, both felids and humans can create very similar mortality patterns that resemble the structure of a living population and show a predominance of prime adults.	In general, the bovid age profiles documented at the site are more similar to mortality profiles created by humans than by felids.
	The mortality profiles from Alcelaphini at DS and one of the lion samples match in the CVA. There is a possi bility that alcelaphines from DS were acquired through confrontational scavenging from lions, also given the high variability in age mortality profiles generated by lions (and humans).	The taphotypes from DS do not overlap with those typical for felids in any case.

A2. Focus on a range of carcass sizes from 1 to 3-4	There are almost 30 bovids represented at DS that reach size 3-4 in their adult stage, as well as five small (size 1-2) bovids and at least five large (size 5) animals.	
	Bovid representation is very similar to that in FLK *Zinj*, almost the same species are represented at both sites in similar proportions.	
	These carcasses show evidence of having been defleshed entirely by hominins, which suggests that meat was sufficiently abundant to be shared.	
B1. Selection of central places	The use of DS as a central place is reflected in the existence of autocthonous taxa (waterbucks) and allocthonous taxa (e.g. wildebeest) at the site.The latter were probably encountered less often, possibly only seasonally.	
	The high bone density inside the site contrasts significantly with the surrounding landscape, and the assemblage is formed of multiple butchered carcasses, which indicates food surplus, and possibly food sharing.	
	Bone clusters are spatially different from those at nonanthropogenic sites, in essence because they are associated with lithics clusters.	
	The clusters of stone tool debris suggest that aside from butchering, knapping activities took place at DS.	Acivities aside from butchering and stone tool manufacture are not evident in the fossil record at DS.
	Skeletal part profiles are relatively unbiased, especially those of small carcasses. The ratio between front and hind limbs is similar to other Paleolithic sites interpreted as central places.	
	The environmental context of the location is characterized by low to moderate competition and trophic dynamics, as indicated by low to moderate degree of ravaging at the site.	
	The depositional time does not exceed two or three years, as evidenced by the subaerial weathering stages on the bone surfaces.	
B2. Selection of referential places	Evidence of repeated occupation at the site by hominins is evidenced in the abundance of skeletal remains and stone tools, and hominin activity in general, as well as the presence of different weathering stages on anthropogenically modified bones.	
	The presence of archaeological material in Level 22A, and the contrast in the density of archaeological materials inside and outside the location also evidences that the location was used repeatedly by hominins.	

	The similarity in the representation of front and hind limbs with sites interpreted as near-kill butchering sites aside from central places, suggest that DS could have also served as a near-kill location, where hominins would have partially processed and consumed the carcasses, while selecting the higher utility parts for transport to a central place. Most of the evidence, especially the presence of complete carcasses, however, points to the use of DS as a central place.
C1. Abundant evidence of butchery	The complete butchering process is evidenced at the site as described in A1, which demonstrates that meat was consumed abundantly. Several fragments present both cut marks and percussion marks. Only 5% of the long bone MNE were complete, and fragmentation ratios are high, suggesting that marrow was intensively exploited. Most bone breakage is attributable to hominins.
D1. Transport of (almost) complete size 3-4 carcasses	The accumulation is autochthonous and undisturbed. All the taphonomic evidence excludes the possibilities of DS being a death site or the result of natural processes. There is a high degree of fragmentation of the assemblage as opposed to the high percentages of complete bones found in natural assemblages, which indicates carcasses were brought into the site. There are abundant axial remains that even appear spatially distributed in 6 to 8 clusters and that show that several carcasses were complete when they were introduced into the site. Small carcass transport seems to have followed an unconstrained strategy; they entered the site complete and were entirely processed at DS. This might be suggestive of short-distance transport from the kill site. In medium-sized carcasses, the appendicular skeleton presents a bias that is not explained in terms of food utility or density-mediated attrition, but seems to reflect particular transport decisions. possibility of long distance transport if DS was used as a near-kill location on occasions.
D2. Collective transport of lithic raw material	There is a variety of raw material types at DS that stem from different sources.

	The amount of lithic remains present clearly exceeds the transport capacity of one individual.
E1. Tools were needed for every subsistence activity	There is a minimum of 15 flakes per postcranial MNI, and there are intensively reduced raw materials from sources that are some kilometers away from the site.
	Materials in various stages of the reduction sequence are present.
F1. Hominins anticipated adaptive needs	The presence of raw materials from distance sources and differential reduction sequences and typologies for tools according to raw material type evidence that hominins anticipated they would need stone tools.

not fit with modern carnivore-made accumulations and by the high amount of lithic artefacts that have been recovered. There are approximately 15 flakes per each MNI represented by long bones (353 flakes for an MNI of 24 including small, medium-sized and large ungulates) along with numerous cores and hammerstones (Díez-Martín *et al.*, in prep.) and, as occurs at FLK *Zinj* and PTK, at DS, bone and lithic clusters also overlap in space and are spatially associated, which means that both types of materials were functionally linked at the time of their deposition. In addition, the low percentage of complete bones and the high fragmentation ratios at DS contrast with the higher percentages of complete long bones and lower fragmentation ratios observed in natural assemblages and some carnivore accumulations.

The "common amenity" scenario (Isaac, 1983) refers to the possibility that other agents besides hominins could have independently also transported food remains to the site. This multiple-agency scenario usually produces a more challenging history of a site's formation, which is usually complex and combines the effect of several taphonomic processes. For example, DK, FLKN and FLKNN are sites where palimpsestic dynamics are evidenced and where the taphonomic information shows that hominins and carnivores used the space without interaction. At FLK *Zinj* only half of the carcasses represented by dentition at the site could be confidently associated with hominin carcass processing activities, while there were a number of isolated bone remains and teeth belonging to suids, elephant, buffalo, giraffe, hippopotamus, Theropithecus, and several complete bones from *Tragelaphus* that lacked hominin-made modifications and could have been naturally deposited (Domínguez-Rodrigo *et al.*, 2007; Domínguez-Rodrigo *et al.*, 2019c). Similarly, the difference between the dental and the postcranial MNI at DS reflects that, although most carcasses were probably part of the anthropogenic accumulation, some ungulates, including suids and hippopotamus, could have a different origin from a hominin agency.

Even though some remains could be the result of independent depositional processes operating at the site in different times, it is true that the palimpsestic signal at DS and FLK *Zinj* is very marginal. Significant carnivore input at the sites should be reflected in a combination of features regarding all or most taphonomic aspects, especially the frequencies and the location of tooth marks, the predominant taphotypes on long bones, bone breakage patterns, and age profiles. Yet, every single taphonomic analysis has yielded unambiguous results that reflect a clear and prevailing anthropic signature, and there are no clear bone modification patterns attributable to felids in the assemblage. Additionally, only two bone fragments in the whole assemblage bear both carnivore- and hominin-inflicted marks, which points to a low degree of competition between carnivores and hominins at the site. In fact, carnivore activity at DS seems to be limited to some bone breakage and ravaging by hyenas, because a portion of the documented green-broken fracture planes and notches are more consistent with static loading and the proportions of shaft circumference types coincide with those of hominin-to-carnivore experiments. Still, most long bone breakage (around 80%) was performed by hominins. Therefore, the scenario of a palimpsest or a "common amenity" place formed by a more or less balanced contribution of carcasses from hominins and carnivores seems very unlikely, even though the occasional input of bones by other agents should not be completely ruled out. All mentioned types of theoretical scenarios except the anthropogenic referential place can thereby be confidently discarded. The taphonomic results of the present study point to hominins as the prime accumulators at DS.

4.2. Early and primary access to meat resources

The taphonomic evidence obtained in this study also indicates that hominins had early access to fully fleshed carcasses and prior to any other carnivores having consumed any significant amount of flesh. The clearest evidence stems from the analysis of bone surface modifications. DS presents a very similar anthropogenic impact and taphonomic signature as FLK *Zinj*, with high frequencies of cut and percussion marks and a very low frequency of tooth marks. Carnivore tooth marks appear in fact even less frequently than at FLK *Zinj*. All the evidence collected from the bone surfaces indicates that the bulk of the activities that were carried out at the site is attributable to hominins, that carnivores only had secondary and marginal access to the remains, and that the degree of ravaging was limited. The presence of cut marks on the ventral side of ribs and some vertebral bodies indicating evisceration or on midshafts and hot zones of meaty long bones demonstrating filleting are especially compelling and conclusive of early and primary access. Yet, the strongest evidence comes

from the joint analysis of the distribution of all three types of bone surface modifications. As already stated in previous sections of this study and elsewhere (e.g. Domínguez-Rodrigo and Pickering, 2010; Domínguez-Rodrigo *et al.*, 2014; Domínguez-Rodrigo, 2015), caution must be exercised when using single isolated bone surface modification variables on different anatomical sections, because they are of limited value due to high variability in the samples and can occasionally yield conflicting results (see Pante *et al.*, 2012). Only the conjoint analysis of several variables and the use of robust statistical methods can help overcome equifinality and leads to less equivocal interpretations of the site. In the case of DS, after correcting the sample of bone surface modifications for poor preservation and dry breakage, both multivariate analyses (MDA or MCVA) and machine learning methods match the sample of bone surface marks invariably with hominin-to-carnivore scenarios.

These results are not at all surprising, considering the growing amount of taphonomic data in the African archaeological record from 2 Ma onward evidencing the systematic butchery of carcasses by hominins, which includes the archaeological deposit from Kanjera South, dated to 2 Ma (Plummer *et al.*, 2009; Ferraro *et al.*, 2013; Parkinson, 2013), FLK *Zinj*, ST4 (Peninj, Tanzania), and several archaeological levels from BK in Olduvai Bed II (levels 1-4) dating from 1.5 to 1.3 Ma, which have yielded very similar taphonomic signatures pointing to early access to carcasses by hominins (Domínguez-Rodrigo *et al.*, 2002; Domínguez-Rodrigo *et al.*, 2009; Domínguez-Rodrigo *et al.*, 2014; Organista *et al.*, 2016; Domínguez-Rodrigo *et al.*, in prep.). The same zooarchaeological or taphonomic pattern is also detected at several sites at Koobi Fora in Kenya with limited archaeological record (FxJj 50, FwJj 14a, FwJj 14b, GaJi 14), and at Swartkrans in South Africa (Bunn *et al.*, 1980; Pickering *et al.*, 2004; Pobiner *et al.*, 2008). Several cut-marked equid mid-shaft long bones and pelvis remains from the site of El-Kherba (Algeria), dated to 1.8 Ma (Sahnouni *et al.*, 2013), also prove that hominins were having early access to carcasses in North Africa at the time of the formation of DS and FLK *Zinj*. Evidence for these activities in several anthropogenically supported sites from the same period in widely separated locations suggests that early and primary access to meat by early *Homo* was geographically widespread by 2 Mya. It is true, however, that in many of the mentioned sites the preservational limitations of the archaeofaunal assemblages preclude more detailed discussions about the function of the sites or the meat-acquisition strategies of hominins, and that the most comprehensive evidence supporting primary access scenarios still comes from Olduvai, in particular from FLK *Zinj* and DS. The present study suggests that there is a very distinct and specific anthropogenic taphonomic pattern detectable at least at two penecontemporaneous sites that indicates that early *Homo* primarily accessed and consumed meat of numerous carcasses, including bulk flesh, brains,

viscerae, marrow and bone grease of terrestrial vertebrates. The archaeofaunal assemblage at FwJj 20 (Koobi Fora), dated to 1.9 Ma, even shows that at this time, hominins exploited a wide variety of vertebrates: the butchered remains found there include turtles and fish, as well as rhinoceroses, hippopotamuses, and crocodiles apart from antelopes (Braun *et al.*, 2010).

Early and primary access to carcasses, evidenced mainly, as mentioned above, in evisceration and defleshing marks on meaty bones on the one hand, and on a lack of typical felid modification patterns on the other hand, leads to one important inference, namely that large quantities of meat were available for hominins. Demonstrating that sufficient meat was acquired by hominins is relevant because it serves to justify interpretations of food sharing (e.g. Isaac, 1978; Domínguez-Rodrigo *et al.*, 2019b). The ungulate skeletal part profile analysis suggests that at least a large part of the carcasses were brought complete or nearly complete to the site, especially small bovids, but also the majority of medium-sized carcasses, which probably means that several individuals collaborated to transport large carcasses into the site. The collective acquisition and transport of abundant animal food could have resulted in its communal consumption. As a matter of fact, the spatial distribution of abundant axial remains in clusters, possibly reflecting the surviving rib cages of some of the mammals, in combination with abundant butchery activities on all anatomical parts, including cut marks and percussion marks that even have similar spatial distributions across the site, reflects that hominins carried out the complete butchering process, intensively exploiting the carcasses for the flesh of the skeleton and the grease and marrow content of the bones, collectively on the same areas. But was the acquisition of animal food a regular day-to-day activity for hominins, or did it take place during isolated episodes over a long period of time? Exactly how much meat is represented at DS?

Domínguez-Rodrigo *et al.* (2019b) recently used similar taphonomic information from FLK *Zinj* as that reported here for DS in conjunction with average estimations of meat weight per carcass for several bovids published by Blumenschine and Caro (1986) to produce an estimate of the amount of flesh represented at that site. Their calculations yielded a minimum value of 377 kg (Domínguez-Rodrigo *et al.*, 2019b). Among African foragers, the amount of meat that is acquired per day varies greatly among and between groups and depends also on the season and camp location (Marlowe, 2010), but it ranges between around 9 and 50 percent of their yearly diet (Wood and Gilby, 2019). Hawkes *et al.* (1991) reported 1.2 kg per hunter-day among the Hadza in the 1980s, although Marlowe's (2010) data from the 1990s and 2000s yielded a lower fraction (Wood and Gilby, 2019). Among the /Gui//Gana foragers from the Central Kalahari, estimations yield 0.3 kg of meat per person per day, similarly as other estimates for the Hadza during the dry season (Lupo, 1993; Bunn *et*

al., 1988). Domínguez-Rodrigo *et al.* (2019b) used this last estimate in order to calculate the amount of time it would have taken the FLK *Zinj* faunal assemblage to accumulate. These authors combined their estimate of the amount of flesh represented at the site with an estimation of group size based on the site's size. According to their results, meat would have been available at FLK *Zinj* for a group of about 18 hominins and for 70 days. At DS, the same procedure yields an estimate of 505 kg available for 39 individuals for 43 days, although the confidence intervals of this calculation provide ranges of 22 to 60 occupants and 28 to 76 days of occupation. (The implications of these estimations of group size for these hominin groups are discussed in a different section of this discussion below). Meat consumption rates per capita per day may have been different for early *Homo* than what is documented for the Hadza, and this estimation may seem somewhat speculative, however, we know from the lack of weathering on the bones that subaerial exposure was minimal and that the site probably formed in less than one or two years. What is more, microwear analyses of the *Parmularius* sample indicate that the assemblage formed either in a single depositional process or in more than one reoccupation during the same season (Domínguez-Rodrigo *et al.*, 2019c). The focus on local fauna, i.e. waterbucks, also suggests that most of the occupation could have taken place during the dry season, which could mean a reduction of the bulk of the occupation to just a few months. The formation of such a large accumulation of carcasses during the dry season makes sense if we consider that among all African foragers hunting productivity is increased during this period of the year. Apparently, among the Hadza, this is due to the more restricted movement of game to fewer sources of water, which makes night-time ambush hunting very effective (Hawkes *et al.*, 2001b; Wood and Marlowe, 2013; Wood and Gilby, 2019). As mentioned above, occupation at FLK *Zinj* also seems to have been short and occurred mostly during the dry season (Domínguez-Rodrigo *et al.*, 2019b). All this suggests that meat was abundantly consumed at these sites on a regular basis, which can only signify that it was an important part of the diet of early humans. In fact, the incorporation of animal meat and marrow increased the quality of the diet of early *Homo* with respect to that of *Australopithecus*, and this is clearly reflected in the hominin fossils attributed to early *Homo* (including *Homo ergaster*) among other things in a reduction of the masticatory system and larger brain sizes.

Apparently, the combination of meat-eating and stone tool use to slice and pound meat would have made selection for a smaller masticatory anatomy possible (Zink and Lieberman, 2016).The regular intake of meat is also argued to have fueled brain size development due to shifts in the relative energy requirements of different organs: since larger brains require more energy, increased energy would have been diverted to brain metabolism at the expense of gut tissue

(e.g. Aiello and Wells, 2002). Early *Homo* is also characterized by larger body sizes and changes in life history, defined by slower rates of growth and maturation (e.g. Pontzer, 2012). Changes toward greater bipedal locomotor economy, speed and endurance would also have increased their home ranges and ultimately also provoked their geographical expansion outside Africa (e.g. Walker *et al.*, 1982; Shipman and Walker, 1989; Leonard and Robertson, 2000; Aiello and Wells, 2002; Antón and Swisher, 2004; Holliday, 2012; Domínguez-Rodrigo *et al.*, 2012; Smith *et al.*, 2012; Pontzer *et al.*, 2016). There is also further evidence of the increasing dependency on meat resources by hominins for example in the discovery of a pathology related to anemia (porotic hyperostosis) on a few cranial fragments belonging to a hominin child, which was probably caused by the mother's meat-deficiency. By 1.5 Mya hominin physiology was already adapted to a regular intake of meat, since some individuals developed a B12-related pathology when it lacked in their diet (Domínguez-Rodrigo *et al.*, 2012). Additionally, toothpick grooves have been found on four fossil cheek teeth attributed to early *Homo*, namely OH 62 (Estalrrich *et al.*, 2020), L. 894 (Boaz and Howell, 1977), and OH 60 (Ungar *et al.*, 2001). These grooves indicate that cleaning interproximal spaces between teeth was a frequent activity, and since meat is proposed as the most likely type of food to become trapped between teeth, especially on molars and premolars (e.g. Ungar *et al.*, 2001; Hlusko, 2003; Bouchneb and Maureille, 2004; Lozano *et al.*, 2013; Estalrrich *et al.*, 2017; Estalrrich *et al.*, 2020), these grooves are also argued to constitute additional evidence for regular meat consumption by early *Homo*. Due to all this, meat and the behaviors related to its acquisition and consumption, including meat sharing, are usually central to the models and hypotheses explaining early human adaptations and the evolution of other derived human traits, including long childhoods, complex cooperation or cooperative breeding (e.g. Isler and van Schaik, 2014; Wood and Gilby, 2019).

In short, the accumulation of numerous carcasses at DS did not occur naturally. Butchery marks appear on the bones in patterns that suggest that substantial amounts of meat and marrow were acquired by hominins before other carnivores appeared on the scene. The behaviors and activities surrounding the obtainment, transport, and consumption of meat that are represented at DS were performed by hominins collectively and regularly and were widespread across Africa during this period of human evolution. All this zooarchaeological and taphonomic information amply reinforces the well-accepted view that meat was an important component of the diet of early *Homo*, something that is also apparent in many anatomical and physiological aspects of the bodies, the brains, and the dentition of early humans and reflected in the available hominin fossil record. The next key question that arises is how these fleshed carcasses were obtained by hominins; in other words, whether hominins engaged

in hunting activities, whether they scavenged by stealing carcasses from felid kills or whether they combined both strategies, as is observed in most contemporary hunter-gatherers, who use a variety of techniques to acquire meat. The next section deals with the available evidence regarding hominin predatory behavior and foraging capabilities.

4.3. Early human hunting and confrontational scavenging

Most researchers agree that meat-eating had a significant impact on the course of human evolution since the emergence of the genus *Homo* around 2.8 - 2.5 Mya (Hill *et al.*, 1992; Bromage *et al.*, 1995; Kimbel *et al.*, 1996; Suwa *et al.*, 1996; Wood and Collard, 1999; Sherwood *et al.*, 2002; Villamoare *et al.*, 2015). The larger brains and body sizes of early *Homo* required more energy than those of other hominin taxa such as *Australopithecus* and *Paranthropus*. These high energetic needs would have been secured by increasing the intake of meat and by sharing food, which is only possible if meat surplus is available. Large amounts of meat could only have been available regularly for hominins if they acquired carcasses either through hunting and/or through confrontational scavenging, because in savanna biomes only marginal carcass resources are available for scavenging, and only for short periods of time during the end of the dry season (e.g. Blumenschine, 1986; Domínguez-Rodrigo, 1997). Additionally, passive scavenging has been seriously questioned by a wealth of zooarchaeological and taphonomic information (Domínguez-Rodrigo, 2015). Given this taophonomic evidence, the question today is rather whether hunting or confrontational scavenging were used more predominantly by hominins, and whether their carcass acquisition strategies are comparable to those of humans today. Modern foragers who live in open and seasonal environments sometimes drive carnivores (lions, leopards, caracals, cheetahs, and wild dogs) off their prey (Yellen, 1977; Hawkes *et al.*, 1991). Among the Hadza, 20% of the meat used to be obtained via scavenging in the 1980s (Bunn *et al.*, 1988; O' Connell *et al.*, 1988), while among the Ju'/hoansi, scavenging contributes around half of this percentage to the diet (Wood and Gilby, 2019). However, they primarily acquire prey through hunting.

Some researchers cannot imagine how early *Homo* would have managed to hunt successfully because they view Oldowan stone tools unsuitable for hunting, and still advocate the view that carcass foraging changed progressively over the course of the evolution of the genus *Homo* (e.g. Pante *et al.*, 2012; Pobiner, 2016; Pante and de la Torre, 2018; Sahle *et al.*, 2017). They argue that hominin carnivory and hominin predatory behaviors evolved gradually from passive scavenging strategies for the obtainment of flesh scraps from felid kills

by Oldowan hominins toward consistent early access to carcasses during the Acheulean (e.g. Cachel and Harris, 1998; Holliday, 2012; Pobiner, 2016). Yet, their research has been severely criticized for using problematic referential data and methods (e.g. Domínguez-Rodrigo *et al.*, 2019a). The opposite view is held here: hominins were successful and regular hunters at least 2 Mya, and small and medium-sized carcass foraging emerged as part of a behavioral set including other behaviors, like food sharing and cooperation (Domínguez-Rodrigo and Pickering, 2017). Interestingly, whenever a strong anthropogenic input is inferred in early Pleistocene archaeofaunal assemblages, the taphonomic evidence points every time to early access to carcasses by hominins, even in older periods in which this evidence in the archaeological record is even more scarce. For example, evisceration marks have been identified at Gona (Ethiopia) at 2.6 Ma (Domínguez-Rodrigo *et al.*, 2005), and at Ain Boucherit (Algeria), which is dated to 2.4 Ma (Sahnouni *et al.*, 2018). It is true that the evidence is not sufficient from 2.6 to 2 Mya to make inferences beyond tentative early access to carcasses, but the subsequent concentrations of lithic artefacts and fossil bones dating from 2.0 Ma and 1.8 Ma like DS and FLK *Zinj*, which also coincide with the appearance of *Homo ergaster* (Feibel *et al.*, 1989; Domínguez-Rodrigo *et al.*, 2015), allow us to test more assumptions and reconstruct a clearer picture of hominin foraging strategies.

At DS, the results from the bovid age profile analysis support hunting, more specifically (but not exclusively), ambush hunting, because the documented mortality profiles fall inside the range of the age structure of a living population, with a predominance of prime adults, which constitute around 60 to 70% of the medium-sized bovid sample. When it appears in the archaeological and ethnographic record, this pattern is usually associated with selective ambush hunting (e.g. Binford, 1978; Stiner, 1990; Bunn and Pickering, 2010). The exact same tendency is observed at FLK *Zinj* for both carcass sizes, especially when using four age classes instead of three. The tendency to hunt high-ranked prey at these early sites also supports that hominins were already efficient hunters, as opposed to the view that their hunting capabilities evolved gradually over the Middle to Upper Pleistocene. Incidentally, hunting scenarios are accepted for several other Lower Paleolithic sites in Eurasia based on similar evidence, like the assemblages of fallow deer in Gesher Benot Ya'aqov (Israel; Rabinovich *et al.*, 2008), and levels TD6-2, TD10.1 at Gran Dolina in Atapuerca (Spain; Saladié *et al.* 2011; 2014; Rodríguez-Hidalgo *et al.* 2015; 2017). At TD10.1 prime-adult individuals dominate the deer mortality profile. This site represents a long-term residential base camp formed probably by very intensive occupations. This preference on high-ranked prey is similar to that documented in other Middle and Late Paleolithic sites across Europe and the Levant (Rodríguez-Hidalgo *et al.* 2015) and coincides with the prey selection

profile that is interpreted as unique for humans (Stiner 1990). Gesher Benot Ya'aqov constitutes an assemblage dominated by a single taxon (Dama dama) where adult individuals are most abundant (Rabinovich *et al.* 2008). At TD6-2 all age groups are represented, but the profile is dominated by immature and adult individuals. Díez *et al.* (1999) suggested that at TD6-2 hominins had had primary access to small and medium-sized animals but had had to scavenge large prey from felids. However, this was contested later by Saladié *et al.* (2014), since no diagnostic evidence was documented that indicated felid activity. If we accept the age mortality profiles from these sites and more recent periods as evidence of hominin predatory behavior, the same should apply for earlier anthropogenic sites, especially if they appear coupled with taphonomic evidence for early access, as is the case of DS.

Age profiles are not the only line of evidence with similar outcomes at DS and at sites from other more recent periods. In fact, one of the most important results obtained in the present study is precisely that several aspects of the taphonomic pattern yielded by the faunal assemblage at DS, in particular the frequencies and location of cut marks, do not differ from those obtained from sites from substantially later periods, where hunting is undisputed. The previously mentioned assemblages are also a good example thereof, because they have been studied thoroughly from a taphonomic perspective. Similar as to what can be observed at DS, in these assemblages, there is evidence for the performance by hominins of all butchering-related activities, which again proves that hominins had early access to abundant meat resources. For example, skinning is evidenced by cut marks on the crania, the metapodials and the phalanges. Detachment of the crania from the postcranial skeleton by cut marks on atlases and cut marks (and in some cases also hack marks) on epiphyses of long bones reveal disarticulation activities. Evisceration is demonstrated by abundant cut marks on the ventral sides of ribs and some vertebrae, and intensive defleshing is evidenced by high percentages of cut (slicing) marks on hot zones of meaty long bones. This demonstrates that carcasses were completely and efficiently processed regularly at these sites, following the same butchery patterns that are also typical in later periods of human evolution (e.g. Rabinovich *et al.* 2008).

The bovid age profiles and the taphonomic and zooarchaeological similarities between DS and other early Pleistocene sites where hunting is accepted are the most important arguments stemming from this study in favor of an early human predatory behavior. However, the fact that the mortality profiles from DS do not consistently overlap with those typical for felid kills is equally important, although occasional overlap is documented with the age profiles created by lions when using three age classes or when using five age classes and considering only the Alcelaphini subsample. However, this match must be taken cautiously, first because lions produce very variable bovid age profiles

depending on certain environmental aspects and seasonality, and secondly, because in the case of DS, these similar profiles do not appear in conjunction with typical felid damage on the bones. Typical modification patterns in felid-consumed carcasses include deep pits on the mesio-lateral sides of the distal femoral troclea, damage on the caudal medial epicondyle of humeri, furrowing of the olecranon of the ulna, on the tibial crest, the pelvic crest, the scapula blade and on the vertebral apophyses, and pits or punctures on vertebral bodies (Gidna *et al.*, 2013; Domínguez-Rodrigo *et al.*, 2015; Domínguez-Rodrigo *et al.*, in prep.). The absence of these patterns in the faunal remains of DS, also reflected in the results of the taphotype study of long bones, argues against scavenging (passive or confrontational). If most carcasses accumulated at DS were the result of aggressive scavenging from felids, these bone modification patterns should be more commonly documented.

The remaining detected evidence at the site that could be pointing to confrontational scavenging is also inconsistent and ambiguous. For instance, the uneven representation of front and hindlimbs in medium-sized carcasses could mean that some of the carcasses were acquired by hominins incomplete. Hominins could have on occasions been able to steal carcasses from felid kills that may have lacked viscera and hindlimbs. However, there is an alternative option, namely that hominins butchered and discarded hindlimbs at the kill site, since they have higher return rates and are more efficiently processed, as a strategy to maximize their individual energetic gain and minimize transport load. Regardless, this only affects a small portion of the assemblage; carcasses seem to have been predominantly acquired complete by hominins.

Evidence from other Bed I sites like FLKN 1-6, FLK 10-15, DK and FLK-NN, where hominins do not seem to have taken advantage of large amounts of complete bones from felid accumulated remains, should not be disregarded. At these sites, complete bones were left unprocessed by hominins. For example, at FLKN 1-6, hominin activity is documented by the presence of lithics in every level of the long sequence spanning hundreds or thousands of years, yet they do not seem to have engaged in exploiting the remains of felid kills. This suggests that scavenging from felids was not a common activity, although the possibility that occasional scavenging may have happened should not be excluded. Even if the mentioned taphonomic signs were reflecting power scavenging, the patterns are not consistent. The taphonomic signal should be more accentuated if the bulk of the assemblage had been acquired through aggressive scavenging. By contrast, the factors pointing to hunting are much more consistent. Thus, it is probable that hunting was the predominant strategy used by hominins to obtain large quantities of meat already by 2 – 1.8 Mya.

Researchers who disagree with this view, admit that hunting would have been a regular activity of hominin lifeways by 1.5 – 1.0 Ma (Pante, 2013; Po-

biner, 2016). Indeed, by this time, in addition to butchering small and medium-sized carcasses, hominins were also systematically exploiting and having primary access to very large ungulates, including Pelorovis, Syncerus or Sivatherium, as has been documented at BK (Domínguez-Rodrigo *et al.*, 2014; Organista *et al.*, 2017). It is true that prior to 1.5 Ma, exploitation of megafauna was rare or sporadic, but the Oldowan sites from 2 - 1.8 Mya are already filled with animals that were heavier, stronger and faster than a single hominin, which should mean that hominin collective predatory capabilities already existed by that time. Killing large animals is traditionally identified as one of the fundamental characteristics of human predatory behavior (when compared to the hunting behavior of other primates) and it illustrates that they acquire enormous amounts of meat. Gui-//Gana foragers have been observed to kill elephants and adult male giraffes (Silberbauer, 1981), and accounts from the early twentieth century describe that the Hadza once hunted hippopotamus and rhinoceros (Wood and Gilby, 2019). This certainly has major implications for food sharing.

The problem that is often posed by those who negate this possibility is that efficient hunting would only have been possible with more advanced technologies. Some have even viewed hunting and the use of efficient hunting technologies as an indication of exclusively modern human behavior (Binford, 1985; Binford, 1988; Klein, 1995; Klein, 2000; McBrearty and Brooks, 2000). Certainly, technology must have played a major role in the evolution of hunting: the use of tools enabled humans to kill aquatic and subterranean prey as well as terrestrial animals, allowing them to exploit many more predatory niches than any other predator (Wood and Gilby, 2019). Technology probably also helped minimize the high metabolic costs that hunting involves, particularly the development of projectile technology. Simple pointed long sticks and spears used as throwing weapons are considered the earliest projectile technology. Contemporary foragers still used untipped and stone or metal-tipped wooden spears in various different hunting strategies to kill prey directly or slowly via blood loss or poisoning (Hitchcock and Bleed, 1997, Bartram, 1997; Woodburn, 1970; Waguespack *et al.*, 2009; Wood and Gilby, 2019). Interestingly, experiments have shown that untipped wooden spears can impact and penetrate prey as efficiently as stone-tipped spears, or even deeper (Wilkins *et al.*, 2014), and that they are very effective as throwing weapons (Domínguez-Rodrigo *et al.*, in prep.). Apparently, producing sharp spears does not require advanced or complex cognitive skills, since even chimpanzees have been observed to use sharpened sticks as hunting tools at Fongoli, where they explore tree cavities to disable and kill galagos (Pruetz and Bertolani, 2007; Pruetz *et al.*, 2015).

The earliest use of wooden spears as throwing weapons is dated to the Middle Pleistocene and documented at Schöningen (Thieme, 1997), Neumark Nord

(Gaudzinski-Windheuser *et al.*, 2018), and possibly Boxgrove (Roberts and Parfitt, 1999), although the existence of wooden technology has been inferred in the Lower Pleistocene from usewear on stone tools and phytoliths (Keeley and Toth, 1981; Domínguez-Rodrigo *et al.*, 2001). It is therefore certainly possible that wooden tipped tools may have been used by early *Homo* and even earlier hominins, and that they could have even preceded the manufacture and use of stone tools (Domínguez-Rodrigo *et al.*, in prep.). Throwing in modern humans is biomechanically enabled by tall and mobile waists and a laterally oriented scapula, apart from a wider humeral torsion and it has been shown that all of these are features already present to a certain degree in *Homo ergaster*. This suggests that this species would have already been capable of throwing spears with control and accuracy (Domínguez-Rodrigo *et al.*, in prep.).

Obviously, if a wooden spear were to be discovered in very old deposits, it would constitute sufficient compelling evidence of hominin predatory capabilities as early as 2 Mya. However, this is unlikely to happen due to preservational issues. Nevertheless, in theory we could expect to find indirect evidence of the use of pointed sticks or spears on the hunted animals in the form of impact marks on the bones. At DS, we have found one very particular mark on the dorsal side of the iliac crest of a left pelvis fragment with associated peeling or flaking underneath it that is very similar to the bone damage created experimentally on pelves by thrusting wooden-tipped spears (Figure 4.1) (Gaudzinski-Windheuser *et al.*, 2018). The documented mark will have to be inspected closely and in detail in the future and compared to experimental marks. If it is finally interpreted as a lesion caused by a wooden spear, it will truly constitute undeniable evidence of early human predatory behavior.

Spears are often used by hunters to impact and wound animals so that they run shorter distances before dying, and they are implemented in various different strategies including prey pursuing and ambush. Even the use of spears by modern foragers for power scavenging has been attested (Bunn, 2001). Truly, using spears or wooden sticks would have provided hominins an adaptive advantage and enhanced their hunting and power scavenging skills.

However, we should not overlook the fact that hominins could also have practiced hunting strategies that are not dependent on technology. Several modern forager groups like the Bushmen San from the Kalahari perform persistence hunting, which consists in pursuing animals during midday for hours in order to drive them to hyperthermia or exhaustion (Liebenberg, 2006). This strategy is very successful, especially in open habitats, yet energetically expensive and time-consuming. Some authors have viewed tracking animals also as a cognitively very complex behavior (Pickering and Bunn, 2007), but it is actually documented in some mammalian carnivores (Lieberman *et al.*, 2007). The idea that hominins could have engaged in persistence hunting to acquire prey

is based on the realization that the anatomy of *Homo erectus* shows numerous adaptations to running, more specifically, endurance running, including sweat glands that enable efficient thermoregulation (Carrier *et al.*, 1984; Bramble and Lieberman, 2004). The skeletal and muscular features include the presence of a nuchal ligament that helps stabilize the head during running, long legs, an expanded gluteus maximus muscle, a long Achilles tendon, the podal plantar arch, and a short forefoot, coupled with the several other anatomical structures that would have enabled arm swinging and trunk rotation while running (Bramble and Lieberman, 2004; Lieberman *et al.*, 2009; Domínguez-Rodrigo *et al.*, in prep.). Ethnoarchaeological evidence shows that endurance running is also used by modern foragers to cover big areas when prey is scarce, and that this enhances their fitness. Archaeologically and ethnographically, persistence hunting could in theory be reflected in more attritional bovid age profiles that resemble those created by cursorial predators. Such is the case of the bovid carcasses from Kanjera South, which overlap considerably with those generated by Kua and Hadza foragers, who sometimes hunt more opportunistically young or old individuals, without waiting to encounter prime adults (Bartram, 1993). Although the possibility that hominins would have confrontationally scavenged from felids has not been completely ruled out at this site, because the age profiles also resemble those sometimes created by lions, Oliver *et al.* (2019) have argued that hominins would have engaged in short chases to hunt the animals accumulated at Kanjera, probably due to the challenges posed by a more open environment than the one that dominated at the Olduvai sites. The fact that the evidence points to ambush hunting at DS and FLK *Zinj*, and to persistence hunting at Kanjera, suggests that hominins might have used different strategies depending on environmental factors (Oliver *et al.*, 2019). Variability in the employed hunting strategies depending on the environment is also typical of modern hunter-gatherers. The fact that similar variation and adaptability in predation strategies were present around 2 Mya also suggests that early Pleistocene hominins were already efficient hunters.

Several authors have identified ambush as the most likely predatory technique used by early hominins (e.g. Bunn and Pickering, 2010; Bunn and Gurtov, 2014). The bovid age mortality profiles documented at DS and FLK *Zinj* certainly lend support to this interpretation. Ambush hunting requires foresight and patience, as well as knowledge of the use of the surroundings by game. The technique used by modern hunter-gatherers consists in searching for fresh signs of prey and selecting locations where these animals are likely to pass in the near future, places that are usually related to the accesses to sources of drinking water (Wood and Gilby, 2019; Domínguez-Rodrigo *et al.*, in prep.). They then hide behind vegetations or artificially constructed hunting blinds and wait for the game to arrive. Based on his own experiments simulating hunt-

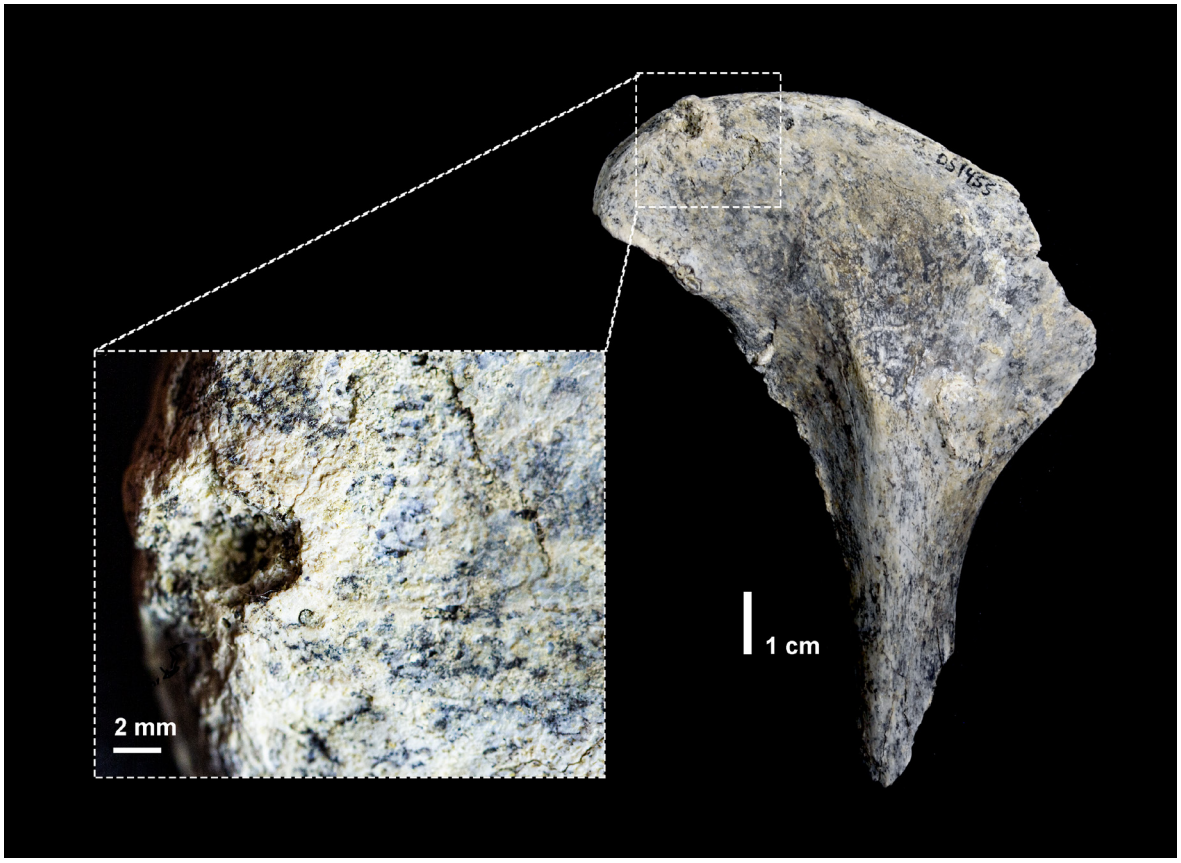

FIGURE 4.1. *Mark surrounded by flaking or peeling on the dorsal side of the iliac crest of a pelvis fragment that bears notable similarities to the bone damage inflicted experimentally on pelves with wooden spears.*

ing with wooden spears, Domínguez-Rodrigo has highlighted that ambushing animals from trees overlying the paths that lead to water sources can be very effective (described in Domínguez-Rodrigo *et al.*, in prep). In general, ambush hunting is practiced by most foragers with such high rates of success (O'Connell *et al.*, 1988; Marlowe, 2010) that some forager groups commonly use this strategy for killing larger game. The Hadza use this technique often and very effectively to hunt zebra, eland, buffalo or impala during the late dry season, when the movements of game are more predictable (Hawkes *et al.*, 2001; Wood and Gilby, 2019). The implementation of this strategy by early humans remains speculative, but it certainly seems plausible, especially at Olduvai, since the environment surrounding the sites seems to have been a wooded habitat with abundant vegetation that could have provided hiding spots for hominins and water sources were nearby. Nevertheless, most modern foragers use a combination of strategies to acquire carcasses, instead of a single technique. For example, the San hunters in the Kalahari and the Hadza stalk prey from hunt-

ing blinds and also pursue prey by foot (Hitchcock and Bleed, 1997; Marlowe, 2010). Oldowan hominins could have behaved similarly in this respect.

Hunting seems to be a behavioral adaptation that is deeply rooted in the phylogeny of humans. In fact, our closest living relatives, the chimpanzees and bonobos are, like humans, among the most carnivorous primates and also show an innate predatory disposition (Domínguez-Rodrigo and Pickering, 2017). Chimpanzees have been observed to prey upon around forty species, although they specialize only on a few small arboreal and terrestrial species - mostly weighing less than 10 kg – including red colobus monkey, galago, duiker, bushbuck and bushpig (Newton-Fisher, 2014; Wood and Gilby, 2019). Chimpanzee hunting has been attested in many instances for example at Gombe and Mahale in Tanzania (Stanford, 1998; Uehara, 1992), Ngogo and Budongo Forest in Uganda (Watts and Mitani, 2002; Newton-Fischer *et al.*, 2002) or at Fongoli in Senegal (Pruetz and Bertolani, 2007; Pruetz *et al.*, 2015). The latter case is especially interesting, because the chimpanzees at Fongoli use sharp sticks and branches to kill galago prey. Bonobos hunt less frequently, but some accounts show that they can be as successful as common chimpanzees (Ihobe, 1992; Hohmann and Fruth, 1993; 2008; Surbeck and Hohmann, 2008; Surbeck *et al.*, 2009). In the genus Pan, this predatory behavior is more common and more expansive in open, seasonal biotopes, where chimpanzees can hunt a wider range of prey (Boesch and Boesch, 1989; Uehara, 1992; Stanford *et al.*, 1994; Stanford, 1996; 1998b; Watts and Mitani, 2001; 2002; Pruetz, 2006; Lwanga *et al.*, 2011; Domínguez-Rodrigo and Pickering, 2017), and hunting frequency seems to be positively correlated with fruit availability, as this provides them a surplus of energy (Mitani and Watts, 2001). Further, chimpanzees have been very rarely observed to passively scavenge, although they sometimes steal carcasses directly from other predators, especially from baboons, by throwing branches and waving their arms (Watts, 2008).

The similarities in the habit of hunting between humans and chimpanzees are most probably homologies, which means that their last common ancestor would have very likely also hunted small prey in groups and occasionally acquired carcasses from other predators (Pickering and Domínguez-Rodrigo, 2010; Duda and Zrzavy, 2013; Wood and Gilby, 2019). A theoretical scenario for the evolution of hominin predatory behavior could have been as follows. The period between 7 and 2.6 Ma is devoid of archaeological record, particularly of evidence of the use of stone tools by hominins to butcher animals, which limits our ability to make inferences, but it can be argued that in the diets of early hominins, meat could have comprised at least the same percentage of the diet as in chimpanzees, at least 1-5% (Wood and Gilby, 2019). It also seems safe to assume that, given the fact that chimpanzees sometimes kill adult conspecifics, the last common ancestor of humans and chimpanzees might have also

been capable of killing larger and dangerous animals (Wood and Gilby, 2019).

As environmental changes turned African woodlands into cooler and drier savanna habitats, early hominins increased their day range and started encountering more terrestrial prey, particularly herbivores (Foley, 1987; 1996). These animals would have mostly congregated near water sources, which would have provided hominins with more opportunities to capture prey, but at higher predation risk. Bunn (2007) has proposed as the first stage of carcass acquisition around 2.6 Mya that hominins would have butchered complete animals at the place of acquisition. At this point, it can be argued that since hominins were capable of knapping stone tools, they may also have been able of manufacturing and using simple wooden implements like chimpanzees do today. These could have been used for different purposes apart from hunting, like digging for food, defense from predators or power scavenging (Wood and Gilby, 2019). Then, from 2 Mya, as evidenced at the sites of Kanjera, Olduvai and Koobi Fora, *Homo ergaster* or their ancestor would have engaged in hunting and power scavenging regularly, which would have given them early and primary access to complete fleshed carcasses. Food consumption would have been delayed in order to transport and share carcasses at a central place, which represents a significant shift in social organization relative to that of earlier hominins and chimpanzees.

4.4. The use of central places by hominins on the Zinj paleolandscape

Aside from determining the degree of involvement of hominins in carcass acquisition and meat consumption at early sites, one of the most important achievements of taphonomic studies in the past decades is having demonstrated that some early sites were created by hominins repeatedly carrying animal carcasses and stones to particular places in the landscape (see discussion in Domínguez-Rodrigo *et al.*, 2007; Domínguez-Rodrigo *et al.*, in prep.). However, the use of these sites as central places has been highly controversial, partly because the concept entails that these places also had a social function in addition to being used for specific activities related to subsistence. This means that hominins could have used these places for sharing food and therefore have stayed at these locations for prolonged periods of time, rather than only have used these spots sporadically as refuge places or stone caches when trying to avoid predation risk. This is viewed as problematic by researchers who conceive early human behavior as similar to that of extant primates and think that hominins lacked the capabilities to obtain abundant meat resources or to confront carnivores.

Simply put, the possibility of using early sites as central places repeatedly for

hominin activities would have been conditioned by two factors. The first would be the amount of food surplus available for hominin consumption, because the use of central places only makes sense if sufficient food is available to be shared. The taphonomic analyses of FLK *Zinj* and DS have widely demonstrated that this condition is met. The second factor would be the degree of carnivore predation risk in the surroundings of the sites. Central places could only have been created if carnivore competition or predation risk was relatively low. This can be assessed by means of reconstructing the paleoenvironment in which the site was formed and by establishing the degree of carnivore ravaging at a site, which can be used as a proxy for carnivore competition. The taphonomic analyses of the Bed I sites showed that carnivores were very active in the lacustrine plain of the former Olduvai lake where these sites formed. Some felids, like leopards, Dinofelis, and solitary lions, were accumulating carcasses at certain locations, probably seeking low-competition settings. The predatory guild was very diverse compared to the carnivore species that are found in modern savannas today, which also suggests that competition among carnivores must have been significant (Domínguez-Rodrigo *et al.*, 2007). Sites were probably located in transitional zones between the alluvial plain and the lacustrine floodplain in closed-vegetation habitats (lacustrine forests), which were probably relatively low-competition habitats (Domínguez-Rodrigo *et al.*, 2007). Nevertheless, if carnivore competition was relatively high, felids and hyenas were arguably very active in the area, and places like FLK *Zinj* and DS, located in closed-vegetation habitats, might not have been such low-competition settings compared to modern closed-vegetation habitats in modern savannas. As a matter of fact, the analysis of several skeletal part ratios to estimate ravaging intensity suggests that the degree of ravaging and carnivore competition were low to moderate at DS. More intensive ravaging is documented at FLKN and DK, which formed in a more open environment. The same inferences can be drawn from bovid taxa representation at the sites. While more species from mixed habitats such as waterbucks (*Kobus*) are predominant at FLK *Zinj* and DS, bovids from more open environments, like *Antidorcas* and *Parmularius* are dominant at FLKN (Domínguez-Rodrigo *et al.*, 2007). Thus, although carnivore competition and ravaging seem to have been ubiquitous during Bed I times, wooded environments would have represented the lowest competition areas, which explains why hominins would have selected these loci for their activities. More detailed recent paleoecological reconstructions further support that DS and FLK *Zinj* were located on a topographically higher platform in a wooded environment dominated by palm and acacia trees (Uribelarrea *et al.*, 2014; Arráiz *et al.*, 2017). The two conditions necessary for the use of central places by hominins are therefore supported.

Apart from the concern regarding acquisition of abundant meat resources

by hominins, the location of the sites in the paleolandscape and the danger posed by the large carnivore guild (Blumenschine *et al.*, 2012), no other arguments have been presented against the use of central places by hominins at Olduvai, and the model has not yet been disproved. On the contrary, there is further evidence from DS and FLK *Zinj* that supports a central-place foraging model. No other site function model explains the simple fact that the accumulations are extremely large. As already mentioned, several species represented at the sites are open-vegetation taxa, like Alcelaphini and Antilopini, that were probably carried across longer distances and brought into the sites from further than the immediate vicinity of the site. The skeletal part profiles suggest that most of the carcasses were introduced partially or fairly complete into the sites, and the lower representation of hind limbs from medium-sized carcasses at DS could be explained by their consumption or extraction of meat at the kill sites by hominins before returning to the central place with the remaining carcass. The other possibility is that some of the carcasses represented at the site could have been acquired incomplete through confrontational scavenging. All the evidence points to DS as a consumption place where carcasses were intensively butchered, and bones were broken for marrow extraction. Such extensive butchering at kill or near-kill sites would only be energetically efficient if central places were several kilometers away. However, the evenness of high-survival element representation suggests short-distance transport. The abundant and diverse stone tool kit represented at the site is also inconsistent with the near-kill butchery model. A near-kill site would contain relatively low frequencies of stone tools relative to the number of carcasses represented. The spatial distribution of all butchering-related activities also shows that carcasses were completely butchered in the same spots.

Bone remains and lithic artifacts at PTK are spatially distributed in a large cluster of similar characteristics as the ones from FLK *Zinj* and DS, which also suggests that PTK was selected by hominins for similar purposes. This does not preclude the use of other locations in the *Zinj* paleolandscape by hominins for other activities. The palimpsests formed at other Bed I sites show that hominins were active in other loci as well. It will be interesting to see whether AGS also served as a central place like the other large anthropogenic sites. This appears to be the case, judging by the similarities in taphonomic attributes observed so far with the other hominin-made assemblages work in progress).

The existence of at least three central places in the *Zinj* paleolandscape in a relatively small area (around 1000 m^2) suggests that hominin groups were very active in the area, just like carnivores. The floodplain, with several (seasonal) fluvial input areas and the nearby location of a freshwater spring would have been an important area of attraction for many species of herbivores, given the presence of accessible water resources. Like modern hunter-gatherers do today,

hominins could have controlled the paths leading to water sources and awaited animals hiding behind vegetation or on the top of trees. Whether these spots were the central places of one or several groups of hominins is unknown, but the high number of carcasses accumulated at the sites in less than one or two years implies that hominins occupied an important position in the predatory guild and that they competed with carnivores, especially felids, for prey. However, the separation of carnivore-made and anthropogenic accumulations in different areas of the lacustrine environment and the general lack of overlap of felid and hominin-induced modifications on the same bones indicates that both agents commonly did not engage in the consumption of the same carcasses (Domínguez-Rodrigo *et al.*, 2007; Domínguez-Rodrigo *et al.*, in prep.).

Incidentally, high degrees of carnivore competition have consequences regarding scavenging opportunities for hominins. First, if carnivores were very active in the Olduvai Bed I environment, the chances for hominins to encounter undisturbed or fleshed carcasses across the *Zinj* paleolandscape, i.e. opportunities for passive scavenging, would have been very low. Second, it has been argued that confrontational scavenging is a far riskier activity than hunting, which would also speak in favor of hunting instead of confrontational scavenging as the predominant predatory strategy followed by hominins during the early Pleistocene. Certainly, carnivores could have posed a major threat for hominins, as they do for modern foragers still today (Treves and Naughton-Treves, 1999). However, the risk of carnivore predation could have also promoted higher cooperative behaviors among hominins and increased sociality, as is observed in fact in several extant primate species (Rose and Marshall, 1996).

4.5. Cooperation and food sharing as the basis of the social organization of early humans

It is likely that defense against predators and foraging for large quantities of meat would only have been effective if hominins engaged in both activities collectively, especially since hominins lacked sophisticated technology in the early Pleistocene. The transport of lithic raw material and large carcasses to central places would also have required a significant degree of cooperation or collaborative participation. Hominins would have engaged in the collective acquisition of food resources with the expectation of benefiting from the shared use of these resources (Domínguez-Rodrigo *et al.*, in prep.). Thus, an outcome of cooperation would have been intentional food sharing (Isaac, 1978). Both intensive cooperation and intentional food sharing are universal features among humans in forager societies. But how exactly did these social behavioral fea-

tures evolve?

It has been argued that increased sociality enabled early *Homo* to cope with the high energetic costs of increased encephalization brought about by a greater reliance on meat-eating. Encephalization would have also led to the need to invest more energy in an increasingly energetically expensive reproductive physiology and in the nurturing of altricial offspring. This would have been possible for females thanks to changes in life history parameters, such as larger inter-birth intervals and prolonged infancy periods, but also thanks to food provisioning by other members of the group (Kramer, 2010; Thompson, 2013). However, this would mainly have been reflected in male provisioning and therefore it mainly explains within-kin cooperation. In order to account for intra-group cooperation and explain the evolution of human social structure, Puurtinen *et al.* (2015; Puurtinen and Mappes, 2009) have suggested that cooperation between non-kin, i.e. intra-group cooperation, could have been triggered by inter-group competition. If this was the case, then natural selection probably would have favored robust male anatomies and larger group sizes. Both of these characteristics can be observed in the paleoanthropological and archaeological record (Domínguez-Rodrigo *et al.*, in prep.). At the same time, a shift in hominin socio-reproductive organization would have had to develop that would have contained or minimized intra-group competition. Domínguez-Rodrigo *et al.* (in prep.) envision two possible models by which this could have occurred, the male philopatric coalition (MPC) and the polygynous reproductive units (PRU). The first is the social structure observed in modern lions and is characterized by several genetically related males controlling a stable female harem. The group functions as an extended family. Males are responsible of group defense, while hunting is a collective and cooperative activity and food is consumed by all members of the group collectively in the same spot (Domínguez-Rodrigo *et al.*, in prep.). Group size does usually not exceed 40 individuals, although the average number of individuals in the pride is around 15 (Schaller, 1972). The second social structure model is based on the association or bonding of several polygynous reproductive units, each containing a maximum of 12 females and subadults. This is the social structure of gelada (Theropithecus gelada) bands. Total group size of these communities can exceed 200 individuals. Several bands sometimes congregate forming herds when their ranging areas overlap. Similar aggregations of bands are observed in human foragers (Domínguez-Rodrigo *et al.*, in prep.).

Which of these social organizations was adopted by hominins? These two types of social structure both predict sexual dimorphism, but they contrast in group size and in a different social use of the space. The answer to this question could therefore potentially be inferred from the archaeological record (Domínguez-Rodrigo *et al.*, in prep.). Group size estimates established based on the size of the anthropogenic early sites from Olduvai predict that hominin groups

were formed by around 13 to 39 individuals. More specifically, according to these estimates, FLK *Zinj* could have been occupied by 18 to 28 individuals (Domínguez-Rodrigo *et al.*, 2019b), PTK by around 13 to 19 individuals (Cobo-Sánchez *et al.*, 2018), and DS by 22 to 39 hominins. These numbers are clearly much more consistent with the MPC model than with the PRU model, and they are also similar to the estimates from the 1.5 Mya footprint trail from Ileret (Kenya), which predicts that *Homo erectus* groups could have been composed of 15 to 23 individuals (Hatala *et al.*, 2016). However, these numbers are probably underestimations, because they result from applying regression models used to predict group size of modern foragers based on the size of their campsites, which means they could be biased, since modern hunter-gatherers show a social structure and use of space different from that of early humans. As a matter of fact, bone refuse accumulated at early sites formed much denser cluster areas than in modern hunter-gatherer campsites, although sites are overall smaller in size than home bases occupied by modern forager groups, especially when excluding low-density scatter areas. This is due to the fact that hominins probably congregated on small areas where food consumption took place collectively. Spatial analyses of the distribution of archaeological remains in all three anthropogenic sites in fact show that bone and lithic artifact clusters are of similar sizes and shapes, reflecting a centripetal use of space by hominins. This is also in line with the predictions of the MPC model and indicates a very cohesive group structure (Domínguez-Rodrigo *et al.*, in prep.).

Conclusions

The appearance of new large anthropogenic sites in Olduvai Bed I at a moment in which novel analytical and statistical methods are available represents an excellent opportunity to address old and new questions regarding the evolution of human behavior, like the meaning of these early sites, the use of the space and the landscape by hominins, and even their social structure. Matters that were once considered elusive or hard to address archaeologically may now be examined in a new light, with more effective taphonomic and spatial statistical approaches as well as with new evidence. Over the years, taphonomic studies have proved to be the answer to most of the questions stemming from the archaeological record. This study lends support to the idea that the examination of each taphonomic aspect of a faunal assemblage from more than one perspective using more than one statistical method as well as the combination of variables help detect hidden information in the fossil record and provide more reliable results. Also, the use of referential analogs and the combination of hypotheses help overcome equifinality and increase the heuristic power of theories. In this study, I have also attempted to solve certain issues by comparing the evidence from DS to the available archaeological and experimental record. Exploring zooarchaeological and taphonomic data from an archaeological site in isolation often does not yield very robust interpretations. One of the most important challenge faced by archaeologists and taphonomists is to find the link between the fossil record and the theories in the form of testable hypotheses.

The interpretation of DS presented here has shown that hominin social dynamics are effectively linked with their subsistence behaviors, and that both can be inferred from the taphonomic analyses and the spatial analysis of the pattern of distribution of food refuse. Based on the taphonomic and spatial evidence from the faunal assemblage of DS, early humans not only obtained and transported food collectively, they probably also engaged in the collective consumption of these resources at very specific reduced areas at the sites. Food was thus probably shared intentionally. Therefore, this study lends support to the theory that early *Homo* subsistence activities relied on high levels of cooperation and that this coordinated behavior resulted in high benefits for the hominin group. The behaviors inferred from these archaeological sites are probably attributable to *Homo ergaster* or to a similar species. Therefore, the re-

sults are also in line with the general agreement among researchers that the appearance of this species marked a significant shift in adaptation from the other hominins. Around 2 Mya, the consumption of meat by hominins increased significantly, and a number of socio-reproductive behaviors that enabled and required meat-eating were also adopted. At that time, hominins appear to have already been part of the predatory guild and very successful hunters. The early archaeological record shows that in spite of their limited technology and their smaller brains compared to those of modern humans, early humans were capable of certain cognitively complex behaviors and were well-adapted to certain forms of hunting and group cooperation, even though their predatory behaviors and social reproductive structures may not have an equivalent in the present. After all, meat-eating, hunting, and cooperation are deeply rooted in our evolutionary history.

6. References

Aiello, L.C., Wells, J.C.K., 2002. Energetics and the Evolution of the Genus *Homo*. Annual Review of Anthropology. 3, 323-338

Aiello, L.C., Wheeler, P., 1995. The Expensive-Tissue Hypothesis: The Brain and the Digestive System in Human and Primate Evolution. Current Anthropology. 36, 199–221.

Altuna, J., Mariezkurrena, K., Ríos, J., San Emeterio, A., 2017. Ocupaciones Humanas en Aitzbitarte III (País Vasco). 26.000-13.000 BP (zona profunda de la cueva). Euskal Kultura Ondare Bilduma.

Antón, S.C., Potts, R., Aiello, L.C., 2014. Evolution of early *Homo*: An integrated biological perspective. Science 345.

Antón, S.C., Swisher, C.C., III, 2004. Early Dispersals of *Homo* from Africa. Annual Review of Anthropology. 33, 271-296.

Aramendi, J., Maté-González, M.A., Yravedra, J., Ortega, M.C., Arriaza, M.C., González-Aguilera, D., Baquedano, E., Domínguez-Rodrigo, M., 2017. Discerning carnivore agency through the three-dimensional study of tooth pits: Revisiting crocodile feeding behaviour at FLK-*Zinj* and FLK NN3 (Olduvai Gorge, Tanzania). Palaeogeography Palaeoclimatology Palaeoecology. 488, 93–102.

Archer, W., Aldeias, V., McPherron, S.P., 2020. What is "in situ"? A reply to Harmand *et al.* (2015). Journal of Human Evolution. 142, 102740.

Ardrey, R., 1976. The hunting hypothesis: a personal conclusion concerning the evolutionary nature of man. Macmillan Publishing Company.

Argote-Espino, D., Solé, J., López-García, P., Sterpone, O., 2012. Obsidian Subsource Identification in the Sierra de Pachuca and Otumba Volcanic Regions, Central Mexico, by ICP-MS and DBSCAN Statistical Analysis. Geoarchaeology 27 (1), 48–62.

Arilla, M., Rosell, J., Blasco, R., Domínguez-Rodrigo, M., Pickering, T.R., 2014. The "bear" essentials: actualistic research on Ursus arctos arctos in the Spanish Pyrenees and its implications for paleontology and archaeology. PLoS One 9, e102457.

Arráiz, H., Barboni, D., Ashley, G.M., Mabulla, A., Baquedano, E., Domínguez-Rodrigo, M., 2017. The FLK *Zinj* paleolandscape: Reconstruction of a 1.84 Ma wooded habitat in the FLK *Zinj*-AMK-PTK-DS archaeological complex,

Middle Bed I (Olduvai Gorge, Tanzania). Palaeogeography Palaeoclimatology Palaeoecology. 488, 9–20.

Arriaza, M.C., Domínguez-Rodrigo, M., 2016. When felids and hominins ruled at Olduvai Gorge: A machine learning analysis of the skeletal profiles of the non-anthropogenic Bed I sites. Quaternary Science Review. 139, 43–52.

Arriaza, M.C., Domínguez-Rodrigo, M., Martínez-Maza, C., Mabulla, A., Baquedano, E., 2015. Differential predation by age and sex classes in blue wildebeest in Serengeti: study of a modern carnivore den in Olduvai Gorge (Tanzania). PLoS One 10, e0125944.

Arriaza, M.C., Domínguez-Rodrigo, M., Yravedra, J., Baquedano, E., 2016. Lions as Bone Accumulators? Paleontological and Ecological Implications of a Modern Bone Assemblage from Olduvai Gorge. PLoS One 11, e0153797.

Arriaza, M.C., Organista, E., Yravedra, J., 2019. Striped hyenas as bone modifiers in dual human-to-carnivore experimental models. Archaeological and Anthropological Sciences.11, 3187–3199.

Asfaw, B., Gilbert, W.H., Beyene, Y., Hart, W.K., Renne, P.R., WoldeGabriel, G., Vrba, E.S., White, T.D., 2002. Remains of *Homo erectus* from Bouri, Middle Awash, Ethiopia. Nature 416, 317–320.

Ashley, G.M., Barboni, D., Dominguez-Rodrigo, M., Bunn, H.T., Mabulla, A.Z.P., Diez-Martin, F., Barba, R., Baquedano, E., 2010. A spring and wooded habitat at FLK *Zinj* and their relevance to origins of human behavior. Quaternary Research. 74 (3), 304-314.

Aslan, A., Behrensmeyer, A.K., 1996. Taphonomy and Time Resolution of Bone Assemblages in a Contemporary Fluvial System: The East Fork River, Wyoming. Palaios 11, 411–421.

Assefa, Z., 2006. Faunal remains from Porc-Epic: paleoecological and zooarchaeological investigations from a Middle Stone Age site in southeastern Ethiopia. Journal of Human Evolution. 51, 50–75.

Attwell, C.A.M., 1980. Age detemination of the blue wildebeest *Connochaetes taurinus* in Zululand. South African Journal of Zoology. 15 (3), 121-130.

Baddeley, A.J., Turner, R., 2005. Spatstat: An R package for analyzing spatial point pattens. Journal of Statistical Software. 12 (6), 1-42.

Baddeley, A., Rubak, E., Turner, R., 2015. Spatial Point Patterns: Methodology and Applications with R. CRC Press.

Badgley, C., 1986a. Counting Individuals in Mammalian Fossil Assemblages from Fluvial Environments. Palaios 1, 328–338.

Badgley, C., 1986b. Taphonomy of mammalian fossil remains from Siwalik rocks of Pakistan. Paleobiology 12, 119–142.

Badgley, C., Behrensmeyer, A.K., 1980. Paleoecology of Middle Siwalik sediments and faunas, northern Pakistan. Palaeogeography, Palaeoclimatology, Palaeoecology. 30, 133-155.

Barboni, D., Ashley, G.M., Dominguez-Rodrigo, M., Bunn, H.T., Mabulla, A.Z.P., Baquedano, E., 2010. Phytoliths infer locally dense and heterogeneous paleovegetation at FLK North and surrounding localities during upper Bed I time, Olduvai Gorge, Tanzania. Quaternary Research. 74, 344–354.

Bartram, Jr., E., L., Marean, C.W., 1999. Explaining the "Klasies Pattern": Kua Ethnoarchaeology, the Die Kelders Middle Stone Age Archaeofauna, Long Bone Fragmentation and Carnivore Ravaging. Journal of Archaeological Sciences. 26, 9–29.

Bartram, L.E., 1997. A Comparison of Kua (Botswana) and Hadza (Tanzania) Bow and Arrow Hunting, in: Knecht, H. (Ed.), Projectile Technology. Springer US, Boston, MA, pp. 321–343.

Bartram, L.E., 1993. An ethnographic analysis of Kua San (Botswana) bone food refuse. Ph.D. University of Wisconsin-Madison.

Bartram, L.E., Kroll, E.M., Bunn, H.T., 1991. Variability in Camp Structure and Bone Food Refuse Patterning at Kua San Hunter-Gatherer Camps, in: Kroll, E.M., Price, T.D. (Eds.), The Interpretation of Archaeological Spatial Patterning. Springer US, Boston, MA, pp. 77–148.

Behrensmeyer, A.K., 1983. Patterns of natural bone distribution on recent land surfaces: implications for archaeological site formation. Animals and Archaeology: 1. Hunters and Their Prey; BAR International series 163, 93–106.

Behrensmeyer, A.K., 1982. Time resolution in fluvial vertebrate assemblages. Paleobiology 8, 211–227.

Behrensmeyer, A.K., 1978. Taphonomic and ecologic information from bone weathering. Paleobiology 4, 150–162.

Behrensmeyer, A.K., 1975. The taphonomy and paleoecology of Plio-Pleistocene vertebrate assemblages east of Lake Rudolf, Kenya. Bulletin of the Museum of Comparative Zoology at Harvard College. 146, 474-578.

Behrensmeyer, A.K., Gordon, K.D., Yanagi, G.T., 1986. Trampling as a cause of bone surface damage and pseudo-cutmarks. Nature. 319, 768-771.

Benito-Calvo, A., de la Torre, I., 2011. Analysis of orientation patterns in Olduvai Bed I assemblages using GIS techniques: Implications for site formation processes. Journal of Human Evolution. 61 (1), 50-60.

Benn, D., 1994. Fabric shape and the interpretation of sedimentary fabric data. Journal of Sedimentary Research. 64, 910-915.

Berger, T.D., Trinkaus, E., 1995. Patterns of trauma among the Neandertals. Journal of Archaeological Sciences. 22 (6), 841-852.

Bevan, A., Lake, M., 2016. Intensities, interactions, and uncertainties: some new approaches to archaeological distributions, in: Bevan, A., Lake, M., (Eds.), Computational approaches to archaeological spaces, pp. 27-53.

Binford, L.R., 1985. Human ancestors: Changing views of their behavior. Journal of Anthropological Archaeology 4, 292–327.

Binford, L.R., 1984. Faunal Remains from Klasies River Mouth. Academic Press, New York.

Binford, L.R., 1983. Long term land use patterns: some implications for archaeology, in: Dunnell, R.C., Grayson, D.K., (Eds.), Lulu linear punctated: Essays in honor of George Irving Quimby, Anthropological Papers of the Museum of Anthropology, University of Michigan 72, pp. 27-53.

Binford, L.R., 1981. Bones: Ancient Men and Modern Myths. Orlando: Academic Press.

Binford, L.R., 1978. Nunamiut Ethnoarchaeology. Academic Press, New York.

Binford, L.R., Bunn, H.T., Kroll, E.M., 1988. Fact and Fiction about the *Zinj*-anthropus Floor: Data, Arguments, and Interpretations. Current Anthropology. 29, 123–149.

Bishop, C.M., 1995. Neural Networks for Pattern Recognition. Oxford University Press.

Bivand, R., Pebesma, E., Gómez-Rubio, V., 2013. Applied spatial data: analysis with R. Springer, New York.

Bivand, R.S., 2010. Exploratory Spatial Data Analysis, in: Fischer, M.M., Getis, A. (Eds.), Handbook of Applied Spatial Analysis: Software Tools, Methods and Applications. Springer Berlin Heidelberg, Berlin, Heidelberg, pp. 219–254.

Blasco López, R., 2011. La amplitud de la dieta cárnica en el Pleistoceno medio peninsular: una aproximación a partir de la Cova del Bolomor (Tavernes de la Valldigna, Valencia) y del subnivel TD10-1 de Gran Dolina (Sierra de Atapuerca, Burgos. PhD Universitat Rovira i Virgili.

Blasco, R., Domínguez-Rodrigo, M., Arilla, M., Camarós, E., Rosell, J., 2014. Breaking Bones to Obtain Marrow: A Comparative Study between Percussion by Batting Bone on an Anvil and Hammerstone Percussion. Archaeometry 56, 1085–1104.

Blasco, R., Fernández Peris, J., 2012. Small and large game: Human use of diverse faunal resources at Level IV of Bolomor Cave (Valencia, Spain). C. R. Palevol 11, 265–282.

Blasco, R., Rosell, J., Gopher, A., Barkai, R., 2014. Subsistence economy and social life: A zooarchaeological view from the 300 kya central hearth at Qesem Cave, Israel. Journal of Anthropological Archaeology 35, 248-268.

Blumenschine, J, R., 1993. A carnivore's view of archaeological bone assemblages. in: Hudson, J. (Ed.), From Bones to Behavior: Ethnoarchaeological and Experimental Contributions to the Interpretation of Faunal Remains. Carbondale, Center for Archaeological Investigations, Southern Illinois at Carbondale, pp. 156-168.

Blumenschine, R.J., Peters, C.R., Masao, F.T., Clarke, R.J., Deino, A.L., Hay, R.L., Swisher, C.C., Stanistreet, I.G., Ashley, G.M., McHenry, L.J., Sikes, N., van

der Merwe, N.J., Tactikos, J.C., Cushing, A., Deocampo, D.M., Njau, J.K., Ebert, J.I., 2003. Late Pliocene *Homo* and hominid land use from western Olduvai Gorge, Tanzania. Science 299, 1217–1221.

Blumenschine, R.J., 1995. Percussion marks, tooth marks, and experimental determinations of the timing of hominid and carnivore access to long bones at FLK *Zinj*anthropus, Olduvai Gorge, Tanzania. Journal of Human Evolution, 29 (1), 21-51.

Blumenschine, R.J., 1991. Hominid carnivory and foraging strategies, and the socio-economic function of early archaeological sites. Philos. Trans. R. Soc. Lond. B Biol. Sci. 334, 211–9; discussion 219–21.

Blumenschine, R.J., 1988a. Reinstating an Early Hominid Scavenging Niche: A Reply to Potts. Current Anthropology 29, 483-486.

Blumenschine, R.J., 1988b. An experimental model of the timing of hominid and carnivore influence on archaeological bone assemblages. Journal of Archaeological Science 15 (5), 483-502.

Blumenschine, R.J., 1986. Carcass consumption sequences and the archaeological distinction of scavenging and hunting. J. Hum. Evol. 15, 639–659.

Blumenschine, R.J., Caro, T.M., 1986. Unit flesh weights of some East African bovids. Afr. J. Ecol. 24, 273–286.

Blumenschine, R.J., Cavallo, J.A., Capaldo, S.D., 1994. Competition for carcasses and early hominid behavioral ecology: A case study and conceptual framework. Journal of Human Evolution 27 (1-3), 197-213.

Blumenschine, R.J., Masao, F.T., 1991. Living sites at Olduvai Gorge, Tanzania? Preliminary landscape archaeology results in the basal Bed II lake margin zone. J. Hum. Evol. 21, 451–462.

Blumenschine, R.J., Peters, C.R., 1998. Archaeological predictions for hominid land use in the paleo-Olduvai Basin, Tanzania, during lowermost Bed II times. J. Hum. Evol. 34, 565–607.

Blumenschine, R.J., Pobiner, B.L., 2007. Zooarchaeology and the ecology of Oldowan hominin carnivory, in: Ungar, P.S., (Ed.), Evolution of the human diet: the known, the unknown, and the unknowable. Oxford University Press, pp. 167-190.

Blumenschine, R.J., Selvaggio, M.M., 1988. Percussion marks on bone surfaces as a new diagnostic of hominid behaviour. Nature 333, 763–765.

Blumenschine, R.J., Stanistreet, I.G., Njau, J.K., Bamford, M.K., Masao, F.T., Albert, R.M., Stollhofen, H., Andrews, P., Prassack, K.A., McHenry, L.J., Fernández-Jalvo, Y., Camilli, E.L., Ebert, J.I., 2012. Environments and hominin activities across the FLK Peninsula during *Zinj*anthropus times (1.84 Ma), Olduvai Gorge, Tanzania. J. Hum. Evol. 63, 364–383.

Boaz, N.T., 1982. Aspects of early hominid emergence. Reviews in Anthropology 9, 313–319.

Boaz, N.T., Behrensmeyer, A.K., 1976. Hominid taphonomy: transport of human skeletal parts in an artificial fluviatile environment. Am. J. Phys. Anthropol. 45, 53–60.

Boaz, N.T., Clark Howell, F., 1977. A gracile hominid cranium from upper member G of the Shungura Formation, Ethiopia. American Journal of Physical Anthropology 46 (1), 93-108.

Boesch, C., Boesch, H., 1989. Hunting behavior of wild chimpanzees in the Tai National Park. American journal of physical Anthropology, 78 (4), 547-573.

Boucher de Perthes, J., 1849. Antiquités celtiques et antédiluviennes: Mémoire sur l'industrie primitive et leurs arts à leur origine. Tome premier. Treuttel et Wurtz, Derache, Dumoulin et Didron, Paris.

Bouchneb, L., Maureille, B., 2004. Sillons d'usure interproximaux: reproduction expérimentale, analyse et application des résultats aux observations sur la lignée néandertalienne. Bulletins et mémoires de la Société d'Anthropologie de Paris 16 (1-2), 37-48.

Brain, C.K., 1983. The Hunters Or the Hunted?: An Introduction to African Cave Taphonomy. University of Chicago Press.

Brain, C.K., 1974. Some suggested procedures in the analysis of bone accumulations from southern African Quaternary sites. Annals of the Transvaal Museum.

Brain, C.K., 1969. The contribution of Namib Desert Hottentots to an understanding of australopithecine bone accumulations. Scientific Papers of the Namib Desert Research Station 39, 13-22.

Bramble, D.M., Lieberman, D.E., 2004. Endurance running and the evolution of *Homo*. Nature 432, 345–352.

Braun, D.R., Harris, J.W.K., Levin, N.E., McCoy, J.T., Herries, A.I.R., Bamford, M.K., Bishop, L.C., Richmond, B.G., Kibunjia, M., 2010. Early hominin diet included diverse terrestrial and aquatic animals 1.95 Ma in East Turkana, Kenya. Proc. Natl. Acad. Sci. U. S. A. 107, 10002–10007.

Braun, D.R., Plummer, T., Ferraro, J.V., Ditchfield, P., Bishop, L.C., 2009. Raw material quality and Oldowan hominin toolstone preferences: evidence from Kanjera South, Kenya. J. Archaeol. Sci. 36, 1605–1614.

Bromage, T.G., Schrenk, F., Zonneveld, F.W., 1995. Paleoanthropology of the Malawi Rift: An early hominid mandible from the Chiwondo Beds, northern Malawi. J. Hum. Evol. 28, 71–108.

Brooks, D.R., McLennan, D.A., . McLennan, D.A., 1991. Phylogeny, Ecology, and Behavior: A Research Program in Comparative Biology. University of Chicago Press.

Brugal, J.P., 1994. Introduction générale: action de l'eau sur les ossements et les assemblages fossiles. Artefacts 9 (Outillage pen elabore en os et en bois de cervides IV), 121-129.

Bunge, M., 1998. Philosophy of Science: From Explanation to Justification. Transaction Publishers.

Bunn, H., Harris, J.W.K., Isaac, G., Kaufulu, Z., Kroll, E., Schick, K., Toth, N., Behrensmeyer, A.K., 1980. FxJj50: An early Pleistocene site in northern Kenya. World Archaeol. 12, 109–136.

Bunn, H.T., 2006. Meat made us human, in: Ungar, P.S., (Ed.), Evolution of the human diet: the known, the unknown and the unknowable. Oxford University Press, pp. 191-211.

Bunn, H.T., 1994. Early Pleistocene hominid foraging strategies along the ancestral Omo River at Koobi Fora, Kenya. J. Hum. Evol. 27, 247–266.

Bunn, H.T., 1991. A Taphonomic Perspective on the Archaeology of Human Origins. Annu. Rev. Anthropol. 20, 433–467.

Bunn, H.T., 1986. Patterns of skeletal representation and hominid subsistence activities at Olduvai Gorge, Tanzania, and Koobi Fora, Kenya. J. Hum. Evol. 15, 673–690.

Bunn, H.T., 1983. Evidence on the diet and subsistence patterns of Plio-Pleistocene hominids at Koobi Fora, Kenya, and at Olduvai Gorge, Tanzania. Animals and archaeology 1, 21–30.

Bunn, H.T., 1981. Archaeological evidence for meat-eating by Plio-Pleistocene hominids from Koobi Fora and Olduvai Gorge. Nature 291, 574–577.

Bunn, H.T., Bartram, L.E., Kroll, E.M., 1988. Variability in bone assemblage formation from Hadza hunting, scavenging, and carcass processing. Journal of anthropological Archaeology 7(4), 412-457.

Bunn, H.T., Ezzo, J.A., 1993. Hunting and Scavenging by Plio-Pleistocene Hominids: Nutritional Constraints, Archaeological Patterns, and Behavioural Implications. J. Archaeol. Sci. 20, 365–398.

Bunn, H.T., Gurtov, A.N., 2014. Prey mortality profiles indicate that Early Pleistocene *Homo* at Olduvai was an ambush predator. Quaternary International 322-323, 44-53.

Bunn, H.T., Kroll, E.M., 1988. A reply to Binford. Curr. Anthropol. 29, 123-149.

Bunn, H.T., Kroll, E.M., Ambrose, S.H., Behrensmeyer, A.K., Binford, L.R., Blumenschine, R.J., Klein, R.G., McHenry, H.M., O'Brien, C.J., Wymer, J.J., 1986. Systematic Butchery by Plio/Pleistocene Hominids at Olduvai Gorge, Tanzania [and Comments and Reply]. Curr. Anthropol. 27, 431–452.

Bunn, H.T., Kroll, E.M., Bartram, L.E., 1991. Bone distribution on a modern East African landscape and its archaeological implications, in: Clark, J.D., (Ed.), Cultural beginnings: Approaches to understanding early hominid life ways in the African savanna. U.I.S.P. Monographien Band 19, 33-54.

Bunn, H.T., Pickering, T.R., 2010a. Bovid mortality profiles in paleoecological context falsify hypotheses of endurance running–hunting and passive scav-

enging by early Pleistocene hominins. Quat. Res. 74, 395–404.

Bunn, H.T., Pickering, T.R., 2010b. Methodological recommendations for ungulate mortality analyses in paleoanthropology. Quat. Res. 74, 388–394.

Cachel, S., Harris, J.W.K., 1998. The lifeways of *Homo erectus*. Early human behavior in global context. Routledge.

Camarós, E., Cueto, M., Teira, L.C., Tapia, J., Cubas, M., Blasco, R., Rosell, J., Rivals, F., 2013. Large carnivores as taphonomic agents of space modification: an experimental approach with archaeological implications. J. Archaeol. Sci. 40, 1361–1368.

Cannon, M.D., 2003. A model of central place forager prey choice and an application to faunal remains from the Mimbres Valley, New Mexico. Journal of Anthropological Archaeology 22, 1–25.

Capaldo, S.D., 1998. Simulating the Formation of Dual-Patterned Archaeofaunal Assemblages with Experimental Control Samples. J. Archaeol. Sci. 25, 311–330.

Capaldo, S.D., 1997. Experimental determinations of carcass processing by Plio-Pleistocene hominids and carnivores at FLK 22 (*Zinj*anthropus). Olduvai Gorge, Tanzania. J. Hum. Evol. 33, 555–597.

Capaldo, S.D., 1995. Inferring Hominid and Carnivore Behavior from Dual-patterned Archaeofaunal Assemblages. Journal of Human Evolution 35 (3), 317-320.

Capaldo, S.D., Blumenschine, R.J., 1994. A Quantitative Diagnosis of Notches Made by Hammerstone Percussion and Carnivore Gnawing on Bovid Long Bones. American Antiquity 59 (4), 724-748.

Carrier, D.R., Kapoor, A.K., Kimura, T., Nickels, M.K., Scott, E.C., So, J.K., Trinkaus, E., 1984. The Energetic Paradox of Human Running and Hominid Evolution [and Comments and Reply]. Curr. Anthropol. 25, 483–495.

Cavallo, J.A., Blumenschine, R.J., 1989. Tree-stored leopard kills: expanding the hominid scavenging niche. J. Hum. Evol. 18, 393–399.

Chaplin, R.E., 1971. The study of animal bones from archaeological sites. Archaeology. Seminar Press.

Chiu, S.N., Molchanov, I.S., 2003. A new graph related to the directions of nearest neighbours in a point process. Adv. Appl. Probab. 35, 47–55.

Cifuentes-Alcobendas, G., Domínguez-Rodrigo, M., 2019. Deep learning and taphonomy: high accuracy in the classification of cut marks made on fleshed and defleshed bones using convolutional neural networks. Sci. Rep. 9, 18933.

Clark, A.E., 2017. From activity areas to occupational histories: new methods to document the formation of spatial structure in hunter-gatherer sites. Journal of Archaeological Method and Theory 24 (4), 1300-1325.

Clark, P.J., Evans, F.C., 1954. Distance to Nearest Neighbor as a Measure of

Spatial Relationships in Populations. Ecology 35 (4), 445-453.

Cleghorn, N., Marean, C.W., 2004. Distinguishing selective transport and in situ attrition: a critical review of analytical approaches. Journal of Taphonomy 2, 43-67.

Cleghorn, N., Marean, C.W., Pickering, T.R., 2007. The destruction of skeletal elements by carnivores: the growth of a general model for skeletal element destruction and survival in zooarchaeological assemblages, in: Pickering, T.R., Schick, K., (Eds.), Breathing life into fossils: Taphonomic studies in honor of C.K. (Bob) Brain. Gosport: Stone Age Institute Press, pp. 37-66.

Coard, R., 1999. One Bone, Two Bones, Wet Bones, Dry Bones: Transport Potentials Under Experimental Conditions. J. Archaeol. Sci. 26, 1369–1375.

Coard, R., Dennell, R.W., 1995. Taphonomy of Some Articulated Skeletal Remains: Transport Potential in an Artificial Environment. J. Archaeol. Sci. 22, 441–448.

Cobo-Sánchez, L., Aramendi, J., Domínguez-Rodrigo, M., 2014. Orientation patterns of wildebeest bones on the lake Masek floodplain (Serengeti, Tanzania) and their relevance to interpret anisotropy in the Olduvai lacustrine floodplain. Quaternary International 322-323, 277-284.

Cohn, J., 1988. Statistical power analysis for the behavioral sciences (2nd ed.). Hillsdale, NJ: Lawrence Erlbaum Associates, Publishers.

Coil, R., Tappen, M., Ferring, R., Bukhsianidze, M., Nioradze, M., Lordkipanidze, D., 2020. Spatial patterning of the archaeological and paleontological assemblage at Dmanisi, Georgia: An analysis of site formation and carnivore-hominin interaction in Block 2. J. Hum. Evol. 143, 102773.

Cortes, C., Vapnik, V., 1995. Support-Vector Networks. Machine Learning 20, 273-297.

Costamagno, S., 2000. Stratégies d'approvisionnement et traitement des carcasses au Magdalénien : l'exemple de Moulin-Neuf (Gironde) / Magdalenian acquisition strategies and carcass processing : the example of Moulin-Neuf (Gironde). Paléo, Revue d'Archéologie Préhistorique 12, 77-95.

Costamagno, S., Fano, M.A., 2005. Pratiques cynégétiques et exploitation des ressources animales dans les niveaux du Magdalénien supérieur-final de El Horno (Ramales, Cantabrie, Espagne. Paléo, Revue d'Archéologie Préhistorique, SAMRA 17, 31-56.

Courtenay, L.A., Yravedra, J., Huguet, R., Aramendi, J., Maté-González, M.Á., González-Aguilera, D., Arriaza, M.C., 2019. Combining machine learning algorithms and geometric morphometrics: A study of carnivore tooth marks. Palaeogeogr. Palaeoclimatol. Palaeoecol. 522, 28–39.

Cressie, N., Read, T.R.C., 1984. Multinomial goodness-of-fit tests. J. R. Stat. Soc. 46 (3), 440-464.

Cronie, O., Van Lieshout, M.N.M., 2018. A non-model-based approach to

bandwidth selection for kernel estimators of spatial intensity functions. Biometrika 105, 455–462.

Dart, R.A., 1959. Further light on australopithecine humeral and femoral weapons. Am. J. Phys. Anthropol. 17, 87–93.

Dart, R.A., 1953. The predatory transition from ape to man. Brill.

Darwin, C., 1871. The descent of man and selection in relation to sex. Murray. London.

Daujeard, C., 2008. Exploitation du milieu animal par les Néanderthaliens dans le Sud-Est de la France. PhD, Lyon.

de Heinzelin, J., Clark, J.D., White, T., Hart, W., Renne, P., WoldeGabriel, G., Beyene, Y., Vrba, E., 1999. Environment and behavior of 2.5-million-year-old Bouri hominids. Science 284, 625–629.

De Juana, S., Domínguez-Rodrigo, M., 2011. Testing analogical taphonomic signatures in bone breaking: a comparison between hammerstone-broken equid and bovid bones. Archaeometry 53 (5), 996-1011.

de la Torre, I., Mora, R., 2005. Unmodified lithic material at Olduvai Bed I: manuports or ecofacts? J. Archaeol. Sci. 32, 273–285.

de los Terreros, J.Y.S., Gómez-Castanedo, A., 2016. Neanderthal and *Homo* sapiens subsistence strategies in the Cantabrian region of northern Spain. Archaeol. Anthropol. Sci. 8 (4), 779-803.

Dennell, R., 1990. Progressive gradualism, imperialism and academic fashion: Lower Palaeolithic archaeology in the 20th century. Antiquity 64, 549–558.

Díez, J.C., Fernández-Jalvo, Y., Rosell, J., Cáceres, I., 1999. Zooarchaeology and taphonomy of Aurora Stratum (Gran Dolina, Sierra de Atapuerca, Spain). J. Hum. Evol. 37, 623–652.

Diggle, P., 2003. Statistical Analysis of Spatial Point Patterns., 2nd edn., Arnold: London.

Diggle, P., Zheng, P., Durr, P., 2005. Nonparametric estimation of spatial segregation in a multivariate point process: bovine tuberculosis in Cornwall, UK. J. R. Stat. Soc. Ser. C Appl. Stat. 54, 645–658.

Dodson, P., 1973. The significance of small bones in paleoecological interpretation. Rocky Mt Geol. 12(1), 15-19.

Domínguez-Rodrigo, M., 2019. Successful classification of experimental bone surface modifications (BSM) through machine learning algorithms: a solution to the controversial use of BSM in paleoanthropology? Archaeol. Anthropol. Sci. 11 (6), 2711-2725.

Domínguez-Rodrigo, M., 2015. Taphonomy in early African archaeological sites: Questioning some bone surface modification models for inferring fossil hominin and carnivore feeding interactions. J. Afr. Earth. Sci. 108, 42–46.

Domínguez-Rodrigo, M., 2012. Critical review of the MNI (minimum number of individuals) as a zooarchaeological unit of quantification. Archaeol. An-

thropol. Sci. 4 (1), 47-59.

Domínguez-Rodrigo, M., 2009. Are all Oldowan Sites Palimpsests? If so, what can they tell us about Hominid Carnivory?, in: Hovers, E., Braun, D.R. (Eds.), Interdisciplinary Approaches to the Oldowan. Springer Netherlands, Dordrecht, pp. 129–147.

Domínguez-Rodrigo, M., 2009. A taphonomic study of bone modification and of tooth-mark patterns on long limb bone portions by suids. International Journal of Osteoarchaeology 19 (3), 345-363.

Domínguez-Rodrigo, M., 2007. Equifinality in carnivore tooth marks and the extended concept of archaeological palimpsests: implications for models of passive scavenging in early hominids, in: Pickering, T.R., Toth, N., Schick, K., (Eds.), Breathing life into fossils: taphonomic studies in honor of CK (Bob) Brain, pp. 255-267.

Domínguez-Rodrigo, M., 2002. Hunting and scavenging by early humans: the state of the debate. Journal of World Prehistory 16, 1–54.

Domínguez-Rodrigo, M., 2001. A study of carnivore competition in riparian and open habitats of modern savannas and its implications for hominid behavioral modelling. J. Hum. Evol. 40, 77–98.

Domínguez-Rodrigo, M., 1999. Meat-eating and carcass procurement by hominids at the FLK *Zinj* 22 site, Olduvai Gorge (Tanzania): a new experimental approach to the old hunting-versus-scavenging debate., in: Ullrich, H., (Ed.), Lifestyles and Survival Strategies in Pliocene and Pleistocene Hominids. Edition Archaea, Schwelm, Germany, pp. 89-111.

Domínguez-Rodrigo, M., 1997. Testing meat-eating in early hominids: an analysis of butchery marks on defleshed carcases. Hum. Evol. 12, 169–182.

Domínguez-Rodrigo, M., 2013. Toward a scientific-realistic theory on the origin of human behavior., in: Domínguez-Rodrigo, M., Stone Tools and Fossil Bones, pp. 11-44.

Dominguez-Rodrigo, M., Alcalá, L., 2019. Pliocene Archaeology at Lomekwi 3? New Evidence Fuels More Skepticism. Journal of African Archaeology 17, 173–176.

Domínguez-Rodrigo, M., Alcalá, L., 2016. 3.3-million-year-old stone tools and butchery traces? More evidence needed. PaleoAnthropology 2016, 46–53.

Domínguez-Rodrigo, M., Alcalá, L., Luque, L., 2009. Peninj: A research project on human origins 1995-2005. Oxbow Books.

Domínguez-Rodrigo, M., Baquedano, E., 2018. Distinguishing butchery cut marks from crocodile bite marks through machine learning methods. Sci. Rep. 8, 5786.

Domínguez-Rodrigo, M., Baquedano, E., Barba, R., Uribelarrea, D., Gidna, A., 2019a. The river that never was: Fluvial taphonomy at Olduvai Bed I and II sites and its bearing on early human behavior. Quaternary International, 526,

26-38.

Domínguez-Rodrigo, M., Barba, R., 2007. New estimates of tooth-mark and percussion-mark frequencies at the FLK *Zinj*anthropus level: the carn., in: Domínguez-Rodrigo, M., Barba, R., Egeland, C., (Eds.), Deconstructing Olduvai: A Taphonomic Study of the Bed I Sites, pp. 39-74.

Domínguez-Rodrigo, M., Barba, R., 2006. New estimates of tooth mark and percussion mark frequencies at the FLK *Zinj* site: the carnivore-hominid-carnivore hypothesis falsified. Journal of Human Evolution 50 (2), 170-194.

Domínguez-Rodrigo, M., Barba, R., Soto, E., Sesé, C., Santonja, M., Pérez-González, A., Yravedra, J., Galán, A.B., 2015a. Another window to the subsistence of Middle Pleistocene hominins in Europe: A taphonomic study of Cuesta de la Bajada (Teruel, Spain). Quat. Sci. Rev. 126, 67–95.

Domínguez-Rodrigo, M., Bunn, H.T., Mabulla, A.Z.P., Ashley, G.M., Diez-Martin, F., Barboni, D., Prendergast, M.E., Yravedra, J., Barba, R., Sánchez, A., Baquedano, E., Pickering, T.R., 2010. New excavations at the FLK *Zinj*anthropus site and its surrounding landscape and their behavioral implications. Quat. Res. 74, 315–332.

Domínguez-Rodrigo, M., Bunn, H.T., Mabulla, A.Z.P., Baquedano, E., Uribelarrea, D., Pérez-González, A., Gidna, A., Yravedra, J., Diez-Martin, F., Egeland, C.P., Barba, R., Arriaza, M.C., Organista, E., Ansón, M., 2014a. On meat eating and human evolution: A taphonomic analysis of BK4b (Upper Bed II, Olduvai Gorge, Tanzania), and its bearing on hominin megafaunal consumption. Quat. Int. 322-323, 129–152.

Domínguez-Rodrigo, M., Bunn, H.T., Pickering, T.R., Mabulla, A.Z.P., Musiba, C.M., Baquedano, E., Ashley, G.M., Diez-Martin, F., Santonja, M., Uribelarrea, D., Barba, R., Yravedra, J., Barboni, D., Arriaza, C., Gidna, A., 2012. Autochthony and orientation patterns in Olduvai Bed I: a re-examination of the status of post-depositional biasing of archaeological assemblages from FLK North (FLKN). J. Archaeol. Sci. 39, 2116–2127.

Domínguez-Rodrigo, M., Bunn, H.T., Yravedra, J., 2014b. A critical re-evaluation of bone surface modification models for inferring fossil hominin and carnivore interactions through a multivariate approach: application to the FLK *Zinj* archaeofaunal assemblage (Olduvai Gorge, Tanzania), 322-323, 32-43.

Domínguez-Rodrigo, M., Cobo-Sánchez, L., 2017a. A spatial analysis of stone tools and fossil bones at FLK *Zinj* 22 and PTK I (Bed I, Olduvai Gorge, Tanzania) and its bearing on the social organization of early humans. Palaeogeogr. Palaeoclimatol. Palaeoecol. 488, 21–34.

Domínguez-Rodrigo, M., Cobo-Sánchez, L., 2017b. The spatial patterning of the social organization of modern foraging *Homo* sapiens: A methodological approach for understanding social organization in prehistoric foragers. Palaeogeogr. Palaeoclimatol. Palaeoecol. 488, 113–125.

Domínguez-Rodrigo, M., Cobo-Sánchez, L., 2017. Spatial simulation and

modelling of the early Pleistocene site of DS (Bed I, Olduvai Gorge, Tanzania): a powerful tool for predicting potential archaeological information from unexcavated areas. Boreas 46 (4), 805-815.

Domínguez-Rodrigo, M., Cobo-Sánchez, L., Aramendi, J., Gidna, A., 2019b. The meta-group social network of early humans: A temporal–spatial assessment of group size at FLK *Zinj* (Olduvai Gorge, Tanzania). J. Hum. Evol. 127, 54–66.

Domínguez-Rodrigo, M., Cobo-Sánchez, L., Yravedra, J., Uribelarrea, D., Arriaza, C., Organista, E., Baquedano, E., 2018. Fluvial spatial taphonomy: a new method for the study of post-depositional processes. Archaeological and Anthropological Sciences 10, 1769-1789.

Domínguez-Rodrigo, M., de Juana, S., Galán, A.B., Rodríguez, M., 2009a. A new protocol to differentiate trampling marks from butchery cut marks. J. Archaeol. Sci. 36, 2643–2654.

Domínguez-Rodrigo, M., Egeland, C.P., Pickering, T.R., 2007. Models of passive scavenging by early hominids: problems arising from equifinality in carnivore tooth mark frequencies and the extended concept of archaeological palimpsests, in: Pickering, T.R., Toth, N., Schick, K. (Eds.), Breathing Life into Fossils: Taphonomic Studies in Honor of C.K. (Bob) Brain. Stone Age Institute Press, Gosport, Indiana, pp. 255-268.

Domínguez-Rodrigo, M., Egido, R.B., Egeland, C.P., 2007. Deconstructing Olduvai: A Taphonomic Study of the Bed I Sites. Vertebrate Paleobiology and Paleoanthropology. Springer

Domínguez Rodrigo, M., Fernández López, S.R., 2011. How can taphonomy be defined in the XXI century? Journal of paleontology 9 (1), 1-13.

Domínguez-Rodrigo, M., García-Pérez, A., 2013. Testing the accuracy of different A-axis types for measuring the orientation of bones in the archaeological and paleontological record. PLoS One 8, e68955.

Domínguez-Rodrigo, M., Lezana, R.M., 1996. Estudio etnoarqueológico de un campamento temporal Ndorobo (Maasai) en Kulalu (Kenia). Trabajos de Prehistoria 53, 131–143.

Domínguez-Rodrigo, M., Lopez-Saez, J.A., Vincens, A., Alcala, L., Luque, L., Serrallonga, J., 2001. Fossil pollen from the Upper Humbu Formation of Peninj (Tanzania): hominid adaptation to a dry open Plio-Pleistocene savanna environment. J. Hum. Evol. 40, 151–157.

Domínguez-Rodrigo, M., Mabulla, A., Bunn, H.T., Barba, R., Diez-Martín, F., Egeland, C.P., Espílez, E., Egeland, A., Yravedra, J., Sánchez, P., 2009b. Unraveling hominin behavior at another anthropogenic site from Olduvai Gorge (Tanzania): new archaeological and taphonomic research at BK, Upper Bed II. Journal of Human Evolution 57 (3), 260-283.

Domínguez-Rodrigo, M., Martínez-Navarro, B., 2012. Taphonomic analysis

of the early Pleistocene (2.4 Ma) faunal assemblage from A.L. 894 (Hadar, Ethiopia). J. Hum. Evol. 62, 315–327.

Domínguez-Rodrigo, M., Pickering, T.R., 2017. The meat of the matter: an evolutionary perspective on human carnivory. Azania: Archaeological Research in Africa 52 (1), 4-32.

Domínguez-Rodrigo, M., Pickering, T.R., 2015. Earliest modern human-like hand bone from a new> 1.84-million-year-old site at Olduvai in Tanzania. Nature 6, 7987.

Domínguez-Rodrigo, M., Pickering, T.R., Bunn, H.T., 2011. Reply to McPherron *et al.*: Doubting Dikika is about data, not paradigms. Proc. Natl. Acad. Sci. U. S. A. 108, E117–E117.

Domínguez-Rodrigo, M., Pickering, T.R., Bunn, H.T., 2010. Configurational approach to identifying the earliest hominin butchers. Proc. Natl. Acad. Sci. U. S. A. 107, 20929–20934.

Domínguez-Rodrigo, M., Pickering, T.R., Diez-Martín, F., Mabulla, A., Musiba, C., Trancho, G., Baquedano, E., Bunn, H.T., Barboni, D., Santonja, M., Uribelarrea, D., Ashley, G.M., Martínez-Ávila, M. del S., Barba, R., Gidna, A., Yravedra, J., Arriaza, C., 2012. Earliest porotic hyperostosis on a 1.5-million-year-old hominin, olduvai gorge, Tanzania. PLoS One 7, e46414.

Domínguez-Rodrigo, M., Pickering, T.R., Semaw, S., Rogers, M.J., 2005. Cutmarked bones from Pliocene archaeological sites at Gona, Afar, Ethiopia: implications for the function of the world's oldest stone tools. J. Hum. Evol. 48, 109–121.

Domínguez-Rodrigo, M., Sánchez-Flores, A.J., Baquedano, E., Arriaza, M.C., Aramendi, J., Cobo-Sánchez, L., Organista, E., Barba, R., 2019. Constraining time and ecology on the *Zinj* paleolandscape: Microwear and mesowear analyses of the archaeofaunal remains of FLK *Zinj* and DS (Bed I), compared to FLK North (Bed I) and BK (Bed II) at Olduvai Gorge (Tanzania), Quaternary International 526, 4-14.

Dominguez- Rodrigo, M., Serrallonga, J., Juan-Tresserras, J., Alcala, L., Luque, L., 2001. Woodworking activities by early humans: a plant residue analysis on Acheulian stone tools from Peninj (Tanzania). J. Hum. Evol. 40, 289–299.

Domínguez-Rodrigo, M., Uribelarrea, D., Santonja, M., Bunn, H.T., García-Pérez, A., Pérez-González, A., Panera, J., Rubio-Jara, S., Mabulla, A., Baquedano, E., Yravedra, J., Diez-Martín, F., 2014c. Autochthonous anisotropy of archaeological materials by the action of water: experimental and archaeological reassessment of the orientation patterns at the Olduvai sites. J. Archaeol. Sci. 41, 44–68.

Domínguez-Rodrigo, D., Pickering, T.R., 2010. A multivariate approach for discriminating bone accumulations created by spotted hyenas and leopards:

harnessing actualistic data from East and Southern Africa. Journal of Taphonomy 8 (2), 155-179.

Domínguez-Rodrigo, M., Yravedra, J., 2009. Why are cut mark frequencies in archaeofaunal assemblages so variable? A multivariate analysis. J. Archaeol. Sci. 36, 884–894.

Domínguez-Rodrigo, M., Barba, R., 2005. A study of cut marks on small-sized carcasses and its application to the study of cut-marked bones from small mammals at the FLK *Zinj* site. Journal of Taphonomy 3 (2), 121-134.

Domínguez-Rodrigo, M., Yravedra, J., Organista, E., Gidna, A., Fourvel, J.-B., Baquedano, E., 2015b. A new methodological approach to the taphonomic study of paleontological and archaeological faunal assemblages: a preliminary case study from Olduvai Gorge (Tanzania). J. Archaeol. Sci. 59, 35–53.

Domínguez-Rodrigo, M., 1999. Flesh availability and bone modifications in carcasses consumed by lions: palaeoecological relevance in hominid foraging patterns. Palaeogeogr. Palaeoclimatol. Palaeoecol. 149, 373–388.

Domínguez-Rodrigo, M., 1997. Meat-eating by early hominids at the FLK 22 *Zinj*anthropus site, Olduvai Gorge (Tanzania): an experimental approach using cut-mark data. J. Hum. Evol. 33, 669–690.

Dominy, N.J., Vogel, E.R., Yeakel, J.D., Constantino, P., Lucas, P.W., 2008. Mechanical properties of plant underground storage organs and implications for dietary models of early hominins. Evol. Biol. 35, 159–175.

Dorman, M., 2014. Learning R for Geospatial Analysis. Packt Publishing Ltd.

Duda, P., Zrzavý, J., 2013. Evolution of life history and behavior in Hominidae: Towards phylogenetic reconstruction of the chimpanzee–human last common ancestor. J. Hum. Evol. 65, 424–446.

Efremov, I.A., 1953. Taphonomie et annales géologiques: 1ère. partie. Annales du Centre d'Études et de Documentation Paléontologique 4, 164.

Efremov, I.A., 1950. Taphonomy and the geological record. Trudy Paleontologicheskogo Instituta 24, 1-177.

Efremov, J.A., 1940. Tap*Homo*ny: a new branch of geology. Pan-Am. Geologist 74, 81-93.

Egeland, A.G., Egeland, C.P., Bunn, H.T., 2008. Taphonomic analysis of a modern spotted hyena (Crocuta crocuta) den from Nairobi, Kenya. Journal of Taphonomy 6, 275-299.

Egeland, C.P., Byerly, R.M., 2005. Application of return rates to large mammal butchery and transport among hunter-gatherers and its implications for Plio-Pleistocene hominid carcass foraging and site use. Journal of Taphonomy 3 (3), 135-158.

Emerson, A.M., 1991. Archaeological implications of variability in the economic anatomy of Bison bison. PhD. Washington State University

Enloe, J.G., 2004. Equifinality, assemblage integrity and behavioral inferences at Verberie. Journal of Taphonomy 2 (3), 147-165.

Enloe, J.G., 2003. Acquisition and processing of reindeer in the Paris Basin. BAR International Series, 1144, 23-32.

Enloe, J.G., 1993. Subsistence organization in the Early Upper Paleolithic: reindeer hunters of the Abri du Flageolet, couche V., in: White, R., Knecth, H., Pike-Tay, A. (Eds.), Before Lascaux: the complex record of the Early Upper Paleolithic, pp. 101-115.

Estalrrich, A., Alarcón, J.A., Rosas, A., 2020. Toothpicking in early *Homo* OH 62 from Olduvai Gorge (Tanzania): An indirect evidence of intensive meat consumption? J. Hum. Evol. 143, 102769.

Estalrrich, A., Fiorenza, L., Menz, U., 2017. Dental behavior and long-term dietary reconstruction of El Sidrón Neandertals derived from molar macrowear patterns. 7th Annual ESHE.

Ester, M., Kriegel, H.P., Sander, J., Xu, X., 1996. A density-based algorithm for discovering clusters in large spatial databases with noise. KDD 96 (34), 226-231.

Faith, J.T., 2007. Sources of variation in carnivore tooth-mark frequencies in a modern spotted hyena (Crocuta crocuta) den assemblage, Amboseli Park, Kenya. J. Archaeol. Sci. 34, 1601–1609.

Faith, J.T., Behrensmeyer, A.K., 2006. Changing patterns of carnivore modification in a landscape bone assemblage, Amboseli Park, Kenya. J. Archaeol. Sci. 33, 1718–1733.

Faith, J.T., Domínguez-Rodrigo, M., Gordon, A.D., 2009. Long-distance carcass transport at Olduvai Gorge? A quantitative examination of Bed I skeletal element abundances. J. Hum. Evol. 56, 247–256.

Faith, J.T., Gordon, A.D., 2007. Skeletal element abundances in archaeofaunal assemblages: economic utility, sample size, and assessment of carcass transport strategies. J. Archaeol. Sci. 34, 872–882.

Faith, J.T., Marean, C.W., Behrensmeyer, A.K., 2007. Carnivore competition, bone destruction, and bone density. J. Archaeol. Sci. 34, 2025–2034.

Farizy, C., David, F., Jaubert, J., 1994. Hommes et bisons du paléolithique moyen à Mauran (Haute-Garonne): XXX supplément à Gallia préhistoire. Vol 30. CNRS éditions.

Feibel, C.S., Brown, F.H., McDougall, I., 1989. Stratigraphic context of fossil hominids from the Omo group deposits: northern Turkana Basin, Kenya and Ethiopia. Am. J. Phys. Anthropol. 78, 595–622.

Fernández-Jalvo, Y., Andrews, P., 2016. Atlas of Taphonomic Identifications. Vertebrate Paleobiology and Paleoanthropology Series. Springer.

Fernández-Jalvo, Y., Andrews, P., 2003. Experimental effects of water abrasion on bone fragments. Journal of taphonomy 1 (3), 145-161.

Fernandez-Jalvo, Y., Sanchez-Chillon, B., Andrews, P., Fernandez-Lopez, S., Alcala Martinez, L., 2002. Morphological taphonomic transformations of fossil bones in continental environments, and repercussions on their chemical composition. Archaeometry 44, 353–361.

Fernández López, S.R., 2006. Taphonomic alteration and evolutionary taphonomy. Journal of taphonomy 4, 111–142.

Ferraro, J.V., Plummer, T.W., Pobiner, B.L., Oliver, J.S., Bishop, L.C., Braun, D.R., Ditchfield, P.W., Seaman, J.W., 3rd, Binetti, K.M., Seaman, J.W., Jr, Hertel, F., Potts, R., 2013. Earliest archaeological evidence of persistent hominin carnivory. PLoS One 8, e62174.

Fiore, I., Bondioli, L., Coppa, A., 2004. Taphonomic analysis of the late Early Pleistocene bone remains from Buia (Dandiero Basin, Danakil Depression, Eritrea): evidence for large mammal and reptile butchering. Rivista Italiana di Paleontologie e Stratigrafia.

Fisher, H.E., 1982. The sex contract: The evolution of human behavior. William Morrow &Company.

Fisher, N.I., 1995. Statistical Analysis of Circular Data. Cambridge University Press.

Foley, R., 1987. Another unique species: patterns in human evolutionary ecology. Longman, London.

Foley, R.A., 2001. The evolutionary consequences of increased carnivory in hominids, in: Stanford, C.B., Bunn, H.T. (Eds.), Meat-eating and human evolution, Oxford University Press, pp. 305–331.

Foley, R.A., 1996. An evolutionary and chronological framework for human social behaviour, in: PROCEEDINGS-BRITISH ACADEMY, vol 88, pp. 95-118.

Frison, G.C., Todd, L.C., 1986. The Colby Mammoth Site: taphonomy and archaeology of a Clovis kill in northern Wyoming. University of New Mexico Press.

Frostick, L., Reid, I., 1983. Taphonomic significance of sub-aerial transport of vertebrate fossils on steep semi-arid slopes. Lethaia. 16 (2), 157-164.

Galán, A.B., Domínguez-Rodrigo, M., 2013. An experimental study of the anatomical distribution of cut marks created by filleting and disarticulation on long bone ends. Archaeometry, 55 (6), 1132-1149.

García, V.A., Egido, R.B., del Pino, J.M.B., 2006. Determinación de procesos de fractura sobre huesos frescos: un sistema de análisis de los ángulos de los planos de fracturación como discriminador de agentes bióticos. Trabajos de prehistoria 63 (1), 37-45.

Gaudzinski, S., 1996. On Bovid Assemblages and their Consequences for the Knowledge of Subsistence Patterns in the Middle Palaeolithic. Proceedings of the Prehistoric Society 62, 19–39.

Gaudzinski, S., Roebroeks, W., 2000. Adults only. Reindeer hunting at the middle palaeolithic site salzgitter lebenstedt, northern Germany. J. Hum. Evol. 38, 497–521.

Gaudzinski-Windheuser, S., Noack, E.S., Pop, E., Herbst, C., Pfleging, J., Buchli, J., Jacob, A., Enzmann, F., Kindler, L., Iovita, R., Street, M., Roebroeks, W., 2018. Evidence for close-range hunting by last interglacial Neanderthals. Nat Ecol Evol 2, 1087–1092.

Gentry, A.W., 2011. Bovidae, in: Harrison, T. (Ed.), Paleontology and Geology of Laetoli: Human Evolution in Context: Volume 2: Fossil Hominins and the Associated Fauna. Springer Netherlands, Dordrecht, pp. 363–465.

Gidna, A., Domínguez-Rodrigo, M., Pickering, T.R., 2015. Patterns of bovid long limb bone modification created by wild and captive leopards and their relevance to the elaboration of referential frameworks for paleoanthropology. Journal of Archaeological Science: Reports 2, 302-309.

Gidna, A.O., Kisui, B., Mabulla, A., Musiba, C., Domínguez-Rodrigo, M., 2014. An ecological neo-taphonomic study of carcass consumption by lions in Tarangire National Park (Tanzania) and its relevance for human evolutionary biology. Quat. Int. 322-323, 167–180.

Gidna, A., Yravedra, J., Domínguez-Rodrigo, M., 2013. A cautionary note on the use of captive carnivores to model wild predator behavior: a comparison of bone modification patterns on long bones by captive and wild lions. J. Archaeol. Sci. 40, 1903–1910.

Gifford, D.P., Kay Behrensmeyer, A., 1977. Observed Formation and Burial of a Recent Human Occupation Site in Kenya. Quat. Res. 8, 245–266.

Giusti, D., Arzarello, M., 2016. The need for a taphonomic perspective in spatial analysis: Formation processes at the Early Pleistocene site of Pirro Nord (P13), Apricena, Italy. Journal of Archaeological Science: Reports 8, 235–249.

Giusti, D., Tourloukis, V., Konidaris, G., Thompson, N., Karkanas, P., Panagopoulou, E., Harvati, K., 2018. Beyond maps: Patterns of formation processes at the Middle Pleistocene open-air site of Marathousa 1, Megalopolis basin, Greece. Quat. Int. 497, 137–153.

Goodall, J, 1986. The chimpanzees of Gombe : patterns of behavior. Cambridge Mass.

Goodall, J, 1963. Feeding behaviour of wild chimpanzees : A preliminary report. Sym. Zool. Soc. Lond. 10, 39–48.

Grayson, D.K., 1989. Bone transport, bone destruction, and reverse utility curves. J. Archaeol. Sci. 16, 643–652.

Grayson, D.K., Delpech, F., 1998. Changing diet breadth in the early Upper Palaeolithic of southwestern France. J. Archaeol. Sci. 25 (11), 1119-1129.

Grayson, D.K., Delpech, F., Rigaud, J.P., 2001. Explaining the development of dietary dominance by a single ungulate taxon at Grotte XVI, Dordogne,

France. J. Archaeol. Sci. 28 (2), 115-125.

Grayson, D.K., Frey, C.J., 2004. Measuring skeletal part representation in archaeological faunas. Journal of Taphonomy 2 (1), 27-42.

Greenacre, M.J., 2010. Biplots in Practice. Fundacion BBVA.

Grimsdell, J.J.R., 1973. Age determination of the African buffalo, Syncerus caffer Sparrman. African Journal of Ecology 11 (1), 31-53.

Guan, Y., 2006. A Composite Likelihood Approach in Fitting Spatial Point Process Models. J. Am. Stat. Assoc. 101, 1502–1512.

Guy, P.R., Sinclair, A.R.E., Norton-Griffiths, M., 1981. Serengeti, Dynamics of an Ecosystem. The Journal of Applied Ecology 18 (1), 336.

Haraway, D.J., 1989. Primate Visions: Gender, Race, and Nature in the World of Modern Science. Psychology Press.

Harmand, S., 2007. Economic behaviors and cognitive capacities of early hominins between 2.34 Ma and 0.70 Ma in West Turkana, Kenya. Mitteilungen der Gesellschaft für Urgeschichte 16 (1).

Harmand, S., Lewis, J.E., Feibel, C.S., Lepre, C.J., Prat, S., Lenoble, A., Boës, X., Quinn, R.L., Brenet, M., Arroyo, A., Taylor, N., Clément, S., Daver, G., Brugal, J.-P., Leakey, L., Mortlock, R.A., Wright, J.D., Lokorodi, S., Kirwa, C., Kent, D.V., Roche, H., 2015. 3.3-million-year-old stone tools from Lomekwi 3, West Turkana, Kenya. Nature 521, 310–315.

Harmand, S., Lewis, J.E., Taylor, N., Feibel, C.S., Boës, X., Prat, S., Roche, H., 2019. Reply to Domínguez-Rodrigo and Alcalá: Interpretation Without Accurate Evidence Is Fantasy. Journal of African Archaeology 17, 177–181.

Harris, J.W.K., Isaac, G., 1976. The Karari Industry: Early Pleistocene archaeological evidence from the terrain east of Lake Turkana, Kenya. Nature 262, 102–107.

Hastie, T., Tibshirani, R., Friedman, J., 2009. The Elements of Statistical Learning: Data Mining, Inference, and Prediction, Second Edition. Springer Science & Business Media.

Hatala, K.G., Roach, N.T., Ostrofsky, K.R., Wunderlich, R.E., Dingwall, H.L., Villmoare, B.A., Green, D.J., Harris, J.W.K., Braun, D.R., Richmond, B.G., 2016. Footprints reveal direct evidence of group behavior and locomotion in *Homo erectus*. Sci. Rep. 6, 28766.

Hawkes, K., OConnell, J.F., 2001. Hunting and nuclear families: some lessons from the Hadza about mens work. Current Anthropology 42 (5), 681-709.

Hawkes, K., O'Connell, J.F., Jones, N.G., 1991. Hunting income patterns among the Hadza: big game, common goods, foraging goals and the evolution of the human diet. Philos. Trans. R. Soc. Lond. B Biol. Sci. 334, 243–50; discussion 250–1.

Hay, R.L., 1976. Geology of the Olduvai Gorge: A Study of Sedimentation in a Semiarid Basin. University of California Press.

Hazelton, M.L., Davies, T.M., 2009. Inference based on kernel estimates of the relative risk function in geographical epidemiology. Biom. J. 51, 98–109.

Hill, A., 1979. Disarticulation and scattering of mammal skeletons. Paleobiology 5, 261–274.

Hill, A.P., 1975. Taphonomy of Contemporary and Late Cenozoic East African Vertebrates. Royal Holloway, University of London.

Hill, A., Ward, S., Deino, A., Curtis, G., Drake, R., 1992. Earliest *Homo*. Nature 355, 719-722.

Hill, M.G., 2002. Paleoindian diet and subsistence behavior on the northwestern Great Plains of North America. PhD, University of Wisconsin - Madison.

Hitchcock, R., Bleed, P., 1997. Each according to need and fashion: spear and arrow use among San hunters of the Kalahari. In Knecht, H. (Ed.), Projectile Technology. Springer, Boston.

Hlusko, L.J., 2003. The Oldest Hominid Habit? Experimental Evidence for Toothpicking with Grass Stalks. Curr. Anthropol. 44, 738–741.

Hodder, I., 1987. The meaning of discard: Ash and domestic space in Baringo. Method and theory for activity area research: An ethnoarchaeological approach, 424-448.

Hodder, I., Orton, C., 1976. Spatial analysis in archaeology. Cambridge University Press.

Hohmann, G., Fruth, B., 2008. New records on prey capture and meat eating by bonobos at Lui Kotale, Salonga National Park, Democratic Republic of Congo. Folia Primatol. 79, 103–110.

Hohmann, G., Fruth, B., 1993. Field Observations on Meat Sharing among Bonobos (Pan paniscus). Folia Primatologica 60, 225-229.

Holliday, T.W., 2012. Body Size, Body Shape, and the Circumscription of the Genus *Homo*. Curr. Anthropol. 53, S330–S345.

Hopkins, B., Skellam, J.G., 1954. A New Method for determining the Type of Distribution of Plant Individuals. Ann. Bot. 18, 213–227.

Huntley, B.J., 1979. Ageing criteria for tsessebe (Damaliscus I. lunatus). South African Journal of Wildlife Research 3 (1), 24-27.

Ihobe, H., 1992. Observations on the meat-eating behavior of wild bonobos (Pan paniscus) at Wamba, Republic of Zaire. Primates 33, 247-250.

Illian, J., Penttinen, A., Stoyan, H., Stoyan, D., 2008. Statistical Analysis and Modelling of Spatial Point Patterns. John Wiley & Sons.

Isaac, B., 1987. Throwing and human evolution. African Archaeological Review 5 (1), 3-17.

Isaac, G., 1978. The Food-sharing Behavior of Protohuman Hominids. Scientific American 238 (4), 90-109.

Isaac, G., 1971. The diet of early man: aspects of archaeological evidence

from Lower and Middle Pleistocene Sites in Africa. World Archaeol. 2, 278–299.

Isaac, G., 1983. Aspects of human evolution. Conference Paper, in: Isaac, B. (Ed.), The archaeology of human origins. Papers by Glynn Isaac, Cambridge University Press.

Isaac, G.L., Harris, J.W.K., Crader, D., 1976. Archaeological evidence from the Koobi Fora formation. Earliest Man and Environments in the Lake Rudolf Basin. University of Chicago Press, Chicago 533–551.

Isler, K., Van Schaik, C.P., 2014. How humans evolved large brains: comparative evidence. Evol. Anthropol. 23, 65–75.

Johnson, E., 1985. 5 - Current Developments in Bone Technology, in: Schiffer, M.B. (Ed.), Advances in Archaeological Method and Theory. Academic Press, San Diego, pp. 157–235.

Kaufulu, Z.M., 1987. Formation and Preservation of Some Earlier Stone Age Sites at Koobi Fora, Northern Kenya. The South African Archaeological Bulletin 42 (14), 23-33.

Keeley, L.H., Toth, N., 1981. Microwear polishes on early stone tools from Koobi Fora, Kenya. Nature 293, 464–465.

Kelsall, J.E., Diggle, P.J., 1995. Kernel Estimation of Relative Risk. Bernoulli 1 (½), 3-16.

Kent, S., Kroll, E.M., Price, T.D., 1991. The Interpretation of Archaeological Spatial Patterning. Springer, Boston, MA.

Kimbel, W.H., Walter, R.C., Johanson, D.C., Reed, K.E., Aronson, J.L., Assefa, Z., Marean, C.W., Eck, G.G., Bobe, R., Hovers, E., Others, 1996. Late Pliocene*Homo*and Oldowan Tools from the Hadar Formation (Kada Hadar Member), Ethiopia. J. Hum. Evol. 31, 549–561.

Klein, D.R., 1999. The Roles of Climate and Insularity in Establishment and Persistence of Rangifer tarandus Populations in the High Arctic. Ecol. Bull. 96–104.

Klein, R.G., 2000. The Earlier Stone Age of southern Africa. The South African Archaeological Bulletin, 107-122.

Klein, R.G., 1999. The Human Career: human biological and cultural origins. University of Chicago Press.

Klein, R.G., 1995. Anatomy, behavior, and modern human origins. Journal of World Prehistory 9, 167–198.

Klein, R.G., 1989. Why does skeletal part representation differ between smaller and larger bovids at klasies river mouth and other archeological sites? J. Archaeol. Sci. 16, 363–381.

Klein, R.G., 1982. Age (Mortality) Profiles as a Means of Distinguishing Hunted Species from Scavenged Ones in Stone Age Archeological Sites. Paleobiology 8, 151–158.

Klein, R.G., 1978. Stone age predation on large African bovids. J. Archaeol. Sci. 5, 195–217.

Klein, R.G., Cruz-Uribe, K., 1991. The bovids from Elandsfontein, South Africa, and their implications for the age, palaeoenvironment, and origins of the site. African Archaeological Review 9, 21–79.

Kortlandt, A., 1980. How might early hominids have defended themselves against large predators and food competitors? J. Hum. Evol. 9, 79–112.

Krajcarz, M., Krajcarz, M.T., 2014. The Red Fox (Vulpes vulpes) as an Accumulator of Bones in Cave-like Environments. International Journal of Osteoarchaeology 24 (4), 459-475.

Kramer, K.L., 2010. Cooperative Breeding and its Significance to the Demographic Success of Humans. Annu. Rev. Anthropol. 39, 417–436.

Kreutzer, L.A., 1988. Megafaunal Butchering at Lubbock Lake, Texas: A Taphonomic Reanalysis. Quat. Res. 30, 221–231.

Kroll, E.M., 1994. Behavioral implications of Plio-Pleistocene archaeological site structure. J. Hum. Evol. 27, 107–138.

Kroll, E.M., Isaac, G.L., 1984. Configurations of artifacts and bones at early Pleistocene sites in East Africa. Intrasite Spatial Analysis in Archaeology. Cambridge University Press, Cambridge, pp. 4–31.

Kruuk, H., 1972. The spotted hyena: a study of predation and social behavior. The University of Chicago.

Kuhn, M., Johnson, K., 2013. Applied Predictive Modeling. Springer, New York, NY.

Kulldorff, M., 1997. A spatial scan statistic. Communications in Statistics - Theory and Methods 26, 1481–1496.

Lam, Y.M., 1992. Variability in the behaviour of spotted hyaenas as taphonomic agents. J. Archaeol. Sci. 19, 389–406.

Lam, Y.M., Chen, X., Pearson, O.M., 1999. Intertaxonomic Variability in Patterns of Bone Density and the Differential Representation of Bovid, Cervid, and Equid Elements in the Archaeological Record. Am. Antiq. 64, 343–362.

Landals, A., 1990. The Maple Leaf Site: implications of the analysis of small-scale bison kills, in: Davis, L., Reeves, B., (Eds.), Hunters of the recent past, pp. 122-151.

Lantz, B., 2013. Machine Learning with R. Packt Publishing Ltd.

Leakey, M.D., 1971. Olduvai Gorge: Volume 3, Excavations in Beds I and II, 1960-1963. Cambridge University Press.

Leakey, M.D., 1967. Preliminary survey of the cultural material from Beds I and II, Olduvai Gorge, Tanzania. Background to Evolution in Africa. University of Chicago Press, Chicago 417–446.

Lee Lyman, R., 2008. Quantitative Paleozoology. Cambridge University Press.

Lee Lyman, R., 1994a. Vertebrate Taphonomy. Cambridge University Press.

Lee Lyman, R., 1994b. Quantitative Units and Terminology in Zooarchaeology. Am. Antiq. 59, 36–71.

Lee Lyman, R., 1992. Anatomical considerations of utility curves in Zooarchaeology. J. Archaeol. Sci. 19, 7–22.

Lee Lyman, R., 1985. Bone frequencies: differential transport, in situ destruction, and the MGUI. J. Archaeol. Sci. 12, 221–236.

Lee, R.B., DeVore, I., 2017. Man the Hunter. Routledge.

Lenoble, A., Bertran, P., Lacrampe, F., 2008. Solifluction-induced modifications of archaeological levels: simulation based on experimental data from a modern periglacial slope and application to French Palaeolithic sites. J. Archaeol. Sci. 35, 99–110.

Leonard, W., Robertson, M.L., 2000. Ecological correlates for home range variation in primates: implications for human evolution, in: Boinski S., Garber PA, (Eds) On the Move: How and Why Animals Travel in Groups, 628-648.

Lê, S., Josse, J., Husson, F., 2008. FactoMineR: an R package for multivariate analysis. J. Stat. Softw. 25 (1), 1-18.

Liebenberg, L., 2006. Persistence hunting by modern hunter-gatherers. Curr. Anthropol. 47 (6), 1017-1026.

Lieberman, D.E., Bramble, D.M., Raichlen, D.A., Shea, J.J., 2009. Brains, Brawn, and the Evolution of Human Endurance Running Capabilities, in: Grine, F.E., Fleagle, J.G., Leakey, R.E. (Eds.), The First Humans – Origin and Early Evolution of the Genus *Homo*: Contributions from the Third Stony Brook Human Evolution Symposium and Workshop October 3 – October 7, 2006. Springer Netherlands, Dordrecht, pp. 77–92.

Lieberman, D.E., Bramble, D.M., Raichlen, D.A., Shea, J.J., 2007. The evolution of endurance running and the tyranny of ethnography: a reply to Pickering and Bunn (2007). J. Hum. Evol. 53, 439–442.

Lockyear, K., 2013. Applying bootstrapped Correspondence Analysis to archaeological data. J. Archaeol. Sci. 40, 4744–4753.

Lozano, M., Subirà, M.E., Aparicio, J., Lorenzo, C., Gómez-Merino, G., 2013. Toothpicking and periodontal disease in a Neanderthal specimen from Cova Foradà site (Valencia, Spain). PLoS One 8, e76852.

Lupo, K.D., 2001. Archaeological Skeletal Part Profiles and Differential Transport: An Ethnoarchaeological Example from Hadza Bone Assemblages. Journal of Anthropological Archaeology 20, 361–378.

Lupo, K.D., n.d. On early hominin meat eating and carcass acquisition strategies, in: Domínguez-Rodrigo, M., (Ed.), Stone Tools and Fossil Bones, pp. 115-151.

Lupo, K.D., O'Connell, J.F., 2002. Cut and tooth mark distributions on large animal bones: ethnoarchaeological data from the Hadza and their implications

for current ideas about early human carnivory, J. Archaeol. Sci. 29 (1), 85-109.

Lwanga, J.S., Struhsaker, T.T., Struhsaker, P.J., Butynski, T.M., Mitani, J.C., 2011. Primate population dynamics over 32.9 years at Ngogo, Kibale National Park, Uganda. Am. J. Primatol. 73, 997–1011.

Lyman, R.L., 1993. Density-mediated attrition of bone assemblages: new insights. From bones to behavior, pp. 324-341.

Lyman, R.L., 1984. Bone density and differential survivorship of fossil classes. Journal of Anthropological Archaeology 3, 259–299.

Lyman, R.L., 1982. 8 - Archaeofaunas and Subsistence Studies, in: Schiffer, M.B. (Ed.), Advances in Archaeological Method and Theory. Academic Press, San Diego, pp. 331–393.

Lyman, R.L., Lee Lyman, R., Houghton, L.E., Chambers, A.L., 1992. The effect of structural density on Marmot skeletal part representation in archaeological sites. Journal of Archaeological Science 19 (5), 557-573.

Madrigal, T.C., Capaldo, S.D., 1999. White-Tailed Deer Marrow Yields and Late Archaic Hunter-Gatherers. J. Archaeol. Sci. 26, 241–249.

Madrigal, T.C., Cregg Madrigal, T., Holt, J.Z., 2002. White-Tailed Deer Meat and Marrow Return Rates and Their Application to Eastern Woodlands Archaeology. American Antiquity 67 (4), 745-759.

Magurran, A.E., 1988. Ecological Diversity and Its Measurement. Princeton University Press.

Manega, P.C., 1994. Geochronology, geochemistry and isotopic study of the Plio-Pleistocene hominid sites and the Ngorongoro Volcanic Highland in northern Tanzania. PhD. University of Colorado at Boulder.

Marean, C.W., 1995. Of taphonomy and zooarcheology. Vertebrate taphonomy. By R. Lee Lyman (1994). Cambridge: Cambridge University Press. 576 pp. 79.95(cloth), 34.95 (paper). ISBN 0-521-45215-5 (cloth), 0-521-45840-4. Evolutionary Anthropology: Issues, News, and Reviews, 4(2), 64-72.

Marean, C.W., Abe, Y., Frey, C.J., Randall, R.C., 2000. Zooarchaeological and taphonomic analysis of the Die Kelders Cave 1 Layers 10 and 11 Middle Stone Age larger mammal fauna. Journal of Human Evolution 38 (1), 197-233.

Marean, C.W., Abe, Y., Nilssen, P.J., Stone, E.C., 2001. Estimating the minimum number of skeletal elements (MNE) in zooarchaeology: a review and a new image-analysis GIS approach. Am. Antiq. 66, 333–348.

Marean, C.W., Bertino, L., 1994. Intrasite Spatial Analysis of Bone: Subtracting the Effect of Secondary Carnivore Consumers. American Antiquity 59 (4), 748-768.

Marean, C.W., Cleghorn, N., 2003. Large mammal skeletal element transport: applying foraging theory in a complex taphonomic system. Journal of Taphonomy 1 (1), 15-42.

Marean, C.W., Frey, C.J., 1997. Animal Bones from Caves to Cities: Reverse

Utility Curves as Methodological Artifacts. Am. Antiq. 62, 698–711.

Marean, C.W., Kim, S.Y., 1998. Mousterian large-mammal remains from Kobeh Cave behavioral implications for Neanderthals and early modern humans. Curr. Anthropol. 39 (S1), 79-114.

Marean, C.W., Rodrigo, M.D., Pickering, T.R., 2004. Skeletal Element Equifinality in Zooarchaeology Begins with Method: The Evolution and Status of the" Shaft Critique." Journal of Taphonomy 2 (1), 69-98.

Marean, C.W., Spencer, L.M., 1991. Impact of Carnivore Ravaging on Zooarchaeological Measures of Element Abundance. Am. Antiq. 56, 645–658.

Marean, C.W., Spencer, L.M., Blumenschine, R.J., Capaldo, S.D., 1992. Captive hyaena bone choice and destruction, the Schlepp effect and olduvai archaeofaunas. J. Archaeol. Sci. 19, 101–121.

Marín, J., Rodríguez-Hidalgo, A., Vallverdú, J., Gómez de Soler, B., Rivals, F., Rabuñal, J.R., Pineda, A., Chacón, M.G., Carbonell, E., Saladié, P., 2019. Neanderthal logistic mobility during MIS3: Zooarchaeological perspective of Abric Romaní level P (Spain). Quat. Sci. Rev. 225, 106033.

Marín, J., Saladié, P., Rodríguez-Hidalgo, A., Carbonell, E., 2017. Neanderthal hunting strategies inferred from mortality profiles within the Abric Romaní sequence. PLoS One 12, e0186970.

Marlowe, F., 2010. The Hadza: hunter-gatherers of Tanzania. University of California Press.

Martín-Perea, D.M., Courtenay, L.A., Domingo, M.S., Morales, J., 2020. Application of artificially intelligent systems for the identification of discrete fossiliferous levels. PeerJ 8, e8767.

Martín-Perea, D.M., Fesharaki, O., Rey Samper, J.J., Arroyo, X., Uribelarrea, D., Cobo-Sánchez, L., Baquedano, E., Mabulla, A., Domínguez-Rodrigo, M., 2019. Mineral assemblages and low energy sedimentary processes in the FLK-*Zinj*, DS, PTK and AMK complex palaeolandscape (Olduvai Gorge, Tanzania). Quat. Int. 526, 15–25.

Mcbrearty, S., Brooks, A.S., 2000. The revolution that wasn't: a new interpretation of the origin of modern human behavior. J. Hum. Evol. 39, 453–563.

McGrew, C, W., 1978. Primates preying upon vertebrates : new records from West Africa (Pan troglodytes verus, Papio papio, Cercopithecus sabaeus). Carnivore 1, 41–45.

McGrew, W.C., Tutin, C.E.G., Baldwin, P.J., 1979. New Data on Meat Eating by Wild Chimpanzees. Curr. Anthropol. 20, 238–239.

McPherron, S.P., Alemseged, Z., Marean, C.W., Wynn, J.G., Reed, D., Geraads, D., Bobe, R., Béarat, H.A., 2010. Evidence for stone-tool-assisted consumption of animal tissues before 3.39 million years ago at Dikika, Ethiopia. Nature 466, 857–860.

Mduma, S.A.R., 1996. Serengeti wildebeest population dynamics: regula-

tion, limitation and implications for harvesting. University of British Columbia, Canada.

Mduma, S.A.R., Sinclair, A.R.E., Hilborn, R., 1999. Food regulates the Serengeti wildebeest: a 40-year record. Journal of Animal Ecology 68 (6), 1101-1122.

Metcalfe, D., Barlow, K.R., 1992. A model for exploring the optimal trade-off between field processing and transport. Am. Anthropol. 94 (2), 340-356.

Metcalfe, D., Jones, K.T., 1988. A Reconsideration of Animal Body-Part Utility Indices. American Antiquity 53 (3), 486-504.

Mitani, J.C., Watts, D.P., 2001. Why do chimpanzees hunt and share meat? Animal Behaviour 61 (5), 915-924.

Mitchell, B.L., Shenton, J.B., Uys, J.C.M., 1965. Predation on Large Mammals in the Kafue National Park, Zambia. Zoologica Africana 1 (2), 297-318.

Moclán, A., Domínguez-Rodrigo, M., 2019. Classifying agency in bone breakage: an experimental analysis of fracture planes to differentiate between hominin and carnivore dynamic and static loading using machine learning (ML) algorithms. Archaeol. Anthropol. Sci. 11 (9), 4663-4680.

Moclán, A., Domínguez-Rodrigo, M., 2018. An experimental study of the patterned nature of anthropogenic bone breakage and its impact on bone surface modification frequencies. Journal of Archaeological Science 96, 1-13.

Møller, J., Syversveen, A.R., 1998. Log gaussian cox processes. Scandinavian journal of statistics 25 (3), 451-482.

Monahan, C.M., 1998. The Hadza Carcass Transport Debate Revisited and its Archaeological Implications. J. Archaeol. Sci. 25, 405–424.

Monahan, C.M., 1996. New zooarchaeological data from Bed II, Olduvai Gorge, Tanzania: implications for hominid behavior in the Early Pleistocene. J. Hum. Evol. 31, 93–128.

Morín, E. 2004. Late Pleistocene population interaction in western Europe and modern human origins: New insights based on the faunal remains from Saint-Césaire, southwestern France, PhD. University of Michigan.

Morlan, R.E., 1994. Bison Bone Fragmentation and Survivorship: a Comparative Method. J. Archaeol. Sci. 21, 797–807.

Newton-Fisher, N.E., 2014. Roving females and patient males: a new perspective on the mating strategies of chimpanzees. Biological Reviews 89 (2), 356-372.

Newton-Fisher, N.E., Notman, H., Reynolds, V., 2002. Hunting of mammalian prey by Budongo Forest chimpanzees. Folia Primatol. 73, 281–283.

Niiniluoto, I., 1987. Truthlikeness, volume 185 of Synthese Library D. Reidel.

Niven, L., 2007. From carcass to cave: large mammal exploitation during the Aurignacian at Vogelherd, Germany. J. Hum. Evol. 53, 362–382.

Niven, L., Steele, T.E., Rendu, W., Mallye, J.-B., McPherron, S.P., Soressi, M., Jaubert, J., Hublin, J.-J., 2012. Neandertal mobility and large-game hunting: the

exploitation of reindeer during the Quina Mousterian at Chez-Pinaud Jonzac (Charente-Maritime, France). J. Hum. Evol. 63, 624–635.

Nilssen, P.J., 2000. An actualistic butchery study in South Africa and its implications for reconstructing hominid strategies of carcass acquisition and butchery in the Upper Pleistocene and Plio-Pleistocene. PhD. Univesity of Cape Town.

Njau, J.K., Blumenschine, R.J., 2006. A diagnosis of crocodile feeding traces on larger mammal bone, with fossil examples from the Plio-Pleistocene Olduvai Basin, Tanzania. J. Hum. Evol. 50, 142–162.

O'Connell, J.F., 1997. On Plio/Pleistocene Archaeological Sites and Central Places. Curr. Anthropol. 38, 86–88.

O'Connell, J.F., Hawkes, K., Blurton Jones, N., 1990. Reanalysis of large mammal body part transport among the Hadza. J. Archaeol. Sci. 17, 301–316.

O'Connell, J.F., Hawkes, K., Jones, N.B., 1988. Hadza Hunting, Butchering, and Bone Transport and Their Archaeological Implications. J. Anthropol. Res. 44, 113–161.

O'Connell, J.F., Hawkes, K., Lupo, K.D., Blurton Jones, N.G., 2002. Male strategies and Plio-Pleistocene archaeology. J. Hum. Evol. 43, 831–872.

Oliver, J.S., 1994. Estimates of hominid and carnivore involvement in the FLK *Zinj*anthropus fossil assemblage: some socioecological implications. J. Hum. Evol. 27, 267–294.

Oliver, J.S., Plummer, T.W., Hertel, F., Bishop, L.C., 2019. Bovid mortality patterns from Kanjera South, Homa Peninsula, Kenya and FLK-*Zinj*, Olduvai Gorge, Tanzania: Evidence for habitat mediated variability in Oldowan hominin hunting and scavenging behavior. J. Hum. Evol. 131, 61–75.

Olsen, S.L., Shipman, P., 1988. Surface modification on bone: Trampling versus butchery. J. Archaeol. Sci. 15, 535–553.

Organista, E., Domínguez-Rodrigo, M., 2016. Did *Homo erectus* kill a Pelorovis herd at BK (Olduvai Gorge)? A taphonomic study of BK5. Archaeol. Anthropol. Sci. 8 (3), 601-624.

Organista, E., Domínguez-Rodrigo, M., Yravedra, J., Uribelarrea, D., Arriaza, M.C., Ortega, M.C., Mabulla, A., Gidna, A., Baquedano, E., 2017. Biotic and abiotic processes affecting the formation of BK Level 4c (Bed II, Olduvai Gorge) and their bearing on hominin behavior at the site. Palaeogeography, Palaeoclimatology, Palaeoecology, 488, 59-75.

Organista, E., Pernas-Hernández, M., Gidna, A., Yravedra, J., Domínguez-Rodrigo, M., 2016. An experimental lion-to-hammerstone model and its relevance to understand hominin-carnivore interactions in the archeological record. J. Archaeol. Sci. 66, 69–77.

Oron, M., Goren-Inbar, N., 2014. Mousterian intra-site spatial patterning at Quneitra, Golan Heights. Quat. Int. 331, 186–202.

Pante, M.C., 2013. The larger mammal fossil assemblage from JK2, Bed III,

Olduvai Gorge, Tanzania: implications for the feeding behavior of *Homo erectus*. J. Hum. Evol. 64, 68–82.

Pante, M.C., Blumenschine, R.J., 2010. Fluvial transport of bovid long bones fragmented by the feeding activities of hominins and carnivores. J. Archaeol. Sci. 37, 846–854.

Pante, M.C., Blumenschine, R.J., Capaldo, S.D., Scott, R.S., 2012. Validation of bone surface modification models for inferring fossil hominin and carnivore feeding interactions, with reapplication to FLK 22, Olduvai Gorge, Tanzania. J. Hum. Evol. 63, 395–407.

Pante, M.C., de la Torre, I., 2018. A hidden treasure of the Lower Pleistocene at Olduvai Gorge, Tanzania: The Leakey HWK EE assemblage. J. Hum. Evol. 120, 114–139.

Pante, M.C., Scott, R.S., Blumenschine, R.J., Capaldo, S.D., 2015. Revalidation of bone surface modification models for inferring fossil hominin and carnivore feeding interactions. Quat. Int. 355, 164–168.

Parkinson, J.A., 2018. Revisiting the hunting-versus-scavenging debate at FLK *Zinj*: A GIS spatial analysis of bone surface modifications produced by hominins and carnivores in the FLK 22 assemblage, Olduvai Gorge, Tanzania. Palaeogeography, Palaeoclimatology, Palaeoecology 511, 29-51.

Parkinson, J.A., 2013. A GIS image analysis approach to documenting Oldowan hominin carcass acquisition: Evidence from Kanjera South, FLK *Zinj*, and neotaphonomic models of carnivore bone destruction. PhD. City University of New York.

Parkinson, J.A., Plummer, T., Hartstone-Rose, A., 2015. Characterizing felid tooth marking and gross bone damage patterns using GIS image analysis: an experimental feeding study with large felids. J. Hum. Evol. 80, 114–134.

Parkinson, J.A., Plummer, T.W., Bose, R., 2014. A GIS-based approach to documenting large canid damage to bones. Palaeogeogr. Palaeoclimatol. Palaeoecol. 409, 57–71.

Pebesma, E.J., 2004. Multivariable geostatistics in S: the gstat package. Computers & Geosciences. 30 (7), 683-691.

Peters, C.R., Blumenschine, R.J., 1995. Landscape perspectives on possible land use patterns for Early Pleistocene hominids in the Olduvai Basin, Tanzania. Journal of Human Evolution 29 (4), 321-362.

Peters, C., van Kolfschoten, T., 2020. The site formation history of Schöningen 13II-4 (Germany): Testing different models of site formation by means of spatial analysis, spatial statistics and orientation analysis. J. Archaeol. Sci. 114, 105067.

Petraglia, M.D., Nash, D.T., 1987. The impact of fluvial processes on experimental sites, in: Natural formation processes and the archaeological record, BAR, pp. 108-130.

Petraglia, M.D., Potts, R., 1994. Water Flow and the Formation of Early Pleistocene Artifact Sites in Olduvai Gorge, Tanzania. Journal of Anthropological Archaeology 13, 228–254.

Pickering, T.R., Bunn, H.T., 2007. The endurance running hypothesis and hunting and scavenging in savanna-woodlands. Journal of Human Evolution, 53 (4) 434-438.

Pickering, T.R., Bunn, H.T., 2013. Meat foraging by Pleistocene African hominins, in: Domínguez-Rodrigo, M. (Ed.), Stone Tools and Fossil Bones: Debates in the Archaeology of Human Origins. Cambridge University Press, pp. 152-173.

Pickering, T.R., Domínguez-Rodrigo, M., 2005. The contribution of limb bone fracture patterns to reconstructing early hominid behaviour at Swartkrans Cave (South Africa): archaeological application of a new analytical method. International Journal of Osteoarchaeology 15 (4), 247-260.

Pickering, T.R., Domínguez-Rodrigo, M., 2013. Can we use chimpanzee behavior to model early hominin hunting?, in: Domínguez-Rodrigo, M. (Ed.), Stone Tools and Fossil Bones. Debates in the Archaeology of Human Origins, pp. 174-198.

Pickering, T.R., Domínguez-Rodrigo, M., Egeland, C.P., Brain, C.K., 2004. Beyond leopards: tooth marks and the contribution of multiple carnivore taxa to the accumulation of the Swartkrans Member 3 fossil assemblage. J. Hum. Evol. 46, 595–604.

Pickering, T.R., Egeland, C.P., 2006. Experimental patterns of hammerstone percussion damage on bones: implications for inferences of carcass processing by humans. Journal of Archaeological Science 33 (4), 459-469.

Pickering, T.R., Egeland, C.P., Domínguez-Rodrigo, M., Brain, C.K., Schnell, A.G., 2008. Testing the "shift in the balance of power" hypothesis at Swartkrans, South Africa: Hominid cave use and subsistence behavior in the Early Pleistocene. Journal of Anthropological Archaeology 27, 30–45.

Plummer, T., Bishop, L., 2016. Oldowan hominin behavior and ecology at Kanjera South,Kenya. J. Anthropol. Sci. 94, 29–40.

Plummer, T., Bishop, L.C., Ditchfield, P., Hicks, J., 1999. Research on late Pliocene Oldowan sites at Kanjera South, Kenya. J. Hum. Evol. 36, 151–170.

Plummer, T., Potts, R., 1995. Hominid fossil sample from Kanjera, Kenya: description, provenance, and implications of new and earlier discoveries. Am. J. Phys. Anthropol. 96, 7–23.

Plummer, T.W., Bishop, L.C., Ditchfield, P.W., Ferraro, J.V., Kingston, J.D., Hertel, F., Braun, D.R., 2009. The Environmental Context of Oldowan Hominin Activities at Kanjera South, Kenya, in: Hovers, E., Braun, D.R. (Eds.), Interdisciplinary Approaches to the Oldowan. Springer Netherlands, Dordrecht, pp. 149–160.

Pobiner, B., 2016. Meat-eating among the earliest humans. Am. Sci. 104 (2), 110-117.

Pobiner, B.L., 2015. New actualistic data on the ecology and energetics of hominin scavenging opportunities. Journal of Human Evolution 80, 1-16.

Pobiner, B.L., 2007. Hominin-carnivore interactions: evidence from modern carnivore bone modification and Early Pleistocene archaeofaunas (Koobi Fora, Kenya; Olduvai Gorge, Tanzania), PhD Rutgers University.

Pobiner, B.L., Braun, D.R., 2005. Strengthening the inferential link between cutmark frequency data and Oldowan hominid behavior: results from modern butchery experiments. Journal of Taphonomy 3 (2-3), 18-26.

Pobiner, B.L., Rogers, M.J., Monahan, C.M., Harris, J.W.K., 2008. New evidence for hominin carcass processing strategies at 1.5 Ma, Koobi Fora, Kenya. J. Hum. Evol. 55, 103–130.

Pontzer, H., 2012. Ecological Energetics in Early *Homo*. Curr. Anthropol. 53, S346–S358.

Pontzer, H., Brown, M.H., Raichlen, D.A., Dunsworth, H., Hare, B., Walker, K., Luke, A., Dugas, L.R., Durazo-Arvizu, R., Schoeller, D., Plange-Rhule, J., Bovet, P., Forrester, T.E., Lambert, E.V., Thompson, M.E., Shumaker, R.W., Ross, S.R., 2016. Metabolic acceleration and the evolution of human brain size and life history. Nature 533, 390–392.

Popper, K., 1972. The Logic of Scientific Discovery, sixth impression (revised). London: Hutchinson.

Potts, R., 1988a. Early Hominid Activities at Olduvai: Foundations of Human Behaviour. Routledge.

Potts, R., 1988b. On an Early Hominid Scavenging Niche. Curr. Anthropol. 29, 153–155.

Potts, R., 1984. Home Bases and Early Hominids: Reevaluation of the fossil record at Olduvai Gorge suggests that the concentrations of bones and stone tools do not represent fully formed campsites but an antecedent to them. American Scientist 72 (4), 338-347.

Potts, R., Shipman, P., 1981. Cutmarks made by stone tools on bones from Olduvai Gorge, Tanzania. Nature 291, 577–580.

Prendergast, M.E., 2008. Forager variability and transitions to food production in secondary settings: Kansyore and Pastoral Neolithic economies in East Africa. PhD. Harvard University.

Prendergast, M.E., Domínguez-Rodrigo, M., 2008. Taphonomic analyses of a hyena den and a natural-death assemblage near Lake Eyasi (Tanzania). Journal of Taphonomy 6 (3-4), 301-336.

Pruetz, J.D., 2006. Feeding ecology of savanna chimpanzees (Pan troglodytes verus) at Fongoli, Senegal. Feeding ecology in apes and other primates, 326-364.

Pruetz, J.D., Bertolani, P., 2007. Savanna Chimpanzees, Pan troglodytes verus, Hunt with Tools. Current Biology 17 (5), 412-417.

Pruetz, J.D., Bertolani, P., Ontl, K.B., Lindshield, S., Shelley, M., Wessling, E.G., 2015. New evidence on the tool-assisted hunting exhibited by chimpanzees (Pan troglodytes verus) in a savannah habitat at Fongoli, Sénégal. R Soc Open Sci 2, 140507.

Puurtinen, M., Heap, S., Mappes, T., 2015. The joint emergence of group competition and within-group cooperation. Evol. Hum. Behav. 36, 211–217.

Puurtinen, M., Mappes, T., 2009. Between-group competition and human cooperation. Proc. Biol. Sci. 276, 355–360.

Rabinovich, R., Gaudzinski-Windheuser, S., Goren-Inbar, N., 2008. Systematic butchering of fallow deer (Dama) at the early middle Pleistocene Acheulian site of Gesher Benot Ya'aqov (Israel). Journal of Human Evolution, 54 (1), 134-149.

Rankin, D.J., Taborsky, M., 2009. Assortment and the evolution of generalized reciprocity. Evolution 63, 1913–1922.

Rendu, W., 2010. Hunting behavior and Neanderthal adaptability in the Late Pleistocene site of Pech-de-l'Azé I. J. Archaeol. Sci. 37, 1798–1810.

Richards, M.P., Schmitz, R.W., 2008. Isotope evidence for the diet of the Neanderthal type specimen. Antiquity 82 (317), 553-559.

Ringrose, T., Ringrose, M.T., 2019. Package "cabootcrs."

Ripley, B.D., 2007. Pattern Recognition and Neural Networks. Cambridge University Press.

Roberts, M., Parfitt, S., 1999. Boxgrove: A Middle Pleistocene Hominid Site at Eartham Quarry, Boxgrove, West Sussex. Geoarchaeology: An International Journal 15 (8), 819-822.

Roche, H., Brugal, J.-P., Delagnes, A., Feibel, C., Harmand, S., Kibunjia, M., Prat, S., Texier, P.-J., 2003. Les sites archéologiques plio-pléistocènes de la formation de Nachukui, Ouest-Turkana, Kenya : bilan synthétique 1997–2001. C. R. Palevol 2, 663–673.

Rodríguez-Hidalgo, A., Saladie, P., Olle, A., 2015. Hominin subsistence and site function of TD10. 1 bone bed level at Gran Dolina site (Atapuerca) during the late Acheulean. Journal of Quaternary Science 30 (7), 679-701.

Rodríguez-Hidalgo, A., Saladié, P., Ollé, A., Arsuaga, J.L., Bermúdez de Castro, J.M., Carbonell, E., 2017. Human predatory behavior and the social implications of communal hunting based on evidence from the TD10.2 bison bone bed at Gran Dolina (Atapuerca, Spain). J. Hum. Evol. 105, 89–122.

Rogers, A.R., 2000. Analysis of Bone Counts by Maximum Likelihood. J. Archaeol. Sci. 27, 111–125.

Rogers, M.J., Semaw, S., 2009. From Nothing to Something: The Appearance and Context of the Earliest Archaeological Record, in: Camps, M., Chauhan, P.

(Eds.), Sourcebook of Paleolithic Transitions: Methods, Theories, and Interpretations. Springer New York, New York, NY, pp. 155–171.

Rose, L., Marshall, F., 1996. Meat Eating, Hominid Sociality, and Home Bases Revisited. Curr. Anthropol. 37, 307–338.

Roura, E.C. i., 2012. High Resolution Archaeology and Neanderthal Behavior: Time and Space in Level J of Abric Romaní (Capellades, Spain). Springer Science & Business Media.

Sahle, Y., El Zaatari, S., White, T.D., 2017. Hominid butchers and biting crocodiles in the African Plio–Pleistocene. Proc. Natl. Acad. Sci. U. S. A. 114, 13164–13169.

Sahnouni, M., Parés, J.M., Duval, M., Cáceres, I., Harichane, Z., van der Made, J., Pérez-González, A., Abdessadok, S., Kandi, N., Derradji, A., Medig, M., Boulaghraif, K., Semaw, S., 2018. 1.9-million- and 2.4-million-year-old artifacts and stone tool–cutmarked bones from Ain Boucherit, Algeria. Science 362, 1297–1301.

Sahnouni, M., Rosell, J., van der Made, J., Vergès, J.M., Ollé, A., Kandi, N., Harichane, Z., Derradji, A., Medig, M., 2013. The first evidence of cut marks and usewear traces from the Plio-Pleistocene locality of El-Kherba (Ain Hanech), Algeria: implications for early hominin subsistence activities circa 1.8 Ma. J. Hum. Evol. 64, 137–150.

Saladié, P., Huguet, R., Díez, C., Rodríguez-Hidalgo, A., Cáceres, I., Vallverdú, J., Rosell, J., Bermúdez de Castro, J.M., Carbonell, E., 2011. Carcass transport decisions in *Homo* antecessor subsistence strategies. J. Hum. Evol. 61, 425–446.

Saladié, P., Rodríguez-Hidalgo, A., Huguet, R., Cáceres, I., Díez, C., Vallverdú, J., Canals, A., Soto, M., Santander, B., Bermúdez de Castro, J.M., Arsuaga, J.L., Carbonell, E., 2014. The role of carnivores and their relationship to hominin settlements in the TD6-2 level from Gran Dolina (Sierra de Atapuerca, Spain). Quat. Sci. Rev. 93, 47–66.

Sánchez, I.C., 2003. La transición de las sociedades cazadoras-recolectoras a pastoras-agricultoras en el mediodía peninsular a través de los restos óseos: los modos de vida y de trabajo de las sociedades cazadoras y productoras. John and Erica Hedges.

Schaller, G.B., 2009. The Serengeti Lion: A Study of Predator-Prey Relations. University of Chicago Press.

Scheel, D., 1993. Profitability, encounter rates, and prey choice of African lions. Behav. Ecol. 4, 90–97.

Schick, K.D., 1984. Processes of Palaeolithic site formation: an experimental study. PhD. University of California, Berkeley.

Schiffer, M.B., 1987. Formation Processes of the Archaeological Record. University of Utah Press.

Schölkopf, B., Williamson, R.C., Smola, A.J., Shawe-Taylor, J., Platt, J.C., 2000. Support Vector Method for Novelty Detection, in: Solla, S.A., Leen, T.K., Müller, K. (Eds.), Advances in Neural Information Processing Systems 12. MIT Press, pp. 582–588.

Selvaggio, M.M., 1994. Carnivore tooth marks and stone tool butchery marks on scavenged bones: archaeological implications. Journal of Human Evolution 27 (1-3), 215-228.

Semaw, S., Renne, P., Harris, J.W., Feibel, C.S., Bernor, R.L., Fesseha, N., Mowbray, K., 1997. 2.5-million-year-old stone tools from Gona, Ethiopia. Nature 385, 333–336.

Semaw, S., Rogers, M.J., Quade, J., Renne, P.R., Butler, R.F., Dominguez-Rodrigo, M., Stout, D., Hart, W.S., Pickering, T., Simpson, S.W., 2003. 2.6-Million-year-old stone tools and associated bones from OGS-6 and OGS-7, Gona, Afar, Ethiopia. J. Hum. Evol. 45, 169–177.

Sept, J.M., King, B.J., McGrew, W.C., Moore, J., Paterson, J.D., Strier, K.B., Uehara, S., Whiten, A., Wrangham, R.W., 1992. Was There No Place Like Home?: A New Perspective on Early Hominid Archaeological Sites From the Mapping of Chimpanzee Nests [and Comments and Reply]. Curr. Anthropol. 33, 187–207.

Sherwood, R.J., Ward, S.C., Hill, A., 2002. The taxonomic status of the Chemeron temporal (KNM-BC 1). Journal of Human Evolution 42 (1-2), 153-184.

Shick, K.D., 1987. Modeling the formation of Early Stone Age artifact concentrations. J. Hum. Evol. 16, 789–807.

Shipman, P., 1986. Scavenging or Hunting in Early Hominids: Theoretical Framework and Tests. Am. Anthropol. 88, 27–43.

Shipman, P., Bosler, W., Davis, K.L., Behrensmeyer, A.K., Dunbar, R.I.M., Groves, C.P., Thackeray, F., Stucky, R.K., 1981. Butchering of Giant Geladas at an Acheulian Site [and Comments and Reply]. Curr. Anthropol. 22, 257–268.

Shipman, P., Rose, J.J., 1988. Bone tools: an experimental approach, in: Scanning electron microscopy in archaeology, pp. 303-335.

Shipman, P., Walker, A., 1989. The costs of becoming a predator. J. Hum. Evol. 18, 373–392.

Silberbauer, G., 1981. Hunter/gatherers of the Central Kalahari. Omnivorous primates, 455-498.

Simpson, C.D., 1966. Tooth eruption, growth and ageing criteria in greater kudu-*Tragelaphus* strepsiceros Pallas. National Museums of Southern Rhodesia.

Sinclair, A.R.E., 1977. The African buffalo; a study of resource limitation of populations. University of Chicago Press.

Sinclair, A.R.E., Arcese, P., Professor Department of Forest Sciences and Director Centre for Applied Conservation Research Peter Arcese, 1995. Serengeti II: Dynamics, Management, and Conservation of an Ecosystem. University of

Chicago Press.

Smith, B.A., Davies, T.M., Higham, C.F.W., 2015. Spatial and social variables in the Bronze Age Phase 4 cemetery of Ban Non Wat, Northeast Thailand. Journal of Archaeological Science: Reports 4, 362–370.

Smith, T.M., Olejniczak, A.J., Zermeno, J.P., Tafforeau, P., Skinner, M.M., Hoffmann, A., Radovčić, J., Toussaint, M., Kruszynski, R., Menter, C., Moggi-Cecchi, J., Glasmacher, U.A., Kullmer, O., Schrenk, F., Stringer, C., Hublin, J.-J., 2012. Variation in enamel thickness within the genus *Homo*. J. Hum. Evol. 62, 395–411.

Speth, J.D., 1987. Early hominid subsistence strategies in seasonal habitats. J. Archaeol. Sci. 14, 13–29.

Speth, J.D., 1983. Bison kills and bone counts: Decision making by ancient hunters. University of Chicago Press.

Spinage, C.A., 1976. Age determination of the female Grant's gazelle. Afr. J. Ecol. 14, 121–134.

Spinage, C.A., 1967. Ageing the Uganda defassa waterbuck *Kobus* defassa ugandae neumann. African Journal of Ecology 5 (1), 1-17.

Stanford, C.B., 1998. The Social Behavior of Chimpanzees and Bonobos: Empirical Evidence and Shifting Assumptions. Curr. Anthropol. 39, 399–420.

Stanford, C.B., 1996. The Hunting Ecology of Wild Chimpanzees: Implications for the Evolutionary Ecology of Pliocene Hominids. Am. Anthropol. 98, 96–113.

Stanford, C.B., Bunn, H.T., 2001. Meat-Eating and Human Evolution. Oxford University Press.

Stanford, C.B., Wallis, J., Mpongo, E., Goodall, J., 1994. Hunting Decisions in Wild Chimpanzees. Behaviour 131, 1–18.

Steele, T.E., 2004. Variation in mortality profiles of red deer(Cervus elaphus) in Middle Palaeolithic assemblages from western Europe. Int. J. Osteoarchaeol. 14, 307–320.

Steele, T.E., Weaver, T.D., 2002. The Modified Triangular Graph: A Refined Method for Comparing Mortality Profiles in Archaeological Samples. J. Archaeol. Sci. 29, 317–322.

Stein, J.K., 1987. Deposits for archaeologists. Ch. 6 in Advances in Archaeological Method and Theory, vol. 2: 337-395.

Stiner, M.C., 2002. On in situ Attrition and Vertebrate Body Part Profiles. J. Archaeol. Sci. 29, 979–991.

Stiner, M.C., 1991. Food procurement and transport by human and non-human predators. Academic Press.

Stiner, M.C., 1990. The use of mortality patterns in archaeological studies of hominid predatory adaptations. Journal of Anthropological Archaeology 9, 305–351.

Stiner, M.C., 1990. The ecology of choice: procurement and transport of animal resources by Upper Pleistocene hominids in west-central Italy. PhD, University of New Mexico.

Straus, L.G., 2019. La Cueva de Las Caldas (Priorio, Oviedo): Ocupaciones Magdalenienses en el Valle del Nalón. Maria Soledad Corchón Rodríguez, Ediciones Universidad de Salamanca.

Surbeck, M., Fowler, A., Deimel, C., Hohmann, G., 2009. Evidence for the consumption of arboreal, diurnal primates by bonobos (Pan paniscus). Am. J. Primatol. 71, 171–174.

Surbeck, M., Hohmann, G., 2008. Primate hunting by bonobos at LuiKotale, Salonga National Park. Current Biology 18 (19), 906-907.

Suwa, G., White, T.D., Howell, F.C., 1996. Mandibular postcanine dentition from the Shungura Formation, Ethiopia: Crown morphology, taxonomic allocations, and Plio-Pleistocene hominid evolution. American Journal of Physical Anthropology: The Official Publication of the American Association of Physical Anthropologists 101 (2), 247-282.

Talbot, L.M., Talbot, M.H., 1963. The Wildebeest in Western Masailand, East Africa. Wildlife Monogr. 3–88.

Taylor, R.D., 1988. Age determination of the African buffalo, Syncerus coffer (Sparrman) in Zimbabwe. African Journal of Ecology 26 (3), 207-220.

Thieme, H., 1997. Lower Palaeolithic hunting spears from Germany. Nature 385, 807–810.

Thomas, D.H., Mayer, D., 1983. Behavioral faunal analysis of selected horizons. The archaeology of monitor valley 2, 353-391.

Thompson, A.M., Raihani, N.J., Hockey, P.A.R., Britton, A., Finch, F.M., Ridley, A.R., 2013. The influence of fledgling location on adult provisioning: a test of the blackmail hypothesis. Proceedings of the Royal Society B: Biological Sciences 280 (1760), 20130558.

Thompson, C.E.L., Ball, S., Thompson, T.J.U., Gowland, R., 2011. The abrasion of modern and archaeological bones by mobile sediments: the importance of transport modes. J. Archaeol. Sci. 38, 784–793.

Titterington, M., 2010. Neural Networks. Encyclopedia of Statistical Sciences.

Todd, L.C., Rapson, D.J., 1988. Long bone fragmentation and interpretation of faunal assemblages: Approaches to comparative analysis. J. Archaeol. Sci. 15, 307–325.

Toots, H., 1965. Random orientation of fossils and its significance. Rocky Mt Geol 4 (2), 59-62.

de la Torre, I., Benito-Calvo, A., 2013. Application of GIS methods to retrieve orientation patterns from imagery; a case study from Beds I and II, Olduvai Gorge (Tanzania). Journal of Archaeological Science 40 (5), 2446-2457.

Toth, N.P., 1982. The stone technologies of early hominids at Koobi Fora,

Kenya: an experimental approach. University of California, Berkeley.

Planton, H.P., Michaux, I.G., 2013. *Tragelaphus* derbianus Giant Eland (Lord Derby's Eland). Mammals of Africa 6, 186-190.

Treves, A., Naughton-Treves, L., 1999. Risk and opportunity for humans coexisting with large carnivores. Journal of Human Evolution 36 (3), 275-282.

Uehara, S, 1992. Characteristics of predation by the chimpanzees in the Mahale Mountains National Park. Human Origins. University of Tokyo Press.

Ungar, P.S., Grine, F.E., Teaford, M.F., Pérez-Pérez, A., 2001. A review of interproximal wear grooves on fossil hominin teeth with new evidence from Olduvai Gorge. Arch. Oral Biol. 46, 285–292.

Uribelarrea, D., Domínguez-Rodrigo, M., Pérez-González, A., Vegas Salamanca, J., Baquedano, E., Mabulla, A., Musiba, C., Barboni, D., Cobo-Sánchez, L., 2014. Geo-archaeological and geometrically corrected reconstruction of the 1.84 Ma FLK *Zinj* paleolandscape at Olduvai Gorge, Tanzania. Quat. Int. 322-323, 7–31.

Valensi, P., Psathi, E., 2004. Faunal exploitation during the Middle Palaeolithic in south-eastern France and north-western Italy. International Journal of Osteoarchaeology 14 (3-4), 256-272.

Venables, W.N., Ripley, B.D., 2002. Modern Applied Statistics with S. Statistics and Computing. Springer Link.

Villa, P., Lenoir, M., 2009. Hunting and Hunting Weapons of the Lower and Middle Paleolithic of Europe, in: Hublin, J.-J., Richards, M.P. (Eds.), The Evolution of Hominin Diets: Integrating Approaches to the Study of Palaeolithic Subsistence. Springer Netherlands, Dordrecht, pp. 59–85.

Villa, P., Mahieu, E., 1991. Breakage patterns of human long bones. J. Hum. Evol. 21, 27–48.

Villmoare, B., Kimbel, W.H., Seyoum, C., Campisano, C.J., DiMaggio, E.N., Rowan, J., Braun, D.R., Arrowsmith, J.R., Reed, K.E., 2015. Paleoanthropology. Early *Homo* at 2.8 Ma from Ledi-Geraru, Afar, Ethiopia. Science 347, 1352–1355.

Voorhies, M.R., 1969. Taphonomy and population dynamics of an early Pliocene vertebrate fauna, Knox county, Nebraska. Laramie: University of Wyoming. Contributions to Geology (Rocky Mountain Geology) 1, 1-69.

Waagepetersen, R.P., 2007. An estimating function approach to inference for inhomogeneous Neyman–Scott processes. Biometrics 63 (1), 252-258.

Waguespack, N.M., Surovell, T.A., Denoyer, A., Dallow, A., Savage, A., Hyneman, J., Tapster, D., 2009. Making a point: wood- versus stone-tipped projectiles. Antiquity 83, 786–800.

Walker, A., Zimmerman, M.R., Leakey, R.E., 1982. A possible case of hypervitaminosis A in *Homo erectus*. Nature 296, 248–250.

Walter, R.C., Manega, P.C., Hay, R.L., 1992. Tephrochronology of Bed I,

Olduvai Gorge: An application of laser-fusion 40Ar39Ar dating to calibrating biological and climatic change. Quat. Int. 13-14, 37–46.

Walter, R.C., Manega, P.C., Hay, R.L., Drake, R.E., Curtis, G.H., 1991. Laser-fusion 40Ar/39Ar dating of bed I, Olduvai Gorge, Tanzania. Nature 354 (6349, 145-149.

Washburn, S.L., 1957. Australopithecines: the hunters or the hunted? Am. Anthropol. 59, 612–614.

Watson, R.M., 1967. The population ecology of the Serengeti wildebeest. PhD, University of Cambridge.

Watts, D.P., 2008. Scavenging by chimpanzees at Ngogo and the relevance of chimpanzee scavenging to early hominin behavioral ecology. J. Hum. Evol. 54, 125–133.

Watts, D.P., Mitani, J.C., 2002. Hunting and meat sharing by chimpanzees at Ngogo, Kibale National Park, Uganda. Behavioural diversity in chimpanzees and bonobos, 244.

Watts, D.P., Mitani, J.C., 2001. Boundary Patrols and Intergroup Encounters in Wild Chimpanzees. Behaviour 138, 299–327.

Weaver, T.D., Boyko, R.H., Steele, T.E., 2011. Cross-platform program for likelihood-based statistical comparisons of mortality profiles on a triangular graph. J. Archaeol. Sci. 38, 2420–2423.

Whallon, R., 1974. Spatial Analysis of Occupation Floors II: The Application of Nearest Neighbor Analysis. Am. Antiq. 39, 16–34.

Whallon, R., Mellars, P., 1978. The spatial analysis of Mesolithic occupation floors: a reappraisal. The Early Postglacial Settlement of Northern Europe, 27-35.

White, T.E., 1953. Observations on the Butchering Technique of Some Aboriginal Peoples No. 2*. Am. Antiq. 19, 160–164.

Wilkins, J., Schoville, B.J., Brown, K.S., 2014. An experimental investigation of the functional hypothesis and evolutionary advantage of stone-tipped spears. PLoS One 9, e104514.

Wolpert, D.H., 1996. The Existence of A Priori Distinctions Between Learning Algorithms. Neural Comput. 8, 1391–1420.

Wood, B., Collard, M., 1999. The changing face of genus *Homo*. Evolutionary Anthropology: Issues, News, and Reviews 8 (6), 195-207.

Wood, B., Gilby, I., 2019. From Pan to man the hunter: hunting and meat sharing by chimpanzees, humans, and our common ancestor, in: Muller, M., Wrangham, R., Pilbeam, D., (Eds.), Chimpanzees and Human Evolution. UCLA, pp. 339-382.

Wood, B.M., Marlowe, F.W., 2013. Household and kin provisioning by Hadza men. Hum. Nat. 24, 280–317.

Woodburn, J., 1970. Hunters and gatherers: the material culture of the no-

madic Hadza.

Woodcock, N.H., 1977. Specification of fabric shapes using an eigenvalue method. Geol. Soc. Am. Bull. 88 (9), 1231-1236.

Yellen, J.E., 1977. Archaeological approaches to the present: models for reconstructing the past. New York. Academic Press.

Yravedra, J., 2006. Tafonomía aplicada a Zooarqueología. UNED ediciones, Madrid.

Yravedra, J., Álvarez-Alonso, D., Estaca, V., López-Cisneros, P., Andrés-Chaín, M., Arrizabalaga, Á., Jordá Pardo, J.F., Elorza, M., Iriarte-Chiapusso, M.-J., Sesé, C., Uzquiano, P., 2017. Selection and Exploitation of Macro-Vertebrate Resources During the Upper Palaeolithic in Northern Spain. New Evidence from Coímbre Cave (Peñamellera Alta, Asturias). Oxford Journal of Archaeology 36 (4), 331-354.

Yravedra, J., Domínguez-Rodrigo, M., 2009. The shaft-based methodological approach to the quantification of long limb bones and its relevance to understanding hominid subsistence in the Pleistocene: application to four Palaeolithic sites. Journal of Quaternary Science 24 (1), 85-96.

Yravedra, J., Lagos, L., Bárcena, F., 2011. A taphonomic study of wild wolf (Canis lupus) modification of horse bones in Northwestern Spain. Journal of Taphonomy 9 (1), 37-65.

Yravedra, J., Rubio-Jara, S., Panera, J., Martos, J.A., 2019. Hominins and Proboscideans in the Lower and Middle Palaeolithic in the Central Iberian Peninsula. Quat. Int. 520, 140–156.

Zink, K.D., Lieberman, D.E., 2016. Impact of meat and Lower Palaeolithic food processing techniques on chewing in humans. Nature 531, 500–503.

7. Appendix

Table 7.1.A) *Parameter values for each machine learning algorithm using the combined dataset including both longitudinal and oblique breakage planes.*

Algorithm	Accuracy	Kappa	Agent	Sensitivity	Specificity	B. accuracy
NNET	0.86	0.74	**C. crocuta**	0.40	0.97	0.69
			C. lupus	0.99	0.92	0.95
			Percussion	0.87	0.85	0.86
SVM	0.85	0.74	**C. crocuta**	0.36	0.97	0.67
			C. lupus	0.98	0.92	0.95
			Percussion	0.87	0.87	0.86
KNN	0.83	0.71	**C. crocuta**	0.34	0.98	0.66
			C. lupus	0.95	0.89	0.92
			Percussion	0.87	0.83	0.85
RF	0.88	0.80	**C. crocuta**	0.51	0.99	0.75
			C. lupus	1.00	0.92	0.96
			Percussion	0.89	0.88	0.89
MDA	0.83	0.70	**C. crocuta**	0.30	0.98	0.64
			C. lupus	0.98	0.87	0.93
			Percussion	0.85	0.85	0.85
NB	0.65	0.30	**C. crocuta**	0.19	0.99	0.59
			C. lupus	0.30	0.98	0.64
			Percussion	0.97	0.29	0.63
PLS	0.83	0.70	**C. crocuta**	0.06	0.99	0.52
			C. lupus	1.00	0.91	0.95
			Percussion	0.90	0.78	0.84

Table 7.1.B) *Classification probabilities obtained using the different algorithms on the combined dataset including longitudinal and oblique fracture planes.*

NNET			
Agent	**C.crocuta**	**C.lupus**	**Hominin**
Classification	66	43	882
%Classification	6.7%	4.3%	89.0%
SVM			
Agent	**C.crocuta**	**C.lupus**	**Hominin**
Classification	52	41	898
%Classification	5.2%	4.1%	90.6%
KNN			
Agent	**C.crocuta**	**C.lupus**	**Hominin**
Classification	46	58	887
%Classification	4.6%	5.9%	89.5%
RF			
Agent	**C.crocuta**	**C.lupus**	**Hominin**
Classification	83	42	866
%Classification	8.4%	4.2%	87.4
MDA			
Agent	**C.crocuta**	**C.lupus**	**Hominin**
Classification	55	62	874
%Classification	5.5%	6.3%	88.2%
NB			
Agent	**C.crocuta**	**C.lupus**	**Hominin**
Classification	33	15	943
%Classification	3.3%	1.5%	95.2%
PLS			
Agent	**C.crocuta**	**C.lupus**	**Hominin**
Classification	8	44	939
%Classification	0.8%	4.4%	94.8%

Table 7.2.A) *Parameter values for each machine learning algorithm using the sample of longitudinal planes <90º.*

Algorithm	Accuracy	Kappa	Agent	Sensitivity	Specificity	B. accuracy
NNET	0.82	0.70	**C. crocuta**	0.47	0.97	0.72
			C. lupus	0.96	0.89	0.92
			Percussion	0.79	0.85	0.82
SVM	**0.79**	**0.64**	**C. crocuta**	0.29	0.97	0.63
			C. lupus	0.98	0.87	0.92
			Percussion	0.75	0.82	0.79
KNN	**0.77**	**0.60**	**C. crocuta**	0.18	0.97	0.58
			C. lupus	0.98	0.82	0.90
			Percussion	0.75	0.82	0.79
RF	**0.80**	**0.65**	**C. crocuta**	0.29	0.98	0.64
			C. lupus	1.00	0.84	0.92
			Percussion	0.75	0.84	0.79
MDA	**0.78**	**0.62**	**C. crocuta**	0.18	0.99	0.58
			C. lupus	1.00	0.87	0.93
			Percussion	0.75	0.79	0.77
NB	**0.70**	**0.49**	**C. crocuta**	0.18	0.99	0.58
			C. lupus	0.84	0.84	0.84
			Percussion	0.75	0.69	0.72
PLS	**0.78**	**0.62**	**C. crocuta**	0.17	0.98	0.58
			C. lupus	1.00	0.84	0.92
			Percussion	0.75	0.81	0.78

Table 7.2.B) *Classification probabilities obtained using the different algorithms on the sample of longitudinal planes <90º.*

NNET			
Agent	**C.crocuta**	**C.lupus**	**Hominin**
Classification	68	20	245
%Classification	20.4%	6.0%	73.6%
SVM			
Agent	**C.crocuta**	**C.lupus**	**Hominin**
Classification	36	19	278
%Classification	10.8%	5.7%	83.5%
KNN			
Agent	**C.crocuta**	**C.lupus**	**Hominin**
Classification	17	32	284
%Classification	5.1%	9.6%	85.3%
RF			
Agent	**C.crocuta**	**C.lupus**	**Hominin**
Classification	43	18	272
%Classification	12.9%	5.4%	81.7%
MDA			
Agent	**C.crocuta**	**C.lupus**	**Hominin**
Classification	14	18	301
%Classification	4.2%	5.4%	90.4%
NB			
Agent	**C.crocuta**	**C.lupus**	**Hominin**
Classification	8	18	307
%Classification	2.4%	5.4%	92.2%
PLS			
Agent	**C.crocuta**	**C.lupus**	**Hominin**
Classification	21	18	294
%Classification	6.3%	5.4%	88.3%

Table 7.3.A) *Parameter values for each machine learning algorithm using the sample of longitudinal planes >90º.*

Algorithm	Accuracy	Kappa	Agent	Sensitivity	Specificity	B. accuracy
NNET	0.78	0.62	**C. crocuta**	0.44	0.94	0.69
			C. lupus	0.93	0.86	0.90
			Percussion	0.77	0.84	0.80
SVM	0.75	0.55	**C. crocuta**	0.33	0.93	0.63
			C. lupus	0.79	0.85	0.82
			Percussion	0.80	0.81	0.81
KNN	0.75	0.53	**C. crocuta**	0.11	1.00	0.56
			C. lupus	0.86	0.80	0.83
			Percussion	0.80	0.73	0.77
RF	0.77	0.59	**C. crocuta**	0.11	0.94	0.53
			C. lupus	1.00	0.85	0.92
			Percussion	0.77	0.84	0.80
MDA	0.71	0.50	**C. crocuta**	0.44	0.93	0.69
			C. lupus	0.89	0.75	0.82
			Percussion	0.66	0.86	0.76
NB	0.54	0.23	**C. crocuta**	0.78	0.68	0.73
			C. lupus	0.21	0.98	0.60
			Percussion	0.66	0.59	0.63
PLS	0.83	0.67	**C. crocuta**	0.11	1.00	0.56
			C. lupus	1.00	0.85	0.92
			Percussion	0.86	0.84	0.85

Table 7.3.B) *Classification probabilities obtained using the different algorithms on the sample of longitudinal planes >90º.*

NNET			
Agent	**C.crocuta**	**C.lupus**	**Hominin**
Classification	31	13	137
%Classification	17.1%	7.2%	75.7%
SVM			
Agent	**C.crocuta**	**C.lupus**	**Hominin**
Classification	**21**	**11**	**149**
%Classification	11.6%	6.1%	82.3%
KNN			
Agent	**C.crocuta**	**C.lupus**	**Hominin**
Classification	**8**	**13**	**160**
%Classification	4.4%	7.2%	88.4%
RF			
Agent	**C.crocuta**	**C.lupus**	**Hominin**
Classification	**3**	**13**	**165**
%Classification	1.7%	7.2%	91.2%
MDA			
Agent	**C.crocuta**	**C.lupus**	**Hominin**
Classification	**30**	**13**	**138**
%Classification	16.6%	7.2%	76.2%
NB			
Agent	**C.crocuta**	**C.lupus**	**Hominin**
Classification	**80**	**0**	**101**
%Classification	44.2%	0%	55.8%
PLS			
Agent	**C.crocuta**	**C.lupus**	**Hominin**
Classification	**7**	**13**	**161**
%Classification	3.9%	7.2%	89.0%

Table 7.4. A) *Parameter values for each machine learning algorithm using the sample of oblique planes <90º.*

Algorithm	Accuracy	Kappa	Agent	Sensitivity	Specificity	B. accuracy
NNET	0.75	0.58	**C. crocuta**	0.36	0.94	0.65
			C. lupus	0.89	0.84	0.86
			Percussion	0.73	0.81	0.78
SVM	0.80	0.66	**C. crocuta**	0.21	0.98	0.60
			C. lupus	1.00	0.81	0.90
			Percussion	0.80	0.88	0.84
KNN	0.82	0.69	**C. crocuta**	0.29	0.99	0.64
			C. lupus	1.00	0.86	0.93
			Percussion	0.82	0.84	0.83
RF	0.80	0.67	**C. crocuta**	0.29	0.97	0.63
			C. lupus	1.00	0.83	0.91
			Percussion	0.76	0.88	0.83
MDA	0.80	0.67	**C. crocuta**	0.36	0.96	0.66
			C. lupus	1.00	0.83	0.91
			Percussion	0.76	0.90	0.83
NB	0.52	0.13	**C. crocuta**	0.07	1.00	0.54
			C. lupus	0.14	1.00	0.57
			Percussion	1.00	0.13	0.56
PLS	0.79	0.64	**C. crocuta**	0.00	1.00	0.50
			C. lupus	1.00	0.83	0.91
			Percussion	0.84	0.81	0.82

Table 7.4. B) *Classification probabilities obtained using the different algorithms on the sample of oblique planes <90º.*

NNET			
Agent	**C.crocuta**	**C.lupus**	**Hominin**
Classification	37	3	263
%Classification	14.1%	1%	86.8%
SVM			
Agent	**C.crocuta**	**C.lupus**	**Hominin**
Classification	13	12	278
%Classification	4.3%	4.0%	91.7%
KNN			
Agent	**C.crocuta**	**C.lupus**	**Hominin**
Classification	14	10	279
%Classification	4.6%	3.3%	92.1%
RF			
Agent	**C.crocuta**	**C.lupus**	**Hominin**
Classification	21	6	276
%Classification	6.9%	2.0%	91.1%
MDA			
Agent	**C.crocuta**	**C.lupus**	**Hominin**
Classification	39	9	255
%Classification	12.9%	3.0%	84.2%
NB			
Agent	**C.crocuta**	**C.lupus**	**Hominin**
Classification	0	0	303
%Classification	0%	0%	100%
PLS			
Agent	**C.crocuta**	**C.lupus**	**Hominin**
Classification	3	5	295
%Classification	0.9%	1.7%	97.4%

Table 7.5. A) *Parameter values for each machine learning algorithm using the sample of oblique planes >90º.*

Algorithm	Accuracy	Kappa	Agent	Sensitivity	Specificity	B. accuracy
NNET	0.83	0.61	**C. crocuta**	0.18	0.95	0.57
			C. lupus	0.83	0.93	0.88
			Percussion	0.90	0.73	0.81
SVM	0.88	0.71	**C. crocuta**	0.09	0.98	0.53
			C. lupus	0.97	0.92	0.94
			Percussion	0.93	0.85	0.89
KNN	0.83	0.59	**C. crocuta**	0.09	0.98	0.53
			C. lupus	0.79	0.92	0.86
			Percussion	0.92	0.70	0.81
RF	0.88	0.70	**C. crocuta**	0.09	0.98	0.54
			C. lupus	0.93	0.93	0.93
			Percussion	0.94	0.80	0.87
MDA	0.91	0.78	**C. crocuta**	0.27	0.99	0.63
			C. lupus	1.00	0.96	0.98
			Percussion	0.95	0.83	0.89
NB	0.78	0.33	**C. crocuta**	0.18	0.99	0.59
			C. lupus	0.24	0.99	0.62
			Percussion	1.00	0.28	0.64
PLS	0.89	0.72	**C. crocuta**	0.00	1.00	0.50
			C. lupus	1.00	0.92	0.96
			Percussion	0.95	0.83	0.89

Table 7.5. B) *Classification probabilities obtained using the different algorithms on the sample of oblique planes >90º.*

NNET			
Agent	**C.crocuta**	**C.lupus**	**Hominin**
Classification	12	7	155
%Classification	6.9%	4.0%	89.1%
SVM			
Agent	**C.crocuta**	**C.lupus**	**Hominin**
Classification	9	8	157
%Classification	5.2%	4.6%	90.2%
KNN			
Agent	**C.crocuta**	**C.lupus**	**Hominin**
Classification	11	7	156
%Classification	6.3%	4.0%	86.7%
RF			
Agent	**C.crocuta**	**C.lupus**	**Hominin**
Classification	11	7	156
%Classification	6.3%	40.2%	89.7%
MDA			
Agent	**C.crocuta**	**C.lupus**	**Hominin**
Classification	9	8	157
%Classification	5.2%	4.6%	90.2%
NB			
Agent	**C.crocuta**	**C.lupus**	**Hominin**
Classification	4	0	170
%Classification	2.3%	0%	97.7%
PLS			
Agent	**C.crocuta**	**C.lupus**	**Hominin**
Classification	0	8	166
%Classification	0%	4.6%	95.4%

Table 7.6. A) *BSM in bone specimens of small ungulate carcasses (size 1 and 2) considering NSP.*

Cortical surface preservation	Correction for dry broken bones (X+(Y/2))		Number of specimens (NSP)	CM	PM	TM
Good			146/490 (29.80%)	8/146 (5.48%)	4/146 (2.74%)	7/146 (4.79%)
	Green (X)	**Dry (Y)**	77.5	8/77.5 (10.32%)	4/77.5 (5.16%)	7/77.5 (9.03%)
	75	5				
Moderate			86/490 (18.25%)	3/86 (4.11%)	2/86 (2.74%)	1/86 (1.37%)
	Green (X)	**Dry (Y)**	42.5	3/42.5 (7.06%)	2/42.5 (4.71%)	1/42.5 (2.35%)
	40	5				
Good+Moderate			232/490 (47.35%)	11/232 (4.74%)	6/232 (2.59%)	8/232 (3.45%)
	Green (X)	**Dry (Y)**	120	11/120 (9.17%)	6/120 (5%)	8/120 (6.67%)
	115	10				
Poor			258/490 (49.25%)	5/258 (2.54%)	3/258 (1.52%)	4/258 (2.03%)
	Green (X)	**Dry (Y)**	138	5/138 (3.62%)	3/138 (2.17%)	4/138 (2.90%)
	116	44				
Total			490/3191 (15.36%)	16/490 (3.27%)	9/490 (1.84%)	12/490 (2.45%)

Table 7.6. B) *BSM in bone specimens of small ungulate carcasses (size 1 and 2) considering NISP*

Cortical surface preservation	Correction for dry broken bones (X+(Y/2))		Number of specimens (NISP)	CM	PM	TM
Good			130/400 (32.5%)	8/130 (6.15%)	4/130 (3.08%)	7/130 (5.38%)
	Green (X)	Dry (Y)	77.5	8/77.5 (10.32%)	4/77.5 (5.16%)	7/77.5 (9.03%)
	75	5				
Moderate			73/400 (18.25%)	3/73 (4.11%)	2/73 (2.74%)	1/73 (1.37%)
	Green (X)	Dry (Y)	42.5	3/42.5 (7.06%)	2/42.5 (4.71%)	1/42.5 (2.35%)
	40	5				
Good+Moderate			203/400 (50.75%)	11/203 (5.42%)	6/203 (2.96%)	8/203 (3.94%)
	Green (X)	Dry (Y)	120	11/120 (9.17%)	6/120 (5%)	8/120 (6.67%)
	115	10				
Poor			197/400 (49.25%)	5/197 (2.54%)	3/197 (1.52%)	4/197 (2.03%)
	Green (X)	Dry (Y)	138	5/138 (3.62%)	3/138 (2.17%)	4/138 (2.90%)
	116	44				
Total			400	16/400 (4%)	9/400 (2.25%)	12/400 (2.75%)

Table 7.7. *BSM on long limb bone specimens per NISP of small sized ungulates (carcass size 1 and 2)*

Cortical surface preservation	Correction for dry broken bones (X+(Y/2))		Number of specimens (NISP)	CM	PM	TM
Good			54/178 (30.34%)	6/54 (11.11%)	4/54 (7.41%)	3/54 (5.56%)
	Green (X)	Dry (Y)	51.5	6/51.5 (11.65%)	4/51.5 (7.77%)	3/51.5 (5.83%)
	51	1				
Moderate			36/178 (20.22%)	1/36 (2.78%)	2/36 (5.56%)	0
	Green (X)	Dry (Y)	26	1/26 (3.85%)	2/26 (7.69%)	0
	24	4				
Good+Moderate			90/178 (50.56%)	7/90 (7.78%)	6/90 (6.67%)	3/90 (3.33%)
	Green (X)	Dry (Y)	77.5	7/77.5 (9.03%)	6/77.5 (7.74%)	3/77.5 (3.87%)
	75	5				
Poor			88/178 (49.44%)	4/88 (4.54%)	3/88 (3.41%)	2/88 (2.27%)
	Green (X)	Dry (Y)	77	4/77 (5.19%)	3/77 (3.9%)	2/77 (2.6%)
	70	14				
Total			178	11/178 (6.18%)	9/178 (5.06%)	5/178 (2.81%)

Table 7.8. *BSM on axial bone specimens per NISP of small sized ungulates (carcass size 1 and 2)*

Cortical surface preservation	Correction for dry broken bones (X+(Y/2))		Number of specimens (NISP)	CM	PM	TM
Good			52/174 (29.89%)	2/52 (3.85%)	0	3/52 (5.77%)
	Green (X)	Dry (Y)	11.5	2/11.5 (17.39%)	0	3/11.5 (26.09%)
	10	3				
Moderate			31/174 (17.82%)	2/31 (6.45%)	0	1/31 (3.26%)
	Green (X)	Dry (Y)	5.5	2/5.5 (36.36%)	0	1/5.5 (18.18%)
	5	1				
Good+Moderate			83/174 (47.70%)	4/83 (4.82%)	0	4/83 (4.82%)
	Green (X)	Dry (Y)	17.5	4/17.5 (22.86%)	0	4/17.5 (22.86%)
	15	5				
Poor			91/174 (52.30%)	1/91 (1.10%)	0	1/91 (1.10%)
	Green (X)	Dry (Y)	10	1/10 (10%)	0	1/10 (10%)
	4	14				
Total			174	5/174 (2.87%)	0	5/174 (2.87%)

Table 7.9. A) *BSM on medium sized ungulates (carcass size 3 and 4) per NSP*

Cortical surface preservation	Correction for dry broken bones (X+(Y/2))		Number of specimens (NSP)	CM	PM	TM
Good			363/1920 (18.91%)	35/363 (9.64%)	36/363 (9.92%)	11/363 (3.03%)
	Green (X)	Dry (Y)	227	35/227 (15.42%)	36/227 (15.86%)	11/227 (4.85%)
	220	14				
Moderate			313/1920 (16.30%)	17/313 (5.43%)	21/313 (6.71%)	10/313 (3.19%)
	Green (X)	Dry (Y)	209.5	17/209.5 (8.11%)	21/209.5 (10.02%)	10/209.5 (4.77%)
	202	15				
Good+Moderate			676/1920 (35.21%)	52/676 (7.69%)	57/676 (8.43%)	21/676 (3.11%)
	Green (X)	Dry (Y)	456.5	52/456.5 (11.39%)	57/456.5 (12.49%)	21/456.5 (4.60%)
	442	29				
Poor			1244/1920 (64.79%)	41/1244 (3.30%)	12/1244 (0.96%)	5/1244 (0.40%)
	Green (X)	Dry (Y)	758	41/758 (5.41%)	12/758 (1.58%)	5/758 (0.66%)
	610	296				
Total			1920/3191 (60.17%)	93/1920 (4.84%)	69/1920 (3.59%)	26/1920 (1.35%)

Table 7.9. *B) BSM on medium sized ungulates (carcass size 3 and 4) per NISP*

Cortical surface preservation	Correction for dry broken bones (X+(Y/2))		Number of specimens (NISP)	CM	PM	TM
Good			289/1360 (21.25%)	33/289 (11.42%)	30/289 (10.38%)	11/289 (3.81%)
	Green (X)	Dry (Y)	167	33/167 (19.76%)	30/167 (17.96%)	11/167 (6.59%)
	160	14				
Moderate			237/1360 (17.43%)	16/237 (6.75%)	16/237 (6.75%)	7/237 (2.95%)
	Green (X)	Dry (Y)	140	16/140 (11.43%)	16/140 (11.43%)	7/140 (5%)
	133	14				
Good+Moderate			526/1360 (38.68%)	49/526 (9.32%)	46/526 (8.75%)	18/526 (3.42%)
	Green (X)	Dry (Y)	307	49/307 (15.96%)	46/307 (14.98%)	18/307 (5.86%)
	293	28				
Poor			834/1360 (61.32%)	31/834 (3.72%)	9/834 (1.08%)	4/834 (0.48%)
	Green (X)	Dry (Y)	443	31/443 (7%)	9/443 (2.03%)	4/443 (0.9%)
	335	216				
Total			1360	80/1360 (5.88%)	55/1360 (4.04%)	22/1360 (1.62%)

Table 7.10. *BSM on long limb bones of medium sized ungulates (carcass size 3 and 4) per NISP*

Cortical surface preservation	Correction for dry broken bones (X+(Y/2))		Number of specimens (NISP)	CM	PM	TM
Good			134/614 (21.84%)	29/134 (21.64%)	28/134 (20.90%)	5/134 (3.73%)
	Green (X)	Dry (Y)	116	29/116 (25%)	28/116 (24.14%)	5/116 (4.31%)
	113	6				
Moderate			114/614 (18.57%)	10/114 (8.77%)	16/114 (14.04%)	5/114 (4.39%)
	Green (X)	Dry (Y)	107	10/107 (9.35%)	16/107 (14.95%)	5/107 (4.67%)
	106	2				
Good+Moderate			248/614 (40.39%)	39/248 (15.73%)	44/248 (17.74%)	10/248 (4.03%)
	Green (X)	Dry (Y)	223	39/223 (17.49%)	44/223 (19.73%)	10/223 (4.48%)
	219	8				
Poor			366/614 (59.61%)	24/366 (6.58%)	9/366 (2.46%)	3/366 (0.82%)
	Green (X)	Dry (Y)	327	24/327 (7.34%)	9/327 (2.75%)	3/327 (0.92%)
	286	82				
Total			614	63/614 (10.26%)	53/614 (8.63%)	13/614 (2.12%)

Table 7.11 . *BSM on axial bones of medium sized ungulates (carcass size 3 and 4) per NISP*

Cortical surface preservation	Correction for dry broken bones (X+(Y/2))		Number of specimens (NISP)	CM	PM	TM
Good			112/596 (18.79%)	4/112 (3.57%)	0	4/112 (3.57%)
	Green (X)	Dry (Y)	40	4/40 (10%)	0	4/40 (10%)
	36	8				
Moderate			105/596 (17.62%)	6/105 (5.71%)	0	2/105 (1.90%)
	Green (X)	Dry (Y)	28	6/28 (21.43%)	0	2/28 (7.14%)
	22	12				
Good+Moderate			217/596 (36.41%)	10/217 (4.61%)	0	6/217 (2.76%)
	Green (X)	Dry (Y)	68	10/68 (14.71%)	0	6/68 (8.82%)
	58	20				
Poor			379/596 (63.59%)	7/379 (1.85%)	0	1/379 (0.26%)
	Green (X)	Dry (Y)	86	7/86 (8.14%)	0	1/86 (1.16%)
	33	106				
Total			596	17/596 (2.85%)	0	7/596 (1.17%)

Table 7.12 A) *CM, PM and TM frequencies according to long bone element and section. Numerator is number of cut-marked, percussion-marked and tooth-marked specimens in each appendicular section. Denominator is total number of specimens in each appendicular section.*

	DS 22B Carcass size 1-2			DS 22B Carcass size 3-4		
	CM	**PM**	**TM**	**CM**	**PM**	**TM**
HUM PSH	0/0 (0)	0/0 (0)	0/0 (0)	1/8 (12.5)	0/8 (0)	0/8 (0)
HUM MSH	4/29 (13.79)	2/29 (6.90)	1/29 (3.45)	7/150 (4.67)	12/150 (8)	1/150 (0.67)
HUM DSH	0/6 (0)	0/6 (0)	0/6 (0)	2/29 (6.90)	0/29 (0)	1/29 (3.45)
RAD PSH	1/7 (14.29)	1/7 (14.29)	0/7 (0)	5/41 (12.20)	1/41 (2.44)	2/41 (4.88)
RAD MSH	3/23 (13.04)	2/23 (8.70)	1/23 (4.35)	12/90 (13.33)	9/90 (7.78)	4/90 (2.22)
RAD DSH	0/2 (0)	0/2 (0)	0/2 (0)	0/9 (0)	0/9 (0)	0/9 (0)
MC PSH	0/3 (0)	0/3 (0)	0/3 (0)	0/13 (0)	1/13 (7.69)	0/13 (0)
MC MSH	0/11 (0)	0/11 (0)	1/11 (9.09)	5/58 (8.62)	9/58 (15.52)	2/58 (3.45)
MC DSH	0/2 (0)	0/2 (0)	0/2 (0)	1/11 (9.09)	0/11 (0)	0/11 (0)
FEM PSH	0/8 (0)	0/8 (0)	0/8 (0)	1/12 (8.33)	0/12 (0)	0/12 (0)
FEM MSH	1/38 (2.63)	3/38 (7.89)	0/38 (0)	11/78 (14.10)	5/78 (6.41)	0/78 (0)
FEM DSH	0/3 (0)	0/3 (0)	0/3 (0)	0/2 (0)	0/2 (0)	0/12 (0)
TIB PSH	0/2 (0)	0/2 (0)	0/2 (0)	0/6 (0)	0/6 (0)	0/6 (0)
TIB MSH	1/44 (2.27)	1/44 (2.27)	0/44 (0)	14/129 (10.85)	11/129 (8.53)	3/129 (2.33)
TIB DSH	0/4 (0)	0/4 (0)	0/4 (0)	0/4 (0)	0/4 (0)	0/4 (0)
MT PSH	0/6 (0)	0/6 (0)	0/6 (0)	0/13 (0)	0/13 (0)	0/13 (0)
MT MSH	1/18 (5.56)	0/18 (0)	1/18 (5.56)	4/42 (9.52)	5/42 (11.90)	0/42 (0)
MT DSH	0/4 (0)	0/4 (0)	0/4 (0)	0/7 (0)	0/7 (0)	0/7 (0)

Table 7.12 B) *CM, PM and TM frequencies according to long bone element and section. Numerator is number of cut-marked, percussion-marked, and tooth-marked specimens in each appendicular section. Denominator is the total number of cut-marked, percussion- and tooth-marked specimens in each element.*

	DS 22B Carcass size 1-2			DS 22B Carcass size 3-4		
	CM	**PM**	**TM**	**CM**	**PM**	**TM**
HUM PSH	0/0 (0)	0/0 (0)	0/0 (0)	1/10 (10)	0/12 (0)	0/2 (0)
HUM MSH	4/4 (100)	2/2 (100)	1/1 (100)	7/10 (70)	12/12 (100)	1/2 (50)
HUM DSH	0/6 (0)	0/6 (0)	0/6 (0)	2/10 (20)	0/12 (0)	1/2 (50)
RAD PSH	1/4 (25)	1/3 (33.33)	0/1 (0)	5/17 (29.41)	1/10 (10)	2/6 (33.33)
RAD MSH	3/4 (75)	2/3 (66.67)	1/1 (100)	12/17 (70.59)	9/10 (90)	4/6 (66.67)
RAD DSH	0/4 (0)	0/3 (0)	0/1 (0)	0/17 (0)	0/10 (0)	0/6 (0)
MC PSH	0/0 (0)	0/0 (0)	0/1 (0)	0/6 (0)	1/10 (10)	0/2 (0)
MC MSH	0/0 (0)	0/0 (0)	1/1 (100)	5/6 (83.33)	9/10 (90)	2/2 (100)
MC DSH	0/0 (0)	0/0 (0)	0/0 (0)	1/6 (16.67)	0/10 (0)	0/2 (0)
FEM PSH	0/1 (0)	0/3 (0)	0/0 (0)	1/12 (8.33)	0/5 (0)	0/0 (0)
FEM MSH	1/1 (100)	3/3 (100)	0/0 (0)	11/12 (91.67)	5/5 (100)	0/0 (0)
FEM DSH	0/1 (0)	0/3 (0)	0/0 (0)	0/12 (0)	0/5 (0)	0/0 (0)
TIB PSH	0/1 (0)	0/1 (0)	0/0 (0)	0/14 (0)	0/11 (0)	0/3 (0)
TIB MSH	1/1 (100)	1/1 (100)	0/0 (0)	14/14 (100)	11/11 (100)	3/3 (100)
TIB DSH	0/1 (0)	0/1 (0)	0/0 (0)	0/14 (0)	0/11 (0)	0/3 (0)
MT PSH	0/1 (0)	0/0 (0)	0/1 (0)	0/4 (0)	0/5 (0)	0/0 (0)
MT MSH	1/1 (100)	0/0 (0)	1/1 (100)	4/4 (100)	5/5 (100)	0/0 (0)
MT DSH	0/1 (0)	0/0 (0)	0/1 (0)	0/4 (0)	0/5 (0)	0/0 (0)

Table 7.13 A) *Percentages for the number of marked bones from each appendicular or bone section in relation to the total number of specimens of that same appendicular or bone section.*

	DS 22B Carcass size 1-2			DS 22B Carcass size 3-4		
	CM	**PM**	**TM**	**CM**	**PM**	**TM**
ULB	5/77 (6.49)	5/77 (6.49)	2/77 (2.60)	22/255 (8.63)	17/255 (6.67)	2/255 (0.78)
ILB	5/70 (7.14)	4/70 (5.71)	1/70 (1.43)	31/253 (12.25)	21/253 (8.30)	9/253 (3.56)
LLB	1/31 (3.23)	0/31 (0)	2/31 (6.45)	10/104 (9.62)	15/104 (14.42)	2/104(1.92)
PSH	1/25 (4)	1/25 (4)	0/25 (0)	7/93 (7.53)	2/93 (2.15)	2/93 (2.15)
MSH	10/163 (6.13)	8/163 (4.91)	4/163 (2.45)	53/547 (9.69)	51/547 (9.32)	10/547 (1.83)
DSH	0/28 (0)	0/28 (0)	0/28 (0)	3/65 (4.62)	0/65 (0)	1/65 (1.54)

Table 7.13 B) *Percentages of cut-marked, percussion-marked and tooth-marked specimens of each appendicular and bone section in relation to the total number of marked specimens of that same appendicular or bone section.*

	DS 22B Carcass size 1-2			DS 22B Carcass size 3-4		
	CM	**PM**	**TM**	**CM**	**PM**	**TM**
ULB	5/11 (45.45)	5/9 (55.56)	1/5 (20)	22/63 (34.92)	17/53 (26.98)	2/13 (15.38)
ILB	5/11 (45.45)	4/9 (44.44)	1/5 (20)	31/63 (49.21)	21/53 (39.62)	9/13 (69.23)
LLB	1/11 (9.09)	0/9 (0)	2/5 (40)	10/63 (15.87)	15/53 (28.30)	2/13(15.38)
PSH	1/11 (9.09)	1/9 (11.11)	0/5 (0)	7/63 (11.11)	2/53 (3.77)	2/13 (15.38)
MSH	10/11 (90.90)	8/9 (88.89)	5/5 (100)	53/63 (84.13)	51/53 (96.23)	10/13 (76.92)
DSH	0/11 (0)	0/9 (0)	0/5 (0)	3/63 (4.76)	0/53 (0)	1/13 (7.69)

Table 7.14 A) *Cut and tooth mark frequencies for axial elements, skull fragments, and mandibles for each carcass size. Numerator is the number of cut-marked and tooth-marked specimens in each element. Denominator is the total number of specimens of each element.*

	DS 22B Carcass size 1-2		DS 22B Carcass size 3-4	
	CM	**TM**	**CM**	**TM**
Rib	4/128 (3.13)	1/128 (0.78)	9/378 (2.38)	3/378 (0.79)
Vertebra indet	0/2	0/2	2/25 (8)	0/25
Cervical vertebra	0/2	0/2	0/18	2/18 (11.11)
Thoracic vertebra	0/9	2/9 (22.22)	3/52 (5.77)	0/52
Lumbar vertebra	1/7 (14.29)	0/7	1/16 (6.25)	0/16
Sacrum	0/0	0/0	0/6	0/6
Caudal vertebra	0/2	0/2	0/5	0/5
Scapula	0/10	0/10	2/51 (3.92)	0/51
Pelvis	0/14	2/14 (14.29)	0/42	2/42 (4.76)
Sternum	0/0	0/0	0/3	0/3
Total axial	5/174 (2.87)	5/174 (2.87)	17/596 (2.85)	7/596 (1.17)
Skull	0/3	0/3	1/16 (6.25)	0/16
Mandible	0/11	0/11	0/51	0/51

Table 7.14 B) *Distribution of CM and TM across the axial elements. Numerator is number of cut-marked, and tooth-marked specimens in each axial element. Denominator is the total number of cut-marked or tooth-marked specimens.*

	DS 22B Carcass size 1-2		DS 22B Carcass size 3-4	
	CM	**TM**	**CM**	**TM**
Rib	4/5 (80)	1/5 (20)	9/17 (52.94)	3/7 (42.86)
Vertebra indet	0/5	0/5	2/17 (11.76)	0/7
Cervical vertebra	0/5	0/5	0/17	2/7 (28.57)
Thoracic vertebra	0/5	2/5 (40)	3/17 (17.65)	0/7
Lumbar vertebra	1/5 (20)	0/5	1/17 (5.88)	0/7
Sacrum	0/5	0/5	0/17	0/7
Caudal vertebra	0/5	0/5	0/17	0/7
Scapula	0/5	0/5	2/17 (11.76)	0/7
Pelvis	0/5	2/5 (40)	0/17	2/7 (28.57)
Sternum	0/5	0/5	0/17	0/7

FIGURE 7.1. *Bone cluster patterns from FLK Zinj, PTK, and areas A, B, and C from DS.*

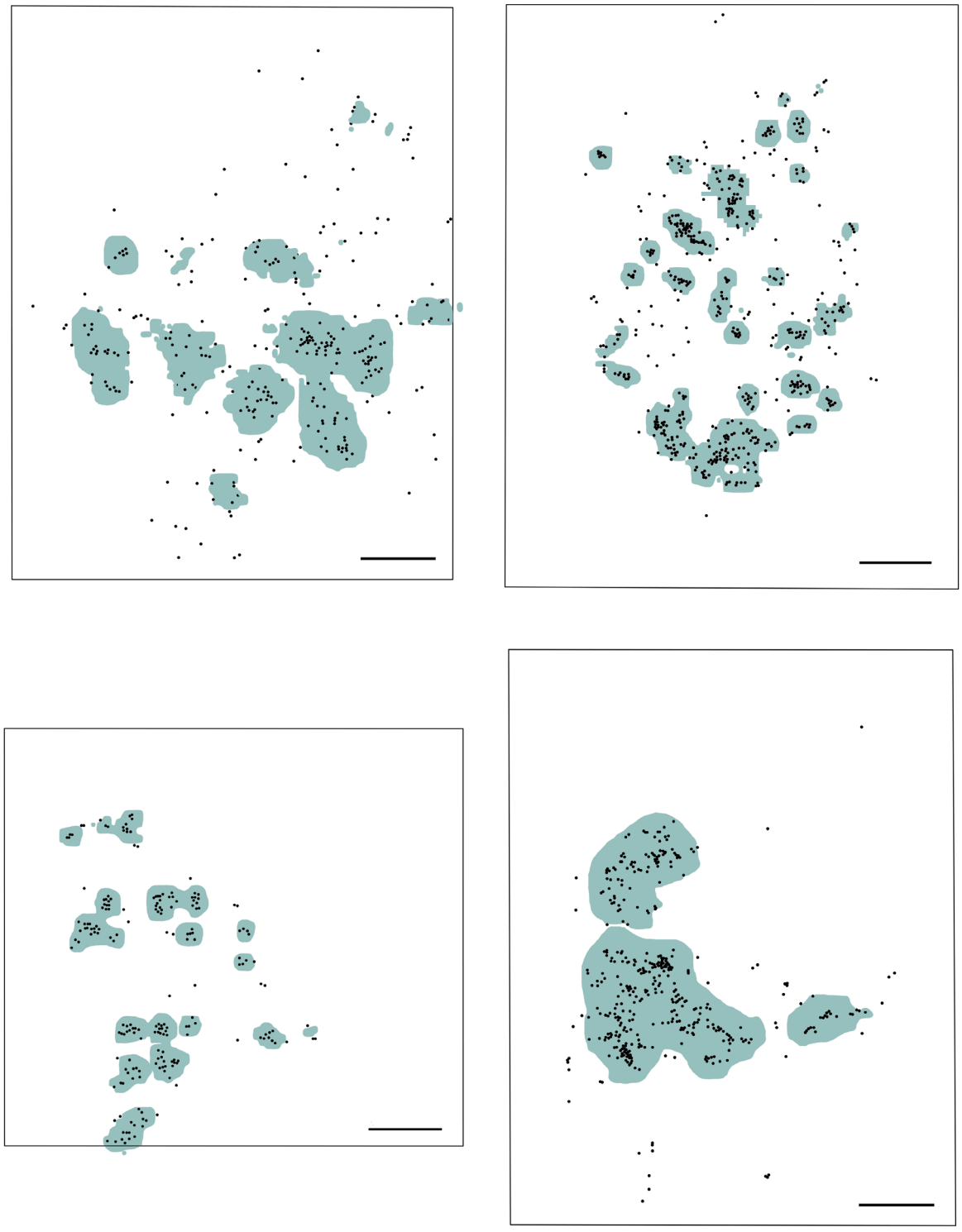

FIGURE 7.2. *Bone refuse cluster patterns from the four hunter-gatherer campsites mentioned in the text.*

FIGURE 7.3. *Lithic cluster patterns from FLK Zinj, PTK, and areas A, B, and C from DS.*

FIGURE 7.4. *Overall cluster patterns from FLK Zinj, PTK, and areas A, B, and C from DS.*

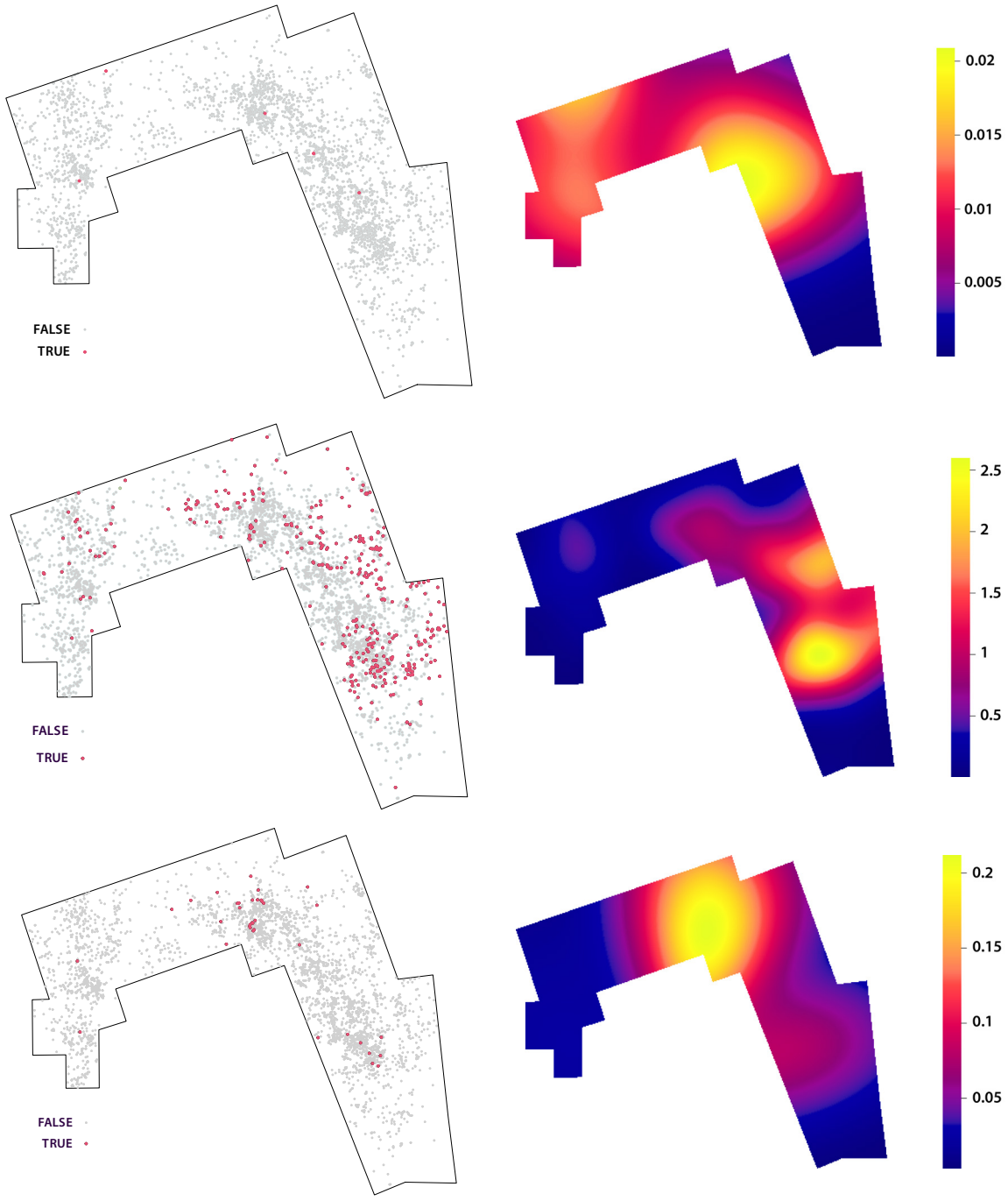

FIGURE 7.5. *Distribution and density maps of the preservation variables abrasion (A), carbonate (B), and water disturbance (C)*

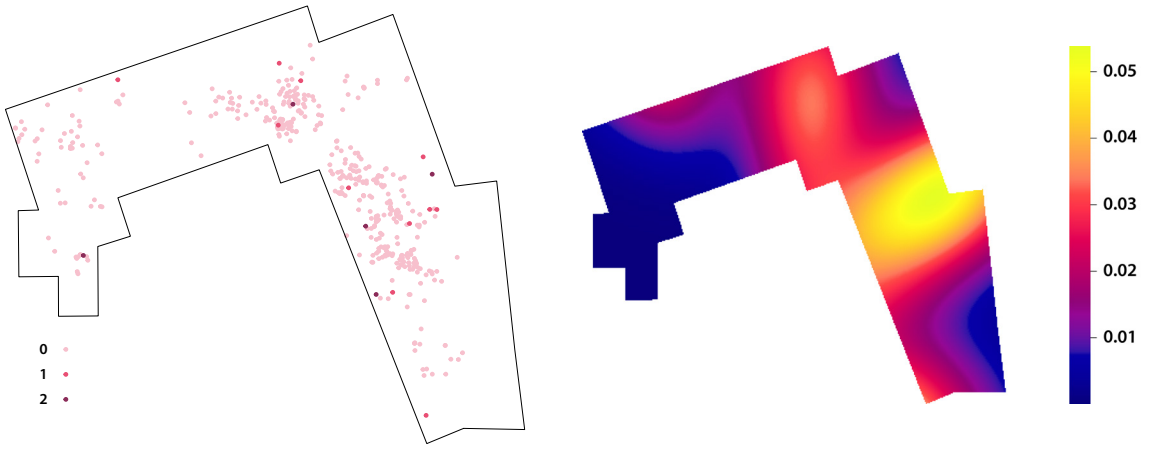

FIGURE 7.6. *Spatial distribution and density map of the weathered specimens at DS.*

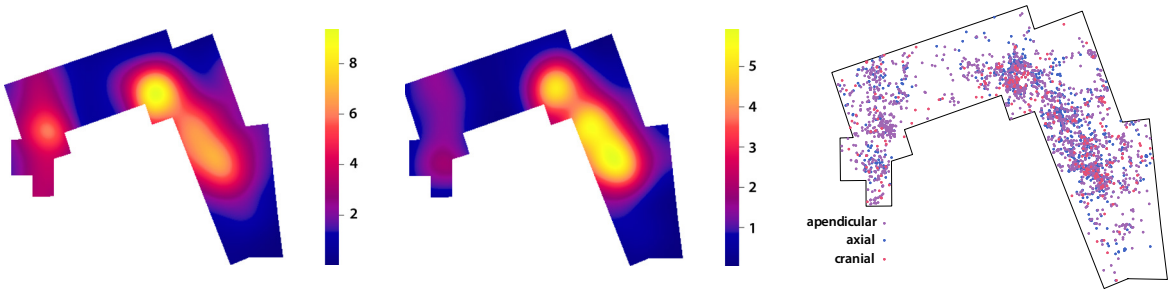

FIGURE 7.7. *Density maps of appendicular and axial specimens, and map of their spatial distribution.*

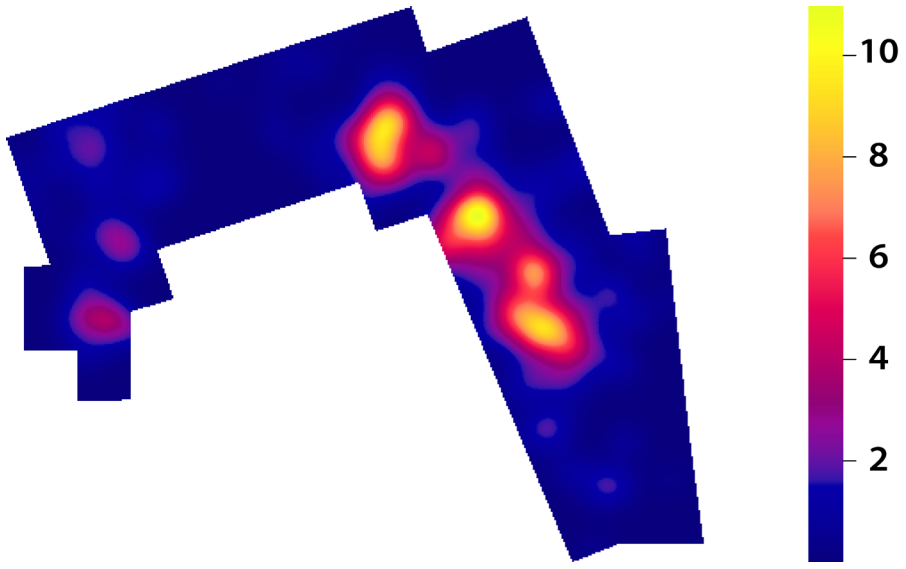

FIGURE 7.8. *Density map of ribs and vertebra remains forming clusters.*

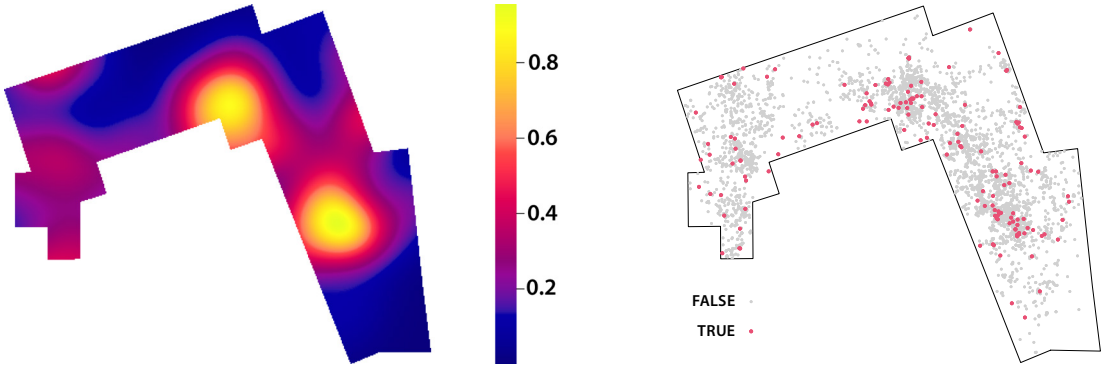

FIGURE 7.8. *Density map and spatial distribution of teeth in the assemblage.*

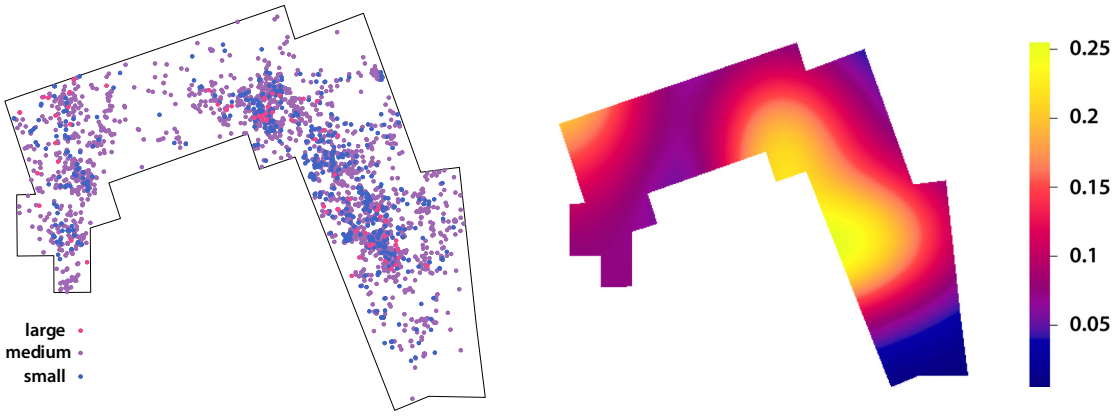

FIGURE 7.9. *Spatial distribution of bone specimens according to carcass size, and spatial density map of the distribution of large carcasses.*

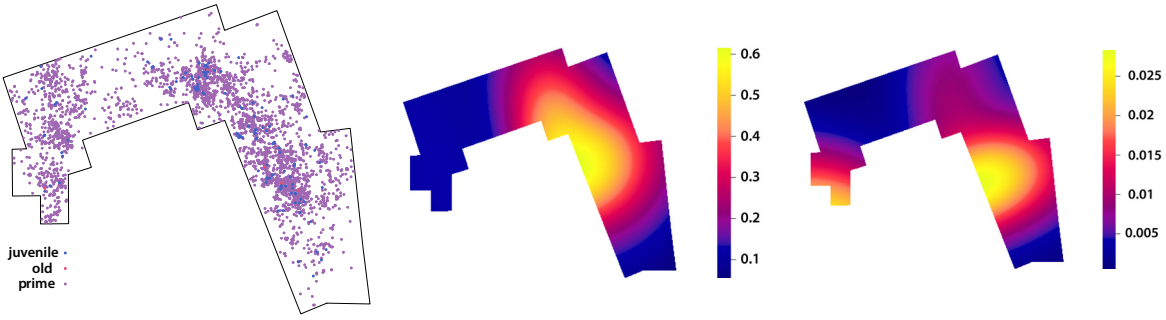

FIGURE 7.10. *Spatial distribution of bone specimens according to bovid age class, and density maps of juvenile and old individuals.*

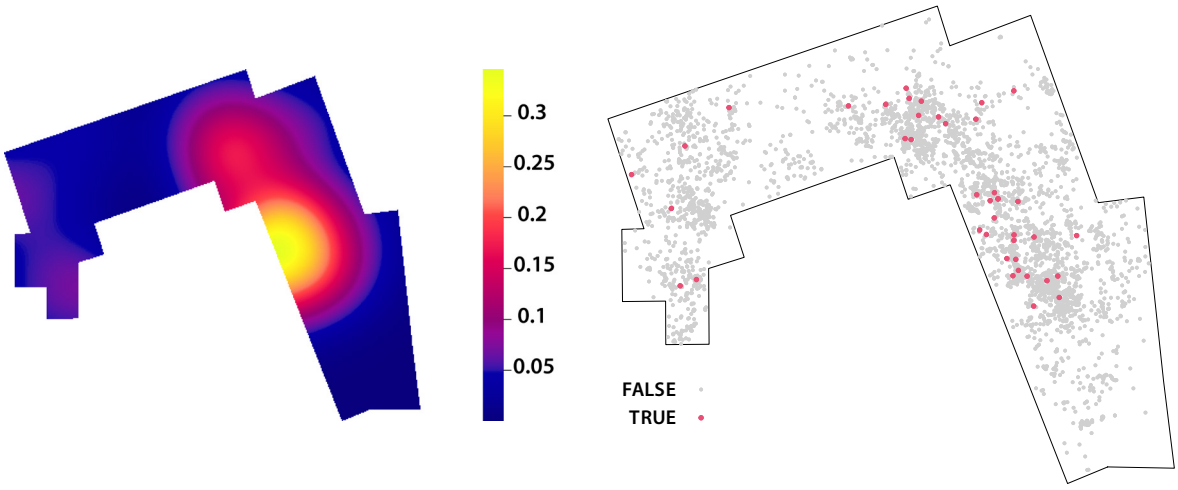

FIGURE 7.11. *Spatial distribution of tooth-marked specimens and density map of these occurrences.*

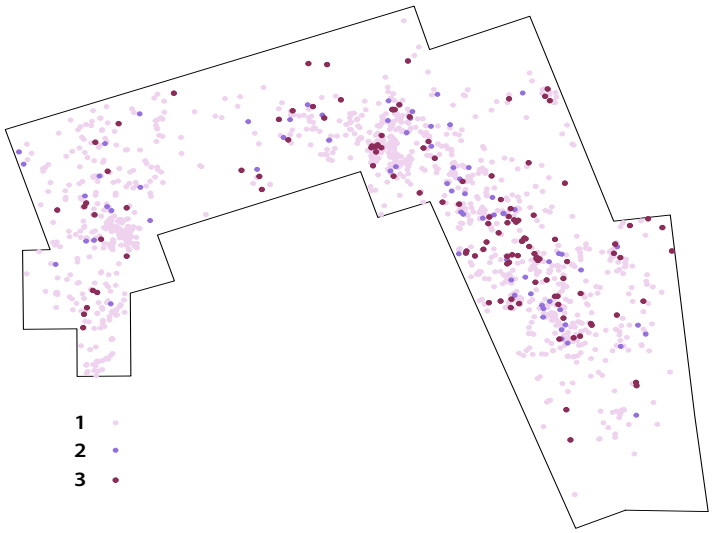

FIGURE 7.12. *Spatial distribution of the different shaft circumference types.*

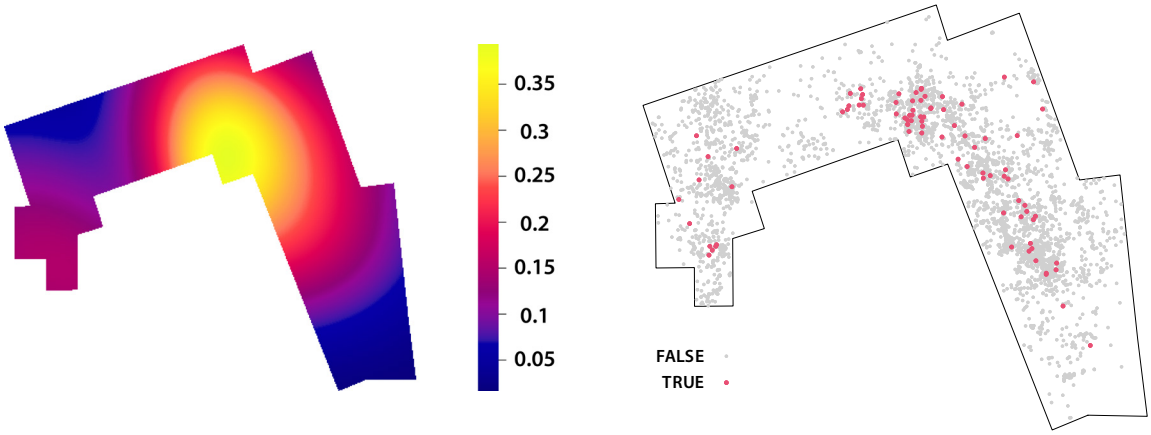

FIGURE 7.13. *Density map and spatial distribution of percussion-marked specimens.*

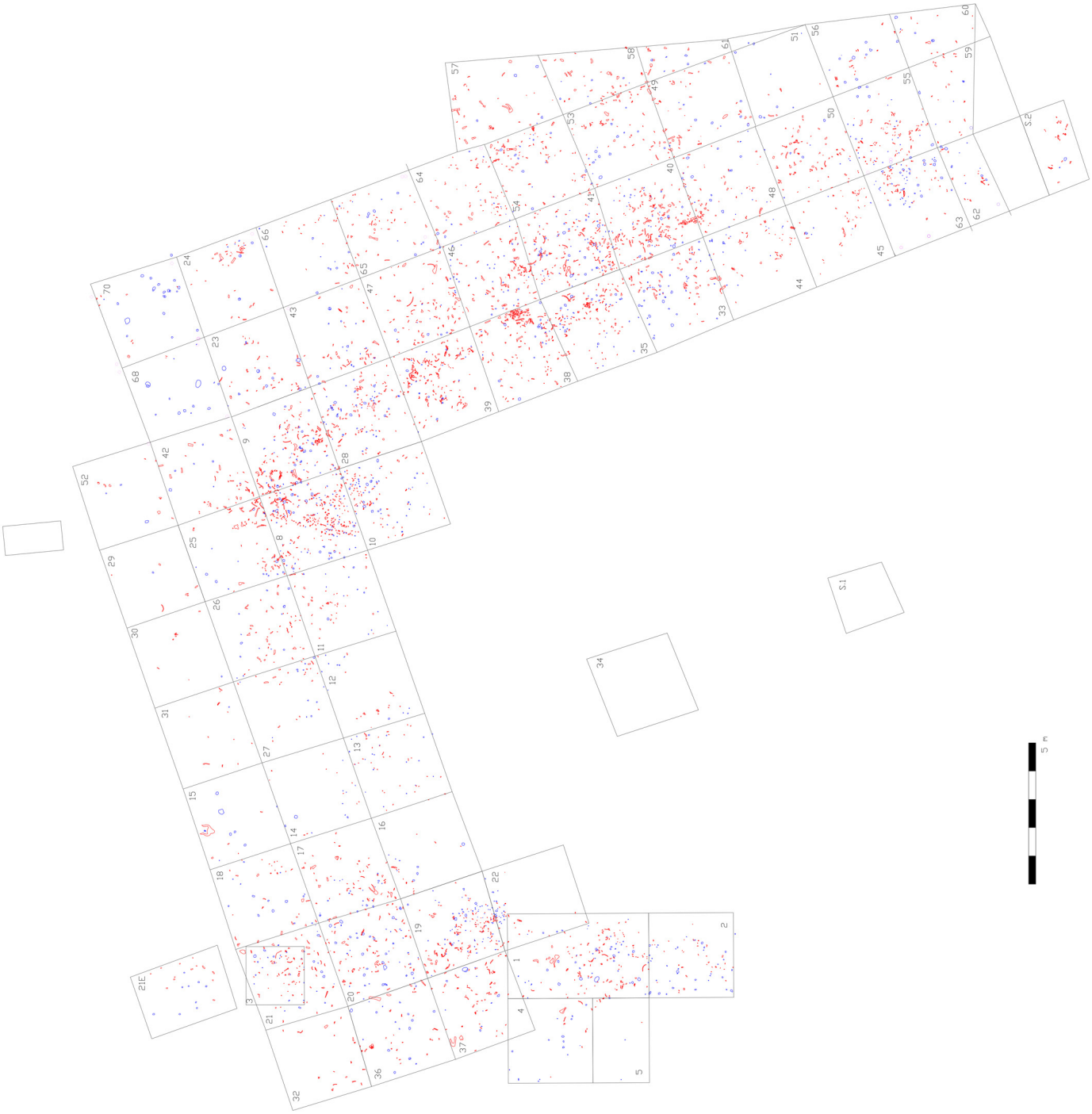

FIGURE 7.14. *Distribution of bone remains (red) and lithics (blue) across the excavated trenches at DS.*